Rainfall-Runoff Modelling in Arid Areas

By

Aisha Mufti Al-Sayyid Hassan Al-Qurashi

A dissertation submitted for the degree of Doctor of Philosophy of the University of London

Department of Civil and Environmental Engineering

Imperial College London

2008

EIBL
LONDON
UNIV.

Declaration of own work

I declare that this thesis

'RAINFALL-RUNOFF MODELLING IN ARID AREAS'

Is my own work and that where any material could be constructed as the work of others, it is fully cited and referenced, and/or with appropriate acknowledgment given.

Aisha Mufti Al-Qurashi

Supervisors:

Prof. Howard S. Wheater

Dr. Neil R. McIntyre

Abstract

Arid areas have distinctive hydrological features substantially different from those of humid areas. The high temporal and spatial distribution of the rainfall, flash floods, absence of base flow, sparsity of plant cover, high transmission losses, high amounts of evaporation and evapotranspiration and the general climatologies are examples of such differences.

The aim of this Ph.D. research is to use advanced tools of model analysis to test some of the current models that consider arid area hydrological characteristics. As most models were mainly developed for other regions, an attempt is made to study their limitations using Omani hydrological data, providing some guidelines for improved rainfall-runoff modelling in arid areas in general and Oman in particular. Two different types of models were selected for this research; KINEROS2, which is an event based, semi-distributed, physically-based model that is considered suitable to be used for arid area conditions, and IHACRES which is a continuous-time, conceptual model, which was applied in both lumped and semi-distributed modes.

These models were applied to hourly and daily data from 25 runoff events during the period 1996-1999 in Wadi Ahin, area 734km^2.

By calibration to each event individually, KINEROS2 could fit a chosen characteristic of the hydrographs well (either volume, peak, or time-to-peak); but in general it could not fit the characteristics together, and there was very high uncertainty in predictions due to the variability of parameter values over events. The lumped IHACRES performed poorly using any selected objective function when fitted over a 2-year calibration period using daily data; and no benefit was noticed using either a more complex version or using the semi-distributed version. However, there was evidence that the semi-distributed IHACRES performs better than any of the other tested models if hourly data is used. The general conclusions are that performance is limited primarily by data constraints and hence the models cannot be assessed fairly; and semi-distributed models with simple process representations may be preferred.

To

My Country…

My Parents…

All who believed in Me

Acknowledgements

I would like at the beginning to thank the Islamic Development Bank, who funded this research and aided in making my dream to contribute to the hydrological community come true. I would like also to thank the Ministry of Regional Municipalities and Water Resources (formal Ministry of Regional Municipalities, Environment and Water Resources) in Oman, who promoted me and gave me study leave for this research.

I would also like especially to thank my supervisors, Professor Howard Wheater whose direction and guidance have had a great effect on the output of this research, and Dr Neil McIntyre whose close supervision and guidance was a great help during the whole study period.

My sincere thanks go to Mr Zahir Al Sulaimani whose support and aid in easing the data collection was extremely helpful. My sincere thanks also go to Carl Unkrich, who kindly provided me with information I needed concerning the KINEROS2 model. The RRMT-L and RRMT-SD versions were introduced briefly by Ilias Pechlivanidis and Barbara Orellana.

I would also like to thank Angela Frederick, Fionnuala Dhonnabhain and Judith Barritt for being very helpful to me during my study period.

My great thanks also goes to my colleagues and friends specially Andrew Ireson, who was a great support and whose friendly manner had a great impact and added not only to my technical knowledge but to my human knowledge too. I wish him all the best in his life and career.

I would never forget to thank my friends John Kay, who was like a God father during the period I spent here, and also Fred Kaul for being there for me whenever I needed them. Their advices and support were invaluable especially during my lows. I would like to thank also my close fried Branka Subotic for providing me with great emotional support every time I felt low. I would like also to thank Max Kigobe for his support in the most critical time on my final stage of my PhD. Sue Hutton and her friendship and advices to cope up with different problems is also much appreciated.

My family, and specially my parents and my sister Khadeeja, and my niece Al-Maha, whose unlimited love and support was the air I needed to continue this research.

I would like to thank my uncle and his family for all the love and support they give me during my stay.

My great thanks go to all who believed in me and were there whenever I needed them with their love, prays, and any kind of support.

List of Papers

1. Al-Qurashi, A. M, and Wheater, H.S. (2005),'Rainfall-runoff in arid areas', WSTA Seventh Gulf Water Conference, Vol 1, 509-526, November.

2. McIntyre, N., Al-Qurashi, A., Wheater, H.S. (2007) Regression analysis of rainfall-runoff data from an arid catchment in Oman. Hydrological Sciences Journal, Vol 52 (6), 1103-1118.

3. Wheater, H.S., Al-Qurashi, A. M. H, McIntyre, N., (2008) 'Hydrological process in wadis-scientific and practical aspects', Proceedings of the 4th International Conference on Wadi Hydrology, Seeb, Oman, 2-4 December 2007, publisher - Ministry of Regional Municiplaities and Water Resources

4. Al-Qurashi, A., McIntyre, N., Wheater H., and Carl Unkrich, (2008),' Flow prediction in an arid catchment in Oman', Journal of Hydrology, Vol 355, 91-105.

5. McIntyre, N., and Al-Qurashi, A., (2008),'Applicability of a semi-distributed rainfall-runoff model to an arid catchment in Oman', waiting for publication.

Paper 1 presents material from chapters 2, and 4. Papers 2, 3 and 4 were co-authored by the author, and present material from chapters 6 and 7. Work similar to that presented in chapter 8 was presented in Paper 5.

Contents

DECLARATION OF OWN WORK 2
ABSTRACT 3
ACKNOWLEDGEMENTS 5
LIST OF PAPERS 7
LIST OF FIGURES 13
LIST OF TABLES 16

CHAPTER 1 22
RAINFALL-RUNOFF MODELLING IN ARID AREAS 22
1.1 INTRODUCTION 22
1.2 THE BACKGROUND TO THE RESEARCH 22
1.2.1 Hydrological features of arid areas 23
1.2.2 Overview on Rainfall-Runoff Modelling 24
1.3 RESEARCH OBJECTIVE 24
1.4 THE STUDY AREA 25
1.5 THE SELECTED RAINFALL-RUNOFF MODELS 25
1.5.1 KINEROS2 26
1.5.2 IHACRES 26
1.6 STRUCTURE OF THE THESIS 27
1.6.1 Chapter One: 27
1.6.2 Chapter Two 27
1.6.3 Chapter Three 28
1.6.4 Chapter Four 28
1.6.5 Chapter Five 28
1.6.6 Chapter Six 28
1.6.7 Chapter Seven 29
1.6.8 Chapter Eight 29
1.6.9 Chapter Nine 30

CHAPTER 2 31
DISTINCTIVE FEATURES OF THE HYDROLOGY OF ARID AREAS 31
2.1 INTRODUCTION 31
2.2 CLIMATE 31
2.2.1 Temperature 32
2.2.2 Sunshine hours 32
2.2.3 Humidity 32
2.2.4 Evapotranspiration 32
2.3 RAINFALL 33
2.3.1 Rainfall generation 33
2.3.2 Spatial and temporal variation of rainfall 33
2.3.3 Annual average rainfall variation 34
2.3.4 Intensity characteristics of storm rainfall 35
2.3.5 Elevation effects on rainfall 36
2.3.6 Effects of seasonality on rainfall 36
2.4 RUNOFF 37
2.4.1 Spatial and temporal variation of runoff 38
2.4.2 Initial losses 39
2.4.3 Hydrograph characteristics 39
2.4.4 Flood peak magnitudes 41
2.4.5 Characteristics of flood events 41
2.5 RAINFALL-RUNOFF RELATIONSHIPS 42
2.5.1 Effects of hydrological processes 42
2.5.2 Effects of watershed physical characteristics 43
2.5.3 Runoff coefficients 46
2.5.4 Difficulties in determining rainfall-runoff relationships 47
2.6 CHANNEL TRANSMISSION LOSSES 48
2.6.1 Definition of transmission losses 48
2.6.2 Importance of transmission losses 49

2.6.3 Factors affecting transmission losse....50
2.6.4 Transmission losses measurements....51
2.7 VEGETATION COVER....52
2.7.1 Effects of vegetation cover on interception....52
2.7.2 Effects of vegetation cover on infiltration....53
2.7.3 Effects of vegetation cover on runoff....53
2.7.4 Effects of vegetation cover on hydrological parameters....53
2.8 EVAPORATION AND POTENTIAL EVAPOTRANSPIRATION....53
2.9 CONCLUSIONS....55

CHAPTER 3....57
RAINFALL AND RAINFALL-RUNOFF MODELLING....57
3.1 INTRODUCTION....57
3.2 AIM OF MODELLING....58
3.3 TYPES OF RAINFALL-RUNOFF MODEL....58
3.3.1 Process Based Classification....59
3.3.1.1 Lumped models:....59
3.3.1.2 Distributed models:....59
3.3.1.3 Deterministic:....59
3.3.1.4 Stochastic:....59
3.3.1.5 Mixed:....59
3.3.2 Time-Scale Based Classification....59
3.3.3 Space-Scale Based Classification....60
3.3.4 Model Structure Based Classification....60
3.3.4.1 Metric Models:....60
3.3.4.2 Conceptual Models:....61
3.3.4.3 Physics-Based Models:....61
3.4 MODEL CALIBRATION....62
3.4.1 Types of Calibration....63
3.4.1.1 Manual calibration:....63
3.4.1.2 Automatic Calibration....63
3.4.2 Verification....65
3.4.3 Sensitivity Analysis....65
3.5 RELIABILITY ESTIMATION....66
3.5.1 Types of Uncertainty....66
3.5.1.1 Natural Uncertainties:....66
3.5.1.2 Data Uncertainty:....67
3.5.1.3 Model–Parameter Uncertainty....67
3.5.1.4 Model-Structure Uncertainty:....67
3.5.2 Reliability Analysis Methods....67
3.6 CURRENT PRACTICE....68
3.7 OVERVIEW ON RAINFALL REPRESENTATION....71
3.7.1 Methods of Estimating Average Rainfall....71
3.7.1.1 Arithmetic mean:....72
3.7.1.2 Isohyetal method:....72
3.7.1.3 Thiessen method:....72
3.7.1.4 Triangulation method:....73
3.7.1.5 Inverse-distance weighted mean:....73
3.7.1.6 Recently developed methods:....73
3.8 CONCLUSION....74

CHAPTER 4....75
APPLICATION OF RAINFALL AND RAINFALL-RUNOFF MODELLING IN ARID-AREAS75
4.1 INTRODUCTION....75
4.2 OVERVIEW OF RAINFALL REPRESENTATION IN ARID AREAS....75
4.3 EFFECT OF ARIDITY ON RAINFALL-RUNOFF MODEL PERFORMANCE....85
4.4 APPLICATION OF DIFFERENT RAINFALL-RUNOFF MODEL TYPES....87
4.4.1 Examples and implication of using Metric Type Models for arid areas....87
4.4.2 Examples and Implication of Using Conceptual Type Models in Arid Areas....93
4.4.3 Examples and implication of using Physically- Based Type Models in arid areas....109
4.5 DISCUSSION OF RESULTS....114
4.6 CONCLUSIONS....118

CHAPTER 5 122
STUDY AREA DESCRIPTION AND ITS HYDROLOGY 122
5.1 INTRODUCTION 122
5.2 OVERVIEW ON OMAN'S LOCATION AND HYDROLOGY 122
5.2.1 Oman's location 122
5.2.2 Oman's General Geomorphology and Geology 123
5.2.3 Oman's General Hydrology 124
5.2.3.1 Climate 125
5.2.3.2 Rainfall 126
5.2.3.3 Runoff 129
5.3 THE SELECTED BASIN 132
5.3.1 Wadi Ahin Topography and Geomorphology 133
5.3.2 Hydrogeology 134
5.3.3 Wadi Ahin Hydrology: 135
5.3.3.1 Rainfall 135
5.3.3.2 Wadi Flow 137
5.3.3.3 The available data for the research 141

CHAPTER 6 145
KINEROS2 MODEL 145
MODEL DESCRIPTION AND INITIAL ANALYSIS 145
6.1 INTRODUCTION 145
6.2 KINEROS2 MODEL 146
6.2.1 Rainfall 147
6.2.2 Interception 148
6.2.3 Hortonian overland flow 149
6.2.4 Channel Routing 151
6.2.5 Infiltration 152
6.3 KINEROS2 INITIAL ANALYSIS 158
6.3.1 The estimation of the parameter values 160
6.3.2 Different plane configurations 163
6.3.3 Rainfall distribution 164
6.3.4 Time interval and durations 164
6.4 THE OBTAINED RESULTS 165
6.4.1 Results using equally divided areas 166
6.4.2 Results using constant size, upper plane 169
6.4.2.1 Results using synthetic rain 169
6.4.2.2 Results using a recorded rainfall event 173
6.5 CONCLUSIONS 178

CHAPTER 7 180
THE KINEROS2 MODEL 180
SENSITIVITY ANALYSIS, CALIBRATION AND VALIDATION 180
7.1 INTRODUCTION 180
7.2 CATCHMENT DIVISION 181
7.3 THE DEFAULT PARAMETER VALUES 182
7.4 LOCAL SENSITIVITY ANALYSIS 184
7.4.1 The selected parameters for the local sensitivity analysis 185
7.4.2 Local sensitivity analysis results 187
7.4.2.1 Effect of using different rainfall interpolations 187
7.4.2.2 Effect of initial condition (S) 188
7.4.2.3 Effect of hydraulic conductivity (*Ks*) 189
7.4.2.4 Effects of coefficient of variation of *Ks* (*Cv*) 189
7.4.2.5 Effects of Manning's coefficient *(n)* 189
7.4.2.6 Effects of capillary drive (*G*), porosity (*Por*), and distribution (*Dist*) 190
7.4.2.7 Effects of volumetric rock fraction (*Roc*) 190
7.4.2.8 Effect of soil layer thickness (*Thic*) 191
7.4.2.9 Effects of microtopography (*Rel* and *Spc*) 191
7.4.2.10 Effects of interception (*Int*) 192
7.4.2.11 Effect of slopes (*Slp*) 193
7.4.3 Discussion of the local sensitivity analysis results 193
7.5 GLOBAL SENSITIVITY ANALYSIS 200
7.5.1 Global sensitivity analysis method 200

7.5.1.1 Model configuration 200
7.5.1.2 Sampled parameters 200
7.5.1.3 Selected events 203
7.5.1.4 Performance criteria 203
7.5.2 Global sensitivity analysis results 204
7.5.2.1 Dotty plots 204
7.5.2.2 Quantification of the sensitivity 208
7.5.2.3 Parameter correlations 210
7.5.3 Discussion of the global sensitivity analysis results 211
7.6 CALIBRATION AND VALIDATION 212
7.6.1 Method of calibration and validation 212
7.6.2 Results - variability of calibrated parameters over events and over objective functions 213
7.6.3 Results - calibration and validation performance 215
7.6.4 Discussion of the calibration and validation results 221
7.7 OVERALL CONCLUSIONS 223
7.7.1 The rainfall interpolation effects 223
7.7.2 The local sensitivity analysis results 224
7.7.3 The global sensitivity analysis results: 225
7.7.4 The calibration and validation analysis results 225

CHAPTER 8 227
THE IHACRES MODEL 227
8.1 INTRODUCTION 227
8.2 IHACRES 227
8.2.1 The non-linear loss module 228
8.2.2 The linear model (UH) 229
8.3 THE RRMT 230
8.3.1 The objective functions 231
8.3.2 Optimisation methods available 232
8.3.3 The semi-distributed version of RRMT (RRMT-SD) 232
8.3.4 Monte Carlo Analysis Toolkit (MCAT) 233
8.4 THE MODEL INPUTS AND THE MODELLING STRATEGY 234
8.4.1 The input data for the lumped RRMT (RRMT-L) 235
8.4.2 The input data for the semi distributed RRMT (RRMT_SD) 236
8.5 THE RESULTS OF RRMT-L 238
8.5.1 Results using the CWI model 238
8.5.2 Results obtained using the Ye model 242
8.6 THE RESULTS OF RRMT-SD 246
8.6.1 Results obtained using the CWI model 246
8.6.2 Results obtained using the Ye model 249
8.7 DISCUSSION OF RESULTS 253
8.8 CONCLUSIONS 263

CHAPTER 9 265
SUMMARY AND CONCLUSIONS 265
9.1 INTRODUCTION 265
9.2 EFFECT OF THE HYDROLOGICAL FEATURES OF ARID AREAS ON RAINFALL-RUNOFF MODELLING 265
9.3 EFFECTS OF RAINFALL ON RAINFALL-RUNOFF MODELLING 267
9.4 RAINFALL-RUNOFF MODELLING AND THEIR APPLICATION IN ARID AREAS 268
9.5 SELECTED MODELS AND THE OBTAINED RESULTS 269
9.5.1 KINEROS2 269
9.5.2 IHACRES 271
9.5.3 Comparison of the performance of the tested models 273
9.6 CONCLUSIONS AND RECOMMENDATIONS 277

REFERENCES: 282

APPENDIX A 299
KINEROS2 299
DOTTY PLOTS 299

APPENDIX B 303

KINEROS2 303
CALIBRATION AND VALIDATION RESULTS 303
4-PARAMETER CASE (SOME PARAMETERS FIXED), G=0 306
6-PARAMETER CASE (SOME PARAMETERS FIXED), G=0 308
11-PARAMETER CASE, G>0 310

APPENDIX C 312
KINEROS2 312
ENSEMBLE RESULTS 312
6-PARAMETERS, G=0 321
11-PARAMETERS, G=0 329

List of Figures

Figure 2.1: Coefficient of variation of annual rainfall as a function of mean annual amount (*After: FAO, 1981*)..... 35
Figure 2.2: Flash flood at Wadi Ghat in Saudi Arabia (*After Walters, 1989*)..... 40
Figure 2.3: Flood Damage in Oman..... 42
Figure 2.4: Distributed channels on the surface of an alluvial fan in Eastern Desert of Egypt (*After Tooth, 2000)*..... 45

Figure 4.1: Flow-Chart of water-balance model structure (*after Mimikou et al., 1992*)..... 85
Figure 4.2: MODHYDROLOG model structure (*after Chiew and McMahon, 1994)*..... 95
Figure 4.3: Pitman Model Structure (*After Hughes, 1995*)..... 98
Figure 4.4: VTI model structure (*After Hughes, 1995*)..... 100
Figure 4.5: Generalized SFB model Structure (*After Ye et al., 1997*)..... 102
Figure 4.6: IHACRES model Structure (*After Ye et al., 1997*)..... 103
Figure 4.7: LASCAM model Structure (*After Ye et al., 1997*)..... 106
Figure 4.8: The Schematic of the integrated modelling procedure (*After Wheater et al., 1997*)..... 108

Figure 5.1: The location of Sultanate of Oman and the administrative regions *(after MWR, 1995)*123
Figure 5.2: Oman's general geology (*after MWR, 1995*)..... 124
Figure 5.3: General morphology of Sultanate of Oman (*After MWR, 1995*)..... 124
Figure 5.4: Greatest recorded flood peaks in Oman compared with world maximum curve developed by Rodier, 1984 *(After MRMEWR, 2001)*..... 130
Figure 5.5: A photo of a falaj in Oman..... 132
Figure 5.6: Wadi Ahin location in relation to Sultanate of Oman and its neighbouring catchments 133
Figure 5.7: Wadi Ahin DEM..... 133
Figure 5.8: Wadi Ahin simplified geological map..... 134
Figure 5.9: The locations of Wadi Ahin rainfall and neighbouring catchments gauges..... 135
Figure 5.10: Some rainfall stations photos in Wadi Ahin catchment..... 136
Figure 5.11: Location of Wadi Ahin flow gauges and the neighbouring catchments gauges..... 137
Figure 5.12: Wadi Ahin flow gauge and its wadi channel..... 139
Figure 5.13: A diagram illustrates the channel cross section at the flow gauge..... 139
Figure 5.14: The used rating curve (1995-99) for Wadi Ahin flow gauge..... 141
Figure 5.15: The rainfall-runoff events of Wadi Ahin for the 1996-99 period..... 142
Figure 5.16: The relationship between the hourly rainfall correlations and distance between rain gauges for the 1996-99 rainfall-runoff events..... 144

Figure 6.1: A simplified diagram of the hydrological processes within KINEROS2 (after http://www.tucson.ars.ag.gov/kineros/)..... 146
Figure 6.2: Diagram illustrates how the catchment can be divided into planes and channels *(after http://www.tucson.ars.ag.gov/kineros/)*..... 147
Figure 6.3: Simplifying diagram to represent rainfall interpolation in KINEROS2 for 3-gauges case 148
Figure 6.4: Notation-finite different grid *(after Woolhiser et al. 1990)*..... 150
Figure 6.5: Scaled basic relation of equation (6.26) *(after http://www.tucson.ars.ag.gov/kineros/)*..154
Figure 6.6: Relation of effective ensemble K_s to coefficient of variation of K_s and scaled rainrate ((http://www.tucson.ars.ag.gov/kineros/)..... 157
Figure 6.7: Variation of C with scaled rainfall rate and $Cv(K_s)$..... 158
Figure 6.8: A flowchart shows the used strategy to test the model's performance using a synthetic catchment with different configurations..... 160
Figure 6.9: Digram shows the assumed synthetic catchment for the case of equal planes (a) and a constant upper plane, and equally divided lower area (b)..... 164
Figure 6.10: KINEROS2 simulations results using equally divided planes, using uniform and non-uniform rain with 5- and 60-min intervals..... 167
Figure 6.11: KINEROS2 simulations results using constant size upper plane and equally divided lower plane, using uniform rain with 5- and 60-min intervals with infiltration..... 169
Figure 6.12: KINEROS2 simulation results using constant size upper plane and equally divided lower plane, using non-uniform rain with 5- and 60-min intervals with no infiltration..... 170
Figure 6.13: KINEROS2 simulation results, using constant size upper plane and equally divided lower plane, using non-uniform rain with 5-min intervals, 2- overall planes, and 4-overall planes..... 171

Figure 6.14: Wadi Ahin, 25 Jan 1997 rainfall event, 5- and 60-min time intervals 174
Figure 6.15: KINEROS simulation results using constant size upper plane and equally divided lower plane, using uniform rain with 5- and 60-min intervals with infiltration 174
Figure 6.16: KINEROS simulation results, using constant size upper plane and equally divided lower plane, using non-uniform rain with 5-and 60-min intervals with no infiltration..... 175

Figure 7.1: The catchment subdivision showing the plane and channel locations..... 181
Figure 7.2: Total rainfall (mm) at each gauge during 07-08 Aug 1996 event..... 185
Figure 7.3: Total rainfall (mm) at each gauge during 25-28 Jan 1997 event 185
Figure 7.4: KINEROS2 output for 07Aug 1996 and 25 Jan 1997 events, using different rainfall interpolations 188
Figure 7.5: Simulation results for 07Aug 1996 and 25 Jan 1997 events, using different values of *S* with *G*=11 and associated values of *Por* and *Dist* 188
Figure 7.6: Simulation results using different values of *Ks* for 07Aug 1996 and 25 Jan 1997 events, using KINEROS2 rainfall interpolation method 189
Figure 7.7: Simulation results for 07Aug 1996 and 25 Jan 1997 events, using different values of *Cv* with *G*=0 and *G*=11 mm 189
Figure7.8: Simulation results for 07Aug 1996 and 25 Jan 1997 events, using different values of *n* with G=0 190
Figure 7.9 Simulation results for 07Aug 1996 and 25 Jan 1997 events, using different types of soil and the corresponding *G, Por* and *Dist* values 190
Figure 7.10: Simulation results for 07Aug 1996 and 25 Jan 1997 events, using different values of *Roc* with *G*=0 and *G*=11 mm..... 191
Figure7. 11: Simulation results for 07Aug 1996 and 25 Jan 1997 events, using different *Thic*, with *G*=0 and *G*=11 mm..... 191
Figure 7.12: Simulation results for 07Aug 1996 and 25 Jan 1997 events, using different *Rel* values when *Spc*=1m 192
Figure 7.13: Simulation results for 07Aug 1996 and 25 Jan 1997 events, using different *Rel* values with *Spc* =10m..... 192
Figure 7.14: Simulation results for 07Aug 1996 and 25 Jan 1997 events, using different values of *Int* with *Ca*=0.1..... 193
Figure 7.15: Simulation results for 07Aug 1996 and 25 Jan 1997 events, using different *Slp* values 193
Figure 7.16: The sensitivity of KINEROS2 to the different parameters, (a) for 07Aug 1996 event and (b) for 25 Jan 1997 event (the straight line is the default peak value) 194
Figure 7.17: The sensitivity of the simulated flow peak of 25 Jan 1997 to different parameter values (a) Effects of changing *n* (b) Effects of changing *Ks* 195
Figure 7.18: Effect on simulated flow peak of change in *Rel* using constant values of *Spc* using the KINEROS2 rainfall interpolation method, (a) for 07 Aug 1996 and (b) for 25 Jan 1997 197
Figure 7.19: Dotty plots for selected calibrated events using OF_5 (*G*=0) for selected events..... 205
Figure 7.20: Dotty Plots of 07 Aug 1996 event using different OFs 206
Figure 7.21: Dotty plots for selected events using OF_5 (11-parameters, *G*>0) 207
Figure 7.22: Dotty plots for selected events using OF_5 for the spatial variation test (6-pairs, *G* =0) 208
Figure 7.23: Illustration of the calculation of the KS statistic from the objective function values. (*adapted from McIntyre et al. 2005*)..... 209
Figure 7.24: Optimum parameter values for each calibrated event, OF_5, 8-parameter case, *G*=0214
Figure 7.25: Optimum parameter values for each calibrated event using OF_5, 11-parameters, *G*>0 214
Figure 7.26: Calibrations and validation results of some selected events using different OFs, 8-parameter case, *G*=0..... 215
Figure 7.27: Calibrations and validation results of some selected events using different calibration OFs, with fixing 4-parameters, *G*=0..... 216
Figure 7.28: Calibration and validation results of some selected events using different OFs, 11-parameter case, *G* >0..... 217
Figure 7.29: Calibrations and validation results of some selected events using different OFs for the spatial variation test (*G* =0)..... 218
Figure 7.30: Validation results for each calibrated event, OF_5, for 8-parameter calibration, *G*=0219
Figure 7.31: Validation results for each calibrated event, OF_5, for fixing 4-parameter calibration, *G*=0..... 219
Figure 7.32: Validation results for each calibrated event, OF_5, 11-parameter calibration, *G*>0 ..220
Figure 7.33: Validation results for each calibrated event using OF_5 for the spatial variation test, *G*=0..... 220

Figure 7.34: Ensemble results for 25 Jan 1997 event, using OF_5 for the 11-paramter test, G>0.....221

Figure 8.1: A simplified diagram of IHACRES' component models (*after Littlewood et al., 1997*).228
Figure 8.2: General structure of RRMT *(from Wagener et al., 2004)* 230
Figure 8.3: The input data for the years 1996-97 used to calibrate the RRMT.....235
Figure 8.4: The input data for the years 1998-99 used to validate the RRMT 236
Figure 8.5: The division of Wadi Ahin into required subcatchments showing the effective hilllopes runoff pathways, and the model's channel network layout 237
Figure 8.6: Dotty plots for the calibration of 1996-97 years using the CWI model with nse* and fm, RRMT-L.....238
Figure 8.7: Model output for the 1996-99 years using the CWI model with nse*, RRMT-L 239
Figure 8.8: Model output for the 1996-99 years (missing out the March 1997 event) using the CWI model with nse*, RRMT-L.....239
Figure 8.9: Model output for the 1996-99 years using the CWI model with fm, RRMT-L 240
Figure 8.10: Calibration and validation results for each year from 1996 to 1999 period using the CWI model, with nse* and fm objective function, RRMT-L.....241
Figure 8.11: Dotty plots for the calibration of 1996-97 years using the Ye model with nse* and fm, RRMT-L.....242
Figure 8.12: Model output for the 1996-99 years using the Ye model with nse*, RRMT-L.....242
Figure 8.13: Model output for the 1996-99 years using the Ye model with nse* (missing out March 1997 event), RRMT-L.....243
Figure 8.14: Model output for the 1996-99 years using the Ye model with fm, RRMT-L.....243
Figure 8.15: Calibration and validation results for 1996 to 1999 period using the Ye model, with nse* and fm, with and without March 1997 event, RRMT-L.....245
Figure 8.16: Dotty plots for the calibration of 1996-97 years using the CWI model with nse* and fm, RRMT-SD 246
Figure 8.17: Model output for the 1996-99 years using the CWI model with nse*, RRMT-SD.....246
Figure 8.18: Model output for the 1996-99 years using the CWI model with nse* (missing out March 1997 event), RRMT-SD.....247
Figure 8.19: Model output for 1996-99 years using the CWI model with fm, RRMT-SD 247
Figure 8.20: Calibration and validation results for 1996 to 1999 period using the CWI model, with nse* and fm, with and without March 1997, RRMT-SD.....248
Figure 8.21: Dotty plots for the calibration of 1996-97 years using the Ye model with nse* and fm, RRMT-SD 249
Figure 8.22: Model output for the 1996-99 years using the Ye model with nse*, RRMT-SD.....250
Figure 8.23: Model output for the calibration period of 1996-99 years using the Ye model, nse* (missing out March 1997 event), RRMT-SD 250
Figure 8.24: Model output for the 1996-99 years using the Ye model with fm, RRMT-SD.....251
Figure 8.25: Calibration and validation results for 1996 to 1999 years using the Ye model, with nse* and fm with and without March 1997, RRMT-SD.....252
Figure 8.26: Calibration and validation results for 1996 to 1999 years using the CWI model and the Ye model, with nse*, RRMT-L.....255
Figure 8.27: Calibration and validation results for 1996 to 1999 period using the CWI model and the Ye model, with fm, RRMT-L.....255
Figure 8.28: Calibration and validation results for 1996 to 1999 period using the CWI model and the Ye model, with nse*, RRMT-SD 259
Figure 8.29: Calibration and validation results for 1996 to 1999 period using the CWI model and the Ye model, with fm, RRMT-SD 259

List of Tables

Table 2.1: Maximum Flood Peaks Reported In Oman 41

Table 5.1: National monitoring network gauges (*after Al-Sulaimani and Al-Obaidani, 2003)*..... 125
Table 5.2: 5 greatest rainfall intensities recorded in Oman durations 15-minutes to 24-hours 128
Table 5.3: General frequency of rainfall intensities for all Oman (Semi-Log analysis for all 1012 station-years (85 Stations) (MWR,1998)..... 128
Table 5.4: Frequency of rainfall intensities for plains, hills and mountains 129
Table 5.5: Wadi Ahin rainfall gauges details..... 136
Table 5.6: Average monthly and annual rainfalls 1975-99 (25 Years) for Wadi Ahin Catchment. 137
Table 5.7: Wadi Ahin flow gauges 137
Table 5.8: Wadi Ahin average monthly and annual flow (*MWR, 2000)* 138
Table 5.9: Flood peak frequencies for all Wadi Gauges in Wadi Ahin catchment (POT Frequency Analysis), (*MWR, 2000*) 138
Table 5.10: Rainfall amounts (mm) for the 1996 -99 events at each rainfall station 143
Table 5.11: Statistics of the runoff events 144

Table 6.1: The parameters used in the test cases..... 162
Table 6.2: The parameter values used in the test cases..... 163
Table 6.3: The percentage of the water balance error (for channel element only) and the event volume errors using different number of planes when equally divided..... 168
Table 6.4: The percent of event volume errors obtained for different number of planes when 1st Plane is constant with synthetic rainfall, uniformly and non-uniformly distributed..... 173
Table 6.5: The percentage of event volume errors for different number of planes when 1st plane is constant with the real-rainfall event, uniformly and non-uniformly distributed..... 177

Table 7.1: Parameters that describe geometry of the different elements 182
Table 7.2: The default values of different parameters used to run KINEROS2 184
Table 7.3: The values used for each tested parameter 187
Table 7.4: The Sensitivity Analysis Results of 07 Aug 1996 Event..... 198
Table 7.5: The Sensitivity Analysis Results of 25 Jan 1997 Event 199
Table 7.6: The KINEROS2 parameters and their ranges used in the global sensitivity analysis ... 201
Table 7.7: Average ranking of importance of parameters to OFs, and overall rank 209
Table 7.8: Correlations between different parameters, using OF_5 210

Table 8.1: The parameters used in SMA model and their ranges..... 234
Table 8.2: The parameters used in the routing model and their ranges..... 235
Table 8.3: The subcatchments characteristics 237

List of Notation

A : cross-sectional area

a^0 : reservoir shape factor to the observed data through optimization

a , b : integers as described in the text

a_i , b_i : coefficients given by Schwartz and Shaw (1975)

Abs : Absolute mean deviation

Ψ : metric potential

ψ_B : soil capillary head

AET : yearly actual evapotranspiration

α : coefficient related to slope and roughness – see Eq (6.16)

B : describes the differences between the volumetric water-holding capacity of the soil and its initial water content

β : constant scale factor with values rarely higher than $\pi/4$ and about always less than 1

BF : baseflow factor

Bs : Bias

C : Chezy friction coefficient

c' : loss rate per unit area

c_1 : weighted factor for the 1st gauge

c_2 : weighted factor for the 2nd gauge

c_3 : weighted factor at the 3rd gauge

Ca : plant (canopy) cover

C_r : constant that is greater than 1, whose values are directly related to the scaled rainfall rate r_* $[r / K_e]$ and $Cv(K_s)$

Cv : Hydraulic conductivity coefficient of variation

$Dist, \lambda$: pore size distribution index, (Corey, 1964)

DPF : lower store depletion factor

E : efficiency

Evp_{max} : maximum limiting rate of evapotranspiration

f : rainfall coefficient

f_* : scaled inflitration

f_c : infiltration capacity

f_{c*} : scaled infiltration capacity

F_p : ponding depth

f_r : Infiltration rate

$f'(t)$: dynamic infiltration rate $f_c(t) - K_t$

g : gravitational acceleration

G : integral capillary drive

G_1 : upper layer soil capillary force

G_l : lower layer soil capillary force

$G(\theta_i, \theta_0)$: effective capillary drive of the shrinking wetting front, which is reduced in relative to the infiltrating G as θ_0 is less than θ_s

G, G_c : Capillary force for plane and channels

γ : proportion of flow lost per unit distance for a given channel element

h : flow depth

h_a : storage of water per unit area (water depth above the plane surface)

$h(j\text{-}i)$: ordinate of GIUH at time j-i

h_w : surface water depth

i : integer as described in the text

I : infiltrated water depth

I_* : scaled infiltrated water depth

I' : cumulative infiltration depth

$I(i)$: effective rainfall intensity at time i

$I(c', a^0)$: A measure of goodness of fit

Int : Interception

$I^{(s)}$: peak of the slow flow

$I^{(q)}$: peak of the quick flow

j : integer as mentioned in the text

Ω : represents the soil type

k : constant of proportionality

K_e : areal effective hydraulic conductivity

K_i : hydraulic conductivity of the initial soil profile, $K(\theta_i)$

K_s : saturated hydraulic conductivity

K_{s1} : upper soil hydraulic conductivity

K_{s2} : lower soil hydraulic conductivity where

Ks, Ks_c: Hydraulic conductivity for plane and channels

l : threshold that introduced by Ye et al (1997), below which no effective rainfall is produce, to be used in low-yielding catchments

L : length of the element

L_h : horizontal projection of the overland flow plane

LK : Likelihood value

L_M : basin data grid sizes

L_R : rainfall resolution

L_R/L_S : storm smearing

L_R/L_W : watershed smearing.

L_s : correlated length of the input rainfall data

L_W : characteristic basin length scale

m : coefficient related to surface roughness. It also indicates if the flow is laminar or turbulent and its value depends on which relationship is used (Mannaing or Chezy law)

M : specific moisture capacity

mf : temperature modulation factor that that controls the sensitivity of $\tau_w(t_k)$ to change in the temperature t_k

μ_e^2 : is the variance of the residuals $e_i = q_i - \hat{q}_i$

n : Manning roughness coefficient

n, n_c : Manning coefficient for the plane and channel

N : integer as described in the text

NDC : fraction of the surface storage capacity that does not drain to the lower store

NSE : Nash Sutcliffe Efficiency

OF : objective function

OF_1 : peak objective function

OF_2 : volume objective function

OF_3 : time to peak objective function

OF_4 : combined objective functions; peak-volume

OF_5 : combined objective peak-volume-time to peak

OF_6 : average performance in terms of flow peak, volume and time to peak that measured over a specified N events

p : peakness factor that introduced by Ye at al (1997) for the low-yielding catchments

P_k : cumulative probability function of K_s, CDF

p_k : the corresponding probability density function, PDF

ϕ, Por : porosity

$\bar{q}_{y,m}$: yearly average monthly runoff (m^3s^{-1})

Q : recorded streamflow (m^3s^{-1})

Q' : simulated streamflow (m^3s^{-1})

$q_c(x,t)$: net lateral inflow per unit length of channel

q_{lo} : overland flow plane horizontal projection

$Q(j)$: surface runoff discharge at time j

q_m : stationarised monthly runoff (m^3s^{-1})

Q_p : peak flow

Q_S : runoff relative sensitivity

Q_t : time-to-peak after beginning of simulation

$Q(t)$: outflow rate, (L/T)

q_q : quick flow

q_s : slow flow

Q_{Vx} : flow volume at location x

ΔQ_v : runoff volume

Q_{VA} : flow volume at location A (x=0)

q_w : discharge per unit width

Q_w : discharge per unit width

$q(x,t)$: inflow rate per unit area

Q_v' : a flow volume that is introduced which always measured over the same time-period to overcome the problem when the Q_v does not represent the full runoff volume

R : rainfall

R_1 : rainfall at the 1st gauge

R_2 : rainfall at the 2nd gauge

R_3 : rainfall at 3rd gauge

r : rate of input at the surface during redistribution, which may be small, negative (evaporation), positive, or 0)

r_* : scaled rainfall rate

$\sqrt{\overline{R}}$: mean of the reference precipitation input over the study period

R_{cv} : coefficient of variation of rainfall

Rel : average micro topographic relief

R_{int} : rainfall intensity

r_{i} : incident precipitation

r_k : total rainfall at time k

R_m : areal monthly precipitation expressed in units of discharge (m^3s^{-1})

$RMSE$: Root Mean Square Error

Roc : %Volumetric Rock

R_r : hydraulic radius

R_v : input rainfall volume

$R(x,t)$: excess rainfall rate in space and time

s : surface store capacity

S : Saturation

S_c : Saturation for channels

σ_q^2 : variance of the observed discharge

SDR_{max}: baseflow threshold for the lower store, defining the depth of water in the lower store at which baseflow ceases.

S_i : initial saturation value

s_k : catchment wetness at time k, with values varying from 0 to 1

Slp : slope

S_{max} : the upper limit of S, the saturation value, known to be less than 1

Spc : average micro topographic spacing

$s(t)$: the storage (L) at time t

t : time

T : reference temperature that is chosen by the model operator

t' : time from start of wetting or rewetting

t_* : scaled infiltration time

t_p : ponding time

Δt : temporal sampling interval

$Thic$: upper soil layer thickness

t_k : temperature at time k

θ : water content by volume

θ_i : water content by volume, when the saturation is at its initial saturation

$\Delta\theta_i$: unit storage capacity, $(\theta_s - \theta_i)$

$\Delta\theta_{i0}$: the water content of the redistributing portion $(\theta_0 - \theta_i)$

θ_s : water content by volume, when the upper limit of S, the saturation value, is S_{max}

θ_w : weighting parameter, with values ranging from 0.6 to 0.8, for the x derivative at the advanced time step

τ_w : catchment drying time constant

u : subscript refers to the upstream surface

$\overline{u}$: average flow velocity

u_k : effective rainfall as the product of incident precipitation r_k and the storage index

u(t) : inflow rate, (L/T)

V^* : dimensionless hydrograph envelope

$volc$: represents the proportion of rainfall, in which the catchment wetness index (s_k) decay occurs by, during the rainfall (r_k) time intervals

$v^{(q)}$: the relative volumetric throughputs for quick flow

$v^{(s)}$: the relative volumetric throughputs for slow flow

W : Woolhiser coefficient

w : width of the element

x : distance

X_i, Y_i : X, Y coordinates for points on map or the observed and simulated recession curve

x_k : streamflow

y, m : subscripts stands for year and month respectively

z : depth of the soil profile

Z : radar reflectivity factor

z_1 : upper soil depth,

$ZMIN$: minimum catchment absorption rate

$ZMAX$: maximum catchment absorption rate

Chapter 1

Rainfall-Runoff Modelling in Arid Areas

1.1 Introduction

Hydrological features of arid areas are different in many aspects from those of humid areas which are caused by a different climate and hence, rainfall regime.

The hydrologic characteristics of arid areas have not been adequately studied, partly due to less frequent runoff events and partly due to very limited data. However, managing the water resources of arid areas is especially challenging. The hydrology of these areas is now receiving more attention.

There are not enough studies that cover all the different hydrological aspects of arid areas even though there are a few studies covering some. There have been few special modelling techniques developed to suit the unique hydrological characteristics and responses of arid areas, despite the fact that they are poorly understood. Hence, techniques used for hydrological design, water resources management, and flood studies have mainly been those developed originally for application in humid areas.

As rainfall-runoff modelling is a very important tool that can be used in assessment and management of hydrological systems (Beven, 2000; Singh et al., 2002; Wheater et al., 2002), some attempts have been carried out recently to test these models and to investigate their performance in different arid areas.

Two models, KINEROS2 and IHACRES, have been chosen from the literature based on their applicability to arid zones. Those models have been tested to evaluate their performance when applied in Oman, shedding light on the problems in modelling, and providing some recommendations.

1.2 The background to the research

The following Section overviews the special hydrological features of arid areas and the applications of different rainfall-runoff models in such areas. The Section also overviews the selected models based on the literature and their application using Omani data.

1.2.1 Hydrological features of arid areas

As mentioned above, any model developed for use in arid areas should be capable of representing the special features of arid zones.

The most important features that need to be considered include those related to climate (Rodier, 1985; Pilgrim et al., 1988; Al-Qurashi, 1995). The climate in arid areas is very different from that in humid areas. The temperature and potential evapotranspiration in arid areas is generally much higher than that in humid areas. The humidity might also be high in arid areas, although it depends on the location of the area relative to the coast. The rainfall characteristics in arid areas are also quite different from those in humid areas.

Arid areas generally do not have continuously flowing streams and the flow channels are mostly dry for most of the year (Pilgrim et al., 1988; Wheater et al., 1997). The rainfall and runoff varies in space and time and partial-area runoff was observed in some arid areas as a result of spatial rainfall distribution (Cordery et al., 1970). The flood hydrographs in arid areas are different in shape and characteristics from those of humid areas (Pilgrim et al., 1988; Walters, 1989; Wheater & Brown, 1989).

Rainfall-runoff relationships in arid areas are complex. The relationship is affected by many factors that may need to be well understood and considered whenever carrying out any analysis or modelling. Hydrological processes, rainfall characteristics, runoff characteristics, transmission losses, all can have great effect on rainfall-runoff relationships. There are some other factors that can affect this relationship and may need to be well represented, such as topography, stream length, catchment size, soil type, fans and reliefs, and vegetation cover (Pilgrim et al., 1988; Rodier, 1985; Nouh. 1990; Al-Qurashi, 1995; Lang et al., 2000).

Transmission loss is the water absorption into the alluvium bed material of the ephemeral channels in the drainage between the upstream and downstream locations (Jordan, 1977; Leonard & Lane, 1990). It is a very important hydrological phenomenon in arid areas that needs to be considered. A number of studies have shown that transmission losses are very high in arid areas (Jordan, 1977; Rodier, 1985; Pilgrim et al., 1988; Leonard & Lane, 1990; Sorman & Abdulrazzak, 1993; Al-Qurashi, 1995, 1999; Wheater et al., 1997).

1.2.2 Overview on Rainfall-Runoff Modelling

Modelling is a very important tool that enables hydrologists to make more comprehensive use of rainfall time series. Rainfall-runoff modelling is also useful for water resources assessment as these models can generate a long representative time series of streamflow volumes from which water supply schemes can be designed. Modelling rainfall-runoff in arid areas can be considered as a key component of studies of the dynamical aspects of arid-zone hydrological processes (Ye et al., 1997). However, there are many different aims for modelling. It can be for management, planning, or research.

Rainfall-runoff models can be divided using many different criteria; process based criteria, time scale, space scale, or model-structure based criteria (Singh, 1995). The different models also vary in complexity from simple models with few parameters to very complex models with many parameters (Beven, 2000, Wheater, 2002). Models that perform well in humid areas are not always suitable for use in arid areas. Selecting the appropriate model can have a great effect on modelling output and the wrong selection can lead to the wrong management decision and planning. Model selection must take due account of the purpose of the modelling, the available data, and the hydrological characteristics of the studied area.

The literature review in **Chapters 3** and **4** discusses the advantages and limitations of each type of model in detail, the different steps and the methods used, and then highlights some of the problems that may be faced when applying the different types of models to arid areas, and how scientists have attempted to overcome these problems.

Good knowledge of rainfall characteristics will help better understanding of the effects of the rainfall data quality and its characteristics on the obtained rainfall-runoff modelling results. Hence, it will help better evaluation of the performance of the used model. It can also aid in understanding the resulting runoff and the rainfall-runoff relationships. The spatial and temporal variations of the rainfall are very high and need to be well understood.

1.3 Research Objective

Many attempts have been made to test watershed models and to investigate their performance in different arid parts. Attempts have been made by hydrologists to modify the currently used models, the majority of which were originally developed for humid areas.

The aim of this PhD research is to use advanced tools of model analysis to test some of the current models that consider arid area hydrological characteristics. As these models were mainly developed for other regions, an attempt is made to study their limitations using Omani hydrological data. Guidelines are provided for improved rainfall-runoff modelling in arid areas in general and Oman in particular. This was carried out by reviewing available models and model types and hence, selecting some models and testing their performance and identifying the main uncertainties using an Omani catchment. Finally, recommendations are provided regarding the suitability of these models or model types and how they might be improved, highlighting any further data that is required, and how uncertainties should be handled in model applications.

1.4 The study area

Oman is known as one of the world's arid areas. It is located in the southeast of the Arabian Peninsula. It is bordered by Saudi Arabia to the west, United Arab Emirates to the northwest, Yemen to the south east and Arabian Sea to the east.

The location of Oman has great effects on its special hydrological characteristics, climate and geology, hence it is important to highlight in the study.

Wadi Ahin which is located in the Sultanate of Oman has been selected for the purpose of this study. Wadi Ahin is situated in Al-Batinah Region north of Oman with catchment area of 810 km^2 to the lowest gauging station. The catchment can be subdivided into two areas; Ahin West (Wadi Ahin nr Hayl) and Ahin East which include Ahin near Majis Kabirah, and left and right channels flow gauges.

Wadi Ahin is classified as having a moderate rainfall regime. The long term annual average is about 152 mm for the upper part of the catchment (Ahin West) and 102 mm for the lower Ahin catchment (Ahin East). The bedrock lithology shows that the catchment consists generally of ophiolite which makes it low permeability.

1.5 The Selected Rainfall-runoff Models

Based on a review that was carried out (see **Section 4.6**) two different model types have been selected for the research; physically based (KINEROS2), and conceptual (IHACRES). An attempt is made to study the benefits and the limitations of each using data from Oman.

1.5.1 KINEROS2

KINEROS2 which is the updated version of the KINEROS model was developed by Woolhiser et al. (1970), Margali (1970), Schreiber (1970), Kilber and Woolhiser (1970), Rovey and Woolhiser (1977), Woolhiser et al. (1990a). One of the most important features of KINEROS is its ability to consider the special hydrological features of arid areas (Michaud & Sooroshian, 1994).

KINEROS2 is an event based, distributed model. It is a kinematic runoff and erosion model that is considered to be a physically-based model as it is based on physical principles of conservation of mass and momentum. It describes the processes of interception, infiltration, surface runoff, and erosion. The model is an 'event-oriented' model, that is, it analyses a specific runoff event due to a defined rainfall occurrence. The model is also considered to be a distributed model as the watershed surface and channel network are represented by a cascade of planes and channels in which each plane is described by a set of parameters, initial conditions, and precipitation inputs, and each channel, by a set of parameters (KINEROS2 Website, 2005).

KINEROS (the old version) was tested in Oman by Wheater (1981) and the results were found acceptable. The same version of the model was also used by Mott MacDonald (1992). However, Michaud and Sorooshian (1994) found some difficulties in applying it to catchment areas larger than 100 km^2. Hence, it was thought to be useful to test the model in a larger catchment with the new updated data in Oman to check its validity and performance and compare it with studies that were carried out in Oman and any other arid areas. Despite Mishaud and Sorooshian's reservations, it was thought important to investigate the performance of a physically-based model with the available data in the selected catchment and to compare its results with the other type of model used in the research.

1.5.2 IHACRES

The IHACRES model undertakes identification of hydrographs and component flows from rainfall, evaporation, and streamflow data (Jakeman et al., 1990, 1992, 1993a, b, 1994; Jakeman & Hornberger, 1993). The model is considered as a lumped hybrid metric/conceptual continuous-time model of average complexity. IHACRES was developed by the Institute of Hydrology (IH) in the United Kingdom and the Centre for Resource and Environmental Studies at the Australian National University (CRES at ANU), Canberra. The aim of the development, as Littlewood et al. (1997) explained, is

to aid in characterising the dynamic relationship between the rainfall and runoff in the selected watershed for the study.

IHACRES is a simple model (only six parameters are used) as it does not conceptualize the spatial variation or distribution of catchment wetness of rainfall. The model consists of two models; a non-linear loss model and a linear unit hydrograph model. The model assumes that there is a linear relationship between the effective rainfall (u_k) and streamflow (Q_k) which allows unit hydrograph theory to be applied. In other words the catchment is conceptualised as a configuration of linear storages either acting in series and or in parallel. The non-linearity observed between the rainfall and the runoff is considered in the non-linear loss model.

To investigate the behaviour of the catchment using the daily data and lumped model, IHACRES model was run within RRMT. RRMT is an Imperial College toolbox that is described in its manual as consisting of a lumped model structures with a high level of parameter identifiability (Wagener et al., 2001). The toolbox includes different moisture accounting models. Those are Catchment Moisture Deficit (CMD) (Evans and Jakeman, 1998), Catchment Wetness Index (CWI), and the Penman model structure (Penman, 1948). Some probability distribution of moisture stores is also included (Wagener et al., 2001). There are also different options to select different objective functions and calibration methods.

A new version of RRMT, RRMT-SD, which is a semi distributed version based on the same concept as the lumped version, was also used to compare the results.

1.6 Structure of the Thesis

The thesis structure is as follow:

1.6.1 Chapter One

Chapter 1 (the current chapter) is an introduction, which highlights the research topics and the model of the different chapters.

1.6.2 Chapter Two

Arid areas have many distinctive features, different from those of humid areas.

This chapter highlights the different hydrological features of arid and semiarid areas that are important to be considered when carrying out any hydrological analysis or watershed modelling in such areas. It covers the following aspects:

- Distinctive features of the hydrology of arid areas

- Rainfall-runoff modelling in arid areas
- Overview on application of rainfall modelling in arid areas
- Overview on application of rainfall-runoff modelling in arid areas

1.6.3 Chapter Three

A rainfall-runoff model requires a reasonably accurate measure of catchment rainfall input to determine the output at the point of interest with acceptable precision (FAO, 1981). Rainfall is the most important input in rainfall-runoff models. Hence, rainfall averaging methods are reviewed in this Chapter.

In general, this chapter discusses modelling aims, techniques, and the different type of models, and highlights some of the limitations of different model types. It also overviews some of the main methods of estimating the average rainfall over the watersheds.

1.6.4 Chapter Four

This chapter discusses some of the rainfall modelling applications in arid areas and their limitations when used in arid areas. It also discusses the rainfall-runoff models that have been tested under arid conditions and the difficulties that were faced due to the special hydrological features of arid areas. Recommendations for the best models for further investigation are provided at the end of this chapter.

1.6.5 Chapter Five

Chapter 5 discussed the location of the study area and its characteristics. It also highlights the reason for its selection. The chapter covers topics that include: general overview on Sultanate of Oman's hydrology, Wadi Ahin catchment and its hydrological characteristics, and the rainfall and wadi flow monitoring network coverage.

Some hydrological analysis of Wadi Ahin is presented in this chapter to provide a better understanding of the selected catchment and put the results obtained from the later modelling in context.

1.6.6 Chapter Six

The literature review of **Chapter 4** led to selection of the KINEROS2 and IHACRES models for this research purpose.

This chapter describes KINEROS2 based on the information in its User Manual on its official web site, direct communication with the developers, and the different studies that were carried out during its development. This is followed by an initial test using a

synthetic catchment to study its performance under different conditions to aid understanding of the model and its limitations and study any possibility to modify the model's code to overcome them or improve its performance.

1.6.7 Chapter Seven

Sensitivity analysis can be described as the procedure to determine the sensitive and insensitive parameters that can affect the model calibration (Sorooshian & Gupta, 1995). It is useful to know which parameters can affect the model performance and its results. Hence, sensitivity analysis was run to determine which parameters are more effective in KINEROS2 (the latest version of KINEROS model that is adopted in this research), to be used in the calibration, and which one are the less effective, so they can be fixed.

The results obtained from the local sensitivity analyses are presented with a discussion of the possible reasons behind them. The obtained results were used as a guide in carrying out the global sensitivity analysis.

Calibration is an important process to select the best parameter sets that can produce simulated values closest to the observed ones. The calibration process consists of two steps; parameter specification where the parameters to be used in the model should be specified, and the parameter estimation where the values of these parameters are determined or estimated based on certain known techniques (Sorooshian & Gupta, 1995).

The chapter discusses the obtained results from the local and global sensitivity analysis using the KINEROS2 model and the model optimisation methods that were used when applied to Wadi Ahin catchment. Comparisons between different results were made to aid in selecting the best objective function. Conclusions from these analyses and a comparison of these results with the results that obtained from any other relative studies then were made.

1.6.8 Chapter Eight

The IHACRES model is the second model that was selected to be investigated for the purpose of this research beside the KINEROS2.

Chapter 8 discusses the theory behind IHACRES and its structure for better understanding of the model based on the IHACRES Manual (2005). The model was applied to the Wadi Ahin catchment and the obtained calibration and simulation results

are discussed. The obtained results were also compared with the other previous studies that were carried out in a similar arid environment.

1.6.9 Chapter Nine

Chapter 9 summarises the obtained results from the carried out research using the two selected models and discusses how this research has fulfilled its objectives.

Some guidelines are provided for improved rainfall-runoff modelling in arid areas in general and Oman in particular. Finally, recommendations are provided regarding the suitability of these models or model types and how they might be improved, highlighting any further data that is required, and how uncertainties should be handled in model applications as this research aimed to.

Chapter 2

Distinctive Features of the Hydrology of Arid Areas

2.1 Introduction

Arid areas have many distinctive features, different from those of humid areas. The high temporal and spatial variability of the rainfall, flash floods, absence of base flow, sparsity of plant cover, high transmission losses, high potential evaporation and evapotranspiration are examples of such differences in hydrological features between arid and humid areas. The quality of data is often poor in many arid areas due to the sparse rainfall and runoff networks, difficulties in accessing the flow gauge sites during storm events, the high variability and irregular occurrence of the flow, the lack of control sections in the changeable flow channels and the difficulty of direct measurement of the flow with the high sediment and debris loads. High transmission losses result from the typically very wide channels (wadis) as they pass through generally quite permeable alluvial plains.

This chapter highlights the different hydrological features of arid and semi-arid areas that are important to be considered when carrying out any hydrological analysis or watershed modelling in such areas.

2.2 Climate

The climate in arid areas, e.g. temperature, evaporation, sunshine hours, humidity and rainfall regime, is very different from that of humid areas. Generally, there are not four clear seasonal divisions in arid areas. In Oman, for example, there are only two seasons: summer, from April to October, and winter, from November to March. The climate in arid areas, however, generally varies both spatially and temporally.

These differences compared to humid areas lead to significant effects on the hydrological characteristics of arid areas (Al-Qurashi, 1995). Also the different climate has important effects on the rainfall pattern and seasonality (Rodier, 1985; Pilgrim et al., 1988).

2.2.1 Temperature

The generally high temperature and the different rainfall regimes have great effects on the evaporation and evapotranspiration in arid areas of the world. For example, in the lowland in Oman the annual mean daily temperature ranges from 26-29 C° with maximum daily temperatures of above 40 C° in summer (MWR, 1995).

2.2.2 Sunshine hours

In arid areas, generally, cloud cover tends to be relatively rare. Daily average sunshine hours in most of Oman, for example, tend to be more than 10 hours a day during the summer months April to September, and average just less than 8 hours a day in winter months. The long sunshine hours, which determine the radiation input, have a strong effect on potential evaporation and evapotranspiration levels.

2.2.3 Humidity

The average annual relative humidity varies from region to region based on its location relative to the coast. For example, in Oman generally it averages about 60% in the Northern coastal parts of Oman (monthly range from 40% to 70%), and up to 70% in the Southern coastal part (monthly range from 50% to 90%), whereas inland and in the desert areas it is around 40% annually with monthly averages from 25% to 55% (MWR, 1995).

2.2.4 Evapotranspiration

Evapotranspiration is the combination of evaporation from soil surface and transpiration from vegetation (Chow et al., 1978). Evapotranspiration is one of the important factors that affect the hydrological processes and it is usually very high in arid and semi-arid areas. It is affected by the temperature, wind velocity, radiation and humidity (Al-Qurashi, 1995). Most high rainfall events generally occur in summer when the potential evapotranspiration is highest, whereas the regions more remote from the tropics tend to have predominantly winter rainfall, when the temperature and the evapotranspiration is low (Pilgrim et al., 1988). More details are represented in **Section 2.8**. Although very high potential evaporation and evapotranspiration result from the high temperatures that tend to prevail in arid regions, the low rainfall tends to limit the actual evaporative effects to only a small proportion of the potential.

Evapotranspiration, soil moisture, and vegetation all depend on the climatological features. Drylands are characterised by a high degree of aridity, reflecting low ratios between precipitation and potential evapotranspiration and by sparse, unevenly

distributed, or temporally variable vegetation cover (Tooth, 2000). Hence, considerations of these differences between humid, arid and semi-arid climates are important in carrying out any hydrological analysis or modelling.

2.3 Rainfall

Rainfall is the major input for the water resources and an understanding of the rainfall characteristics is critically important in estimating average and maximum flows in wadis as well as groundwater recharge. The generally short period of available rainfall records and the sparse coverage and quality of the available data, however, make it difficult to carry out comprehensive studies and modelling. Most arid areas are located in developing countries where there tends to be, in general, limited rainfall network coverage, and hence limited available data resources.

2.3.1 Rainfall generation

Rainfall in many arid areas results from squall lines and convective cloud mechanisms producing storms typically of short durations, relatively high intensity and limited areal extent. Arid zone rainstorms may develop in the presence of irregular cloud cover associated with large-scale air masses, or they may develop within band-type cloud patterns (FAO, 1981). For example, scattered convective showers over the eastern mountains of Oman sometimes occur due to penetration of shallow monsoon currents moving inland towards United Arab Emirates. However, other rainfall mechanisms can cause rainfall in Oman such as cold frontal troughs, which are common in winter, tropical cyclones which sometimes move from the Arabian Sea and advection of deep layers of cold air moving from central Asia through the Arabian Gulf to the southeast of Oman (MWR, 1995). The latter can cause heavy rainfall.

2.3.2 Spatial and temporal variation of rainfall

Rainfall is generally sparse in arid areas. There can be many years without any significant rainfall, but on the other hand there can also be distinctly wet years with several severe events. The rainfall, however, tends to be more variable in space and time compared to humid areas (Pilgrim et al, 1988, Wheater et al., 1991a, b; Al-Qurashi, 1995). It is notable that rain gauge densities in Walnut Gulch in USA, for example, which are about 1 per 2km^2, showed highly localised rainfall occurrence with spatial correlations of storm rainfall of 0.8 at 2km separation, and close to zero at 5-20km spacing (Wheater & Weshah, 2002). Osborn and Renard (1973) recommended 300-500m separation between rainfall gauges to be able to capture the localised rainfall in

arid areas, which is obviously difficult in practice. In Saudi Arabia, the typical spacing between rainfall gauges at five experimental basins of a five-year intensive study (Dames & Moore, 1988) was 10km. The study shows that on 51% of rain days, only one or two rain gauges out of 20 experienced rainfall, but the sub-daily data showed even more spotty results.

However, the rainfall pattern in other arid areas can be very different. Studies in New South Wales, Australia, have shown spatially extensive, low intensity rainfalls (Cordery & Pilgrim., 1970). The HAPEX-Sahel project based on Niamy and Niger showed that 80% of total seasonal rainfall was found to fall as widespread events which covered at least 70% of the 100 rain gauge network (Lebel et al., 1997).

2.3.3 Annual average rainfall variation

The annual average rainfall in arid and semi arid areas could be a misleading value due to the high variability in rainfall in time and space. Such an average could be seriously influenced by a single day with a high rainfall total. The coefficient of variation of annual or seasonal point rainfall is in general negatively correlated with the mean annual rainfall (FAO, 1981), **Figure 2.1.** For example, in an arid part of Australia, a one day rainfall event of 750mm was recorded in a tropical cyclone while a total of 4mm was recorded at the same site in the whole of another year (Pilgrim et al., 1988). In Oman, the average annual rainfall varies from about 50mm in Central Oman to more than 300mm in the mountain areas in the North. The highest recorded daily cyclonic rainfall events were 424 mm (13/06/1977) in Masirah, 286mm (05/06/1890) in Muscat and 186mm (12/11/1966) in Salalah (MWR, 1998). It should be noted that these amounts were most probably for less than 12 hours but it was difficult to determine the duration as all the available records at the time were for daily recording gauges only. A more severe event has hit Oman recently, in 2007, which is still under study by the time of writing up this thesis, in which daily rainfall in excess of 800mm was reported.

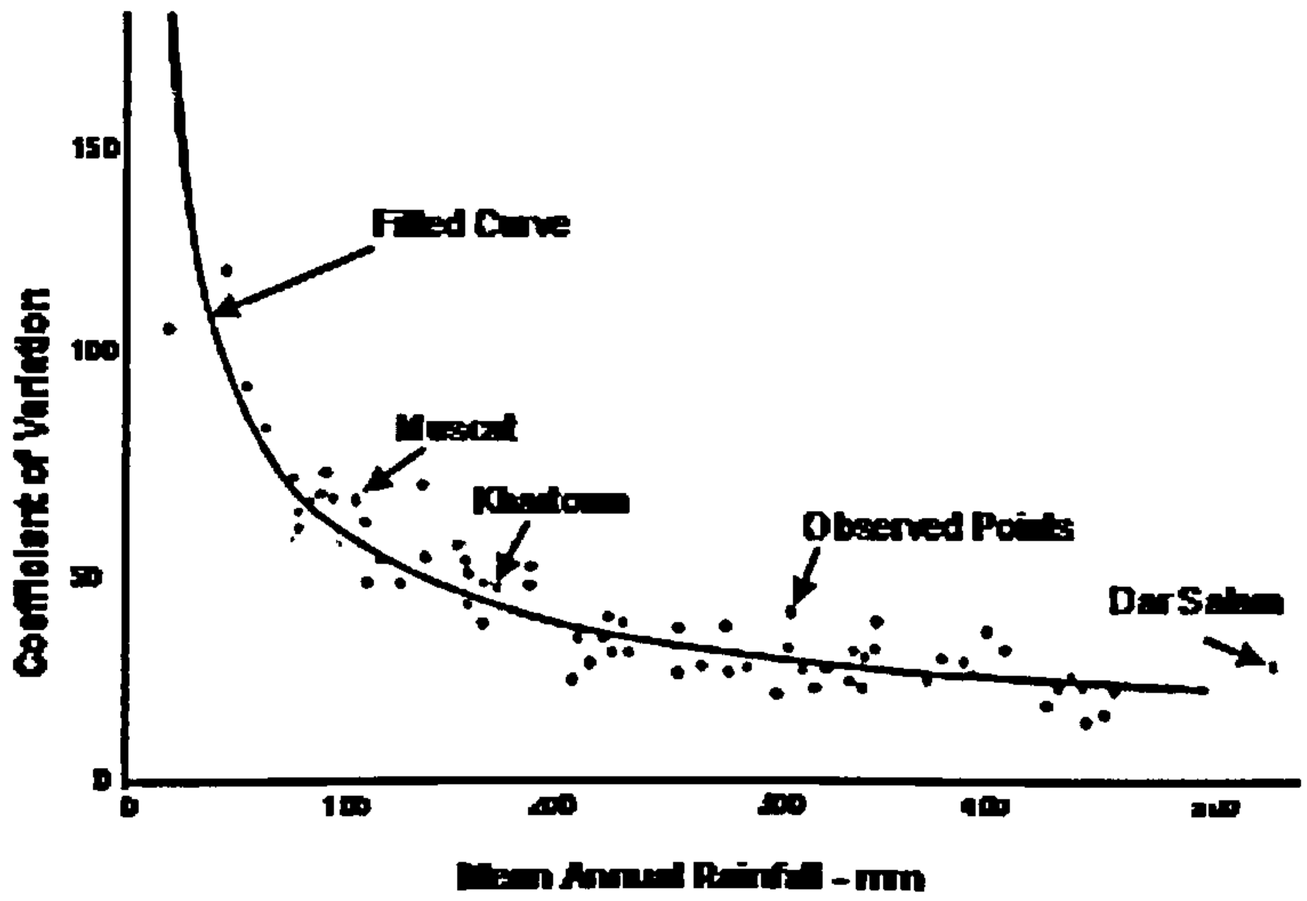


Figure 2.1: Coefficient of variation of annual rainfall as a function of mean annual amount (*After: FAO, 1981*)

2.3.4 Intensity characteristics of storm rainfall

Generally the rainfall in arid areas tends to be very localized. Often intense rainfall of short duration falling on bare land with limited or sparse vegetative cover generates Hortonian excess overland flow that can be enhanced by surface crusting (Wheater et al., 1997).

Renard et al. (1970), in a study of the three storms that produced the largest runoff peaks on record at Alamogordo Creek experimental watershed in northeastern New Mexico (in the arid part of USA) since 1955 (5 June 1960; 16 June 1966; and 21-24 August 1966), found that the first two storms were centred on the watershed. The 6-hour, 50-year return period maximum point rainfall was exceeded at one of the rain gauges within two hours during both these events and the 1-hour maximum value at the same rain gauge for both storms exceeded the 100-year (return period) value. For the August storm, at another rain gauge, the maximum 6-hour rainfall was estimated as a 1000-year event. However, it was found that almost all of the runoff producing rainfall at this station fell in about 2 hours. Osborn and Lane (1971) in their study on depth-area relationships for thunderstorm rainfall in southeast Arizona, found that the maximum storm rainfall for 16 selected events ranged from 36 to 88 mm, all lasting for less than two hours.

An analysis of rainfall intensities and duration in Oman shows that as the return period increases, the maximum sub-daily rainfall total tends to become a smaller proportion of the daily total. This reflects the fact that most recorded storms tend to be of short duration, but as return periods increase, the storm durations tend to increase (MWR, 1998).

2.3.5 Elevation effects on rainfall

Rainfall is generally affected by elevation. Drissel and Osborn (1968) demonstrated this well-known characteristic in their study area (Walnut Gulch, USA), i.e. that the distribution of mean annual rainfall over the entire watershed is not random and an orographic effect is clearly indicated, which is demonstrated by most isohyetal maps

A hydrological study in Oman (MWR, 1998) shows clear elevation effects for both counts of rainy days and rainfall amounts. Hence, the rainfall stations were classified based on their elevations as mountain (≥ 800m above mean sea level), hill (neither mountainous nor plain), and plain stations (those within relatively flat areas, with no significant nearby hills). Intensity-duration analyses were carried out based on this classification. The analysis shows that the hill category values tend to lie between mountain and plain values, being closer to the plains values for shorter durations and moving towards the mountain values as the durations increase. The mountain category data start at higher values for the average rainfall intensities and rise at a slightly lower rate than the hill category data for 6- and 12-hours durations, where the hill category crosses over eventually to exceed the mountain values (MWR, 1998).

However, Wheater and Brown (1989) and Wheater et al. (1991a, b) in their study in Saudi Arabia did not find clear effects of elevation on individual rainstorm depth, but noted a strong relationship between the frequency of raindays and elevation.

2.3.6 Effects of seasonality on rainfall

Seasonal effects are very clear from some studies carried out for various arid areas. The winter and summer rainfall in arid areas were found by several authors to be different in characteristics (Al-Qurashi, 1995, Mourits & Abdin Saleh, 2002; Hofman & Rambo, 1995; Drissel & Osborn, 1968). The summer events seem more intense with short duration and more localised. The generated floods can be severe and sometimes cause severe and flashy floods that can result in considerable damage.

Wheater et al. (1997) in a Saudi Arabia study found that there are significant differences in correlation of spatial rainfall between the summer and winter seasons. However, a study in Wadi Al Jizi in Oman showed a very low summer and winter spatial rainfall correlation, but winter correlations from October to March were much higher (Hofman and Rambo, 1995).

A study of the greatest recorded rainfall events and rainfall intensities in Oman (MWR, 1998) showed that the summer month of July predominated as the most likely month for

severe rainfall intensities, whereas the results of Al-Qurashi (1995) showed April to be the predominant month. It should be noted that Al-Qurashi used a shorter period of records and the analyses were carried out only for one basin compared to the MWR nationwide study. Both studies agree that intense rainfall is associated with the summer season. However, Al-Qurashi (1995) showed in her study, that for high storm intensities for longer durations, of 12 to 24 hours, the winter month February predominates. This finding was consistent with the expectation that in arid areas, generally events with lower intensities but longer durations and larger rainfall volumes tend to be associated with winter frontal storms, whereas shorter durations with greater intense tend to be associated with summer convective storms.

The rainfall studies in Southeast Arizona and New Mexico show seasonal patterns too (Osborn et al., 1979; Renard, et al., 1970). Drissel and Osborn (1968) in their study on variability in rainfall producing runoff from a semiarid rangeland watershed, Alamogordo Creek in New Mexico, found that the summer convective storms produce about 80% of the annual rainfall, with over 50% of the annual total occurring in June, July and August. Most thunderstorms occur in summer due to the combination of moist air moving into the region from the Gulf of Mexico and the strong convective heating. It was also noted that most of these thunderstorms occur in the late afternoon or early evening producing high-intensity, short-duration rains of limited areal extent. Summer rainfall was found as highly variable from year to year and over the different parts of the watershed (Osborn & Hickok, 1968). Osborn and Hickok (1968) explained in their study that the winter storms result from weak cold fronts producing relatively low-intensity rainfall which agrees with the studies carried out in Saudi Arabia and Oman.

It should be borne in mind that the type of rainfall is influenced by the type of the rainfall mechanism, for example, the winter storms can be severe if caused by a cyclone (Al-Qurashi, 1995). As there could be more than one type of runoff-producing thunderstorm, it might be advisable to differentiate between these events when analysed.

2.4 Runoff

Estimation of runoff is an essential component in the management of water resources (Chiew & McMahon, 1994). It is important to achieve a reliable estimate of stream flows for various purposes, for example reservoir yield analysis, gap-filling missing records, determining rainfall losses, predicting future responses and better understanding of hydrological processes and potential for flood protection.

The predominant runoff mechanism is generally Hortonian overland flow, where the rate of rainfall exceeds the potential rate of infiltration (Pilgrim et al, 1988; Wheater et al., 1997). In combination with high intensity, short duration and convective rainfall, extensive overland flow is expected to be generated.

In most arid areas, baseflows or continuous flows are rare, and flow channels are generally dry for most of the year, with flashy floods expected after short intense rainfall which might last for a few hours to not more than a few days.

Rodier (1985) in his study on the aspects of arid zone hydrology has determined the factors he believed to be affecting the runoff as below:

- Climatological factors
- Physiographic conditions
- Hydrographic degeneration (distribution of the main channel downstream to many unclear flow paths, which geomorphologists refer to as braided channels).

However, runoff in arid areas has some special characteristics, and these are discussed further in the remainder of this section.

2.4.1 Spatial and temporal variation of runoff

The generated runoff is likely to be highly localised in space and reflects the spottiness of the spatial rainfall fields, occurring on only parts of a catchment (Wheater, 2002; Walters, 1989). Pilgrim et al. (1988) in their study in Western Australia found that a further key cause of this phenomenon was spatial differences in infiltration capacity; areas producing runoff were in valley bottoms and along stream channels. The Cordery et al. (1983) study (also in western New South Wales) however, did not find clear evidence on this phenomenon. It should be noted that runoff spatial occurrence varies not only from one area to another, but also from one event to another.

As runoff in arid areas tends to vary in space and time, annual average discharge can be misleading. Drissel and Osborn (1968) showed that the total runoff in a studied watershed at New Mexico was 0.8 mm in 1964, whereas in 1960 it was 59 mm, and about 60% of total runoff from 1956 through 1965 was produced in 1960. This is not uncommon in arid areas as it is normal to have many years of effectively no flow and then a sequence of one or more wet years. Hence, it should not be surprising to have a water shortage in the arid areas in one year and severe floods with huge amounts of flow volume in another year.

2.4.2 Initial losses

The initial loss is the maximum amount of precipitation that can occur under specific conditions without producing runoff. The initial losses in arid areas are different from those in humid areas. For example, in the humid New South Wales, an average depth of 35 mm is required before runoff starts but up to 125 mm is required under dry antecedent conditions (Pilgrim et al., 1988), compared to only 16 mm of rain in a storm (as intensity of more than 5 mm per hour) in a study in the arid western New South Wales (Cordery et al., 1983).

In Oman, the initial losses were estimated to be 8 mm by some studies, but Al-Qurashi (1995) found that runoff events were observed for less than this value at Wadi Ahin. It can be assumed that these values vary from one part in the basin to another due to partial area runoff in arid areas. Hence, further investigations are necessary. Adequate rainfall network coverage will also be needed for better assessment of this process.

2.4.3 Hydrograph characteristics

In deserts where precipitation occurs as short, intense showers, flash floods are the typical result. The hydrographs in arid and semi-arid areas tend to be flashy with short time bases and steep rising and falling limbs (Pilgrim et al., 1988; Walters, 1989; Wheater & Brown, 1989). This is demonstrated in **Figure 2.2**. For small catchments the rise time could be as little as 15-30 minutes, showing a brief period of peak flow, and relatively slow decline. For example, Schreiber and Kincaid (1967) and Osborn and Lane (1969) found that runoff was strongly correlated to the maximum 15-minute intensity of rainfall. Osborn and Renard (1973), however, found that for large watersheds runoff was best correlated to the maximum 30-minute rainfall for both peak discharge and total storm runoff but the best correlations between the point rainfall and peak and total discharge were for the very small watersheds.

Schick (1988) in his review of the characteristics of flashy floods in rocky arid catchments of the Southern Negev and Sinai, found that the flow rises from significant levels to high, short flood peaks within several minutes. Osborn and Renard (1973) showed in their study on Walnut Gulch in Arizona that runoff-producing rainfall seldom lasted for more than 30 minutes at any point. The study also indicates that the average duration of flow for individual storms events is relatively short (of the order of one-hour) on the very small watersheds within Walnut Gulch and it is considerably longer (up to 6-hours) on the larger watersheds. The variations in durations between similar sized watersheds were referred, by the authors, to the differences in the alluvial

channels; the amount of transmission losses increases with the increase of the amount of the channel alluvium. Walters (1989) in his study on Wadi Ghat in Saudi Arabia, describing the event of April 1985, showed that after a mild increase from zero to 660m^3/s in 2.5 hour, there was a rapid increase in discharge from 660 to 3200m^3/s in one hour and then a rapid decrease to 660m^3/s in the following 40 minutes with a total flood volume of 19.3Mm^3.

It was noted that the channel storage and peak discharge affect transmission losses. The higher discharges have greater wetted perimeter and consequently higher transmission losses, a large part of which occur on the rising part of the hydrograph and thereby shortening the rise time.

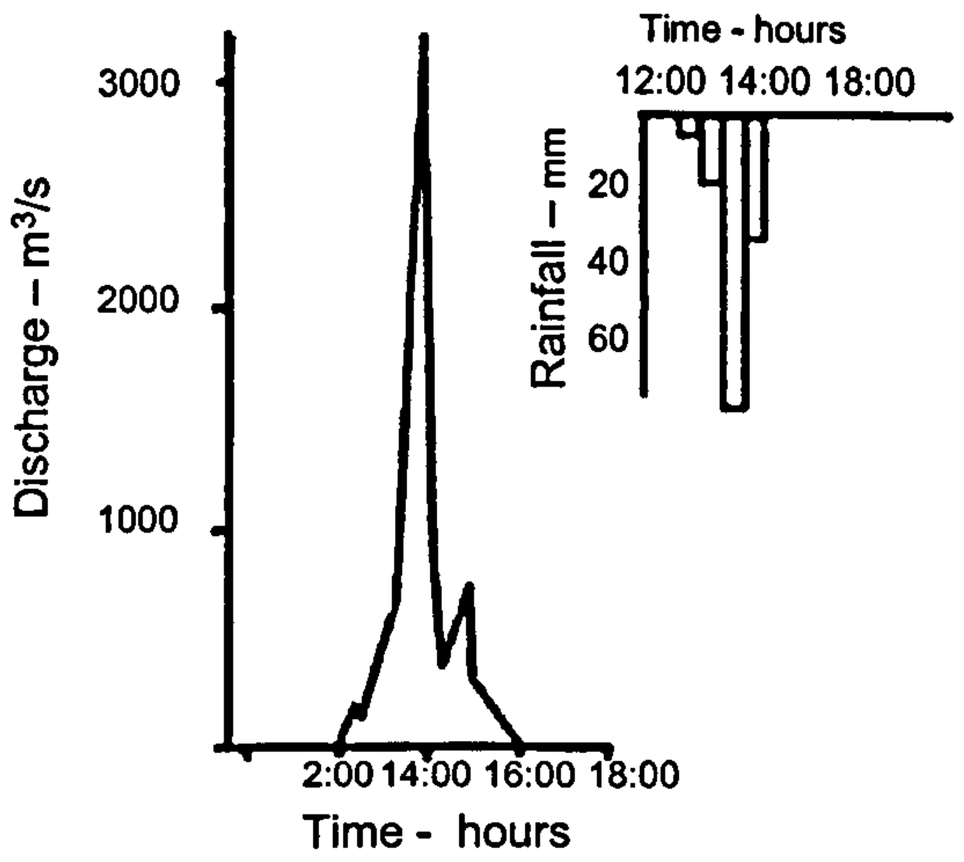


Figure 2.2: Flash flood at Wadi Ghat in Saudi Arabia (*After Walters, 1989*)

It should be noted that rainfall intensity has a great effect on the shape of the hydrograph. Minshall (1960) in his study in the Midwest of the USA found that rainfall intensity has some effects on geometry of the unit hydrograph and showed that the rise time decreased with increasing peak discharge. The rise time of the runoff hydrograph, decreases with the channel distance traversed by the runoff.

The situation might not be the same in arid areas. Renard et al. (1966) in their study of Walnut Gulch, found that the time of rise decreases with increasing size of drainage basin. They attributed this to transmission losses during rising stages and presence of overriding translatory waves as the flow moves through the channel. Renard et al. (1966) showed that storm pattern and sequence dominate watershed parameters in influencing the shape of the runoff hydrograph. He believed that the peak discharge affects the rise time of the runoff hydrograph through its effects on channel storage.

Higher peak discharge and its associated channel storage effects tend to increase the rise time at a downstream station.

2.4.4 Flood peak magnitudes

Flood peaks in arid areas can be very high. Flood peaks of up to 1650m^3/s were observed in the Southern Negev and Sinai (Schick, 1988). However, in Oman much higher peaks have been observed. A study on "Wet periods in Oman in recent decades" (MWR, 2000b) showed in March 1997, a remarkable flood filled Hawasinah Recharge Dam and overtopped its spillway with a massive peak outflow of 2,760m^3/s, causing devastation and loss of lives downstream.

Table 2.1 shows some of the floods that were reported in different parts of Oman. It should be noted that the floods of Wadi Andur and Ghudun were most probably a result of a cyclone.

Table 2.1: Maximum Flood Peaks Reported In Oman

Wadi Name	Catchment Area (km^2)	Flood Peak (m^3/s)	Flood Date
Wadi Dayqah at Mazara	1,711	9,500	1927
		7,750	1965
		5,190	1982
Wadı Ibra	687	5,140	1927
Wadı Halfayn at Izki	270	4,130	1951
Wadı Muaydin at Birkat al-Mauz	197	3,580	1951
Wadı Andur	884	8,250	1977
Wadi Ghudun	1,937	10,600	1977
		10,400	1983

2.4.5 Characteristics of flood events

It should be noted that even though floods are rare in arid areas, when they occur these tend to be very high and the volume is considerable, e.g. in Egypt, during the flood of 12-17 November 1996, 154.5Mm^3 was discharged to the river Nile, which is equivalent to the average daily release from Aswan Dam (Abu Zeid, 1997).

The occasional severe floods in an otherwise arid environment can cause considerable damage to both life and property, as **Figure 2.3** below demonstrates.



Figure 2.3: Flood Damage in Oman

Surface water flow from the mountainous watersheds tends to be ephemeral and generally occurs as brief periods of relatively intense flood flow closely associated with individual storm events. Drainage of mountain watersheds following major rainfall events may cause one or two months of surface flow. The varied nature of flow in ephemeral stream channels reflects the full range of climatic and drainage basin characteristics, notably type and distribution of rainfall, infiltration capacity of surface material, antecedent moisture conditions and local topography. On the other hand, as the flood moves downstream, the flood volume is reduced by losses from the flood hydrograph through bed infiltration (Wheater, 2002), in particular through wide wadi channels as these traverse often permeable downstream flood plains.

The resulting runoff in the arid area is one of the most important factors in infiltration and recharge of ground water aquifers. The magnitude and frequency of recharge from ephemeral streams is the amount of infiltration into the wadi bed as the flood wave progresses in the downstream direction. Alluvium channels usually infiltrate a large volume of flood flow (Sorman & Adbulrazzak, 1993).

2.5 Rainfall-Runoff Relationships

The rainfall-runoff relationship in arid areas is complex and does not seem to be very well understood, at least to date. However, there are many factors that affect this relationship. These factors include effects of hydrological processes and the effects of physical characteristics of the watershed. Some details on the effects of these factors are explained below.

2.5.1 Effects of hydrological processes

Hydrological processes, such as type of runoff-producing storms, have clear effects on the rainfall-runoff relationship (Pilgrim et al., 1988).

Lang et al. (2000) showed in his study that the hydrological processes in arid areas are dominated by the high rainfall intensities, prevailing low infiltration rates of the rocky terrain and high infiltration rates of the sandy/gravely alluvial beds in ephemeral watercourses. Schreiber and Kincaid (1967) in their study, using a stepwise multiple linear regression equation found that average runoff increases as precipitation amount increases, decreases as crown spread of vegetation increases and decreases as antecedent soil moisture increases.

2.5.2 Effects of watershed physical characteristics

The physical features of watersheds have great effects on the rainfall and runoff and their relations. Many studies have investigated the effects of different catchment physical characteristics on rainfall and runoff (Rodier, 1985; Pilgrim et al., 1988; Nouh, 1990; Al-Qurashi, 1995). It is important to understand the effects of physical features on the hydrological process and the rainfall-runoff relationship as these can make it possible to transpose hydrological characteristics from known gauged catchments to unknown (ungauged) catchments.

It should be noted that the effects of physical catchment features are more direct on runoff than in rainfall. The physical features affect mostly the effective rainfall rather than the total rainfall, even though the total rainfall will be affected by the orographical and the elevation of the location. The physical features can also affect the amount of initial losses that can affect the effective rainfall. Some of the physical characteristics that can affect the rainfall-runoff relationships are described below:

- ***Effect of Elevation:*** As mentioned previously, a clear relation was found between the number of rainy days and the elevations (Wheater in Saudi Arabia, 1991a, b), and other studies show a good relation between the amount of rainfall and the elevation (MWR, 1998).

- ***Stream length:*** It is one of the important parameters and found to have a well known correlation with the size of the catchment, where the stream slope is inversely related to the main stream length and thus the catchment size (Pilgrim et al., 1982; Al-Qurashi, 1995). The stream length affects the runoff magnitude. The transmission losses generally increase with the increase of the stream length, and so the flood magnitude decreases (Al-Qurashi, 1995; MWR, 1998, 2002).

- ***Effect of stream slopes:*** Rodier (1985) explained in a study the effects of land slope as well as river bed slope on runoff. He states that runoff appears only if the slope of the

ground has a significant value. The flood can move a longer way with a significant continuous slope as the stream channel may avoid hydrographic degeneration (main channel deviation into many unclear channels). The surface characteristics and hence runoff potential of areas with different average slopes are likely to be quite different (Pilgrim et al., 1988). A study carried out in Oman (MWR, 1998) found that the floods are affected significantly by the catchment area, slope and the percentage of alluvium (or alternatively percentage of mountain).

• ***Catchment size:*** Renard et al. (1970), and Nouh (1990) all believed that the basin size affects the rainfall-runoff relationship and showed that the hydrological responses of small catchments are different and more variable than those of large catchments. Fogel and Duckstein (1973) stated that the smaller the watershed, the greater the correlation between rainfall and runoff. Fogel and Duckstein (1973) referred this to the variability of the convective storms in time and space which increases with the increase of the area as well as the channel storage and transmission losses. Goodrich (1990) explained that the basin-average depth of runoff decreases with increasing watershed area due to partial area storm coverage as well as the increased channel losses. Osborn and Renard (1973) referred this to the limited areal extent of thunderstorm rainfall and because of increasing magnitude of channel abstractions for the largest watersheds.

Nouh (1990) has investigated 32 catchments in Saudi Arabia for determining the effect of the catchment size on the accuracy of the performance on the geomorphological rainfall-runoff models using a model based on the geomorphological instantaneous unit hydrograph (GIUH). The study considered the effects of basin slope, size of catchment, and soil type. The results showed the size of the catchment has a great effect on the accuracy of the model. The accuracy decreases as the size of the catchment increases. It was noted that the increase of basin size can increase the rainfall measurement errors which will significantly affect the runoff simulation (Goodrich, 1990; Nouh, 1990).

• ***Effect of soil type:*** Soil type and geology were found among the parameters that affect the rainfall-runoff relationships and the hydrological response (Pilgrim et al., 1982). The study, which was carried out in New South Wales, Australia, found that these effects are more significant in small catchments than larger ones where the catchment size was found to be affected by the geomorphological features. Rodier (1985) presents an explanation in his study of the effect of the soil type on the runoff and recharge. He believes that knowledge of the nature of the soil and subsoil are important for the prediction of runoff or the recharge of aquifers. In addition to that, Pilgrim et al. (1988)

stated that the soil's surficial properties play a primary role in runoff production, as saturation of the surface soil occurs relatively rarely. Other features which were believed to have effects are hydrophobic soils, armouring, dispersive soils, cracks, scald or claypan areas, sand dunes and bare surface rock (Rodier, 1985; Pilgrim et al., 1988).

• ***Effect of fans and relief:*** The relief and fans are believed to have effects on the rainfall-runoff relationship (Pilgrim et al, 1988). The amount of alluvium in the channel has great effects on this relationship, as studies in Walnut Gulch by Osborn and Renard (1973) and the nationwide study carried out in Oman showed (MWR, 1998).

Pilgrim et al. (1988) showed that the differences in average relief have several important effects on the hydrology of arid and semiarid regions, as in regions with little relief there is often no integrated drainage network. Pilgrim believed that the size and hydrological importance of alluvial fans also depend on relief. The relative importance of fans with different degrees of relief will cause differences in hydrological characteristics (French, 1987, Pilgrim et al., 1988).

The fans have also some effects on rainfall runoff relationships. Fans can be defined as low cones of alluvial material where the central point lies at the mouth of a gully or ravine and the material spreads out onto the adjoining plain. French (1987) believed that fans are a feature of drainage networks in most arid regions and are related to the high sediment loads carried by streams in arid and semiarid regions. They form where slopes and hence the velocities decrease. The high relief can lead to occurrence of alluvium fans which are expected to provide high storage capacities that can absorb large volumes of water and recharge local aquifers.



Figure 2.4: Distributed channels on the surface of an alluvial fan in Eastern Desert of Egypt (*After Tooth, 2000)*

• ***Effect of vegetation cover:*** The effects of vegetation cover, which changes with time and rainfall amounts and duration, are also among the factors and parameters that influence the rainfall-runoff relationships. Similarly land use can affect the hydrological processes. Cultivated land for agricultural use tends to reduce the runoff but if the cultivated area in the valley replaces a dense bush of thorn trees, the floods may flow more easily downstream (Rodier, 1985). Urbanisation affects the runoff, which generally increases with the increase of urbanised area.

2.5.3 Runoff coefficients

Many studies discussed runoff coefficients in different watersheds in arid areas. The time series of annual runoff coefficients is interesting because the variability of this ratio gives an overview of the behaviour of the annual water balance over time (Neil et al., 2003). However, it was noted that most of the studies were not able to obtain such a runoff coefficient that can be adopted with confidence for any catchment. In fact, where there are very wide and generally unsaturated permeable wadi channels, runoff rates and so runoff coefficients decrease as flows proceed downstream, inevitably making the concept of runoff coefficients as used in more humid regimes of limited value for arid areas. Investigation of this issue showed that the coefficients also vary from one event to another and from one season to another (Al-Qurashi, 1995). As an example, Gibb (1976) in the study carried out for Oman, assumed typical ranges of 17 to 20% for the monthly values but 25 to 35% were used for more specific cases for the hard-rock areas. Wheater and Bell (1983) found the runoff coefficient ranges from 1 to 121% for Wadi Aday in northern Oman, whereas the runoff coefficients obtained by Al-Qurashi (1995) in her study for Wadi Ahin in northern Oman ranged from 7 to 42% for the upper catchment gauge and 0.3 to 4% at the lower gauge for the summer events, and ranged from 3 to 21% for the upper gauge and up to 1% for the lower catchment in the winter. The latter study showed that the seasonality can have great effects on runoff coefficients that should be taken into account.

In another study in the region but for Saudi Arabia, Wheater and Brown (1989) found that the runoff coefficients ranged between 6 to 80%. Walters (1989) in his study on wadi Ghat watershed in Saudi Arabia obtained a runoff coefficient of 27% for April 1985 event, whereas Sorman and Abdulrazzak (1993) found that these coefficients varied in the range of 1 to 7% for the runoff depth ranging from 2 to 18 mm. In another study in the region and at north-east Libya, De Vera (1984) found the range of the coefficient varies between 0.01 to 83%. On the other hand, in India, in Luni Basin,

Sharma and Vangani (1982) obtained runoff coefficients that vary between 0.1 to 63%. Osborn and Renard (1973) in their study in Walnut Gulch watershed in USA, assumed 'onsite runoff' may average as much as 20 to 25 % of summer rainfall. However, Michaud and Sorooshian (1994) suggested an average of 11 % of rain from the validation storms became runoff at the watershed outlets. Hence, there is no one specific runoff coefficient that can be used for each individual catchment with any confidence and more investigations seem to be necessary.

Obtaining the runoff coefficients can be difficult. In the eight watersheds Osborn and Renard (1973) analysed they were not able to obtain any really good rainfall-runoff correlation. The study of Fogel and Duckstein (1973) also could not obtain any good relationship after numerous trials using different parameters even though much better correlation was obtained for the smaller watersheds. Fogel and Duckstein (1973), however, showed in their study that the runoff coefficient is a function of both the characteristics of the watershed and the rainfall intensity for a given drainage basin. The authors believed that for very small watersheds, a simple linear relationship appears to be adequate for estimation of runoff volume from convective storm rainfall. They also stated that any equation that uses only the depth of storm rainfall as the independent variable has limited applicability for estimating runoff.

Osborn and Lane (1969) referred the correlation of runoff to the rainfall intensity to the condition of the normally dry surface, which allows an increase in the rate of infiltration. The authors found that there was a negative correlation on one of the watersheds they selected between runoff and antecedent rainfall. They also found that there were no significant correlations between any of the precipitation variables and duration, lag time or rise time of the runoff hydrograph. However, the authors were aware of using only runoff-producing events in their analysis, therefore rendering runoff equations that are biased. The runoff coefficient is also affected largely by the transmission losses. The latter is not well understood or measured, hence it is one of the reasons for the difficulty in determining the runoff coefficient values in arid areas.

2.5.4 Difficulties in determining rainfall-runoff relationships

Many studies showed that the rainfall-runoff relationship shows a high degree of scatter (Brown, 1987; Al-Qurashi, 1995). Furthermore, some studies showed runoff occurrence with no recorded rainfall (Wheater & Brown, 1989; Al-Qurashi, 1995). There could be many reasons for this, which we do not fully understood, as the hydrology of arid areas is still under investigation. El-Hames and Richards (1994) and Al-Qurashi (1995)

explained that the climate conditions in arid regions are very variable and the rainfall and flood events are infrequent, hence even long periods of records may only contain very few events.

The poor relationship between rainfall and runoff in different watersheds in arid and semi-arid areas can be also explained by the spatial and temporal distribution of both rainfall and runoff (Pilgrim et al., 1988; Rodier, 1985; Wheater et al., 1991a, b; Al-Qurashi, 1995). However, the short period of records and the poor quality of the data together with insufficient network coverage makes rainfall-runoff modelling a challenging task.

The complex relationship of rainfall and runoff in arid areas is reflected in the rainfall-runoff modelling. Low yielding catchments present great difficulties in analysing and modelling rainfall-runoff relationships (Chiew & McMahon, 1994; Ye et al., 1997).

Baseflow also can cause great difficulties in modelling rainfall-runoff. Ye et al. (1997) believed that in cases where baseflow is relatively small but sustained, it makes the largest contribution to catchment water yield, thus the estimation of the model parameters controlling baseflow in such situations is critical but difficult.

2.6 Channel Transmission Losses

Transmission losses are a very important phenomenon in studying stream flow and groundwater recharge in arid areas. There are many studies that discussed this phenomenon and its importance in arid areas (Jordan, 1977; Rodier, 1985; Pilgrim et al., 1988; Leonard and Lane, 1990; Sorman & Abdulrazzak, 1993; Al-Qurashi, 1995; Wheater et al., 1997).

2.6.1 Definition of transmission losses

Transmission losses can be defined as the water absorption into the alluvium bed material of the ephemeral channels in the drainage between the upstream and downstream locations (Jordan, 1977; Leonard and Lane, 1990). The amount of the reduction depends on the amount of runoff in the drainage area between the locations.

However, these losses can be divided into different types; some as recharge, some that are added to soil moisture storage, and some that are stored temporarily in the saturated zone in the stream bank material (Jordan, 1977). The processes of transmission losses however, are complex and not yet fully understood. Infiltration experiments can be carried out in wadi alluvium to determine hydraulic properties and may show highly

transmissive profiles, but point measurements were found to be inappropriate to explain observed response from real runoff event (Parissopoulos & Wheater, 1992a).

2.6.2 Importance of transmission losses

Understanding the transmission loss phenomenon and assessing it is important in modelling surface and groundwater. Transmission losses can be considered as one of the main causes of the great variation of runoff coefficients. Analysis of these losses can aid stream flow modelling and flood forecast (Jordan, 1977). The studies in Walnut Gulch in U.S.A and other arid parts all showed that it can represent a very large amount, and it is not unusual to have a high flood in the upper stream of the catchment and barely any flood at the downstream gauge (Cordery et al., 1983; Al-Quarshi, 1995; Wheater et al., 1997). Due to this phenomenon, water is lost, as flood waves travel through the normally dry stream channel systems or networks. Thus, runoff volumes and flood peaks are reduced (Renard et al., 1970).

The infiltration into the wadi bed is important in recharging the alluvial aquifers. Sorman and Abdulrazzak (1993) in their analysis of groundwater rise due to transmission losses in Saudi Arabia estimated that on average of 75% of bed infiltration reaches the water table. Transmission losses and their resulting groundwater recharge were believed to be the key issue for water resources management in ephemeral stream systems (Wheater et al., 1997). Wheater (2002) assumes the differences between the flood transmission losses and the groundwater recharge are expected to be small but will depend on residual moisture stored in the unsaturated zone and its subsequent drying characteristics. He also suggested that if the water table approaches the surface, relatively large evaporation losses may occur.

Transmission losses are also an important component of the water budget because surface water yields are reduced, riparian vegetation and wildlife are affected, and local aquifers are recharged. Therefore, prediction of flood peaks and calculation of water budgets for watersheds in arid areas require quantification of the impacts of transmission losses on components of the hydrologic cycle (Leonard & Lane, 1990). However, this phenomenon can also be used to increase the amount of recharge at certain locations by construction of flood detention structures which can slow the transmission of the flood and lead to the focusing of recharge on particular locations as in the Batinah plain of northern Oman to prevent flow from being lost to the sea or to the desert interior (Wheater et al., 1997).

BIBL LONDON UNIV.

2.6.3 Factors affecting transmission losse

Transmission losses between stations might be expected to be highly variable from one event to another (Jordan, 1977; Sorman and Abdulrazzak, 1993; Al-Qurashi, 1995). There are many factors affecting the amount of the transmission losses.

The differences could be due to varying in antecedent moisture conditions, differences in runoff to the stream between gauging stations, differences in alluvial materials, and differences in geometry of channels and flood plains. Wheater and Brown (1989) believed that the duration of the flow and the spatial extent of surface wetting affect infiltration more than the flow magnitude.

Osborn and Renard (1973) explained in their study that the transmission losses are related to channel length and wetted parameter, hydrograph characteristics, volume and porosity of alluvium and amount of clay in suspension in the water infiltrating into alluvium. Renard et al. (1966) believed that most transmission losses occur during the rising part of the hydrograph and have a pronounced effect on the hydrograph shape; the longer the reach of channel traversed, the more pronounced the effect of transmission loss in shortening the rise time. They also noticed that the coarse alluvial beds near the surface dry out rapidly between runoff events. Osborn and Renard (1973) showed that the relationship between mean annual runoff and area changes for different physiographic and climatic provinces. Transmission losses thus affect runoff per unit area, causing a decrease in runoff with increasing drainage area except where there is groundwater discharge.

In another study, it was noted that the presence of silt lenses within the alluvium have important effects on surface infiltration as well as sub-surface redistribution (Parissopoulos & Wheater, 1990). In practice, spatial heterogeneity is likely to introduce considerable complexity to the infiltration process and to up-scaling from point properties (Wheater et al., 1997). Parissopoulos and Wheater (1990) illustrated this using two-dimensional simulation and showed that significant reduction in infiltration rates occur once hydraulic connection is established with an underlying water table. In a series of two-dimensional numerical experiments it was also shown that infiltration opportunity time was more important than high flow stage influencing infiltration, and that hysteresis effects were generally small (Parrissopoulos & Wheater, 1992b).

Wallace and Lane (1978) attempted to relate the volume of available storage potential within the alluvium in the bed of a channel network to stream orders and lengths, to

enable estimation of potential losses but found that the available storage volume was much greater than the potential supply in runoff events. Wheater et al. (1997) found in his study in Walnut Gulch, that the events examined had a maximum value of average transmission loss of 4076 m^3/km in comparison with the estimate of Lane et al. (1971) of 480-6700 m^3/km as an upper limit of available alluvium storage. Telvari et al. (1998) in a study of Fowler's Gap catchment in Australia also discussed the role of the available storage. The study shows that 7000 m^3 of overland flow becomes transmission loss. Hence, once the alluvium storage is satisfied, two thirds of overland flow is transmitted downstream. Two sources of transmission losses were suggested: loss could be occurring direct to the bed but limited by available storage, or losses could occur through the banks during flood events (Telvari et al., 1998).

2.6.4 Transmission losses measurements

There is no specific technique to measure transmission losses up to date. Transmission losses in Walnut Gulch, USA were measured by determining the difference between the upstream flood volume and that of the downstream (Jordan, 1977). In Alamogordo Creek watershed, losses were estimated by comparing the inflow and outflow hydrographs and volumes for individual storms for channel reaches having little or no unmeasured tributary inflow (Renard et al., 1966; Osborn & Renard; 1973). Renard et al. (1966) however, stated that, the transmission losses in the case of Alamogordo Creek watershed are considerably smaller because of the fine-textured channel alluvium present.

Mathematical modeling of transmission losses has been limited. However, there are now a few models, and hydrologists are attempting to develop or improve some of the existing models to define the transmission losses. One of the models was used by Lane et al. (1971) to predict downstream hydrographs using regression techniques and a three-parameter gamma distribution to represent the inflow and outflow hydrographs at some location in Walnut Gulch watershed.

Hughes and Sami (1992) in their study from a 36.6 km^2 semiarid catchment in South Africa had monitored soil moisture using a neutron probe following two flow events. It was found that at some locations immediate response occurred throughout the profile but at others a response near surface was followed by delayed response at depth which was also evidence of the heterogeneity.

Analysis of observed flood flows at different locations can allow some quantification of losses, and studies by Walters (1990) and Jordan (1977) provide evidence that the rate

of loss is linearly related to the volume of surface discharge. However, Wheater et al. (1997) in an analysis of transmission losses between 2 pairs of flow gauges on Walnut Gulch catchment for a 10-year sequence of data, found that a simple linear model of transmission loss as proportional to upstream flow was inadequate.

Wheater (2002) in his study on hydrological process in arid and semi-arid areas believed that it is very difficult to assess the transmission losses. He suggested that, where deep unsaturated alluvial deposits exist the simple linear models as developed by Jordan (1977) and implicit in the results of Walters (1990) may be applicable, but where alluvial storage is limited, this must be taken into account. Wheater (2002) explained that it is not possible at present to extrapolate from in-situ point profile hydraulic properties to infer transmission losses from wadi channels.

2.7 Vegetation Cover

The rainfall in arid and semiarid areas is very sparse and has a great variation from one location to another and from one time to another, and so has the runoff. The vegetation cover also changes with time as it depends on the rainfall. The density of vegetation may be very different after a wet period from that after a prolonged dry period. Rodier (1985) showed that in the valleys the vegetation can become dense after rainfall, and this impedes the flow during floods. There is also a wide variation in the soil water balance at a scale related to plant spacing (Pilgrim et al., 1988).

2.7.1 Effects of vegetation cover on interception

Interception is highly significant in arid areas, mainly where runoff is due to low intensity rainfall and where the plant cover is varying with time (Pilgrim et al., 1988). The interception varies greatly with time and space in arid and semiarid regions due to the variation of the vegetation cover which complicates the description of the process and modelling of interception (Pilgrim et al., 1988). The vegetation affects the interception but these effects are very small in determining the micro-hydrology at a site when the rain occurs at high intensities during thunderstorms (Al-Qurashi, 1995). Pilgrim et al. (1988) suggest that even with their different rates of evaporation, the lumping of interception and surface soil water together in a single store may be more reasonable in arid regions than in humid zones due to the generally longer periods between rainfall events. However, interception data are very few in arid areas and very little is known about it.

2.7.2 Effects of vegetation cover on infiltration

The vegetation cover has an important effect on infiltration and recharge beside the flow velocity, interception, and evapotranspiration. The vegetation usually occurs where the infiltration capacity is high (Al-Qurashi, 1995).

2.7.3 Effects of vegetation cover on runoff

The spatial and temporal aspects of the runoff and soil water are likely to have a greater impact on the spatial and temporal runoff and soil water variations in arid areas than in humid regions. The sparse coverage of vegetation has also a great effect on the soil erosion, and it can lead to high sediment runoff coefficients. Tooth (2000) stated that the typical sparse or uneven distribution of dryland vegetation can exert a significant influence on hillslope runoff and sediment transport processes.

There are many studies giving examples of the increase of runoff and sediment from the dryland hillslopes under conditions of decreased vegetation cover (Laird & Harvey, 1986; Graf, 1988; Thornes, 1990; Florsheim et al, 1991; Abrahames et al., 1995). Vegetation cover however, often fluctuates in response to periods of above and below average rainfall, periodic fire or grazing effect, with implications for hillslope runoff and erosion (Graf, 1988, Cooke et al., 1993, Thornes, 1994; Tooth, 2000).

2.7.4 Effects of vegetation cover on hydrological parameters

Vegetation cover has also some effects on other parameters that can affect the hydrological responses of the watershed such as the roughness coefficients, the soil characteristics and evapotranspiration. Hence, it affects both effective rainfall and runoff.

The complexity of the vegetation cover over space and time increases the difficulty of modelling rainfall-runoff and defining other affected parameters in arid areas (Pilgrim et al., 1988).

2.8 Evaporation and Potential Evapotranspiration

The potential evapotranspiration rate is defined (Chow et al., 1988) as 'the evapotranspiration that would occur from a well vegetated surface when moisture supply is not limiting'. Evaporation and evapotranspiration were defined by Bedient and Wayn (1988), as 'the process by which water in its liquid or solid state is transformed into water vapour, which mixes with the atmosphere. Evapotranspiration is considered separately as the combined loss of water vapour from the surface of plants (transpiration) and the evaporation of moisture from soil'.

Potential evapotranspiration was the key factor that was used by UNESCO (1979) to determine and classify the arid areas. However, the values of potential evaporation are generally much higher in arid areas than in humid areas (Mourits & Saleh, 2002).

- ***Potential evaporation*** in arid areas is very high as mentioned previously. Rodier (1985) believed that if the mean annual precipitation is 100 mm it could evaporate entirely if the average annual precipitation does not include any heavy rainfalls. Potential evaporation was estimated to be about 2200 mm/year for Lake Chad in Africa compared to 2700 at Najran in Saudi Arabia (Rodier, 1985). Rodier believed it is very difficult to estimate daily evaporation in arid areas, especially for a whole basin which is much more difficult than at a point.

Rodier (1985) explained that the evaporation from a free water surface is similar to pan evaporation. He also believed that for a given climate, the annual evaporation from a reservoir surface may vary broadly in relation to the reservoir depth, the area, the shape, the exposure to prevailing winds.

- ***Evapotranspiration*** is the combination of evaporation from soil surface and transpiration from vegetation (Chow et al., 1988). It varies for a given climate with the type of vegetation cover. The values therefore can vary from one place to another in the same country. The vegetation cover in arid areas is sparse and different in wet periods than in dry periods, hence the evapotranspiration varies. In Oman, the potential evapotranspiration was found to vary from one region to another. In the Interior (inland) it is in the order of 3,000 mm /year, on Al Batinah coast (Northern Oman) was 2100 mm/year, whereas, in Salalah Plain (Southern Oman), it was 1,700 mm/year (MWR, 1995).

The effects of seasonality were shown by Al-Qurashi (1995), in her study for Wadi Ahin in Northern Oman, to vary significantly for the potential evapotranspiration values in the winter season and summer. Mott MacDonald (1991) in their study for Oman obtained values in the range of 1.7-5.0 mm/day for winter whereas they ranged from 2.2 to 6.9 mm in summer. Saleh and Sendil (1984) in their study to estimate the evapotranspiration under arid conditions in Saudi Arabia, compared 4 different sites using four empirical methods. The results showed that some of the empirical methods give significantly lower estimates under extremely arid conditions than was shown by direct lysimeter measurements. These results agreed with another study by Saleh (1988) in other sites in Saudi Arabia.

Pilgrim et al. (1988) believe that in arid areas, evaporation from bare soil assumes a greater importance than transpiration from plants, due to the greater area of bare soil and the frequency of small rainfall events which allow bare soil to return water to the atmosphere without major pathway impedance. Rose (1968) assumed that as soils dry, soil water transport in the vapour phase becomes more significant, and the diurnal rate of evaporation is significantly affected by soil temperature gradients.

Evaporation and evapotranspiration values could affect the flood duration time and baseflow (Al-Qurashi, 1995). However, in the case of flash floods with high velocities and short durations evaporation and evapotranspiration can generally be ignored without any significant effects on the results of flood magnitude (Parissopoulos & Wheater, 1992a, b; Al-Qurashi, 1995).

2.9 Conclusions

Arid areas have distinctive hydrological features. This chapter has discussed the most distinct hydrological features of arid areas which are expected to affect any hydrological study and should be considered. It is important to consider these features in any rainfall-runoff modelling for arid areas.

Important features that need to be considered include climate effects. The climate in arid areas is very different from that of the humid areas. The temperature, evaporation and evapotranspiration in arid areas are much higher than in humid areas. The humidity can also be quite high, although it depends on the location of the area relative to the coast.

The rainfall characteristics in arid areas are also rather different and these characteristics need to be fully understood and considered in any hydrological modelling and analysis. It also varies highly in space and time. Some studies show clearly the effects of seasonality. The summer events seem to be more intense and localized than winter ones, which are less intense and can be more distributed over larger areas. Elevation affects the rainfall in both the number of the rain days and the rainfall depth. On the other hand, the annual average rainfall can be misleading and needs to be carefully examined to ensure that a few extreme high rainfall events in a few days do not bias the long term average.

Arid areas generally do not have continuous stream flow and the flow channels are mostly dry most of the year. However, when runoff does occur it can be very high with floods that are very flashy in nature. Such floods can cause tremendous damage when channel capacity is limited. It was also noted that runoff varies in space and time and

partial-area runoff could be significant in some arid areas. The flood hydrographs in arid areas are often different in shape and characteristics from those of humid areas, typically showing rapid peak rise and short recession, and often lasting for a few hours only. Relative to catchment area, flood peak magnitudes can also be very high (up to more than 10,000 m^3/s in Oman). Flood volumes also can be very large, with millions of cubic meters were recorded in one day in Oman stations.

Rainfall-runoff relationships in arid areas were discussed in this chapter. It was shown that this relation is complex. The relation is affected by many factors that need to be well understood and considered when carrying out any analysis or modelling. Hydrological processes such as the type of runoff-producing storm, rainfall characteristics, runoff characteristics, transmission losses, all have great effects on rainfall-runoff relationships. There are some other factors that can affect this relationship and need to be well understood, such as watershed physical characteristics. These characteristics include; elevations, stream length, slope, catchment size, soil type fans and reliefs, and vegetation cover.

The difficulty in understanding rainfall-runoff relationships was reflected in the difficulty in obtaining a runoff coefficient. In that transmission losses in arid are so high in typically permeable wadi courses, runoff rates depend more on length of channel upstream than the basin rainfall and soil types as in more humid regimes. The runoff rate reduces downstream in such circumstances, and so no unique runoff coefficients can be expected. The literature review for arid areas showed that it was very difficult to obtain any runoff coefficient that can be used in hydrological analysis with any confidence. Hence, using any coefficient without more investigation can result in taking the wrong decision in water resources planning and management.

Transmission loss is a very important hydrological phenomenon in arid areas, and can be very high. These losses are very important in groundwater recharge and should not be ignored in any surface or groundwater modelling. In such circumstances this phenomenon is not yet fully defined, and further investigation is necessary. It is also very important that this phenomenon is taken into account when selecting a suitable model for use in any arid areas.

Overall, it is clear that any hydrological study that ignores the special hydrological features of arid regions can easily obtain misleading or wrong results. Hydrological models should take into account these features, and models that were originally developed for humid areas should be reviewed and modified as necessary.

Chapter 3

Rainfall and Rainfall-Runoff Modelling

3.1 Introduction

The development of rainfall-runoff models can be regarded as a revolution in the hydrology and water resources field.

Watershed models are important in water resources assessment, development and management (Singh et al., 2002), and flood studies. Some models can generate a long representative time series of streamflow volumes from which water supply schemes can be designed. They can be used to analyse the quantity and quality of streamflow, reservoir system operations, groundwater development and protection, surface water and groundwater conjunctive use management, water distribution systems, water use, and a range of water resources management activities (Wurbs, 1998). Watershed models are also used to quantify the impacts of watershed management strategies, linking activities within the watershed to water quantity and quality for environmental and water resources protection (Singh et al., 2002) and flood design. Beven (2001) stated there is a limited range of measurement techniques and a limited range of measurements available in space and time, therefore there is a need to extrapolate from the available measurements to assess the likely impact of future hydrological change. These models can differ in type and complexity but are routinely used for water management in humid areas.

This chapter discusses modelling aims, techniques, and the different type of rainfall-runoff models, and highlights some of the limitations of different model types.

On the other hand, a thorough knowledge of rainfall is a very important input to rainfall-runoff models. The importance of such knowledge has been widely recognised. Selecting the most suitable method for determining the average rainfall of the study area is very important to obtain better results and to ensure that the selected rainfall-runoff model performs reliably. Hence, this chapter also discusses the different techniques that are used in estimating the rainfall inputs. Specific applications for arid areas are discussed in **Chapter 4**.

3.2 Aim of Modelling

Watershed models, generally, are used to understand dynamic interactions between climate and land-surface hydrology (Singh et al., 2002).

Modelling rainfall-runoff in arid areas can be considered as a key component of studies of the dynamical aspects of arid-zone hydrological processes (Ye et al., 1997).

There are many different reasons for modelling, depending on the problem that needs to be investigated. However, the different aims of modelling can be summarised, based on Singh et al. (2002) and Beven (2001), in the following points:

- To predict or extrapolate from known measurements in both space and time, particularly to ungauged catchments where measurements are not available.
- To improve and understand the existing hydrological system and determine the effects of hydrological management decisions and their possible impacts on the future. For example, models can be used for varied purposes, such as planning and designing soil conservation practices, irrigation water management, wetland restoration, stream restoration, and water-table management, at field scale. At large scale, models can be used for flood protection projects, rehabilitation of aging dams, flood plain management, water-quality evaluation, and water-supply forecasting.
- To assess the impact of change in climate and water resources.
- For research reasons, models can be used for demonstrating a theory, improving understanding of the hydrological process, and development of new areas of science.

Modelling has become a very important tool and the development of new models or improvements of old models to cover new aspects should be expected due to the increase in computer capability together with additional data and hydrological knowledge. Singh et al. (2002) suggest that the models, in future, will play an increasing role in water resources planning, development, and management.

3.3 Types of Rainfall-Runoff Model

Rainfall-runoff modelling started in 1930s with the introduction of unit hydrographs. In the 1960s continuous, conceptual models were introduced, but with the increased power of computers, physically-based models were introduced in the 1970s. Currently, many different models are in use and the number is on the increase as the science is developing and computer power is advancing. Models can be classified based on; the process description, scale, and technique of solutions (Singh, 1995). They can also be classified based on land-use (agricultural, urban, forest and range land) or model-use

(planning models, management models, prediction models) (Singh, 1995). However, discussing the details of the latter is beyond the aim of this literature review and only the main classifications of the models are discussed below.

3.3.1 Process Based Classification

Singh (1995) explained that models can be classified based on the description of the hydrological processes that contribute to the watershed output. Based on these criteria, the model can be classified as shown below:

3.3.1.1 Lumped models: In lumped models, the hydrological processes are described for the entire watershed without any subdivisions, using differential equations or empirical algebraic equations. As these types of models are generally expressed by ordinary differential equations, spatial variability of process, input, boundary conditions and watershed geometric characteristics are not taken into account (Singh, 1995).

3.3.1.2 Distributed models: In distributed models, the spatial variability of processes, input, boundary conditions, and/or watershed characteristics are taken into account (Singh, 1995). However, it should be noted that even though the rainfall-runoff process is distributed, there are some other variables and processes that might be used which are not, such as some input variables and boundary conditions.

Singh (1995) explained that the models can be classified based on the process also as:

3.3.1.3 Deterministic: in which the results are determined through known relationships between the states and events, and in which a given input will always produce the same output, if all the components are deterministic.

3.3.1.4 Stochastic: in which the results are determined by using one or more random variables to represent uncertainty about a process, or in which a given input will produce an output according to some statistical distribution, if any of the components are stochastic.

3.3.1.5 Mixed: if the model components are described by a mix of deterministic and stochastic components.

3.3.2 Time-Scale Based Classification

Singh (1995) explained that the time scale may be defined by the time intervals that used for input and internal computations, or by those used for output and calibration of

the model, for example, models can be classified based on the interval as sub-daily, daily, monthly, or yearly. Models can also be classified as event-based models (one event is simulated, or continuous (a series of events plus intervening periods are simulated continuously).

3.3.3 Space-Scale Based Classification

This type of classification depends on the spatial scale of the watershed. Many hydrologists use the catchment size as a base for this classification in which the catchments can be classified as; small (area up to 100 km^2), medium (100-1000 km^2), and large (>1000 km^2). This can seem very arbitrary, so Singh (1995) suggests not classifying the watersheds based on the area but rather based on the homogeneity of the watershed characteristics. Singh points out it will be difficult to find a watershed that is homogeneous in all its characteristics which means all watersheds would be either medium or large based on this criterion. However, it should be noted that in reality, the small size watersheds commonly show great heterogeneity, and hence such classification does not seem to be very applicable.

3.3.4 Model Structure Based Classification

Wheater et al. (1993) has classified the models into three types, based on the model structure and its description of hydrological processes. These three types of the models are described below:

3.3.4.1 Metric Models

These types of models are based on observations and try to understand the system's characteristic response from those data. The metric approaches include the unit hydrograph theory for catchment-scale simulation that was developed by Sherman (1932). The model synthesises streamflow responses to rainfall by a loss function and a linear model, satisfying the basic requirements of hydrological modelling. Wheater et al. (1993) believe that the major strength of the method is in analysis. However, the unit hydrograph is only one (simple) example of the metric type of model. A more general set of time series analysis models can also be used.

Wheater (2002b) believes that a simple model such as a metric model can be enough if the aim is to estimate the runoff events from the available rainfall data and climatic inputs at a catchment-scale. It should be noted that this type of model does not consider land use change directly as it considers only the range of observed data (Wheater,

2002b), hence, other type of models can be introduced if this is among the modelling aims.

3.3.4.2 Conceptual Models

This type of model is normally more complex than metric models. A conceptual model represents all of the component hydrological processes perceived to be of importance in catchment-scale input-output relationships (Wheater et al., 1993).

This type of model is believed to have been started when the Stanford Watershed Model was developed by Crawford and Linsley (1966). Many conceptual models have been developed since, and even though these models vary considerably in complexity they are always based on a representation of internal storages which is generally associated 'explicitly' with particular hydrological components (Wheater et al., 1993).

The essential features of all of these models are that the model structure is specified a priori, according to the perception of the important component processes.

Conceptual models, as known, do not have directly measurable parameters and generate continuous flow sequences using usually simple hydrological relationships (Wheater, 2002b). Hence, this type of model overcomes the event-based models' problems, which depends on unit hydrographs, as metric models. It should be noted that many metric models are based on events, but some can be used for continuous simulations. However, this type of model needs to be calibrated to establish reasonable parameter values, and hence problems in determining a unique local objective value can occur in some cases due to 'equifinality' (a problem resulting from over parameterisation of model), data limitations and models structure faults which can affect its performance (Wheater, 2002b).

Wheater et al. (1995) stated that 'the model complexity very often exceeds the information content of the available data, the ill-conditioning, or identifiability problem'. They recommended that model complexity should be reduced by an appropriate degree; this could be achieved by use of identification statistics or sensitivity analysis and by holding insensitive parameters constant or formally re-structuring the model, but this approach can move the model towards the metric approach.

3.3.4.3 Physics-Based Models

This type of model represents the component processes within hydrological models in a more classical mathematical-physics form, based on continuum mechanics, through

numerical solution of the relevant equations of motion using a finite difference or finite element spatial discretisation (Wheater et al., 1993). The first model was developed by Freeze (1972), in which finite difference methods were used to solve Richards equation for unsaturated flow in two dimensions to represent hillslope processes. The St-Venant equations of gradually varied unsteady flow were used to represent the streamflow. Similar mathematical formulations were used in models such as the Institute of Hydrology Distributed Model (IHDM) and the Systems Hydrologique Europeen (SHE) model, but with more complete micrometeorological process representation (Wheater et al., 1993).

Even though models of this type are a powerful compilation of the relevant idealised processes, they do have some problems. Wheater et al. (1993) believe that the major problems are in the representation of subsurface processes, such as representing natural soils in the numerical solution scheme of these models as homogeneous elements which is not true as the soil types in reality are generally structured and heterogeneous. The second problem Wheater et al. (1993) highlighted in their study concerns 'observability' as the parameters of physics-based models are measurable in design, but in practice this cannot be achieved at the required scale for model discretisation. These measurements are made at a point and, for most parameters extensive field investigation is considered impractical and can be very expensive (Wheater et al., 1993). Hence, practically, for any specific catchment there will be a large number of unknown parameters that need to be estimated, which affects the uncertainties in the model parameters and performance. The other problem that Wheater et al. (1993) discussed is that the parameters cannot be uniquely identified in calibration using the observed input-output data as the degrees of freedom are so large.

3.4 Model Calibration

Model calibration is an important process and stage in the modelling procedure. It has a great effect on how successful the application of the hydrological model is. Model calibration, for conceptual hydrologic models, was described by Sorooshian and Gupta (1995) as the process of selecting suitable values of model parameters such that the behaviour of the watershed can be simulated closely.

There are two types of model parameters in some models; physical parameters and process parameters (Sorooshian & Gupta, 1995). The physical parameters are those parameters that represent the physical properties of the watershed such as the watershed areas, surface slopes, etc. These parameters are usually measurable. However, there are

some other parameters that are related to soil characteristics and related to the infiltration process such as the hydraulic conductivity and porosity, which are measurable in theory but difficult to measure in practice. The process parameters are the immeasurable parameters that represent watershed characteristics such as average depth of soil moisture storage, coefficient of nonlinearity controlling rate, etc. (Sorooshian & Gupta, 1995).

The calibration process consists of two steps:

- ***The parameter specification***: This is done when the model is selected, where the physical parameters to be used in the model should be specified if the measured values are available. Hence, it can be used with more confident, and calibration might not be needed in such cases (Sorooshian & Gupta, 1995).

- ***The process parameter estimation***: In this type, a range of values is assumed and the optimum value can be determined through the calibration procedure (Sorooshian & Gupta, 1995).

3.4.1 Types of Calibration

There are two ways to carry out the model calibration as described below:

3.4.1.1 Manual calibration

In manual calibration, the adjustment of the parameter values is carried out by the user through a trial and error process. Sorooshian and Gupta (1995) and Wheater (2005) showed that manual calibration has some weaknesses as it is difficult to determine the best fit or to determine a clear point that defines when the calibration is completed. This is usually left to each modeller, hence it is subjective as different results can be obtained by different modellers. As the modeller will tend to consider various aspects of model fit during the manual calibration process, it may be considered to be multi-objective calibration; however, subjectivity ad lack of consistency between modellers in their fit.

Recent work has brought some of the benefits of manual calibration into the area of automatic calibrations. Multiple objective functions are now being used within automatic calibration criteria is an issue to extract more information from available data as Wheater (2005) stated.

3.4.1.2 Automatic Calibration

In this method, the calibration is carried out with the aid of computers to speed up the procedure. The use of the computer helps to overcome the problem of availability of

model calibration experts and also to overcome the subjectivity which is a problem in manual calibration (Sorooshian & Gupta, 1995).

However, it should be noted that there is no fully automatic calibration procedure yet and some manual decisions are still needed, for example specifying the range of the parameter values and the objective function (Sorooshian & Gupta, 1995).

Sorooshian and Gupta (1995) showed that there are five main elements in automatic calibration:

- ***Objective Function***: It was defined by Sorooshian and Gupta as 'an equation that is used to compute a numerical measure of the difference between the model-simulated output and the observed watershed output'. There are many different equations that can be used for an objective function. The most common objective functions used are that based on the Least Squares Methods and Maximum Likelihood Methods.

- ***Optimisation Algorithms***: Sorooshian and Gupta (1995) have defined the optimisation algorithms as 'a logical procedure that is used to search the response surface which is described by the objective function in the parameter space, constrained to the allowable ranges on the parameters, for the parameter values that optimise the numerical value of the objective function'.

There are many different methods for optimisation using computer aids. However, the optimisation methods or strategies can be classified as 'local search' methods and 'global search' methods.

- ***Local search method*** consists of three main steps; selecting the direction to move in parameter space, deciding on the moving distance, and deciding on the termination time when no further improvement can be achieved (Sorooshian & Gupta, 1995). As the termination point depends on the point of start, it is difficult to know if the global minimum function has been achieved (Sorooshain & Gupta, 1995).

- ***Global search method*** can be classified into three categories; deterministic, stochastic or a combination of the two (deterministic and stochastic). Deterministic strategies require that certain criteria related to the continuity of the function and its derivatives should be satisfied to obtain the global solution, which is difficult to obtain. However, stochastic and combination methods seem to be more commonly used in the hydrologic models currently as mentioned by Sorooshian and Gupta, (1995). It should be noted that, even with using automatic calibration, it is difficult to obtain a single set

of optimal parameters and there could be other sets that can be considered as good as the selected one (Beven, 2001).

The uniform random search, URS, the simplest stochastic global method and is very commonly used. In this method, the modeller searches for the optimum parameter values through a uniform random sampling of the parameter space within the range of possible values for each parameter. The modeller must choose these ranges, and the number of random samples taken. This method was adopted in the Wadi Ahin study.

- ***Termination Criteria***: there are different criteria that are used to determine the termination point when the optimum solution has been obtained. These criteria include: function convergence and parameter convergence. In function convergence the optimisation should be terminated if the algorithm is no longer able to improve the function value, whereas in parameter convergence, it is terminated when the algorithm is unable to change the parameter values and improve the function value significantly. Furthermore, the optimisation could be also terminated if the computer time is limited (Sorooshian & Gupta, 1995).

3.4.2 Verification

Verification is used to test the performance of the model calibration by using a set of input-output data that is not used in the calibration process (Sorooshian & Gupta, 1995). The verification procedure helps to detect any biases that might be caused by the estimated values of the used parameters during the calibration procedure. If the model cannot obtain a good fit to the validation data then the entire calibration procedure and any assumptions that were made during the model selection and calibration might need to be reviewed.

3.4.3 Sensitivity Analysis

Sensitivity analysis can be described as the procedure to determine the sensitive and insensitive parameters (Sorooshian & Gupta, 1995). It is useful to know which parameters can affect the model performance and its results. There are two types of sensitivity analysis as described by Beven (2001); the local sensitivity analysis, where the best estimate of the parameter set or an identified optimum parameter set are identified or evaluated in the immediate region, and the global sensitivity analysis which is believed to give better estimates of the parameters within the model structure. There are many known global sensitivity analysis methods such as: generalized

sensitivity analysis (GSA), regionalized sensitivity analysis (RSA), the Horyberger-Spear-Young (HSY) method, or the GLUE method (Beven, 2001).

In this research: local and global sensitivity analysis both were carried out, where in the local sensitivity analysis the sensitive parameters were determined manually by fixing all the parameters except the tested one to check its effects on the model performance and obtained results, whereas in the global sensitivity analysis all the sensitive parameters were varied simultaneously using URS method to identify the near optimum parameters values (see **Section 3.6.2**).

3.5 Reliability Estimation

Reliability estimation is very important in hydrological modelling, especially when the model is used outside the range of conditions in which the model was successfully calibrated and verified (Melching, 1995). In such a situation it is very important that the hydrologists are sure that the model is reliable. Reliability can also be used to determine the dominant sources of uncertainty that affect the reliability of model output. Reliability analysis can also be used as a guide for data collection to aid in enhancing the model reliability and utility with a suitable data-collection cost (Melching, 1995). Melching et al. (1991) (taken from Melching, 1995) believed that the reliability estimates are also very important to assess model verification and to select the appropriate model. Beven (1989) believed that finding a realistic way for predicting uncertainty is very important.

3.5.1 Types of Uncertainty

Beck (1987) found that uncertainty was affected by model structure, model parameters, and uncertainty that is related to estimates of the future behaviour, and suggested reducing modelling uncertainty by using properly designed experiments and monitoring programs.

Melching (1995) and Beven (2001) mentioned some types of uncertainty as mentioned below;

3.5.1.1 Natural Uncertainties: This describes the uncertainty arising from natural random effects which include the random temporal and spatial fluctuations that always affect the physical process of runoff generation, such as rainfall. The amount of uncertainty depends on quality and type of the data used to describe the random effects.

3.5.1.2 Data Uncertainty: The uncertainty in any of the data that is used to run the hydrological model which includes; precipitation, streamflow, evapotranspiration, and watershed morphology can affect the uncertainty of the model. The errors in the boundary conditions are among the errors that can affect the obtained results too.

3.5.1.3 Model–Parameter Uncertainty: The uncertainty in model parameter values can have great effects on modelling results. For calibrated models, the data uncertainty is reflected in model parameter uncertainty. The model calibration results can be used to estimate the values of the standard deviation as well as the distribution of the basic variables for the representative storms that were selected by the modeller. However, there are many difficulties in obtaining unique and 'conceptually' realistic parameter values by model calibration as was discussed by Sorooshian and Gupta (1995).

3.5.1.4 Model-Structure Uncertainty: Melching (1995) and Beven (2001) believed that the uncertainty of model-structure has great effects on the representation of the physical runoff process. The approximate nature of the model has significant effects on runoff features such as the peak, the time to the peak, the runoff volumes, etc. These effects can affect results in different ways and degrees as explained by Melching (1995).

3.5.2 Reliability Analysis Methods

Melching (1995) believes that for all uncertainty sources that might affect the reliability of the used model, the joint probability distribution should be obtained. However, this can be a difficult task, generally, and possible only for linear models with identically distributed parameters. Therefore, Melching suggests the combination of uncertainties in the basic variables of the watershed model into measures of overall model-output reliability should be carried out in approximate way. There are many methods for analysis of uncertainties, of which the Monte Carlo simulation method is the most commonly used.

Monte Carlo Simulation (MCS) is used to assess the output reliability of many hydrological models. In this method probability distributions are proposed for the uncertain variables, and random values are generated according to their probability distribution, and the model is executed using each random sample (Melching, 1995). The statistics such as mean, standard deviation, skewness, etc, and the empirical probability distribution of the model output can be determined by repeating the random

generation of variable values and model execution steps many times. In order to improve the sampling accuracy, stratified sampling methods such as Latin Hypercube Sampling (LHS) (Melching, 1995) can be used. The selected distributions of the samples should reflect the feasible parameter values for that particular tested case, as explained by Beven (2001). The URS method introduced previously is a simple method of MCS where the parameters are assumed to be uniformly distributed.

As well as the MCS, methods of reliability analysis includes the Mean Value First-Order Second-Moment Method, and the advanced First-order second-moment method, Rosenblueth's Point Estimation method, and Harr's Point-Estimation method as mentioned by Melching (1995). However, those are, generally not suitable for non-linear rainfall-runoff models, and MCS is the preferable method.

It should be noted that the parameters' sensitivity and their closeness to the optimum values can be identified when using the Monte Carlo sampling method by using dotty plots. The dotty plots as defined by Beven (2001) are the scatter values that represent the parameter value against the selected objective function value, where each dot represents one model run and their numbers is equal to the Monte Carlo sampling number. Hence, the dotty plots can be used to identity the parameters near optimum values. Furthermore, the dotty plots can also aid in identifying the behavioural and the non behavioural samples, where the obtained values are not close to the near optimum value. However, the same behaviours can be obtained from different models (Beven, 2001). Hence, it should be noted that the good or bad results from using any model should not depend on a behaviour of any individual parameter but the whole selected set of parameters due to the interactions between them (Beven, 2001).

3.6 Current Practice

There are many different types of models that are used in different countries. The selected type of model depends on the hydrological characteristics of that country or area, the aim of the modelling, the amount of complexity that can be accepted and the availability of data. There were also several investigations carried out recently to evaluate and discuss the different available models; their reliability, limitations and future directions (Singh et al., 2002). The current practice shows that the currently used models have many different limitations that need to be investigated and improved. The problems, which are not yet sorted out entirely, include a shortage of data.

Having more than one set of parameter values (as can be the case when manual calibration is carried out) following calibration, makes it difficult to know which is the

best set to apply when making prediction or relating parameter values to the catchment characteristics. The current computer power makes it easier to determine a unique best fit parameter and also makes it easier to analyse the model uncertainty, for example using a generalized sensitivity analysis and the GLUE method (Beven, 2001). This can be considered as one of the most important developments in hydrological practice (Wheater, 2002b). However, the generalized likelihood uncertainty estimation (GLUE) can be affected by data errors and model structure uncertainty (Wheater, 2002b).

Wheater believes that stochastic tools that been developed recently, have allowed more detailed analysis of model structure and parameter uncertainty. This was found useful in extracting maximum information from the available data through parameter-efficient models, allowing formal determination of model parameter uncertainty, and providing the capability to produce confidence limits (Wheater, 2002b). However, further investigation seems to be required as each model or method has its own limitations that need to be overcome or improved.

Wheater (2002b) discussed the limitations of different types of models. In his study, he showed that the conceptual models can be used to simulate the hydrologic response based on available calibration data but regarding simulating the effect of land use change, the physically-based models may be more suitable because they use parameters that are more closely related to actual physical properties. These models can be used in modelling ungauged catchments and can in theory determine the effects of any catchment change. In practice, there are some problems these types of models can face which include the fact that the laboratory-based processes of small scale nature may not represent the actual watershed response and the soil characteristics (Grayson et al., 1992; Wheater, 2002b). In particular, macropore flow in some physically-based models is neglected due to lack of relevant theory and the appropriate data. Hence, Wheater (2002b) suggests fundamental research to investigate the appropriate process representation and parameterisation at a given scale.

Grayson et al. (1992a, b) believe that the measured parameter values used in physically based models do not present the real catchment response, hence these parameters lose their physical significance and there is a danger in misuse or misinterpretation of the resulting values. It is dangerous to use this type of model for a different purpose from what it was developed for or in different conditions from where these models have been tested (Grayson et al., 1992a, b, Wheater, 2002b).

More complex models with a large number of parameters have been developed recently (Perrin et al., 2001) even though experience does not show that these models always give the best results, compared to the simple models with less parameters (Perrin et al., 2001; Michaud & Sorooshian, 1994; Chiew & MacMahon, 1994).

New techniques have been applied in modelling, recently, such as Geographical Information System (GIS), remotely sensed data and environmental tracers, which have contributed important advances in watershed modelling (Singh et al., 2002).

Singh et al. (2002) discussed some of the models commonly used in different countries. It was shown that, in USA, HEC-HMS is considered the standard model in the private sector for the drainage systems design and quantifying the effect of the land-use change on flooding, whereas the NWS (National Water System) model is the standard model used for flood forecasting. The standard model that is adopted by the Environmental Protection Agency is HSPF, whereas the standard model adopted for water resources planning and management works by USGS is the MMS Model. UBC and WATFLOOD models are the currently adopted models in Canada, for hydrologic simulation whereas, in Australia, the adopted models are the RORB and WBN for flood forecasting, drainage design, and evaluating the effect of land use change. TOPMODEL and SHE are the commonly used models in many European countries for hydrologic analysis though in Scandinavian countries, the HBV model is more common for flow forecasting whereas in Italy the ARNO, LCS, and TOPKAPI models are the more common models. On the other hand, the Tank model is more common in Japan whereas, the Xinanjiang model is the most common in China.

Arid areas recently have begun to receive some more attention from both hydrologists and governments. Scarcity of the water resources made it essential to study the available resources. Currently, better understanding is being gained from experimental watersheds in America such as Walnut Gulch in Arizona and Alamogordo Creek in New Mexico. There are also some other studies carried out in the arid part of Australia (the eastern part). Many studies were carried out recently in the Middle East, such as Saudi Arabia, Egypt, Jordan, Oman, Yemen and others. The rapid development in these countries and the importance of water management has led to attempts to better understand the water resources. Moreover, there is a programme on wadi hydrology run by UNESCO in which more detailed studies and data from different arid countries in the Middle East are being analysed for better understanding of their hydrology. This programme beside the other scattered ones in different parts of the arid zones provide

hope that a better understanding will be reached and that analysis tools will be developed that take into account the particular hydrological features of arid and semiarid areas.

The literature review that follows in **Chapter 4** shows that many models have been tested recently under the arid conditions to check their performance. GIUH (a metric type model), IHACRES (a conceptual type model), and KINEROS (a physically based model) were among those which showed promising results. In general, very few models have been developed particularly for arid areas. Hence, no doubt more work will need to be carried out to investigate the validity of these models by testing them in many different arid areas. As most of the current used models in arid areas were originally developed for humid areas use, they might not always consider the special hydrological features of arid areas. The main problem the hydrologists are facing when modelling arid zones is the shortage of the appropriate, good quality data. The network coverage, in addition, can be also an obstacle to obtain reliable results.

3.7 Overview on Rainfall Representation

A rainfall-runoff model requires a reasonably accurate measure of catchment rainfall input to determine the output at the point of interest with acceptable precision (FAO, 1981). However, watershed models are not yet very efficient and when they produce poor results, it is difficult for the modellers to know which to blame; the poor estimate of rainfall or the model structure (Andreassian et al., 2001).

Most of the techniques that are used in rainfall modelling were developed originally for humid areas. It seems difficult to judge the applicability of these techniques to arid areas due to the quality of the data and the short period of records, besides the limited understanding of all the hydrological features.

The subsection below discusses the main methods of estimating the average rainfall.

3.7.1 Methods of Estimating Average Rainfall

The determination of the average rainfall in any hydrological analysis and modelling is very important. Toth et al. (2000) showed that rainfall estimation is a very difficult task and that uncertainties affect the performances of both stochastic and deterministic rainfall models. The method used for estimating the spatial average rainfall is important, as each method has its advantages and disadvantages, and can work better in certain circumstances than other methods. Available methods are discussed briefly below:

3.7.1.1 Arithmetic mean

The arithmetic mean is the most common and simplest methods for determining the spatial average rainfall.

In this method, all the rainfall values for the selected period and duration are summed for all the selected rainfall gauges and then divided by the number of the gauges. As can be easily seen, there is no consideration for the effects of the spatial distribution of rain gauges or the effect of the topography. This method can be useful for preliminary studies, to get a general feeling of the average rainfall over the studied area (Mosapha, 2001). This method can be reliable in the case of even distribution of the rainfall gauges and where there are no topographic effects plain areas. This method can be more reliable when the rainfall is more spatially uniform; as uniformity often increases with the time-scale, then this method is more likely to be suitable for monthly or annual estimates (Mosapha, 2001). However, for rainfall fields that are significantly non-uniform, e.g. at small time-scales, or where topography affects the climate, it is believed that good coverage of rainfall gauges is necessary to obtain reliable rainfall estimate.

3.7.1.2 Isohyetal method

This is a frequently used method of estimating spatial average rainfall. In this method contour lines are drawn to connect the points with equal precipitation. These points must be judged from the available gauged values. The average rainfalls between each of these contour lines are estimated and multiplied by the areas between the contours and then summed for the overall average rainfall over the catchment. This method gives a good idea of storm morphology and a map of the rainfall pattern can be produced reasonably accurately (Bedient & Huber, 1988).

It should be noted that this method takes account of the areal distribution of rainfall and the orographic effects, and it is a more suitable method for areas with variation in topographical terrain.

An improvement to the method was suggested by considering the length of the isohyets in the computation of the average rainfall between the contours but it is time and labour-consuming (Shaw & Lynn, 1972). However, the isohyetal method needs good rainfall network coverage, otherwise it will be very difficult to draw suitable and accurate contours.

3.7.1.3 Thiessen method

This is another reliable method, if a good rainfall network is available. In this method all rainfall stations in the catchment are connected by lines. These lines then are

bisected by perpendicular lines forming polygons around each gauge. The relative contribution of each gauge to the catchment rainfall is the ratio of the area of the polygon of that gauge to the total area of the catchment. This method is used widely in hydrological studies and believed to be a reasonably accurate method though it does not consider orographic effects. There is no need to redraw polygons for each storm, as in the isohyetal method, which makes it much easier to use. Once the polygons have been plotted, it can be used for the catchment so long as there are no changes in the rain gauge network for that catchment

3.7.1.4 Triangulation method

This method is close to the Thiessen method as it depends on connecting the rainfall gauges and does not consider the orographic effects. It also depends on connecting the rainfall gauges by straight lines to form network of triangles. The triangles that are constructed should be as close to equilateral as possible (Mosapha, 2001). The areas of the constructed triangle are used as weighting factors that are multiplied by the arithmetic means of the rainfall values from the three rain gauges located at the vertices of each triangle.

3.7.1.5 Inverse-distance weighted mean

To estimate rainfall at a point, the weighted average of the measured rainfall at the nearby gauges is used. The weights are proportional to the inverse of the distance of the gauge to that point (Mosapha, 2001). The distance may be raised to a power. In theory this can give a spatial distribution of rainfall which can be integrated to give a spatial average.

3.7.1.6 Recently developed methods

There are some other methods that have been recently used for determination of spatial rainfall characteristics such as Kriging, Multiquadric, Bi-Cubic spline methods, and others. These methods are more complicated than the above-mentioned ones. Brief descriptions of some of these methods are given below:

- ***Kriging method***: in this method the spatial correlation of the observations structure is predicted explicitly and modelled using a variogram. Hence, the unsampled locations are also predicted (Syed et al., 2003).
- ***Multiquadric method:*** this method depends on the minimum energy concept of mathematical physics. The rainfall surface is represented by summation of many individual quadric surfaces (Syed et al., 2003). The rainfall value at any unsampled rain

gauge, can be obtained by summing all the contributions from the quadratic surfaces centred at all other data points (Shaw & Lynn, 1972).

- ***Bi-Cubic Splines:*** this is another mathematical technique. It depends on interpolating smoothly between the different points (or gauges) considering the functional continuity and slope and curvature continuity throughout the interpolation (Shaw & Lynn, 1972). The spline fit is accomplished by connecting each pair of (*X,Y*) forms with the adjacent points by part of a third-order polynomial.

3.8 Conclusion

The chapter has discussed the aim of modelling, overviews the history of modelling, modelling techniques, and current practice. In general, the chapter summarise the different steps and the methods used and then highlights some of the problems the different type of models are facing and how to overcome these problems with some suggestions for future work to improve model performance.

Calibration of models is a very important process to select the appropriate parameter set. There is a danger of obtaining good fits for the wrong reasons, in which case the predictions can be misleading. Therefore, it is very important that the modeller has a good understanding of the calibration techniques and how to use them. Verification should always be carried out whenever possible to test the adopted assumptions and values. Sensitivity analysis is another procedure that should be carried out to detect the parameters which can affect the model results more than others, and reliability/uncertainty analysis, usually using MCS, should be used to determine effect of model parameter uncertainty on model type.

Rainfall is a very important input to rainfall-runoff models. Good understanding of rainfall will help better understanding of effects of the rainfall data quality and its characteristics and hence, better evaluation of the performance of the used model. It can aid in understanding the resulting runoff and the rainfall-runoff relationships.

The selection of the appropriate interpolation rainfall method for determining the average rainfall over the study area is very important as it can have great effects on the obtained results. There are many different interpolation methods as shown in this chapter and it is up to the modeller to select the suitable method to his study area based on it characteristics and the available data.

For the purpose of this research different methods are to be tested to prove its great effects on the output results as will be shown in the following chapters.

Chapter 4

Application of Rainfall and Rainfall-Runoff Modelling in Arid-Areas

4.1 Introduction

Modelling is a very important tool that enables hydrologists to make more comprehensive use of rainfall time series as mentioned previously in this report. Modelling rainfall-runoff in arid areas can be considered as a key component of studies of the dynamical aspects of arid-zone hydrological processes (Ye et al., 1997). Rainfall-runoff modelling aids the hydrologists to understand the hydrological process much better. Thus, rainfall-runoff modelling is an important science field which needs more investigation.

Very few models have been developed that are specifically for arid areas, and work needs to be carried out to investigate their validity. However, a number of watershed models have been tested recently to check their validity when applied in arid areas, with some modifications being made to consider the special hydrological characteristics of arid areas.

This chapter discusses the different rainfall and rainfall-runoff models that have been tested under arid conditions and the difficulties that were faced due to the special hydrological features of arid areas. Recommendations for the best models for further investigation are provided at the end of the chapter.

4.2 Overview of Rainfall Representation in Arid Areas

Rainfall characteristics in arid areas have been discussed in detail in **Chapter 2.** These characteristics have great effects on the runoff produced and it is very important they are well understood for a better understanding of the errors in modelled runoff. They are also very important when selecting a suitable model and understanding the modelling results.

Rainfall-runoff modelling requires a reasonably accurate measure of catchment rainfall input to determine the output at the point of interest with acceptable precision (FAO, 1981). The watershed models used for arid areas are not yet very efficient. Hence, it is difficult for the modellers to know, when they produce poor results which to blame; the

poor estimate of rainfall or the model structure (Andreassian et al., 2001), or the poor network coverage.

Pilgrim et al. (1988), Wheater et al. (1991a. b), and Al-Qurashi (1995) all highlighted the importance of rainfall data quality and its significant effect on the reliability of rainfall-runoff modelling.

However, among the studies that discuss the effects of the rainfall quality on rainfall-runoff modelling, not all agree on its importance e.g. the studies of Krajewski et al. (1991), Storm et al. (1988) and Chow (1978) attached less significance. Some of the most detailed studies that demonstrate this critically important issue are Singh and Woolhiser (1976), Wilson et al. (1979), Hamlin (1983), Dawdy and Bergman (1969). There is no attempt made here to discuss all these studies in detail as they cover both arid and humid areas but only some to shed light on how important these effects can be. In addition, there are many studies that investigated the spatial and temporal variation of rainfall in arid areas using point rainfall measurements and its implications for rainfall and rainfall-runoff modelling and representation, where some of these studies will be discussed below.

The Section below reviews some rainfall applications and discusses the different rainfall aspects that need to be considered when rainfall-runoff modelling is carried out, the different rainfall measuring techniques that are used, and their effects on the obtained results.

Michaud and Sorooshian (1994b) carried out a study that aimed to investigate the effects of rainfall-sampling errors on simulations of desert flash floods. The study was constructed using the Walnut Gulch catchment in the southwestern United States. Two sets of rainfall gauges were tested. The first is the sparse 'ALERT' type network (1 gauge / 20 km^2). For this type of data the authors explained that tipping bucket rain gauges were used in which a signal is given whenever the bucket is full and tips, so short interval records can be obtained (up to1-min). There were 8 gauges in this set. The second is the data from the next generation weather radar (NEXRAD) digital precipitation estimates which represent 4 × 4 km pixels together with 58 rainfall gauges. All precipitation data has 1-hour resolution.

The observed data were sampled in different ways and the obtained results then were used as input to the research version of the distributed rainfall-runoff model (KINEROS) that was developed by Goodrich (1990). Different tests were carried out on the observed rainfall; checking the effects of the areal and sparse rain gauge sampling

errors, checking accuracy of average rainfall over the basin, and the comparison of the simulated and observed peak flow values.

The study came forward with some interesting results. The rainfall average for the 4 × 4 km pixels resulted in underestimation of runoff, which was explained by the coarse coverage of this grid leading to small cells of high rainfall intensity being missed. In the ALERT type network (one gauge / 20 km^2) the errors were also high and the obtained values were only 58% of the observed peak on average. This was referred to the inadequate rain-gauge network. It was also found that the resulting runoff was reduced, compared to the observed flow, which can be referred to the high infiltration in arid and semi-arid areas, which might not been represented properly using the 1-hour time interval.

Another study in which rainfall data quality was discussed and the research version of KINEROS was used is Faures et al. (1995). The study aimed to test different rainfall measurement uncertainties and to gain a better understanding on how spatial rainfall variability impacts the performance of runoff models for small catchments, and assessment of the impact of wind on precipitation observations. In the course of this study, the effect of measurement and data processing errors, and the influence of inclination on runoff modelling were studied.

The authors selected the KINEROS model as it allows that surface runoff production results from precipitation excess above infiltration (Hortonian mechanisms). Therefore, the authors believed it to be suitable for use in Walnut Gulch where the watershed has a deep water table and the subsurface flow does not have any notable effects on runoff generation. The other important reason was that the model accounts for spatial and temporal variability of rainfall. The rainfall input used in the modelling was in the form of 'breakpoint rainfall data' (i. e. digitized chart records) from multiple raingauges, as described by the authors, with minimum time step of 1- minute.

The model was calibrated by adjusting soil saturated hydraulic conductivity (*Ks*) and the Manning's roughness coefficient (*n*), and it was verified using an independent sample of 20 events. The model performance was judged using the Nash-Sutcliffe (1970) efficiency for peak runoff rate (E_Q) and runoff volume (R_V). Two modifications were applied. The first was an adaptation of a method in which the effect of temporal rainfall intensity distribution on the overland flow model element can be computed. To gain this, a nearby recording gauge hyetograph was scaled with the value obtained from the averaging measurements from the nearby non-recording gauge to enable the model

to consider the information that is provided by the non-recording gauge. The second modification was made to compute the hydrologic rainfall from the vertical rainfall observations. The hydrologic rainfall, as defined by Faures et al. (1995) is 'the amount of water that actually reaches the ground' whereas the vertical is 'the meteorological' rainfall observation.

The authors explained that the recording gauges trace the accumulated rainfall depth as a function of time where the trace is digitized at breaks in slope. The rainfall intensities were obtained by subtracting the accumulated depth at different breakpoints and then dividing the result by the time increment, therefore the temporal variability of the rainfall hyetograph increases in relation to the frequency of the breakpoints. As the rainfall intensity is the main cause of the runoff generation in arid areas, the authors believed it is very important to study how the digitization of the rainfall variations can affect the prediction of the runoff.

The study showed that digitisation of recording rain gauge charts, which resulted in a variation coefficient of maximum rainfall intensity of 9 to 26%, does affect the estimated values of runoff in the rainfall-runoff modelling. The coefficients of variation for runoff volumes ranged in this study between 1.5 to 2.5%, whereas they ranged from 3.2 to 5.5% for peak runoff rate. The study showed that the effect of the wind and, hence the resulting rainfall inclination, is affected by the topography of the watershed. The study also illustrated that the percentage measurement errors can affect the smaller events more than the large events and so the relative variation of runoff volume of the small events is much higher than that for larger storms. The authors believed that the uncertainty in runoff volume estimation is affected highly by the number of input rain gauges, whereas the locations of the gauges, generally, effect the modelling of the storm hydrograph.

The authors suggested using non-recording gauges if only one recording gauge is available in the studied catchment so long as it is a small catchment. It should be borne in mind that assuming a uniform rainfall with dependence on only one single rain gauge can lead to large uncertainties in runoff estimation (Faures et al., 1995). The effects of spatial and temporal variation of rainfall and runoff is very high even for small catchments, hence caution in necessary in such cases (Wheater 1991a, b; Al-Qurashi, 1995). However, Faures et al. (1995) emphasised the importance of knowledge of the spatial rainfall variability on the same or smaller scale if distributed catchment modelling is to be used for small-scale watersheds.

Lopez (1996) carried out a very interesting study on the effect of the uncertainty in spatial distribution of rainfall on catchment modelling. The author investigated the effect of uncertainty on the prediction of runoff volume, peak runoff, and sediment yield.

Lopez used an event-based distributed model. The model considers the processes of interception, depression storage, infiltration-excess, overland flow, channel flow, and non-equilibrium sediment transport. The author did not mention the name of the model used but from the model description and the governing equations, it seems very similar to KINEROS model (if it is not KINEROS).

The study involved using the Walnut Gulch watershed. Walnut Gulch has a very dense rain gauge network, hence the author found it easy to obtain the required rainfall data. 10 weighing-type recording gauges either within or adjacent to the study area were used to measure three storm events of different size. Lopez (1996) studied the effects of rain gauge network density on the obtained simulations, effect of spatial arrangement of rain gauges, effect of rainfall spatial variability, and effect of network density on computed areal rainfall.

It was found that the network density has a great effect on the modelled runoff volume, peak runoff, and sediment yield. Reducing the rain gauge numbers can result in a high percentage error, but the percentage of errors obtained are different depending on the different number of gauges used (e.g. using five gauges results in a different error from that using six or nine and so on) due to the spatial and temporal variation of rainfall. Lopez also illustrated how the location of each gauge is important due to its weighting areas. He explained that the spatial arrangement of each gauge (location of the gauge) can affect the obtained results, which depend on the location of rain gauge that is used and will vary from one storm to another due to the differences in storm distribution. The study also shows that the point rainfall measurements may not be able to describe sufficiently the spatial and temporal distribution of the rainfall unless the rain gauge density is high. However, the percentage error varies from one event to another depending on the amount of spatial variation of rainfall at each event. On the other hand, the study shows that using Thiessen polygons was successful in estimating the average rainfall at the watershed scale but was not able to estimate the spatial variation of the rainfall at the scale of the model's 'computational elements'.

Andreassian et al. (2001) carried out a study where the impact of imperfect rainfall knowledge on the efficiency and the parameters of watershed models were investigated.

This study, though not directly relevant to arid areas, shows how a model can be sensitive to the rainfall data quality. The chosen sites were all French watersheds but with different climate regimes, one of which was Mediterranean.

Three continuous daily watershed models, GR3L, and modified versions of IHACRES (IHAC) and TOPMODEL (TOPMO), were used by Andreassian et al. (2001) to study the effect on model efficiency and parameter behaviour associated with improvements in rain gauge network characteristics. To study the relationship between the quality of the areal rainfall and the capacity of the models to simulate daily flows for the selected watersheds, a large number of subsets of the total rain gauge network were randomly generated. Sensitivity analysis showed that a good result was obtained for one of the watersheds with only one rain gauge. This can be true only where uniform rainfall dominates. The sensitivity analysis showed that improved rainfall estimates generally improved model results. On the other hand, models respond differently when calibrated using different sets of rainfall data but the three models showed a significant ability to cope with imperfect rainfall estimates. The criteria that were used to check the efficiency of the models were based on Gore index and the streamflow-based Nash and Sutcliff efficiency criterion. The Gore index can be obtained by the following formula;

$$GORE = 1 - \frac{\sum_{i=1}^{N}(\sqrt{R_i^E} - \sqrt{R_i})^2}{\sum_{i=1}^{N}(\sqrt{R_i} - \sqrt{\bar{R}})^2}$$

where N is the number of time steps (i) of the period, $\sqrt{R_i^E}$ is the estimated precipitation input, R_i is the rainfall at time step i, and $\sqrt{\bar{R}}$ is the mean of the reference precipitation input over the study period.

It was shown that GR3J, IHAC, and TOPMO were capable of reacting to improved accuracy in rainfall input both by increased performance and reduced variability of efficiency (Andreassian et al., 2001).

Wheater and Brown (1989) carried out a study on rainfall characteristics for southwest Saudi Arabia. Short-term data from a comprehensive hydrometric network (100 SIAP autographic rain gauges over five wadis with an average density of one gauge over 50 to 150 km^2). Hourly time series data were used. Intensity-duration-frequency analysis was carried out using a station-year approach, grouping gauges to form composite records.

The analysis showed a complex regional pattern of rainfall intensity characteristics. The authors found that the frequency of rainday occurrences, which were directly related to elevation, were the main difference between the point rainfall characteristics for a certain network.

Wheater et al. (1991a) carried out another study in Saudi Arabia. Hourly data from the same network of 100 autographic rain gauges from five wadis in southwest Saudi Arabia were used. The overall objectives of the rainfall modelling were to summarise the essential characteristics of the hourly rainfall in a stochastic formulation, which would provide the basis for generation of synthetic rainfall sequences as input to a distributed hydrological model. The hydrological model, calibrated with respect to the observed point rainfalls from the gauge network, was used to explore water resource management options as an aid to policy assessment. The model was developed to reproduce both the spatial distribution of rainfall event and the temporal (hourly) sequence. With respect to temporal scale, individual events were observed to occur on a timescale of hours or less, and representation of the rainfall variability at the hourly level was believed to be important. Extended simulations were required and thus the marked seasonality of response needed to be incorporated. Therefore, a 'multivariate approach' based on observed characteristics of the data was adopted.

The authors pointed out that other studies (see Wheater et al., 1991a) in arid areas have used different approaches but in the present study a clustered approach was proposed in which a set of index gauges was selected for each storm and used as the basis for the generation of a set of localised raincells.

The study faced a problem in defining the raincell due to the available network density which was too low and caused severe problems of model identification. A detailed analysis of the observed spatial and temporal rainfall properties was therefore carried out and from those results a simpler and more direct model was identified. A rainfall model was formulated as a two-stage process, firstly, the occurrence of a catchment rainday was simulated and secondly, the locations of the rainfall occurrence and the point temporal characteristics were generated (Wheater et al., 1991a).

The model successfully reproduced the observed seasonality of monthly occurrence and the distribution of rainday inter-arrival times. The frequency distributions of number of gauges effective during a rainday and the number of raindays at individual gauges were also reproduced. In addition, point rainfall characteristics such as the distribution of event durations, hourly depths and start times were also reproduced. However, a

difference of 7% between the simulated average annual rainfall and the observed mean for the same period was obtained. There was also systematic underestimation of the occurrence of multiple-gauge events for the high and low elevation groupings. The authors assumed that this was a reflection of the weak spatial dependence, which was not included in the model.

There is another study that Wheater et al. (1991b) carried out on gauges of a longer period of record in the same region (outside the previous study area) after some modifications to the stochastic model (Wheater et al., 1991a) guided by the 'discrepancy' between the long-term and short-term annual rainfall. The model was adjusted empirically to consider the long-term results. The calibration data were shown to have lower than average rainday occurrence. The model reproduced the basic spatial and temporal characteristics of hourly and daily rainfall, and mean annual rainfall. The consistent pattern of the regional variability was also identified. It should be noted that the model did face difficulties in estimating the extreme events which are rare in arid areas but of great importance. However, the authors stated that further work is required to address in detail issues of persistence and variability at the annual timescale.

In another study, Julien and Moglen (1990) have used a one dimensional, kinematic wave, finite element model to investigate the spatial variability effects on the overland flow hydrographs. The authors found that the effects of the temporal distribution of precipitation are higher than the spatial distribution effects. Ogden and Julien (1993) carried out a study to verify the finding of Julien and Moglen (1990) using two semi-arid watersheds, Macks Creek (southwestern Idaho) and Tylor Arroyo (southeastern Colorado). In addition Ogden and Julien (1993) wanted to quantify the effects the temporal variation of precipitation can have on the one dimensional overland flow method. The authors were keen also to study the runoff relative sensitivity Q_s caused by the influences of the spatial and temporal variation of rainfall as a function of rainfall duration, temporal resolution of rainfall data, and the runoff time to equilibrium. In addition to that, the authors also wanted to validate the temporal variability in the one-dimensional model using two-dimensional simulations. The relative sensitivity was defined in the study as 'the total volume of outflow variability over 50 Monte Carlo simulations normalized by the rainfall volume and the coefficient of variation of rainfall, R_{cv}' and can be obtained through the following formulas:

$$Q_s = V^* / R_{cv}$$

where V^* is called the dimensionless hydrograph envelope and is calculated using the following formula:

$$V^* = \Delta Q_v / R_v$$

where ΔQ_v is the runoff volume and can be determined as shown below:

$$\Delta Q_v = \sum_{\tau=0}^{\infty} (q_{\max} - q_{\min})_\tau \, w \Delta t$$

where $q_{\max}$ is the upper discharge and $q_{\min}$ is the lower discharge of the hydrograph envelope for the obtained results from the Monte Carlo simulations, and Δt is the temporal sampling interval.

R_v is the input rainfall volume and can be obtained using the following formula:

$$R_v = q_w q_{lo} \Delta t \sum_{\tau=0} R(\tau)$$

where q_w is the runoff plane width, q_{lo} is the overland flow plane horizontal projection, and R is incident rainfall intensity.

The variables that govern the one-dimensional overland flow as described by Ogden and Julien (1993) are the length of the horizontal projection of the overland flow plane (L_h), the flow depth (h), the average flow velocity ($\bar{u}$), the surface slope Slp_o, the excess rainfall rate in space and time $R(x,t)$, the discharge per unit width (q_w), the roughness coefficients of the plane (n), and the gravitational acceleration (g). The details of the channel routing equations are not discussed in this thesis and can be obtained directly from the study. However, it is useful to know that the selected model, CASC (Julien et al., 1988), is a one-dimensional model that ignores infiltration. The authors believed that it would be impossible to separate the effects of the temporal and spatial variability of the rainfall from those of the infiltration, hence the assumption was made that all the rainfall was considered as excess rainfall. The algorithm used in the study was as adopted in the Julien and Moglen study (1990), in which the simulation of time varying storms, and stationary storms with variable overland flow parameters were achievable.

On the other hand, CASC2D (Julien & Saghafian, 1991), the two-dimensional runoff simulation model, which is used in this study does consider the infiltration and uses the three-parameter Green and Ampt model (1911) for infiltration and the diffusive wave formulations for channel routing (see Ogden & Julien, 1993, for details). However, in Ogden & Julien (1993) study, the channel routing was neglected and all flow was

modelled as overland flow to avoid the substantial computational effort that would be needed for channel routing. A precipitation model of Rodriguez-Iturbe and Eagleson (1987) was used to generate two-dimensional rainfall fields. Monte Carlo methodology was used by applying 50 samples of spatially variable rainfall fields to each watershed.

However, Ogden and Julien (1993) found that the relative sensitivity to spatial variability of both overland flow geometries was tested according to the temporal resolution of the rainfall data and rainfall duration. It was found that the relative sensitivity increases with the rainfall duration and the temporal resolution in both simulations regardless of the size of the catchment. This confirms the results that were obtained by Julien and Moglen (1990) on their study on the two-dimensional overland flow. For one-dimensional overland flow, it was found that as the temporal sampling interval and rainfall duration increase, the effect of the temporally variable rainfall on the relative sensitivity increases. It was also found that the temporal resolution of rainfall data does affect the relative sensitivity in both one and two dimension simulations. The relative sensitivity increases with the increase of the square root of temporal resolution of the rainfall data. In contrast, the relative sensitivity decreases with the increase of rainfall duration.

There was an interesting study that was carried out on Wadi Ghulaygi in Sultanate of Oman (Wheater et al., 1997). The model was described later in this report in some detail and the model structure was shown in **Figure 4.8**. The model consists of two parts - a rainfall model and rainfall-runoff model. The rainfall model was the same model that was used in Saudi Arabia studies (Wheater et al., 1991, a, b). It was used to provide the daily rainfall input to the rainfall-runoff model. This model presented a very good link between all the hydrological components and showed how the runoff is linked to the rainfall and how both affect the groundwater recharge. However, such models also carry errors from one step to another, and any inappropriate assumption or hypothesis will affect the other linked models.

All the above discussed studies agree on the importance of the rainfall quality, rainfall errors, rainfall interpolation method, and the rainfall network coverage has great impact on the model results and need to be considered when rainfall or rainfall runoff modelling is carried out.

4.3 Effect of Aridity on Rainfall-Runoff Model Performance

The basin aridity is known to affect the performance of the used model. Mimikou (1992) has carried out a study to investigate the effect of the aridity on the performance of the models. Mimikou has tested two models to study the influence of basin aridity on the efficiency of runoff predicting models; a monthly ***water balance model*** (Mimikou et al., 1991) and the second is an autoregressive ***empirically fitted rainfall-runoff model of Kalman filter type*** (Mimikou, 1983). Some elements of the models were modified to enable the model to consider the amount of rainfall, rainfall trend if increasing or decreasing, and any existence of significant snow during the current or previous month. The ***water balance model*** is based on a conceptualization of the physical processes in the basin. **Figure 4.1** shows the flow chart of the model.

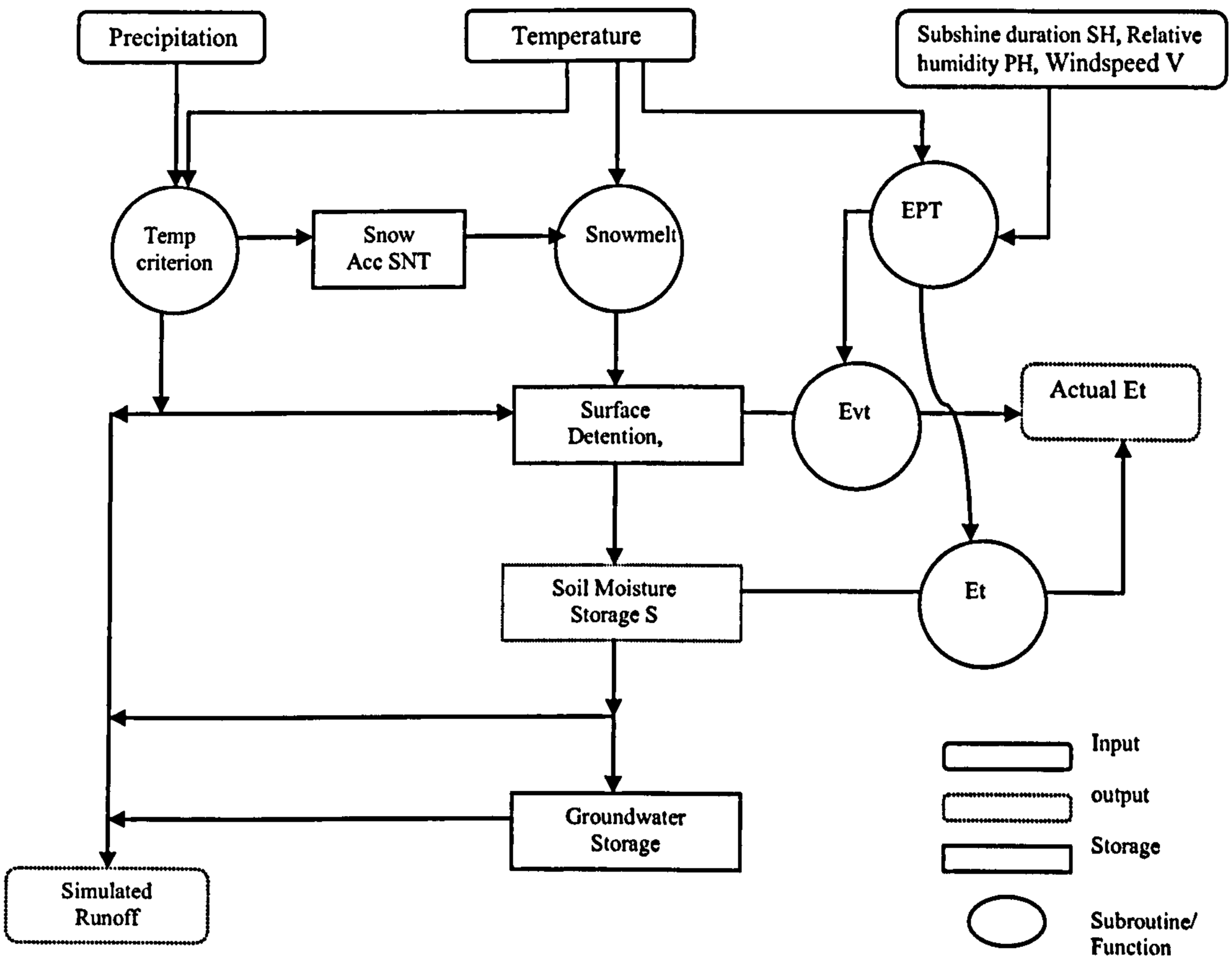


Figure 4.1: Flow-Chart of water-balance model structure (*after Mimikou et al., 1992*)

Empirically fitted rainfall-runoff model of Kalman filter type (blackbox type) relates the input to the output without any representation of the physical character of the rainfall-runoff process. The basic equation is:

$$\overline{q}_{y,m} = \overline{q}_m + a_i.Q_{y,m-1} + b_i.R_{y,m} \quad (\text{for } m = 1, Q_{y,m-1} = Q_{m-1,12})$$

where y and m stand for year and month respectively and $\overline{q}_{y,m}$ (m^3s^{-1}) is the estimated average monthly runoff; $\overline{q}_m$ (m^3s^{-1}) is the yearly average monthly runoff (averaging over the calibration period); $Q_{y,m}$ (m^3s^{-1}) is the stationarized monthly runoff; $R_{y,m}$ is the areal monthly precipitation expressed in units of discharge (m^3s^{-1}) , and a_i and b_i are coefficients given by Schwartz and Shaw (1975).

Monthly data were used for both models. The input data for the water balance model used in this study include; precipitation, hydrometreological data; temperature, sunshine duration, minimum relative humidity, and day time wind speed. The output includes estimates of surface runoff, soil moisture storage, and actual evapotranspiration. For the empirically fitted Kalman filter type model additional input data needed were areal precipitation and runoff time series with information about snow content of precipitation. The models were tested using data from five representative basins situated in mountainous central and northern Greece.

The results show that the aridity seems to have some influence on the model performance. Aridity was correlated with the performance of the models. The author has used the inverse property, basin humidity which is expressed by the index R/AET, where R is the yearly precipitation and AET is the yearly actual evapotranspiration which was computed from the long-term water balance equation

$$R = AET + Q$$

where, Q is the yearly basin runoff.

If $R/AET \geq 1$ then the basin is considered arid.

In the empirically fitted model, the efficiency, using the Nash and Sutcliffe (1970) equation, increased with the increase of aridity (as the autoregressive characteristics of the runoff series are more significant), whereas the efficiency increases with the increases of humidity in the water balance model. The author referred this to the recursive nature of the Kalman filter model type as it is based on the preservation of the runoff autoregression. The autocorrelation characteristics of the runoff series become more significant as the basin aridity increased. On the other hand, for the water-balance model, the added algorithms to the model structure to reconstruct the relation between the rainfall and the runoff process added some model uncertainty in case of arid conditions whereas the relation is simpler in the case of humid conditions leading to

better efficiency. However, the author believes that both models are equally good in case of moderate conditions.

4.4 Application of Different Rainfall-Runoff Model Types

Different model types have been tested in various parts of arid areas to study some of the hydrological aspects. Some of the studies which have been carried out in different parts of the USA, Australia, Saudi Arabia, Oman, etc. are discussed in this Section.

4.4.1 Examples and implication of using Metric Type Models for arid areas

The use of metric models started some time in 1930s, even though the model structures were different from those usually used now. These types of model are the simplest hydrological models as they require less information regarding the physical characteristics of the studied watershed (Holder, 1985). Although these models are metric, the parameters may have some physical interpretation. The unit hydrograph method (time-series rainfall-runoff models) or regression equations (non-time-series rainfall-runoff models) can be used.

In this section, different examples are given from different metric models. It should be noted that most of these models depend on the unit hydrograph method even though different names are used.

- ***Use of regression equations***

Osborn and Lane (1969) carried out a study on rainfall-runoff relationships for very small semi-arid watersheds. The study was carried out using some sub-catchments of Walnut Gulch, Southern Arizona in USA. The areas of the sub-catchments ranged from 2.3 km^2 to 44.5 km^2. The rainfall-runoff relationships were developed using three years of data.

A simple linear regression model was used to predict runoff volume, runoff duration, and hydrograph lag-time. The used regression model was developed originally by Schreiber and Kincaid (1967) to predict on-site runoff from short-duration convective storms using stepwise multiple linear regression equations. The Osborn and Lane (1969) study was carried out to investigate the effect of the other parameters that Schreiber and Kincaid did not investigate. Schreiber and Kincaid (1967) studied the effect of five independent variables; total storm rainfall, maximum 5-min intensity, antecedent soil moisture, basal area, and crown spread of vegetation, and the dependent variable was the runoff volume. Osborn and Lane, on the other hand, included some

additional parameters; maximum depth 5-, 10-, 20-, and 30-min intervals, and duration of total storm rainfall, and runoff-producing rainfall (rainfall that resulted in runoff) as the independent variables, whereas the dependent variables were runoff peak rate, total volume of runoff, rise time, lag time, and runoff duration.

The antecedent soil moisture was determined using Linsley et al. (1949) equations. However, as only the runoff-producing events were used in the analysis, the authors found that the runoff equations were dominated by the total precipitation term. The authors believed that if all the events above a certain threshold value were selected then the total precipitation might not be the most important factor and the shorter rainfall duration might be of greater significance.

The study showed that runoff volumes were most strongly correlated to total rainfall. Furthermore, it was found that the peak rate of runoff was most strongly correlated to the maximum 15-min rainfall depth, the flow duration was most strongly correlated to watershed length, and lag-time was most strongly correlated to watershed area.

The authors suggested that the linear regression models such as used in their study might not be able to predict the hydrograph's properties accurately for the extreme events therefore further investigation was required in the larger subcatchments in the Walnut Gulch catchment than what was tested in this study. The authors were also aware of using many high frequency events but an inadequate number of low-frequency events. Hence, a suggestion was made to separate the low frequency events using a different set of equations in the analysis. The authors also suggested developing different equations to be used for estimation of water yield as distinct to those to be used for flood estimates.

In another study on the Walnut Gulch watershed, Osborn and Renard (1969) explain how difficult it is to develop rainfall-runoff relationships from small watershed data, as the events can be so different from each other, and hence it is difficult to select a typical hydrograph for design purposes. The authors had carried out analysis of two major runoff events in which the analysis showed that the hydrographs of the storms were highly different due to different storm intensities. The durations of the events were also different with one storm having 60-min duration, and the other having only 30-min. This is not surprising as it is very common in arid areas to have great differences from one event to another and more investigation is required using long period of record, when available, to select a typical hydrograph that serves the purpose of the study.

In another study, Lane et al. (1971) developed a method for predicting the outflow hydrograph in which the volume and peak discharges of the outflow hydrographs were both predicted using the volume of the inflow hydrographs. This approach was thought to be useful to determine the transmission losses. A reach in the Walnut Gulch experimental watershed was selected for the study. The inflow and the outflow hydrographs were represented by a 3-parameter gamma distribution. The authors emphasized defining the hydrologic system in terms of its effects on the outflow hydrograph parameters; hence, a number of events were selected to derive the regression equations to predict the parameters of the outflow hydrographs. To develop relationships between the parameters of the outflow hydrograph and the parameters of the inflow hydrograph, multiple linear regression analysis was used. To fit the theoretical distribution to the outflow hydrograph, Lane et al. (1971) described two methods that were adopted using the parameters that were obtained from the first part. The first method was to relate the mean and the mode of the theoretical distribution to the time to centroid and time to peak of the hydrograph to obtain the values of the first two parameters of the theoretical distribution, whereas the third parameter was determined from the time of the beginning of runoff in relation to the used time scale.

The second method determined the shape of the hydrograph through deriving two parameters of the theoretical distribution. This is done by relating the difference between the mean and the mode of the distribution to the difference between the time to centroid and time to peak of the outflow hydrograph. The third parameter was obtained in the same way as that used in the first method.

The authors found the developed method successful and both methods that were used to fit the gamma distribution were acceptable. However, the gamma distributions were found to work better with a single peak event. The study showed interesting results regarding the transmission losses. The transmission losses and, hence the outflow volume, were found to be related to the volume of the flood rather than the peak discharge. On the other hand, the antecedent channel moisture indices did not have significant effect on the outflow hydrograph or the losses. The authors suggested using this study as a guide for estimating the transmission losses and recommended further work to be carried out to study the other parts of the watershed to obtain regression equations so that the coefficients of these equations could be related to the physical characteristics of the streams. Hence, a regional description of the transmission losses could be obtained.

• ***Use of the unit hydrograph method***

Wheater and Brown (1989) carried out a study in Saudi Arabia testing the performance of the unit hydrograph method in the region. Eleven storms from 1984 and 1985 data were selected for detailed analysis. One millimeter, 10-minute unit hydrographs were derived for each of the events individually. The separation of baseflow was not thought necessary as the flows were ephemeral.

The obtained unit hydrographs were described by the authors as reasonable, except for one event, although the very steep rising limbs were sometimes associated with initial instability. The individual unit hydrographs showed high variability, therefore extensive analysis of this variability was undertaken by the authors. The results showed that no consistent relationship could be determined to explain the variability of the unit hydrograph in terms of rainfall or antecedent conditions. The results of an overall unit hydrograph that was obtained from the combined set of all the events were also found to be poor.

One of the greatest difficulties faced in the study was the selection of suitable runoff coefficients. The range of the runoff coefficients in this study varied from 5.9% to 79.8%. The analysis could not explain the scatter in the rainfall-runoff volume relationship in terms of rainfall depth, maximum intensities, temporal distribution or antecedent conditions. The authors referred the variation of hydrographs for the different events and the variation in the runoff coefficients to the highly localised rainfall and transmission losses. This is a well known problem in arid areas as was discussed in detail in **Chapter 2** of this report.

Stewart (1986), in her study in Saudi Arabia, showed that raingauges 8-10 km apart showed negligible correlation and the same was found by Osborn et al. (1979). Wheater and Brown (1989) suggested two solutions to this problem. The first solution was to increase the density of the raingauges, which is not practical for large basins, and the other suggested solution was to use flood frequency analysis in design. However, this can specify the peak discharge but not the problem of the hydrograph shape as was mentioned by the authors (Wheater & Brown, 1989).

• ***Use of Geomorphologic Instantaneous Unit Hydrograph (GIUH)***

Nouh (1990) carried out a study using 32 catchments in Saudi Arabia using the geomorphological instantaneous unit hydrograph (GIUH). The model was developed by Singh and Aminian (1984) but some modifications were applied by Allam et al. (1989) to include the infiltration losses. The model was found appropriate for small size humid

catchments and there was a need to test it in arid conditions (Nouh, 1990). The model was based on Rodriguez-Iturbe and Valdes (1979) and Gupta et al. (1980) and it incorporates the two-term Philip infiltration equation and is based on the convolution of the GIUH with the effective rainfall. According to the model, the direct runoff hydrograph *Q(j)* is computed as follows:

$$Q(j) = \sum_{i=0}^{j} h(j-i)I(i)\Delta t, j = 0,1,2,...$$

where *Q(j)* is the surface runoff discharge at time *j*, *i* is numerical time step into the past, *h(j-i)* is the ordinate of GIUH at time *j-i*, *I(i)* is the effective rainfall intensity at time *i*, and Δt is the discretization time interval used for discretizing the Rainfall Hyetograph and Instantaneous Unit Hydrograph.

The author explained that the effective rainfall hyetograph was computed by subtracting the infiltration rates from the gross rainfall hyetograph. The SCS curve number method was used to estimate the direct runoff volume. The author assumed the ratio of volume of initial abstraction to potential maximum retention to be a constant value, equal to 0.25, as was estimated from a previous study (Nouh, 1986).

Nouh (1990) investigated the effect of catchment characteristics such as catchment size, shape, slope, and catchment infiltration rate on the accuracy of the model. The results showed that the most effective catchment characteristics are the size of the catchment, the infiltration rate, and slope. The model accuracy was found higher for low infiltration rate catchments and catchment areas of less than 400 km^2. Hence, the GIUH was not recommended for use a large catchment or those with high infiltration rates (Nouh, 1990).

Nouh (1990) investigated the effect of the rainfall characteristics such as the spatial variation of the rainfall, the temporal variation, and the total rainfall depth and dry period between successive storms on the model performance. The spatial and temporal variations and intensity of the rainfall were found to affect the performance of the model. In addition, the length of the dry periods also has some effect. The results also showed that the model has higher accuracy in estimating the total runoff volumes than the peak discharge.

In another example, Sorman and Abdulrazzak (1993b) carried out a study, using the same geomorphologic instantaneous unit hydrograph (GIUH). The study was conducted using thirteen representative catchments in Saudi Arabia aiming to determine the flood

hydrographs. It is considered as an important study in water resources assessment in the country. The data used were related to geomorphologic parameters, hydraulic parameters, hydrologic characteristics, soil parameters, and climatologic parameters, whereas the model was as described previously (Nouh, 1990).

Sorman and Abdulrazzak (1993b) explained that the calibration of the model showed that the peak discharge and time to peak seem to be highly affected by the flood velocities and hydraulic conductivities

It was concluded from this study that the most dominant parameters in estimating the flood hydrographs were the soil porosity, pore-size index, and saturated hydraulic conductivity, flow velocity, and ground water table levels. The authors believed that this model is a useful tool that can be used to estimate the flood hydrographs in ungauged catchments. The results of this study seem to be much more promising than those of the previous study by Nouh (1990) in which the model was found less successful in estimating the flood peak when used in larger catchments. However the data availability is very important to use this model.

- ***The Sharma and Murthy (1996) model***

Another example of the studies that have been carried out using the metric method is the study of Sharma and Murthy (1996). The study considers the hydrological characteristics of flood hydrographs in arid areas (see **Chapter 1**). The hypothesis that was made by the authors is based on the belief that the time to peak is short in relation to the overall flow duration. Thus, the outflow hydrographs in arid areas can be simulated by selecting a series of flow peak values and attaching to these properly shaped recession curves. The upland basins flow hydrographs were simulated through a combination of regression and differential equations techniques, where the regression analysis were used to model the rising limb and a conceptual analog of discharge from a single leaky reservoir was used to model the recession portion. Sharma and Murthy (1996) believed that the representation of any arid upland basin with a single discharge reservoir can be considered as the simplest way to simulate the behaviour of the ephemeral channel network. It was also found that it is necessary that the design of the reservoir configuration and outflow rate reflects the effect of the topography and the physical mechanisms during the flow recession.

The data set used in the study was taken from six representative upland basins in India. It consisted of ephemeral flow hydrographs (51 hydrographs) for the period of seven years (26 June 1980 to 13 June 1987). Discrete observed flow values at 30-min intervals

were compared with the model results. The selected events were such that none of the selected flow events exceeded 50-hour and the recession curves were selected such that there is no indication of any new flood peak and the flow depth is less than 5% of the flood peak.

Graphical relationships were obtained between the peak discharge-effective rainfall-basin area, and time to peak-effective rainfall-basin area for the studied basins and these relationships were used to predict the rising limb of the ephemeral flow hydrographs. The recession flow was obtained by fitting the model parameters c' (loss rate per unit area), a^0 (reservoir shape factor) to the observed data through optimisation. A measure of goodness of fit was defined to compare the model and observed curves using the following equation

$$I(c', a^0) = \left[1/(N-1)\sum_{i=2}^{N}(X_i - Y_i)^2\right]^{1/2}$$

where X_i and Y_i are the points on the observed and simulated recession curves and N is number of points on the curves.

Based on this study, Sharma and Murthy (1996) believed that their model which consists of two main parameters; loss rate, and reservoir shape were found to have values lying in a narrow range, hence it was suggested that the recession curves seem to have characteristic shapes. The model is believed to be helpful to understand the runoff generation processes. It can also be used successfully in predicting runoff yield, extending recession curves if there any part is missing, and to produce the stream flow record.

4.4.2 Examples and Implication of Using Conceptual Type Models in Arid Areas

The basics of conceptual type models are described in **Chapter 3.** However, it should be noted that there is some overlap for some models with the physically-based model category in the way they consider some of the physical characteristics of the watershed and include physically measured parameters. Overlap with metric models is possible too.

- ***Use of the MODHYDROLOG model***

MODHYDROLOG is used to estimate runoff from rainfall and potential evapotranspiration data. The model was first developed by Porter and McMahon (1975) and was called HYDROLOG. This version was tested on six catchments in southeastern

Australia. The groundwater algorithm was further modified by Chiew and McMahon (1991) to improve the simulation of 'the stream-aquifer interaction' and the 'groundwater seepage processes', and the new version was called MODHYDROLOG (Chiew & McMahon, 1991).

The model includes many component parts to simulate the hydrological processes with some parameters that are related to the physical characteristics of the watershed. MODHYDROLOG includes 19 parameters, and Porter and McMahon (1976) recommended values for some of the parameters based on their experience on some Australian catchments. However, Chiew and McMahon (1991) suggested that the parameters should be optimised when required. The model also takes spatial variation into account by providing the facility to apply the model individually to subareas within each catchment but the spatial variation was not allowed in this study as the model parameters were calibrated against the stream flow records that are available at the catchment outlet only. The model structure is shown in **Figure 4.2.**

The model performance was investigated for different hydrological conditions. It was tested in tropical conditions by Brown (1987) and in arid conditions by Wong and Mustinove (1987).

Chiew and McMahon (1994) carried out a study using the MODHYDROLOG to test 28 Australian catchments of different climatic and physical characteristics, using monthly time steps. Their study investigated the physical basis of the model and the possibility of relating the model parameters to the physical and climatic characteristics of the catchment. The study also investigates the possibility of using the model without any calibration.

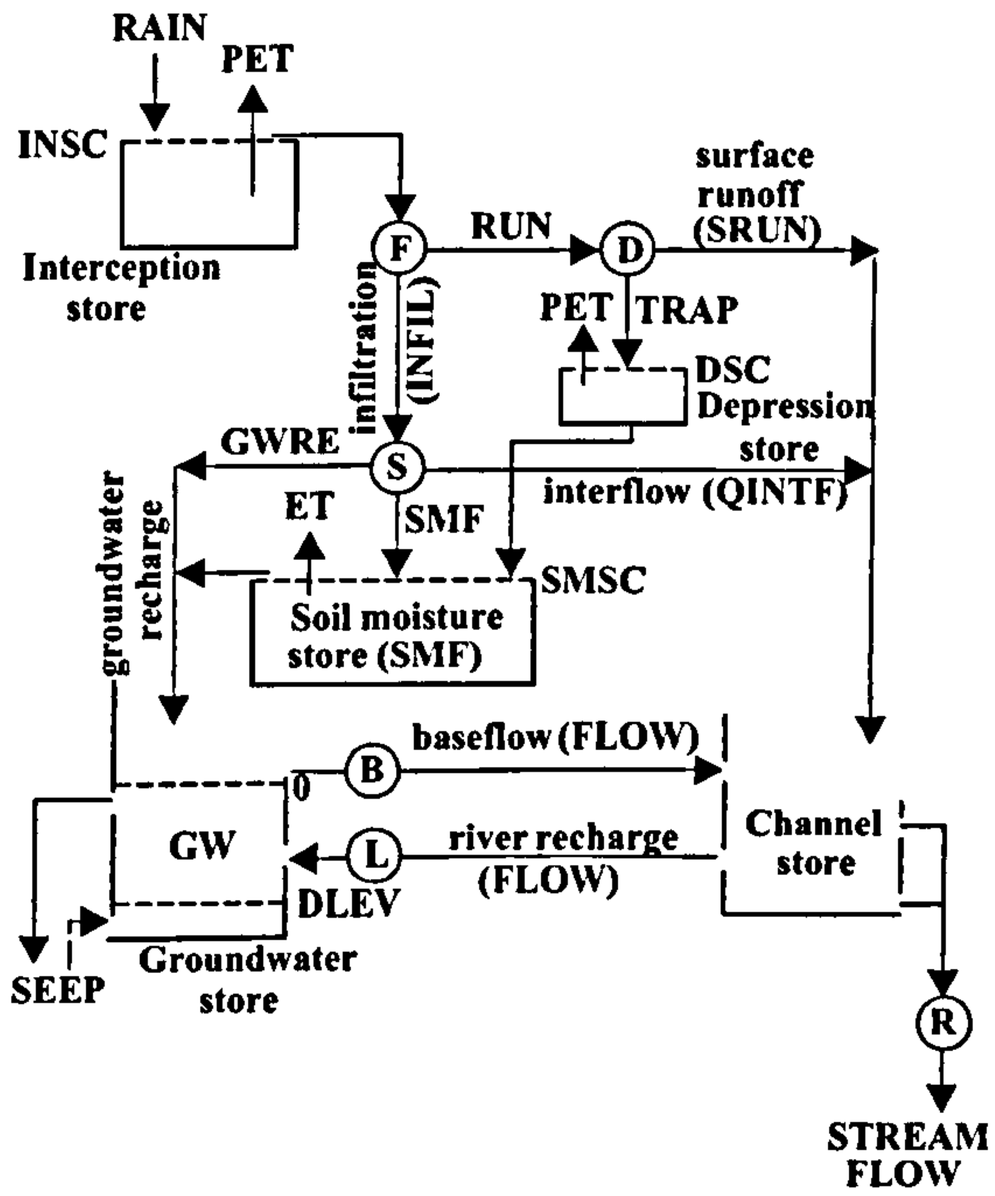


Figure 4.2: MODHYDROLOG model structure (*after Chiew and McMahon, 1994)*

The analyses were applied using four simulations on each catchment with different numbers of model parameters that were optimised in the model calibration. The authors pointed out that sensitivity studies on the relative importance of the parameters in this model have been carried out by Chiew and McMahon (1990) for semiarid catchments and by Wong and Mustinove (1987) for arid catchments but the calibrated parameters values are not recommended for use other than in the areas for which they have been calibrated. The objective function used is the following:

$$OF = \sum_{i=1}^{N} (\sqrt{Q_i'} - \sqrt{Q_i})^2$$

where Q_i' and Q_i are the simulated and recorded streamflow (m^3s^{-1}), respectively, of month i, and N is the number of months in the model simulation. To ensure realistic parameter values, the lower and upper limits for each parameter were set during the calibration process.

The efficiency, E, is determined through the following equation:

$$E = \frac{\sum_{i=1}^{n} (Q_i - \bar{Q})^2 - \sum_{i=1}^{n} (Q_i' - Q_i)^2}{\sum_{i=1}^{n} (Q_i - \bar{Q})^2}$$

where Q_i' and Q_i as defined above and $\overline{Q}$ is the mean monthly recorded flow. The E=0.6 was considered to be satisfactory, whereas E=0.8 is considered to be acceptable (Cheiw & McMahon, 1993b).

The monthly streamflow volumes that were estimated by the model with different numbers of optimised parameters, and the volumes estimated without model calibration were then compared to determine if the model parameters can be successfully estimated using the catchment physical and climatic characteristics, and if the model has to be calibrated for all applications, or how many model parameters need to be optimised to obtain an adequate simulation of stream flow. The study tested four different optimisation cases: all 17 parameters; 9 parameters; 4 parameters and no optimisation.

In comparison of runoff volumes estimated with different numbers of model parameters optimized, it was found that some parameters are more important than others, and the use of all the 17 model parameters is not necessary. The results showed that, optimising 9 parameters give results as good as those estimated using 17 parameters in approximately 70% of the selected catchments but the quality of the monthly flows estimated when 4 parameters are optimized is considered to be the same as those estimated using 17 parameters in about 50% only of the catchments. Furthermore, in the 4-parameter case, it was found that the flow estimates for 15 of the 28 catchments were still considered to be acceptable for typical application. On the other hand, the results obtained when no calibration was carried out (using the parameter values that recommended based on the catchment physical and climatic characteristics) was very poor, and only 7 out of the 28 catchment considered to be acceptable.

Compared with the simulations when 17 and 9 parameters are optimized, the interflow and deep seepage processes were not simulated when only 4 model parameters were optimized. The authors explained that simulating the deep seepage is not necessary in this case as this is needed only where the runoff coefficients are low. However, it seems that the model does not perform well with fewer than 9 parameters. The quality of the flows that were estimated by optimizing 4-parameters was poorer than those obtained by optimizing 17 or 9 parameters in dry catchments with low runoff coefficients (only 50% of the results were found acceptable using 4 parameters as mentioned above).

The study shows clearly that it is always more difficult to simulate runoff in semiarid and arid catchments when compared to the wetter catchments. The authors referred this to the processes governing the relationship between rainfall and runoff in arid

catchments, where runoff is a small proportion of rainfall and where streams are ephemeral and hence, generally more complicated than in wet catchments.

The Chiew and McMahon (1994) study showed that the streamflow volumes estimated without any model calibration are significantly poorer than the estimates obtained through model calibration as only 7 of the 28 catchments were considered to be acceptable without calibration.

Important parameters should always be calibrated against stream flow data where possible. Another important finding about the model is that, although the selected MODHYDROLOG generally gives satisfactory estimates of runoff, it has some difficulty in simulating long periods of zero flows followed by flow peaks in ephemeral streams in arid catchments. This poses the question of the suitability of using this model in arid areas.

The study of Chiew et al. (1993a) on eight catchments throughout Australia compared the results of MODHYDROLOG with simpler conceptual models and time series equations. The study found that MODHYDROLOG generally performs better or as well as other commonly used rainfall-runoff models (Stanford model, Sacramento model and Boughton model) as the results of studies of Moor and Mein (1975), and Weeks and Hebbert (1980) showed. The study showed that MODHYDROLOG gives much better estimates of stream flow in general. However, the problem of MODHYDROLOG performance in arid areas remains and further studies in this matter seem to be required.

- ***Use of the Pitman model***

The **Pitman model** is a conceptual monthly model that was developed by Pitman (1973). The model was used widely for the design of small and large water supply schemes as well as more general surface water availability assessments within Southern Africa. This model has also been used in surface water resources assessment projects for the whole of South Africa in which regional guidelines for the estimation of parameter values of the Pitman model were developed (Hughes, 1995).

Pitman model has two main functions that generate runoff. The first is a symmetrical triangular distribution, defined by two parameters, representing the catchment absorption rate (*ZMIN* and *ZMAX*). This defines that if the rainfall in any iteration step ($\Delta t = 0.25$ months usually) is greater than $ZMIN^* \Delta t$, then some runoff occurs. The other function is mainly controlled by a maximum moisture storage parameter. If the storage level exceeds this value all further rainfall becomes runoff.

Hughes (1995) believes that the moisture storage is depleted by evapotranspiration and drainage using a non-linear soil moisture runoff formulation. As this equation is based on a non-linear relationship between current soil moisture storage and runoff from soil moisture, the last mechanism is not usually relevant when the model is applied to arid and semi-arid areas where sub-surface flow plays only a minor role due to intermittent rain events and high evaporation rates. Once the runoff is generated by either of these functions it must reach the catchment's outlet, as there are no loss functions except those related to artificial abstractions (Hughes, 1995).

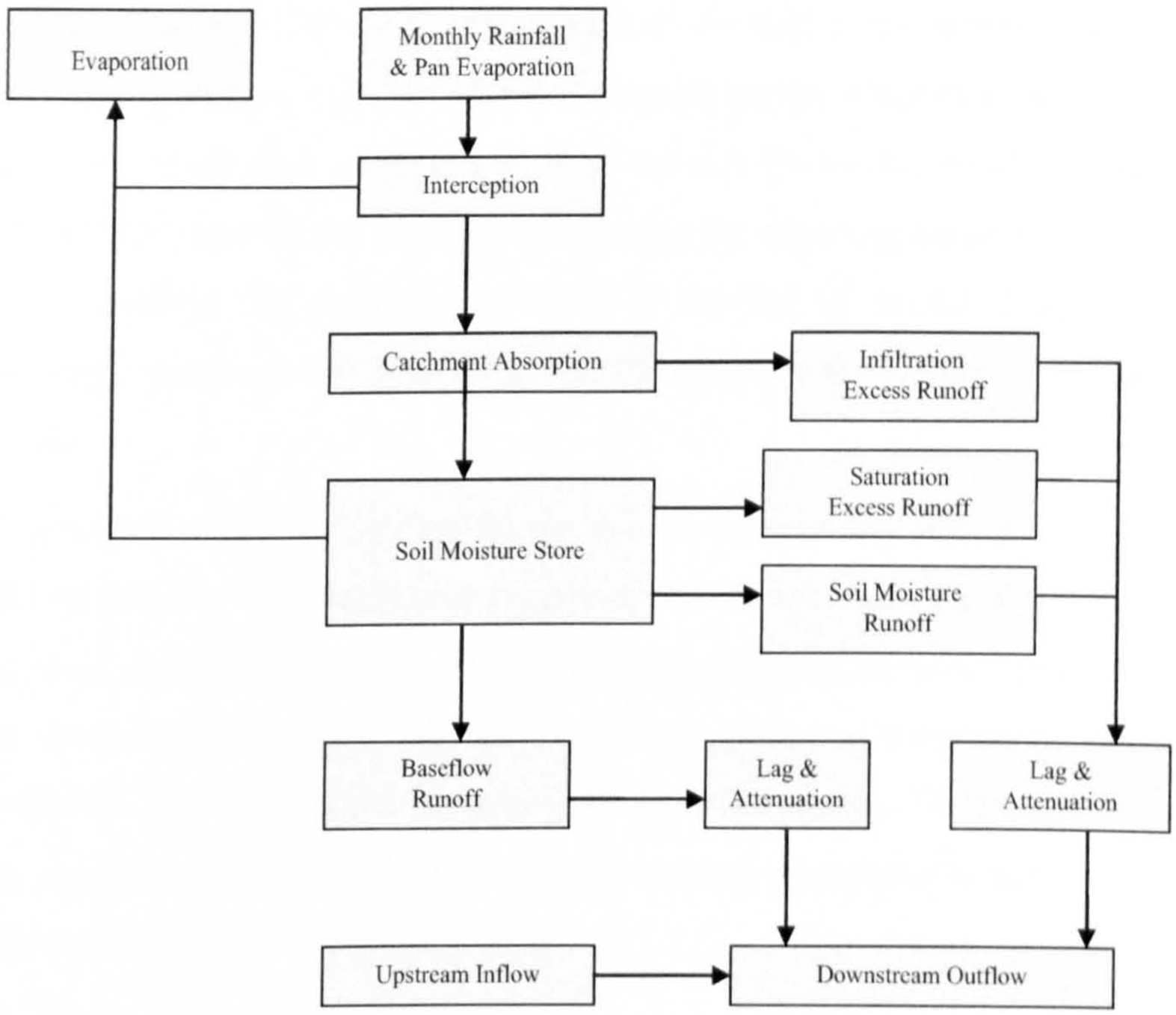


Figure 4.3: Pitman Model Structure (*After Hughes, 1995*)

Hughes (1995) explained that despite the widespread use of the Pitman model in some regions such as Africa, the model seems to have some problems when used in the more arid zones. The problems were grouped by Hughes into two main categories; those related to the way in which the model represents catchment runoff generation processes and those associated with the nature of the rainfall input to the model. Hughes (1995) illustrated that two main hydrological processes are commonly missing in such models. The first problem is regarding the capability of the model to allow for runoff generated in upstream sub-catchments to be lost through re-absorption into storages lower down, whereas the second problem is regarding the capability to allow for vegetation changes that are usually affected by the variations in seasonal rainfall amounts.

Hughes (1995) applied the model to two basins to demonstrate the type of problems this model can face when applied to arid or semiarid areas. The first area was the Mosetse River in Botswana, using monthly data from two stations. The months of January 1972 and 1974 were selected for more detailed analysis of the model rainfall input compared to the available knowledge of the actual rainfall.

It was noted from this study that regardless of the data quality, the model representation of the excess rainfall for some events (especially the 1972 event) resulted in exceeding the thresholds of the catchment absorption by a greater degree than occurred in reality, and hence the simulated flow was overestimated for this event, whereas in other cases the model appears to have significantly underestimated the maximum rainfall leading to underestimation of the flow of 1981 and 1987 events. Therefore, an effort was made by Hughes (1995) to improve the model performance by applying some modifications that can help to decrease the simulated flow for a number of events. Hughes suggested including some functions to allow for runoff re-infiltration when the catchment is relatively dry.

When the model was applied to Nata River in Botswana, it was found that a reasonably acceptable fit between simulated and observed flows could only be obtained by setting the storage and absorption parameters for the upstream areas to values much higher than the lower sub-area. The author was aware that the potential evaporation demand was misrepresented (only scarce data were available for the study). This might have had an important impact on the simulation of those runoff components related to storage thresholds in the model.

- ***Use of the VTI model***

Hughes (1995) investigated a daily time-step VTI model that was developed by Porter and McMahon (1971) in six catchments in Botswana. The model structure is shown in **Figure 4.4**.

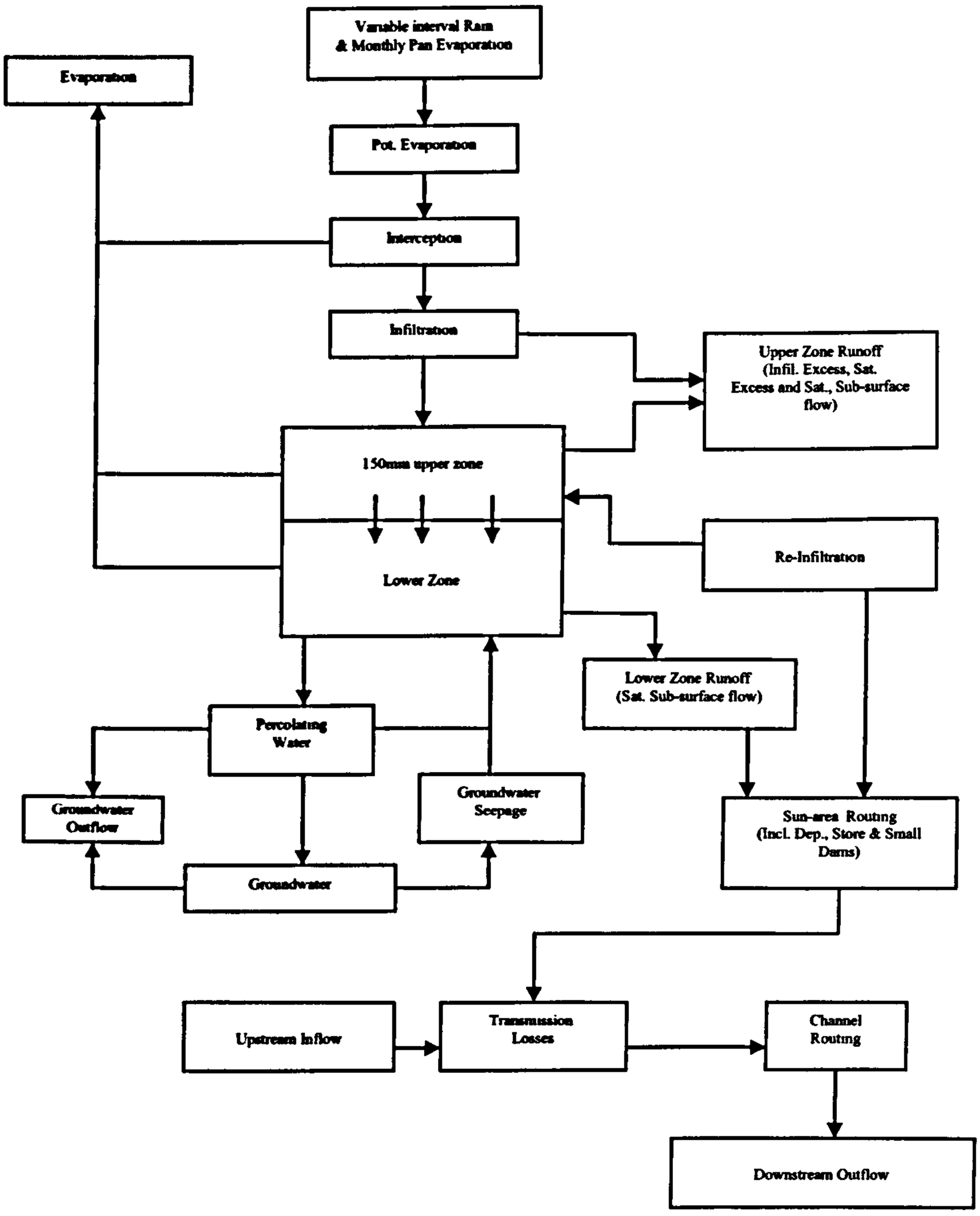


Figure 4.4: VTI model structure (*After Hughes, 1995*)

The author believed that the most important element of the model is the ability of the model to generate the runoff either by infiltration excess processes or by saturation excess. Another important facility this model provides is that it has a transmission loss routine that allows water that has reached the channel system to be re-infiltrated if sufficient capacity exists in the transmission loss storage zones.

The catchment needed to be divided into sub-areas but there was little information to indicate if the main model parameters need to be different across the sub-areas and there was no information to quantify any differences. Hence, the used parameter values are the same for the different sub catchments within the total catchment. As a result, variation in the rainfall input for the sub-areas due to the distribution of the rain-gauges has little differences (Hughes, 1995).

Even though the results for the monthly values were better than for the daily, the monthly values were not highly accurate. The daily model requires much more calibration effort without ensuring better results (SMEC, 1991). Hughes (1995) explained the difficulty of being confident about the model performance when the rainfall data quality is questionable. This is believed to be the situation in many other arid areas. The other issue that needed to be considered was that the best calibration parameter values were dependent on rainfall input, hence longer periods were needed for calibration.

- ***Use of the GSFB model***

The Generalized SFB model (**GSFB**) is a modified version of Boughton's (1984), SFB model. It uses concurrent daily rainfall and potential evaporation data as inputs to estimate monthly streamflow. The model requires the specification of seven model parameters; the surface store capacity (*S*), the daily infiltration capacity (*F*), and the baseflow factor (*B*). The other four parameters, which are fixed only in the original model SFB, are the fraction of the surface storage capacity that does not drain to the lower store, *NDC*; the maximum limiting rate of evapotranspiration, Evp_{max}; the lower store depletion factor, *DPF*; a baseflow threshold for the lower store, SDR_{max} defining the depth of water in the lower store at which baseflow ceases. The model structure is shown in **Figure 4.5**.

Ye et al. (1997) carried out a study in Australia using different hydrological models to test their performance in low-yielding ephemeral catchments. The study includes the GSFB model. Ye et al. (1997) obtained estimates for seven of the GSFB model parameters (*S, F, B, NDC, DPF, SDR, C*) using a simulated annealing algorithm (Kirkpatrick et al., 1983; Press et al., 1992).

Despite the fact that GSFB uses a daily time step for computation, the model was calibrated on the basis of fitting monthly flows only in the study. The objective function for the GSFB model was the sum of the square of the differences between the square roots of observed and modelled monthly runoff. The Nash Sutcliffe efficiency was obtained as shown below:

$$E = 1 - \mu_e^2 / \sigma_q^2$$

where μ_e^2 is the variance of the residuals $e_i = Q_i - Q'_i$ between the model discharge Q'_i and the discharge observations Q_i, and σ_q^2 is the variance of the observed discharge.

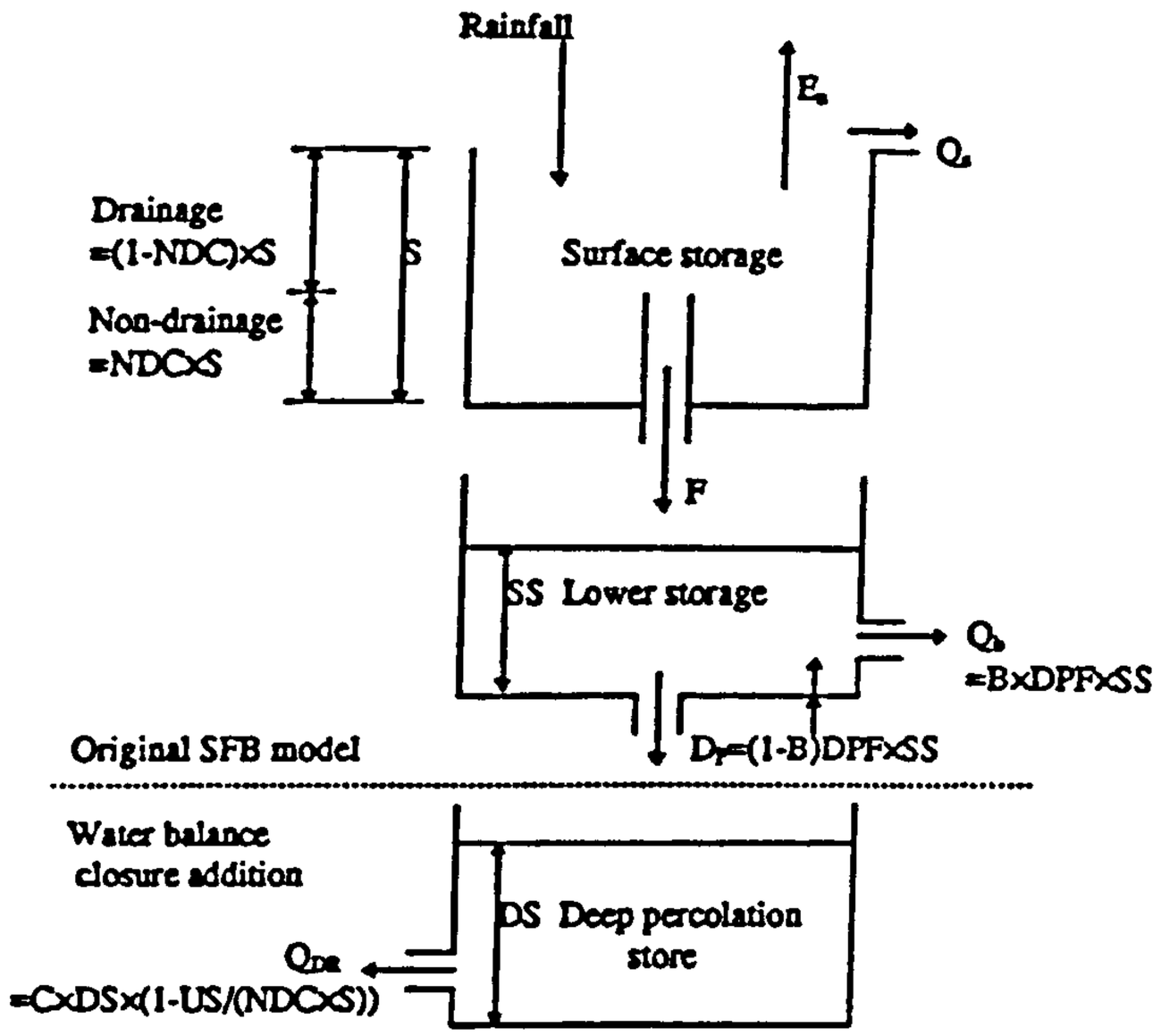


Figure 4.5: Generalized SFB model Structure (*After Ye et al., 1997*)

However, the study obtained poor results on a daily basis compared to monthly. The efficiency values were negative in five out of six cases that were studied, indicating large errors. However, the results showed that on a monthly basis the model performance has improved.

It was believed that it might be an adequate model if the interest is only in monthly river flows, but it is not recommended for daily prediction. This may be due to its calibration using monthly data which might not be suitable as this model requires daily data. Ye et al. (1997) noted that the model was designed to perform in monthly time-step although it uses daily climatic input. However, Ye et al. found that when the performance of GSFB was compared with IHACRES and LASCAM models, the results were poorer compared to the other two models. Overall, GSFB is not recommended for use with a daily time-step or for low-yielding areas. The authors found that GSFB is better for the wetter catchments as its performance decreases with the decrease of catchment yield.

- ***Use of the IHACRES model***

The IHACRES model undertakes identification of hydrographs and component flows from rainfall, evaporation, and streamflow data (Jakeman et al., 1990, 1991. 1993a, b, 1994a, b; Jakeman & Hornberger, 1993). The model is considered as a hybrid metric/conceptual model of average complexity.

The model structure was devised to be able to consider different types of catchments and climatologies and at the same time to be statistically accurate. IHACRES utilizes two concepts of unit hydrograph theory; that precipitation is transformed to effective rainfall and the relationship between effective rainfall and total streamflow is conservative and linear.

The model loss involves calculation of an index of catchment storage s_k at each time step k. The effective rainfall u_k is typically computed for humid areas as the product of incident precipitation r_k and the storage index. However, for the low-yielding catchments for the study of Ye et al. (1997), two extra parameters p (peakness factor) and l (threshold below which no effective rainfall is produced) were required to generate u_k from

$$u_k = [s_k - l]^p r_k \text{ if } s_k > l, \text{ otherwise, } u_k = 0$$

Ye et al. (1997) explained that in the low-yielding catchments examined in their study and for catchments with no regular baseflow, only one linear store is needed to explain streamflow and using a single store required only one additional parameter to those in the loss model so that the total number of parameters used to model the three selected catchments was only six.

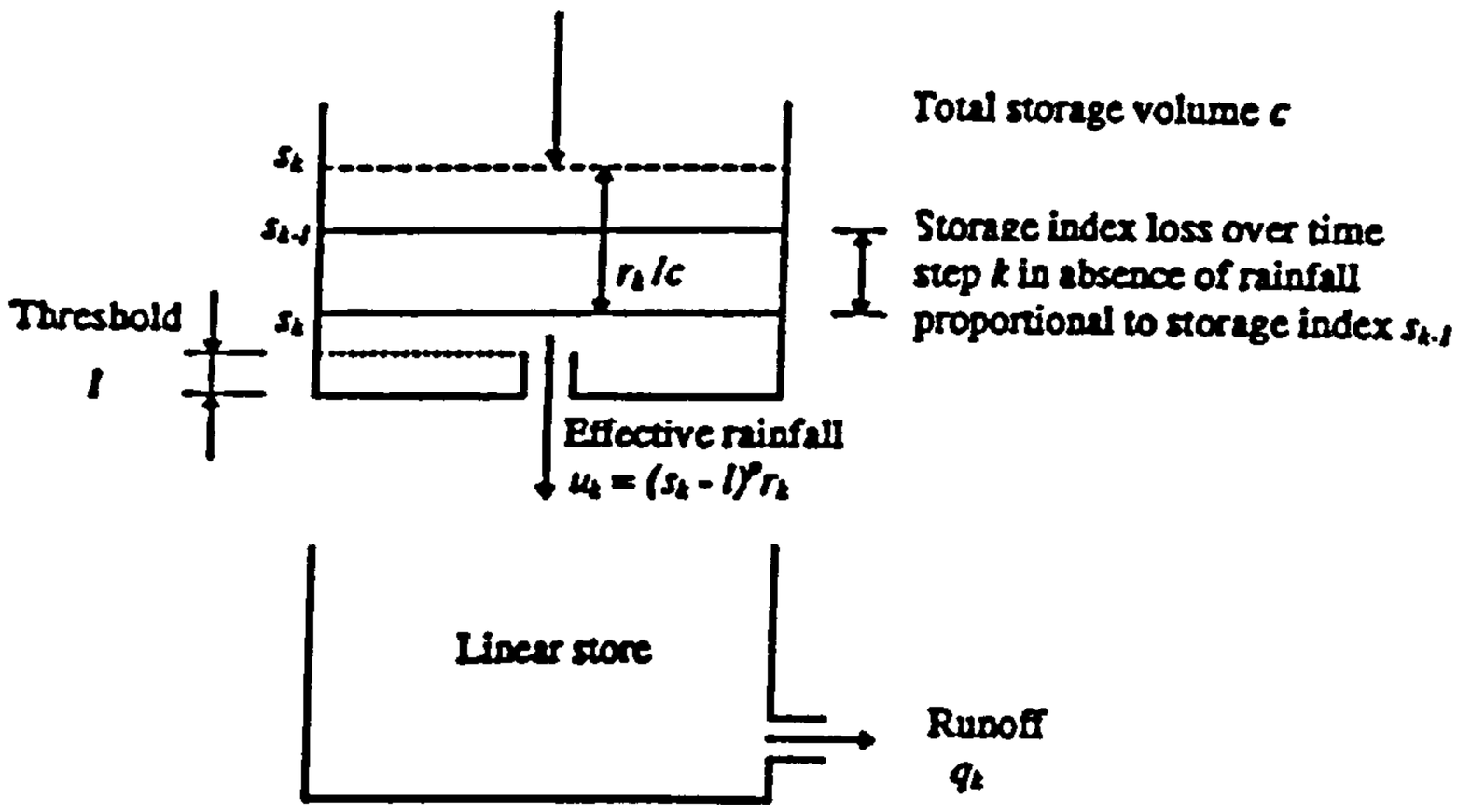


Figure 4.6: IHACRES model Structure (*After Ye et al., 1997*)

Ye et al. carried out a study using the IHACRES using three low-yield catchments in Australia. The model was calibrated using two periods, each of 5 years. The first period is drier than the second period. Three assessment criteria were used as shown below

Absolute mean deviation:

$$ABS = N^{-1}\sum_i |Q_i - Q_i'|$$

Bias:

$$Bs = N^{-1}\sum (Q_i - Q_i') = N^{-1}\sum_i e_i$$

The efficiency was obtained through the Nash Sutcliffe equation described before.

The results were found to be reasonable with efficiency ranging from 82 to 90% when the model was used with daily data, but the performance of the model increased when used for monthly analysis. It was also noticed that the model had less bias than the GSFB and LASCAM models when tested on the same catchments and data periods. This was, however, due to the consideration of the bias explicitly in its calibration as one of the performance indicators (Ye et al., 1997). IHACRES was found to be of adequate performance in all tested cases. IHACRES was also found to be adequate when applied to independent time series for both monthly and daily time steps.

The IHACRES model was used in another study that is relevant to this research, the Post and Jakeman study (1999). The authors tested this lumped conceptual rainfall-runoff model at a daily time-step using 16 small (less than 1 km^2) catchments in Australia. The study attempted to understand the controls on catchment-scale hydrologic response to landscape attributes. Therefore, each of the 16 catchments was considered to be ungauged, and a prediction of the daily streamflow of that catchment made based on the relationships between landscape attributes and hydrologic response characteristics derived using the other catchments. The results ranged from very good to poor. The study showed that regional relationships between hydrologic response characteristics and landscape attributes could be used to predict the daily streamflow of an ungauged catchment from an appropriate rainfall and temperature time series. The poor results of some catchments were referred to the insufficient understanding of the relationships between the landscape attributes and the hydrologic response characteristics. On the other hand, there was no clear effect of the catchment size on the performance of the tested models. Overall, IHACRES performed very well in calibration and was considered sufficient for runoff estimation.

Evans and Jakeman (1998) also used the IHACRES model but with a modification. The authors introduced the catchment moisture deficit (CMD) to the model to utilise a water balance approach that extracts information from catchment-scale time series data

available on precipitation, energy-related variables and stream discharge. The modified model adopts the hydrograph identification approach used in the linear module of the rainfall-runoff model IHACRES but replaces the statistically based non-linear evapotranspiration loss module by a catchment moisture deficit accounting scheme.

The structure of IHACRES model was described earlier in this section, which shows that it consists of linear streamflow routing model and non-linear loss model. For the linear model, Evan and Jakeman adopted two stores in parallel for humid catchments and one store for semiarid catchment based on the Ye et al. (1997) study that was described earlier.

However, it should be noted that the authors did not have adequate ET data available, hence no direct assessment of ET estimates could be made. Three small catchments were tested, two of them are humid catchments (Coweeta catchments in North Carolina, USA), whereas the other is a semiarid catchment (Scott Creek in South Australia).

The obtained results from the model calibration were found to be good, even though the model had some difficulty reproducing hydrograph recessions in one of the humid catchments. The model does have some difficulties in determining a clear CMD value. However, the authors believe that by using this semi-physical approach, the physical interpretation of the parameters will be made easier than with the statistical approach in the unmodified IHACRES. It was also believed that this approach could be used to provide the land surface feedbacks for a climate model.

Croke and Jakeman (2004) introduced a new revised version of the non-linear part of IHACRES model that was used in the Evans and Jakeman (1998) study reviewed above. The new version was developed to aid in estimating flows in ungauged basins and for applications where time-series estimates of actual evapotranspiration are required. This modified model has only 3 parameters that are related to the climate data. The new version was applied to the same catchments that were used by Evans and Jakeman (1998). The results showed lower R^2 values for the calibration periods but better performance for the simulation period.

- ***Use of the LASCAM model***

The LASCAM model (Sivapalan et al., 1994a, b) has been developed to predict the impact of land use and climate change on the daily trends of streamflow and salinity in the forested water supply catchments of southwestern Western Australia. The model was designed to consider the unique soils and climate of the region and is sensitive to the hydrological processes operating in the water supply catchments.

Figure 4.7 illustrates the model structure.

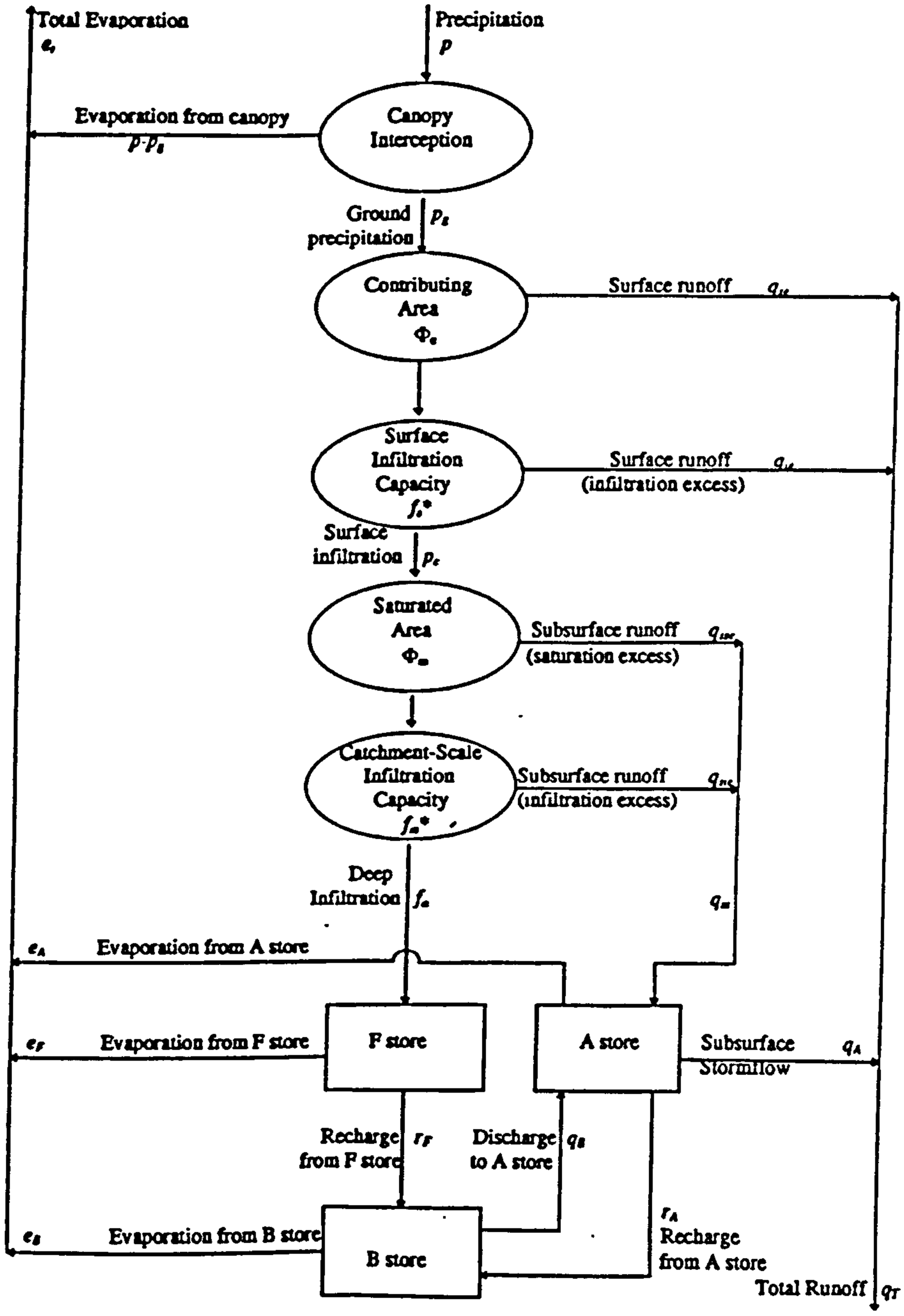


Figure 4.7: LASCAM model Structure (*After Ye et al., 1997*)

The model has 22 parameters, which describe each of 17 potential flux paths and the initial volumes of the three soil moisture stores that represent the permanent deep groundwater system. LASCAM is designed to predict salt export as well as streamflow, hence a large number of parameters is required.

Ye et al. (1997) used this model to check the performance of conceptual rainfall-runoff models in low-yielding ephemeral catchments ranging in size from 0.82 to 517 km^2. It

should be noted the version of the model used in that study did not use all facets of the full LASCAM model. It was operated as a lumped-catchment model with no spatial distribution of runoff generation, without activating the streamflow routing algorithm.

The input data were also not distributed, but were taken as catchment means. Furthermore, leaf area index was kept constant in time and with no consideration of the vegetation change effect.

The results of the study of Ye et al. (1997) showed that LASCAM provided the best model fit statistics overall compared to the other two models (GSFB and IHACRES models) in both wet and dry periods.

In general the LASCAM model was found adequate for simulations on independent time series, for monthly and daily time steps for all selected catchment, when compared with GSFB and IHACRES. Comparing the results of Ye et al. (1997) with other studies, the study contrasts with Michaud and Sorooshian (1994) and Hughes (1995), which both indicated that simpler models do not yield inferior accuracy to more complex models. On the other hand, Chiew and McMahon (1994) found better results using more complex model MODHYDROLOG.

- ***Use of Conceptual Integrated Models***

Wheater et al. (1997) used an integrated type of model in their study. The study was to evaluate the daily time-step rainfall-runoff components and was constructed using data from the experimental basin at Walnut Gulch, USA. **Figure 4.8** shows the developed model structure.

The used model was developed by Wheater et al. (1995) for the evaluation of different options for recharge management in Wadi Ghulaji in northern Oman based on the improved understanding of the arid area hydrology. The model was described by the author as a distributed model, based on a simple multivariate model of raingauge rainfall. This model was used to provide stochastic input sequences to a daily rainfall-runoff model. The rainfall-runoff model conceptualises the catchment as a network of planes and channels, with consideration of the differences between jebel (mountains) and alluvial planes.

The model includes a number of options to represent runoff from the plane elements, including the US Soil Conservation Service (SCS) method. The channels are represented as a series of one-dimensional elements and the transmission loss is

represented as a linear function of upstream discharge using the Jordan (1977) equation shown below:

$$\frac{dQ_{Vx}}{dx} = -kQ_{Vx}$$

where; x = distance downstream; Q_{Vx} = flow volume at location x; and k = constant of proportionality, which can be expressed as:

$$Q_{Vx} = Q_{VA}\,(1-\gamma)^{x}$$

where Q_{VA} is the flow volume at A (x=0) and γ represents the proportion of flow lost per unit distance for a given channel element.

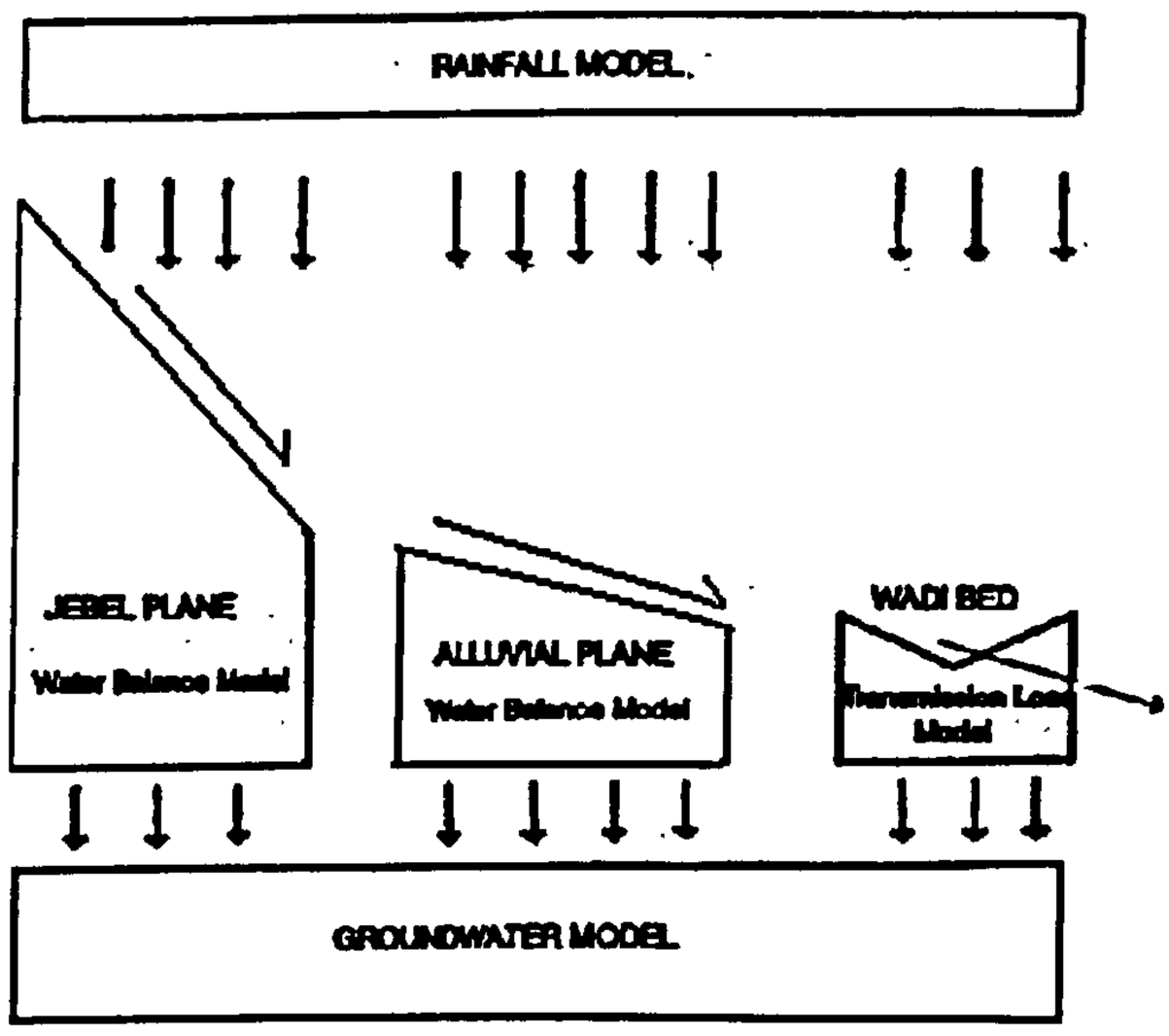


Figure 4.8: The Schematic of the integrated modelling procedure (*After Wheater et al., 1997*)

Transmission losses provide groundwater recharge to the distributed multi–layer groundwater flow model (MODFLOW). It was suggested that including the channel width can improve Jordan's relationship (Walter, 1990; Sorman & Abulrazzak, 1993a). Hence, the effect of the increased wadi width was allowed by increasing γ downstream (Wheater et al., 1995).

The developed model was tested by detailed assessment of one of the components, the rainfall–runoff model using data from the intensively monitored Walnut Gulch catchment in Arizona. The original model was applied with constant γ, and the SCS

option for runoff generation was applied using a single value of curve number for each sub-basin and the two parameters were calibrated for each sub-basin for the selected events. The model was modified to incorporate the observed relationship between transmission loss and upstream discharge with no considerations of spatial variability in γ, using the following equation:

$$\gamma = 118.8(Q_{VA})^{-0.71}$$

Some simple curve number modification was also applied according to the season and 5-day antecedent precipitation. Wheater et al. (1995) noticed significant improvements when those modifications to antecedent conditions and transmission losses were applied. The authors found the performance of the calibrated daily flow model encouraging. Clear relationships were observed between flow volumes and hydrographs peaks. Hence, the simulated flood volumes could be used to estimate flood peak response. The multivariate modelling approach of Wheater et al. (1995) was used as a first attempt to represent rainfall variability, but it was considered desirable in future to have a full stochastic spatial-temporal rainfall (Wheater et al., 1997).

4.4.3 Examples and implication of using Physically- Based Type Models in arid areas

Physically-based models are very useful in many manners as was described previously in this report. Examples of some models in use are discussed in this Section.

- ***Use of KINEROS model***

KINEROS is considered to be a physically-based model as it is based on physical principles of conservation of mass and momentum. The model is also considered to be a distributed model as the watershed surface and channel network are represented by a cascade of planes and channels in which each plane may be described by its unique parameters, initial conditions, and precipitation inputs, and each channel, by unique parameters.

KINEROS is an 'event-oriented' model that does not include components that describe evapotranspiration and soil water movement between storms. Hence, it does not have the ability to maintain a hydrological water balance between storms. It has the ability to calculate the surface runoff for a single event or surface runoff and erosion if there is a need to calculate the latter parameter but the initial soil moisture conditions will be required in such cases.

Wheater for the Royal Oman Police (ROP) (1981) carried out a study using KINEROS. The study was conducted in assessment of the 3 May storm that hit Wadi Aday in Northern Oman and caused severe damage. The catchment was split into about seven planes and three channels based on soil type even though it was not explained comprehensively in the report.

As the model allows only for a single rainfall input, the continuing loss was represented by using a runoff coefficient of 0.75 to reduce the hard rock sub-areas by 25%, whereas for the gravel hills, the area reduction was 50%, using a runoff coefficient of 0.50. The author found it necessary to use separate input because of the difference in the losses in hard rock areas and these from that of gravel areas.

The obtained results showed a good agreement between the observed peak discharge and that obtained by the model though this was partly due to the adjustment of roughness coefficients. In addition, the model obtained about the same time to peak that was given by eye witnesses. It was also found that the estimated initial peak value was similar to the lower peak that was observed at the beginning of the flood. However, comparing the results obtained using KINEROS to those obtained by the time-area approach the author believed that KINEROS obtained better results. The author referred this to the fact that the model is physically-based in which the effects of flood routing due to the channel storage and overland flow are explicit.

Michaud and Sorooshian (1994a) in their study comparing simple versus complex distributed runoff models on a mid-sized semiarid watershed have also used KINEROS. KINEROS was compared to the simpler lumped models that are based on the SCS method.

The study was constructed using data for the Walnut Gulch, USA. Six events were selected for model calibration, and an additional 24 events for validation, of which 20 were the largest peak flows during 1957-1973, whereas the other four were slightly smaller peak flows from the same period. Eight rain-gauges with a minimum time step of 1-min were used. Daily rainfall data (6-8 months prior to each storm for the complex model and 5 days prior to each storm for the simple model were used to estimate initial soil water content for each event.

The models were calibrated using rainfall from eight rain-gauges and observed flows at the watershed outlet. The models were validated by comparing simulated and observed peak flow, runoff volume, time to peak, and the ratio of peak flow to volume (because it

is a measure of runoff routing ability). Sensitivity analyses of KINEROS were also performed.

The authors illustrated that the lumped SCS model performed very poorly without calibration. The un-calibrated version predicted runoff for only two of the 24 events but the calibrated version was more accurate, though it still under-predicted the peak flow by more than 50% on average. The authors, however, expected the poor performance of the lumped model as it does not take into account the spatial variations in rainfall and runoff that are important under the prevailing conditions.

Overall, it was found that the simulations were disappointing for all the calibrated models, especially in simulating peaks and volumes, though KINEROS was much better in comparison to the distributed SCS model in simulating peak flows and volumes. On the other hand, both SCS models were not able to accurately simulate peak flows or runoff volumes for individual events. However, the calibration increased the performance of the SCS models slightly.

The authors believed that the disappointing performance of the complex model (KINEROS) could be due to its non-linearity in its routing routine as the input error does not affect the performance of linear routing model accuracy as much as in the case of non-linear routing models. Michaud and Sorooshian (1994a) showed that a rapid convergence to an optimum parameter set was obtained for the SCS model representing at least a local minimum of the objective function, whereas it was not clear if convergence was obtained in the KINEROS case due to its computational constraints and significant interaction of the parameters. The data quality effects on the modelling results were questionable too. The very important finding in this study is that the KINEROS can not cope with medium to large size watersheds, which have catchment areas of more than 100 km^2. These could be due to the spatial variation of the rainfall in arid and semi-arid areas bearing in mind that the rainfall measurement errors may increase with increasing the catchment size. It was also noted that the runoff in these regions decreases as the catchment size increases due to partial area coverage and increased channel losses (Goodrich, 1990). The authors believed that the simulations of runoff in such areas are more difficult at 100 km^2 than for a smaller catchment of few hectares. Michaud and Sorooshian (1994a) explained that in larger basins, the channel processes need to be simulated adequately and not only the hillslope processes. They also believed that the characterization of some of the parameters and hydrological characteristics such as spatial rainfall variation, initial soil water contents, and

watershed characteristics is much more difficult compared to humid areas and the physical realism might be compromised in complex models if they have insufficient spatial resolution.

The authors found it difficult based on this study to decide on the best type of models and the model complexity level that can be accepted to model arid areas with catchment areas for more than 100 km^2 sizes due to the unexpectedly poor results of KINEROS. Complex models were found to perform well in small well-instrumented catchments and this study found that complex model can give better results without calibration though it is not suggested to use uncalibrated models in ungauged catchments as the parameter uncertainty is very high. However, the authors believe that simple models are important where limited data are available. The rainfall accuracy is essential to improve the models accuracy (Michaud & Sorooshian, 1994a)

Another study in which KINEROS was used is Faures et al. (1995) in which the research version of KINEROS model that was developed by Goodrich (1990) was used. The aim of the study and the study area, and the input data were described in **Chapter 3**. However, it seems difficult to evaluate the performance of KINEROS from this study as the authors concentrated on discussing the effects of the rainfall errors and importance of rainfall knowledge rather than the evaluation of KINEROS performance. The performance of the model seems to be acceptable to the authors.

- ***Use of an Integrated Physical-Based Model***

El-Hames and Richards (1998) developed a physically-based model that they believed to consider the hydrological features of arid areas that can produce flash floods and the associated transmission losses. The model was tested in a catchment in south-western region of Saudi Arabia.

The model consists of two submodels; a hillslope, to calculate excess rainfall simulating one-dimensional infiltration using Richards' equation, and overland flow routing using the kinematic wave approach.

The infiltration component considers the excess rainfall on slopes and aid in calculating the transmission losses. The Richards' equation of flow of unsteady-saturated flow in the 1-D vertical direction was used as shown below:

$$M(\Psi)\frac{\partial \Psi}{\partial Z} = \frac{\partial}{\partial Z}\left(K(\Psi)\frac{\partial \Psi}{\partial Z} + K(\Psi)\right)$$

where:

M : specific moisture capacity

Ψ : a metric potential

t : time

K : hydraulic conductivity

Z : depth of the soil profile

The overflow routing component was important to route the excess rainfall over hillslopes towards river channels. El-Hames and Richards (1998) explained that overflow routing is different from channel routing as the shallow water flow can be very fast due to the steep slope. El-Hames believed the best method to be used is the kinematic wave method which can consider the shallow flows successfully and is numerically stable in describing the rapid flow depth.

The model was tested and calibrated through testing and calibrating its sub-models; the hillslope and the channel routing sub-models. Three rainfall-runoff cases in Wadi Tabalah were used to test and calibrate the model. The parameters of the overland flow generation routing were the only parameters that were adjusted during the first major sub-model routing (channel model) and then were fixed through the following simulations, during the second sub model (hillslope model), as it is difficult to adjust these parameters afterwards due to the spatial variation of the channel network and its system input-ouput.

Reasonable results were obtained by the model for peak flows, initial time of rise, time to peak and runoff volumes. However, the model seems to miss one of the peaks in one of the simulated events. The author explained this as being due to the inadequate time-interval as only hourly data were available for the analysis.

The sensitivity analysis showed that the output hydrograph shape and volume are greatly affected by initial soil moisture content, the soil saturated hydraulic conductivity, and the Manning roughness coefficient. These findings were found by the authors to agree with the study of Placios-Velez and Cuevas (1992).

However, the developed model was found to be sensitive to the rainfall error associated with rainfall bursts and an adequate time sequence needs to be used which may not be always available in arid areas (El-Hames & Richards, 1998). The results also showed that the infiltration amount is about 88% of the rainfall volume. The model was recommended to be used for determination of transmission losses. The model was considered by the authors as the first physically-based model that is capable of simulating the dynamic transmission loss during hydrograph translation.

The model showed good results with minimum calibration for the selected watershed which was of medium size (170 km^2). Even though the authors believe that this model can be used as a prediction tool in ungauged catchments of medium size if the appropriate required data is available, the model should be tested in other arid parts before deciding to adopt it as a prediction tool. However, this model can not be used in personal computers as it needs a very long CPU time for running the simulation, especially to determine the infiltration.

4.5 Discussion of Results

In this section a review of the discussed models above highlights the advantages and the disadvantages of these models. The investigation of the different studies that were carried out in arid areas showed that there are some expected problems that could be referred to the distinctive arid areas features, such as the high spatial and temporal variations of rainfall and runoff and also the high transmission losses beside the other features that were discussed in detail in **Chapter 2** of the thesis. Furthermore, it was also noted that different type of models are facing different problems based on their structure, complexity, and the data availability and quality.

The general problems and limitation of metric type models were discussed in detail in **Chapter 3** of this thesis. However, the metric type of models seems to be simpler in general than the other model types such as the conceptual and physically-based models and the parameters can be identified more easily. However, for the event based models, selecting the representative event seems to be a problem. The selection of the suitable type of model is a challenge in its own for the hydrologists as the type of model that can be successful for one area and under a certain conditions might not be successful in another application.

The review showed that there are some problems in using each type of model that need to be considered. Osborn and Lane (1969) suggested that the linear regression models might not always be able to predict the parameters accurately for extreme events, hence it was suggested to treat the low frequency events separately, using a different set of equations.

On the other hand, in using a unit hydrograph method, selecting a representative event can be very difficult as different events can have different hydrographs, storm durations and discharge peaks as Osborn and Lane (1969) showed. Wheater and Brown (1989) also faced some problems in their study as the individual unit hydrographs showed high variability, and they were unable to determine a consistent relationship to explain that

variability. Selecting a runoff coefficient was also among the problems faced by Wheater and Brown. The variation of the runoff coefficients and the transmission losses were found to have great effects on the hydrograph shape and analysis. The unit hydrograph method however, can be used in the analysis of individual or discrete events but not for continuous simulations or predicting effects of changes.

On the other hand, the GIUH seems to be an advanced metric model. GIUH was used by Nouh (1990) and Sorman and Abdulrazzak (1993a, b) who used sites in Saudi Arabia, as discussed previously. The model was found to be highly affected by some parameters that needed to be directly measured from the field, which makes it difficult to use in catchments with limited data. The results that were obtained by the model in this study seem to be acceptable. In addition, a methodology was suggested to estimate the peak discharge for ungauged catchments. However, model results showed that peak discharge and time to peak are highly affected by flood velocities and hydraulic conductivities. Groundwater levels were also found to have some effects on the results. On the other hand, Nouh (1990) found that the model performance is affected by the catchment size and does not recommend using this model for catchments with areas greater than 400 km^2 and for the high infiltration rate catchments.

The report also discussed the application and results of six conceptual models namely; MODHYDROLG, Pitman model, VTI, GSFB, IHACRES, and LASCAM model.

MODHYDROLG was applied to many different catchments in Australia of which many were arid catchments. The results seem to be satisfactory in most cases and the model can be considered suitable for simulating stream flow in general. The model is basically a conceptual model with many physically-based parameters. However, the model uses 19 parameters, which makes it among the more complex models that need a large amount of data. Chiew and McMahon (1994) had to adjust some parameters and adopt some recommended values from other studies. The model was found adequate to be used with optimisation of only 9 parameters.

The studies showed that modelling arid and semi-arid catchments was more difficult than modelling the wetter catchments due to the processes governing the relationship between rainfall and runoff in arid areas. The most important finding about this model was the difficulty it is facing in simulating long periods of zero flows that were followed by peaks. This puts its suitability under question. It might be necessary to investigate the reasons and check the possibility of overcoming this problem.

The Pitman model is a monthly time-step conceptual model that is used widely in Africa. Hughes (1995) highlighted that this model has some problems when used in arid catchments. The model can overestimate the catchment absorption and storage threshold. Hence, it underestimates the maximum runoff. Some modifications were found necessary to adjust this problem. However, although the modifications that Hughes (1995) has applied to the model have improved the performance of the model, but the difficulties in adopting this model in arid and semi-arid areas remained. However, the input data quality was questionable. Hence the effect of the data quality on the model performance should also be considered. This problem is an important problem that needs to be considered when studying arid areas.

VTI is another model that was discussed in the report. The model has high ability in generating the runoff beside the facility it has in providing a transmission loss routine. Both facilities are important for modeling arid areas. The application that was reviewed in this report (Hughes, 1995) did not obtain highly accurate results, though it was difficult to know weather that was due to the model structure or the data quality. However, the model needs a large number of data that might not always be available in arid areas.

GSFB, on the other hand is a simple conceptual model. It has only 8 parameters that need to be specified in which some of these parameters can be fixed as mentioned above. However, Ye et al. (1997) showed poor results and the model's performance in dry conditions was questionable.

IHACRES is another conceptual model that was reviewed. It is considered to be a hybrid metric/conceptual model of average complexity. The model was tested in some low yield catchments in Australia (Ye et al., 1997). It should be noted that the effective rainfall model is typically used for humid areas but the authors did introduce two extra parameters for use in low-yield catchments (**Section 4.3.2**). The model showed high performance and accuracy, though the performance increases when used for monthly rather than daily analysis. In another study (Post & Jakeman, 1999), it was found that regional relationships between hydrologic response characteristics and landscape attributes could be used to predict the daily streamflow of ungauged catchments from an appropriate rainfall and temperature time series. However, the study showed some inadequate results for some catchments. The authors explained this by the poor understanding of the relationships between the landscape attributes and the hydrologic response characteristics.

Evans and Jakeman (1998) introduced the catchment moisture deficit (CMD) to the model and tested it in selected wet catchments in USA and semi-arid catchments in Australia. However, the authors were not able to use the appropriate ET values as data were not available. However, the model was believed to be suitable to provide the land surface feedbacks for a climate model. Further modifications to IHACRES were also carried out by Croke and Jakeman (2004), regarding the non-linear part of the model and the new version was tested on the same catchments that Evans and Jakeman (1998) used. The performance of the model improved but at present the modified models do not seem to be adequate to be adopted till further investigations are carried out to determine their performance in different areas, as well as understanding the modified model's limitations.

LASCAM is the last conceptual model that has been reviewed. This model was developed to predict the impact of land use and climate change on the daily trends of streamflow and salinity in forest supply catchments in Australia. It has 22 parameters (in which there are 17 potential flux paths). Hence, the model can be considered as a highly complex model that needs a high amount of data. LASCAM was tested by Ye et al. (1997) as was discussed in **Section 4.3.2.** The model seems to be suitable to be used for other arid areas if adequate data were available.

The report has also reviewed some physically based models that were used in dry conditions. KINEROS can be considered as one of the most important models developed to consider arid conditions. Wheater (1981) has used the model for a study in Sultanate of Oman, in which the model was found to perform successfully. The obtained results were found to be in a good agreement with the calculated peak discharge. The estimated time to peak was also found to be accurate. However, Michaud and Sorooshian (1994) in their study found that the model can not cope with medium to large catchment areas (greater than 100 km^2). As this contrasts with the study of Wheater (1981), it is a surprising finding that needs to be investigated further. As KINEROS is one of the most important models for arid areas and refine a finding which challenges its applicability is very important and must be assessed further. Investigation to determine the reasons behind the model's poor performance is essential to study the reasons and implications and to apply any possible improvement to overcome this problem.

El-Hames and Richards (1998) have developed another physically-based model that they claim to be suitable for use in arid areas as it considered the spatial hydrological

characteristics of these areas. The model was tested in Saudi Arabia and successful and reasonable results were obtained. The model has good ability to determine the transmission losses. However, the model was found to be sensitive to the rainfall bursts, and adequate time sequence is important but this is not always available in arid areas. However, the model can not be run with a personal PC as it needs a long CPU time for running the simulation. The model will need more investigations before judging its ability to represent arid areas and understanding its strong and weak points.

Reviewing the applications of the different models and model types showed that the performance of the model can be different from one model to another based on many factors. The model that can be successfully used in one area might not be suitable to be used in another area. Therefore, care should be taken to select the suitable model type with the acceptable complexity. It should be noted that selecting a complex, sophisticated model might not be of any benefit if the model does not consider the hydrological characteristics of the area and the values of the effective parameters can not be identified. The model selection needs to consider the size of the catchment, availability of data, climatic conditions, and the use of the results.

4.6 Conclusions

Rainfall data quality is very important to consider when carrying out rainfall-runoff modelling. Rainfall errors have been found to have remarkable effects on the results of rainfall-runoff modelling. Rainfall errors can be caused by instrument malfunction and accuracy, human errors, rainfall network coverage, etc. These errors will affect the calculated runoff and will lead to variable accuracy of outflow results. Investigation of the rainfall data to find out the source of this variability before using it in any model is advisable. It is important to determine how much effect each error source has. However, it is very important to bear in mind that, although the rainfall errors are important, there are some other errors such as those caused by the model structure and the estimation of the parameters values (Michaud & Sorooshian, 1994b). Lopez (1996) explained that the uncertainty in the spatial distribution of rainfall has great effects on the identification of the parameters in any distributed model.

From these studies it can be seen that it is obvious that rainfall errors will affect the rainfall-runoff modelling results but determination of the exact amount of error is not an easy task. The data quality in arid areas is generally questionable and this makes it even more difficult when modelling arid areas.

The difficulties in rainfall modelling were clear in many studies. (Wheater, 1991a,b) study faced a problem in defining the raincell whereas, in another study difficulties were found in estimating the extreme events which are rare in arid areas but no doubt of great importance, and having great effects on the annual properties.

It was found that lumped models can obtain different results from distributed models. Krajewski et al. (1991) in his study using a distributed model found that the model has higher response to temporal resolution of the input precipitation data than that of the spatial resolution. On the other hand, Krajewski et al. believed that the lumped models generally underestimate peak flows compared to the distributed models. However, it was suggested that the two-dimensional physically based models are more applicable to modelling the problems of optimal and spatial resolution (Krajewski et al, 1991). Ogden and Julien (1993) believe that the reason behind the failure of some of the hydrologic models in reflecting the effect of spatial and temporal rainfall variability is the application of single parametric values to rainfall intensity in space and time. Both models tested by Ogden and Julien (1993), the one-dimensional and the two-directional models, assumed a uniform rainfall intensity distribution over the whole catchment and have used a uniform distribution to allow the rainfall intensity to vary with time.

The review discussed some applications based on point estimate of rainfall, and a few based on radar estimates. From all the studies conducted in arid areas, it seems difficult to capture the rainfall that falls in different parts of the catchment, and even studies using relatively high density networks have shown how difficult that could be. Using radar seems to be a good alternative, potentially able to capture any rainfall at any part of the catchment at any time. However, that will depend on the radar resolution but it should be borne in mind that radar technology is very expensive and not all arid areas can afford it; besides that, a dense coverage of rainfall gauges would still be preferable to apply any necessary correction for rainfall amounts recorded by the radar. Also, radar can not effectively be applied in mountainous regions.

It can be concluded that rainfall characteristics in arid areas are more complicated in some aspects than the humid areas and have great effects on rainfall-runoff modelling. The quality and the network coverage make it a challenging task. Nevertheless, good knowledge of the rainfall characteristics together with a skilled modeller is important to obtain good rainfall-runoff relationships.

This chapter also reviewed different studies that were carried out in rainfall-runoff aspects in arid areas. The different models that were used and their performance were

discussed and the different problems were highlighted. The model's performances were found to be affected by many factors which include;

- The purpose of the study and how suitable the selected model for fulfilling this purpose
- The model type (metric, conceptual or physically-based model)
- The complexity of the model structure and the used parameters
- The hydrological characteristics of the studied areas
- The data availability
- The data quality
- The sufficiency of the modeller's experience in the used model and the studied area

All these factors are important to select the appropriate model to be used. The performance of the model and the obtained results can be affected negatively if the inappropriate model was selected.

The report showed that the different types of models that were discussed each have advantages and disadvantages, though some of the models seem inappropriate for use in arid areas as they do not consider the important hydrological characteristics such as the spatial and temporal variation of the rainfall and runoff or the infiltration losses beside the other factors.

Based on the review of the models and their documented applications in the literature, three models had been reported as being suitable in arid zones, and would be good to be further investigated as they represent the three different model types that represent; the metric, conceptual, and the physically-based types of model. These models are the GIUH, IHACRES, KINEROS. However, due to the time limitations, and as IHACRES is a hybrid metric/conceptual model, the GIUH model, which is representing metric models, was excluded and it was decided to focus on the two other models: KINEROS and IHACRES in the modelling study using data from a catchment in Oman. The two selected models are briefly described:

- **IHACRES**: This was found to be potentially appropriate to represent the conceptual type models. It is a hybrid metric/conceptual model of average complexity. The model structure was constructed to consider the different types of catchments and climatologies. The model has been applied to some dry regions and was found appropriate. Hence, it might be appropriate to test it using Oman's data to invistigate its performance in other arid parts.

- **KINEROS:** This model was found appropriate to be investigated as a physically-based model. This model was developed to consider the spatial hydrological characteristics of the arid areas. The model was tested in Oman by Wheater (1981) and found appropriate, whereas Michaud and Sorooshian (1994a) found some difficulties in applying it for catchment areas larger than 100 km^2. It will be useful to test the model in a catchment with the new data in Oman to check its validity and performance. The model is a discrete event model that is believed to have been improved recently to consider continuous events. It will be very useful to test the version of the model and check its performance and study its limitations.

The details of these models and their applications using Omani data are discussed in the following chapters.

Chapter 5

Study Area Description and its Hydrology

5.1 Introduction

The literature review of **chapter 2** discussed the most distinct hydrological features of arid areas which are expected to affect any hydrological study and should be considered. It is important to consider these features in any rainfall-runoff modelling for arid areas.

Chapter 4 reviewed different studies that were carried out in rainfall-runoff aspects in arid areas. The different models that were used and their performance were discussed and the different problems were highlighted.

Based on these reviews, it is recommended to investigate two different model types that represent conceptual and physically-based model types. The validation and limitations of each of these models can be investigated through their application using data from an arid area. As Oman is classified as arid, a study site that is located in Oman was thought to be suitable to be used.

This Chapter describes the selected site and its hydrological characteristics.

5.2 Overview on Oman's Location and Hydrology

5.2.1 Oman's location

The Sultanate of Oman is one of the arid countries that located in the southeast of the Arabian Peninsula. It is located in the southeast of the Arabian Peninsula. It is neighboured by Saudi Arabia from the west, United Arab Emirates from the northwest, Yemen to the south east and the Gulf of Oman and the Arabian Sea from the east.

Figure 5.1 shows the location of Sultanate of Oman.

Figure 5.1 also shows the administrative regions that Oman is divided into namely; Muscat Governorate, Musandam Governorate, Dhofar Governorate, Al-Batinah Region, Dakhliyah Region, Dhahirah Region, Al-Wusta Region, and Al-Sharqiyah Region.



Figure 5.1: The location of Sultanate of Oman and the administrative regions *(after MWR, 1995)*

The location of Oman has great effects on its hydrological characteristics, climate, and geology, hence it is important to highlight these in this study.

5.2.2 Oman's General Geomorphology and Geology

There is a mountain chain of about 700 km length that runs along the coast from Musandam to Sur (Al-Sharqiyah Region), rising to about 3000m. This mountain chain divides Oman's wadis into two types; wadis to the north of the chain that drain to the coast, and the wadis that drain to the south of the chain to the interior plain (inland) or the desert.

The origin of Oman's geology and structure is believed to lie in the formation of the Arabian Plate about 800 million years ago, where sediments of different age were deposited, and then experienced different periods of folding and faulting. The rock outcrop age ranges from 800 million years to recent formations and the character varies from metamorphic and igneous to sedimentary.

The general geology of Oman is shown in **Figure 5.2**, whereas, the general geomorphology is shown in **Figure 5.3**.

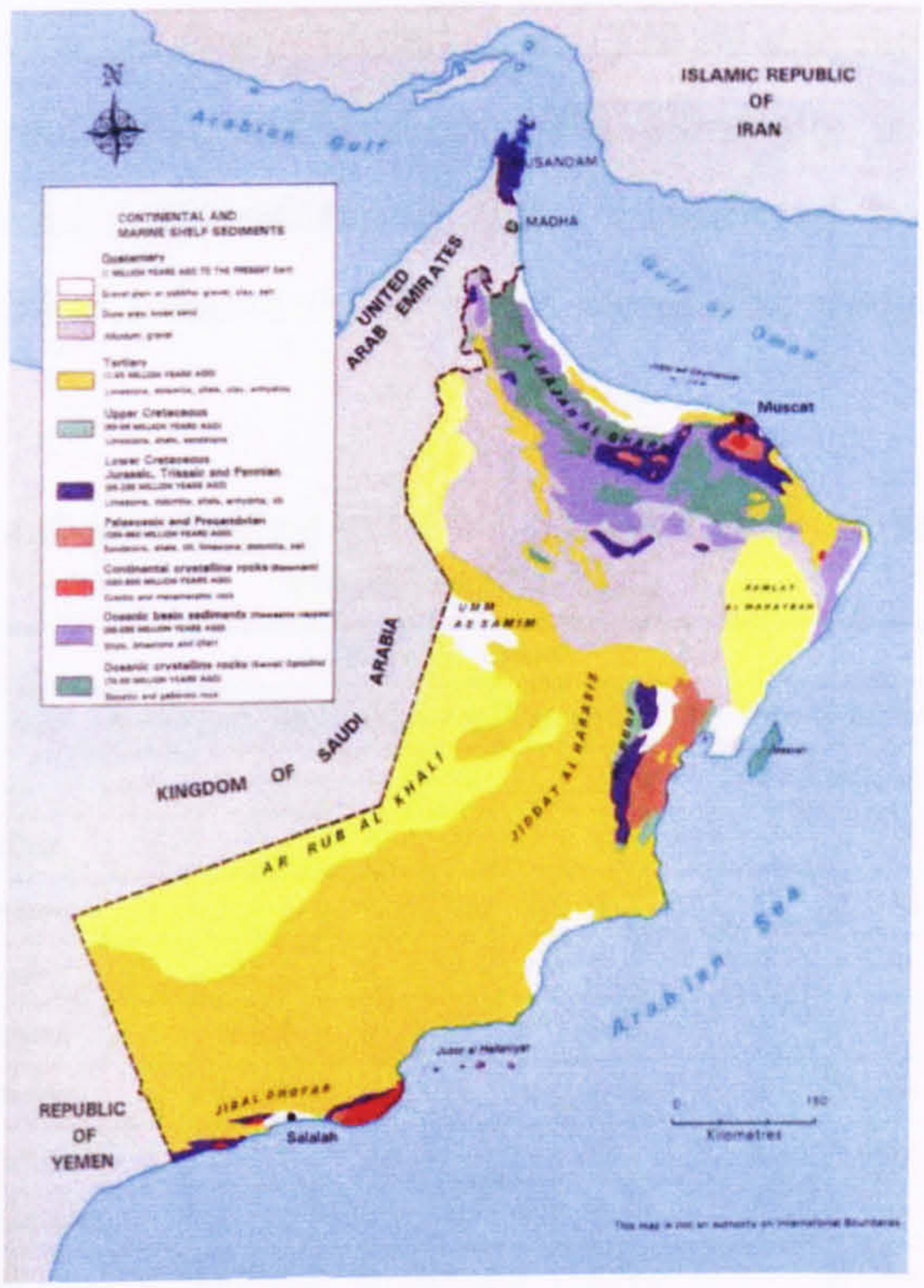


Figure 5.2: Oman's general geology (*after MWR, 1995*)

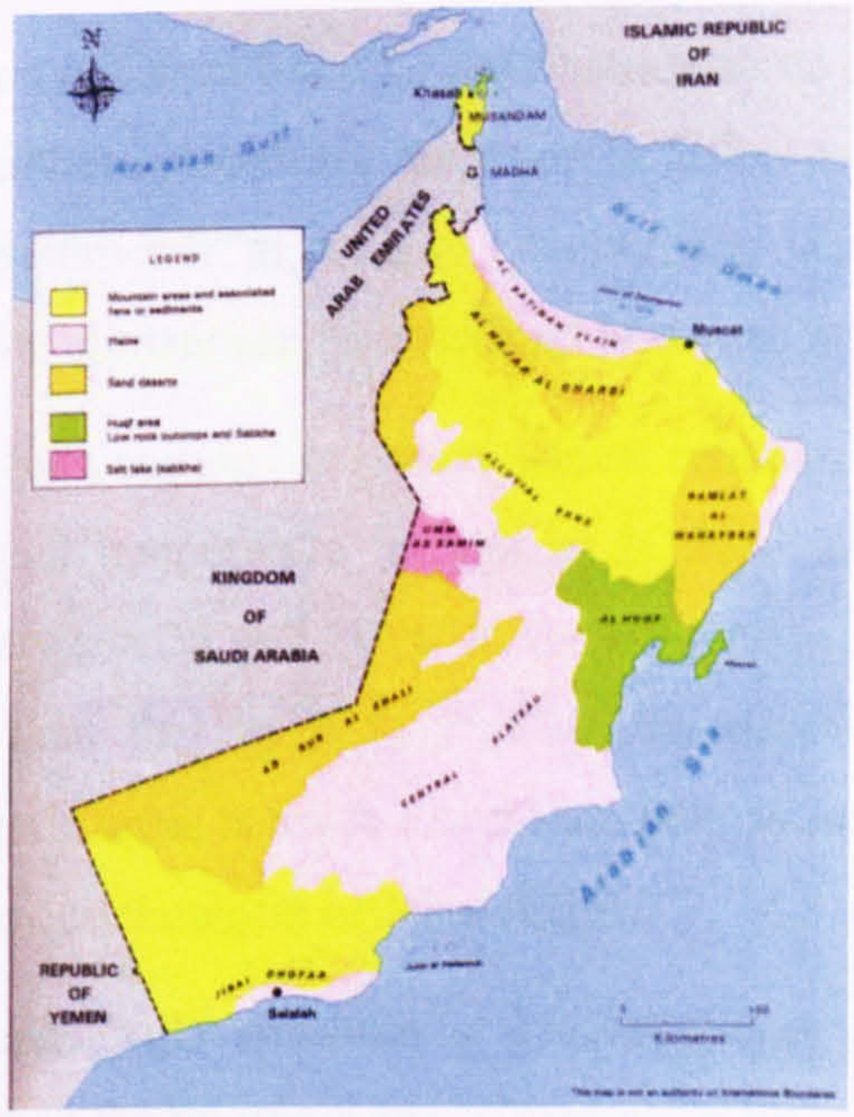


Figure 5.3: General morphology of Sultanate of Oman (*After MWR, 1995*)

5.2.3 Oman's General Hydrology

Oman is classified as an arid country. Hence, the hydrological characteristics are generally similar to these of other arid areas as have been described in detail in **chapter 1**.

Continuous data collection in Oman started from 1970 though there was one rain gauge in Muscat for which records started in about 1894. Generally, the monitoring network collects: climate, rainfall, surface runoff, aflaj (traditional irrigation system), and groundwater data. **Table 5.1** shows the different monitoring gauges that are distributed nationwide.

Table 5.1: National monitoring network gauges (*after Al-Sulaimani and Al-Obaidani, 2003)*

National Monitoring Points											
Region	Wadi Flow	Peaks	Dams	Rain Gauges	Wells	Aflajes	Springs	Khawrs	Discharge	Salinity	Total
Muscat	15	5	1	34	176	17	5	0	0	56	309
S. Batinah	23	1	4	31	130	73	16	0	0	98	376
N. Batinah	29	7	4	56	229	24	0	0	0	60	409
Musandam	4	0	1	14	90	1	0	0	0	0	110
Ad Dhahirah	18	0	1	32	519	89	0	0	0	123	782
Ad Dhakhliyah	19	1	5	51	354	113	6	0	0	189	738
N. As Sharqiyah	13	1	0	43	211	169	0	0	40	171	648
S. As Sharqiyah	5	4	1	17	143	40	0	0	0	85	295
Dhofar	10	0	1	63	217	0	37	11	139	488	966
TOTAL	136	19	18	341	2069	526	64	11	179	1270	4633

5.2.3.1 Climate

The geographical location of Oman has a large influence on its climate. It is located in a zone where different weather systems are dominant in different seasons. There are only two seasons in Oman: Summer from April to October, and Winter, from November to March (MWR, 1995). The climate can be described briefly as below:

- ***Temperature:*** The temperature in Oman varies considerably from one area to another. The mean annual temperature in Muscat is from 30 to over 40° C during summer whereas it is between 26 and 29° C in the lowland areas, as in the Dakhliyah Region, and is higher than that by 6 to 8° C in the desert areas. However, the temperature in the mountain areas is much lower than that; snow can occur in the winter in Jabel Shams sometimes, to the north of Jabel Akhdar.

- ***Daily sunshine hours:*** Daily sunshine is generally over 10 hours except in the mountain areas as well as in the Southern area (Dhofar), in Khareef time (from mid June to mid September) where the sunshine is less.

- ***Wind Velocity:*** Wind velocities (at 2 m above the ground level) are generally in the range of 2 to 3 m/s.

- ***Evapotranspiration:*** The high temperature and low humidity cause high evaporative conditions in the interior (inland areas). The mean potential evapotranspiration is very

high and it could be up to 3,000 mm per annum in the inland areas (areas far from the Coast), in Al-Batinah is about 2,100 mm, whereas in Salalah Plain it is about 1,700 due to the influence of the monsoon.

- ***Meteorological Stations:*** There are several meteorological stations in the Sultanate of Oman. Most of these stations are operated by the Ministry of Transportation and Communication although there are some that are operated by the Ministry of Regional Municipalities, Environment and Water Resources, the Ministry of Agriculture and Fisheries, and the Petroleum Development of Oman (PDO). These stations are located mainly in Muscat, Al-Batinah, and Al-Sharqiyah regions.

5.2.3.2 Rainfall

Rainfall in Oman varies widely through time and space, as in other arid areas. The long-term annual average rainfall amounts vary from 50mm in central Oman to 300mm in the mountain area in the north and Dhofar. There is a great variation in the rainfall amounts from one year to another. For example, one dry year can be followed by a series of two or three wet years.

- ***Rainfall generation mechanisms:*** The principal mechanisms causing rainfall in Oman, as described in MWR (1995), could be classified as the following:

a) Cold frontal troughs: this mechanism occurs normally in the central and southern parts of Oman. It is more common in winter and early summer. It is associated with the eastward moving extra-tropical depressions that originate largely over the North Atlantic Ocean or Mediterranean Sea.

b) Tropical cyclones: these cyclones move from the Arabian Sea and affect mostly the southern and eastern coast. They occur in the Dhofar Governorate and Masirah Island more than in Muscat Governorate. These are not very common but when they do occur, usually between May and December, they can cause very heavy rainfall.

c) Advection of a deep layer of cold air moving from central Asia through the Arabian Gulf to the southeast of Oman. This layer can cause heavy rainfall and can occur about three times on average per year.

d) On-shore monsoon currents: this type is caused by the surface air flow over the Arabian Sea dominated by the strong southwesterly current which feeds the monsoon circulation of south Asia. Mostly, the Dhofar Governorate is the one that is affected by this mechanism. Extensive stratiform cloud and frequent drizzle (called Khareef season)

occurs in Dhofar when an off-shoot of this flow and another air stream originating over the Gulf of Aden mix together.

e) Scattered convective showers over the eastern mountains sometimes occur due to penetration of shallow monsoon currents moving inland towards UAE. This affects the Dhofar Mountains during June and July causing high humidities, low potential evaporation and semi-persistent fog.

- ***Rainfall Monitoring Network:*** There are over 300 rainfall stations as can be seen in **Table 5.1** spread over the different regions in Oman.

Most of the old, long term, stations recorded daily data but an attempt was made recently to update all these stations and new automatic stations were installed. The quality of the data varies considerably though the newer stations show better data quality than the old ones in general.

- ***Rainfall Frequency Analysis:*** Rainfall frequency analysis showed that very high events can occur in Oman. 1-hour rainfall of 84mm was reported in the Muscat vicinity in Nov 1997 in Luzugh and 74 mm at Amyrat, whereas the greatest 1-day rainfall was 424mm in Masirah Island on 13th Jun 1977, and 286mm in Muscat in June 1890 (both before continuous records began). These events are not expected to be a result of a 24-hour steady rainfall. They are expected to have 12-hour totals of at least 212 mm and 143 mm respectively, which are higher than the greatest 12-hour rainfall that have been officially recorded in Oman (MWR, 1998).

Table 5.2 shows the maximum rainfall intensities recorded in Oman at any rainfall recording station for 15, 30-min, 1, 2, 3, 6, 12, and 24-hrs.

The method used was peak-over-threshold where the total number of peaks where made to equal to the number of years on record of flood peaks, using a lumped station-year approach. A log-normal frequency distribution was derived. Individual station analyses for stations of a record period of more than 10-years were also carried out to be compared with the results obtained from the station year approach (MWR, 1998).

This analyses show that there are very considerable differences between the frequencies derived for different stations, for example the 50-yr, 6-hr rainfall is 45mm at Al-Fulayj whereas it is 114mm at Al-Muqayfah. This shows that there is a need to differentiate between areas of low and high rainfall intensity characteristics (MWR, 1998). **Table 5.3** shows the general rainfall frequency for all the recording stations in Oman.

Table 5.2: 5 greatest rainfall intensities recorded in Oman durations 15-minutes to 24-hours

Rank	1	2	3	4	5
15 Minutes					
Rainfall (mm)	48	43	39	37	37
Location	Darsait	Ibra	Sayh Khatum	Nizwa	J Harim
Date	3.5.81	10-11.4.90	5.12.91	7-8.7.82	20.7.88
30 Minutes					
Rainfall (mm)	74	69	52	52	52
Location	Darsait	Ibra	Nizwa	Nuway	J Hayl
Date	3.5.81	10-11.4.90	7-8.7.82	27.7.95	25-27.7.95
1 Hour					
Rainfall (mm)	84	76	74	72	70
Location	Darsait	Ibra	J Shams	Nuway	Al Khadrah
Date	3.5.81	10-11.4.90	27.28.7.88	27.7.95	21-22.7.90
2 Hours					
Rainfall (mm)	90	88	81	77	77
Location	Darsait	J Shams	Ibra	Nuway	Madruj
Date	3.5.81	7-9.7.94	10-11.4.90	27.7.95	27.7.88
3 Hours					
Rainfall (mm)	98	96	95	83	79
Location	Ibra	Darsait	J Shams	Izki	Madruj
Date	10-11.4.90	3.5.81	7-9.7.94	24-26.2.90	27.7.88
6 Hours					
Rainfall (mm)	109	106	101	99	97
Location	Ibra	Al Muqayfah	J Bani Jabir	Darsait	Izki
Date	10-11.4.90	30.3.97	7.6.96	3.5.81	24-26.2.90
12 Hours					
Rainfall (mm)	129	119	118	115	112
Location	Dahiyah	Izki	J Shams	Al Muqayfah	Qahlah
Date	23-26.2.82	24-26.2.90	21-25.7.95	30.3.97	25-27.2.90
24 Hours					
Rainfall (mm)	152	137	135	133	131
Location	J Shams	Dahiyah	Yanbu	As Sabukh	Al Khan
Date	21-25.7.95	23-26.2.82	16-19.2.88	16-21.2.88	16-19.2.88

Table 5.3: General frequency of rainfall intensities for all Oman (Semi-Log analysis for all 1012 station-years (85 Stations) (MWR,1998)

Duration hours	Rainfall (mm) for the Following Return Periods:						
	Av	5-yr	10-yr	20-yr	50-yr	100-yr	200-yr
0.25	15	19	22	25	29	32	35
0.5	20	26	31	36	42	47	52
1	25	32	38	45	54	60	67
2	28	36	43	50	60	67	74
3	30	39	47	54	65	72	80
6	34	44	53	62	74	83	92
12	39	50	61	73	88	99	111
24	44	58	71	85	104	118	132

The investigation showed that the best criterion for categorising the stations was the terrain. Hence, the stations were classified as: mountain (with elevation over 1000 m. a. m. s. l.), hills (close to hills or mountains), and plain stations (close to the coastal areas). It was noticed from the analysis that the mountain stations have higher average annual rainfall intensities and tend to have slightly less steep frequency plots than hill stations,

whereas plains stations tend to start low and remain relatively low. **Table 5.4** shows a summary of the frequency analyses within these categories.

Table 5.4: Frequency of rainfall intensities for plains, hills and mountains

Plains Areas (287 Station-Years, 21 Stations)							
Duration hours	Rainfall (mm) for the Following Return Periods:						
	Av	5-yr	10-yr	20-yr	50-yr	100-yr	200-yr
0.25	13	16	20	23	27	31	34
0.5	17	21	26	30	36	41	45
1	20	25	31	36	44	50	55
2	22	28	35	41	49	56	62
3	24	31	38	45	54	62	69
6	28	35	43	51	61	69	77
12	31	39	48	57	69	78	87
24	35	44	56	68	83	94	106
Hill Areas (504 Station-Years, 41 Stations)							
Duration hours	Rainfall (mm) for the Following Return Periods:						
	Av	5-yr	10-yr	20-yr	50-yr	100-yr	200-yr
0.25	15	18	21	24	28	31	35
0.5	21	26	31	36	43	48	53
1	25	32	38	45	54	61	67
2	28	36	43	50	60	67	74
3	31	39	47	55	65	73	81
6	35	44	53	63	76	86	96
12	39	50	62	75	91	104	116
24	44	57	71	86	105	120	135
Mountain Areas (221 Station-Years, 22 Stations)							
Duration hours	Rainfall (mm) for the Following Return Periods:						
	Av	5-yr	10-yr	20-yr	50-yr	100-yr	200-yr
0.25	18	21	24	27	31	34	37
0.5	24	29	34	39	45	50	55
1	31	38	44	51	59	66	72
2	35	43	50	58	67	75	82
3	37	45	53	61	71	78	86
6	42	51	59	68	79	88	97
12	48	59	70	80	94	104	114
24	56	70	83	96	113	125	138

However, it should be noted that the data period of record that was used is very short (less than 10-years in some stations and less than 20-years in most of the rest) and it is necessary to review these results when long period data is available in the future.

5.2.3.3 Runoff

There are no continuous rivers in Oman but wadi channels that are dry except if there is a heavy rainfall event, when there is flow. The general runoff characteristics are mostly the same as in other arid areas as described in **Chapter 2.**

It would appear that very large floods indeed can occasionally occur in Oman in the order of 50% to 90% of the world maximum as **Figure 5.4** shows. The highest floods relative to world maximum can probably only relate to relatively small catchments with times of concentration of a few hours. The heavy long duration storms of several days which occur in some monsoonal countries are not very normal in Oman. Hence beyond

catchment areas of 2,000km^2 or so, the percentage of world maximum would be expected to drop off for Oman (MWR, 2000a).

However, it is also possible that some of the highest floods in Oman have resulted from landslips within gorges, which dammed the gorges but after subsequent breaches, flood waves may have passed downstream. They may not all therefore have reflected natural flood conditions (MRMEWR, 2001).

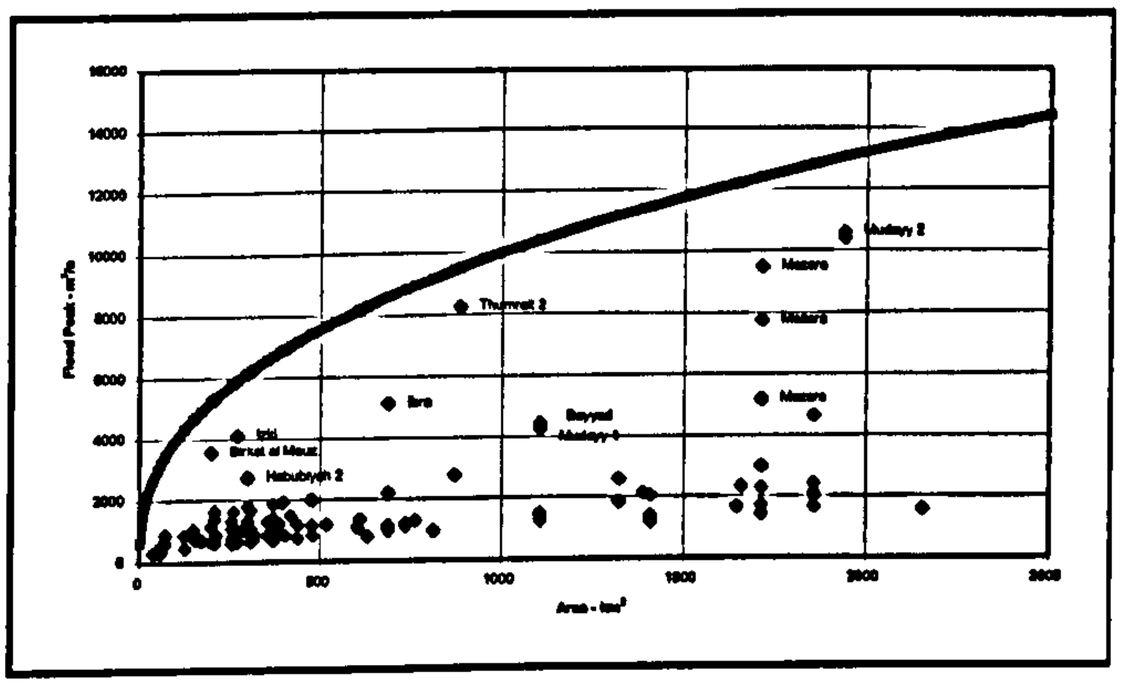


Figure 5.4: Greatest recorded flood peaks in Oman compared with world maximum curve developed by Rodier, 1984 ***(After MRMEWR, 2001)***

- ***Flow Monitoring Network:*** There are over 150 wadi gauge stations that are spread out over different hydrological basins in Oman (see **Table 5.1**).

Mainly, there are three different types of wadi gauges; datapod recording type (electronic data loggers with pressure transducers), bubble gauges with chart recorders, and stilling well-float type gauges with chart recorders.

Indirect measurement such as slope-area measurement and flow through culverts method are often used after floods and the obtained values are used to verify the gauged peak discharge, and to replace it during gauge failures. Indirect measurements are also used in plotting the rating curves for high flood peak values while the low flows are obtained by direct measurements such as current meter measurements. However, it should be noted that direct wadi flow measurement is difficult in most arid areas due to the difficult access to the wadi during floods, channel geometry, high sediment loads, and the flash nature of floods, etc. (Al-Qurashi, 1995). The direct way of measurement, therefore is not always appropriate as the flow gauges can be washed away during severe floods.

- ***Flood Frequency Analysis:*** Flood frequency analysis is very important for forecasting the frequencies of future floods. It is also very important in design of hydraulic structures and flood protection schemes. However, it is not any easy task due

to the spatial and temporal variation of rainfall and runoff, short period of records, and quality of the available data. It is very difficult to identify the appropriate statistical distribution for describing the data and to estimate the parameters for the selected distribution. In arid areas, where normally low to moderate floods are dominant, the possibility of a sharp upward curvature may appear due to a high peak that can occur infrequently. The suggestion was made to eliminate the zero flood peaks from the flood frequency calculations to compute a provisional frequency curve for the remaining years and then adjusting the exceedance frequency by the ratio of the number of years with runoff. It was also suggested that in the upward curvature, only the upper half (medium to high flow) of annual events should be fitted with a theoretical frequency curve. Detecting the outliers (data points that depart significantly from the trend of the remaining data) was found to be difficult as the coefficients of the variation of annual flood peak are high, records are short and the potential for measurement error is high (MWR, 2000a).

Flood peaks and flows in flash flood wadis are usually difficult to measure directly, hence empirical equations or indirect measurements are used and therefore measurements errors are much higher. The use of regionalization techniques for flood estimation incorporating unbiased estimators of probability weighted moments which is known as L-moments were found useful. The regional flood frequency analysis for a number of combinations of regional groupings in order to identify areas of homogeneity with respect to flood characteristics was carried out (MWR, 1998). These criteria included; topography (hill, mountain, and plain), administrative regions, catchment areas, catchment rainfall. It was found that the topographic criteria seem to be the best criteria to be adopted.

- ***Aflaj:*** Aflaj (single is falaj) are old irrigation systems that have been used for hundred of years in Oman. **Figure 5.5** shows a picture of one of these aflaj. Mainly, there are three different types of aflaj; dawudy which originates from the groundwater table; ghayli which depends on wadi baseflow; and ayni which depends on springs. The flow in aflaj is measured using current meters. Aflaj as can be seen can be either groundwater like dawudy and spring type, or surface water (from wadi) as ghayli type.



Figure 5.5: A photo of a falaj in Oman

5.3 The Selected Basin

Wadi Ahin basin was selected for this research. Wadi Ahin is located in Al-Batinah Region which is considered to be one of the most populated regions in Oman. It is one of the catchments that have been studied intensively from different aspects (Mott MacDonald, 1991, 1992; Al-Qurashi, 1995), as it is well covered by hydrological data compared to the other catchments in Oman. These studies were serving different aims ranging from Master Plan project or groundwater scheme, to research purposes. This was found to be useful as some essential data and information for the modelling can be extracted from these previous studies, and used for comparison with some new results.

The total catchment area of this catchment upto Majis Kabirah is. The catchment can be subdivided into two areas; Ahin West (up to Wadi Ahin nr Hayl, 734km^2) and Ahin East which include Ahin near Majis Kabirah (879km^2) and left and right channels flow gauges, see **Figure 5.6**.

Wadi Ahin is classified as having a moderate rainfall regime. The long term annual average is about 152mm for the upper part of the catchment (Ahin West) and 102mm for the lower Ahin catchment (Ahin East).

The bedrock lithology shows that the catchment consists generally from ophiolite which makes its permeability low.

Figure 5.6 show the catchment general location and its subdivisions, whereas **Figure 5.7** shows the DEM of Wadi Ahin catchment.

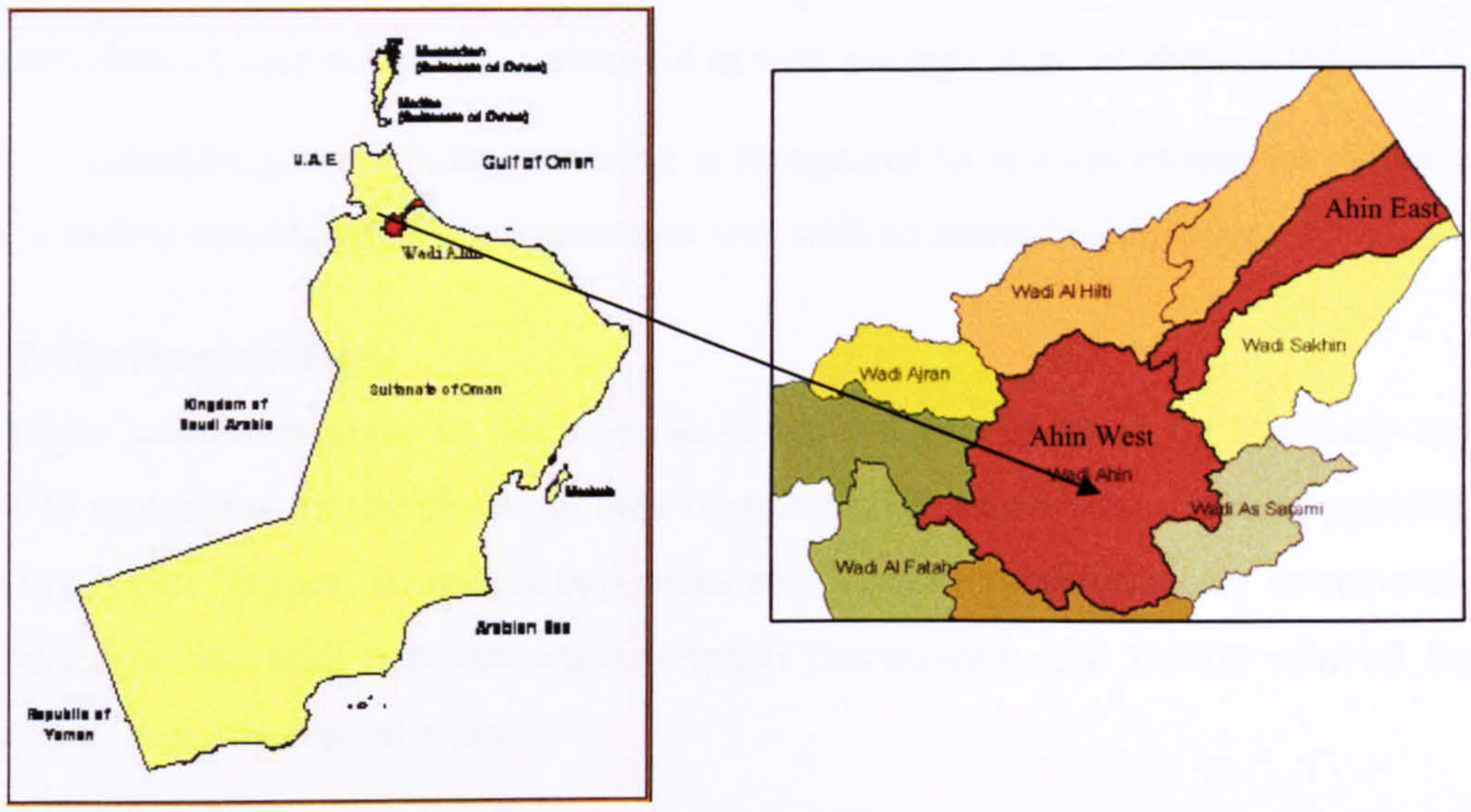


Figure 5.6: Wadi Ahin location in relation to Sultanate of Oman and its neighbouring catchments

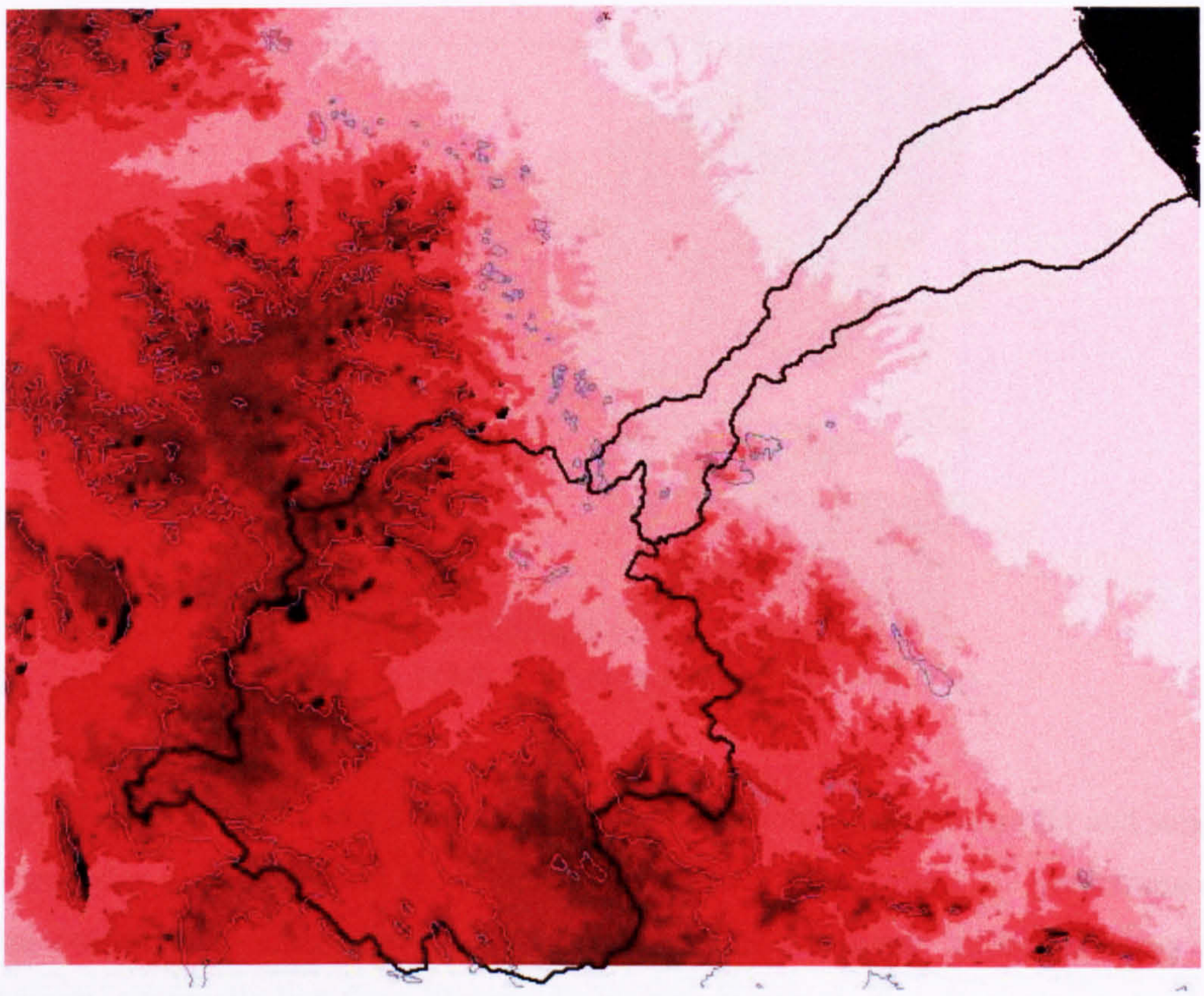


Figure 5.7: Wadi Ahin DEM

5.3.1 Wadi Ahin Topography and Geomorphology

The wadi channels are better defined in the upper catchment than in the coastal areas, where the wadi flows in a series of channels that are more difficult to define. Elevations range from greater than 1,300 m in mountain areas to near sea level on the plains. The

typical channel slope in the upper catchment ranges from 0.1% to 0.32%. The width of the main channel near the gauge is about 54 m with average slope of about 0.16%.

Only 1 distinctive goemorphological zone is recognised in this catchment; an ophiolite zone, which is considered as a mountainous area with an impermeable layer.

5.3.2 Hydrogeology

The upper catchment areas in Shinas-Liwa-Sohar are characterised by relatively low ophiolite mountains. In the piedmont area irregular hills and narrow ridges of ophiolite and Hawasinah Nappes, Aruma Group rocks and Tertiary limestones, are interspersed with thin alluvial wadi deposits which expand downstream into thicker alluvial fan deposits to form the coastal plain.

The simplified geology is shown in **Figure 5.8.** It illustrates the major geological and physiographic characteristics of the study area.

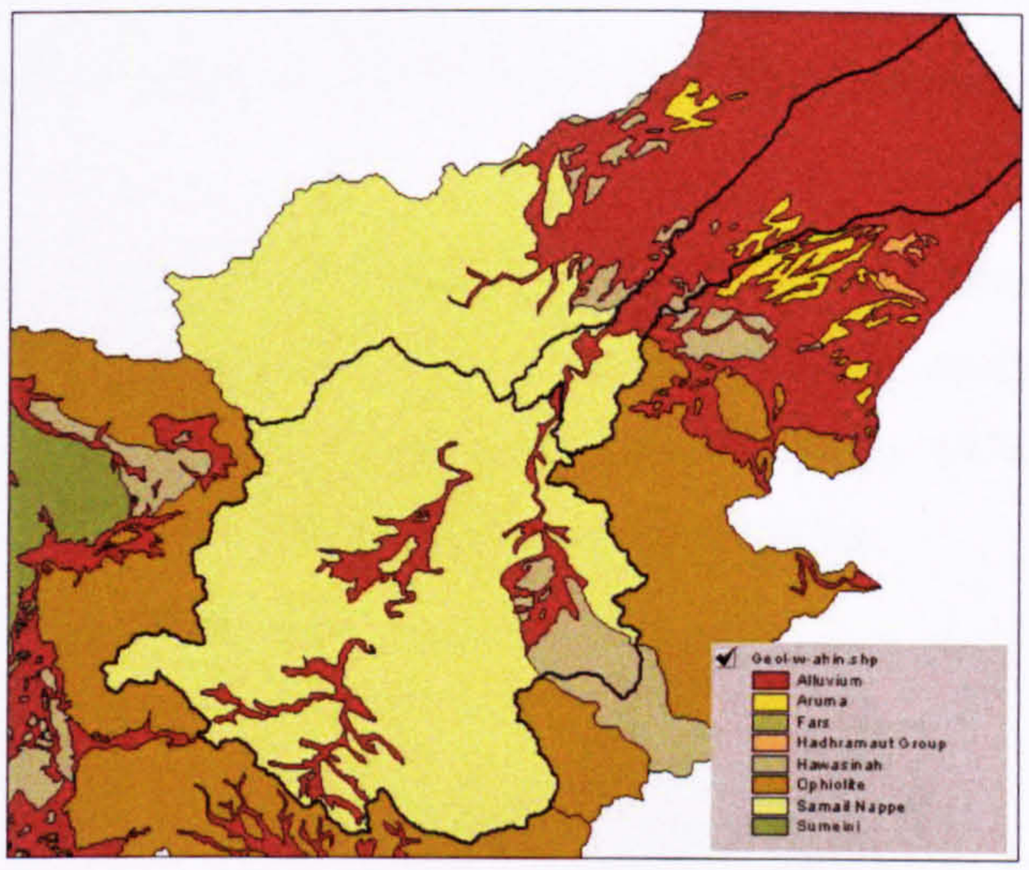


Figure 5.8: Wadi Ahin simplified geological map

- **Aquifer systems**

Alluvial deposits within the coastal plain collectively form the main aquifer and supply the majority of groundwater in the area. Groundwater abstractions are predominantly concentrated in shallow alluvium near the coast. In the upper catchment areas the alluvium is typically less than 20 m thick, ranging in composition from clay to boulder and in many instances has been weakly to strongly cemented. Well yields vary considerably depending upon the nature of the wadi deposits, their saturated thickness and degree of sorting and cementation.

- ***Fractured Hawasina sediments and Samail Nappe ophiolite*** tend to produce poor and unpredictable yields and are generally considered to be inferior aquifers. However

seepage from storage within the ophiolites is now recognised to be an important source sustaining aflaj and supplementing flow in the alluvium. Many villages, almost all of the aflaj, and a significant number of wells are located within the ophiolite jabals, indicating that these rocks have an important water resource function.

- ***The Hajar Super Group (HSG) rocks*** are not represented except for small outcrops of **Aruma Group** limestone, calcarenite and marl which have very limited development potential.

5.3.3 Wadi Ahin Hydrology

5.3.3.1 Rainfall

There are 10 rainfall gauges within the catchment. The locations of these gauges are shown in **Figure 5.9** together with the gauges in the neighbouring catchments, whereas photos of some of these gauges are shown in **Figure 5.10**. The details of these gauges are shown in **Table 5.5.** It should be noted that Tawi Badr rainfall station is used in the analysis as it is located in the border of Al Jizi and Ahin basins to represent the high elevation terrains.

All of the gauges are automatic except two (Haybi and Al Ghuzayfah) which are standard daily gauges, hence cannot be used for short duration analysis. Unfortunately, these gauges have the longest records (both established in 1974). However, these stations can be used as guides for determining storm locations.

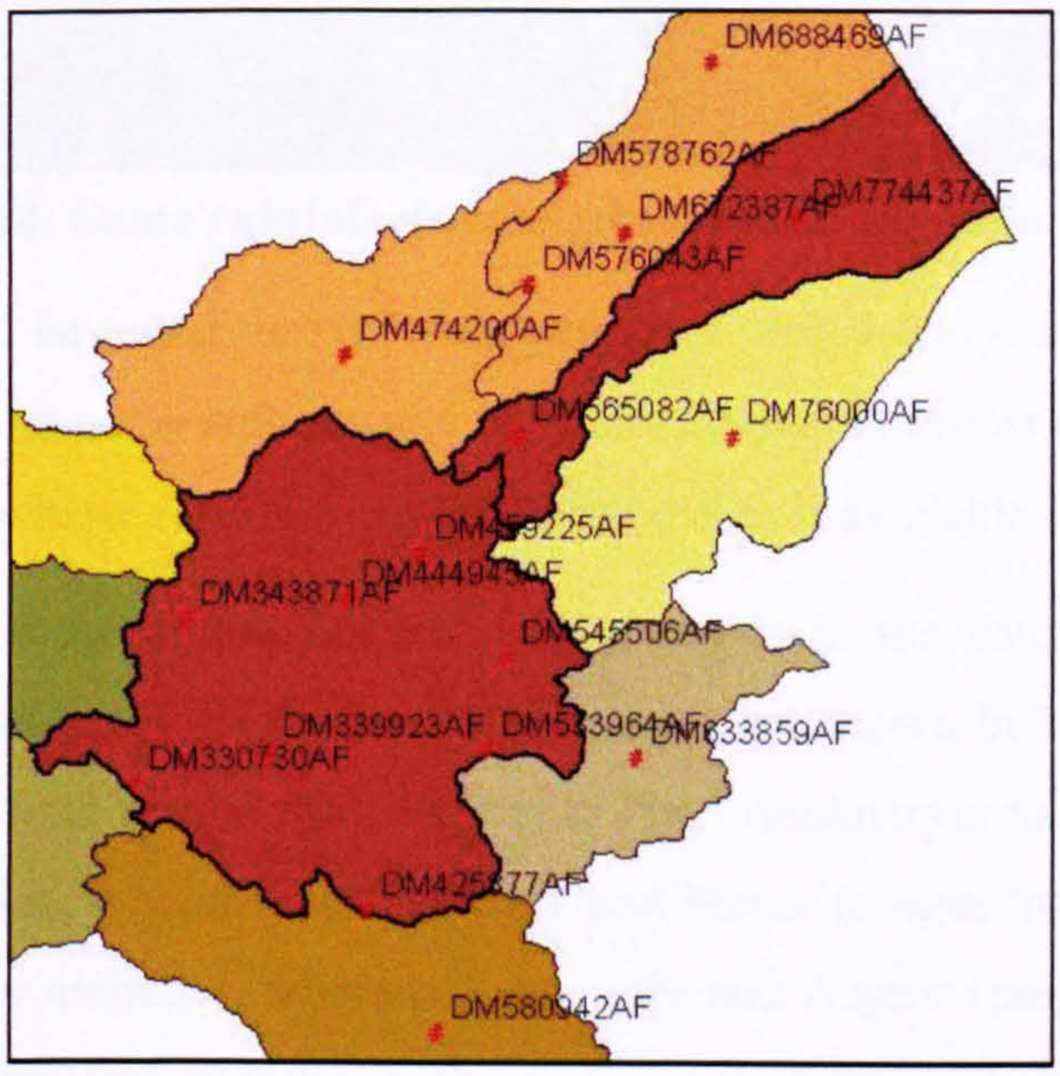


Figure 5.9: The locations of Wadi Ahin rainfall and neighbouring catchments gauges

Table 5.5: Wadi Ahin rainfall gauges details

Staion Id	Station Name	Basin	UTM-E	UTM-N	Zone	Type1	Ele(m)	Inspec.Freq	Begin of records
*DM330730AF	Tawi Badr	Al Jizi	430200	2637000	40	CASE	890	mon	10.01.95
DM339923AF	Al Waqbah	Ahin	439200	2639300	40	CH	750	mon	10.08.1983
DM343871AF	Al Hayl	Ahin	433700	2648100	40	CASE	890	mon	10.01.1995
DM425877AF	Al Masarah	Ahin	445700	2628700	40	CASE	910	mon	10.01.1995
DM444945AF	Qufays	Ahin	444400	2649500	40	CH	570	mon	1.10.1983
DM459225AF	Al Ghuzayfah	Ahin	449200	2652500	40	SD	520	daily	1.01.1974
DM533964AF	Al Khadd	Ahin	453600	2639400	40	CASE	1010	mon	25.04.1995
DM545506AF	Haybi	Ahin	455000	2645600	40	SD	540	daily	5.03.1974
DM565082AF	Hayl Ashkhariyin	Ahin	455800	2660200	40	CH	300	mon	4.07.1983

(a) Qufays Rainfall Station **(b) Khad Rainfall Station**



(c) Waqbah Rainfall Station **(d) Hayl Ashkhariyyin Rainfall Station**

Figure 5.10: Some rainfall stations photos in Wadi Ahin catchment

However, it should be noted that the data period of record that was used is very short (less than 10-years in some stations and less than 20-years in most of the rest) and it is necessary to review these results when long period data is available in the future.

To shed light on some of the rainfall characteristics in the catchment, the average monthly rainfall values for all the long term gauges are shown in **Table 5.6.** The table shows that annual total ranges from 98 mm at Hayl Ashkharyin to 143 at Al-Waqbah. For the winter season, it seems that February and March (ranges from 16-41 mm) have the highest monthly averages, whereas April, July and August (ranges from 4-17 mm) seem to be the dominant months in the summer though much less than the winter months.

Table 5.6: Average monthly and annual rainfalls 1975-99 (25 Years) for Wadi Ahin Catchment

Station	Station ID	Elev. m	25-Year Average Monthly and Annual Rainfalls - mm												
			Oct	Nov	Dec	Jan	Feb	Mar	Apr	May	Jun	Jul	Aug	Sep	Total
Hayl	DM271711B	520	1	1	6	12	41	23	13	2	2	7	4	2	116
Kitnah	DM260958B	650	1	0	7	14	35	23	12	2	1	12	10	3	121
Al Waqbah	DM339923A	750	3	1	4	13	29	31	12	5	5	15	17	8	143
Qufays	DM444945A	570	4	1	4	11	27	27	12	4	4	13	13	4	125
Haybi	DM545506A	540	9	3	2	11	28	25	12	4	5	15	14	11	140
Ghuzayfah	DM459225A	520	5	3	6	11	29	21	14	4	1	12	11	4	120
Ashkharyin	DM565082A	300	6	5	8	7	24	16	12	3	1	9	4	3	98

Note: 1. Data sets are all gap-filled to the water-year 1996. Some gaps occur since then.
2. The water-year for N Oman is Oct to Sep, for S Oman it is January to Dec

5.3.3.2 Wadi Flow

Wadi Ahin is one of the important catchments in Al-Batinah Region as has been explained previously. There are four wadi flow gauges within the catchment; one representing the upper catchment (Hayl), and three downstream (Majis Kabirah, Ahin left channel, and Ahin right channel). The details of these gauges are shown in **Table 5.7** and the flow gauge locations are shown in **Figure 5.11**.

It should be noted that the station DM4445808AD, shown in **Figure 5.11,** seems to be a temporary station that was established for flow monitoring to serve the studies carried out for Ahin dam, which is located few kilometres from Wadi Ahin near Hayl flow station. An attempt was made to get hold of its data but seems to be, unfortunately, lost.

Table 5.7: Wadi Ahin flow gauges

Station id	Station Name	Basin	UTME	UTMN	Type	DA	Elevation	Begin of records
DB 554869 AD	AHIN NEAR HAYL	Ahin	4546	26588	v	734	300	1.10.84
DB 872977 AD	AHIN NEAR MAJIS KABIRAH	Ahin	4828	26796	v	879	9	10.05.85
DB 875654 AD	AHIN LEFT CHANNEL NEAR KHISHDAH	Ahin	4855	26764	v	NA	9	1.01.84
DB 875650 AD	AHIN RIGHT CHANNEL NEAR KHISHDAH	Ahin	4856	26760	v	NA	9	1.01.84

Note: v means continuous recording station

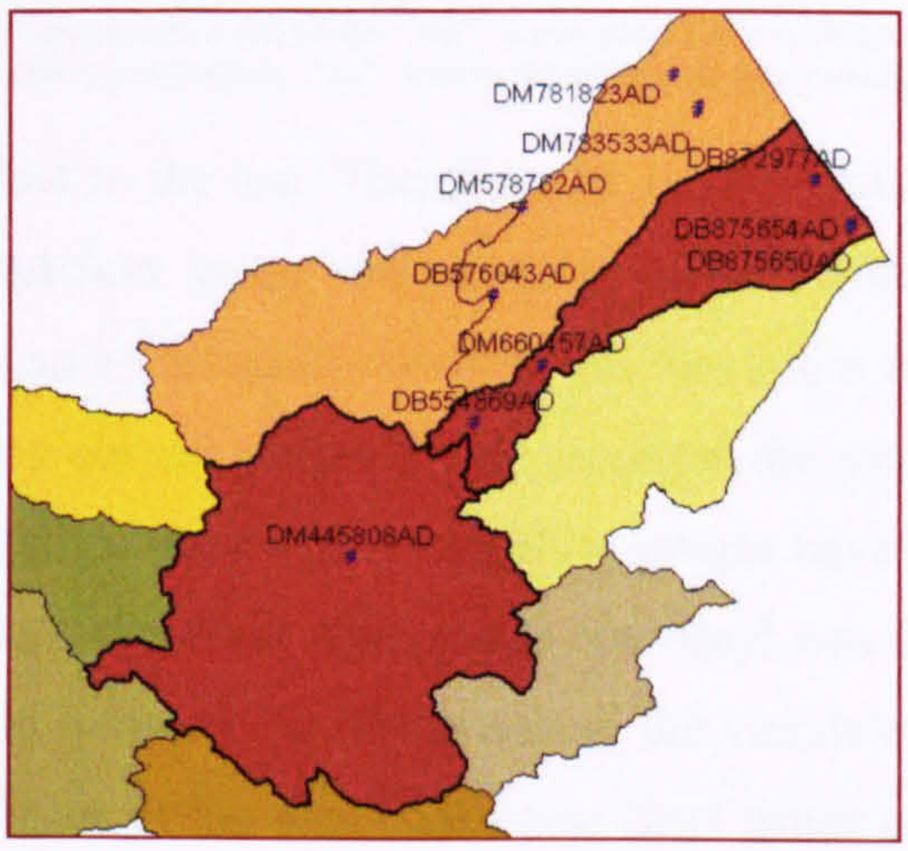


Figure 5.11: Location of Wadi Ahin flow gauges and the neighbouring catchments gauges

The annual total flow, as can be seen from **Table 5.8**, is about 29Mm^3 at Hayl, measuring the upstream part of the catchment, but only 0.9Mm^3 at Majis Kabirah, 2.1Mm^3 at the left channel, and 2.3Mm^3 at the right channel of the Kishdah gauges in which the total downstream flow will be only 5.3Mm^3. This highlights the amount of transmission loss between the upstream and the downstream channel. However, it should be noted that the catchment areas for the gauges at the Kishdah (the left and right channels) are unknown hence, the runoff per unit area can not be determined there.

The average monthly and annual flows are shown in **Table 5.8,** and the flood frequency analyses of all the wadi gauges are shown in **Table 5.9.**

Table 5.8: Wadi Ahin average monthly and annual flow (*MWR, 2000)*

Entire Period of Records (Usually to End of 1999)															
St No	Station	Wadi	Area km^2	Average Monthly and Annual Flows (Mm^3)													
				Oct	Nov	Dec	Jan	Feb	Mar	Apr	May	Jun	Jul	Aug	Sep	Annual
SS12	Hayl	Ahin	734	0.76	0.46	0.60	1.40	1.86	10.51	2.13	0.66	0.74	2.08	2.16	6.09	29.4
SS13	M Kabirah	Ahin	879	0.00	0.00	0.03	0.02	0.17	0.35	0.05	0.03	0.00	0.24	0.04	0.01	0.9
SS14	Khishdah 1	Ahin	-	0.01	0.00	0.34	0.06	0.76	0.26	0.25	0.06	0.02	0.20	0.11	0.02	2.1
SS15	Khishdah 2	Ahin	-	0 03	0 04	0 17	0 50	0 79	0 50	0 13	0.02	0 01	0 11	0.03	0 00	2.3
St No	Station	Wadi	Area km^2	Average Monthly and Annual Runoff (mm)													
				Oct	Nov	Dec	Jan	Feb	Mar	Apr	May	Jun	Jul	Aug	Sep	Annual
SS12	Hayl	Ahin	734	1.04	0.63	0.81	1.90	2.53	14.32	2.91	0.90	1.00	2.84	2.95	8.29	40.1
SS13	M Kabirah	Ahin	879	0.00	0.00	0.04	0.02	0.19	0.40	0.05	0.03	0.00	0.27	0.04	0.01	1.1
SS14	Khishdah 1	Ahin	-	-	-	-	-	-	-	-	-	-	-	-	-	-
SS15	Khishdah 2	Ahin	-	-	-	-	-	-	-	-	-	-	-	-	-	-

Table 5.9: Flood peak frequencies for all Wadi Gauges in Wadi Ahin catchment (POT Frequency Analysis), (*MWR, 2000*)

No.	Terr-ain Class	Plot Cate-gory	Station	Wadi	Station ID	Region	Period of Record	Area km^2	Mean (MAF) m^3/s	Return Period - yrs					Max World m^3/s
										5	10	20	50	100	
										Flood Peak Frequencies - m^3/s					
SS12	np	a	Hayl	Ahin	DB554869AD	N Batinah	82-99	734	405	574	765	955	1207	1398	1430
SS13	p	a,D	M Kabirah	Ahin	DB872977AD	N Batinah	83-99	879	59	115	221	326	465	570	9497
SS14	p	a,D	Khishdah 1	Ahin	DB875654AD	N Batinah	83-97	936	82	127	164	201	250	288	9739
SS15	p	a,D	Khishdah 2	Ahin	DB875650AD	N Batinah	83-99	-	37	59	77	96	120	138	NA

Notes : 1. Data period is since station installation, not including prior historic flood estimates made at some stations
2. Mean is mean of annual flood series, not peak-over-threshold (POT) series
3. "p" means wadi gauging station in the plains, "np" is non-plain (hills or mountains)
4. "a" refers to acceptable plot/trendline, "na" means not acceptable (poor trend)

The flow used to be lost to the sea. Therefore, in 1992 a recharge dam was installed downstream of the Hayl flow gauge and upstream of the coastal wadi flow gauges to capture the flow so it can be released slowly to get maximum recharge downstream of the dam area. Hence, the coastal gauges do not represent the natural wadi flow after the dam construction, and all of these three wadi flow gauges have been removed recently due to that reason. Hence, the Wadi Ahin gauge near Hayl was the gauge that was used here for the comparison between the observed and the simulated flows obtained using the selected models. Photos of the Wadi Ahin near Hayl gauge and its site are shown in **Figure 5.12.**



Figure 5.12: Wadi Ahin flow gauge and its wadi channel

The Wadi Ahin gauge near Hayl is located on the right bank, 200m upwadi from a road crossing, and about 1.5km southwest of Hayl village, covering a drainage area of 734km^2. Its elevation is about 300m (above mean sea level) as the topographic map shows. The gauge started in February 1983, measuring peaks only but continuous records started from October 1984 up to date.

The channel bed (see **Figure 5.12**) consists of sand and small cobbles and it bends from the gauge. The right bank is steep with irregular rock cliffs. The left bank is re-cemented conglomerate overlain above medium flows with boulders or large cobbles with the lower end of the reach subject to scour and fill.

Figure 5.13 shows the channel cross section at the gauge vicinity (the PZF point represents the point of zero flow at the cross section).

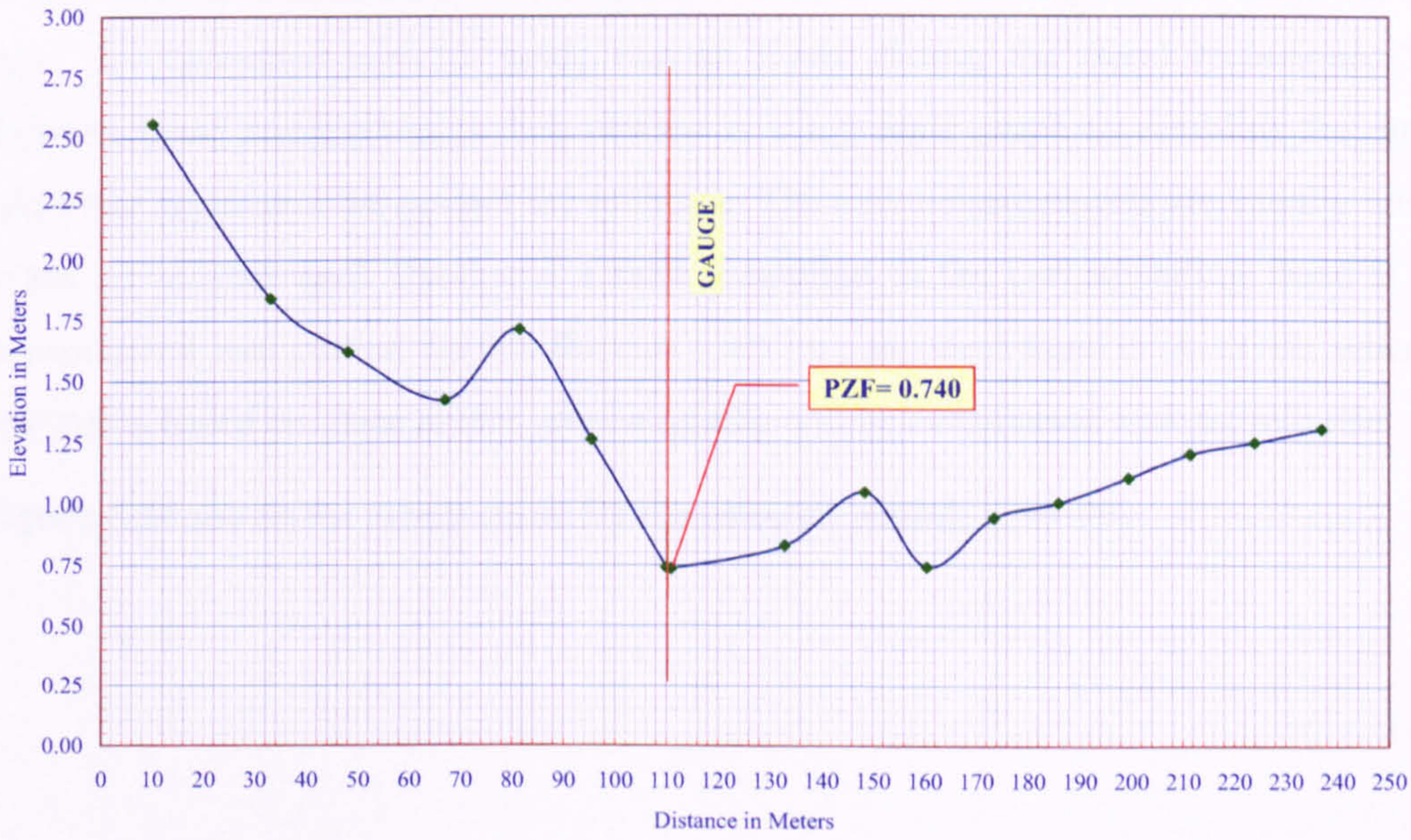


Figure 5.13: A diagram illustrates the channel cross section at the flow gauge

The gauge consists of a water-stage recorder and crest-stage gauge. The water-stage recorder is of an Omnidata Datapod Model II electronic dataloger recorder type,

housed in a capped steel pipe casing anchored in concrete beneath the wadi bed near the right bank and interfaced with a 15-meter Druck pressure transducer in a double screen, gravel packed assembly attached to the exterior of the steel pipe housing. Crest-stage gauges, CSI-1 and 2, are near the datapod, whereas, CSI-3 and 4 are upwadi and downwadi respectively from the datapod.

The CSI gauges are used to aid in determining the high flood marks when the wadi channel survey is carried out after any major flood. They are used to determine the longitudinal flood section of the channel. The obtained flood marks are important in the slope area measurements calculations, which are carried out after high floods to amend the recorded flood peaks, and update the rating curves that are used to convert the measured gauged heights to its corresponding discharge.

The slope-area measurement depending on the Manning equation for computing streamflow which makes use of the physical characteristics of the channel, surface elevations at time of peak discharge, and channel roughness coefficients. The data required for a slope-area measurement are obtained through a field survey of a reach of the channel. The survey includes the elevation and location of high-water marks corresponding to the peak stage, cross sections of the channel along the reach, and selection of a roughness coefficient.

As the slope area measurements, in general, are used for the high floods only, the low flows are measured directly using current meter during the flood recessions. The obtained flood measurements then plotted in a log scale graph to establish the rating curve that suppose to be unique for each site. The new measurements are usually added to the curve after each flood and a shift is applied to the corresponding flood if the measurement was plotted outside the curve until a consistent trend is observed, where a new curve based on these recent measurements will be constructed and put into use.

Figure 5.14 shows the rating curve for the selected period, 1996-99.

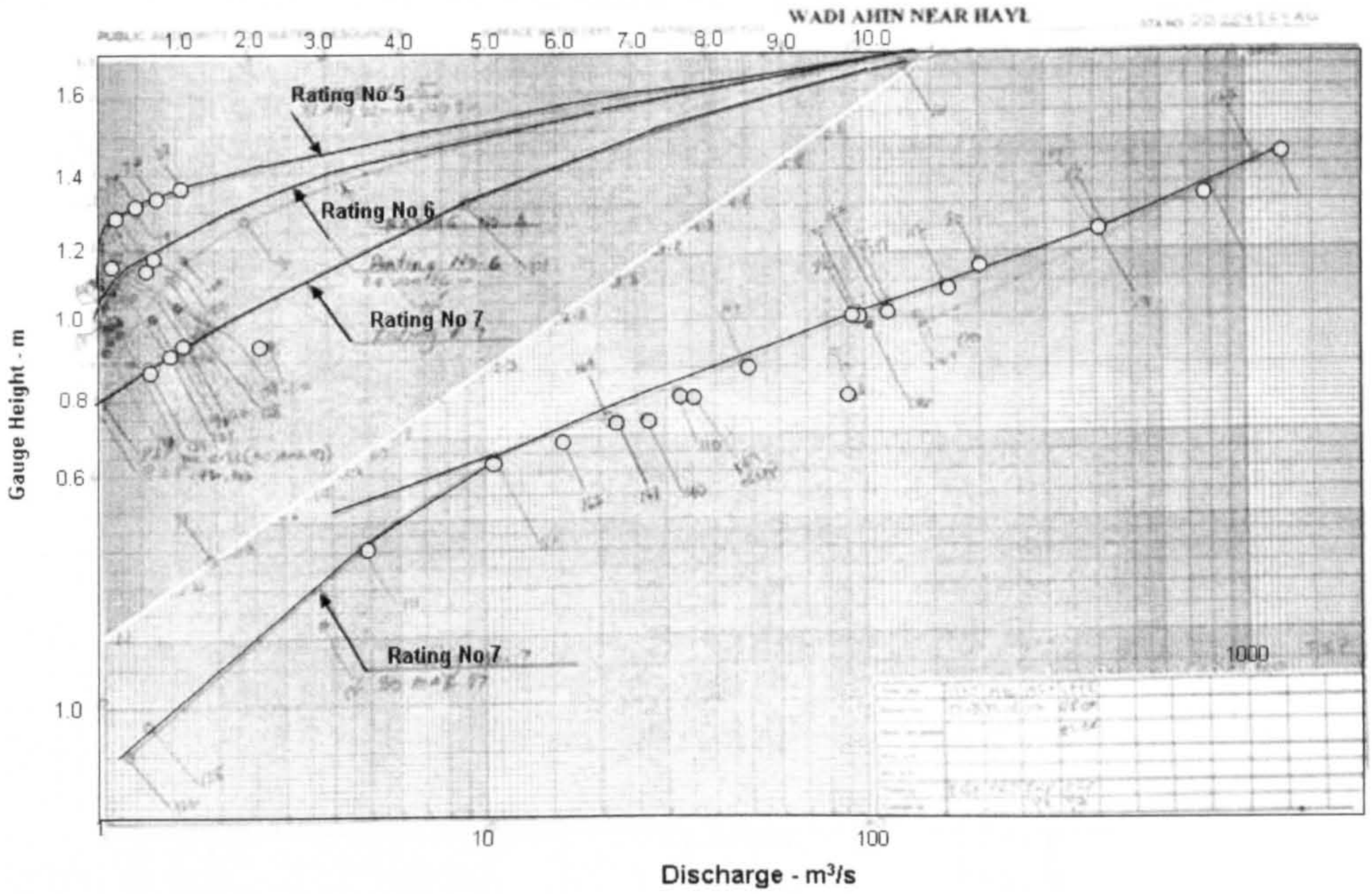


Figure 5.14: The used rating curve (1995-99) for Wadi Ahin flow gauge

The maximum discharge, during the period 1996-99, was 1,120m^3/s which was recorded for the 30 March 1997 flood with gauge height of 5.97m, whereas the minimum was 0m^3/s on many days each year. Outside this period of record; the maximum discharge, 1,220m^3/s, occurred sometime during 1977, based on slope-area measurement with a gauge height 6.15m.

5.3.3.3 The available data for the research

Hourly, daily and monthly data for the period from 1996 to 1999 have been gathered from the Ministry of Regional Municipality and Water Resources (MRMWR) in the Sultanate of Oman. The metrological data was obtained from the same Ministry where Sohar metrological station was used, as it was the closest to Wadi Ahin catchment.

It should be noted that the hourly data was available only for the automatic gauges of the DP type that works with pc chips. As the timing for the chart based gauges was found to be questionable for some events, an enquiry was made about these events with the Ministry in Oman. It was found that it is impossible to get hold of the charts earlier than 2000. Hence, it was impossible to check the accuracy of the event timing for these gauges but as most of the locations have been updated by automatic gauges of the DP type, this problem should not have great effects on Wadi Ahin, in general. However, the Hayl Ashkharyin and Haybi gauges are standard gauges with only daily records, and hence they were excluded from the analysis of KINEROS2.

Thirty rainfall events have been selected for the period 1996-1999. However, two of these events (08 Jul 1996, 22 Apr 1996) were excluded due to the doubtful quality of data. **Figure 5.15** shows the rainfall-runoff time-series for the remaining 28 events.

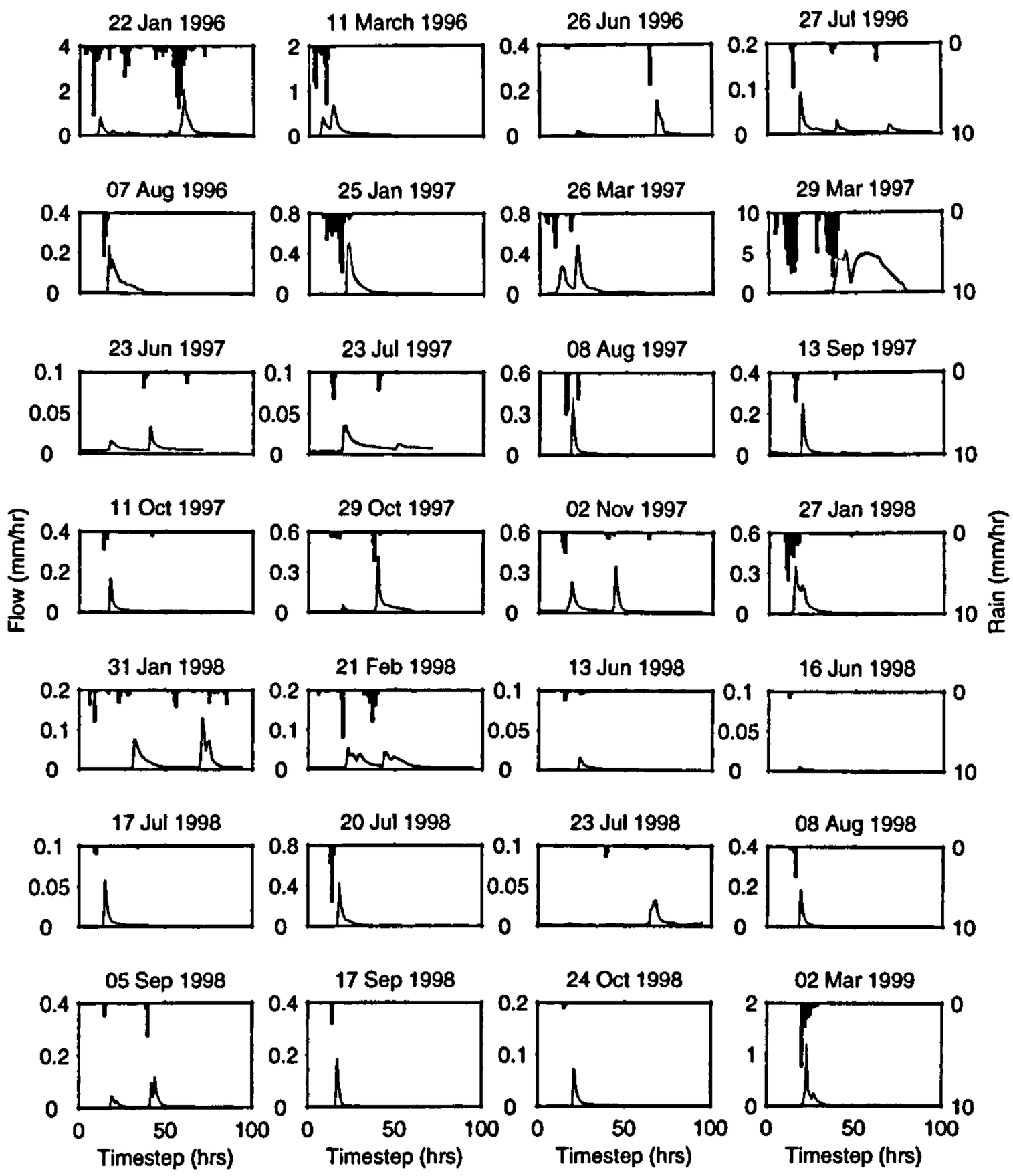


Figure 5.15: The rainfall-runoff events of Wadi Ahin for the 1996-99 period

Table 5.10 shows the rainfall amounts for each event for the used period, 1996-99, for the different rainfall stations. Consideration of the rainfall intensity and spatial distribution might help understand the controls on model performance and the parameter sensitivity analysis results. The events were classified into high intensity, widely spread rainfall events (shown in the table as h. w), medium intensity widely spread (shown as m. w), low intensity widely spread (shown as l. w), high intensity localised (shown as h. l), medium intensity localised (shown as m. l), low intensity localised (shown as l. l).

Table 5.10: Rainfall amounts (mm) for the 1996 -99 events at each rainfall station

Evnt No	Rf Dist	Event Date	DM565082AF	DM444945AF	DM343871AF	DM330730AF	DM339923AF	DM425877AF	DM533964AF
1996 Events									
*	h. w	22-28/01/1996	28	73	65.2	62 6	61 5	73 6	63 2
E1	h. w	11-12/03/1996	25	19 5	20 8	23	14	16 4	26
E2	h. l	26-30/06/1996	2 5	5	0 6	0	1.5	0	27 6
*	l. l	08-09/07/1996	0	0	0	1 2	0	6 8	0 6
E3	m. l	27-30/07/1996	7	16 5	12 2	3	3 5	22 4	13
E4	h. l	07-08/08/1996	0	0	3 2	5 2	34 5	21.8	0
1997 Events									
E5	h. w	25-28/01/1997	14	26 5	55.4	41 6	38 5	29	37.4
*	h. w	26-31/03/1997	41	78 5	57	155 8	81	175 8	89
*	h. w	22-23/04/1997	13 5	12 5	20	30.8	0	26 2	34 2
E6	m. w	23-25/06/1997	0	4	10 2	11 2	0	8 8	0
E7	l. w	03-05/07/2007	0	7 5	0 6	0	6	36	7 2
E8	h. l	08-10/08/1997	0	22 5	2 8	0	14	37.2	14 6
E9	l. w	13-15/09/1997	0	0	9 6	3 8	18 5	2 8	5 8
E10	l. w	11-14/10/1997	6 5	2	16	0 4	0	4	0
E11	h. w	29-31/10/1997	46 5	8 5	14 6	17	11.5	27	19 8
E12	m. w	02-04/11/1997	19	0	14.4	0.2	7 5	1 6	16 2
1998 Events									
E13	h. w	27- 29/01/98	12	21 5	41 4	12 8	28 5	20 8	20 4
E14	m. w	31/01- 04/02/98	12	17 5	14 8	11 2	9	64 6	16
E15	h. w	21/02-24/02/98	13	12	12 8	29 8	22 5	30	22 6
E16	l. w	13-15/06/98	0	1 5	8 6	0 6	7	0	4 4
E17	l. l	16-18/06/98	0	0	0	0	0	0	7
E18	m. l	17-19/07/98	0	0	0 4	0	11	9 4	0
E19	h. l	20-22/07/98	0	16 5	22 4	26 8	6 5	0	0
E20	m. l	23-26/07/98	0	10 5	8 4	1 2	2	0	1 2
E21	h. l	08-09/08/98	0	20 5	3 8	0	3 5	0	6 4
E22	h. l	05-08/09/98	0	3 5	1 2	0	0	0	30
E23	l. l	17/09/1998	0	0	0	0	0	0	14
E24	h l	24-25/10/98	0	0	0 8	0	2 5	0	2 8
1999 Events									
E25	h. l	02- 03/03/99	41	29	0	0	30 5	0	0
	l. l	28/09- 01/10/99	0	1	0	0	0	0	0

Statistics of the events are given in **Table 5.11.** Measuring the time lags between peak rainfall and peak flow is complicated because some events contain more than one rainfall and flow peak, and in other cases more than one rain peak can be associated with the single flow peak. However, 37 lags are relatively distinct and lie between 2 and 9 hours; 27 of these lie between 2 and 4 hours. Eight of the ten largest events in terms of rainfall volume were in the winter months January-April. This period also had relatively uniform rainfall (a greater proportion of the gauges had significant rainfall). There is an exceptional event from 26 March – 1 April 1997. The estimated return period of that peak flow is 85 years, and the runoff coefficient is 1.48, clearly due to under-measurement of rainfall or over-estimation of flow. Excluding that event, the runoff coefficients ranged from 0.02 to 0.33, with a mean of 0.15.

An attempt was made to check the relation between the distance between the rainfall stations and the correlation of the recorded rainfall. The spatial correlations of hourly rainfall are plotted in **Figure 5.16.** However, there is no clear relation between the two though it was noticed that the rainfall events are more frequent in the high elevation stations compared to the others with lower elevations.

Table 5.11: Statistics of the runoff events

Date	Peak rainfall at any gauge	Peak gauge-average rainfall	Total rainfall (sum of gauge-average)	No. gauges with	Rainfall centroid distance from flow gauge	Base flow	Runoff coeff.	Time lag of peak
	(mm/hr)	(mm/hr)	(mm)	< 2mm rain	(km)	(mm/hr)		(hrs)[a]
22-Jan-96	17	8	61	0	23	0 001	0.29	4,3 and 3
11-Mar-96	16	6	21	0	20	0 001	0 28	4
26-Jun-96	28	4	5	4	18	0	0.13	4
27-Jul-96	16	4	11	0	22	0 001	0 06	4,3 and 7
07-Aug-96	31	5	9	3	28	0.003	0.15	3
25-Jan-97	12	7	35	0	24	0	0.08	4
26-Mar-97	40	8	97	0	25	0.001	1.48	4,4 and 4
23-Jun-97	8	2	5	3	28	0 004	0.04	4
03-Jul-97	15	3	8	3	27	0 003	0 05	7
08-Aug-97	27	5	13	2	24	0 002	0 09	4
13-Sep-97	17	3	6	2	25	0 003	0.13	4
11-Oct-97	15	2	4	3	19	0.002	0 16	4
29-Oct-97	26	4	9	2	16	0.003	0.15	2 and 2
02-Nov-97	18	3	8	3	16	0 017	0.33	4
27-Jan-98	17	6	22	0	22	0.003	0 09	4
31-Jan-98	22	4	21	0	24	0.003	0.05	9
21-Feb-98	16	6	20	0	24	0 003	0 04	3 and 7
13-Jun-98	4	1	5	4	23	0	0 02	9
16-Jun-98	5	1	1	6	19	0 001	0.02	6
17-Jul-98	6	1	2	5	26	0.001	0 09	5
20-Jul-98	22	7	10	3	25	0.001	0.13	4
23-Jul-98	9	1	3	4	20	0	0 1	6
08-Aug-98	21	4	5	3	17	0 001	0.09	3
05-Sep-98	8	4	1	6	20	0 001	0 15	4
17-Sep-98	14	2	2	6	19	0 001	0.17	3
24-Oct-98	2	1	1	5	22	0 001	0 26	6
02-Mar-99	23	6	14	4	12	0	0 21	3

a. Where more than one value is given, the values refer to different rainfall bursts/flow peaks within the same event

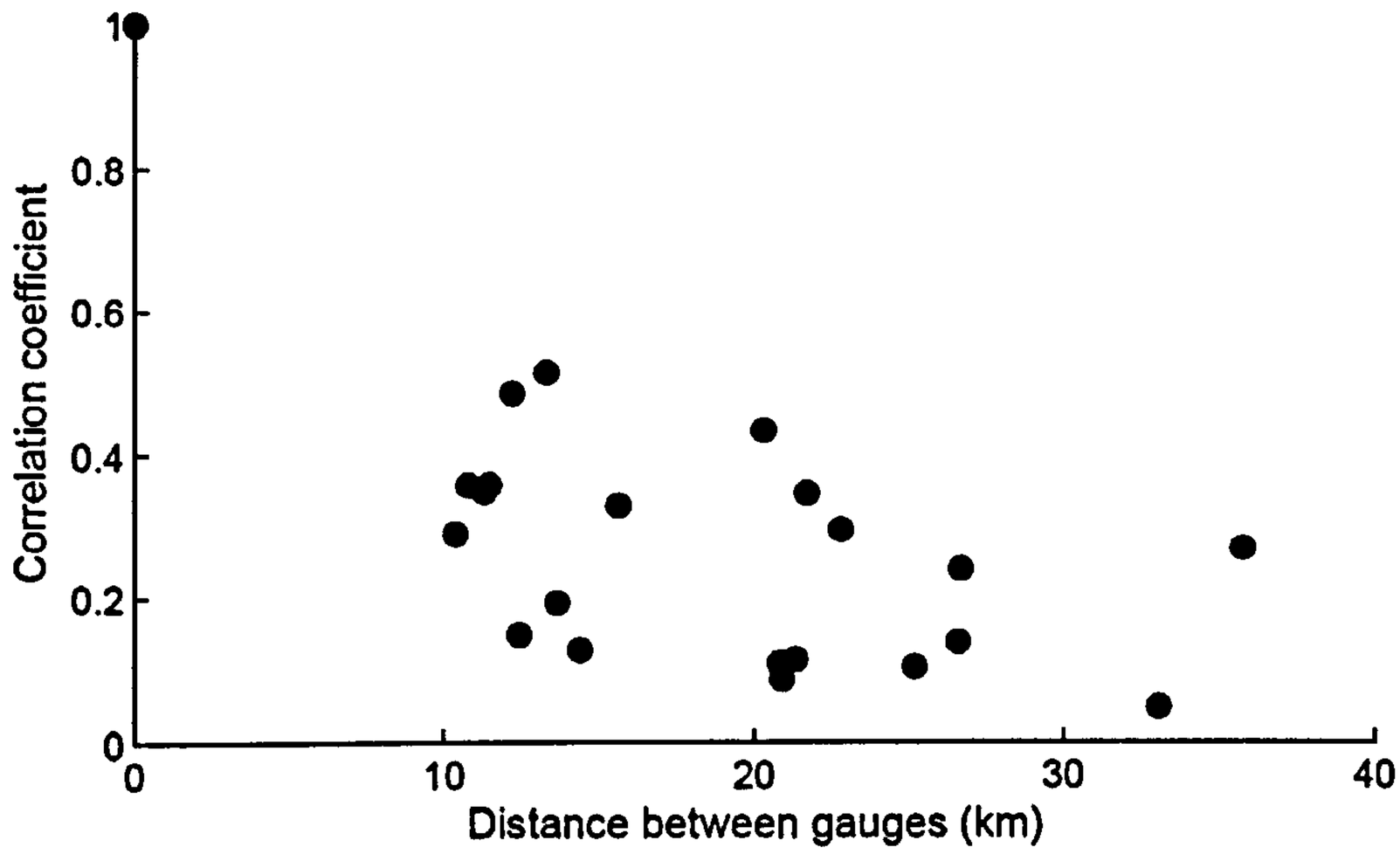


Figure 5.16: The relationship between the hourly rainfall correlations and distance between rain gauges for the 1996-99 rainfall-runoff events

Chapter 6

KINEROS2 Model

Model Description and Initial Analysis

6.1 Introduction

The literature review carried out in **Chapter 4** discusses the application of different models in arid areas. The literature review led to selection of the KINEROS and IHACRES models for this research purpose.

The KINEROS2 model (the latest version of KINEROS) is believed to be a suitable model to be tested on the selected study catchment, the Wadi Ahin, in the Sultanate of Oman (see **Chapter 5**) based on the structure and previous reports that show some suitability for modelling arid areas. KINEROS2 is a distributed, physically based model that was specially developed in the USA for use in arid conditions, though it was thought to not be entirely suitable for catchments larger than 100km^2 (Mishaud & Sorooshian, 1994). The model has been used in some arid areas, and in catchments larger than that size, with some success, and therefore an attempt will be made to investigate the performance of this model in the selected catchment to understand the possible reasons behind such conclusions, and to consider any necessary amendments to the model algorithms for possible improvements.

This chapter describes KINEROS2, based on the information on its official web site and the different studies that were carried out during its development. This is followed by an initial test using a synthetic catchment to study its performance under different conditions to aid understanding of the model and its limitations and study any possibility to modify the model's code to overcome them or improve its performance.

6.2 KINEROS2 Model

KINEROS was developed by the scientists of the United States Department of Agriculture, Agricultural Research Service, (USDA-ARS) in Tucson, Arizona. The model was based on significant work that was carried out during the 1970's (Woolhiser et al., 1970; Morgali, 1970; Schreiber, 1970; Kilber & Woolhiser, 1970; Rovery et al., 1977a, b). Further work was carried out by Woolhiser et al. (1990) to extend the model capability. However, the model was recently further developed and the new version, KINEROS2, which is used in this research, has emerged.

One of the most important features of KINEROS2 is its ability to consider the special hydrological features of arid areas (Michaud & Sorooshian, 1994). The model is also believed to be useful for determining the effects of various artificial features such as small detention reservoirs, or lined channels, on flood hydrographs.

KINEROS2, as its original version, is event based, describing the processes of interception, infiltration, surface runoff and erosion. The model is a physically-based model that is simulating flow and erosion, using the kinematic wave equation describing overland and channel flow (see http://www.tucson.ars.ag.gov/kineros/).

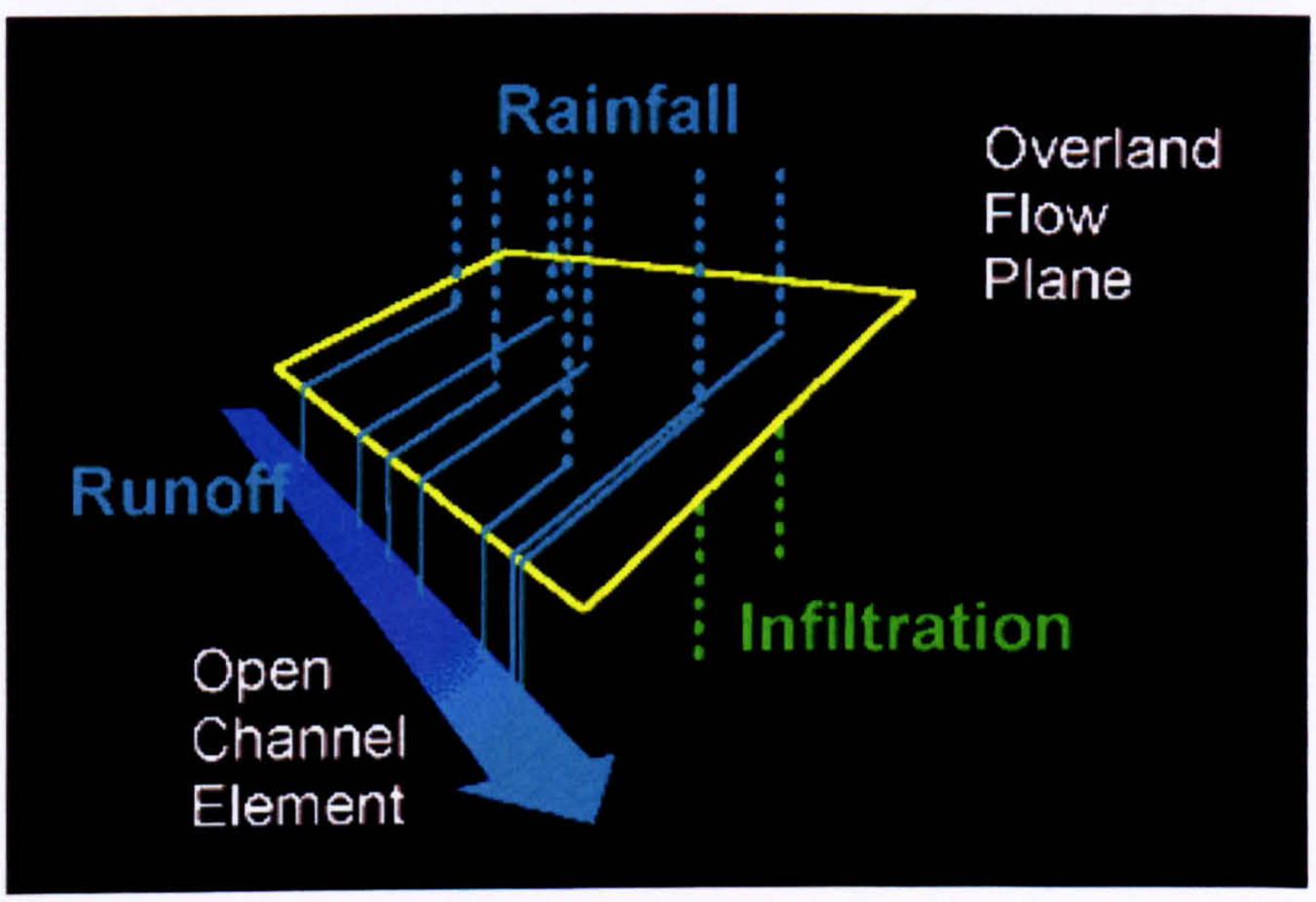


Figure 6.1: A simplified diagram of the hydrological processes within KINEROS2 (after http://www.tucson.ars.ag.gov/kineros/)

The model is also considered to be a distributed model as the watershed surface and channel network are represented by a cascade of planes and channels which can be called elements in which each plane may be described by its unique parameter values, initial conditions, and precipitation inputs, and each channel by its unique parameter values. The parameters and initial condition are assumed to be uniformly distributed

over each element but can vary from one element to another (Mishaud & Sorooshian, 1994). The watershed is divided, using soil type map and DEM, into channels, and into planes that contribute lateral flow to the channels. Hence, these maps are very important tools in defining the flow channels' paths and the extent of the planes. **Figure 6.2** illustrates how the catchment can be divided.

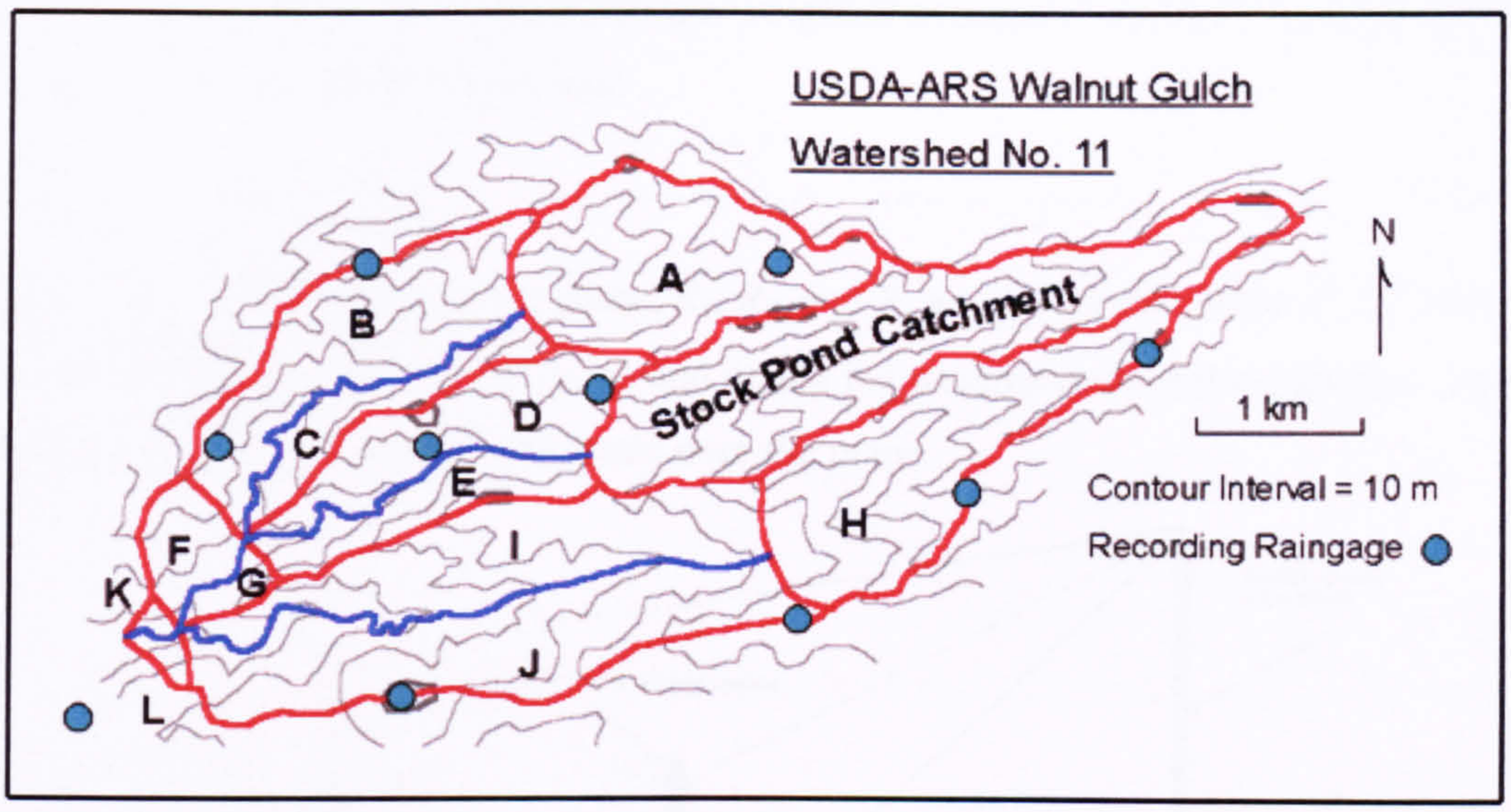


Figure 6.2: Diagram illustrates how the catchment can be divided into planes and channels *(after http://www.tucson.ars.ag.gov/kineros/)*

Many modifications and additions have been made to the original KINEROS model. Erosion and sediment transport and pond element components, the infiltration component and model input have all been modified (and the representation of the spatial variability of rainfall) since it was first developed as mentioned above.

The theory and the different components of KINEROS2 are discussed below based on the KINEROS2 web site, (http://www.tucson.ars.ag.gov/kineros/), direct communication with the developers, and the model code. However, the sediment and reservoir routing have not been discussed as they have not been used in the study.

6.2.1 Rainfall

KINEROS2 provides a special procedure for rainfall interpolation where it considers the spatial and temporal variability of rainfall. The rainfall for input to each plane and channel is estimated by interpolation from up to twenty rain gauge locations. The location of each element is represented by a single pair of x, y coordinates, which are normally the areal centroid of that element.

The details of rainfall interpolation computation in KINEROS2 are summarised below:

Within the KINEROS2 code, the rain gauge data are spatially interpolated. For each model plane (**e.g. Figure 6.3**), a centroid coordinate is specified by the user. At each time-step the ordinates of the rainfall at the three nearest surrounding gauges (or, in special cases, the nearest 2 gauges) are used to define a planar surface, and the average rainfall is computed as the ordinate of this surface over the plane's centroid (Woolhiser et al., 1990). This is formulated into the weighted average of the three gauged values, where the three weights sum to one:

$$R = c_1 R_1 + c_2 R_2 + c_3 R_3 \quad \text{..... (6.1)}$$

where R is the rainfall over the plane, R_1, R_2, and R_3 are the rainfall at the 1st, 2nd, and 3rd gauge respectively, and the c_1, c_2, and c_3, are the weights each of these gauges. This weighted average is applied uniformly over the plane

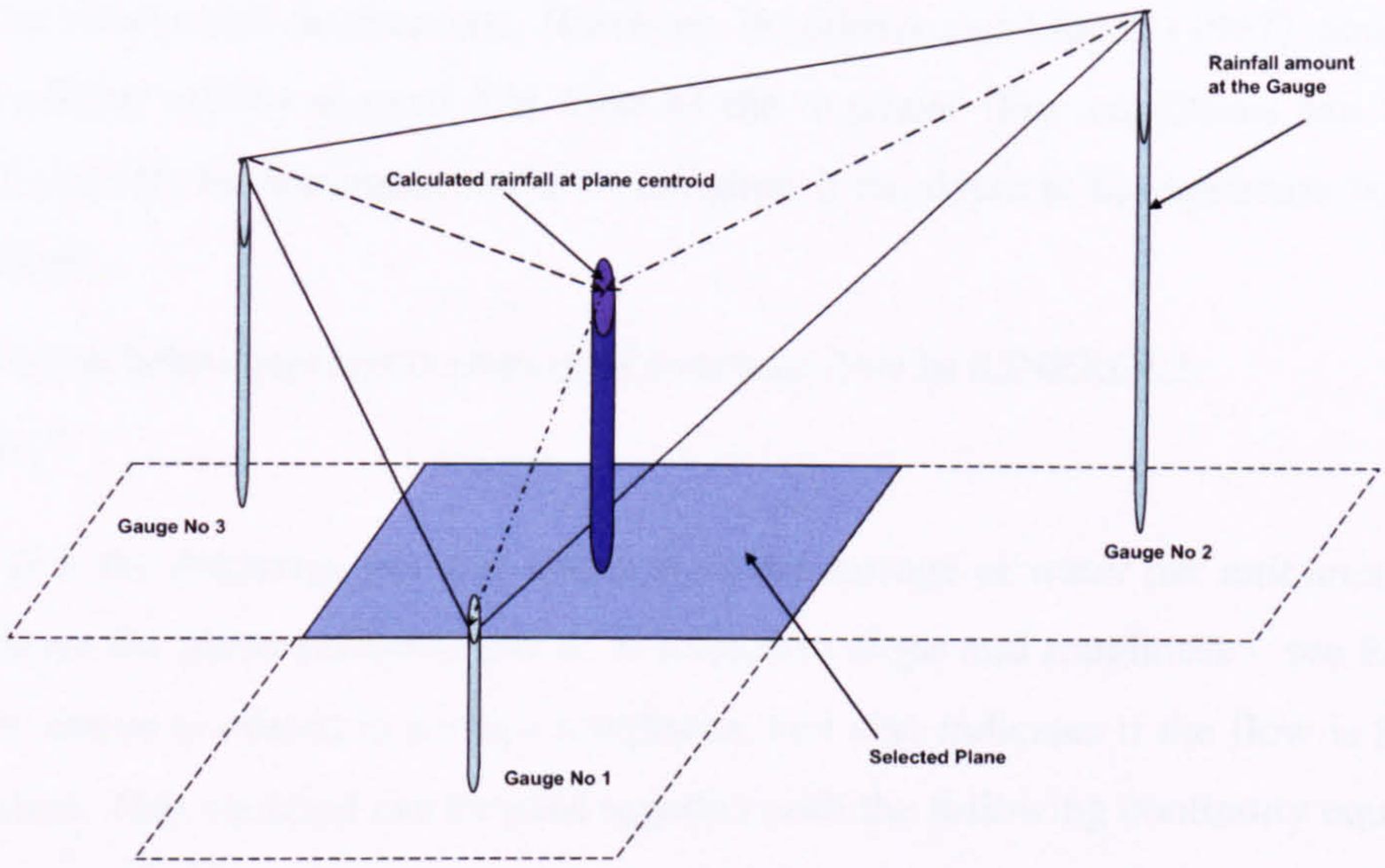


Figure 6.3: Simplifying diagram to represent rainfall interpolation in KINEROS2 for 3-gauges case

6.2.2 Interception

Interception (I) is the amount of rainfall that can be held by plant surfaces without reaching the soil surface. It is known to be affected by the type of vegetation cover and its density, vegetation growth stage, and wind velocity (Woolhiser et al., 1990). In KINEROS2, two parameters are controlling the effect of interception; the interception depth which reflects the average depth of rainfall that is held by the vegetation type or types in the study area, and the fraction of the surface covered by interception vegetation.

The effective rainfall rate is determined by reducing the actual rainfall rate by this fraction until the actual rainfall depth equals the interception depth. It should be noted

that the rainfall is reduced at the beginning of the event until the rainfall accumulation equals the interception depth. In cases where there is more than one event modelled in sequence, the interception amount is deducted from the first event only under the assumption that the interception depth is exceeded in the first event.

6.2.3 Hortonian overland flow

Hortonian overland flow is believed to be a complicated three dimensional processes in microscale but can be viewed as a one-dimensional flow process at a larger scale (see the KINEROS2 web site).

It is important to bear in mind that the kinematic wave equation which is adopted in the model for the flow routing is only a simplified form of the de Saint Venant equations and cannot consider complexities such as backwater or attenuation of waves, unless they form shocks that do attenuate. However, Woolhiser and Liggett (1967), and Morris and Woolhiser (1980) showed that most of the overland flow conditions can be well approximated by the kinematic wave formulation if the depth at the upstream boundary was defined.

The equation below represents routing of overland flow in KINEROS2:

$$Q_w = \alpha h_a^{\ m} \quad \text{.....} \quad (6.2)$$

where, Q is the discharge per unit width, h_a is the storage of water per unit area (water depth above the plane surface), and α is related to slope and roughness – see Eqs (6.8 and 6.9), and m is related to surface roughness, and also indicates if the flow is laminar or turbulent. This equation can be used together with the following continuity equation:

$$\frac{\partial h}{\partial t} + \frac{\partial Q}{\partial x} = q(x,t) \quad \text{.....} \quad (6.3)$$

where t is time, x is the distance along the slope direction, and $q(x,t)$ is the inflow rate per unit area. By combining the above two equations, the following equation can be obtained:

$$\frac{\partial h}{\partial t} + \alpha m h^{m-1} \frac{\partial h}{\partial x} = q(x,t) \quad \text{.....} \quad (6.4)$$

To solve Eq (6.4), the upstream boundary conditions need to be specified by specifying the depth *(h)*, which can be determined if the upper boundary is a flow divide, using the following equation:

$$h(0,t) = 0 \quad \text{.....} \quad (6.5)$$

In case of having another element contributing then the upper boundary condition would be specified based on continuity, using the following equation:

$$h(0,t) = \left[\frac{\alpha_u h_u(L,t)^{m_u} w_u}{\alpha w}\right]^{\frac{1}{m}} \quad \text{..... (6.6)}$$

where subscript u refers to the upstream surface, w is the width and L is the length of the upstream element. The initial condition can be specified as a unit storage.

The numerical solution that is adopted in the model to solve the kinematic wave equations (6.4) is carried out using a four-point implicit method as shown below:

$$h_{j+1}^{i+1} - h_{j+1}^{i} + h_j^{i+1} - h_j^{i} + \frac{2\Delta t}{\Delta x}\left\{\theta_w\left[\alpha_{j+1}^{i+1}\left(h_{j+1}^{i+1}\right)^m - \alpha_j^{i+1}\left(h_j^{i+1}\right)^m\right] + (1-\theta_w)\left[\alpha_{j+1}^{i}\left(h_{j+1}^{i}\right)^m - \alpha_j^{i}\left(h_j^{i}\right)^m\right]\right\}$$
$$-\Delta t\left[\bar{q}_{j+1} + \bar{q}_j\right] = 0 \quad \text{.....(6.7)}$$

where, θ_w is a weighting parameter, with values ranging from 0.6 to 0.8, for the x derivative at the advanced time step, $\bar{q}$ is the average flow, i represent the increment in time, and j the increment in space. **Figure 6.4** below represents the notation for the finite difference grid.

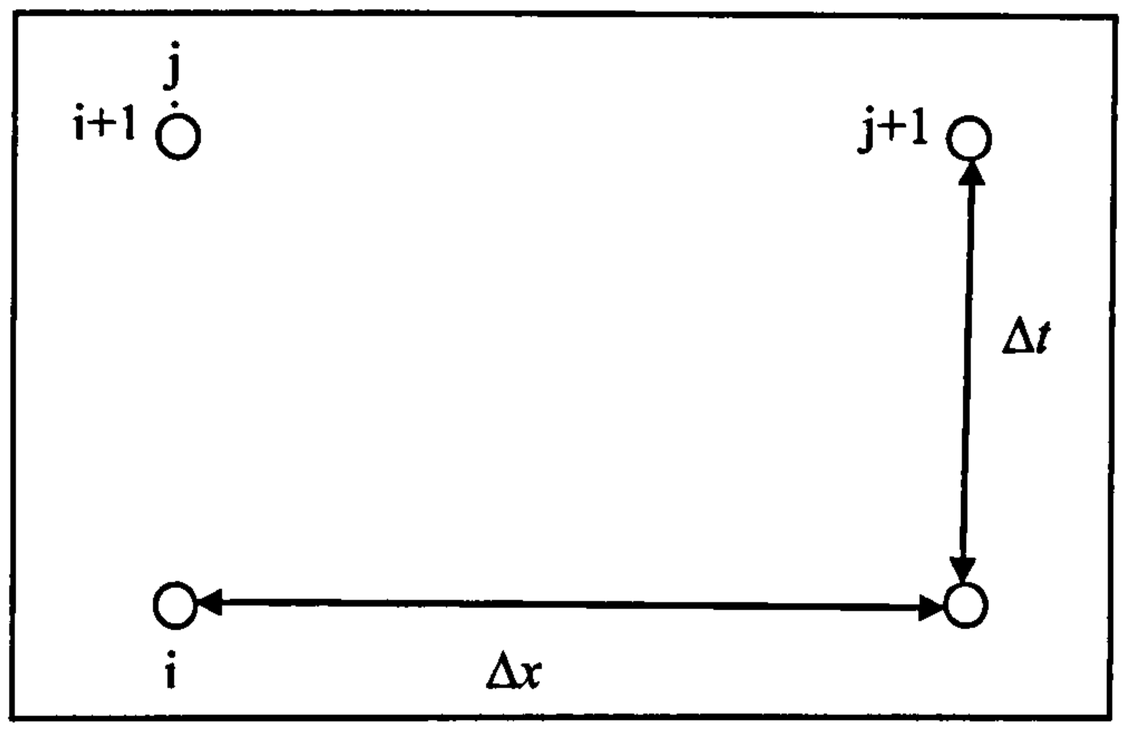


Figure 6.4: Notation-finite different grid *(after Woolhiser et al. 1990)*

There are two options provided in KINEROS2 for determining α and m in equation (6.7) as shown below:

1. The Manning hydraulic resistance law:

$$\alpha = 1.49 Slp^{1/2}/n \quad \text{and } m = 5/3 \quad \text{..... (6.8)}$$

where Slp is the slope, n is Manning roughness coefficient (using English units).

2. The Chezy law in which:

$$\alpha = CS^{1/2} \quad \text{and} \quad m = 3/2 \quad \text{.....(6.9)}$$

where, C is the Chezy friction coefficient.

It should be also noted that KINEROS2 developers have introduced two parameters; relief and spacing to describe the effects of the microtopography on the shape of the hydrograph, especially during the recession (Woolhiser et al., 1997). The relief geometry is assumed to have the maximum elevation with the area that is covered by the surface water and varies linearly with its elevation, whereas the spacing, the mean distance between relief elements, was introduced to specify the relief scale. It is believed that these two parameters aid in determining the water loss through infiltration during the recession where the soil is covered by the flowing water.

It should be noted that the overland response characteristics are controlled by the slope, slope length, and the hydraulic resistance parameters together with the rainfall intensity and infiltration characteristics (Woolhiser et al., 1990).

6.2.4 Channel Routing

In KINEROS2, the free surface flow in channels is represented by the kinematic approximation using the unsteady gradually varied open channel flow equations. The rainfall that falling over the channels is used directly, and indirectly through using the planes that are assumed to be covered completely by uniformly distributed flow that varies in time (see the KINEROS2 official web site). The channel is receiving these lateral inflows from the adjacent planes.

The continuity equation used for a channel receiving lateral flow is Eq (6.3) which can be rewritten under the kinematic assumption, where Q can be expressed as a function of A, as in the following equation:

$$\frac{\partial A}{\partial t} + \frac{dQ}{dA}\frac{\partial A}{\partial x} = q_c(x,t) \quad \text{.....(6.10)}$$

where, A is the cross-sectional area, Q is the channel discharge, and $q_c(x,t)$ is the net lateral inflow per unit length of channel. The relation between Q and A under the kinematic assumption can be expressed through the following equation:

$$Q = \alpha R_h^{\,m-1} A \quad \text{.....(6.11)}$$

where, R_h is the hydraulic radius and m is a constant and its value depends on which relationship is used (Manning or Chezy law).

It should be noted that KINEROS2 allows compound channels where the over bank flow can be considered. In such case, two independent kinematic equations are used but with the same datum and water level and with no energy transfer between the main channel and the overbank one. Each section will need to have its own parameters that describe its geometry and infiltration characteristics. The model has also the facility to add a baseflow to the modelled channel. In such cases, it is assumed that there is no infiltration through that channel. The upstream boundary condition is either Q=0 or the flow output from the upstream channel element.

The kinematic equations for channels can be solved through a four point implicit technique as shown below:

$$\frac{A_{j+1}^{i+1}-A_{j+1}^{i}+A_{j}^{i+1}-A_{j}^{i}}{\Delta t}+\frac{\theta_w\left(Q_{j+1}^{i+1}-Q_{j}^{i+1}\right)+\left(1-\theta_w\right)\left(Q_{j+1}^{i}-Q_{j}^{i}\right)}{\Delta x} \quad \text{..... (6.12)}$$
$$-0.5\left[q_{c\,j+1}^{\,i+1}+q_{c\,j}^{\,i+1}+q_{c\,j+1}^{\,i}+q_{c\,j}^{\,i}\right]=0$$

where, θ_w is a weighting factor for the space derivative, and q_c is the channel flow. A_{j+1}^{i+1} and Q_{j+1}^{i+1} refer to $A\left(d_{j+1}^{i+1}\right)$ and $Q\left(d_{j+1}^{i+1}\right)$, which are dependent on the channel geometry and depth only. The unknown depth d_{j+1}^{i+1} is solved by using Newton's iterative technique.

6.2.5 Infiltration

Infiltration rate (f_r) is one of the important variables in KINEROS2 but its process is quite complicated with many variables that have effects on it. The infiltration in KINEROS2 is determined based on the Smith and Parlange (1978) model. The infiltration capacity (f_c) based on this study is determined as shown in the following equation:

$$f_c = K_s\left[1+\frac{\Omega}{\exp(\Omega I/B)-1}\right] \quad \text{..... (6.13)}$$

where I is the infiltrated water depth, K_s is the saturated hydraulic conductivity, and Ω represents the soil type. B describes the differences between the volumetric water-holding capacity of the soil and its initial water content and can be obtained through the following equation:

$$B=(G+h_w)(\theta_s-\theta_i) \quad \text{..... (6.14)}$$

where G is the net capillary drive (discussed below), h_w is the surface water depth, and $(\theta_s - \theta_i)$ is the unit storage capacity, $\Delta\theta_i$. θ in general is known as the water content by volume, which equals ϕS, where S is the degreed saturation and ϕ is the porosity. Hence, θ_s is ϕS_{max} when the upper limit of S is S_{max}, which is known to be less than 1, whereas θ_i is ϕS_i, where S_i is the initial saturation. It should be noted that, the initial relative saturation of the upper soil layer, S_i is a scaled value of water content. If the used S_i value is 1, then the water content equals the porosity, ϕ.

The initial rainfall amounts can be entirely infiltrated to the soil, if the intensity is below the maximum rate of infiltration capacity (f_c) or infiltrability. The infiltrability is 'the limiting rate at which water can enter the soil surface' (Hillel, 1971), (taken from KINEROS2 web site; *www://tucson.ars.ag.gov/kineros*), and it is believed to be a dynamic term compared to the capacity. The f_c can become limiting at a point called ponding which occurs at a time called the ponding time t_p, with a ponding depth called F_p. Eq. (6.13) approaches the Green-Ampt relation when Ω is near 0 as in case of sand, whereas it represents the Smith-Parlange (1978) infiltration equation when Ω is near 1 as for a well-mixed loam. As most soils are best described by a value of Ω near 0.85, KINEROS2 adopts it as the default value.

The most important relations that need to be considered to understand the infiltrability relations can be described in scaled terms for f_*, I_*, and t_*, taking $h_w = 0$, are the following:

$$f_* = \frac{f_r - \bar{K}_s}{\bar{K}_s} \quad \text{.....(6.15)}$$

$$I_* = \frac{I}{G\Delta\theta} \quad \text{.....(6.16)}$$

$$t_* = t\frac{\bar{K}_*}{G\Delta\theta} \quad \text{.....(6.17)}$$

where the bars indicates the use of the areal mean value of K_s. In this case, the rain rate is also re-scaled based on the same base as f_r. Hence, $r_* = (r - \bar{K}_s)/\bar{K}_s$.

In the light of these, the spatial variation of the f_{c*} parameters can be represented by the equation below, and hence Eq (6.13) can be re-written as:

$$f_{c\bullet} = \frac{\Omega}{\exp(\Omega I_\bullet) - 1} \quad \text{..... (6.18)}$$

Figure 6.5 illustrates how Eq (6.18).

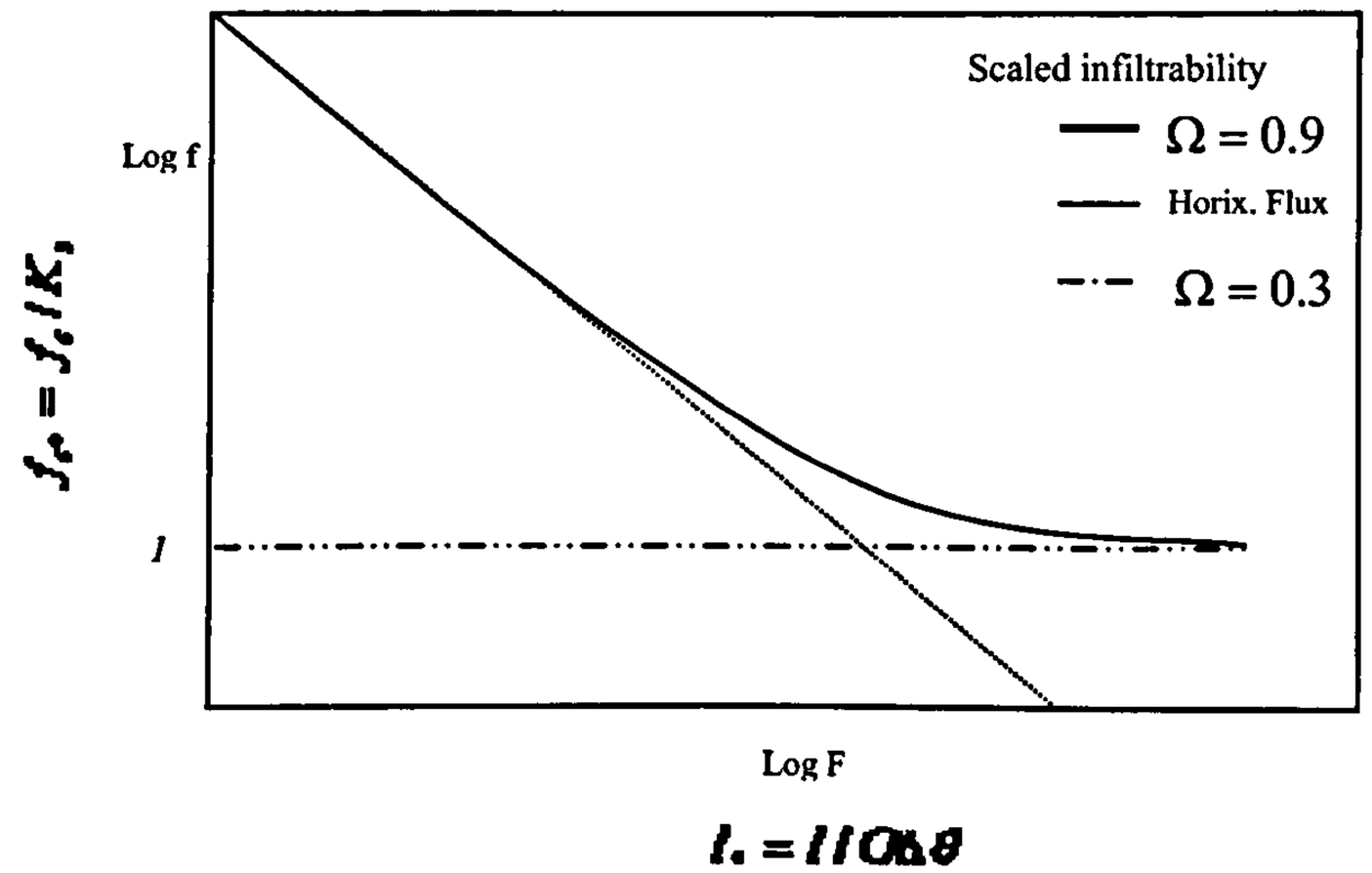


Figure 6.5: Scaled basic relation of equation (6.26) ***(after http://www.tucson.ars.ag.gov/kineros/)***

The infiltration process in KINEROS2, is controlled by three main parameters; the field effective saturated hydraulic conductivity, *Ks*; the integral capillary drive, *G*; and the porosity, ϕ. Another parameter that is added to KINEROS2 is the pore size distribution index, λ (Corey, 1964), (see; *www://tucson.ars.ag.gov/kineros*), where its values can be taken from the statistical study of soil texture of Rawls et al. (1982), (see; *www://tucson.ars.ag.gov/kineros*), which provides a guideline for estimation of this new parameters.

The net capillary drive parameter *G*, is defined as:

$$G = G(0) = \int_{-\infty}^{0} \frac{K(\psi)}{K_s} d\psi \quad \text{..... (6.19)}$$

The upper limit in the above equation is assumed to be 0 (when the used *G* is with no subscript). However, the upper limit changes for redistribution case, where the relation $K(\psi)$ is taken from soil characteristic relation of Brooks and Corey for simplicity as shown below:

$$\frac{K(\psi)}{K_s} = \left(\frac{\psi_B}{\psi}\right)^{2+3\lambda} \quad \text{..... (6.20)}$$

Hence, Eq (6.19), when it is integrated using Eq (6.20), becomes:

$$G = \frac{\psi_B^{(2+3\lambda)}}{-1-3\lambda} \quad \text{.....(6.21)}$$

where ψ is the metric potential and ψ_B is the air entry potential. The value of ψ_B can be determined using Eq (6.21), as the values of G and λ can be estimated based on the soil texture type as can be found in the literature review (Woolhiser et al , 1990).

Cv, was another parameter that was added to KINEROS2, for better description and analysis of the infiltration process, which describes the spatial variation in the soil hydraulic conductivity, K_s.

The infiltration computations are discussed below with the aid of the model official web site and some of the previous studies used to develop the model, as will be pointed out when necessary.

KINEROS2 has the ability to deal with the case where two soil layers exist. In such case and with upper soil depth z_1, one of the layers will be the most restrictive layer, either the upper or the lower based on the relative values of the hydraulic conductivity of each, K_{s1} and K_{s2} where the layer with the lowest value is, generally, the most restrictive one. However, the two soil layers may act identically if the products $(G_1)(K_{s1})$ and $(G_2)(K_{s2})$ are equal (Smith et al, 1990), where K_{s1} and K_{s2} are the hydraulic conductivity of the upper layer and the lower layer respectively, and the G_1 and G_2 are the capillary force for the upper layer and the lower layer respectively. This can occur under very high rainfalls that are occurring over a soil of a shallow surface layers for a short time infiltration (only). However, in this research, one soil layer was assumed for simplicity as there was no enough information to assume there are two. Hence, the relations between the different parameters in this case were not thought to be necessary to be discussed here.

KINEROS2 has also the ability to recover the infiltrability in cases where more than one period of runoff-producing rainfall occurs within one modelled event, where the soil is drying significantly between periods. A method for redistribution/reinfiltration that is described in Smith et al. (1993) and Corradini et al. (1994) was adopted for such cases and the change in water content at the surface can be expressed by the following equation:

$$\frac{d\theta}{dt} = \frac{\Delta\theta_{i0}}{I}\left[r - K_i - \left(K(\theta_0) + \frac{\beta p K_s \Delta\theta_{i0} G(\theta_i, \theta_0)}{I}\right)\right] \quad \text{.....(6.22)}$$

in which $\Delta\theta_{i0}$ is $\theta_0 - \theta_i$, the water content of the redistributing portion, θ_i is the original water content below the redistribution front, r is the rate of input at the surface during redistribution, which may be small, negative (evaporation), positive, or 0), p is an effective depth factor, and $G(\theta_i, \theta_0)$ is the effective capillary drive of the shrinking wetting front, which is reduced in relative to the infiltrating G as θ_0 is less than θ_s. β is a constant scale factor with values rarely higher than $\pi/4$ and about always less than 1. β can be determined through the following equation:

$$\beta = \frac{1}{Z(\theta_i - \theta_i)} \int_0^Z (\theta - \theta_i) dz \quad \text{.....(6.23)}$$

where Z is the lowest extent of wetting. Eq. (6.23) is solved using the Runge-Kutta method.

In addition, KINEROS2 also has the ability to deal with the situations where initial, low rainfall to occurs before a runoff-producing period. This can change the effective "initial" soil water content used in the infiltration calculations. The model is using a method based on 'soil dynamics studies' to estimate the change in the effective θ_i that is caused by the initial slow rainfall ($r < K_s$). The method is based on the soil properties and the relative value of rainfall rate as described in Corradini et al. (1994).

The model also deals with the very wet initial conditions where the soil profile becomes wet following a short period of redistribution with high initial content of the upper soil and where it is necessary to include the steady flux of the water that already exists to the total infiltration flux. To deal with such situation, Eq (6.13), (Smith et al. 1993) has been modified, and I is determined through the following relation:

$$I' = (I - K_i t') \quad \text{..... (6.24)}$$

where I' is the cumulative infiltration depth (see Smith et al., 1993), and can be obtained through:

$$I'(t) = \int_0^t f' dt \quad \text{..... (6.25)}$$

$f'(t)$ is the dynamic infiltration rate $f_c(t) - K_i$, K_i is the hydraulic conductivity of the initial soil profile, $K(\theta_i)$, and t' is the time from start of wetting or rewetting.

KINEROS2 has also the ability to deal with the cases where the study area is heterogeneous, in which the K_s has a random distribution. Where there are some values of $K_s > r$, in which the area that is not contributing to the runoff is increasing with the decrease of r, the model attempt to determine the value of K_e as the areal effective value to represent this situation. The K_e value is increasing with the value of r and can be determined through the following equation:

$$K_e = [1 - P_k(r)] + \int_0^r k p_k(k) dk \quad \text{..... (6.26)}$$

where, P_k is the CDF (cumulative probability function) of K_s, and p_k is the corresponding PDF (probability density function). The lognormal PDF, the relation between the r_*, K_s, and $C_v(K_s)$, are demonstrated in the figure below:

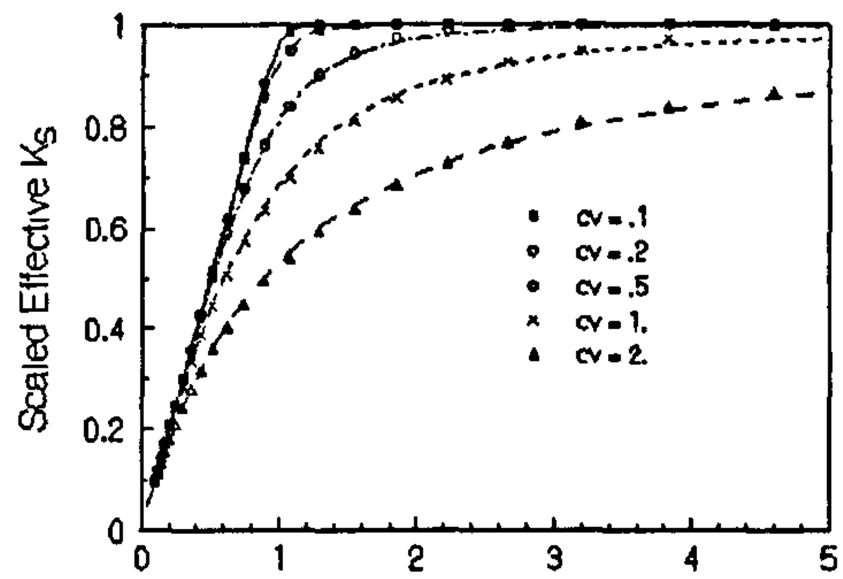


Figure 6.6: Relation of effective ensemble K_s to coefficient of variation of K_s and scaled rainrate (http://www.tucson.ars.ag.gov/kineros/)

Hence, and from the above Figure, the K_e value can be determined through the equation:

$$K_e = \left[1 + \left(\frac{1}{r_*}\right)^p\right]^{-\frac{1}{p}} \quad \text{..... (6.27)}$$

where, $p = 0.7 + \frac{1.2}{C_v^{1.2}}$

To establish a relationship for infiltration of the heterogeneous surface as a whole, the surface ensemble behaviour can be described in scaled terms based on the K_e through the following equation:

$$\frac{f_{c*} - 1}{r_* - 1} = \left\{1 + \left[\frac{r_* - 1}{\Omega}\left(\exp(\Omega I_*) - 1\right)\right]^c\right\}^{-\frac{1}{c}} \quad \text{..... (6.28)}$$

in which C_r is a parameter greater than 1, whose values are directly related to the scaled rainfall rate r_* [r / K_e] and $Cv(K_s)$. The figure below illustrates how the value of C_r can be estimated as a function of $Cv(K_s)$.

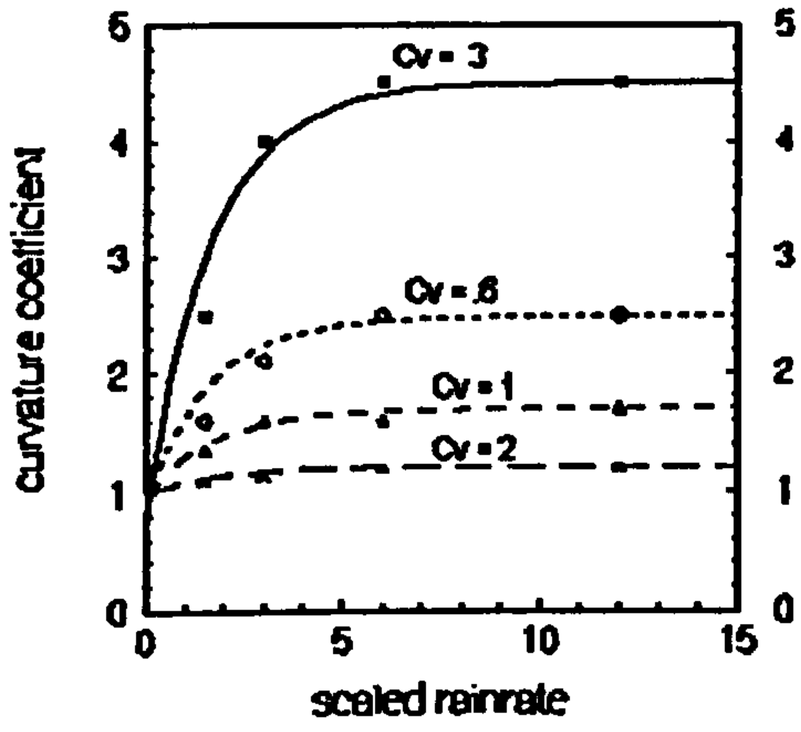


Figure 6.7: Variation of C with scaled rainfall rate and $Cv(K_s)$, (http://www.tucson.ars.ag.gov/kineros/)

Hence, for $C(r_*,Cv)$, C_r can be obtained as follow:

$$C_r = 1 + \left[0.75(C_v)^{-1.3}\right]\left[1 - \exp(0.1 - r_*)\right] \quad \text{..... (6.29)}$$

Hence, these highlight that the infiltration is controlled in KINEROS2 model by three main parameters; the field effective saturated hydraulic conductivity, *Ks*; the integral capillary drive, *G*; and the porosity, ϕ. The interrelationship between these parameters seems a bit complex due to the fact that there are many parameters that need to be considered to determine the values and the effects of these parameters as described above. However, all of the three parameters are input parameters where the modeller has to specify their values to enable the model to calculate the infiltration rate for his study catchment.

6.3 KINEROS2 Initial Analysis

KINEROS2 was tested to study its behaviour under different configurations such as different numbers/sizes of planes, rainfall distributions, and different rainfall data time intervals and durations, using a simple synthetic catchment.

The test was also carried out to check the effects of numerical errors on the model performance, using different numbers of planes in series to represent the same overall hill-slope length. The overall length was selected as the same as the longest plane length used for the Wadi Ahin catchment simulations, which was 20,000m.

The tests also aimed to understand the response of the model to different plane configurations, in particular the effect of numerical errors associated with plane length. Preliminary tests on the Wadi Ahin catchment showed that the model gives a warning, such as 'based on length and parameter *clen*, the numerical increment of 1080.5 m. is too large for realistic numerical solution of the flow equation, and may give misleading results', if Δx was greater than 30m. The new user manual (see, *www://tucson.ars.ag.gov/kineros*) highlights that the numerical solution that is used in KINEROS2 (KINEROS2, version 3.2, Dec 2003) to solve the kinematic wave equations using the four-point implicit finite difference method is usually unconditionally stable but its accuracy depends highly on the size of space and time steps, Δx and Δt. Furthermore, KINEROS2 allows a maximum of 20 numerical elements per plane, implying a maximum recommended plane length of 600m. However, the actual maximum plane length required to achieve acceptable numerical errors is difficult to ascertain as it depends also on hydraulic parameters, infiltration, and rainfall rates. As the chosen number of planes in series is arbitrary, based on the developer's opinions, the tests here help to find out the reasonable number of planes to be used and the effects of errors associated with the spatial discretisation, and to find out the optimum plane length to reduce spatial complexity without getting significant numerical errors.

Another objective for the tests was to understand the effects of simple spatial distributions of rainfall on the model response. This was done by running the model using a uniform rainfall distribution (using the data specified for one rainfall gauge over the entire synthetic catchment), and non-uniform rain (assuming the same rain event over the upper plane only and no rain on the rest of the catchment).

The model response to infiltration was also checked. This was carried out by running the model with the above-mentioned configurations, under saturated conditions (no infiltration was allowed and hence only the kinematic wave component of the model is being tested), and then non-saturated conditions (allowing infiltration).

The model was also tested in the case where there is a consistent flow input from the upper plane, to look at the effect of the downstream plane size and numbers in this case (as opposed to the first test where input flow is distributed over all planes). This is carried out through the second case that is shown in the flowchart in **Figure 6.8.**

Figure 6.8 demonstrates the different configurations that were used to examine the different response of the model and the strategy that is followed, in running these tests.

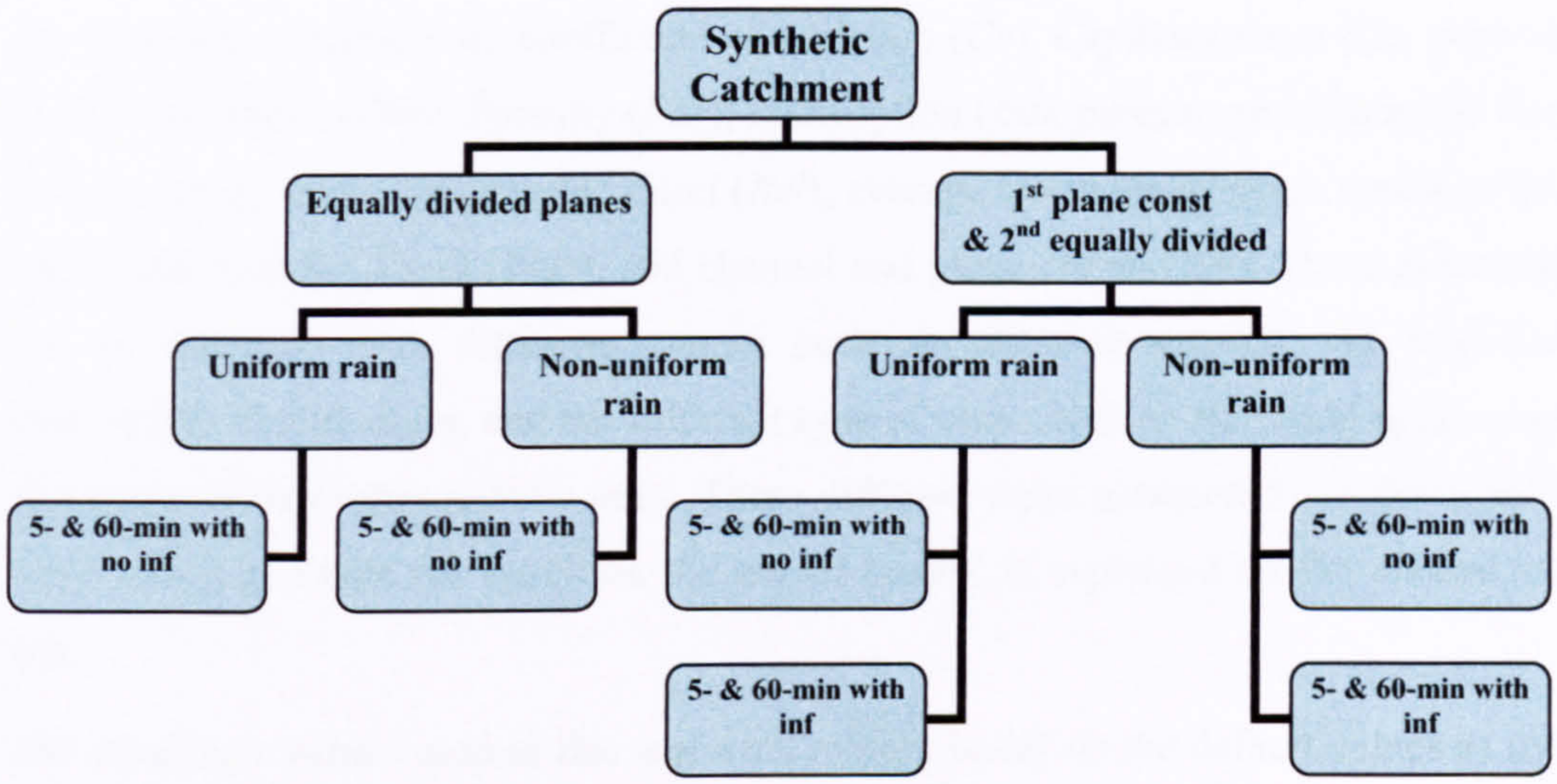


Figure 6.8: A flowchart shows the used strategy to test the model's performance using a synthetic catchment with different configurations

Both catchment configurations, shown in **Figure 6.8**, were run with synthetic and recorded data from Wadi Ahin with 5- and 60-min time intervals, however only a selection of representative results are reported here.

Where possible, the results of KINEROS2 were compared with an analytical solution of the kinematic wave equation (Lane and Shirley 1981, taken from Parlange et al. 1981). However, this analytical solution is only applicable to uniform rainfall with the no-infiltration tests. The analytical solution was obtained using the same synthetic catchment as that used to run KINEROS2 but with no channel (see below for details). The assumed channel length for the synthetic catchment that is used to run KINEROS2 is only 100m which is negligible compared to the catchment size with a 20,000m length. Hence, the KINEROS2 and the analytical solutions are in practice comparable. The details of selected tests are specified and discussed below.

6.3.1 The estimation of the parameter values

For KINEROS2 to be run requires many different parameters that describe each element. These parameters are of three types. Global parameters are not particularly related to any specific element (such as *clen* which describes the longest single channel element or contiguous cascade of planes, temperature, sediment diameters and densities that are required if sediment is to be modelled). Then, there are plane parameters (the parameters that are related to the individual plane elements) and channel parameters (the individual channel element parameters). Those parameters (for both element types) includes the hydraulic conductivity (K_s), Initial Saturation *(S)*, Mannings Coefficient

(n), Hydraulic conductivity coefficient of variation (*Cv*), Capillary force *(G),* pore size distribution index (*Dist*), Porosity (*Por*), Interception (*Int),* percentage Volumetric Rock (*Roc*), average micro topographic relief (*Rel*), average micro topographic spacing (*Spc*), upper soil layer thickness (*Thic*), and channel and plane slopes (*Slp*). These parameters can be obtained from different sources such as site measurement, the modeller's knowledge, the literature, and the different type of maps such as the topographic maps, soil maps, or any other relative ones. These different input parameters are described in some detail in **Table 6.1** based on the model guides as explained on the official web site.

The parameter values used in this test were mainly based on the default values as used by Mott MacDonald (1992) in a previous study on the Wadi Ahin, see **Table 6.2.** The used value for the *clen* was 100 m, as was suggested by the developer.

It should be noted that the values of hydraulic conductivity (K_s) and initial Saturation (*S)* were set to prevent any infiltration in the no-infiltration case. The capillary force *(G),* porosity *(Por),* and distribution *(Dist),* which were chosen for the same soil type, as they were found to be linked to each other. It should also be noted that using G=0 sets the infiltration to a constant rate, equal to K_s, and hence all the parameters become redundant, that are are linked to the infiltration computation.

Table 6.1: The parameters used in the test cases

Parameter	Symbol	Units	Definition	Comments
Parameters Used in Both Elements				
Upstream	Up		Identifier of the upstream element when applicable	Can be determined from the catchment division map
Length	*Le*	m	plane or channel length	Can be calculated from the catchment map
Width	Wi	m	Width of the plane or channel bottom	Can be calculated from the catchment map for planes and from cross section survey for the channel
Slope	*Slp*	-	plane or channel slope	Can be determined from the catchment DEM
Manning	*n*	$sm^{-1/3}$	Manning roughness coefficient	Can be determined from the literature and the site
Chezy	*Ch*		Chezy conveyance factor	Can be determined from the literature and the site
*X			Representative x coordinates	Can be determined from the map or the site
*Y			Representative y coordinates	Can be determined from the map or the site
Saturation	*S*		Initial degree of soil saturation	Can be determined through measurement or previous studies
Saturated hydraulic conductivity	*Ks*	mm/hr		Can be determined through measurement or previous studies
Capillary drive	*G*	mm	Mean capillary drive, Zero value sets the infiltration to a constant rate that equal to Ks	Can be determined through measurement or literature
Variation of *Ks*	*Cv*	-	Coefficient of variation of Ks	Can be determined through measurement or literature
Distribution	*Dist*	-	Pore size distribution index, Used for redistribution of soil moisture during unponded intervals	Can be determined through measurement or literature
Porosity	*Por*	-	Soil porosity	Can be determined through measurement or literature
Rock	*Roc*	-	Volumetric rock fraction, if Ks is estimated based on texture class, it has to by multiplied by (1-Rock) to reflect this volume	Can be determined through measurement or literature
Parameters Used for Planes Only				
Relief	*Rel*	mm	Average micro-topographic relief	Can be determined from the map or
Spacing	*Spc*	m	Average micro-topographic	Can be determined from the map or
Interception	*Int*	mm	rainfall amount lost through interception	Can be determined from the map (land cover maps) or the site
Canopy Cover	*Ca*	-	Fraction of surface covered by interception cover (rainfall reduced by this amount till accumulating the interception length	Can be determined from the map (land cover maps) or the site
Thickness	*Thic*	mm	Upper soil layer thickness	
Parameters Used for Channels Only				
Lateral			Identifier of elements contributing lateral flow when applicable (applies to channel element)	Can be determined from the catchment division map
Type	*Ty*		Channel type; simple or compound	Can be determined from cross-section survey
Qb	*Qb*	m^3/s	Base flow discharge at end of channel, when applicable	Can be determined from available data
SS1, SS2	*SS1, SS2*		Bank side slopes	Can be determined from cross-section survey
Rwidth	*RW*		Rainfall on the channel area if desirable	Can be determined from available data or modeller judgment
Woolhiser coeff.	*W*	-	David Woolhiser's effective wetted perimeter function	Can be determined from literature
Wcoeff	*Wcoeff*		Optional override of coefficient in the Woolhiser function	Can be determined from literature
Rainfall interpolation non-linearity	*f*	-		Can be determined through the calibration or modeller's judgment

Note:

a. In plane no. 9 the default ks value was 31.22mm/hour, in plane no. 10 it was 20.8 mm/hour; in all others it was 3.7mm/hour

b. In 4 channel reaches, default s value was 0.05; in all other channel it was 0.45.

c. In channel no. 1, default θ value was 0.15; in all other channel it was 0.44.

d. *No need to specify the coordinates if one gauge is used

Table 6.2: The parameter values used in the test cases

Par	Values- Planes		Values- Channel	
	No Inf	With Inf	No Inf	With Inf
Slp	0.09	0.09	0.001	0.001
n	0.035	0.035	0.036	0.036
Cv	0.1	0.1	na	na
Thic	500	500	na	na
S	1	0.45	1	0.45
Rel	20	20	na	na
Spc	10	10	na	na
Ks	0	3.7	0	41.7
G	0	11	0	11
Dist	0.6	0.25	0.6	0.25
Por	0.1	0.463	0.15	0.436
Roc	0	0	0	0

6.3.2 Different plane configurations

A synthetic catchment was assumed with total length of 20,000m, the longest length for the largest plane in Wadi Ahin catchment, and a channel with an arbitrary length of 100m with 50m width and 4 m depth, a slope of 0.09, and roughness coefficient of 0.035, where the geometry of the assumed channel was selected based on the channel geometry of the Wadi Ahin channels. As the behaviour of the channel is not one of the objectives of the tests, the channel length was deliberately set to be very small compared to plane lengths. This will also ease the comparison of the model's results with those obtained by the analytical analysis.

The planes were divided in two ways as shown below:

- **Equal area planes**: In this configuration the total synthetic catchment area of 2,000,000m^2 (20,000m length and 100m width) was divided lengthwise into equal area planes using 2, 4, 8, 16, and 32 planes, keeping the parameter values for each plane the same. **Figure 6.9a** shows a diagram that illustrates the synthetic catchment used in this test (not to scale).

- **Constant area upper plane:** In this configuration, the synthetic catchment was assumed to consist of two areas. The upper area is of 100,000m^2 (1000m length and 100m width) and was represented by one plane only, whereas the lower area is of 2,000,000m^2 (20,000m length and 100m width). It should be noted that the lower area here is the one that is divided into different numbers of equally sized planes each time, keeping the 1st plane constant, see **Figure 6.9b**.

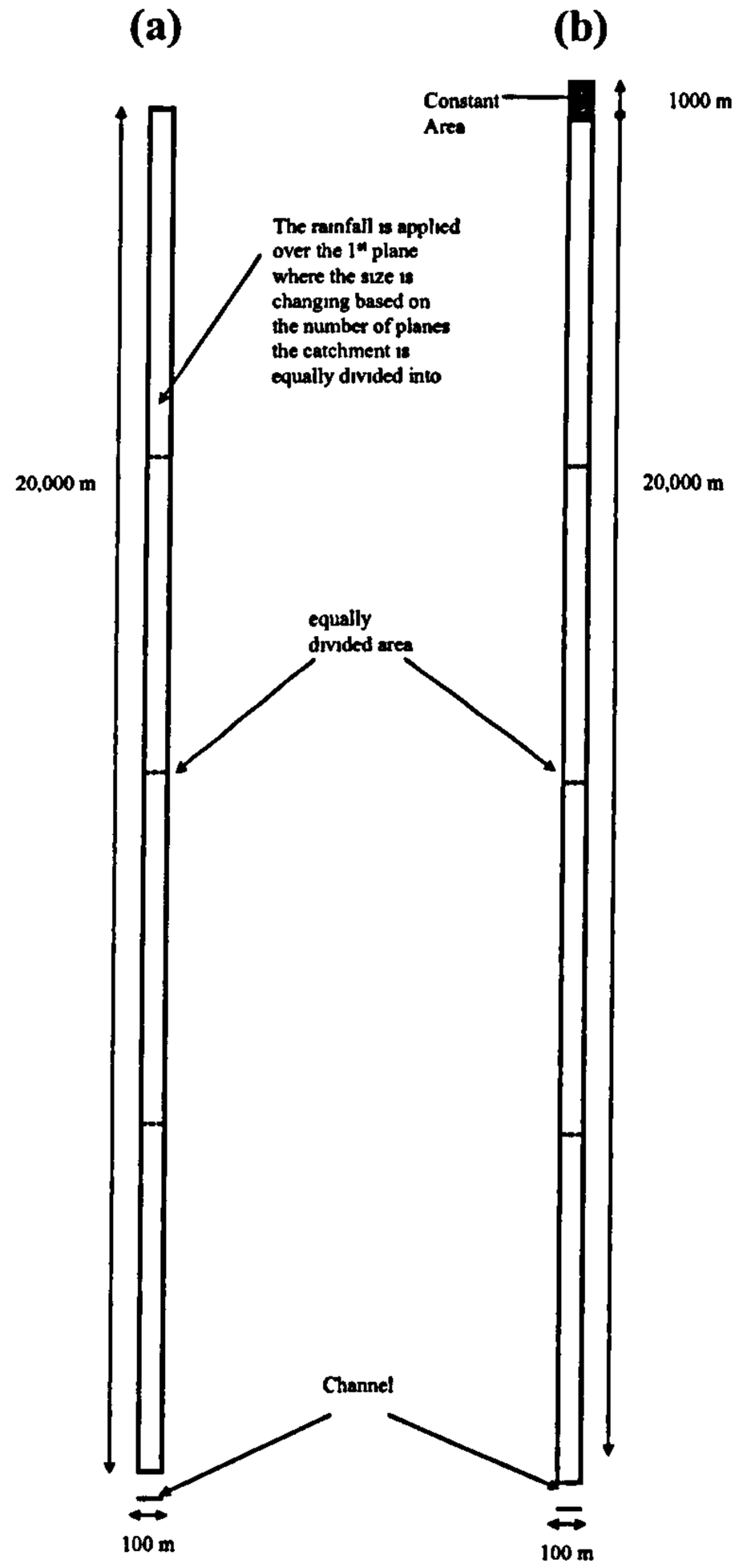


Figure 6.9: Digram shows the assumed synthetic catchment for the case of equal planes (a) and a constant upper plane, and equally divided lower area (b)

6.3.3 Rainfall distribution

The model was run assuming uniform and then non-uniform rainfall spatial distribution as described above, using a 10 mm rainfall event distributed uniformly over the first time-step. The model was also run using a real, recorded, rainfall event (25 Jan 1997 event) at one of the Wadi Ahin rain gauges (Tawi Badr gauge, DM330730AF). Both events were run with the different plane configurations that were explained in **Section 6.3.2.**

6.3.4 Time interval and durations

The model response to different input data time intervals was also tested, by assuming a total amount of 10mm, falling in the 1st 5-min duration, using 5-min intervals, and assuming the same amount (10mm) falling in the 1st 60-min duration, using 60-min time interval.

Using calculation time step that is too large may cause some instability in computation as the wave hydrograph can travel through the subreach with length of Δx in a time that is less than the time interval, Δt, selected by the modeller. Hence, KINEROS2 provides a Courant adjustment facility to overcome this problem by computing a temporary estimate of outflow volume. By using this facility, the outflow volume of each element based on the computational time step is compared to the volume computed using the values stored at each user time step, where the difference should be less than 1% for any element or a warning is given in the output results. A large discrepancy indicates that the input time step is too large.

6.4 The Obtained Results

The model was run using the above mentioned configurations and was assessed based on the 'water balance errors' and the 'event volume error' which indicates that there are no overall problems with the adopted time steps or the plane divisions. These errors may result from the numerical errors associated with the space and time grid discretisation. In addition, the results were also assessed by comparison with analytical solution, and when using different plane sizes.

- ***Water balance error***

KINEROS2 determines water balance errors for each element through checking the rainfall on the element, the inflow, infiltration amounts, stored volumes and the outflow from that element, hence, the differences between the inflow, outflow and storage are used to check the water balance error. The inflow volume is computed by integrating the outflow hydrograph from the upstream element, using trapezoidal integration using the user-specified time step (equal time intervals). On the other hand, the outflow volume is computed using the internal time step, which can be smaller than the user time step due to the Courant adjustment, if enabled, or due to a rainfall breakpoint falling within the user time step. Hence, the inflow volume from an element may not match the outflow volume from the upstream element. This indicates that the user time step that is used is too large. However, the program compares these two values and prints a warning in the event summary if they differ by more than 10%. It should be noted, if the individual element water balance errors are small but of the same sign, they can add up to a relatively large overall error in the event summary and conversely, the individual water balance errors can be large but of different signs so they can cancel each other resulting in a misleadingly low overall event error. However, the water balance error is useful to be checked for each individual element to keep track of the

model's performance at each element to tackle where the problem occurred if the overall models performance was not acceptable.

- ***Event volume error***

The model also checks the event volume error for each simulated event (overall value). In this case, the element storage volume is the area under the depth profile at the end of the simulation. The infiltrated volume, as for the outflow volume, is computed using the internal time step and not the user-specified time step. The infiltration can be estimated over a particular time step or steps in some cases, where these estimations can be poor. Poor infiltrated volume estimates typically occur when flow is advancing or receding and part of the surface has no water depth and if a large *dx* increments (long planes) is used than this problem increases tremendously.

In our case, this was checked for each simulated event and the obtained errors are reported in each case. In general, this is the error that the modeller needs to consider to assess the model's overall performance in simulating any event with no problems. However, it should be noted that a poor volume balance does not necessarily indicate numerical problems as can be seen from above as these can be due to many different reasons.

6.4.1 Results using equally divided areas

KINEROS2 was first run with equally divided areas using uniform and non-uniform rain with both 5- and 60-min rainfall durations and time intervals with no infiltration (under saturated catchment conditions).

The obtained results (simulated flow in m^3/s) for the different number of planes; 1, 2, 4, 8, 16, and 32 planes denoted by P1-P32, are shown in **Figure 6.10a, b, c,** and **d**. The figure also shows the results obtained using the analytical solution (shown in the **Figure 6.10a,** and **6.10c,** for 5- and 60-min uniform rain as AnalSol).

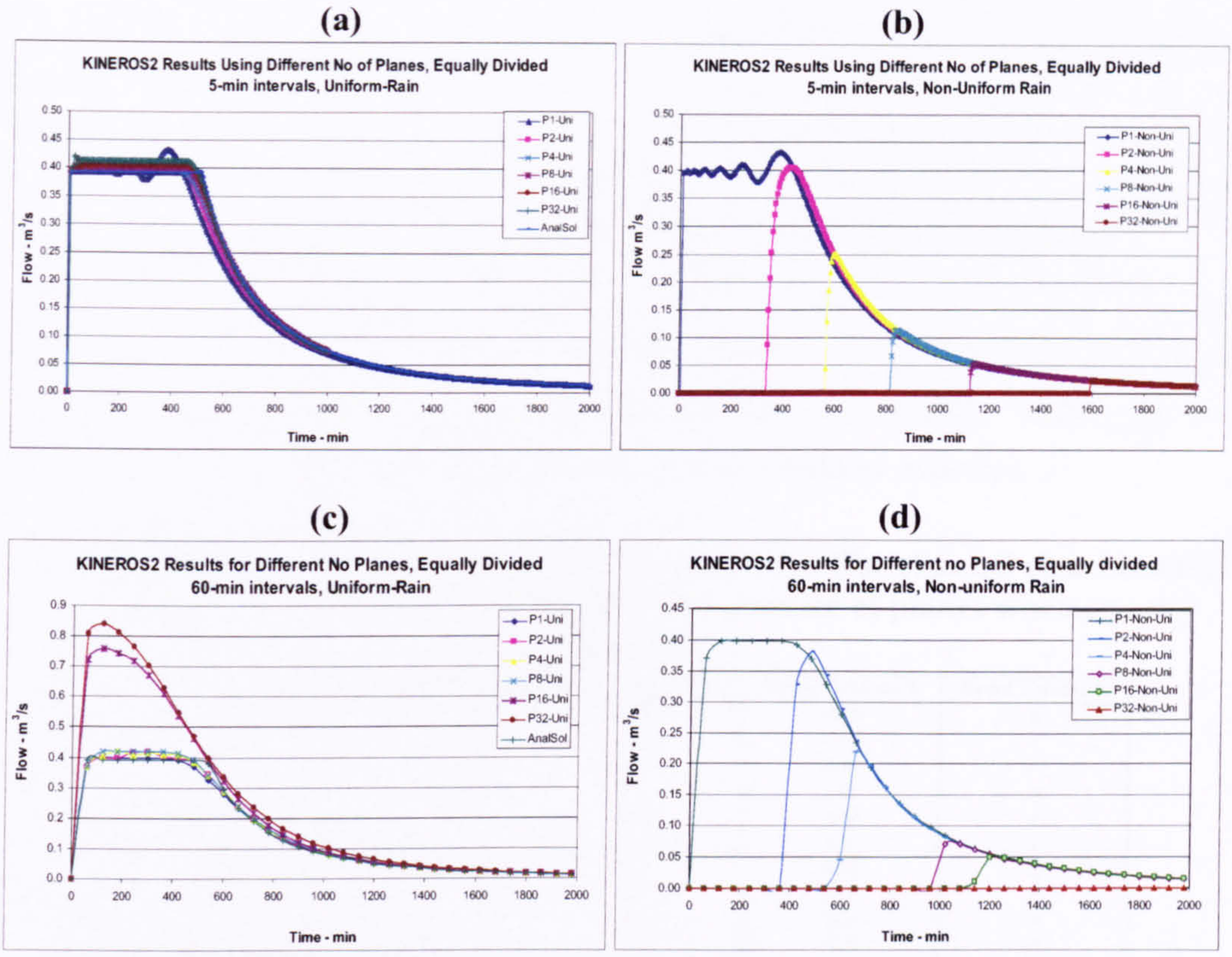


Figure 6.10: KINEROS2 simulations results using equally divided planes, using uniform and non-uniform rain with 5- and 60-min intervals

The results of 5-min simulations (10mm of rain on the 1st 5-min time interval) for the tested catchment show that the flood peaks simulated using different numbers of planes with the same total size have only slight differences, when uniform rain was applied. The figure shows that, with using just one plane, some instability in flood peak values occur as can be seen in **Figure 6.10a** and **b.** It was also found that there were only slight differences in the obtained peaks, which were close (0.39-0.41 m^3/s) to that obtained using the analytical solution for the kinematic wave equation (0.39 m^3/s), when applied to the same configuration.

The simulations for the 60-min duration (10mm of rain on the 1st 60-minute time interval) with the uniform rain are shown in **Figure 6.10c**.

The results show that there is only slight difference in the obtained flood peaks for the different number of planes up to 8 equal area planes from that obtained using 5-min intervals. However, for some unclear reason, the flood peak increased when the catchment was divided into 16- and 32- planes. This could be due to the large input time step as the durations of the flows from the upper planes are short relative to the time step, resulting in large distortion of the hydrographs as described above.

The obtained results for the non-uniform case for the 5-min intervals are shown in **Figure 6.10b**, and for the 60-min intervals are shown in **Figure 6.10d.**

The results show that the flood peaks decrease as the number of planes increases. This is due to the fact that the rainfall volumes are decreasing with the increasing number of planes as the rainfall was applied to the upper plane only, for which its size decreases with the increased number of planes. However, it can be seen clearly from the figures that the flood peaks from the 5-min interval test are slightly higher than the corresponding peaks from the 60-min interval test as would be expected.

Table 6.3: The percentage of the water balance error (for channel element only) and the event volume errors using different number of planes when equally divided

Duration	Rainfall Distribution	Plane Nos	Water Balance %	Event Volume %
5-min	Uniform	P-1	-0.05	3
		P-2	0.07	1
		P-4	0.07	<1
		P-8	0.07	<1
		P-16	0.07	1
		P-32	0 07	2
	Non-Uniform	P-1	-0.03	3
		P-2	-0.02	4
		P-4	-0.04	<1
		P-8	-0.06	10
		P-16	-0.06	25
		P-32	0 62	32
60-min	Uniform	P-1	0.1	2
		P-2	0.01	2
		P-4	0.01	4
		P-8	0	4
		P-16	0.17	42
		P-32	0	53
	Non-Uniform	P-1	0.01	2
		P-2	0.01	5
		P-4	0.05	6
		P-8	0.11	11
		P-16	0.2	44
		P-32	0 68	<1

The event volume error for the 5-min, uniform rain in this configuration, using one plane (total plane length of 20,000m), was 3%, which is generally an acceptable percentage value. The percentage of errors for the 5-min, uniform rain distribution were smaller, generally, than that obtained when the non-uniform rain was applied. However, the percentage of errors when 16- and 32- planes were used, were the worse of all (25 and 32% for P-16 and P-32, respectively).

The event volume error using 60-min, uniform rain, was 42% for P-16, and 53% for P-32, compared to 2, 2, 4, and 4%, for P-1, P-2, P-4, and P-8, respectively, see **Table 6.3**. The analytical solution shows that the flood peak is around $0.39 m^3/s$, but the obtained peak values for P-16 and P-32 are about double than the calculated correct value, which means that there was a problem and these results can not be considered acceptable.

6.4.2 Results using constant size, upper plane

The model was run using this configuration (see **Figure 6.7**), with synthetic and real recorded events under different conditions. The results are discussed below. It should be noted that no analytical solution was found in the literature for this scenario to compare with.

6.4.2.1 Results using synthetic rain

The model was run under saturated conditions (no infiltration) and unsaturated conditions (allowing for infiltration), see **Table 6.2**. The results of the simulations using uniform rain and no infiltration were found very similar to those shown in **Figures 6.10a** and **6.10c**. This was expected as these two sets of tests are the same except that there is an additional area of 100,000m^2 (the upper plane in the latter test with the constant area). However, it was found useful for comparison purposes with the other different runs for this configuration to re run the uniform rain as the infiltration was allowed using this configuration only.

The simulations were run allowing for infiltration to check its effects on the obtained results with the different plane divisions and rainfall distributions and the results are shown in **Figure 6.11a** and **b** for the 5- and 60-min time intervals using the uniform rain.

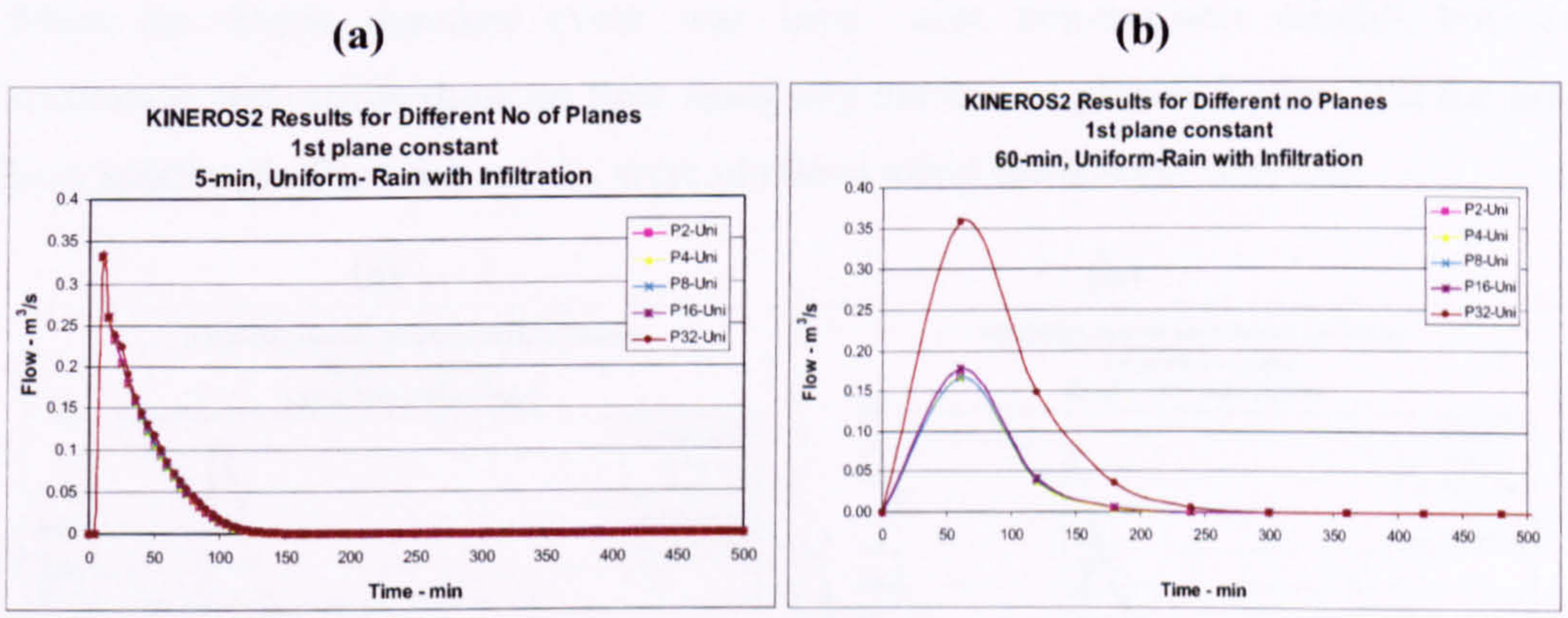


Figure 6.11: KINEROS2 simulations results using constant size upper plane and equally divided lower plane, using uniform rain with 5- and 60-min intervals with infiltration

The results of the simulations using 5-min duration, uniform rain, **Figure 6.11a,** shows that the flood peaks and the recessions are affected by using different number of planes. It was noticed that, even though the plane sizes except P-1 and the parameter values are the same for all the planes, the infiltration amounts were different for different planes (as you would expect).

Figure 6.11b shows the results using 60-min intervals for the same configurations, with uniform rainfall distribution, allowing for infiltration. The flood peak values are very close for the different number of planes except when using 32- planes. The flood peak has significantly increased using 32- planes for no obvious reason. The figure shows that, the hydrographs have faster recessions compared to the no infiltration cases.

The model was run using the 5- and 60-min interval, non-uniform rainfall distribution using the same plane configurations without infiltration. **Figure 6.12a** and **b** show the resulting simulation.

Figure 6.12a shows that the model responses are different from those obtained using the uniform rainfall distributions. The flood peak values for the 5-min time intervals are decreasing with the increased numbers of the planes as well as the time to peak for P-2, and P-4 but are close to each other for P-8 to 32. The obtained flood peak values for P-2 and P-4 were found to be unacceptable (recall that the upstream input flow from the 1st plane is the same in all cases). This can be due to the large Δx which seems to not be able to define the advancing waveform very well. This is believed to be caused by numerical difficulty in modelling the advancing flow. The difficulty occurs at the front, where the solution is forced to zero at some intervals of Δx rather than finding the value of x where depth is zero (Unkrich, *pers. comm.*).

When the 5-min duration event was used, with non-uniform rainfall but with infiltration, the results show no flow using any number of planes. It seems all the flows have infiltrated. The same results were obtained using the 60-min intervals.

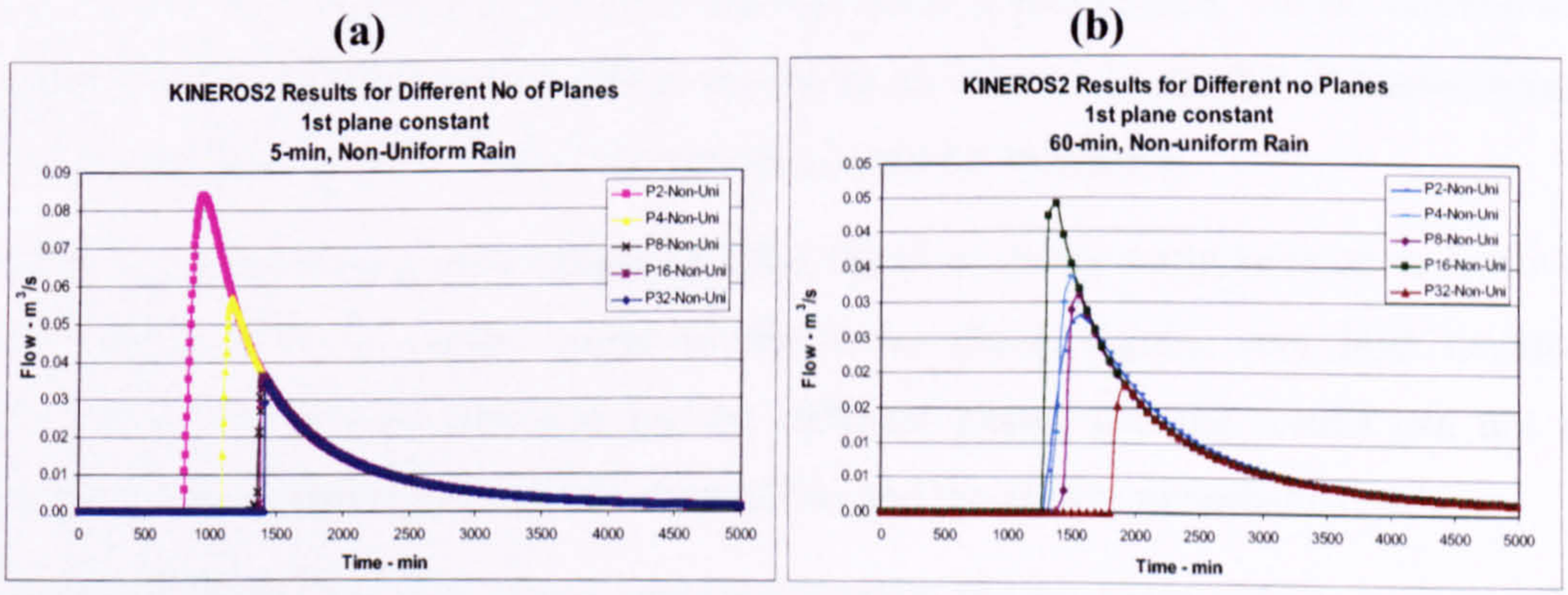


Figure 6.12: KINEROS2 simulation results using constant size upper plane and equally divided lower plane, using non-uniform rain with 5- and 60-min intervals with no infiltration

The results of using 60-min, non-uniform rain and no infiltration, show that the flood peaks have no consistent change that can be linked easily to the increased number of planes. As can be seen from **Figure 6.12b**, the flood peak is higher when 4-planes were

used from that obtained using 2-planes but lower than that obtained using 8-planes and then increases remarkably when 16-planes were used but decreased largely using 32-planes.

An attempt was made to deduce the cause of the problem by studying the flow routing from one plane to another, to highlight where the problem started. Hence, the outflow at the end of each plane is plotted. **Figure 6.13a** below shows the flow from different planes as it goes downstream, when total of 2 planes were used whereas, **Figure 6.13b** shows the flood routing when total of 4 planes were used.

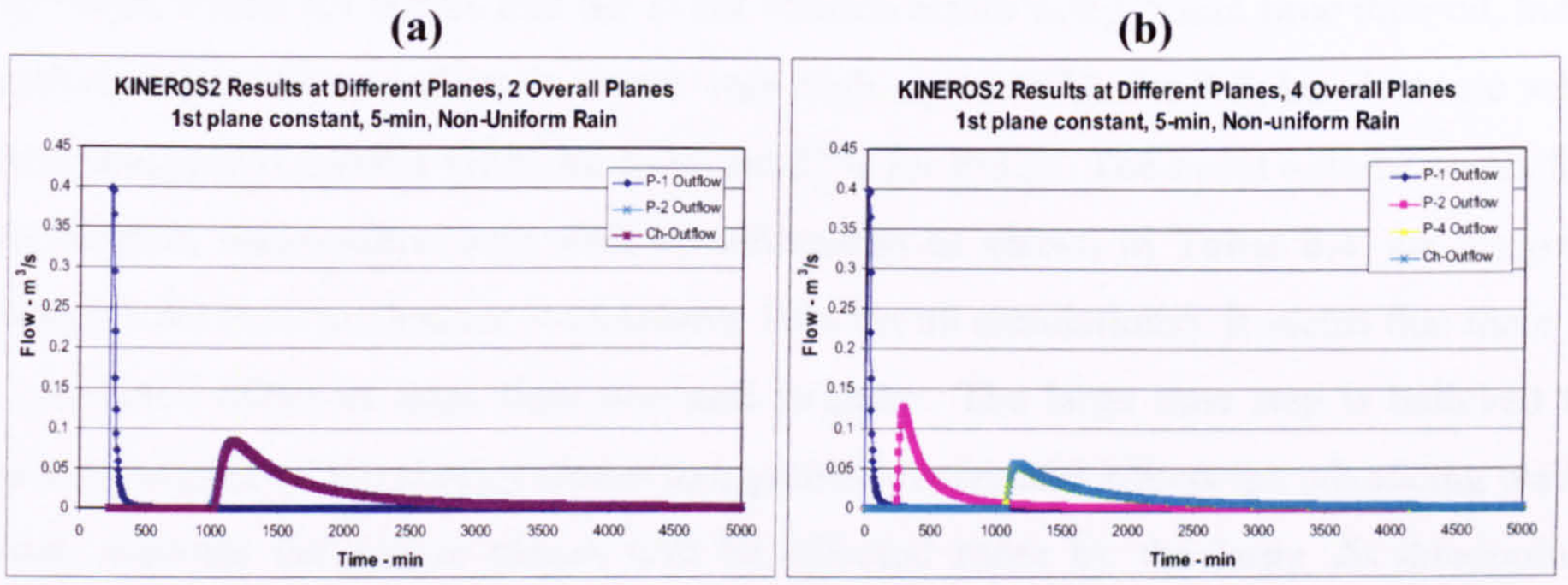


Figure 6.13: KINEROS2 simulation results, using constant size upper plane and equally divided lower plane, using non-uniform rain with 5-min intervals, 2-overall planes, and 4-overall planes

Figure 6.13a shows that the flow is decreasing as it moves downstream from the 1st plane to the next one. It was noticed that the parameters were set to have no infiltration but a very high negative infiltration value was obtained from the 2nd plane which shows that there is a kind of bug in the code and the result is problematic. As the rainfall was applied to the upper plane only, there should be no increase in rainfall amounts, hence, the flow volume in the 2nd and 4th planes should not be increasing.

When four planes were used (**Figure 6.13b**), the flow shows some increase as it moves downstream from the upper plane to the lower plane. Again, very high negative infiltration values were obtained for the different planes and the results can not be accepted due to high event volume error (47%) and the clearly unrealistic results.

Table 6.4 shows that the volume percentage errors for the event volume summary for the 5-min time intervals using uniform rain with no infiltration are all in the acceptable range (<1% to 2%). However, in the case for 60-min, it was up to 53% for P-32, whereas the least was obtained when P-2 was used (2%). The error was increasing with the increased number of planes.

The errors for 5-min, uniform with infiltration are less than 1% for all cases except for P-32 when it was 2%. In contrast, the event volume error for the 60-min, uniform rain with infiltration was ranging from 12% for P-2 to 5% for P-4 and 42% for P-32, see **Table 6.4**. It seems that the large input time step has greater effects when larger plane numbers are used. This could be because the durations of the flows from the upper planes is short relative to the used time step, resulting in large distortion of the hydrograph as was explained before. However, the infiltration seems to alter the flow sufficiently, hence the 16-plane case did not suffer a noticeable effect as can be seen.

However, **Table 6.4** shows that the event volume errors using 5-min time interval, non-uniform rain, with no infiltration were very high, up to 187% for P-2, but decrease with increasing plane number (18% for P-16 but 27% for P-32). The event volume errors for the 60-min, non-uniform rain with no infiltration as shown in **Table 6.4**, are ranging from 1% for P-32 to 58% for P-16 (above 10% for all simulations). It seems that there is a combined effect of large time step and large Δx. The large time step is believed to have an impact on the shorter planes to a greater degree and affects the advancing wave front, whereas the longer planes will be affected more by the large Δx standpoint. Hence, the overall effects are unpredictable (as concluded by the discussion with Unkrich).

The volume error for 5-min, non-uniform rainfall with infiltration were ranging from 6% for P-32 to 50% for P-2 but the error was 5% for P-8 and P-16. The errors were very high for the 60-min time interval too, though it showed unclear trend (from 23% for P-2, 9 for P-4, 7 for P-8, 28 for P-16, and 24% for P-32.

Table 6.4 shows that the event volume error is, generally, high for all cases with the non-uniform rain with no clear trends with the increased number of planes.

Table 6.4: The percent of event volume errors obtained for different number of planes when 1st Plane is constant with synthetic rainfall, uniformly and non-uniformly distributed

Duration	Rainfall Distribution	Plane Nos	Event Volume %
5-min	Uniform (No Infiltration)	P-1	
		P-2	<1
		P-4	<1
		P-8	<1
		P-16	1
		P-32	2
	Uniform (with Infiltration)	P-1	
		P-2	<1
		P-4	<1
		P-8	<1
		P-16	2
		P-32	<1
	Non-Uniform (No Infiltration)	P-1	
		P-2	187
		P-4	47
		P-8	39
		P-16	18
		P-32	27
	Non-Uniform (with Infiltration)	P-1	
		P-2	50
		P-4	9
		P-8	5
		P-16	5
		P-32	6
60-min	Uniform (No Infiltration)	P-1	
		P-2	2
		P-4	5
		P-8	7
		P-16	40
		P-32	53
	Uniform- (with Infiltration)	P-1	
		P-2	12
		P-4	5
		P-8	<1
		P-16	2
		P-32	42
	Non-Uniform (No Infiltration)	P-1	
		P-2	9
		P-4	14
		P-8	12
		P-16	58
		P-32	1
	Non-uniform (with Infiltration)	P-1	
		P-2	23
		P-4	9
		P-8	7
		P-16	28
		P-32	24

6.4.2.2 Results using a recorded rainfall event

The model was tested with the above-mentioned configuration (constant upper plane and equally divided lower planes) using the synthetic catchment but with the real

recorded event of the 25th Jan 1997 using the rainfall from one gauge, Tawi Badr (DM330730AF), from the Wadi Ahin catchment. The model was run with 5-min and 60-min intervals with uniform and the non-uniform rainfall distributions with and without allowance for infiltration.

Figure 6.14a shows the rainfall distribution for 5-min intervals, whereas **Figure 6.14b** shows the rainfall distribution for 60-min interval.

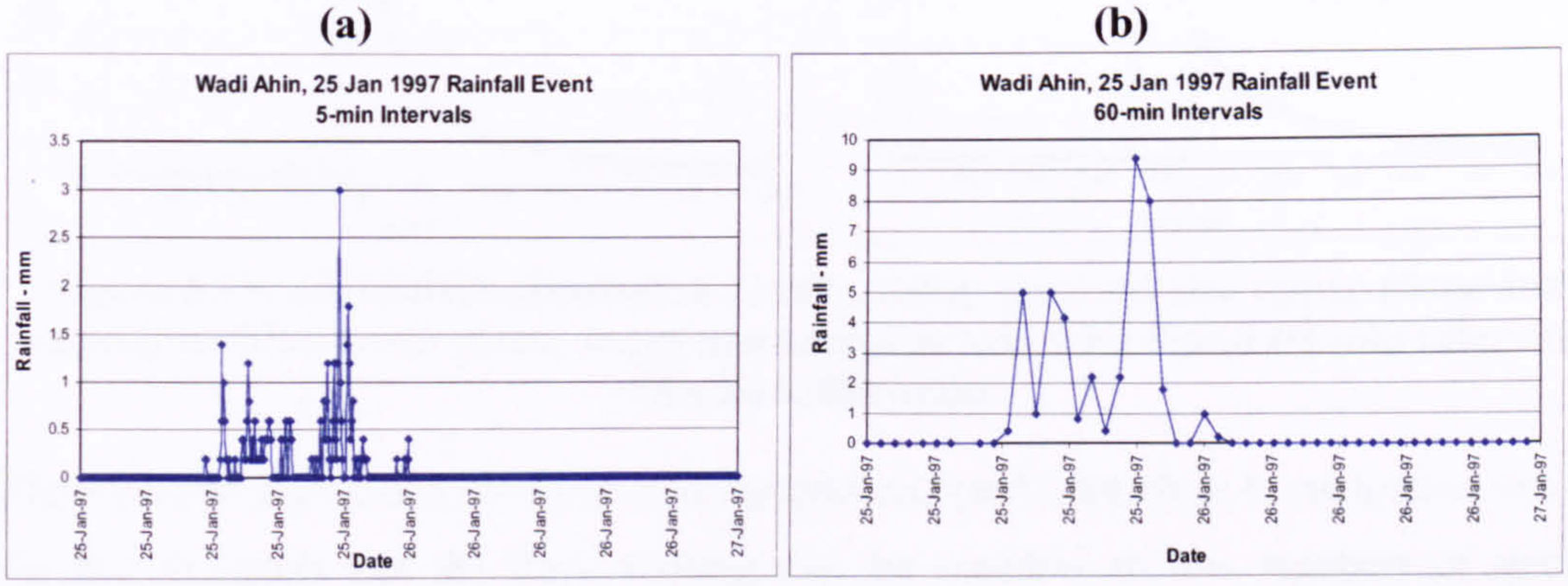


Figure 6.14: Wadi Ahin, 25 Jan 1997 rainfall event, 5- and 60-min time intervals

The model was run using 5- and 60-min intervals with a uniform rainfall distribution, with infiltration and the results are shown in **Figures 6.15a** and **6.15b.** The simulations with non-uniform rain showed that there are hardly any differences when subdividing the catchment into more planes. Hence, they have not been presented.

Figure 6.15a, shows that there are small differences in the flood peak values from those obtained when no infiltration was allowed.

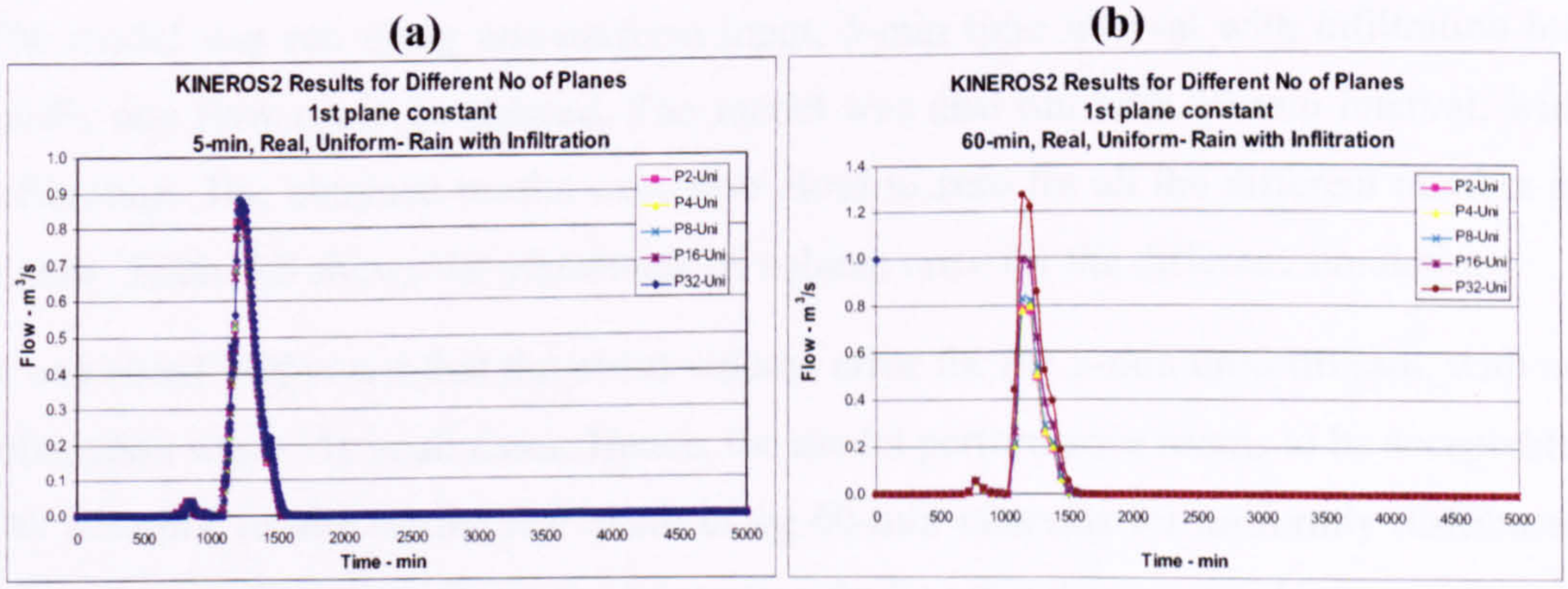


Figure 6.15: KINEROS simulation results using constant size upper plane and equally divided lower plane, using uniform rain with 5- and 60-min intervals with infiltration

The simulations of 60-min, uniform rain show different responses when the simulations were run with infiltration, **Figure 6.15b**. The flood peak using 32- planes resulted in the highest flood peak value compared to all the others, for no obvious reason.

The results of the model simulations, using 5- and 60-min, non-uniform rainfall distribution are shown in **Figures 6.16a** and **6.16b** with no infiltration.

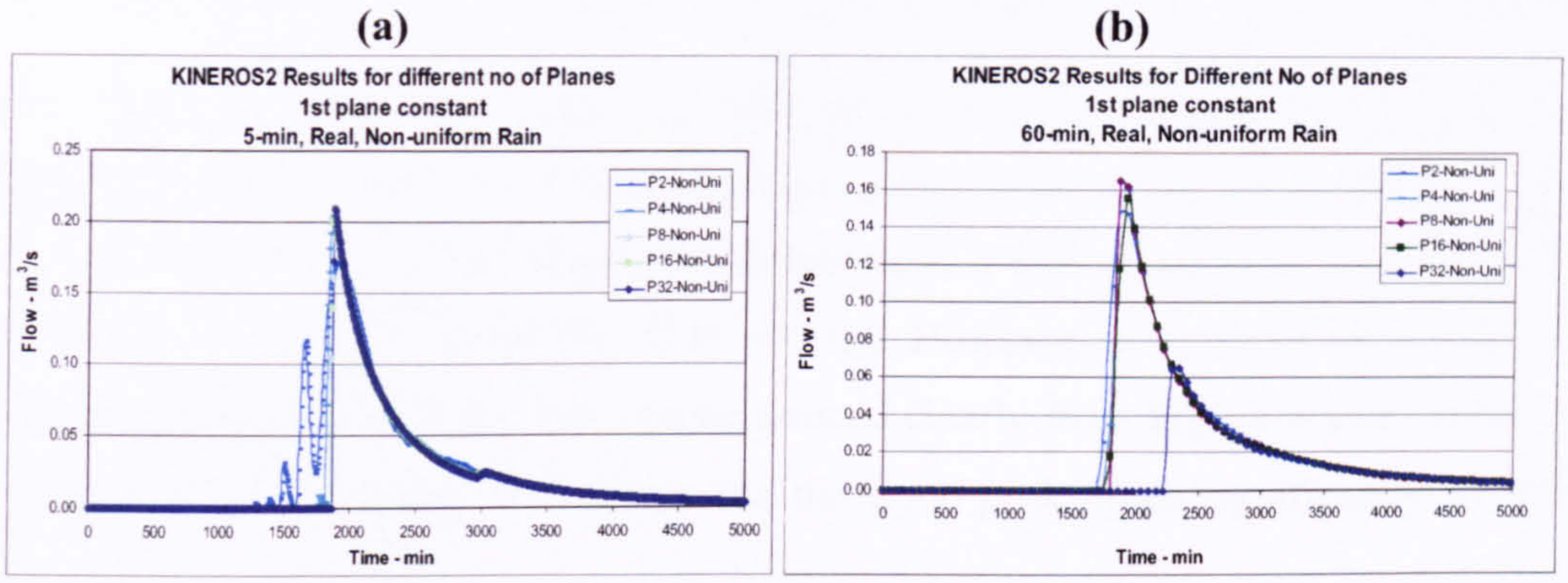


Figure 6.16: KINEROS simulation results, using constant size upper plane and equally divided lower plane, using non-uniform rain with 5-and 60-min intervals with no infiltration

Figure 6.16a shows that the flood hydrographs and peaks are close to each other except for P-2. It seems that the flood routing may be sensitive to low numbers of spatial elements with high length. This can be caused by the Δx value and Δt used values as mentioned before.

However, the non-uniform rainfall simulations for the real events for the 60-min intervals with no infiltration are shown in **Figure 6.16b**. The figure shows that the flood peaks using the 60-min rainfall intervals are less than those obtained using 5-min intervals. The flood peaks are slightly different for different numbers of planes. However, the difference was quite high using 32-planes.

The model was run using non-uniform input, 5-min time interval with infiltration but hardly any flow could be noticed. The model was also run with 60-min interval, with infiltration. The obtained results were also close to zero for all the different number of planes. **Table 6.5** shows the percentage of volume error for the different simulations.

It was noted in this test that the event volume error for the 5-min uniform rain, with no infiltration was <1% in all cases. Hence, the model performance seems to be acceptable. The obtained results for the real event using 60-min intervals for uniformly distributed rain with no infiltration, shows the interesting finding that the event volume summary is increasing with the increasing number of the planes (from <1% for P-2 to 4% for P-16). The event volume summary error was <1% for P-2 and, P-4, and P-8 but jumped to 4% for P-16 and to 9% for P-32.

The simulations using 5-min, uniform rain, with infiltration, showed the volume errors were all <1%. However, when 60-min was used, it was found that, the errors were <1% for P-2 to P-8 but increased to 8% for P-8 and to 12% for P-32.

The simulation errors for 5-min, non uniform, with no infiltration, appeared to vary randomly with the variation of plane numbers. It was 8% for P-16, 4% for P-4 but up to 12% for P-2. In the case of using 60-min intervals, it was the highest also for the P-2 (7%) but it was the lowest for P-16 (<1%). However, it jumped up to 50% in unexpected results for P-32. This can be noticed clearly from **Figure 6.16b**, where the obtained flood peaks has close values but the flood peak drops significantly for P-32 case.

The obtained results for the 5-min intervals, non-uniform rain, when allowing for infiltration, were from 2% for P-16 to 7% for P-4. These errors are slightly high but it dropped to <1% for P-32, the event volume errors, for 60-min, non-uniform rainfall, with infiltration, were also high. They were ranging from 2% for P-8 to 15% for P-2 and 5% for P-8 but 4% for P-32. This shows clearly that increasing number of planes is not leading to a general decrease in volume errors as was expected.

Table 6.5: The percentage of event volume errors for different number of planes when 1st plane is constant with the real-rainfall event, uniformly and non-uniformly distributed

Duration	Rainfall Distribution	Plane Nos	Event Volume %
5-min	Uniform (No Infiltration)	P-1	
		P-2	<1
		P-4	<1
		P-8	<1
		P-16	<1
		P-32	<1
	Uniform (with Infiltration)	P-1	
		P-2	<1
		P-4	<1
		P-8	<1
		P-16	<1
		P-32	<1
	Non-Uniform (No Infiltration)	P-1	
		P-2	12
		P-4	4
		P-8	10
		P-16	8
		P-32	6
	Non-Uniform (with Infiltration)	P-1	
		P-2	6
		P-4	7
		P-8	<1
		P-16	<1
		P-32	<1
60-min	Uniform (No Infiltration)	P-1	
		P-2	<1
		P-4	1
		P-8	2
		P-16	4
		P-32	9
	Uniform (with Infiltration)	P-1	
		P-2	<1
		P-4	<1
		P-8	<1
		P-16	4
		P-32	12
60-min	Non-Uniform (No Infiltration)	P-1	
		P-2	7
		P-4	3
		P-8	3
		P-16	<1
		P-32	50
	Non-Uniform (with Infiltration)	P-1	
		P-2	15
		P-4	8
		P-8	2
		P-16	4
		P-32	4

6.5 Conclusions

The KINEROS2 model was run for a simple synthetic catchment (a series of planes of total length 20,000m, feeding a short channel) using different configurations: different numbers of planes in series, different rainfall distributions, and different rainfall time intervals. It was also run with and without infiltration to test the model's performance under different conditions. The model responses were compared to study the effects of the numerical errors on the obtained flood peak values.

The results show that using different numbers and sizes of planes have different effects based on the configuration but no clear pattern was noticed. However, the tests show that KINEROS2 was having some problems in coping with a single plane length of 20,000 m in some cases (**Figure 6.10a** and **b**) but seems to give reasonable results in other cases for both 5- and 60-min time intervals (**Figure 6.10c** and **d**) for the uniform rainfall distribution test. The tests also show that, using smaller lengths did not prove to be always the solution as can be noticed from the results, e.g. when 16 and 32 planes were used (**Figures 6.10c, 6.11b, 6.12b, 6.15b**). The event volume errors were increasing in some cases with the increasing size of planes (**Tables 6.1, 6.2,** and **6.3**). Using large size planes, where Δx is large (**Figure 6.12a**), shows a problem for some cases.

It was also found from the test that using large input time steps may cause a loss of information regardless of whether the time step is adjusted using the Courant adjustment. One possible explanation is that, when larger numbers of planes are used, such as in some cases when 16 and 32 planes, the duration of flows from the upper planes is short relative to the time step, resulting in large distortion of the hydrographs. In some other cases, there is a combined effect of large time step and Δx. It is believed that the large time step will impact the shorter planes to a greater degree and can cause some problems in determining the right location of the advancing front. Hence, the longer planes will be more affected by the large Δx.

The results of using the real rainfall event shows that there is no effect of using a different number of planes with uniform rain for both 5- and 60-min intervals but there is slight effect when non-uniform rain is applied. However, in the cases where infiltration is allowed, the flood peaks seem to be slightly affected by both the number of planes and the time intervals, see **Figures 6.15a** and **6.15b**.

The amount of rainfall and its duration have some effects on the obtained results and the model performance. This was evident when the model was run with infiltration, (**Table 6.3** and **6.4**), when a very small amount of flow is running to a rather large channel. Hence, the water balance errors were high in such cases for some individual elements when the model was run with non-uniform rain with infiltration. In addition, the relatively high event volume balance errors for the non-uniform rainfall in some cases can be caused by the numerical difficulty in modelling the advancing flow. The difficulty occurs at the front, where the solution is forced to zero at some interval of Δx rather than finding the value of x where depth is zero, as has been mentioned before. The rainfall distributions (uniform and non-uniform) were found to have some effects on the obtained results, as was expected, but some results were not easily explained as there are many factors affecting them.

From the tests reported in this chapter, the tested configurations and rainfall distributions do have effects on the obtained results, but the model's response was not easy to predict. However, using a 5-min time interval did not show any better results compared to the results using a 60-min interval in most cases. Hence, each case needs to be studied individually. The user might need to run the model with different sizes of planes with close observation of the obtained hydrographs and the percent of errors until the optimum length is reached for his or her study area as was done here where the effect of using the longest length was tested using different configurations. The accepted error percentage should not exceed 1% in theory, based on the developer's advice. However, this might not be always possible and the user might need to accept a higher percentage of error. In our case, up to 30% can be thought reasonable due to the quality of the data and the rainfall network coverage. However, this is will depend also on the used objective function and the comparison between the observed and the simulated hydrographs, as the next chapter shows.

Local sensitivity analysis to check the effect of different parameter values on the model behaviour will be addressed in the next chapter for further investigation of controls on the model's performance.

This primary test lead to further subdivision of some planes of the Wadi Ahin catchment to avoid the negative effects of using large plane sizes, with close observation of the event volume errors during any simulation. As there was no clear advantage for using 5-min time interval in our case, the research was carried out using 60-min time interval.

Chapter 7

The KINEROS2 Model

Sensitivity Analysis, Calibration and Validation

7.1 Introduction

Sensitivity analysis can be described as the procedure to determine which parameters most affect the model results and performance (Sorooshian & Gupta, 1995). This may guide the calibration process (for example identifying the less important parameters which may be fixed) and may lead to better understanding of how the model is working. The analysis will also be used in this chapter to look at how the spatial nature of the rainfall event affects the importance of parameters and the model performance. Initial local sensitivity analysis of the KINEROS2 model was followed by more extensive global sensitivity analysis, calibration and validation tests.

The local sensitivity analyses were run using two differently-distributed rainfall events, perturbing all parameters which were considered to be uncertain around a default value, one at a time.

The global sensitivity analysis was carried out through uniform random sampling of the parameter space, and looking at the shape and statistics of plots of model outputs against parameter values ('dotty plots'). 25 events from the years 1996-1999 were used. This analysis also provided estimates of the optimum parameter sets, allowing calibration and validation.

The model performance was measured using five different objective functions: peak flow, event volume, time to peak, a combination of peak flow and volume, and a combination of peak flow, volume and time to peak. This chapter describes the local and global sensitivity analysis and discusses the results obtained. At all stages the one-layer subsurface was used (see **Section 6.3**) and the Courant adjustment was applied (see **Section 6.4**). With some exceptions, noted below, the parameters were assumed to be uniform over the catchment for the sensitivity analyses.

7.2 Catchment division

The catchment was subdivided into 20 plane elements and 8 channel elements based on the Digital Elevation Model (DEM), soil type and geological maps (see **Figure 7.1** for the catchment divisions and **Table 7.1** for the elements' details). The catchment was, primarily, divided in systematic way but further subdivisions were introduced later which affected the numbering system. **Table 7.1** shows characteristics such as the length, slope, width, and area of the each element.

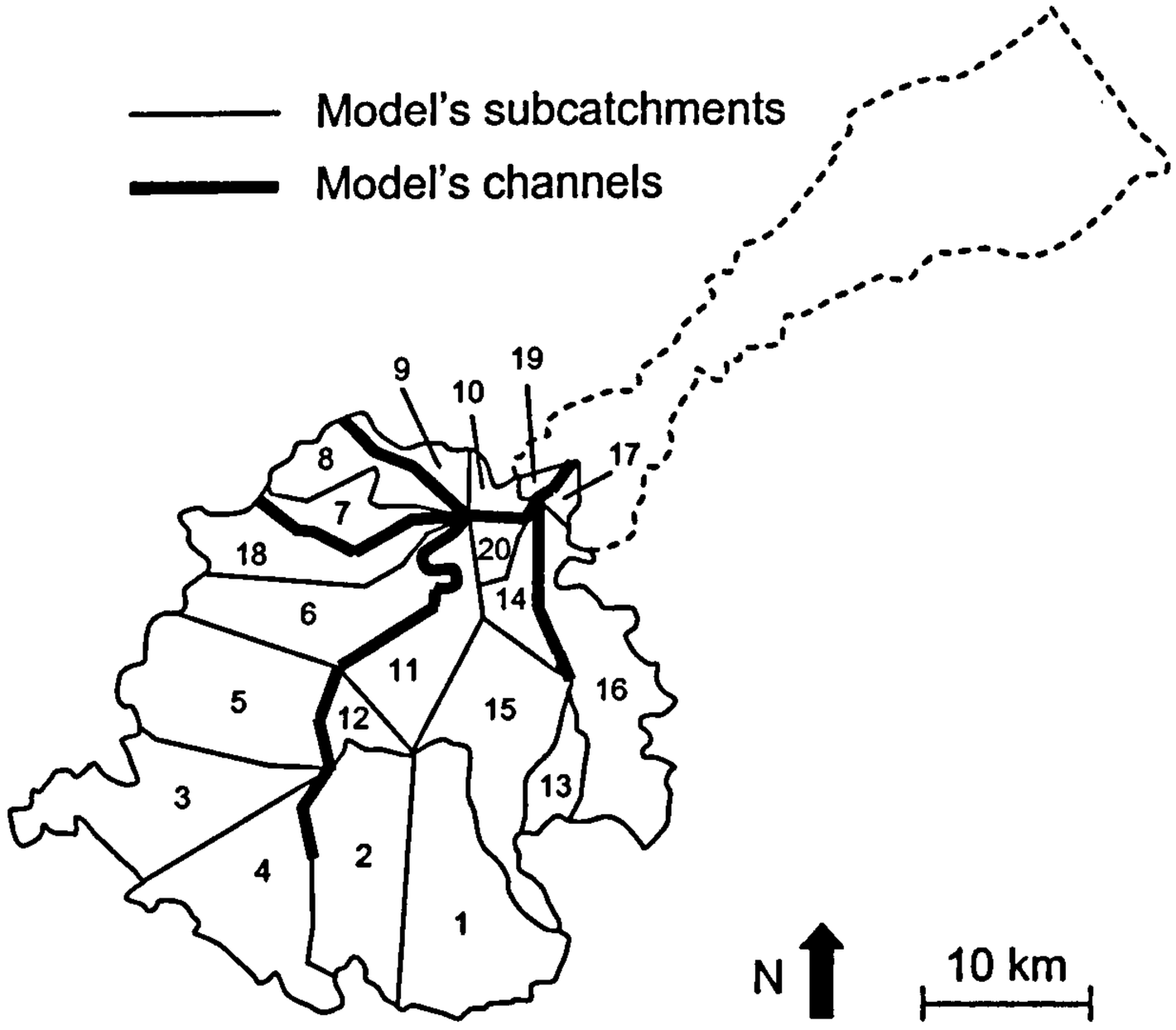


Figure 7.1: The catchment subdivision showing the plane and channel locations

Table 7.1: Parameters that describe geometry of the different elements

Element	Length (m)	Width (m)	Area (km^2)	Slope
Planes				
1	15127	5611	84.4	0.04
2	12073	5534	66.4	0.03
3	12459	5163	63.9	0.03
4	10778	6157	66	0.06
5	1789	40547	72.1	0.35
6	14060	3884	54.3	0.05
7	11175	1798	20	0.06
8	8520	2882	24.4	0.09
9	695	17618	12.2	0.92
10	3473	2461	8.5	0.05
11	12541	3233	40.3	0.04
12	4276	2964	12.6	0.09
13	7851	1907	14.9	0.11
14	19674	910	17.8	0.01
15	16305	3933	63.7	0.06
16	18336	3645	66.4	0.05
17	2616	1298	3.4	0.06
18	12372	2952	36.3	0.07
19	2710	326	0.9	0.01
20	3429	1630	5.6	0.05
Channels				
1	5526	50	0.3	0.041
2	5887	50	0.3	0.041
3	14726	50	0.7	0.012
4	12646	50	0.6	0.055
5	8410	50	0.4	0.073
6	10302	60	0.6	0.012
7	4618	60	0.3	0.016
8	2922	60	0.2	0.02

7.3 The Default Parameter Values

Before discussing the parameters, it should be noted that the model requires definition of two inputs which are common to all elements: the type of units (Metric or English) that are adopted, and the *Clen* (the characteristic length which generally equals the longest single channel element or contiguous cascade of planes, which KINEROS2 uses to define the numerical grid size for planes and channels, for example a small value of *Clen* means a relatively fine spatial grid).

For the purpose of estimating their default values, and their inclusion in the sensitivity analysis and calibration, the model parameters fall into six categories:

1) The geometry parameters (plane width, length, and area; channel cross-section width, side-slope, and length) which are assumed to be measurable from the DEM and are not included in the sensitivity analysis or calibration. In practice, the plane areas are easily measured from the DEM, however estimation of the length and width needed some judgement because the planes delineated from the DEM are not rectangles (see **Figure 7.1**). The channel cross-section shapes also need some judgement based on knowledge

of the wadis; due to the very limited data on cross-sections they were all assumed to be the same shape based on the cross-section survey data that were available at the flow gauge site near the catchment outlet only, as shown in **Figure 5.13.** The survey cross section was used as a guide and to obtain the side slopes and the width as the model is assuming a trapezoidal section. Also, it should be noted that only the major wadis were represented as channels, not the extended channel network.

2) The average slope of each plane, which although measurable from the DEM, is considered to contain significant uncertainty due to the difficulty of estimating a value which is effective at the scale of the planes. The default value is taken as the measured value and a slope factor parameter, *Slp,* is included in order to adjust measured slope to effective slope.

3) Parameters which contain significant uncertainty due to the difficult or impossible task of measuring their values over large scales. These parameters need to be adjusted in the sensitivity analysis and calibration. They are: initial degree of soil saturation (*S*), saturated hydraulic conductivity (*Ks*), coefficient of variation of *Ks* (*Cv*), Manning's coefficient (*n*), capillary length scale (*G*), volumetric rock fraction (*Roc*), porosity (*Por*), and the pore size distribution index (*Dist*). Their default values are taken from the previous study of Wadi Ahin by Mott Macdonald (1992), who estimated the values based on calibration in Wadi Ahin and using calibrated values from other catchments. Some of these values were fixed following the results of the local sensitivity analysis. There are also the relief (*Rel*) and the Spacing (*Spc*), which were not included in the KINEROS version that was used by Mott MacDonald (1992) study.

4) Parameters which, although uncertain, were fixed at default values that were thought to be reasonable, in order to keep the analysis to a more manageable size. This included the canopy cover (*Ca*), the interception loss (*Int*), and the soil layer thickness (*Thic*), which were fixed at the default value.

5) The rainfall interpolation parameter *f*. This was introduced after the local sensitivity analysis and is defined in **Section 7.6.**

6) Parameters that describe the flow routing directions. Those were described by identifying which planes or channels contribute to each element laterally and longitudinally. The required information was obtained directly from the digital elevation maps (DEM). This depends largely on how the modeller has divided sub-catchments into channel and plane elements, and the topography of the catchment which controls the flow routing direction. Hence, this information was obtained from the DEM and its

sensitivity was not thought necessary to be tested as the flow directions are clear from the DEMs, see **Figure 5.7,** and the topographic maps.

The default values of the parameters are listed on **Tables 7.1** and **7.2. Table 7.2** also lists the source of the default value.

Table 7.2: The default values of different parameters used to run KINEROS2

Parameter	Symbol	Units	Default value (planes)	Default value (channels)
Manning's coefficient	*n*	$sm^{-1/3}$	0.035	0.036
Relief (micro-topography)	*Rel*	mm	20	NA
Relief spacing (channel micro-topography)	*Spc*	m	10	NA
Woolhiser coeff.	*W*	-	NA	0.15
Saturated hydraulic conductivity	*Ks*	mm/hr	3.7[a]	41.7
Capillary drive	*G*	mm	0	0
Variation of *ks*	*Cv*	-	0.1	NA
Initial saturation	*S*	-	0.45	0.45[b]
Soil porosity	*Por*	-	0.1	0.44[c]
Ditribution (pore size distribution)	*Dist*	-	0.6	-
Interception depth	*Int*	mm	2	NA
Rock cover	*Roc*	-	0	0
Canopy cover	*Ca*	-	0	NA
Soil layer thickness	*Thic*	mm	500	NA
Rainfall interpolation non-linearity	*f*	-	1	NA
Slope factor	*Slp*	-	1	NA

a. In plane no. 9 the default Ks value was 31.25mm/hour, in plane no. 10 and 15 it was 20.8 mm/hour; in all others it was 3.7mm/hour
b. In 4 channel reaches, default value was 0.05; in all other channel it was 0.45
c. In channel no. 1, default value was 0.15; in all other channel it was 0.44

7.4 Local Sensitivity Analysis

The model was run using different rainfall interpolations as mentioned before with the default parameter values shown in **Tables 7.1** and **7.2** to check the effect of rainfall and the different interpolations on the model results.

The model then was run with the different parameter values as shown in **Table 7.2** using mainly the KINEROS2 rainfall interpolation.

The analyses were run for each of the two events, 07 August 1996 and 25 January 1997, which were chosen because they had markedly different spatial variance of rainfall. The 07 August 1996 event **(Figure 7.2)** is a local storm, concentrated in the north-east part of the catchment and there was no rainfall recorded on the lower part of the catchment, whereas the 25 Jan 1997 is a widespread event **(Figure 7.3)**, distributed over the whole catchment, although the maximum rainfall was recorded in the south-west part (Wadi Ahin near Hayl).

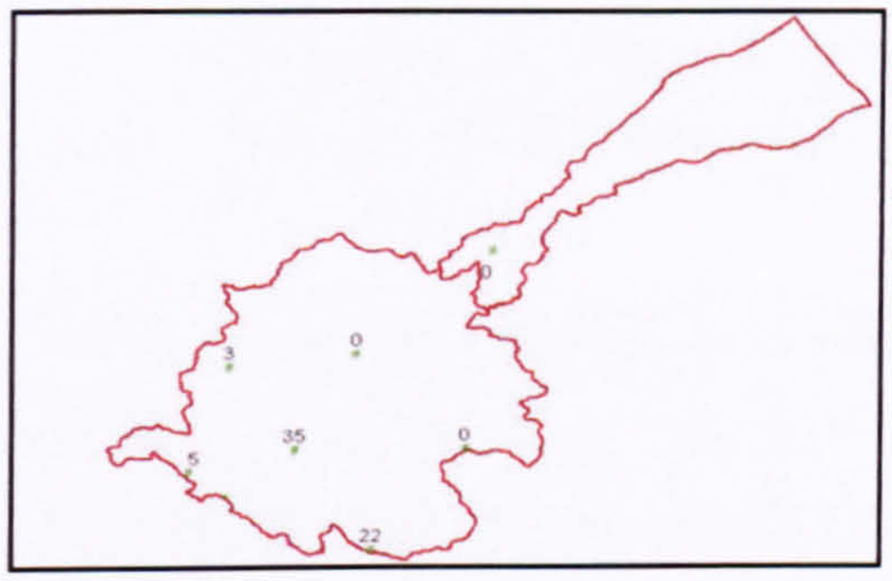


Figure 7.2: Total rainfall (mm) at each gauge during 07-08 Aug 1996 event

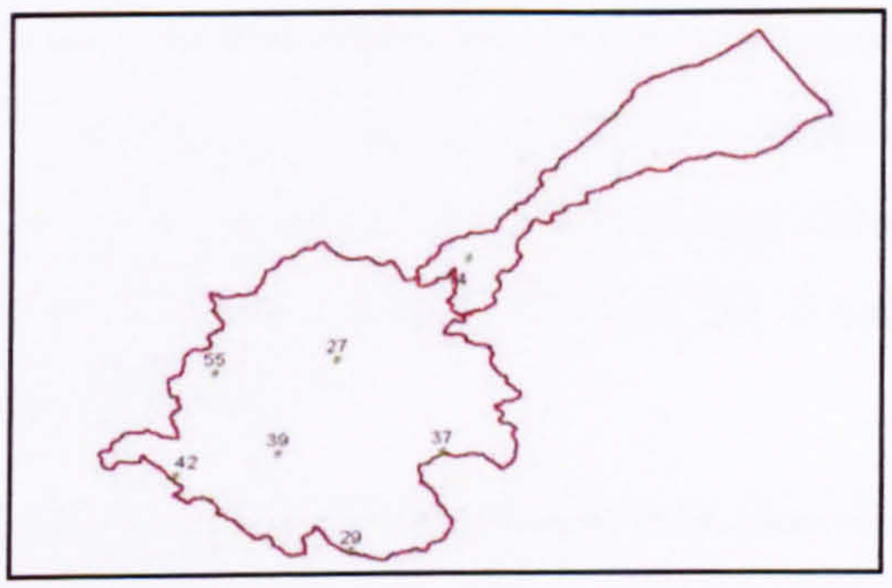


Figure 7.3: Total rainfall (mm) at each gauge during 25-28 Jan 1997 event

7.4.1 The selected parameters for the local sensitivity analysis

Table 7.3 shows the values that were used for each tested parameter. The values were selected in such a way that their effects and the model's sensitivity to their values can be identified, while maintaining physically plausible values. The values were varied uniformly across the catchment.

KINEROS2 includes a 'multiplier' facility for some parameters (*Ks*, *n* or *Chezy* used coefficients, *Cv, G,* and *Int*) which allows the values of those parameters over the whole catchment to be multiplied by a specified factor, rather than having to change the value for each element individually. Using this facility was especially convenient for *Ks* in this study because its default values were not uniform across the catchment. The multiplier was also used when the change was to be applied to both types of elements, the channels and the planes.

As the vegetation cover is very sparse and limited, and as there was not enough information on the exact percentage of its coverage, the percentage of vegetation cover (*Ca*) was assumed to be nil in all the runs except when the interception parameter sensitivity was tested when *Ca* was set to 0.1.

Perturbing the values of *G, Dist*, and *Por* individually led to the model crashing in some cases. This is thought to be because of the strong inter-dependency of these parameters and maintaining plausible combinations of values requires all three to be changed

simultaneously. Hence, the combinations of values *G, Dist*, and *Por* used in the sensitivity analysis were based on the soil texture table in the KINEROS2 manual (after Woolhiser, 1990).

One combination used was G=11 mm (the recommended value for a sandy loam soil type) and the corresponding *Dist* and *Por* values were 0.25 and 0.463, respectively. Some other types of soil textures were also used, as **Table 7.3** shows.

In the G=0 case, which leads to have a constant infiltration that equals to *Ks*, the *Por* and *Dist* values used were the default values. It should be noted that the G value also affects the sensitivity of the models result to the initial condition, S, as no sensitivity to this parameter should be expected when G=0. Furthermore, the model code is set so that if S is greater than 0.95, the model automatically sets the G value to zero and assumes only one soil layer of infinite depth.

The model's sensitivity to the rainfall interpolation was also checked, using the default parameter values. Three different interpolation methods were tested; *a)* the KINEROS2 interpolation method (see **section 7.5.2.1** for details of this method), *b)* for each plane, using the rainfall from a single gauge which is within that plane or the closer from the neighbouring planes, and *c)* assuming uniform rainfall over the whole catchment. The uniform rainfall was determined using the spatially averaged, area-weighted, rainfall from method (a):

$$R^t = \frac{1}{A_T}\sum A_i R_i^t \qquad \text{.....(7.1)}$$

where R^t is the catchment's uniform rainfall at time-step t, R^t_i is the rainfall for plane number i at time-step t, and A_i is the area of plane number i and A_T is the whole catchment area.

Table 7.3: The values used for each tested parameter

Parameter	Used Values for Each Element	
	p	Ch
Ks (mm/hr)	0 0.37 0.74	0 4.17 8.34
S	0 0.45 0.8 1	0 0.45 0.8 1
n	0.0035 0.035 0.04	-
Cv	0 0.1 0.5 0.9 1	0 0.1 0.5 0.9 1
G, Dist, Por (G; mm)	5, 0.69, 0.437 11, 0.25, 0.463 20, 0.23, 0.501	5, 0.69, 0.437 11, 0.25, 0.463 20, 0.23, 0.501
Int (mm)	1 2 2.8	NA
Roc	0.2 0.4 0.8	NA
Spc (m)	20 40 80	NA
Rel (mm)	20 50 100	NA
Spc/Rel	1/ 20.0 1/50.0 1/100.0 1/ 1000.0 10/20.0 10/50.0 10/100.0 10/1000.0	NA
Thic (mm)	1000 5000 10000	
Slp	0.1 0.5 0.8	0.1 0.5 0.8

Note:
P: plane
Ch: channel

7.4.2 Local sensitivity analysis results

7.4.2.1 Effect of using different rainfall interpolations

The two selected events were run using the three different methods of rainfall interpolation; the KINEROS2 interpolation method (the label in the figures shows it as KINOUT-C), the weighted average rainfall method (shown in the figures as KINOUT-Wavg), and by selecting one rain gauge for each plane. For the latter method, two realisations were used to show how arbitrary this method could be - two different rain gauges were assigned to the planes where more than one gauge was considered valid (shown in the Figure as S1 and S2). All parameters were fixed at the default values for

the rainfall sensitivity analysis. **Figures 7.4a** and **b** show the results for the 07 Aug 1996 and the 25 Jan 1997 events with all the different rainfall interpolations.

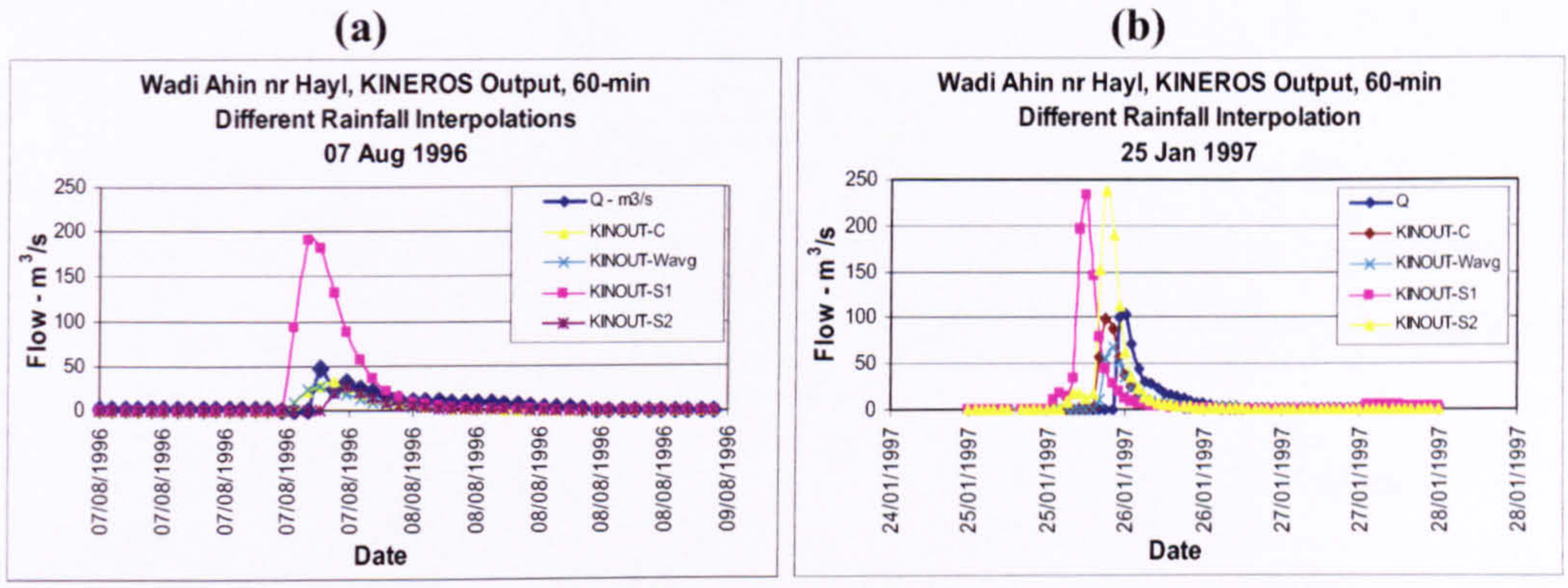


Figure 7.4: KINEROS2 output for 07Aug 1996 and 25 Jan 1997 events, using different rainfall interpolations

For the purpose of this research and for all the other sensitivity analysis tests, the KINEROS2 method was adopted (called centroid method and shown in the figures as KINOUT–C-).

7.4.2.2 Effect of initial condition (S)

The initial condition effect was tested by varying the initial saturation values, *S*, using values of 0, 0.8 and 1.0, in addition to the default value (0.45 for most elements). It should be noted that using the default G = 0 means that the infiltration will be set to a constant value equal to the *Ks*, which is expected to affect the importance of the initial condition. Therefore, the sensitivity to *S* was tested first with the default *G* value (*G* = 0) and then using *G* = 11 mm and associated values of *Por* and *Dist* (**Figure 7.5a** and **b)**. These parameter changes were applied to both elements, planes and channels, together.

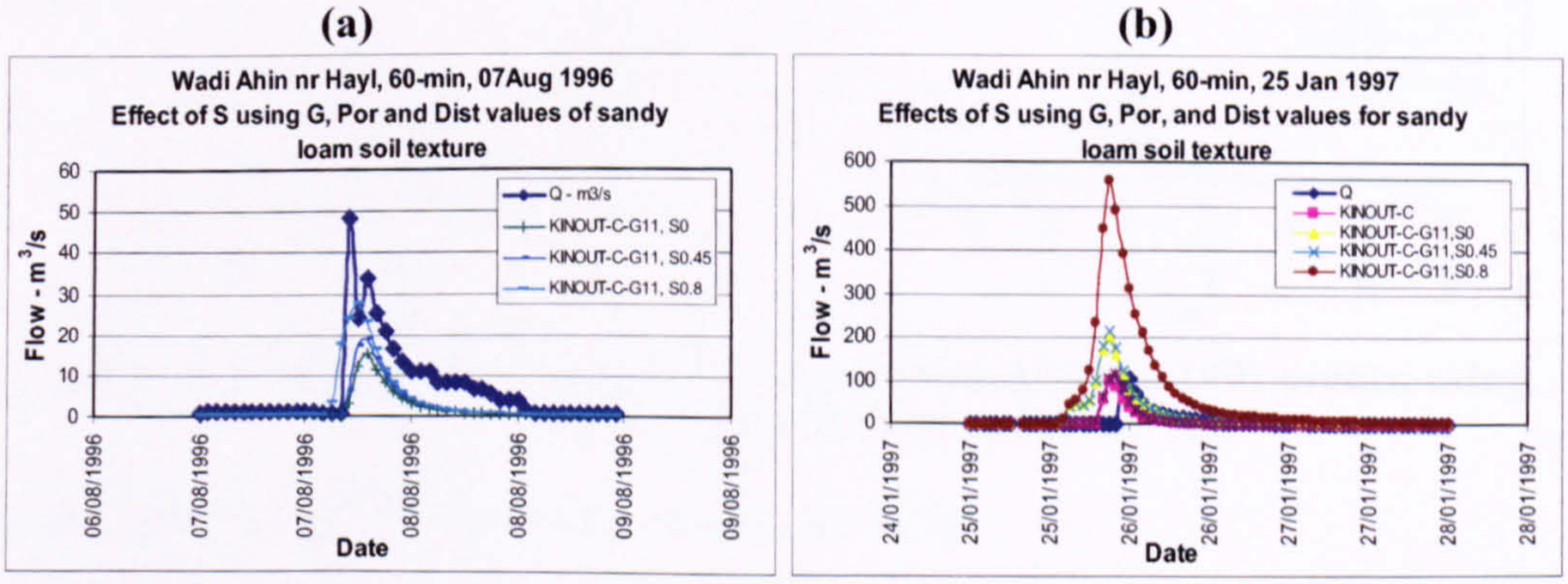


Figure 7.5: Simulation results for 07Aug 1996 and 25 Jan 1997 events, using different values of *S* with *G*=11 and associated values of *Por* and *Dist*

7.4.2.3 Effect of hydraulic conductivity (*Ks)*

Figure 7.6a and **b** below show the effects of using different *Ks* multipliers for the two tested events. For example, the label *Ks*=0.37 mm/hr means that the model was run using a multiplier =0.1, hence the *Ks* value for planes changed from 3.7 mm/hr (the default value) to 0.37 mm/hr, and from 41.7 mm/hr to 4.17 mm/hr for the channels. As the results show that the model is very sensitive to any small change, it was believed there is no need to use larger numbers to prove the models sensitivity to this parameter.

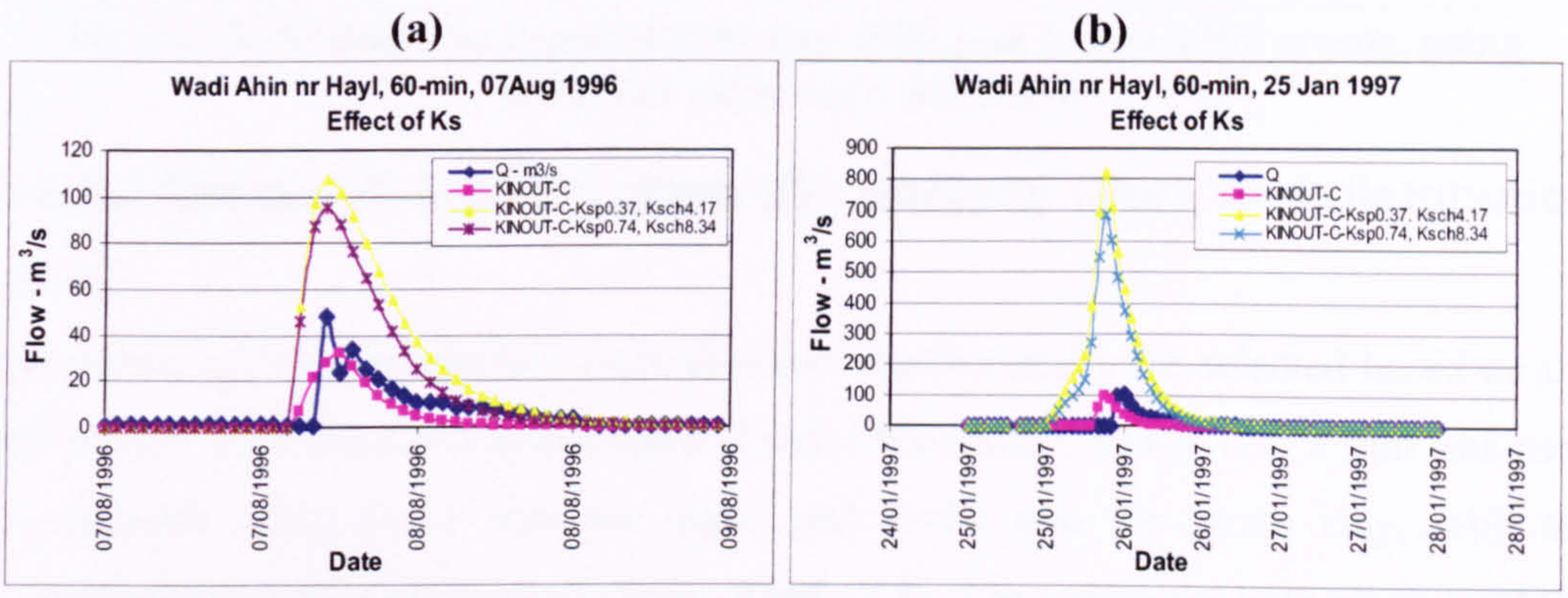


Figure 7.6: Simulation results using different values of *Ks* for 07Aug 1996 and 25 Jan 1997 events, using KINEROS2 rainfall interpolation method

7.4.2.4 Effects of coefficient of variation of *Ks* (*Cv)*

The effect of perturbing *Cv* (*Cv* = 0, 0.1, 0.5, 0.9 and 1.0 applied to both planes and channels) was tested for both events, for both *G*=0 and *G*=11 mm (with associated values of *Por* and *Dist*). **Figure 7.7a** and **b** show the results.

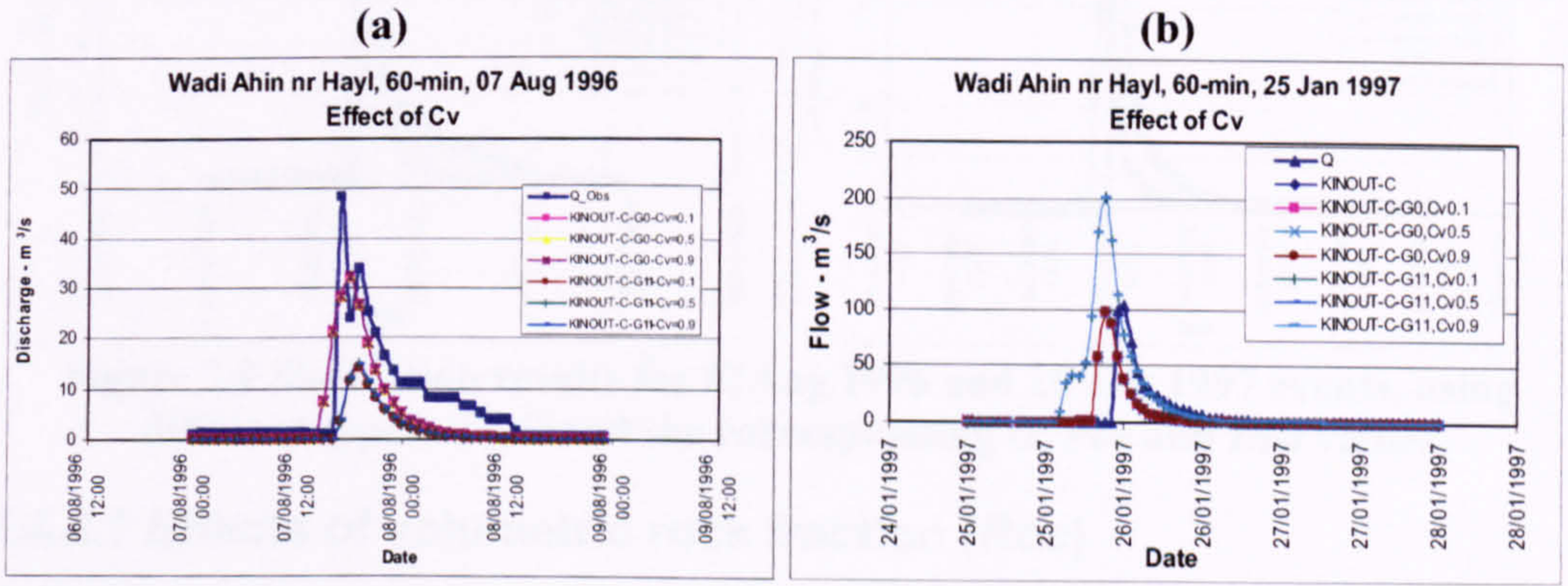


Figure 7.7: Simulation results for 07Aug 1996 and 25 Jan 1997 events, using different values of *Cv* with *G*=0 and *G*=11 mm

7.4.2.5 Effects of Manning's coefficient *(n)*

The effect of perturbing Manning's coefficient (n = 0.0035 and 0.04) for the planes was tested for both events. Results are shown in **Figures 7.8a** and **b**.

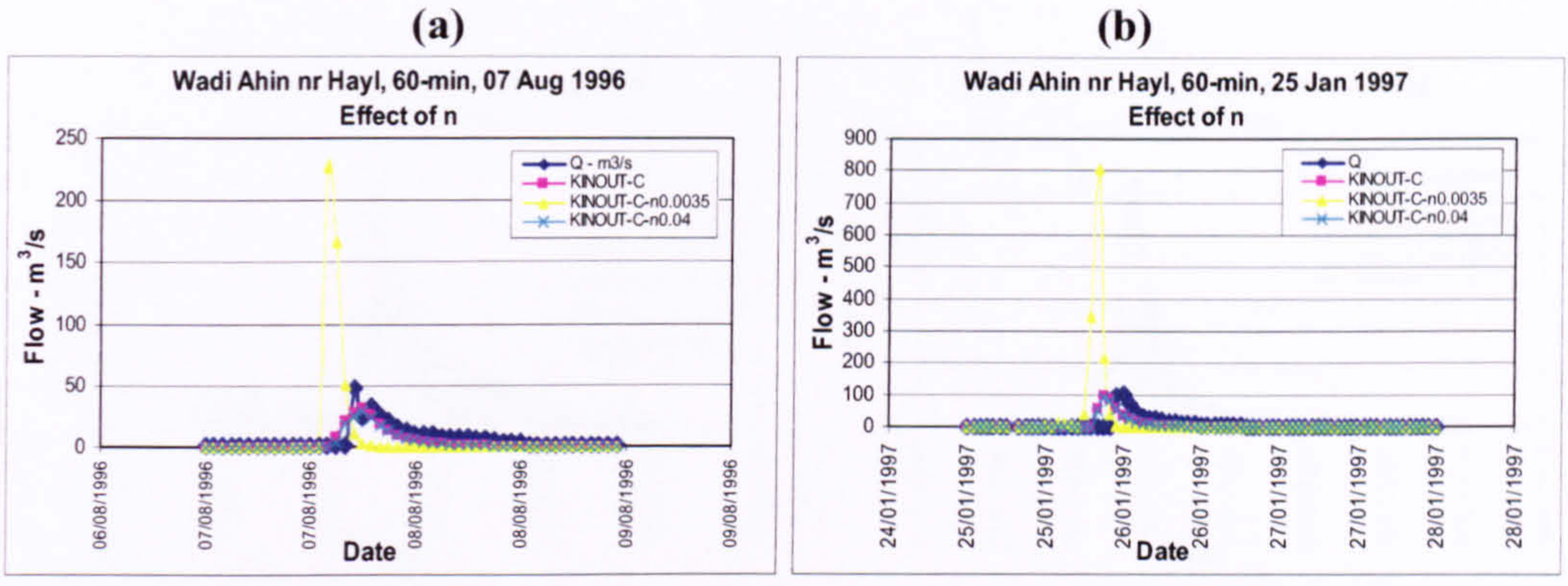


Figure7.8: Simulation results for 07Aug 1996 and 25 Jan 1997 events, using different values of *n* with G=0

7.4.2.6 Effects of capillary drive (*G*), porosity (*Por*), and distribution (*Dist*)

The values of these parameters were changed together and were selected based on the soil texture from the KINEROS2 manual (after Woolhiser, 1990). G = 5 mm was used to represent sand, G=11 mm for loam, and G=20 mm for sandy clay, with the corresponding values of *Por* and *G* (see **Table 7.3**). The values for both planes and the channels were changed together.

Figure 7.9 shows the results.

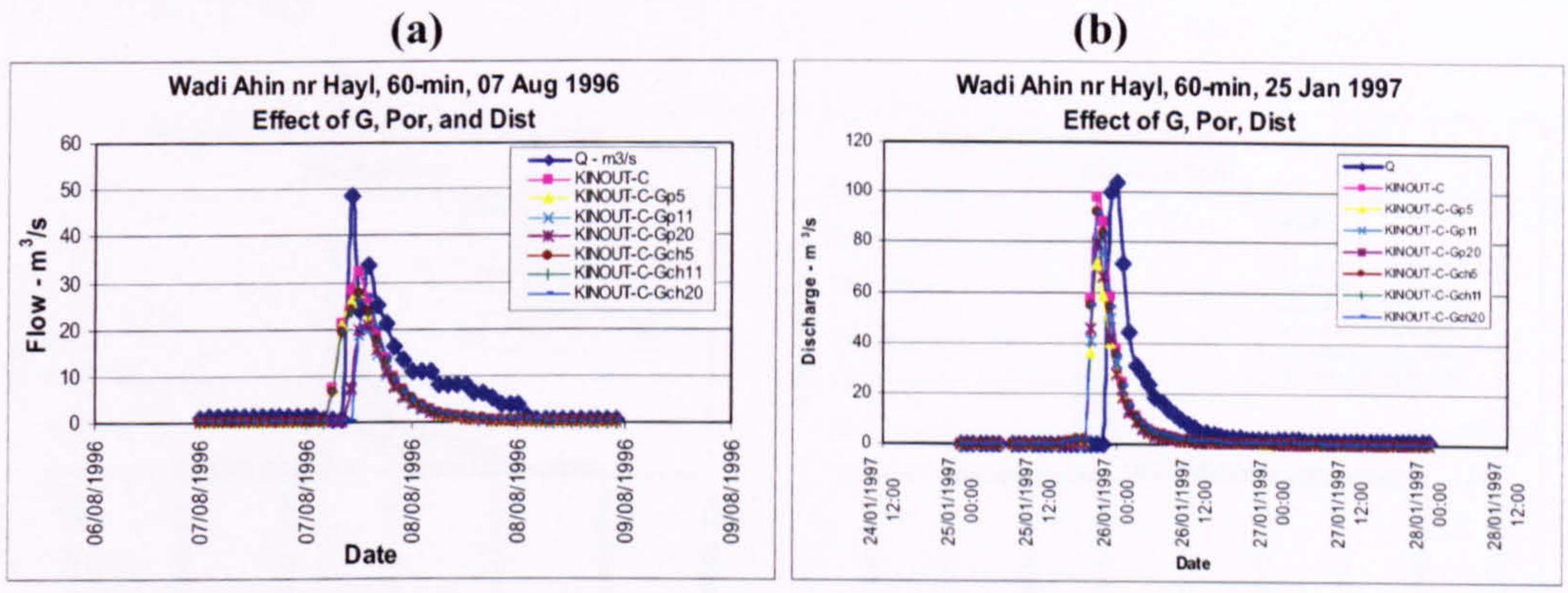


Figure 7.9 Simulation results for 07Aug 1996 and 25 Jan 1997 events, using different types of soil and the corresponding *G, Por* and *Dist* values

7.4.2.7 Effects of volumetric rock fraction (*Roc*)

Figure 7.10a and **b** show the results obtained using different *Roc* = 0.2, 0.4, and 0.8 (for planes) when G=0, and those when using G=11 mm.

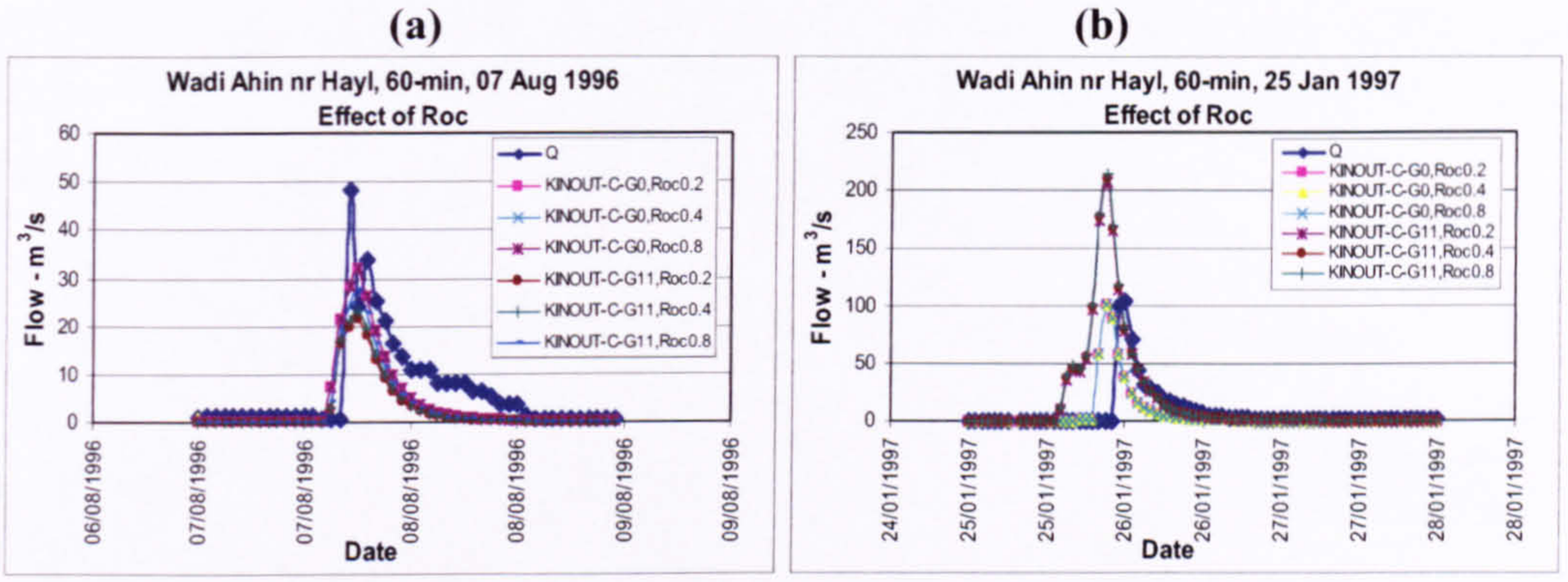


Figure 7.10: Simulation results for 07Aug 1996 and 25 Jan 1997 events, using different values of *Roc* with *G*=0 and *G*=11 mm

7.4.2.8 Effect of soil layer thickness (*Thic)*

The figure below shows the effect of using different values of thickness of the upper soil layer (*Thic*) with *G*=0 and *G*=11 mm. For *G* = 11 mm, the values of *Thic* used were 1000, 5000 and 10000 mm, as **Figure 7.11** shows. For *G* = 0, KINEROS2 assumes one layer of infinite thickness. Hence, any layer thickness assigned will have no effects, as the results below approves.

The test shows that there is a clear effect on the flood peaks obtained between the two cases (*G* = 0, *G* = 11 mm) for both events but a constant value was obtained for each case (*G*=0, *G*=11).

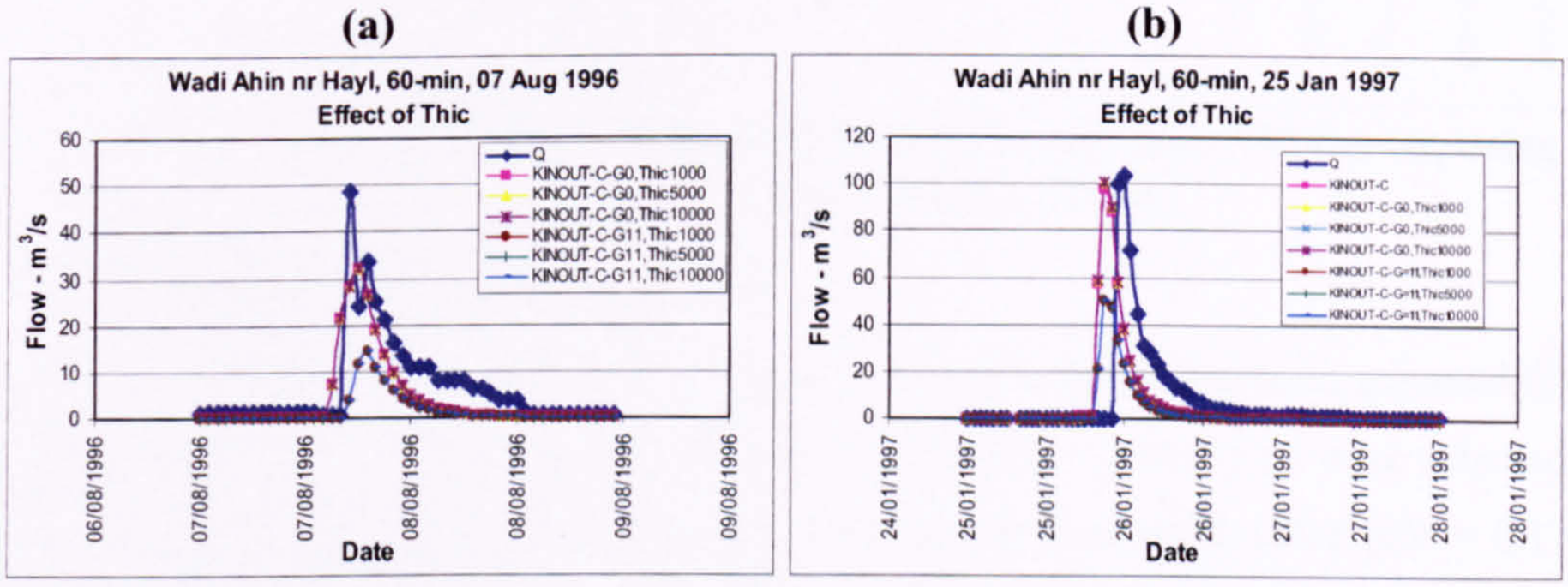


Figure7. 11: Simulation results for 07Aug 1996 and 25 Jan 1997 events, using different *Thic*, with *G*=0 and *G*=11 mm

7.4.2.9 Effects of microtopography (*Rel* and *Spc*)

The effects of the microtopography parameters, relief (*Rel*) and spacing (*Spc*), have been checked by changing *Rel*, keeping the *Spc* as the default value, then changing *Spc*, keeping the *Rel* as the default value. Finally, *Rel* was changed while fixing *Spc* to 10m.

Figure 7.12 shows the model results using *Rel* values of 20, 50, 100 and 1000 mm with *Spc* =1 m, for the 07 Aug 1996 and 25 Jan 1997 events, whereas **Figure 7.13** shows the results using the same values of *Rel* but with *Spc*=10 m (the default value).

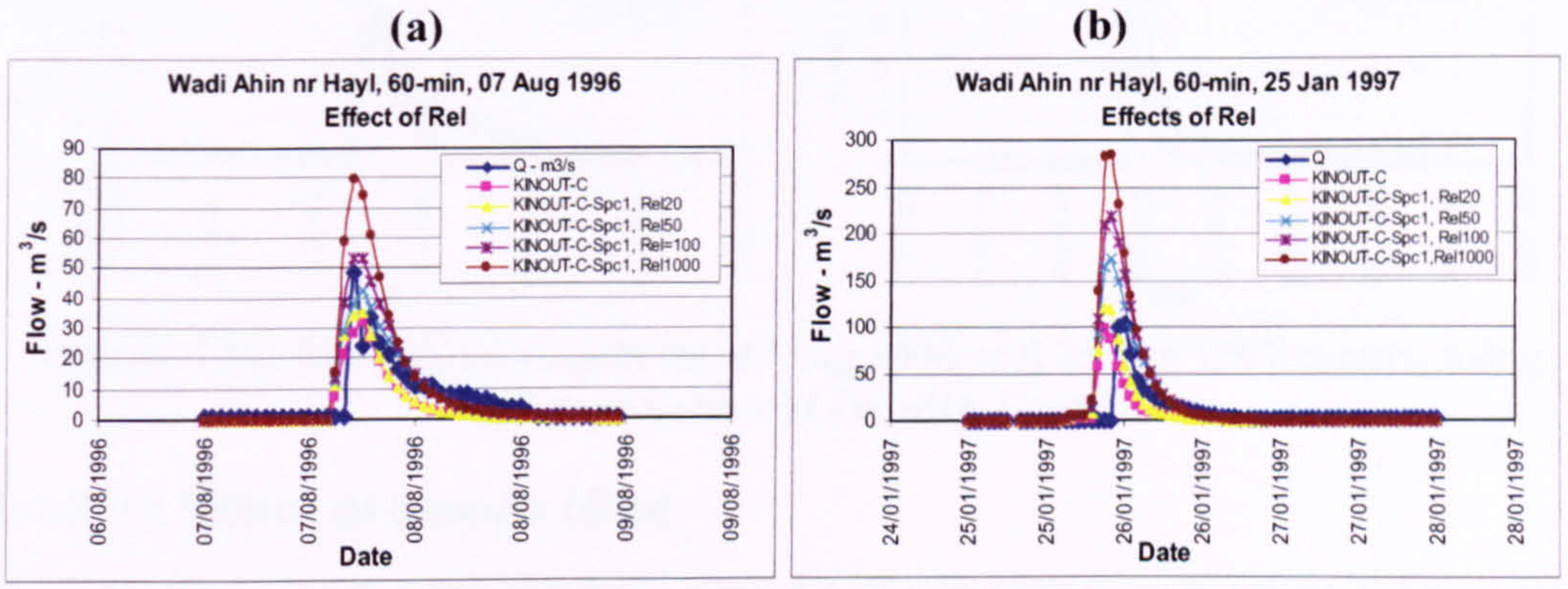


Figure 7.12: Simulation results for 07Aug 1996 and 25 Jan 1997 events, using different *Rel* values when *Spc*=1m

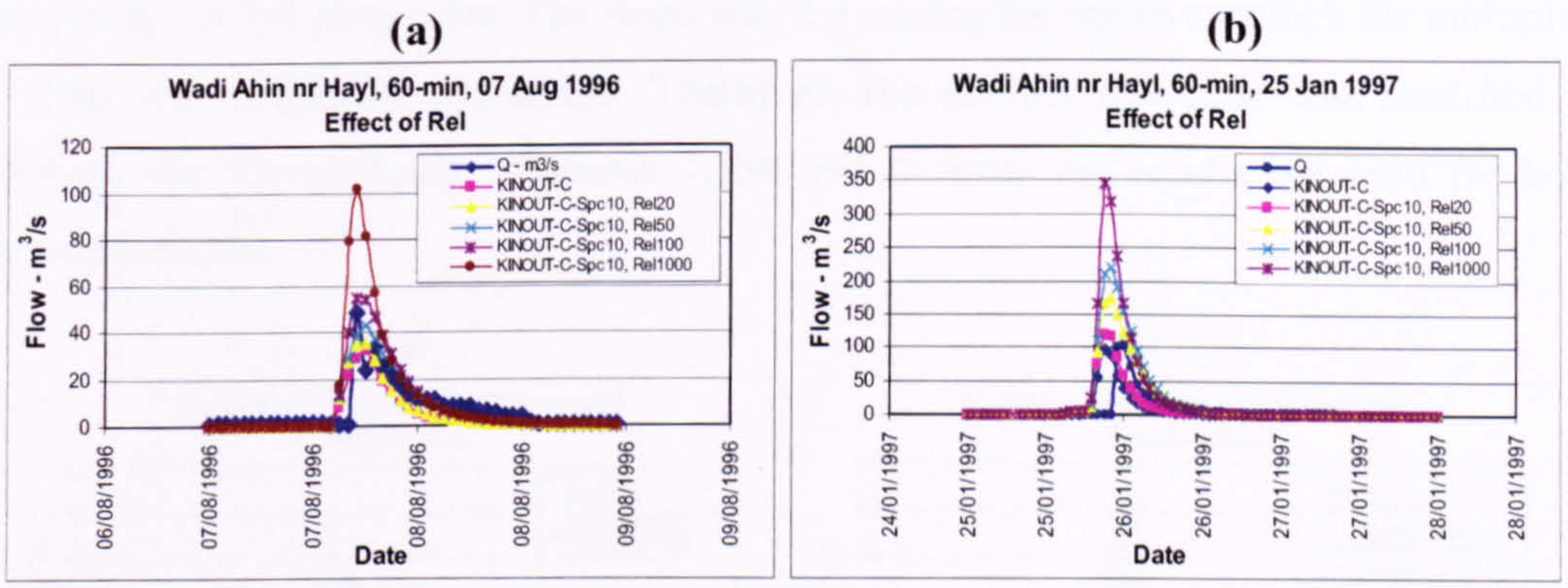


Figure 7.13: Simulation results for 07Aug 1996 and 25 Jan 1997 events, using different *Rel* values with *Spc* =10m

7.4.2.10 Effects of interception (*Int*)

Different values of interception (*Int* = 1mm, 2mm and 2.8mm) based on assumed types of vegetation cover (grass, meadow grass, and alfa alfa, respectively) were selected to test effects on the model results. Canopy cover is set to a small value (*Ca* = 0.1) to allow some effects (interception loss is factored by *Ca*). The results are shown in **Figures 7.14a** and **b,** below.

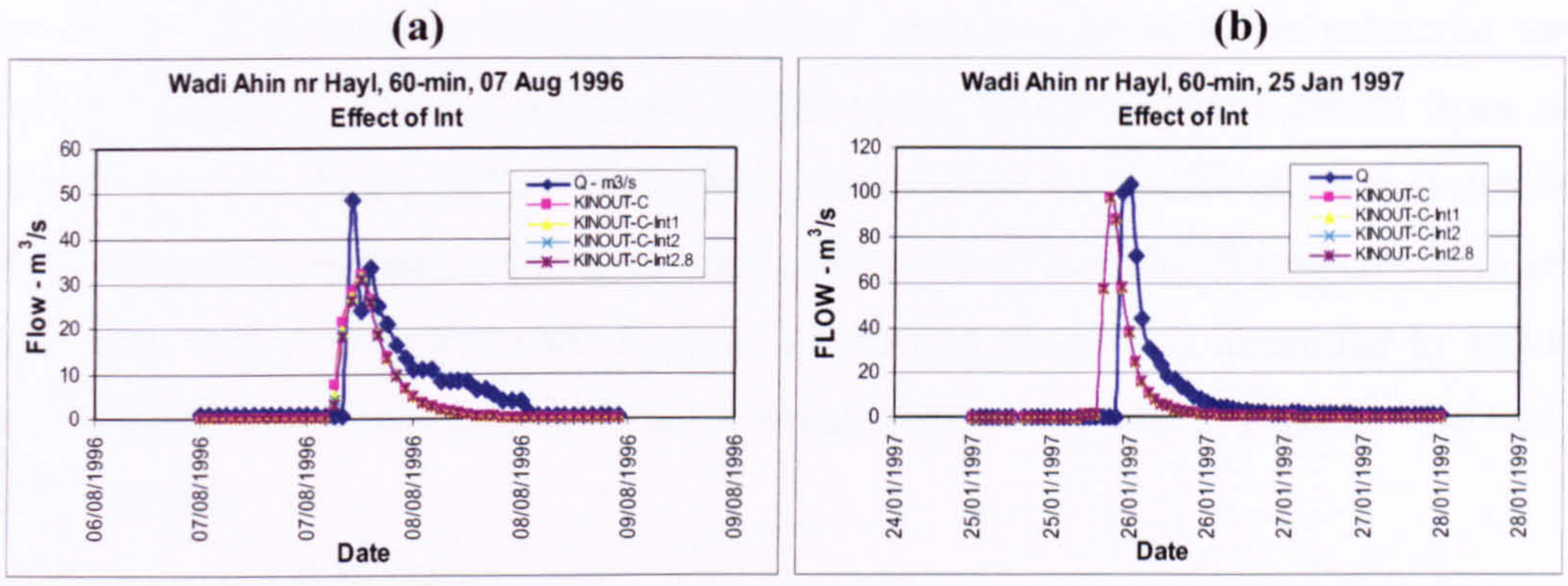


Figure 7.14: Simulation results for 07Aug 1996 and 25 Jan 1997 events, using different values of *Int* with *Ca*=0.1

7.4.2.11 Effect of slopes (*Slp*)

The effects of slopes were checked using the *Slp* multiplier with values ranging from 0.1 to 0.8. The chosen range was thought to be suitable to demonstrate any model sensitivity to this parameter. The slope was not among the inputs to which the multiplier facility was originally applicable. Therefore, the KINEROS2 code was modified to include the *Slp* multiplier. **Figures 7.15a** and **b** show the results obtained for both selected events.

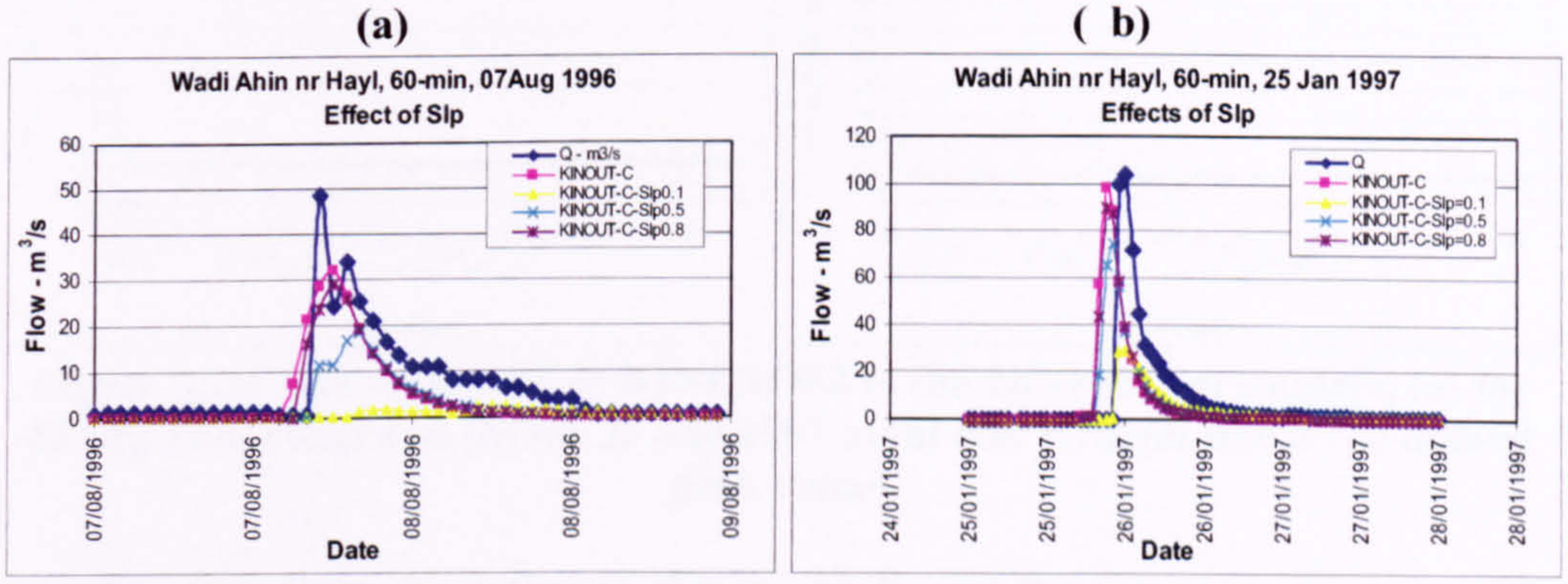


Figure 7.15: Simulation results for 07Aug 1996 and 25 Jan 1997 events, using different *Slp* values

7.4.3 Discussion of the local sensitivity analysis results

The rainfall interpolation clearly has great effect on the results as shown by **Figure 7.5a** and **b.** The obtained values are shown in **Tables 7.4** and **7.5** below. It was noted that the assumption of uniform rainfall smoothes the rainfall intensity, hence the simulated hydrograph is low compared to the observed. The KINEROS2 method is also expected to spatially smooth the rainfall, but to a lesser extent, and this is evident in the results. On the other hand, assigning one gauge per plane over-estimates the flood peaks. This is likely to be because the high rainfall intensities at a single gauge are applied over the whole plane which will tend to intensify (in time) the spatial average rainfall. Of course,

the effect will depend on the spatial-temporal rainfall distribution, in particular how well the gauged rainfall represents the spatial value, which will be different from one event to another. Hence, this method could over-estimate the rainfall in some events but under-estimate it in others, bearing in mind how localised the rainfall generally is in arid areas. The high sensitivity to the location of the rain gauge was illustrated by testing two different sets of rain gauges for some plane elements (shown in **Figures 7.4a** and **b** as S1 and S2).

The results of the sensitivity analysis for the different parameters show that there are some parameters that have more effects than others, as was expected. This provides important guidance as to which parameters merit attention in calibration and sensitivity analyses.

Figures 7.16a and **b,** below, show the effects of the different parameters for both selected events (using the KINEROS2 rainfall interpolation method).

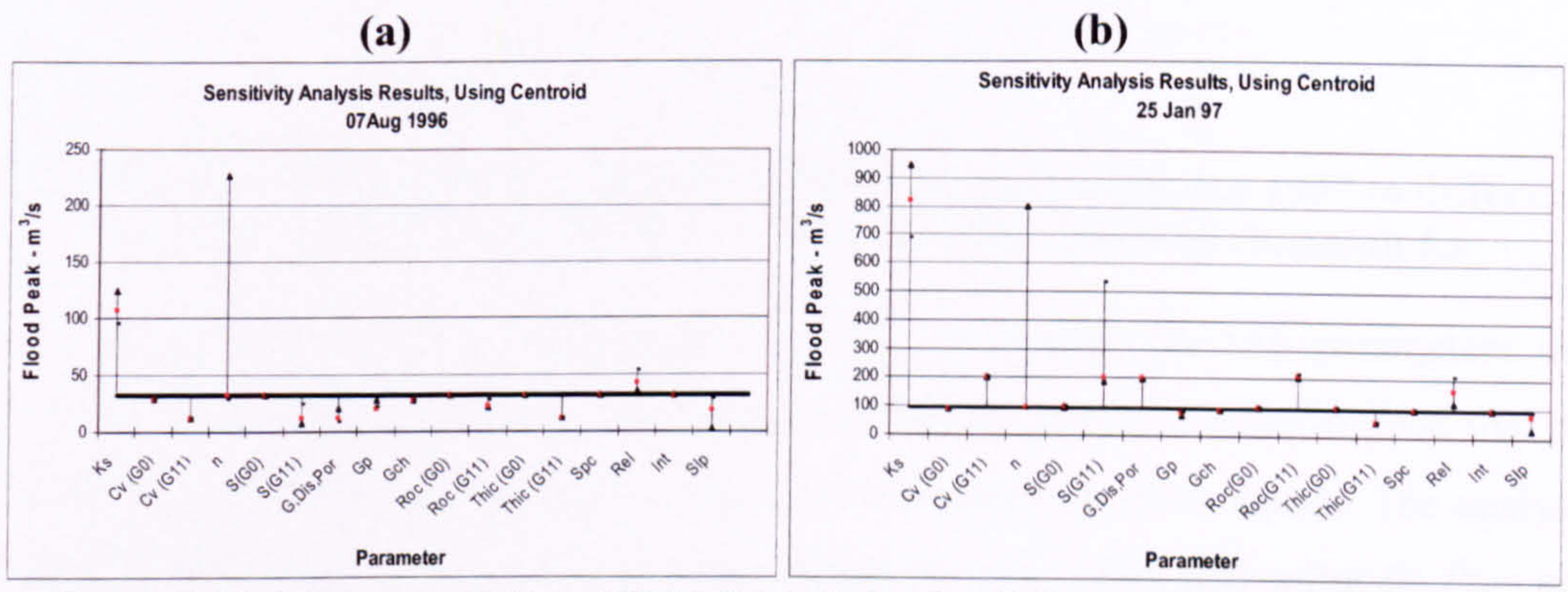


Figure 7.16: The sensitivity of KINEROS2 to the different parameters, (a) for 07Aug 1996 event and (b) for 25 Jan 1997 event (the straight line is the default peak value)

It is very clear from these figures that *n* and *Ks* are the most sensitive parameters followed by the *G* values and then *Rel*, and *Slp*. The initial condition *S* also has some effect. However, that does not mean the other parameters do not have any effects but effects are either relatively small, or are dependent on the locality of the perturbations, and not shown up using the chosen default parameter values.

Figures 7.17a and **b** demonstrate the large effects of *n* and *Ks* on the results of the 25 Jan 1997 event. Similar effects were obtained for the 07 Aug 1996 event. The flood peak is decreasing highly with the increase of the *n* values as demonstrated below. The Manning's coefficient, *n*, which describes the roughness of the planes/channels, is known to be a very important factor in determining the flow and has great effect on the

flow velocity (for example, Beven, 2001; Al-Qurashi et al., 2008). Hence, its effects were expected.

The flood peaks decrease with the increase of the *Ks* values. The field effective saturated hydraulic conductivity, *Ks*, is one of the main parameters that control the infiltration process. Hence, this effect was expected. However, the change of the coefficient of variation of *Ks*, *Cv*, has only a slight effect on the results as **Tables 7.4** and **7.5** show. This was found to be also true for the percentage of the volumetric rock fraction, *Roc*.

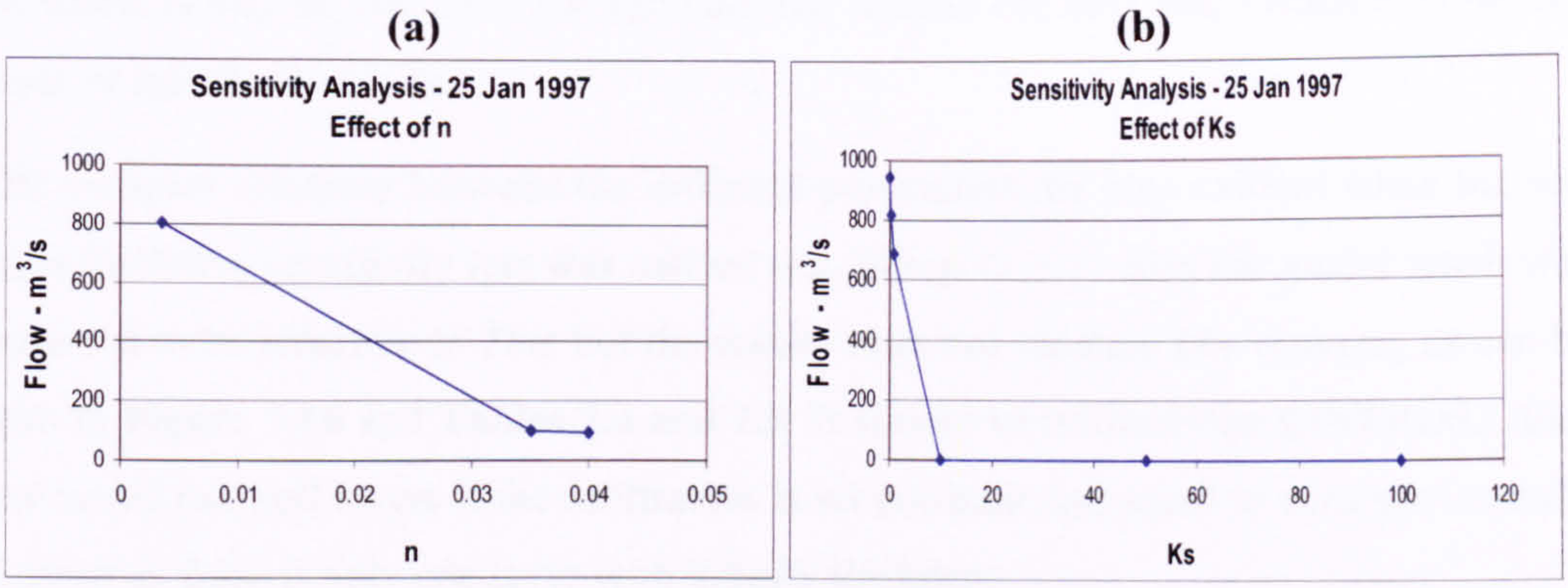


Figure 7.17: The sensitivity of the simulated flow peak of 25 Jan 1997 to different parameter values (a) Effects of changing *n* (b) Effects of changing *Ks*

The capillary drive, *G*, and soil porosity, *Por*, are among the key parameters that KINEROS2 depends on for determining the infiltration. Hence, it is no surprise that the results show how sensitive the model could be to changes in their values. The analysis has been run with two options: using the default *G* value (=0), and using *G, Por,* and *Dist* values corresponding to a sandy loam soil (*G* = 11 mm, *Por* = 0.463, and *Dist* = 0.25). In the first case, the infiltration is assumed by the model to be of a constant rate that is equal to *Ks*. In addition, the model in this case assumes there is only one soil layer of infinite thickness and ignores any other specified thicknesses. In this case, and as the results show, there are no effects of changing any value of any parameter that is used in the infiltration calculations, including the initial saturation, *S*. When the *G*, *Por* and *Dist* values were changed based on the soil type, it was noticed that the other infiltration parameters do have significant effects on the results.

The effects of the variation of *S* were clear when tested with *G* = 11 mm. Generally, the flood peaks were increasing with higher initial saturation values. However, the nature of the sensitivity varied from one event to another. The flood peaks of the 07 Aug 1996 event increased with increased *S* values, to the upper limit, *S*=1. However, this was not the same for the 25 Jan 1997 event, where the flood peaks increased till *S* = 0.8, but

decreased rapidly when $S = 1$. This is believed to be due to the differences in the rainfall amounts between the two events, where in the first case it could be that the wetting front did not reach the bottom of the upper soil layer, or this might have happened only late in the event so the soil did not reach the saturation point. On the other hand, in the second case, the rainfall intensity and duration were much higher and the possibility that the soil layer became saturated during the event is high, but when the higher *S* value of 1 was used, the capillary drive, *G,* was set automatically to 0 by the model. Hence, the infiltration rate automatically became constant and equal to *Ks* and the default soil layer thickness *(Thic)* of 500 mm was ignored and instead the soil was assumed to be one layer of infinite thickness.

The complex relations between the different parameters are also evident when the soil layer thickness sensitivity test was carried out. When $G = 11$ mm the model result was expected to be sensitive to *Thic* but the results does not indicate any changes, as can be seen in **Figure 7.16** and **Tables 7.4** and **7.5**. It should be noticed that KINEROS2 does not model two soil layers if the infiltration is set constant and equal to zero but instead , it assumes there is only one layer with infinity thickness.

The model was run with a value of *Spc* =1 m and then *Spc* = 10 m, varying *Rel* each time. **Figures 7.18a** and **b** show the effects of these changes on the flood peaks for both tested flood events. The results show the importance of these parameters and their interaction.

Figure 7.18a shows that using higher values of *Spc* increases the obtained flood peaks but the amount of this change varies based on the used value of the *Rel*. The differences in the results for the lower part of the graph for the event of 07 Aug 1996 seem to be hardly noticable but increase with the increase of the flow. **Figure 7.18b** shows that the case is different in the event of 25 Jan 1997. The effect of the changes in the value of *Spc* (1m or 10m) does not show clearly when the values of *Rel* are less than 100 mm but then there is clear difference in the obtained flood peak values, as the figure shows. This indicates that the effect of *Spc* is clear when the *Rel* is higher, which is logical.

The micromorphology is believed to have some effects on the flow and the wetted perimeter determination, and these effects are known to be different in low flow compared to high flow conditions, and therefore the infiltration process is affected accordingly.

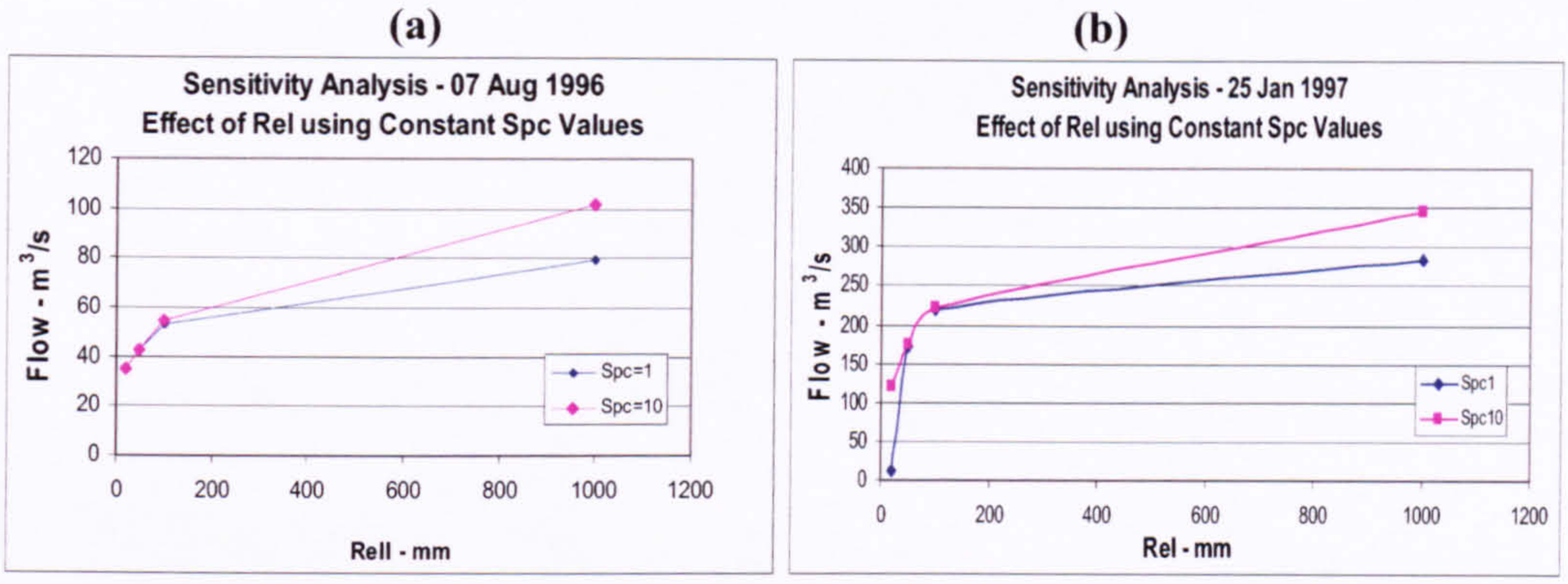


Figure 7.18: Effect on simulated flow peak of change in *Rel* using constant values of *Spc* using the KINEROS2 rainfall interpolation method, (a) for 07 Aug 1996 and (b) for 25 Jan 1997

Tables 7.4 and **7.5,** below, show the obtained results for the two tested events, when different parameter values were used. It should be noted that the local sensitivity analysis was carried out to test the effects on the obtained flood peaks only and not the time to peak or flood volumes as the main aim is to test the parameters sensitivity rather than the best obtained hydrograph for simplicity and as the flood peak can be considered as the most important output in the flood studies. The assessment of the obtained hydrograph was carried out when the global sensitivity analysis was carried out.

Table 7.4: The Sensitivity Analysis Results of 07 Aug 1996 Event

Parameter	Element type	Parameter Value	Obtained Flood Peak (Centroid)
Observed Flood Peak= 48.5 m^3/s			
Ks	P/Ch	0	124.18
		0.37/ 4.17	107.51
		0.74/ 8.34	95.58
	All	10	4.27
		50	0.23
		100	0.23
Cv (G=0)	P	0.1	19.14
		0.5	29.14
		0.9	29.14
Cv (G=11)		0.1	11.44
		0.5	11.84
		0.9	12.12
Manning	P	0.0035	226.54
		0.035	32.19
		0.04	29.04
Sat (G=0)	All	0	32.17
		0.45	32.17
		0.8	32.17
		1	32.17
Sat (G=11)	All	0	7.05
		0.45	11.68
		0.8	23.52
		1	32.36
G, Dist, Por	P	5, 0.69, 0.437	28.076
		11, 0.25, 0.463	19.86
		20, 0.23, 0.501	20.96
	Ch	5, 0.69, 0.437	27.67
		11, 0.25, 0.463	27.4
		20, 0.23, 0.501	26.97
	All	5, 0.69, 0.437	20.64
		11, 0.25, 0.463	11.68
		20, 0.23, 0.501	8.3
Rock% (G=0)	All	0.2	32.17
		0.4	32.17
		0.8	32.17
Rock% (G=11)		0.2	21.64
		0.4	23.29
		0.8	27.91
Soil Layer Thickness (G=0)	P	1000	32.17
		5000	32.17
		10000	32.17
(G=11)		1000	11.68
		5000	11.68
		10000	11.68
Space (m)	P	20	32.17
		40	32.17
		80	32.17
Relief (mm)	P	20	35.34
		50	42.65
		100	54.16
Space/Relief	P	1/ 20.0	35.33
		1/50.0	42.56
		1/100.0	53.47
		1/ 1000.0	79.78
		10/20.0	35.33
		10/50.0	42.64
		10/100.0	54.61
		10/1000.0	101.85
Slope	P, Ch	0.1	2.66
		0.5	18.67
		0.8	28.75
Interception	P	1	31.90
		2	31.49
		2.8	31.15

Note: * shows the default value and its relative result.
The S value is 0.05 for channel no 4.

Table 7.5: The Sensitivity Analysis Results of 25 Jan 1997 Event

Parameter	Element type	Parameter Value	Obtained Flood Peak (Centroid)
Observed Flood Peak= 104 m^3/s			
Ks	P, Ch	0	945.22
		0.37, 4.17	821.05
		0.74, 8.34	686.91
	All	10	0.24
		50	0.24
		100	0.24
Cv (G=0)	P, Ch	0.1	92.45
		0.5	92.45
		0.9	92.45
Cv (G=11)		0.1	201.3
		0.5	201.35
		0.9	201.44
Manning	P	0.0035	804.85
		0.035	98.12
		0.04	93.21
Sat(G=0)	All	0	96.18
		0.45	98.89
		0.8	98.89
		1	98.89
Sat(G=11)	All	0	188.32
		0.45	203.61
		0.8	533.63
		1	97.17
G, Dist, Por	P	5, 0.69, 0.437	71.38
		11, 0.25, 0.463	81.17
		20, 0.23, 0.501	79.81
	Ch	5, 0.69, 0.437	92.31
		11, 0.25, 0.463	91.92
		20, 0.23, 0.501	91.34
	All	5, 0.69, 0.437	198.51
		11, 0.25, 0.463	203.61
		20, 0.23, 0.501	193.14
Rock% (G=0)	All	0.2	100.79
		0.4	100.79
		0.8	100.79
Rock% (G=11)	All	0.2	206.53
		0.4	209.44
		0.8	214.48
Layer Thickness (G=0)	P	1000	100.79
		5000	100.79
		10000	100.79
(G=11)		1000	50.54
		5000	50.54
		10000	50.54
Space (m)	P	20	98.09
		40	98.10
		80	98.11
Relief (mm)	P	20	120.66
		50	165.1
		100	209.54
Space/Relief	P	1/ 20.0	120.67
		1/50.0	173.71
		1/100.0	219.22
		1/ 1000.0	283.99
		10/20.0	120.81
		10/50.0	174.24
		10/100.0	221.68
		10/1000.0	346.24
Slope	P, Ch	0.1	29.34
		0.5	74.7
		0.8	89.88
Interception	P	1	98.11
		2	98.06
		2.8	98 05

Note: * shows the default value and its relative result.
The S value is 0.05 for channel no 4.

7.5 Global Sensitivity Analysis

The local sensitivity analysis, presented above, has provided useful insight into relative effects of the KINEROS2 parameters, and has allowed development of knowledge about how the model functions. However, it can not be regarded as a complete analysis because only two events were used and results are conditional on the assumed default parameter values. A more complete, global sensitivity analysis is now applied to 25 events, to test the hypothesis that the local sensitivity analysis was successful in identifying the globally important parameters. The analysis is also expected to deliver more insight into the functioning and limitations of KINEROS2 and the results will also be used for the calibration.

7.5.1 Global sensitivity analysis method

The global sensitivity analysis was carried out using the Monte Carlo method. 20,000 random samples are drawn from a uniform distribution specified for each parameter. The parameter distributions are assumed independent of each other at this stage. For each of the 20,000 parameter sets, the model is run for each event, and the performance (the measured fit to defined characteristics of the hydrograph observed at the Hayl flow gauge) is recorded. The response of these performance measures (i.e. objective functions) over the parameter space is visualised using dotty plots, and is quantified using statistics of the response surface. This is a common method of global sensitivity analysis (Beven and Binley, 1992; Wagener et al., 2004; McIntyre et al., 2004).

7.5.1.1 Model configuration

The model was configured as described previously for the local sensitivity analysis test (using a single soil layer, with the planes and channels shown in **Figure 7.1**.

7.5.1.2 Sampled parameters

In order to reduce the sampling problem to a manageable size, *Por*, *Cv*, *Int*, *W*, *Roc, Spc* and *Ca* were fixed at the values in **Table 7.2,** leaving up to 11 parameters to be sampled (for planes: *Ks*, *G*, *n*, *Rel*, *S*, *Slp*, *f*; and for channels: Ks_c, G_c, n_c, S_c). These 11 parameters were chosen based on the results of the local analysis. *f* is an additional parameter, explained below.

The uniform distributions of these 11 parameters are defined by the ranges in **Table 7.6.** These ranges reflect the range of values in the literature (Woolhiser et al., 1990;

KINEROS2 web site; Mott MacDonalds, 1992), consistent with the nature of the soils in Wadi Ahin.

Table 7.6: The KINEROS2 parameters and their ranges used in the global sensitivity analysis

Parameter	Symbol	Units	Default value (planes)	Range (planes)	Default value (channels)	Range (channels)
Manning's coefficient	*n*	$sm^{-1/3}$	0.035	0.01-0.1	0.036	0.01-0.1
Relief (micro-topography)	*Rel*	mm	20	10-100	NA	NA
Relief spacing (channel micro-topography)	*Spc*	mm	10	-	NA	NA
Woolhiser coeff.	*W*	-	NA	NA	0.15	-
Saturated hydraulic conductivity	*Ks*	mm/hr	3.7 [a]	0-10	41.7	20-50
Capillary length scale	*G*	mm	0	0-500	0	0-500
Variation of *ks*	*Cv*	-	0.1	-	NA	NA
Initial saturation	*S*	-	0.45	0-0.5	0.45 [b]	0-0.5
Soil porosity	*Por*	-	0.1	-	0.44 [c]	-
Ditribution (pore size distribution)	*Dist*	-	0.6	-	-	-
Interception depth	*Int*	mm	2	-	NA	NA
Rock cover	*Roc*	-	0	-	0	-
Plant cover	*P*	-	0	-	NA	NA
Soil layer thickness	*Thic*		NA	500	-	500
Rainfall interpolation non-linearity	*f*	-	1	0-10	NA	NA
Slope factor	*Slp*	-	1	0.5-1	NA	NA

Note:

a. In plane no. 9 the default ks value was 31.22mm/hour, in plane no. 10 it was 20.8 mm/hour; in all others it was 3.7mm/hour
b. In 4 channel reaches, default value was 0.05; in all other channel it was 0.45.
c. In channel no. 1, default value was 0.15; in all other channel it was 0.44.

The KINEROS2 rainfall interpolation method was adopted, because it provided the opportunity to parameterise the rainfall estimation, by adding a rainfall parameter *f* into the KINEROS2 code, and hence test the sensitivity of performance to rainfall within the Monte Carlo experiment.

Within the original KINEROS2 code (see **Chapter 6**), the rainfall over a plane is estimated as the weighted average of the three (or in special cases, two) nearest gauged values (Eq 7.2), where the three weights sum to one. For the Wadi Ahin model, a parameter (*f*) was added into the weighting (Eq 7.3). The *c* is the weight related to the gauge from the centroid and *f* controls the weight given to the nearest rain gauge. For example, $f = 0$ means that the three gauges are weighted equally, $f = 1$ is the KINEROS2 default, $f = 10$ weights almost entirely to the nearest gauge. Clearly, this one-parameter model does not aim to produce a realistic spatial rainfall field, but allows a limited exploration of the sensitivity of results to assumptions within the rainfall interpolation.

$$R = c_1 R_1 + c_2 R_2 + c_3 R_3 \quad \text{.....(7.2)}$$

$$R = \frac{c_1^f R_1 + c_2^f R_2 + c_3^f R_3}{c_1^f + c_2^f + c_3^f} \quad \text{.....(7.3)}$$

where R is the rainfall over the plane, R_1, R_2, and R_3 are the rainfall at the 1st, 2nd, and 3rd gauges respectively.

Knowing that sampling 11 parameters simultaneously is ambitious, with regards to achieving a good coverage of the 11-dimensional parameter space, initially the sampling problem was reduced by assuming G=0, G_c=0, and Slp=1. G=0 fixes the infiltration rate equal to the saturated hydraulic conductivity (*Ks*) and was the default value used by Mott Macdonald (1998). This leaves only 8 parameters to sample (n, n_c, *Ks*, Ks_c, S, S_c, *Rel* and *f*). Then four parameters were fixed to their optimum values that obtained from the 8-parameter case (S, S_c, *Rel* and *f*), leaving only 4-parameters, before running the model with the 11-parameters.

Finally, the Monte Carlo sensitivity analysis experiment was repeated, introducing some spatial variability into *Ks*. The catchment was divided into three different areas based on the soil and geology, with three independently sampled values of *Ks (Ks1, Ks2,* and *Ks3)*. These three areas are plane numbers 9, 10, and 15 and the ranges of *Ks1*, *Ks2*, and *Ks3* were 0 to 10 mm/hour, 20 to 40 mm/hour, and 10 to 30 mm/hour, respectively. For this experiment, the values of all the other parameters except n, Ks_c, and n_c are fixed to the default values.

7.5.1.3 Selected events

Hourly data for 30 events from 1996 to 1999 were considered (see **Chapter 5, Section 5.3.3.3**). **Figure 5.15** shows the rainfall-runoff time-series for these events, whereas the rainfall details of these events are shown in **Table 5.10**.

Three of these events (08 Jul 1996, 22 Apr 1996 and 28 Sep 1999) were excluded due to the doubtful quality of data. However, on running the Monte Carlo sampling, only 25 events were found suitable for analysis. For many of the remaining events, the model was crashing for certain parameter sets. These parameter sets were missed out from the analysis. The number missed out in this way was small (for example, in the 8-parameter case, at most 1017 and on average 131 out of the 20,000). However, in one event (26 March 1997) KIINEROS2 crashed without producing any output at all, for reasons which are not clear, but suspected to be linked with instability at high values of initial saturation. The 26 March 1997 has an exceptionally high runoff, with an observed runoff coefficient of 148%. The 22 Jan 1996 event was also excluded because KINEROS2 often crashed when attempting to simulate it (for example, there were 2516 crashes out of the 20,000 for the 8-parameter sensitivity analysis). This was a high multiple-peak event that is different from the other events. However, the latter two events were included in a similar study, Al-Qurashi et al. (2008) for comparison purposes to check the effects of including these two events. In that study, the range of S was estimated from 0 to 0.5.

7.5.1.4 Performance criteria

The global sensitivity analysis evaluates the variation of model performance over the sampled parameter space (i.e. the performance response surface). The performance, for each event individually, was measured using five different objective functions. These are: fit to peak flow (OF_1), fit to runoff volume (OF_2), fit to time-to-peak (OF_3), fit to peak and volume (OF_4), and fit to peak, volume, and time-to-peak (OF_5):

$$OF_1 = \left| \frac{Q_p' - Q_p}{Q_p} \right| \quad \text{.....(7.4)}$$

$$OF_2 = \left| \frac{Q_v' - Q_v}{Q_v} \right| \quad \text{.....(7.5)}$$

$$OF_3 = \left| \frac{Q_t' - Q_t}{K_t} \right| \quad \text{.....(7.6)}$$

$$OF_4 = \frac{1}{2}(OF_1 + OF_2) \quad \text{.....(7.7)}$$

$$OF_5 = \frac{1}{3}(OF_1 + OF_2 + OF_3) \quad \text{.....(7.8)}$$

where Q_p is the observed peak flow, Q_v is the observed flow volume, and Q_t is the observed time-to-peak after beginning of simulation (all observations are at the Hayl gauge). Q_p', Q_v' and Q_t' are the corresponding simulated values. It should be noted that, in some cases, flow gauging ceased before the end of the runoff (the water level in the wadi may have been below the minimum recording level of the gauge), so Q_v does not necessarily represent the full runoff volume; however Q_v' is always measured over the same time-period as Q_v. In OF_3, K_t is a representative time-scale (because Q_t - Q_t' is not dependent on the scale of Q_t unlike the equivalent terms in OF_1 and OF_2). K_t = 4 hours is chosen, as this is the most common time lag between peak rainfall and peak runoff (see **Table 5.11**).

The average performance in terms of combined flow peak, volume and time-to-peak was measured over a specified N events (e.g. N=24 for the validation in **Section 7.7**):

$$OF_6 = \frac{1}{N}\sum_{i=1,N} OF^i{}_4 \quad \text{..... (7.9)}$$

$$OF_7 = \frac{1}{N}\sum_{i=1,N} OF^i{}_5 \quad \text{..... (7.10)}$$

7.5.2 Global sensitivity analysis results

7.5.2.1 Dotty plots

Dotty plots (plots of objective function value against parameter value, where each dot represents one of the 20,000 samples) were plotted for all events for the sampled parameters. The dotty plots show a univariate projection of the response surface, hence showing which parameters have less effect on the used objective function over the sampled range. They show the location of the optimum sampled parameter values, and the peakedness of the response surface around this optimal value illustrates the identifiability of the parameter. The plots show the concentration of sampling around the optimal value, indicating the adequacy of the sampling for accurately estimating the optimal value. The plots also assist in determining whether an appropriate range of values has been assumed for each parameter (the five optimal values should be within the sampled range).

Figure 7.19 shows the dotty plots using OF_5 for some selected events, for the case where G=0 and Slp=1 (8-parameter sampling). The red dot indicates the sample with the lowest objective function value (lowest possible value, indicating perfect performance is zero). The y-axis is truncated at OF_5 = 0.3 (equivalent to 30% error) for 07 August 1996 and 25 January 1997, 1 for 23 July 1998, and 0.5 for 02 March 1999, hence, any samples which led to poorer performance are excluded from the plots.

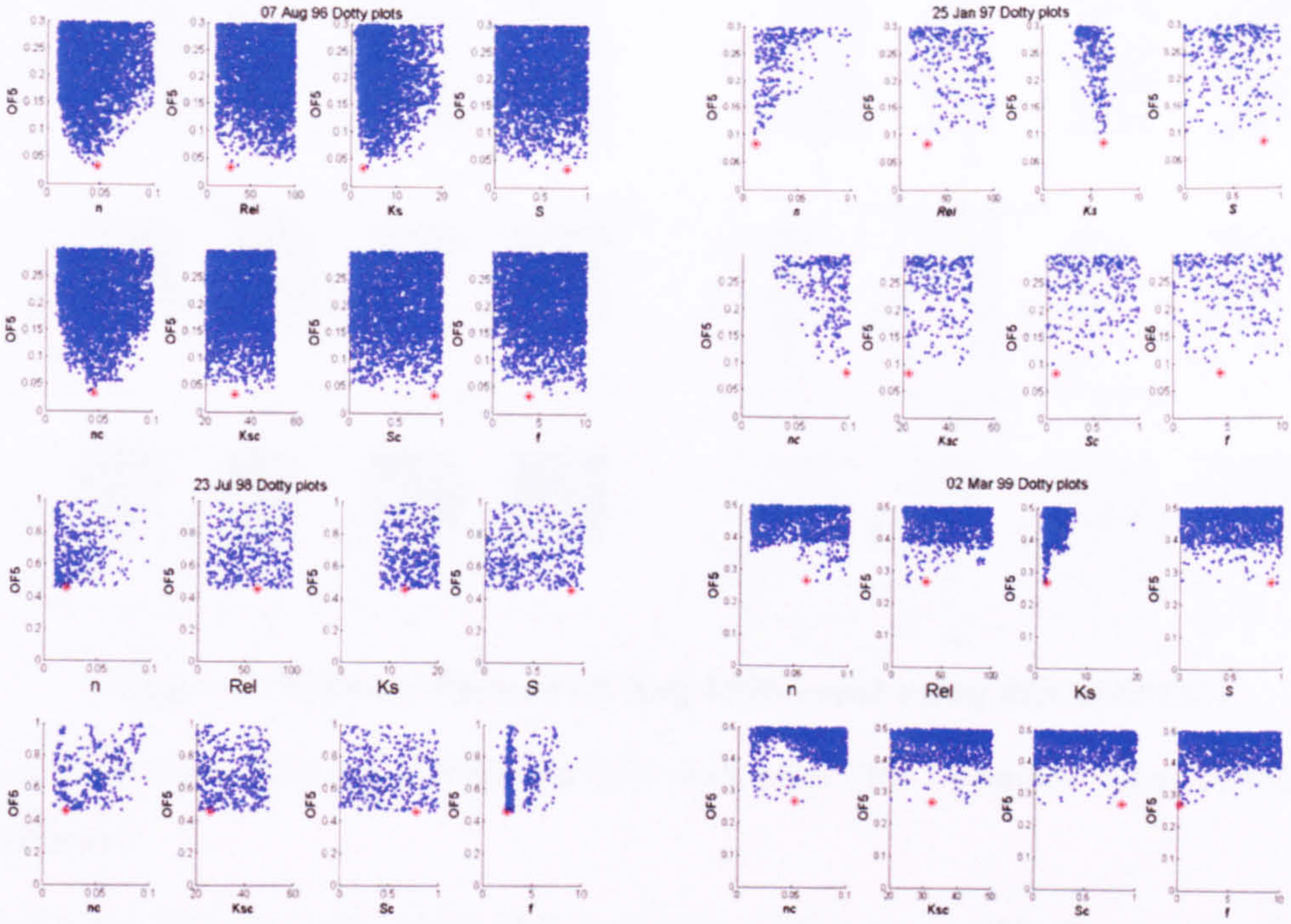


Figure 7.19: Dotty plots for selected calibrated events using OF_5 (G=0) for selected events

The model was run using different OFs to check the effect of using different OFs on the sensitivity. The results for the 07 Aug 1996 event are shown in **Figure 7.20** (only OF_1 to OF_4 as OF_5 is shown in **Figure 7.19** for this event).

The dotty plots show that some parameters cause a greater response than others, and their optimum values are better defined than others in general, e.g. *n* values, *Ks*, and to a lesser extent the *Rel*.

It was expected that the initial degree of saturation, *S*, will also have better defined values but the dotty plots show it is less well defined. The unclear definition of *S* could be related to the assumption that the capillary drive *G* was zero in this case. Hence, the infiltration is assumed to be constant and equal to *Ks* and therefore, all the parameters related to the infiltration process are not expected to show any effects.

The dotty plots show that in general the sampled optimum values of the parameters (the red dots) are different from one event to another (see also **Section 7.7.2**).

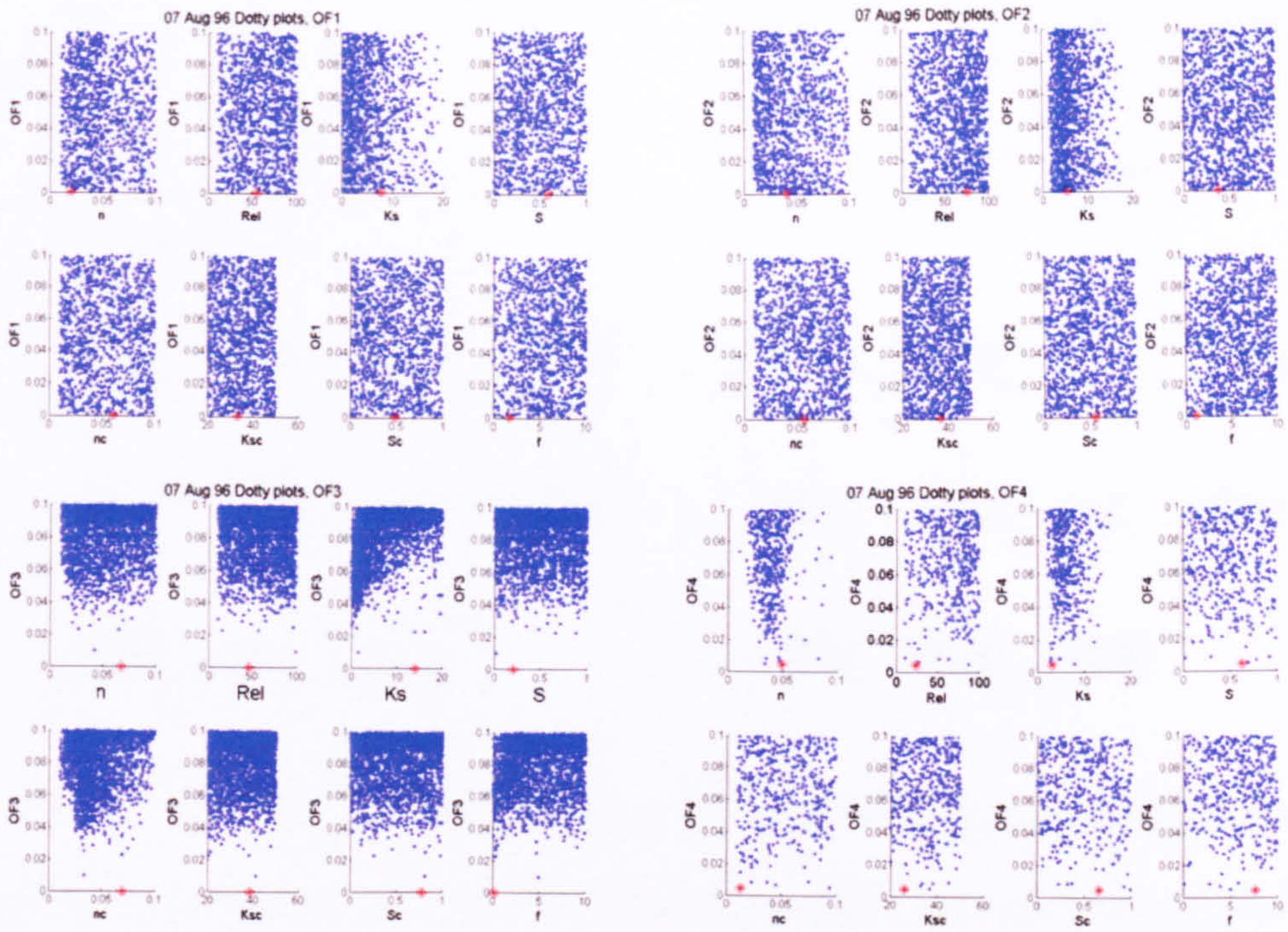


Figure 7.20: Dotty Plots of 07 Aug 1996 event using different OFs

The results show that using different OFs does affect the optimum value of the used parameters.

Results for OF_1 and OF_2 show that optimum performance (OF=0) can be achieved across the full range of parameter values. This shows that either of these, alone, is not an adequate calibration criterion. When considering OF_4 and OF_5, although the dotty plots were different shapes across events (**Figure 7.19** and **7.20**), n, n_c, Ks, and to some extent Rel consistently appear to be the most sensitive parameters.

Dotty plots of OF_5 for some selected events for the 11-parameter sampling (G>0) are shown in **Figure 7.21**.

The shape of the dotty plots varies from one event to another, and also depends on the performance measure used, but generally Ks and n produce the greatest response in performance and are the most identifiable parameters. However, all the other parameters show some slight effects especially for Aug 1996 event, as the figure demonstrates.

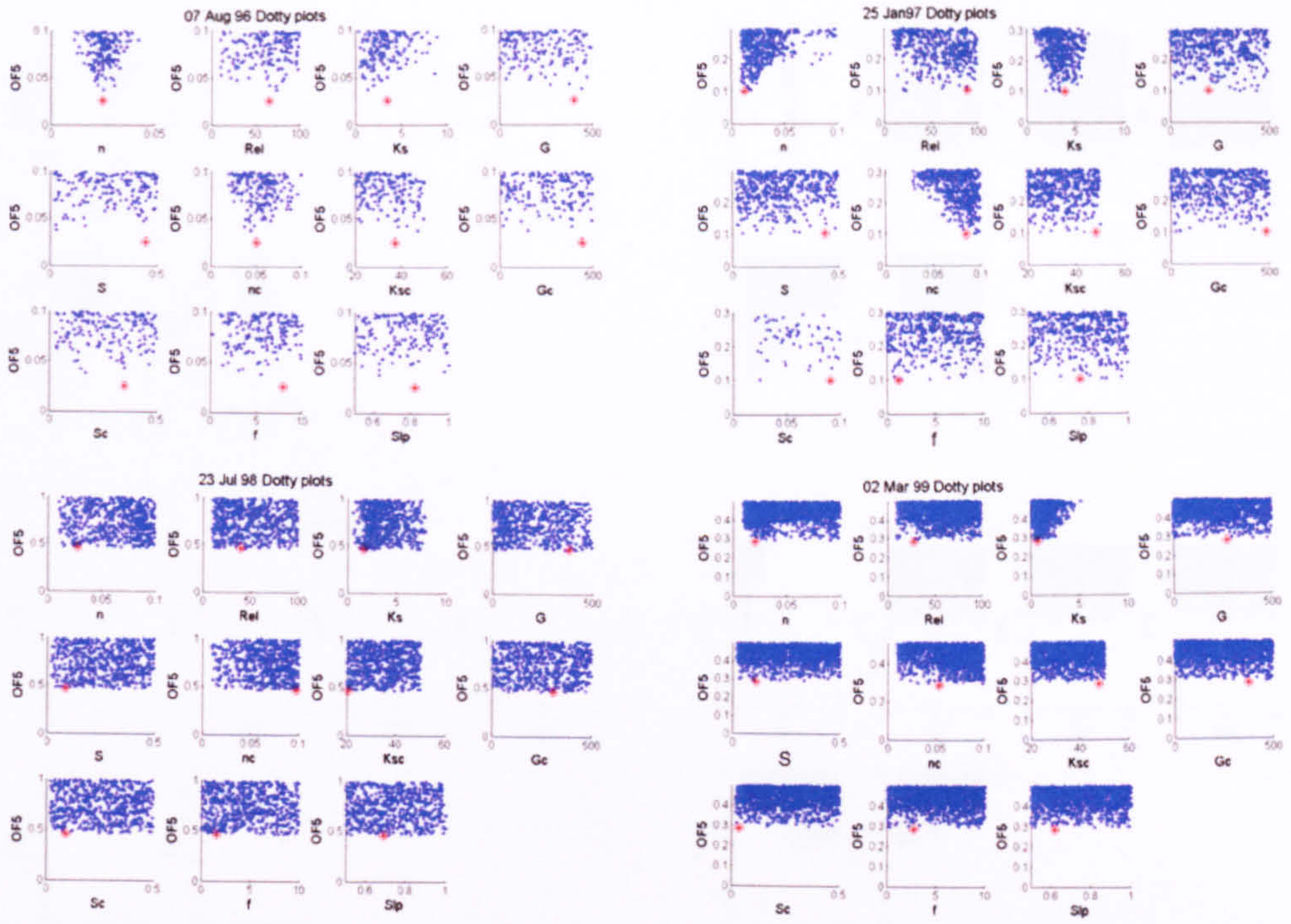


Figure 7.21: Dotty plots for selected events using OF_5 (11-parameters, G>0)

Dotty plots for some selected events for the case of spatial variation of *Ks* are shown in **Figure 7.22**. The figures show that the effects are varying from one event to another, as in the above cases, but generally *Ks1*, *n*, and n_c are the most identifiable parameters compared to the others. This could be due to the fact that *Ks1* represents a much larger area than *Ks2* or *Ks3*. The effects of *n,* for both channels and planes, are important in this case but the effects vary strongly from one event to another.

The outcomes from the dotty plots are: the primary importance of *n* and *Ks* are confirmed; n_c and *f* are the next two most important overall. It should be noted, however, that the variability of the estimated optimum parameter values is high over events and this appears to be random, except for optimum values of *Ks* which were relatively consistent over events and always show the strongest effects.

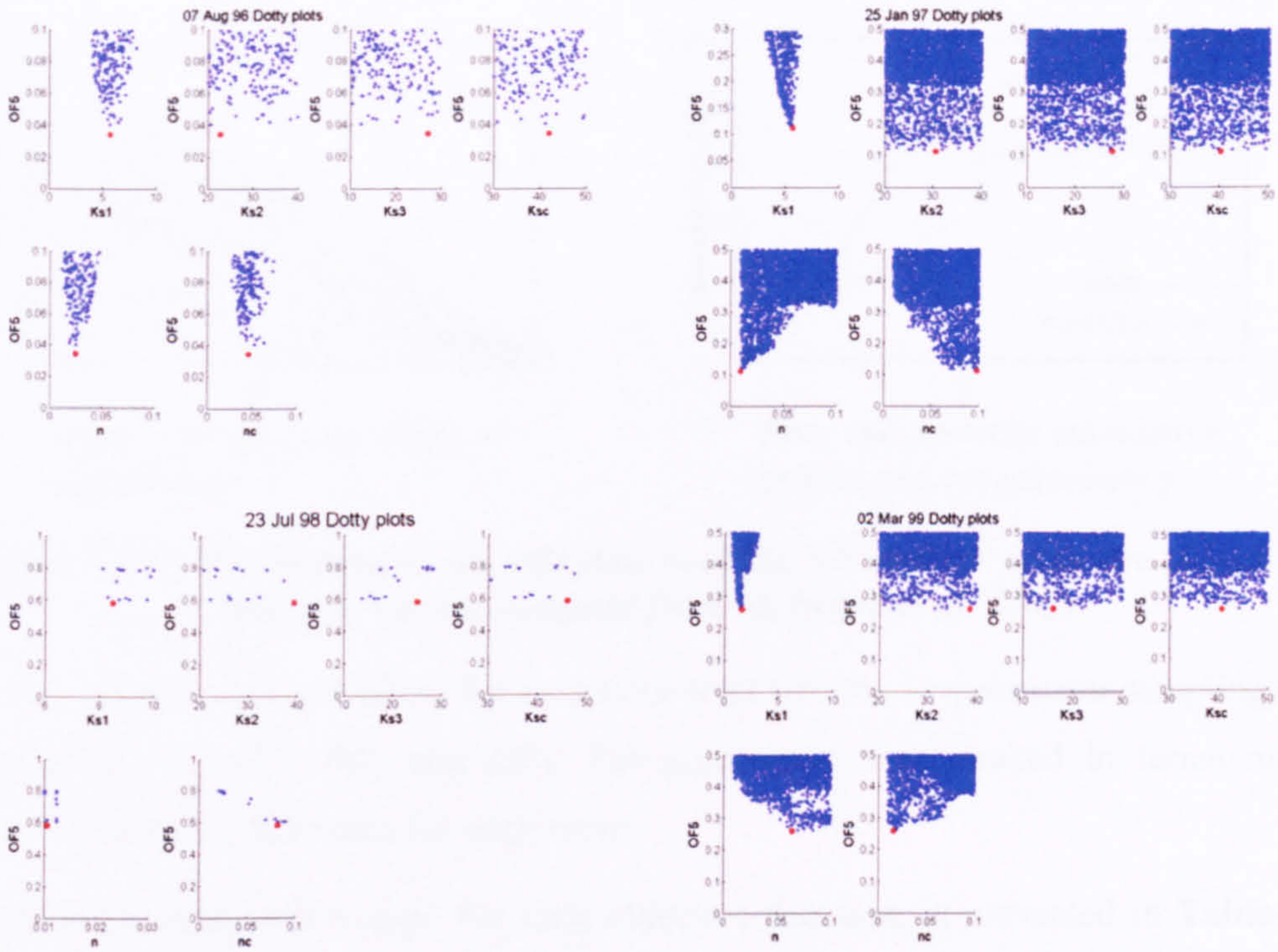


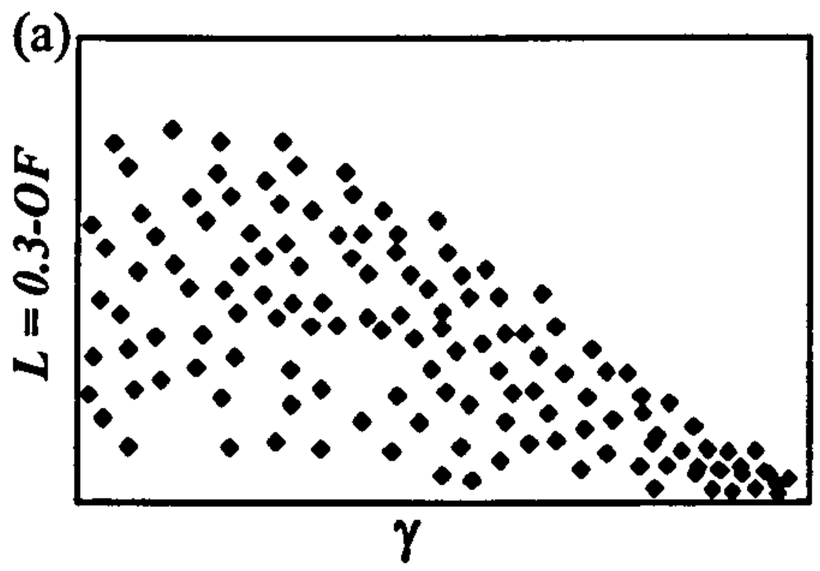
Figure 7.22: Dotty plots for selected events using OF_5 for the spatial variation test (6-pairs, G =0)

7.5.2.2 Quantification of the sensitivity

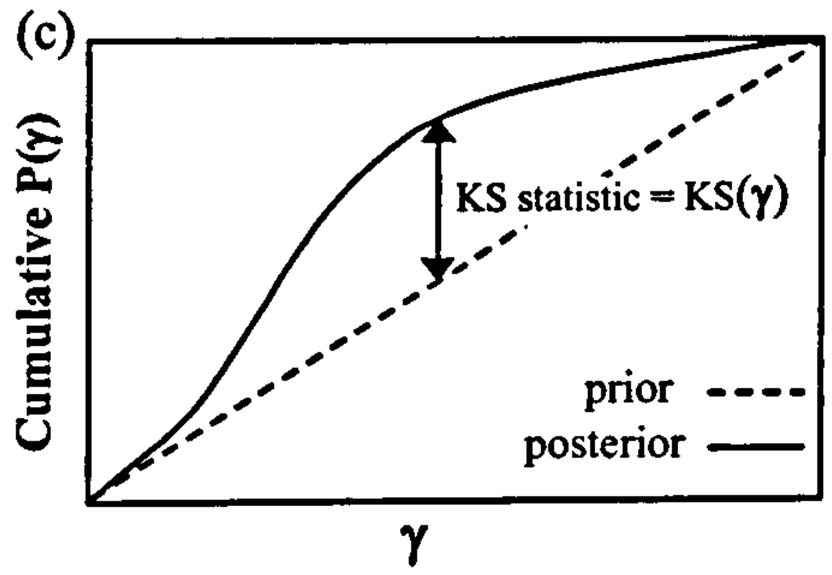
The Kolmogorov-Smirnov (KS) statistic is often used as a statistic which summarises the shape of the dotty plot (McIntyre et al. 2005). This statistic is a measure of how much the posterior parameter distribution (the cumulative values of performance over the parameter range) deviates from a uniform prior distribution. For example, if a parameter has no influence on the performance, then the dotty plot will appear flat and the KS statistic will be zero, while a peaked dotty plot will produce a high KS value. The method of calculation is shown in three steps below. The first step is conversion of performance measure to a likelihood value LK. In this case, LK is defined as:

$$LK = 0.3 - OF \quad \text{if OF} < 0.3\text{, otherwise LK} = 0 \qquad (7.11)$$

The threshold of 0.3 is chosen to represent a 'good' result. The second step converts the dotty plot of likelihoods for a parameter into a posterior cumulative probability distribution for that parameter by calculating the cumulative likelihood then normalising so that the maximum value is one. The cumulative distribution of the prior uniform distribution is a straight line, and the maximum difference between the prior and posterior is the KS statistic.



Scatter-plot of L over range of parameter γ



Prior and posterior cumulative distributions of parameter γ

Figure 7.23: Illustration of the calculation of the KS statistic from the objective function values. (*adapted from McIntyre et al. 2005*)

The KS statistic was calculated for each parameter (for the 11-parameter sampling), for each event, for OF_1, OF_2 and OF_3. The parameters were ranked in terms of the significance of the KS value for each event.

The average rank over events, for each objective function, is presented in **Table 7.7,** together with an overall rank based on the average of these averages.

Table 7.7: Average ranking of importance of parameters to OFs, and overall rank

	$OF_1(Q_p)$	$OF_2(Q_v)$	$OF_3(Q_t)$	Overall rank
n	3.0 (0)	3.8 (2)	3.9 (0)	2
Rel	5.2 (1)	5.4 (1)	6.7 (0)	6
Ks	2.0 (0)	1.1 (0)	2.2 (0)	1
G	4.4 (0)	2.6 (2)	4.0 (0)	3
S	6.1 (0)	5.8 (2)	6.3 (1)	7
n_c	3.8 (0)	8.1 (3)	1.6 (0)	4
Ks_c	9.3 (5)	9.1 (6)	8.7 (2)	10
S_c	9.6 (5)	8.6 (4)	9.2 (4)	11
G_c	8.5 (7)	8.7 (5)	9.7 (5)	9
f	5.7 (0)	5.0 (2)	6.0 (0)	5
Slp	8.4 (0)	7.7 (0)	7.8 (1)	8

In the case of OF_1, OF_2 and OF_3 respectively, two, two and six events were omitted in the calculation of average ranks because there were few (less than 100) parameter sets giving good performance (OF < 0.3). *Ks* is found to be the most influential parameter overall, followed by *G*, *n*, n_c and *f*, and there were only small variations in rank between objective functions. All the parameters had significant KS statistics, in other words they all had some effect.

7.5.2.3 Parameter correlations

It should be noticed that the dotty plots only illustrate the uni-variate projection of the response surface. This means that if the response surface includes significant bi-variate or multi-variate effects, then the importance of a parameter may be under-estimated by viewing the dotty plot. In the extreme case that two parameters have equal or opposite effects on the performance measure (i.e. are strongly correlated) then the dotty plots may not show their effects at all. The same limitation applies to the KS statistic, which is a uni-variate statistic as applied above. Therefore, the dotty plots and KS statistic values are supplemented by a parameter correlation analysis.

The correlation between two parameters was calculated for each OF, considering only the parameter sets which are 'good' (OF<0.3). This aims to identify bi-variate 'ridges' on the response surface, indicating where two parameters varied together cause stronger effects than if they are varied one at a time.

Analysis of correlations between different parameters was carried out for different events. **Table 7.8** shows the results obtained for different tested events.

Table 7.8: Correlations between different parameters, using OF_5

Pars	*n*	*Rel*	*Ks*	*G*	*S*	n_c	Ks_c	G_c	S_c	*f*	*Slp*
07 August 1996											
n	1.000	0.098	-0.516	-0.076	-0.014	-0.431	-0.067	0.017	0.043	-0.021	0.129
Rel	0.098	1.000	0.231	0.030	-0.014	-0.059	0.025	-0.034	-0.025	0.004	-0.027
Ks	-0.516	0.231	1.000	-0.248	0.089	0.172	-0.040	-0.031	-0.016	0.141	0.017
G	-0.076	0.030	-0.248	1.000	0.065	0.012	-0.012	-0.001	0.021	0.049	-0.022
S	-0.014	-0.014	0.089	0.065	1.000	0.003	-0.034	-0.034	0.036	0.006	0.034
n_c	-0.431	-0.059	0.172	0.012	0.003	1.000	-0.024	-0.039	-0.008	0.048	0.006
Ks_c	-0.067	0.025	-0.040	-0.012	-0.034	-0.024	1.000	0.026	0.015	-0.023	-0.030
G_c	0.017	-0.034	-0.031	-0.001	-0.034	-0.039	0.026	1.000	0.021	0.010	-0.042
S_c	0.043	-0.025	-0.016	0.021	0.036	-0.008	0.015	0.021	1.000	-0.014	0.000
f	-0.021	0.004	0.141	0.049	0.006	0.048	-0.023	0.010	-0.014	1.000	0.015
Slp	0.129	-0 027	0 017	-0 022	0 034	0 006	-0 030	-0 042	0 000	0 015	1 000
25 January 1997											
n	1.000	-0.078	-0.553	-0.004	0.001	0.097	0.067	0.004	0.058	-0.028	0.099
Rel	-0.078	1.000	0.367	-0.069	0.010	0.148	-0.056	-0.022	-0.064	0.009	0.040
Ks	-0.553	0.367	1.000	-0.596	0.083	-0.099	-0.150	0.010	-0.023	0.192	0.025
G	-0.004	-0.069	-0.596	1.000	-0.021	-0.014	-0.026	-0.039	-0.009	0.088	0.008
S	0.001	0.010	0.083	-0.021	1.000	-0.075	0.153	-0.076	0.013	-0.016	0.012
n_c	0.097	0.148	-0.099	-0.014	-0.075	1.000	-0.008	-0.017	-0.072	-0.019	0.096
Ks_c	0.067	-0.056	-0.150	-0.026	0.153	-0.008	1.000	0.069	0.029	-0.012	-0.041
G_c	0.004	-0.022	0.010	-0.039	-0.076	-0.017	0.069	1.000	-0.041	-0.029	-0.002
S_c	0.058	-0.064	-0.023	-0.009	0.013	-0.072	0.029	-0.041	1.000	0.028	0.056
f	-0.028	0.009	0.192	0.088	-0.016	-0.019	-0.012	-0.029	0.028	1.000	0.092
Slp	0 099	0 040	0 025	0 008	0 012	0 096	-0 041	-0 002	0.056	0 092	1 000
27 January 1998											
n	1.000	-0.192	-0.172	-0.121	0.016	0.008	-0.030	0.048	-0.024	0.134	0.001
Rel	-0.192	1.000	0.163	0.090	-0.025	-0.054	-0.053	-0.004	-0.138	-0.132	-0.057
Ks	-0.172	0.163	1.000	-0.735	0.122	0.164	-0.169	-0.107	0.001	0.451	0.172
G	-0.121	0.090	-0.735	1.000	0.064	-0.132	-0.004	0.078	0.026	-0.302	-0.036
S	0.016	-0.025	0.122	0.064	1.000	0.115	0.026	-0.001	0.005	0.044	0.035
n_c	0.008	-0.054	0.164	-0.132	0.115	1.000	0.034	0.026	-0.114	0.297	0.156
Ks_c	-0.030	-0.053	-0.169	-0.004	0.026	0.034	1.000	-0.067	-0.043	0.023	-0.116
G_c	0.048	-0.004	-0.107	0.078	-0.001	0.026	-0.067	1.000	0.118	0.027	-0.004
S_c	-0.024	-0.138	0.001	0.026	0.005	-0.114	-0.043	0.118	1.000	-0.066	0.055
f	0.134	-0.132	0.451	-0.302	0.044	0.297	0.023	0.027	-0.066	1.000	0.119
Slp	0 001	-0 057	0.172	-0 036	0 035	0.156	-0 116	-0 004	0 055	0.119	1.000

Table 7.8 shows that there are stronger correlations between some parameters than others but the relative strengths are different from one event to another. Strong negative correlations consistently exist between *n* and *Ks*, *Ks* and n_c and *Ks* and *G;* strong positive correlation consistently exists between *Ks* and *Rel*, and *Ks* and *f*. Recognizing such relationships aid in better understating the obtained results and the optimum parameter values when carrying out global sensitivity analysis.

7.5.3 Discussion of the global sensitivity analysis results

The global sensitivity analysis of the 11-parameters found that they were all significantly affecting all objective functions over the tested events, although the effects were varying from one event to another and one performance measure to another. The finding that the parameters governing hillslope infiltration rates, *Ks* and *G*, and the Manning's roughness, *n*, are consistently the most important confirms previous research in arid and semi-arid catchments (e.g. Sorman and Abdulrazzak, 1993; El-Hames and Richards, 1998; Yatheendradas et al., 2007; Al-Qurashi et al., 2008). The parameters governing channel infiltration (Ks_c, G_c and S_c) were found to be the least significant parameters. This relative insensitivity can be explained by the limited channel bed area compared to the planes (**Table 7.1**). Grayson et al. (1992) show that an extended channel network would be expected to increase importance of channel bed infiltration. Initial saturation of the channel soil (S_c) was the second least significant parameter, and that of the planes was ranked the seventh out of 11 parameters (see **Table 7.8**). It should be noted that the initial saturation was varied only over the range 0-0.5 for the case of using $G>0$ because of numerical stability problems at higher values, although this range is believed to be reasonable for the Wadi Ahin events.

The correlation between some parameters was strong, particularly between *Ks* and the other relatively important parameters, for example the roughness parameter *n*, as **Table 7.7** shows. This is believed to be because the main function of *n* is to control flow velocity and residence time, and hence cumulative infiltration loss. On the other hand, correlations between slope parameter, *Slp,* and roughness, *n,* were found to be less than expected.

The results were consistent with the results in Al-Qurashi et al. (2008), where the two large additional events were included to give a total of 27 events.

The local sensitivity analysis shows clearly which parameters are sensitive and need to be considered in the model's calibration but it can not show how definable the parameter is as the global sensitivity analysis using the Monte Carlo simulation method. It should

be noted that in the local sensitivity analysis all parameters but the tested one were fixed, and hence, the obtained results and the tested parameter are not affected by the other parameters as in the global one. Therefore, it was not surprising to see some parameters shows less sensitive than what was found in the local sensitivity analysis such as the *Slp* and *Rel*.

7.6 Calibration and validation

7.6.1 Method of calibration and validation

The lowest value of any objective function (OF_1-OF_7) out of the 20,000 samples is an approximation to the best possible performance of the model, as measured by that particular objective function. The associated parameter set sample is an approximation to the best parameter set, for that objective function. In other words, the random sampling experiment acts as a calibration. Therefore, the experiments explained previously result in a 'best' parameter set for each event, for each of objective functions OF_1-OF_5; and a 'best' parameter set over a number of events (OF_6-OF_7).

The optimum parameters sets derived for each of the other 25 events are used individually to produce an ensemble of predictions for each event. Taking the average of the ensemble, but where the parameter sets which achieved objective function value is less than 0.3 during calibration, are allowed to contribute to the ensemble, rather than all 25. The obtained results using this criterion were shown under OF_8.

As previously described, this was repeated for the 8-parameter experiment, the 11-parameter experiment, and the spatially varied parameter experiment. Also, a calibration was done when fixing the values of *f*, *S* and S_c, as well as *Slp* (at the measured value) and *Rel (*at the average value).

The performance is assessed in two different ways. Firstly, as a visual assessment, the time-series of observed and simulated flow were plotted for selected events. Secondly, as a more general measure, the number of events for which 'good' performance (OF<0.3) was achieved was counted. For example, the simulated value of peak flow must be within 30% of the observed value, as defined by Eq 7.4, to be counted. This 0.3 value is arbitrary, however is considered to be a reasonable tolerance given the limited accuracy of rainfall and flow gauging.

The validation for each event is done using two different approaches: 1) using the best parameter set obtained using OF_6 as the calibration criteria (the event being validated is missed out from the calculation of OF_6 so that it is a true validation test); 2) using the

ensemble of 24 parameter sets obtained from calibration to the other 24 events, and the average of the ensemble is used as the validation result.

A benchmark for the validation performance is that achieved using the default parameter set (i.e. based mainly on Mott Macdonald, 1992).

7.6.2 Results - variability of calibrated parameters over events and over objective functions

Ideally, the best parameter set would be identical over all 25 events. This would imply: 1) that the physical nature of the system as parameterised in KINEROS2 was not changing over events (implying that both the actual physical system was not significantly changing, and that the KINEROS2 parameterisation accurately represents that system); 2) that the calibration technique was sufficient to consistently identify the parameter set which represents that system; and 3) that the rainfall-runoff data sets were sufficiently accurate so as not to require compensatory changes in the parameter values over events.

Furthermore, ideally, the best parameter set would be the same from one objective function to another. This would imply that KINEROS2 was able to produce the best fits simultaneously to peak flows, flow volumes and time to peak, with one parameter set. However, the optimum parameter values were found, in general, to vary widely over the events and over the OFs. **Figure 7.24** shows the parameter variation over events, using the OF_5 objective function, for the 8-parameter case. The only calibrated parameter which may be considered as reasonably consistent over events is *Ks*.

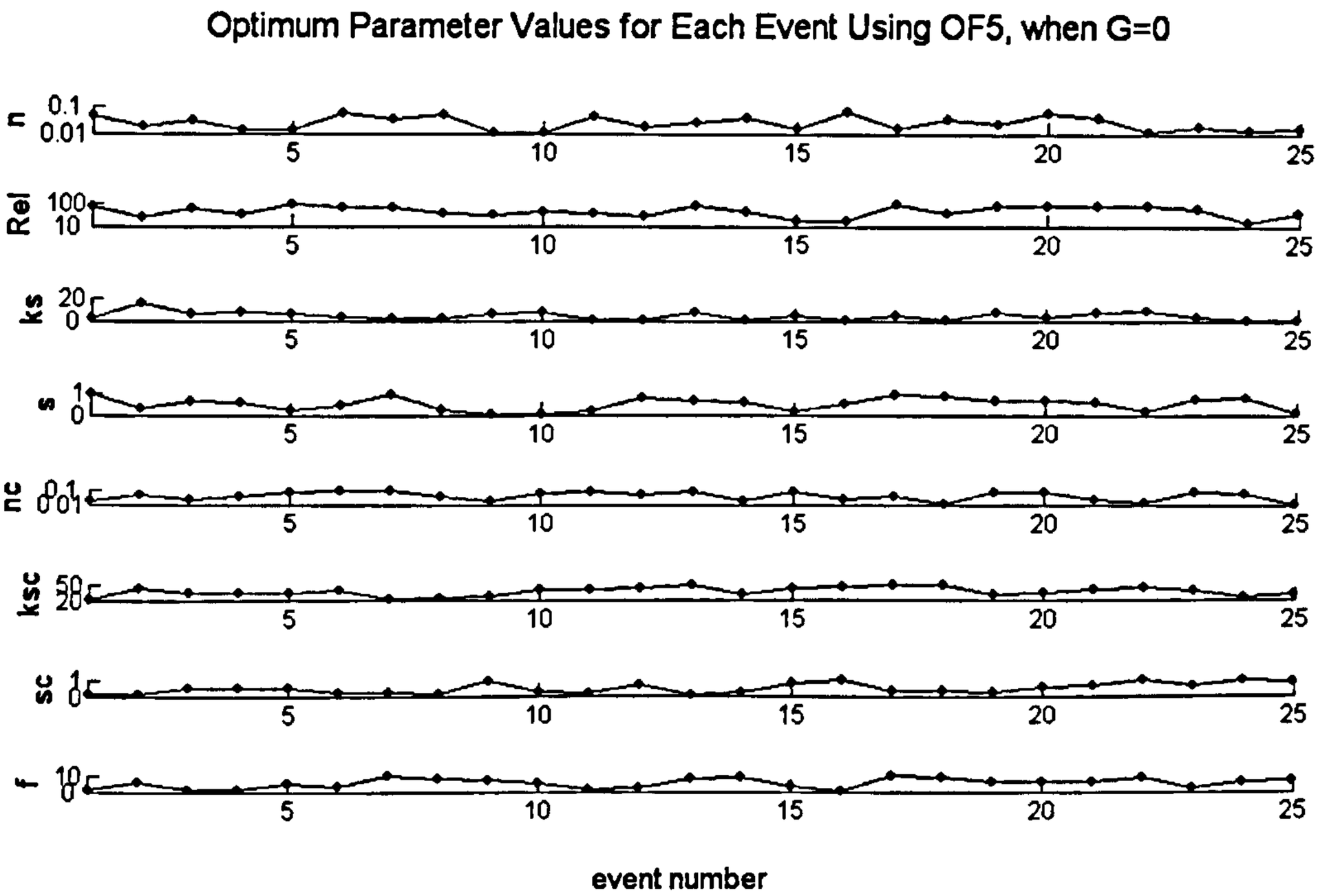


Figure 7.24: Optimum parameter values for each calibrated event, OF_5, 8-parameter case, G=0

For the 11-parameter case (**Figure 7.25**), except *Ks* and S_c, none of the parameters seem to be reasonably consistent over events. However, *n* does seem reasonably consistent except for some events where the values were increasing for no clear reasons.

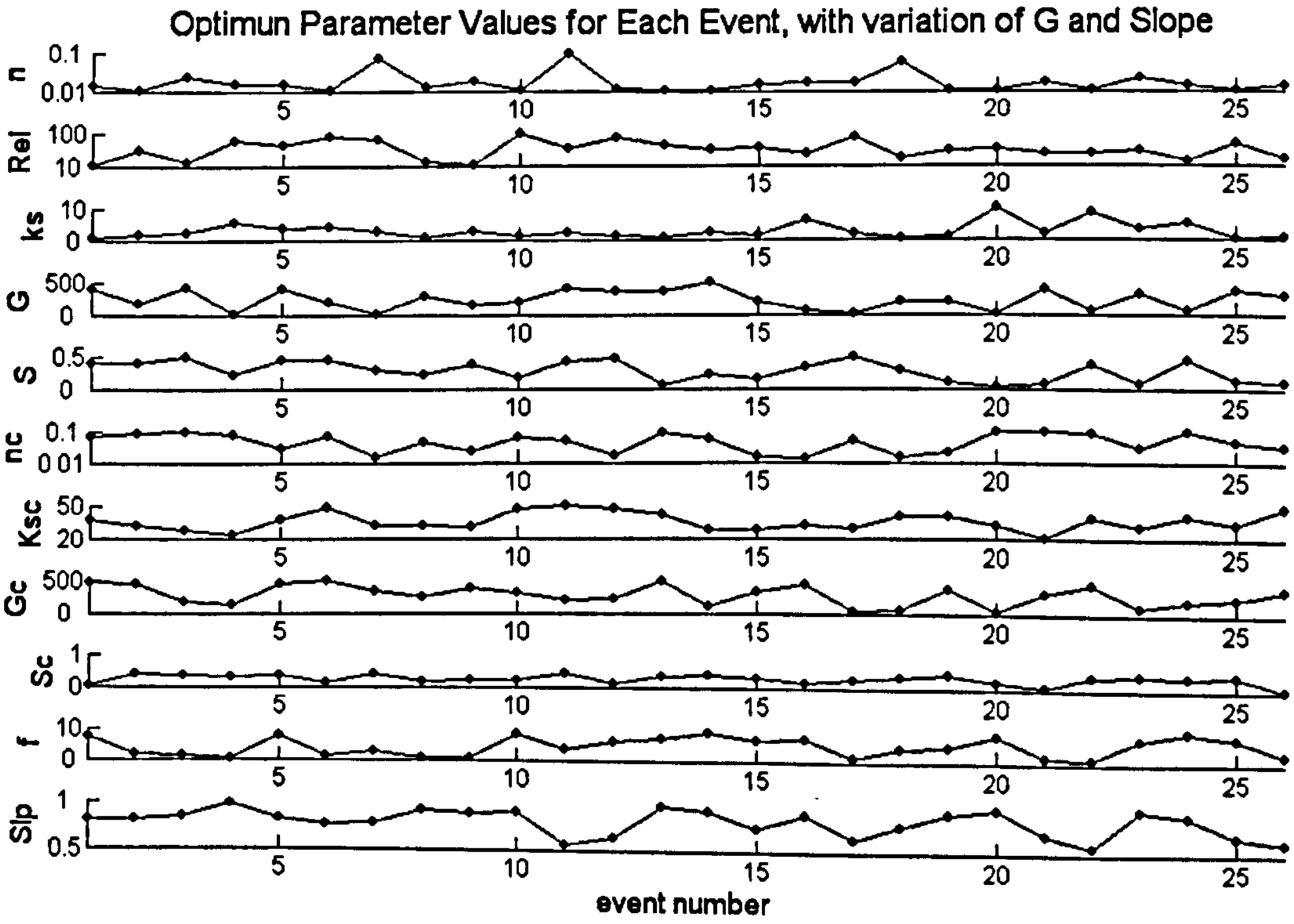


Figure 7.25: Optimum parameter values for each calibrated event using OF_5, 11-parameters, G>0

The same general result – that the best parameter values varied with event - was found when some parameters were fixed, and when the two *Ks* was varied spatially, and when the two additional events were added (see also Al-Qurashi et al., 2008).

It is very clear as the figure shows that the best parameter set for any event is not necessary applicable to be used for another event successfully.

7.6.3 Results - calibration and validation performance

Figures 7.26 shows the calibration (CAL.) and validation (VAL.) hourly time-series results for two selected events for the 8-parameter (G =0) case. Plots entitled (a)-(d) are calibration results using OF_1, OF_2, OF_4 and OF_5 as the calibration criteria, and those entitled (e) and (f) are validation results using OF_6 and OF_7 as the calibration criteria, while (g) is the ensemble average using OF_5 as the calibration criteria (called OF_8 to distinguish between it and the calibration results using OF_5), and (h) is the result using the default parameter set. Note that these calibration results (a-d) use the best parameter set for each event individually, not the best parameter set over all events, hence the results are good.

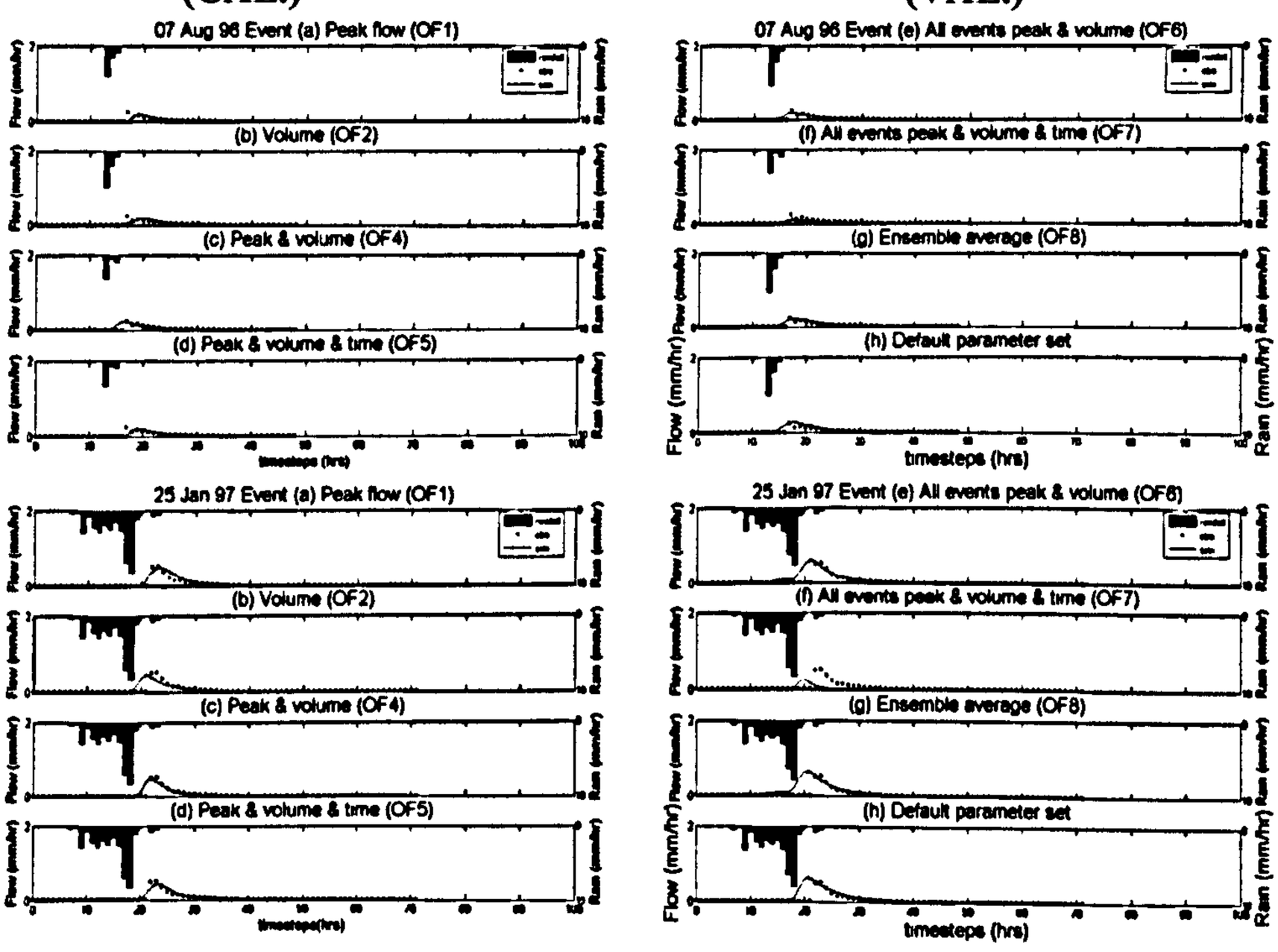


Figure 7.26: Calibrations and validation results of some selected events using different OFs, 8-parameter case, G=0

The calibration results show that all the events have OF_1, OF_2, OF_3 <0.3 and 23 events for OF_4 have less than 0.3, and 7 events using OF_5.

The prediction exercise was repeated while fixing S, S_c, Slp, and f at the values identified from the first calibration. The obtained results are shown in **Figure 7.27**.

This did improve the prediction performance slightly using OF_5: for example, 10 good results ($OF_5 < 0.3$) compared to 7 events for the previous case. On the other hand, all the calibration results for OF_1, OF_2, OF_3 and OF_4 were <0.3.

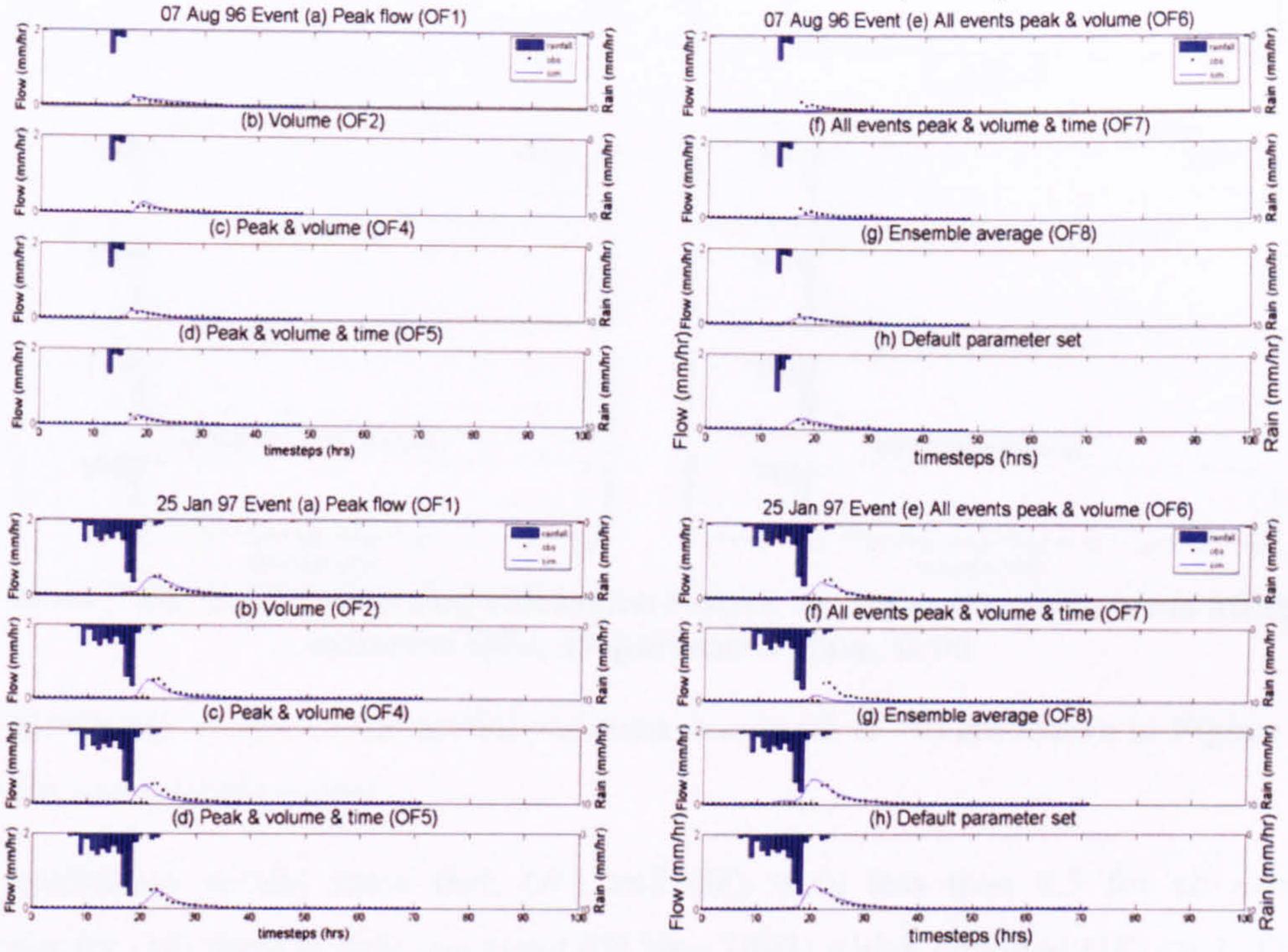


Figure 7.27: Calibrations and validation results of some selected events using different calibration OFs, with fixing 4-parameters, G=0

The simulation results for the 11-parameter case (G>0) for two selected events are shown in **Figure 7.28** for the calibration and validation.

The calibration results show that OF_1, OF_2 and OF_3 were less than 0.3 for all events, whereas there are 2 events which obtained OF_4 less than 0.3 and 9 for OF_5.

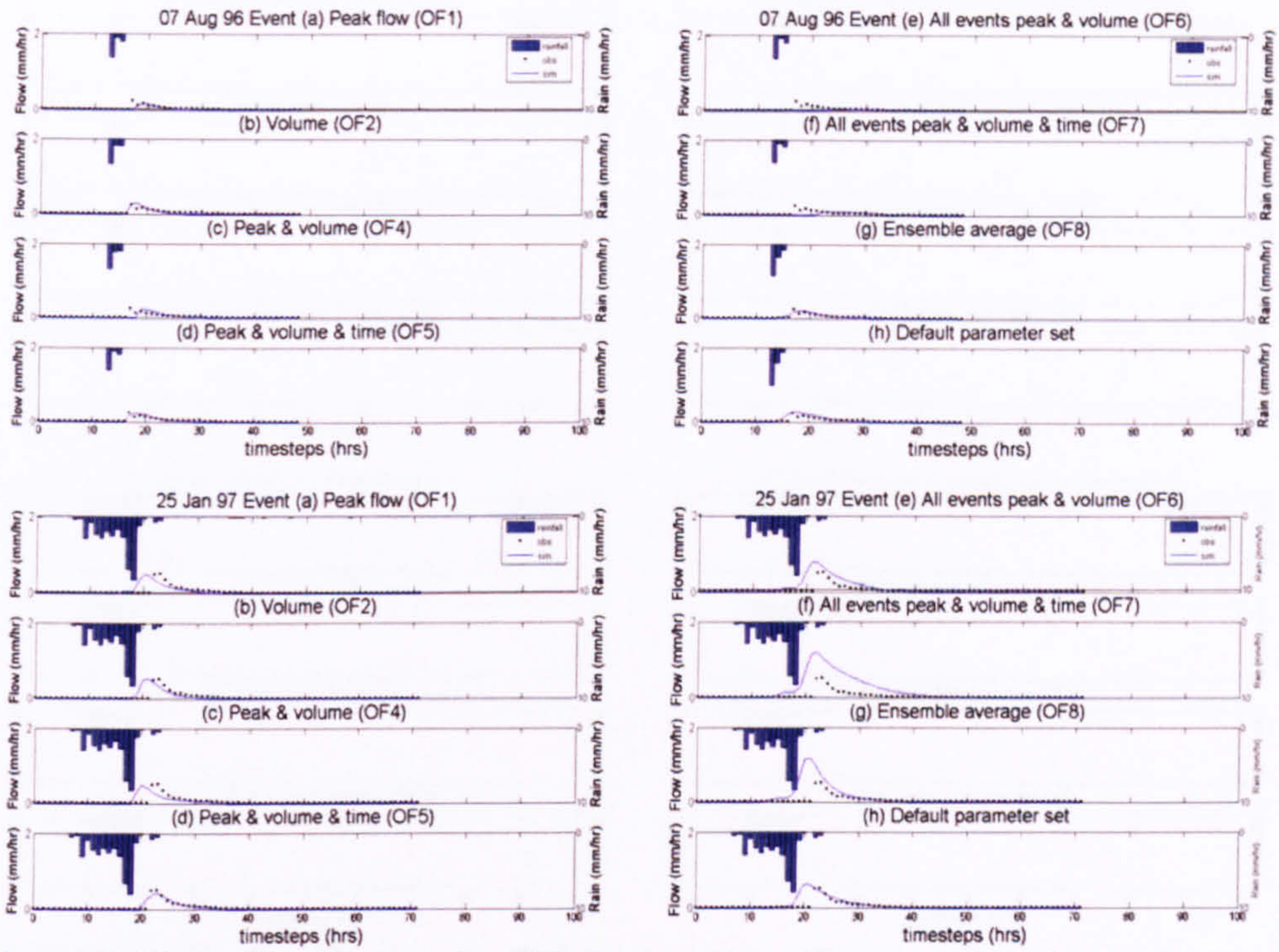


Figure 7.28: Calibration and validation results of some selected events using different OFs, 11-parameter case, $G>0$

The simulation results for the spatial variation case (with $G=0$) are shown in **Figure 7.29** for two selected events.

The calibration results show that, OF_1 and OF_2 were less than 0.3 for all events, whereas for OF_3 there is only one event (02 Nov 1997) which obtained $OF_3<0.3$. There were 20 events with calibration OF_4 values less than 0.3 compared to only 6 events for OF_5. This reflects largely the problems with achieving good fits to time-to-peak.

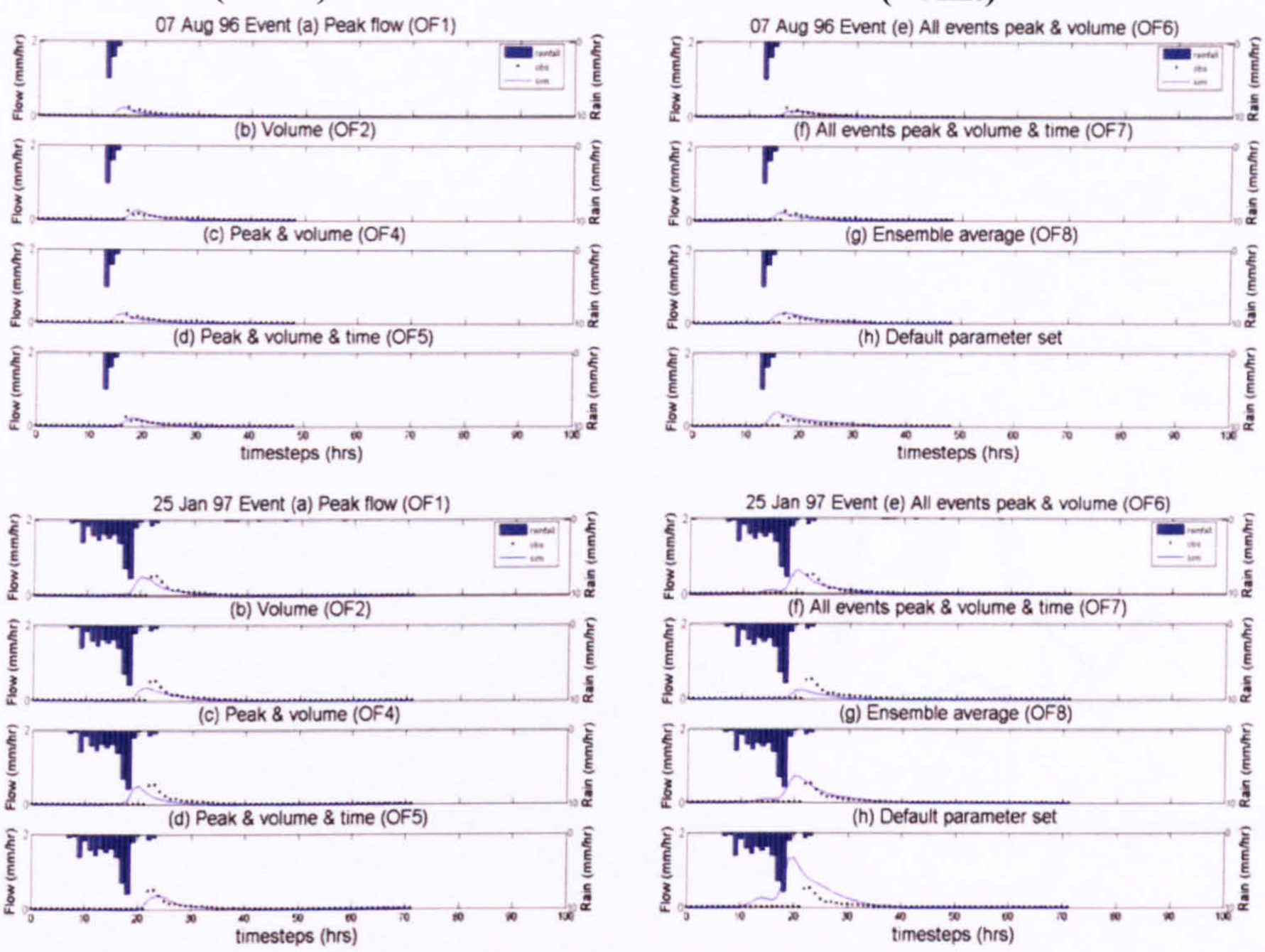


Figure 7.29: Calibrations and validation results of some selected events using different OFs for the spatial variation test (G =0)

Figure 7.30 is a plot of the OF_5 value over all 25 events for the 8-parameter calibration. It shows four lines: the minimum OF_5 values achieved in calibration of each event individually; the OF_5 values achieved using the default parameter set (the benchmark); the OF_5 values achieved using the best parameter set over all the other events (i.e. the validation result); the average of the ensemble of results using the best parameter set from each of the other events. This shows that, while the calibration has obtained 7 events with $OF_5 < 0.3$, only one event has obtained $OF_5 < 0.3$ in the validation when OF_7 was used and none when the OF_8 (the ensemble average) was used.

Figure 7.31 gives the same data in the case where 4 parameters were fixed. The validation results show that there were 10 good results that obtained values <0.3 (using OF_5) but none using the other OFs.

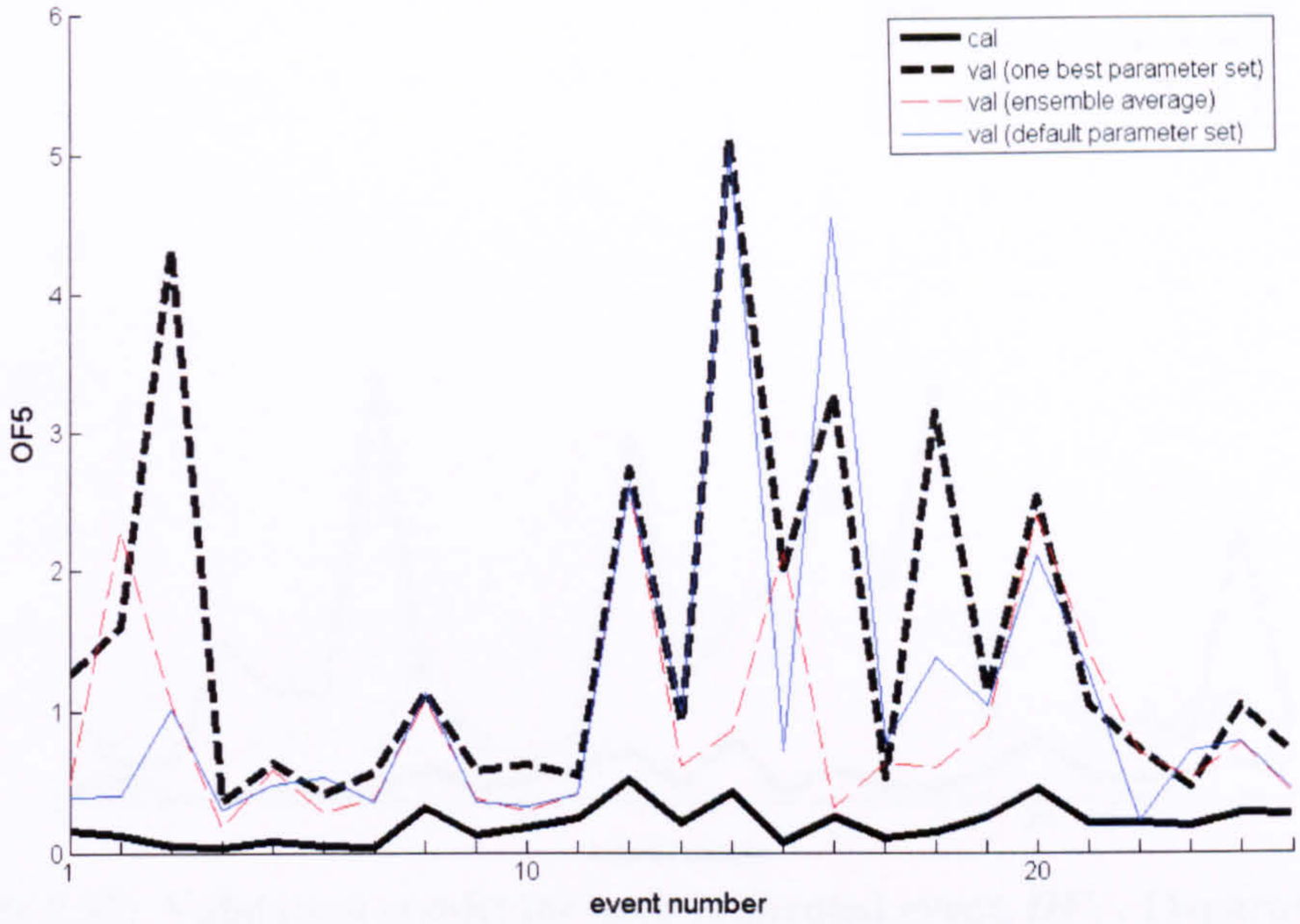


Figure 7.30: Validation results for each calibrated event, OF_5, for 8-parameter calibration, G=0

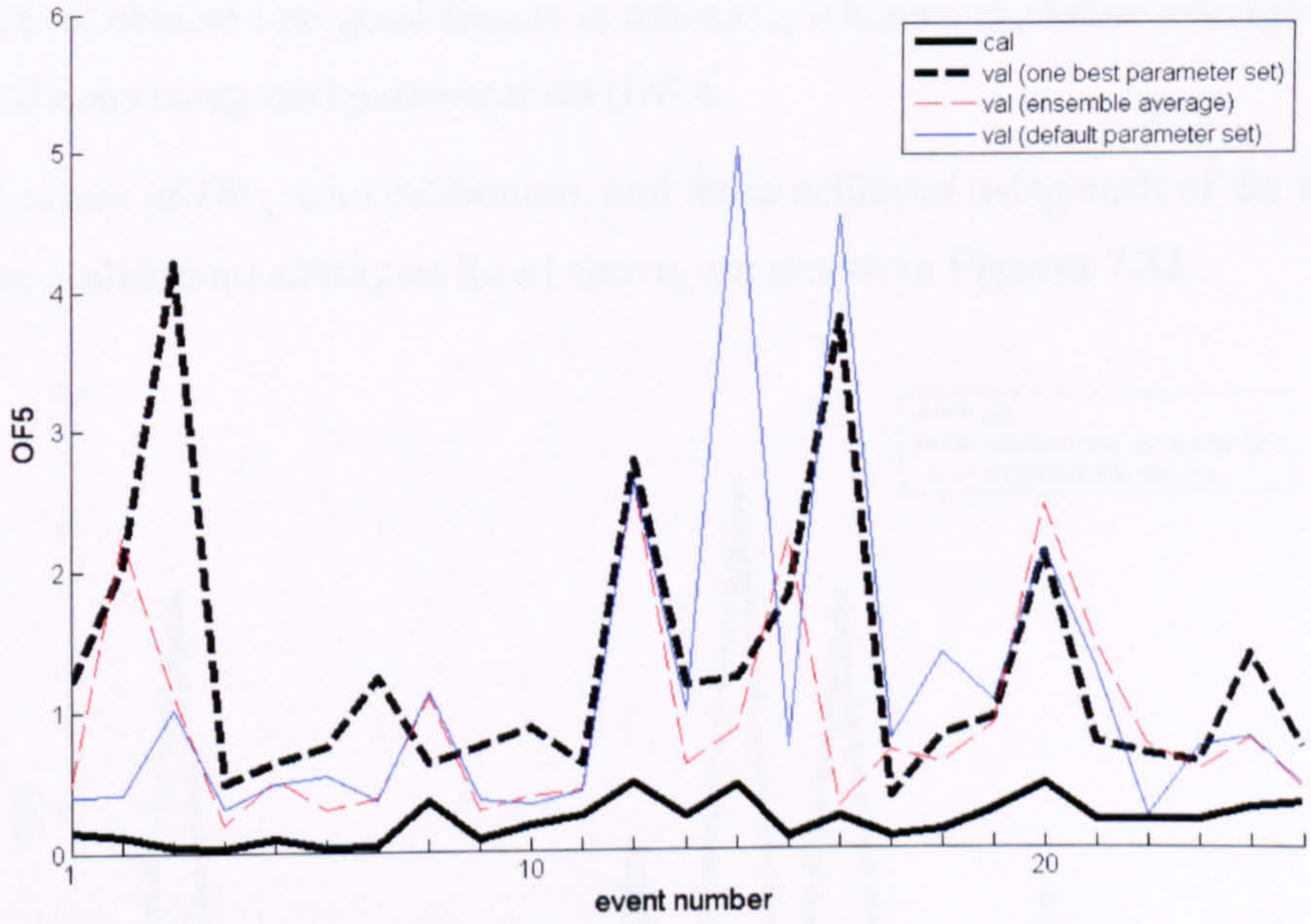


Figure 7.31: Validation results for each calibrated event, OF_5, for fixing 4-parameter calibration, G=0

Figure 7.32 shows the validation result for the 11-parameter calibration case using OF_5. The results show that the obtained results vary from one event to another, as in the above cases. The best results were obtained when each event was calibrated using single OF (OF_1-OF_3).

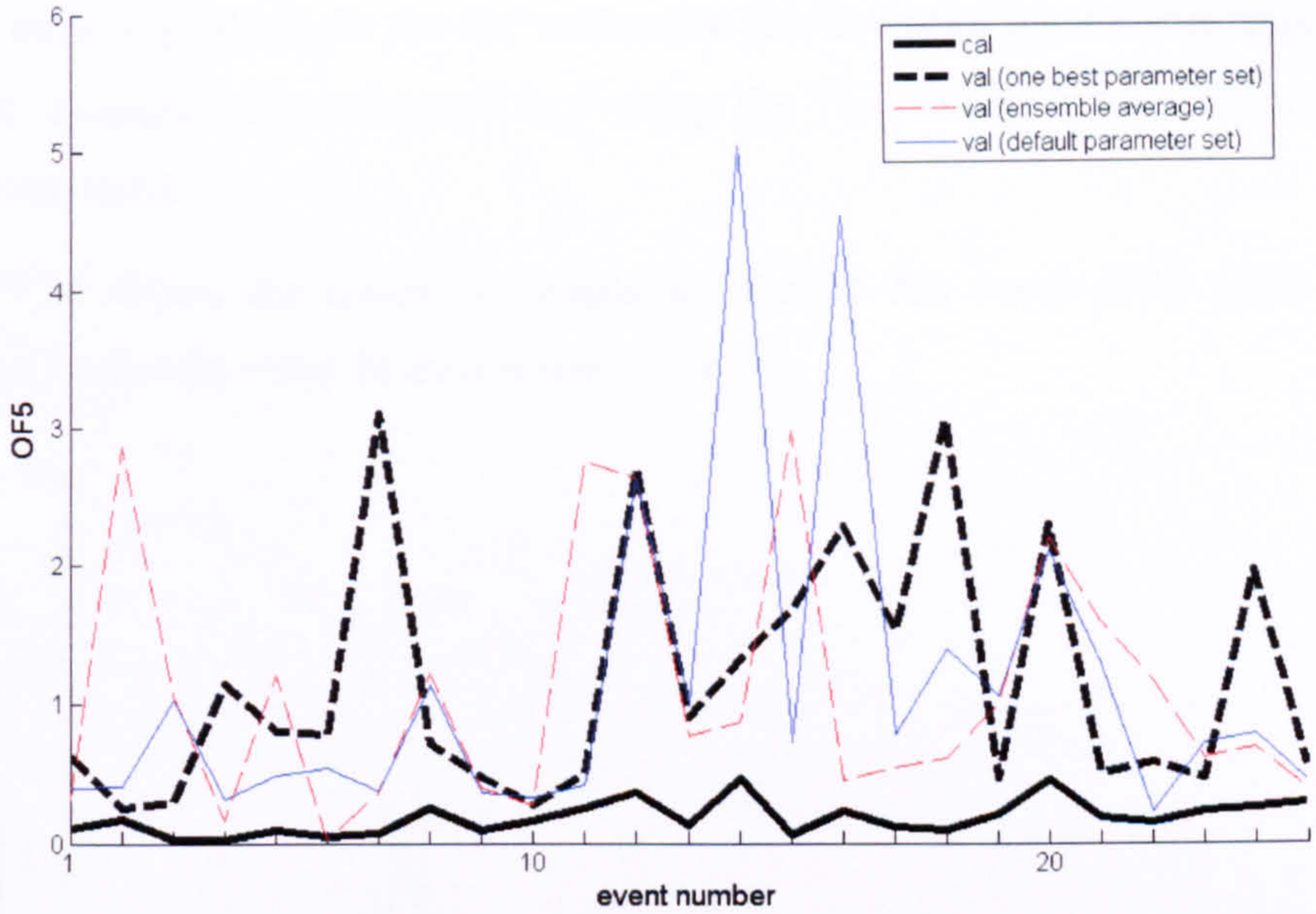


Figure 7.32: Validation results for each calibrated event, OF_5 , 11-parameter calibration, G>0

There were 9 good results obtained when using OF_5. The validation using one best parameter set obtained no good results in this case, whereas ensemble average obtained only 2 and none using best parameter set (OF_7).

The best values of OF_5 from calibration, and those achieved using each of the first three prediction (validation) strategies listed above, are shown in **Figures 7.33**.

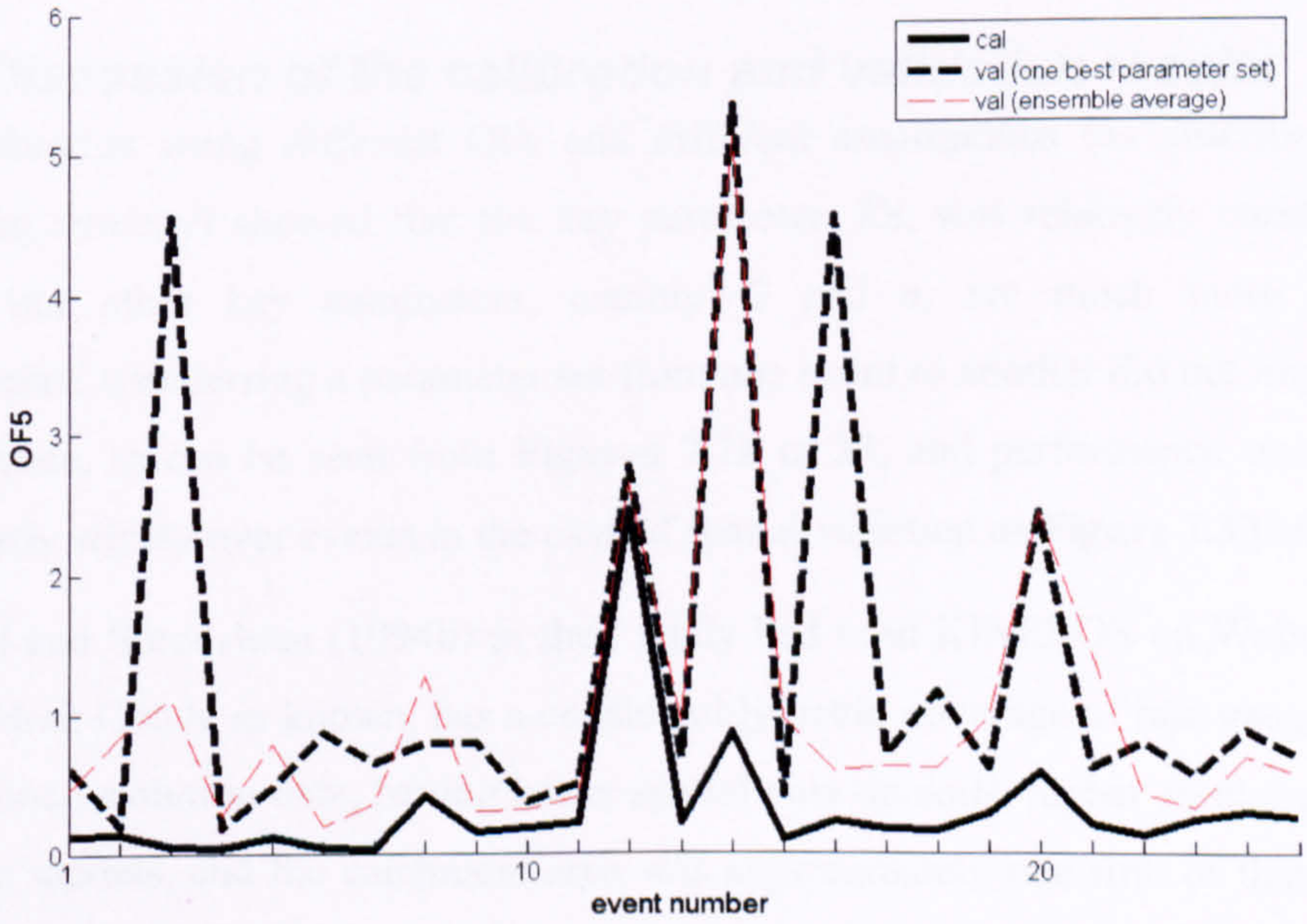


Figure 7.33: Validation results for each calibrated event using OF_5 for the spatial variation test, G=0

The performances over the 25 events when the spatial variation was used did not generally improve upon the 11-parameter version, e. g., the parameter set using OF_5-

optimal gave 6 good results for the calibration run but none for the validation and the ensemble average runs, compared to 9 using the 11- parameter case when the OF_5-optimal was used.

Figure 7.34 shows the ensemble results for the 25 Jan event 1997 when the best parameter set for the other 24 events was used.

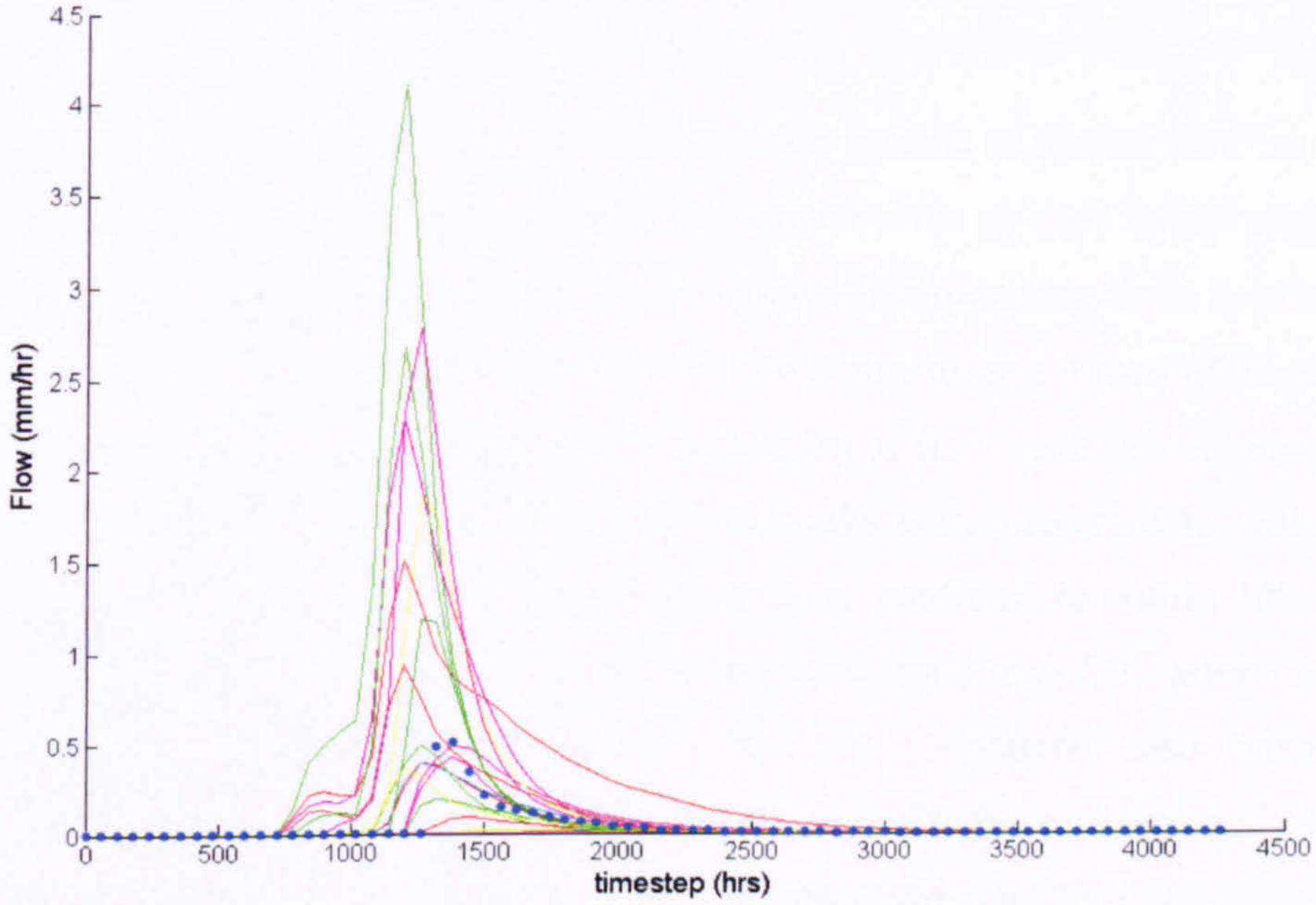


Figure 7.34: Ensemble results for 25 Jan 1997 event, using OF_5 for the 11-paramter test, $G>0$

7.6.4 Discussion of the calibration and validation results

The calibration using different OFs and different assumptions (as described in the modelling strategy) showed that the key parameter, *Ks*, was relatively constant over events, but other key parameters, notably *G* and *n*, are much more variable. Furthermore, transferring a parameter set from one event to another did not improve the performance, as can be seen from **Figures 7.26** to **33,** and performance was varying particularly widely over events in the case of spatial variation as **Figure 7.33** shows.

Michaud and Sorooshian (1994b) in their study had used KINEROS on Walnut Gulch data. Walnut Gulch, as known, has a considerably better coverage of rain gauges with a higher time-resolution data, having better spatial data on soils, higher resolution digital elevation models, and the catchment area was approximately one fifth of that of Wadi Ahin. They found that the validation root mean square error (RMSE) for peak flows was 79% of the mean observed peak, with four out of 24 predicted peaks overestimated by more than 100% for Walnut Gulch. This study shows the validation RMSE (11-parameters, OF_6 calibration criterion) for 25 events was 163% with only two peaks

overestimated by more than 100%. Al-Qurashi et al. (2008) found the best validation peak flow RMSE error (achieved using a 5-parameter calibration to OF_1) was 147% of the mean observed peak, and none of the calibrated 27 peaks overestimated by more than 100%, although only 7 of the peaks were predicted to within 30%. Given the much poorer spatial data available for Wadi Ahin, the comparison with the results from Walnut Gulch (Michaud & Sorooshian, 1994b) is not disappointing, and might be attributed to the less localised rainfall (see Wadi Ahin correlations in **Figure 5.16**).

McIntyre et al. (2007) previously applied regression models to predict flood peaks and volumes in Wadi Ahin, using substantially the same events as used in this chapter but splitting some of the longer events into two events, incorporating three events which would not run in KINEROS2 due to numerical problems, to give a total of 34 events in their regression. They found that, by linear regression of flow peak and volume against gauge-average rainfall, 16 of 34 observed flow peaks were predicted to within 30% (OF<0.3), and 11 of 34 observed flow volumes were predicted to within 30%. Using KINEROS2, the best results in this chapter were obtaining 5 out of 25 using OF_6 in 8-parameters and 11- parameters cases and 4 in the 4- parameters case (when some parameters were fixed). However, the best validation results obtained were only 4 out of 25 in the 11-parameter case and 6-parameter case (the spatial variation case), using OF_7. The best results using OF_6 were 8 out of 25 in this research.

A potential benefit of a distributed simulation model over a lumped empirical model is the theoretical ability to significantly improve predictions by accounting for the spatial-temporal nature of the rainfall and rainfall-runoff processes. However, application of KINEROS2 has failed to do so.

The KINEROS2 performance varied based on the adopted OF criterion. The model was found to be able to obtain acceptable results using OF_1, OF_2 and OF_3 (were <0.3 in all cases) but its performance decreases when combined OFs were used (e.g OF_4, and OF_5). The worse results were obtained using OF_5 (only 7 good results using 11 parameters with G>0 and 6 when G =0, and 5 for the spatial variation case).

The peak, volume and time of peak are all considered important, but the model's performance was found poor in general and the reasons for the limited performance are not proven though the poor rainfall coverage is among the expected reasons. Also, the rainfall interpolation method was shown in the local sensitivity analysis to have a great effect on the results. The rainfall parameter, f, provided a limited exploration of the possible realisations of spatial rainfall. The use of a space-time stochastic rainfall model

for generation of rainfall scenarios would allow more extensive analysis of the sensitivities of KINEROS2, and could be used to demonstrate that rainfall estimation problems are over-riding, which can not be concluded from this study or Al-Qurashi et al. (2008), although is indicated by Yatheendradas et al. (2008). However, there is likely to be significant bias in the estimate of areal rainfall because the gauges in Wadi Ahin are biased towards lower elevations, and this may be the cause of the estimated runoff coefficient of 1.48 for the March 1997 event. A stochastic model which includes elevation adjustment is therefore recommended. Chandler and Wheater (2002) and Yang et al. (2005) provide such a model for daily rainfall; for subdaily rainfall further development of continuous space-time Poisson process models might be required (Wheater et al., 2005).

7.7 Overall Conclusions

Local sensitivity analysis was run using the KINEROS2 model to define the most effective parameters.

The sensitivity analysis was carried out using two events: 07 Aug 1996, and 25 Jan 1997, which have different rainfall distributions and intensities. The model's sensitivity to different rainfall distribution, intensity, and interpolation method was analysed. The analysis shows that the model output is sensitive to many parameters but some parameters have higher effects than others. **Tables 7.4** and **7.5** show, clearly, how the flood peaks vary with the variation of some parameter values.

The overall conclusions can be briefed in the following points:

7.7.1 The rainfall interpolation effects

Three different rainfall interpolation methods were tested: the KINEROS2 method, the weighted average of the gauges to produce uniform rainfall over the whole catchment, and the selected gauges method. The results show that the model is very sensitive to the rainfall input and the rainfall interpolation method. The uniform rainfall produced poorer matches to observed flow compared to the other two, and the selected gauge method was found to be very arbitrary method and the flow results depend heavily on the assigned rainfall gauge and the rainfall distribution for each event. The simulations show clearly that spatial distribution of the rainfall input over the catchment affects results, and a suitable method of calculating areal rainfall from gauged rainfall is a very important factor. However, it was found that the KINEROS2 produces a reasonably

good base for the further steps in the research as it does take into account the three (or in cases two) closest rain gauges.

7.7.2 The local sensitivity analysis results

- The model is very sensitive to the *n* values and the analysis shows that the flood peaks decreases with the increase of the *n* values.
- The *Ks* parameter is one of the key parameters for the infiltration calculation in the model and the change in its values was found to have great effects on the model's results.
- *Cv* (the coefficient of variation of *Ks*) was found to have a very slight change (only if $G>0$).
- The effect of the volumetric rock fraction (*Roc*) was found to have no effect when $G=0$ but there was a slight effect when $G=11$ mm.
- The mean capillary drive, *G*, and the pore distribution index, *Dist*, and the porosity, *Por*, are linked strongly. Hence, the values of these parameters were changed together, based on the soil texture (Woolhiser, 1990). It was found that the obtained results are affected by the change in these three parameters.
- The soil layer thickness was tested when the default value $G=0$ and with $G=11$ mm, with the corresponding *Por* and *Dist* values for the sandy loam soil texture. It was found that, even though the obtained flood peaks were different when the *G* values were different but there was no change in the obtained flow values for each case with the variation of *Thic*.
- The analysis shows that changing the relief (*Rel)* values has some noticeable effects on the flood peak values and effects are linked to the value of spacing (*Spc)* used. It was found that there is no effect or only a slight effect when changing the *Spc* value with constant *Rel* value, but much higher effect when changing the *Rel* value but using a constant *Spc* value. The flood peaks are increasing with the increase of the *Rel* and this effect was greater when a higher *Spc* was used.
- The change in the interception values has a slight effect on the model's output.
- The test shows that the slope (*Slp)* has a significant effect on the results.

- The initial condition which is represented by the saturation values (for both elements) was also found to have some effects on the obtained results, when *G* was allowed to vary.

Hence, all of the effective parameters were selected for further investigation by carrying out a global sensitivity analysis through the uniform random sampling method (Monte Carlo). This also allowed estimation of the optimum parameter sets that give the best fit to the observed hydrographs.

7.7.3 The global sensitivity analysis results

Global sensitivity analysis was run using the Monte Carlo method, with 20,000 parameter samples for 25 events from Wadi Ahin from 1996-1999, using different objective functions representing peak flow, flow volume and time-to-peak performances. The random sampling experiment was also used to approximate the optimal parameter sets for these objective functions.

The study shows that the factors found to most affect the volume and peak performance were generally consistent with those previously identified in the literature – infiltration rates in the hillslopes, the Manning's roughness in hillslopes and channels, and the rainfall interpolation parameter.

7.7.4 The calibration and validation analysis results

- The calibration results for each event independently, using the best of the sampled parameter sets, shows that the KINEROS2 was able to accurately simulate independently flow peak, flow volume and time to peak, for almost all events for all the tested cases, but the case is different using the combined OFs (e.g OF_6, and OF_7).

- The parameter sets which were estimated to be optimal for individual events did not perform well when transferred to other events. The parameter set which gave best calibration performance over any combination of 24 events did not generally produce acceptable performance (defined as within 30% of observed) when used to predict the 25^{th} event.

- The parameter sets identified for the events individually were used to produce an ensemble of predictions. This produced very high uncertainty and the average of the ensemble was a very poor representation of the observed flow data.

- KINEROS2 does not produce high performance in predicting the time to peak, peak, and volume in all cases if a combined OF is used (such as OF_4 and OF_5) and as mentioned before it was more successful when each event was calibrated individually using single OF measure (such as OF_1, OF_2 and OF_3).

- Various objective functions (peak and volume and time, peak and volume, peak only, and volume only) were tried, as well as a second experiment where the infiltration model was made more complex by setting G > 0, and a third experiment which allowed spatial variability in the infiltration rate, but the same general conclusions were reached.

- The work carried out proves that KINEROS2 is a very sophisticated model and might be considered to be over parameterized. Hence, most of these parameter values might be difficult to be identified in most arid areas, as these areas generally suffer from the lack of the essential data such as the rainfall and flow data.

- From this analysis, it was found that the validation results were poor, and hence, it is difficult to transfer the optimum parameter from one event to another even in the same catchment. Therefore, it is difficult to recommend regionalization of the results using KINEROS2. Further analysis using more catchments might be important to study this issue.

- There is still some unclear behaviour of KINEROS2 that needs to be investigated further, as the time limits prevented this to understand the reasons for the model crashing when using certain parameter value combinations.

- The potential value of KINEROS2 and other distributed rainfall-runoff models lies mainly in their ability to simulate spatially and temporally continuous runoff. However it is difficult to see how a useful level of accuracy can be achieved in arid and semi-arid regions using typically available data sets which suffer from poor quality and network coverage.

Chapter 8

The IHACRES Model

8.1 Introduction

The general objective of this chapter is to assess the applicability of a simple conceptual continuous-time model, IHACRES, to modelling rainfall-runoff at a daily time-step in Wadi Ahin. The specific aims are: to assess the performance of the model in terms of time-series fit and volume balance; to test whether a modified version of the model performs better; to test whether a semi-distributed version of the model performs better than the spatially lumped version; to evaluate the volume performance relative to that of the event-based modelling done using KINEROS2; to discuss the difficulties of applying IHACRES to Wadi Ahin and how this might be overcome with additional analysis.

Daily data were used (rather than the hourly data used in the KINEROS2 application) because only daily flow data, not hourly, were available in continuous-time format for Wadi Ahin.

This chapter introduces IHACRES and describes its structure. Then, the application of the model to the Wadi Ahin catchment, using both lumped and semi-distributed versions, is presented. The calibration and validation results are discussed and recommendations are made.

8.2 IHACRES

IHACRES was developed by the Institute of Hydrology (IH) in the United Kingdom and the Centre for Resource and Environmental Studies in the Australian National University (CRES at ANU), Canberra (Jakeman et al., 1990; Littlewood and Jakeman, 1994). It is a metric-conceptual rainfall-runoff model, normally applied as a lumped model. The main aim of its development, as Littlewood et al. (1997) explained, was to aid in characterising the dynamic relationship between the rainfall and runoff in the selected watershed. As inputs, the IHACRES model uses time-series of rainfall, potential evaporation or temperature, and streamflow (Jakeman et al., 1990, 1991, 1993a, b, 1994a, b; Jakeman & Hornberger, 1993). Any time-step may be used, although the model has normally been used with daily data.

The IHACRES model consists of two component models: the non-linear loss model and the linear routing model as shown in **Figure 8.1.**

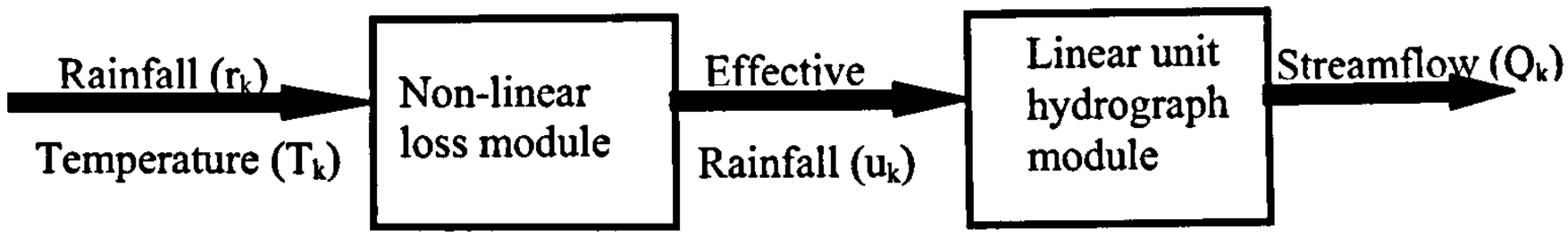


Figure 8.1: A simplified diagram of IHACRES' component models (*after Littlewood et al., 1997*)

The model assumes that there is a linear relationship between the effective rainfall at time-step k (u_k) and streamflow (Q_k) which allows the unit hydrograph theory to be applied. The catchment routing is conceptualised as a configuration of linear storages acting in series and/or parallel, hence this configuration defines the unit hydrograph shape. The non-linearity observed between the rainfall and the runoff is considered in the non-linear loss model, using the catchment wetness index concept, described below.

8.2.1 The non-linear loss module

The non-linear module (the loss module) is the part that estimates the effective rainfall. It is believed that the effective rainfall at time-step k (u_k), generated from the input rainfall (r_k) depends on the catchment wetness index (s_k). The following equations define how r_k and u_k are related to each other, and how s_k is estimated (Littelewood et al., 1997):

$$u_k = r_k s_k \quad \text{.....} \quad (8.1)$$

$$s_k = volc.r_k + \left(1 - \frac{1}{\tau(T_k)}\right) s_{k-1}, \quad \text{.....} \quad (8.2)$$

$$\tau(T_k) = \tau.e^{mf(refp - T_k)}, \qquad \tau(T_k) > 1 \quad \text{.....} \quad (8.3)$$

where $\tau(T_k)$ is the catchment drying time constant at temperature T (°C) at time-step k; $\tau(refp)$ is the catchment drying time constant at a reference temperature *refp* (°C). $\tau(T_k)$ controls the rate of the decay of the catchment wetness index (s_k) in the absence of rainfall. The parameter *mf* (the temperature modulation factor) is the parameter that controls the sensitivity of $\tau(T_k)$ to temperature. *volc* is the volume forcing constant, representing the increase in *s* associated with one unit of rainfall. The value of *volc* may be set such that the volumes of effective rainfall and observed stream flow are the same over the model calibration period. The other parameters, which are usually calibrated

are τ_w and *mf*. The user manual suggests using $s_0 = 0$ as an initial condition, assuming that the simulation begins when the catchment is dry

Ye et al. (1997) introduced two additional parameters (both of which need calibrated) to the loss function in order to model the behaviour of low-yielding ephemeral catchments. Hence, the effective rainfall (u_k) becomes:

$$u_k = (s_k - l)^p . r_k, \qquad \text{if } s_k > l, \text{ otherwise, } u_k = 0 \quad \text{.....(8.4)}$$

where l is the threshold below which no effective rainfall is produced, and p is a peakiness factor.

In this chapter, the original catchment wetness index loss model is called the CWI model and the extended version developed by Ye et al. (1997) is called the Ye model.

8.2.2 The linear model (UH)

In principle, IHACRES can include any configuration of linear routing stores. However, two stores in parallel is believed to adequately represent catchment-scale routing for many, if not most, natural regimes that consist of baseflow and storm flow components at the daily time-scale. Baseflow can be represented by the slow flow (large residence time) store; and storm flow can be represented by the quick flow (small residence time) store. This routing model is defined as follows:

$$S_q = k_q \cdot Q_q \quad \text{.....(8.5a)}$$

$$S_s = k_s \cdot Q_s \quad \text{.....(8.5b)}$$

where S_q and S_s are the storages (mm) in the fast and slow reservoirs respectively, Q_q and Q_s are the outflows (mm/Δt) from the fast and slow reservoirs, and k_q and k_s are the residence times (Δt) of the fast and slow reservoirs.

The rates of change of the storages are defined by the equations:

$$\frac{dS_q}{dt} = u_q - Q_q \quad \text{.....(8.6a)}$$

$$\frac{dS_s}{dt} = u_s - Q_s \quad \text{.....(8.6b)}$$

where u_q and u_s are the inflows to the fast and slow reservoirs respectively. The pair of equations 8.5a and 8.5b are solved in discrete time as,

$$Q_{q,k} = u_{q,k}\left(1 - e^{-\Delta t / kq}\right) + Q_{q,k-1} e^{-\Delta t / kq} \quad \text{.....(8.7)}$$

where subscript k is the time-step number. The same solution method applies to Equations 8. 6a and 8. 6b. The inflow to the fast flow reservoir u_q is equal to the effective rainfall u multiplied by a split parameter $\%q$.

$$u_q = \%q \cdot u \quad \text{.....(8.8)}$$

$$u_s = (1 - \%q) \cdot u \quad \text{.....(8.9)}$$

The IHACRES literature usually uses the discrete-time parameters, for example for the fast store, $a = e^{-\Delta t / kq}$ and $b = 1 - e^{-\Delta t / kq}$. However, in this chapter, k_q and k_s are used for consistency with the parameterisation used in the RRMT software.

8.3 The RRMT

For the purpose of this research, the IHACRES model was run through the rainfall-runoff modelling toolbox (RRMT), which was developed by Wagener et al. (2004).

RRMT is a flexible modelling tool, which contains a choice of simple conceptual model structures. The modeller can choose the model structure that serves his aims (Wagener et al. 2004). The general structure of RRMT is shown in **Figure 8.2.**

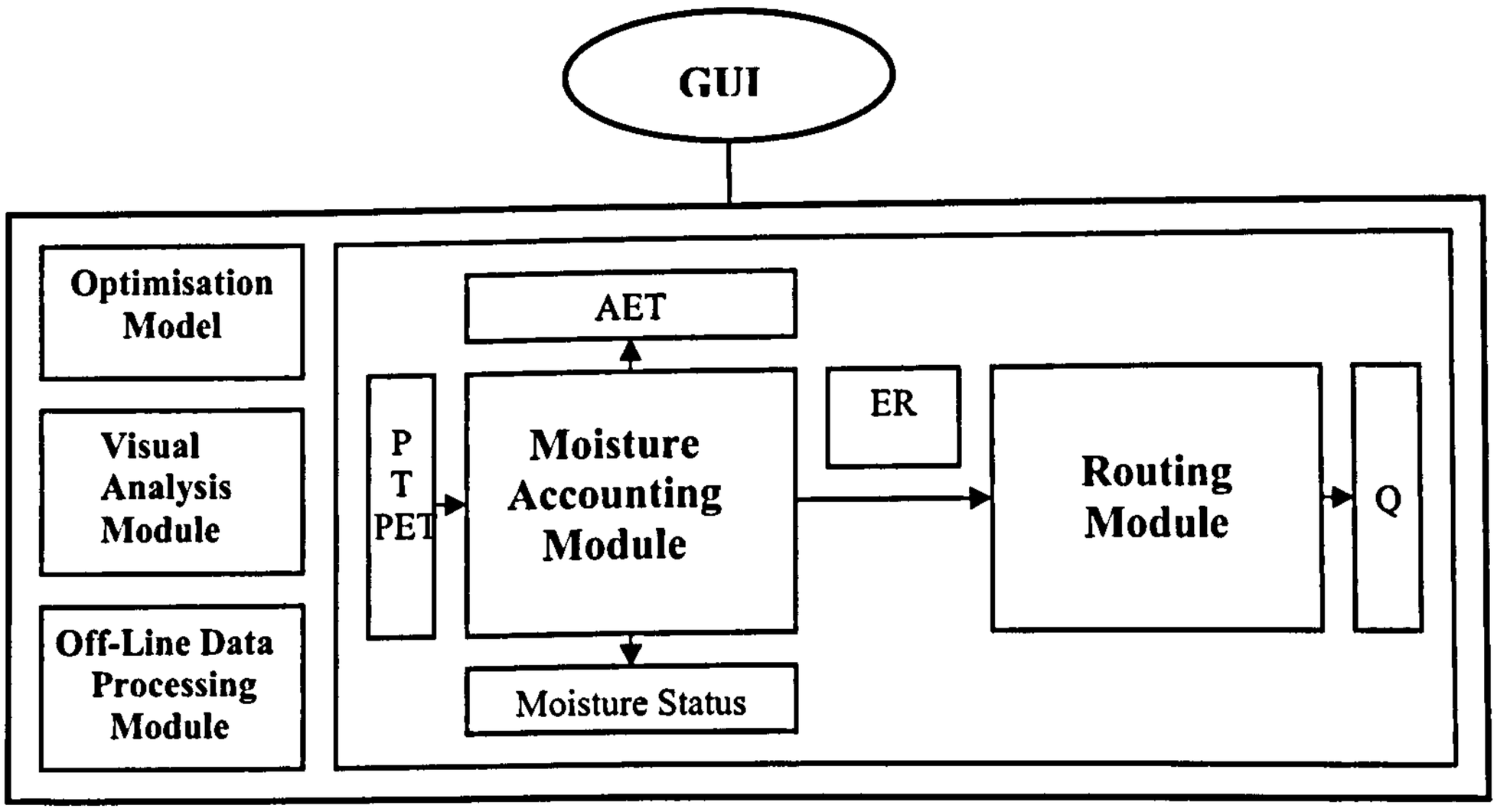


Figure 8.2: General structure of RRMT *(from Wagener et al., 2004)*

The model structures, as shown in the figure above, generally consist of a soil moisture accounting module and a routing module.

Recently, a new version of RRMT was developed where the main catchment is subdivided into sub-catchments (the semi distributed version, RRMT-SD, (Orellana et al., 2008) and options for channel routing are included.

8.3.1 The objective functions

There are many different objective functions (OFs) that can be selected in the RRMT to measure the model performance. The different OFs that are used in the Wadi Ahin application are as mentioned below:

a) Nash Sutcliffe Efficiency, nse:

$$\text{nse} = 1 - \frac{\sum_{i=1}^{N}(Q_i' - Q_i)^2}{\sum_{i=1}^{N}(Q_i - \overline{Q}_i)^2} \quad \text{.....(8.10)}$$

where Q' is the simulated flow, Q is the observed flow, $\overline{Q}$ is the mean observed flow, and N is the total number of time-steps in the calibration period with observations of flow.

The optimum (maximum) value of nse is 1.0. The RRMT always defines the optimum as the minimum value of the objective function. Therefore in its plots, it uses nse* = 1-nse, which has a minimum value of zero. It should be noted that nse gives a higher weight to fitting the peaks (by squaring the residuals).

b) Root Mean Square Error, RMSE:

$$RMSE = \sqrt{\frac{1}{N}\sum_{i=1}^{N}(Q_i - Q_i')^2} \quad \text{.....(8.11)}$$

RMSE for medium flows, fm, is used for the purpose of this research. This measure is the same as RMSE except that the observed flow values that are used in calculating the OF are between low and high threshold values that are selected by the modeller. Hence, assuming the upper threshold is fixed suitably, this measure is not biased by the high flood peaks. The high threshold used in this study is 8.5 mm/day, selected such that it can eliminate the extreme event of March 1997, whereas the low flow threshold used is 0.1mm/day, selected to eliminate the periods of any baseflow less than 0.1 mm/day from the model assessment to check the models performance when especially low flows are omitted as well as especially high flows.

These objective functions (RMSE within thresholds, and nse) have been commonly used for calibration and assessment of continuous-time rainfall-runoff models (e.g. Wagener et al., 2001; Al-Qurashi et al., 2008).

8.3.2 Optimisation methods available

The RRMT includes two automatic optimisation methods: the Uniform Random Search, and the Shuffled Complex Evolution (Duan et al., 1992).

The uniform random search was adopted in the research, as it generates data for a global sensitivity analysis, and it provides approximations to the optimum parameter sets for all the chosen objective functions. It is a simple, known method that was found to serve the purpose of this research with no problems.

8.3.3 The semi-distributed version of RRMT (RRMT-SD)

The new, semi-distributed, version of RRMT (RRMT-SD) mainly uses the same functions and concepts that are used in the lumped version. However, the catchment is subdivided into a number of subcatchments, which are linked together by a channel network. The objective of this new software is to allow the spatial variations in inputs (rainfall, potential evaporation or temperature, and model parameters) to be represented, and also to allow generation of outputs at interior points in the catchment. In the case of Wadi Ahin, the objective of applying RRMT-SD was to represent the effects of the spatial variation in rainfall (parameters and temperature were assumed to be uniform over the catchment).

The conceptualisation of the rainfall-runoff model for each subcatchment in RRMT-SD consists of a soil moisture accounting (SMA) function, a hillslope routing function and the channel routing function. The SMA and hillslope routing are applied for each subcatchment independently (in effect, several lumped models running in parallel). The channel routing then models the flow accumulation according to the specified channel network, starting from the upstream subcatchments to the catchment outlet. The available channel routing functions are a linear reservoir (1 parameter), a time-delay (1 parameter) and a kinematic wave (2 parameters) (Orellana et al., 2008).

For the Wadi Ahin application, the SMA and hillslope model structures were the same as used for the lumped modelling (the CWI and Ye models, defined by Eqs 8.1-8.4; and two parallel linear stores, defined by Eqs 8.5-8.9).

The one-parameter time-delay was used for channel routing because it is simple and numerically efficient (unlike the kinematic wave option) and it represents channel travel

time while maintaining the peakiness of the flood (unlike the linear reservoir option). The time-delay function is defined as:

$$Q_d(t) = Q_u\left(t - \frac{L}{c}\right) + \int_{x=0}^{x=L} q\left(t - \frac{x}{c}\right)dx \quad \text{.....(8.12)}$$

where Q_d (m^3s^{-1}) is the flow output at the downstream end of a subcatchment's channel, Q_u (m^3s^{-1}) is the flow input to the upstream end of that channel (i.e. the flow accumulated from all upstream catchments), L (m) is the channel length, c (ms^{-1}) is the celerity parameter, q (m^2s^{-1}) is the hillslope runoff which is assumed to be uniformly distributed over L, t (s) is time, x (m) is distance from the downstream end of a channel to the upstream end. As the model operates on discrete time-steps, $Q_u(t\text{-}L/c)$ and $q(t\text{-}x/c)$ are estimated by linear interpolation between the values at the two surrounding discrete time-steps. The integration of q is done numerically using a space increment, $\Delta x = L/20$. Although there is only one parameter to be calibrated (c), the user needs to specify the channel length L for every subcatchment.

Like RRMT, RRMT-SD includes the options of the uniform random search or the Shuffled Complex Evolution method for parameter estimation. For the Wadi Ahin application, the uniform random search was used, as mentioned before. The objective functions specified in **Section 8.3.1** were used (nse* and fm).

When using RRMT-SD instead of RRMT, the parameter estimation problem is potentially much greater because there can be a different parameter set for each subcatchment. However, in the Wadi Ahin application, the parameters are assumed to be uniform across the catchment. Therefore, moving from the lumped to semi-distributed version there is only one additional parameter, the wave celerity (c). It is hypothesised that the ability to represent the spatial rainfall effects will result in a significant improvement in performance over the lumped version.

8.3.4 Monte Carlo Analysis Toolkit (MCAT)

RRMT provides the option to use the Monte Carlo Analysis Toolkit (MCAT, Wagener et al., 1999, 2002a) to assist in investigating the model performance in terms of parameter sensitivity and identifiability (Wagener et al., 2001). The MCAT provides a number of options for visualising the sampled model parameters and model outputs that aid in analysing the model uncertainty. In the Wadi Ahin application, the MCAT was used to generate scatter plots of performance against parameter values ('dotty plots').

8.4 The Model Inputs and the Modelling Strategy

The IHACRES model was run through the RRMT (RRMT-L) and the semi distributed version (RRMT-SD), as mentioned above, to compare the results. The two versions of the model were run using 1996-97 for calibration and 1998-99 for validation with and without the rare event of March 1997.

The uniform random sampling procedure consisted of taking 20,000 parameter set samples from within the specified ranges of the parameters (**Table 8.1**), running the model for each and calculating the objective functions for each.

Two objective functions were used to assess the simulation results in calibration and validation, nse* and fm. These were supplemented by viewing the time-series plots to visually assess the fits. The OF_2 (volume objective function) that is used to assess the KINEROS2 results was also used to compare the results. The OF_1 (peak objective function) was not considered to be applicable in this case for comparison with the KINEROS2 results, as an hourly time-step was used in the KINEROS2 but a daily time–step is used in IHACRES. Also, the exact flood peak values can not be expected to be determined when using the daily time-step as the flood can start and end in the same day in arid areas (see **Chapter 1**). The same is also correct for the OF_3 (time to peak objective function). The time to peak, as reported in the literature is generally ranging from 15-30 min only (Schereiber and Kincaid, 1969; Osborn and Lane, 1969; Al-Qurashi, 1995). In the Wadi Ahin case, 4-hours was the most commonly recorded lag between peak rainfall and peak flow.

The used parameter ranges are shown in **Table 8.1** for the CWI and the Ye SMA models, and in **Table 8.2** for the routing model. These ranges are the default ranges specified in the RRMT. If the best parameter values are outside these ranges, then this would be noted in the dotty plots, and the ranges could be changed.

Table 8.1: The parameters used in SMA model and their ranges

Parameter	Symbol	Range
Time constant of catchment losses	τ	1-40 (dt)
Reference parameter	*refp*	0-10 (°C)
Modulation factor	*mf*	0-5 ($°C^{-1}$)
Initial moisture state of catchment	*s0*	0-1 (-)
Volumetric constant	*volc*	0.005-0.1 (dt/mm)
*Celerity wave	*c*	0.5-1 (m/s)
**Threshold value	*l*	0-15 (-)
**Peakness factor	*p*	0-2 (-)

* channel routing parameter that is used in RRMT-SD only
** additional pars for use with Ye et al. (1997) model

Table 8.2: The parameters used in the routing model and their ranges

Parameter	Symbol	Range
Time constant quick flow reservoir	k_q	1-15 (dt)
Time constant slow flow reservoir	k_s	15-400 (dt)
fraction of flow through quick flow reservoir	$\%q$	0-1 (-)

Note: dt is the time step that is used in running the model. It is one day in our case

8.4.1 The input data for the lumped RRMT (RRMT-L)

The input file that was required to run the lumped version of the RRMT model (RRMT-L) was the average daily rainfall and air temperature over the whole catchment.

The average rainfall was calculated using the KINEROS2 rainfall interpolation method by running the KINEROS2 model with the daily rainfall data and then calculating the catchment average rainfall using Equation 7.1 (**Section 7.5.1**). The idea was to eliminate the effects of using different rainfall interpolations in making comparisons between the IHACRES and the KINEROS2 results. The daily temperature data were obtained from the Sohar metrological station, which is the nearest meteorological station to the Wadi Ahin catchment.

Figure 8.3 shows the input daily rainfall, flow, temperature, and the potential evaporation for the calibration period, 1996-97, whereas **Figure 8.4** shows the input data but for the validation period, 1998-99.

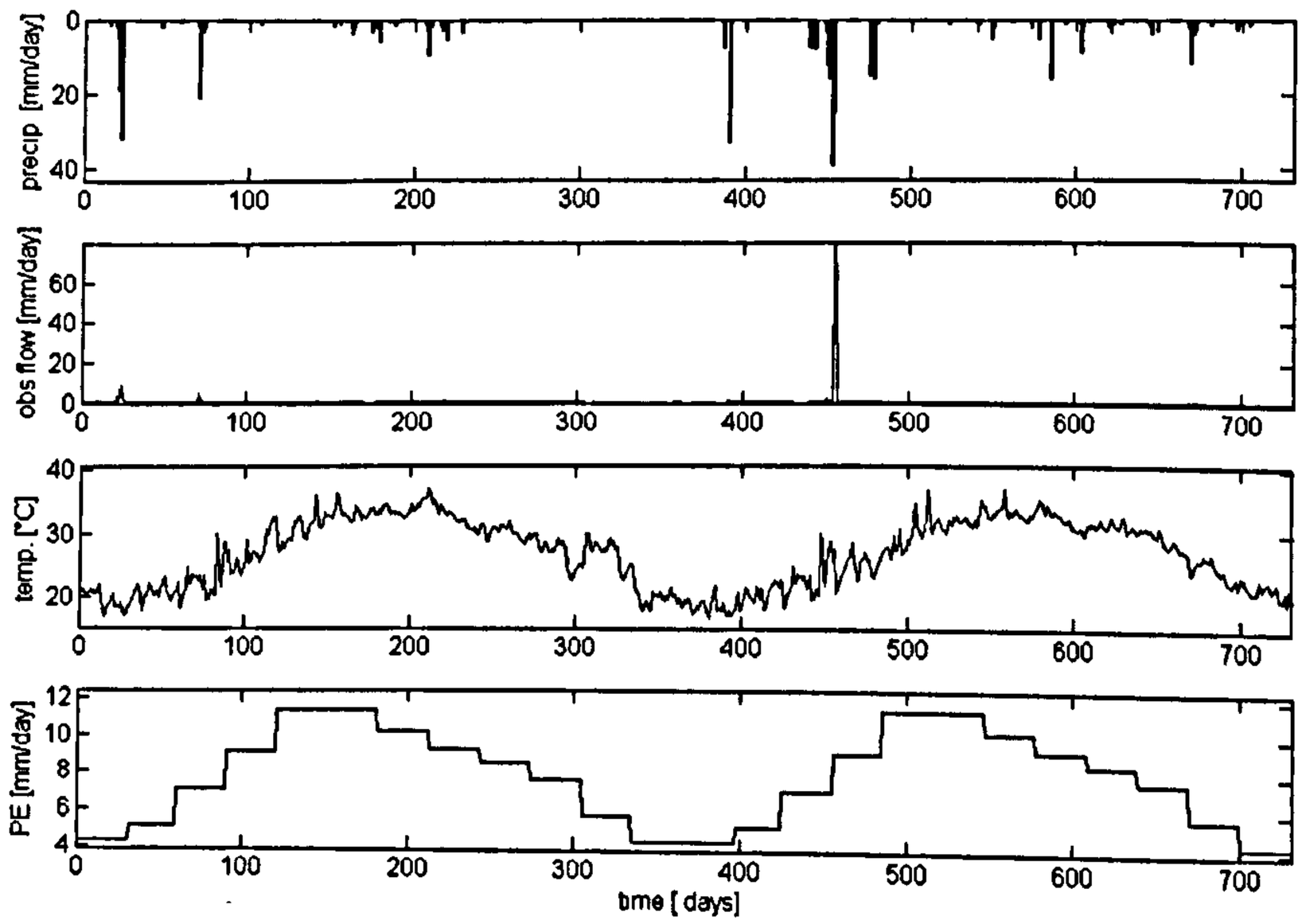


Figure 8.3: The input data for the years 1996-97 used to calibrate the RRMT

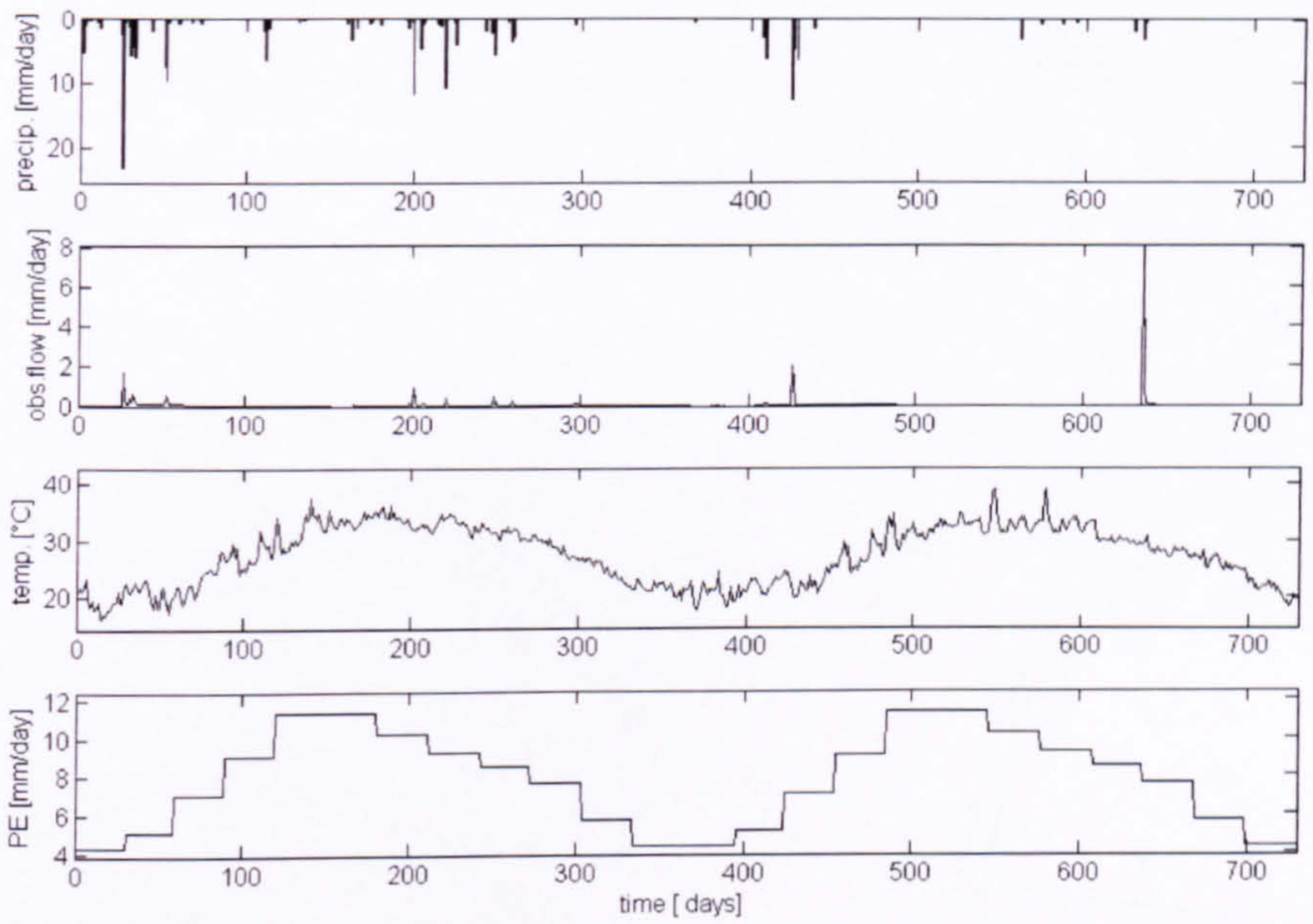


Figure 8.4: The input data for the years 1998-99 used to validate the RRMT

8.4.2 The input data for the semi distributed RRMT (RRMT_SD)

Because of the spatial dimension, more input files were needed for RRMT-SD. For every subcatchment, time-series of rainfall and temperature were needed; and also flow for the Hayl subcatchment. Also, every subcatchment requires a number to identify it, the number of the immediately upstream catchment (if it exists), the subcatchment area, and the channel length.

Wadi Ahin was subdivided into 20 subcatchments which correspond exactly to the planes used in the KINEROS2 application. This allows a more straightforward comparison between the performances of the two models because the spatial rainfall distribution during events is identical. However, this was slightly complicated because RRMT-SD only permits one subcatchment to be associated with each channel length, whereas in the KINEROS2 model two planes were often associated with one channel element. This was overcome where necessary by introducing artificial channel lengths to the RRMT-SD model, which run in parallel with the primary channel lengths, and which lead to the same downstream channel (**Figure 8.5b**). Although conceptually not very satisfactory, using two parallel channels is mathematically identical to using a single channel, because the channel routing model is linear. It should be noted that there is no attempt in either KINEROS2 or in RRMT-SD to represent the distributed channel network other than the main wadis (the effect of the smaller channels is lumped into the plane/hillslope routing).

Figure 8.5a shows the division of Wadi Ahin into the subcatchments for application of RRMT-SD, along with the conceptualised hillslope flow directions; and **Figure 8.7b** shows the channel network.

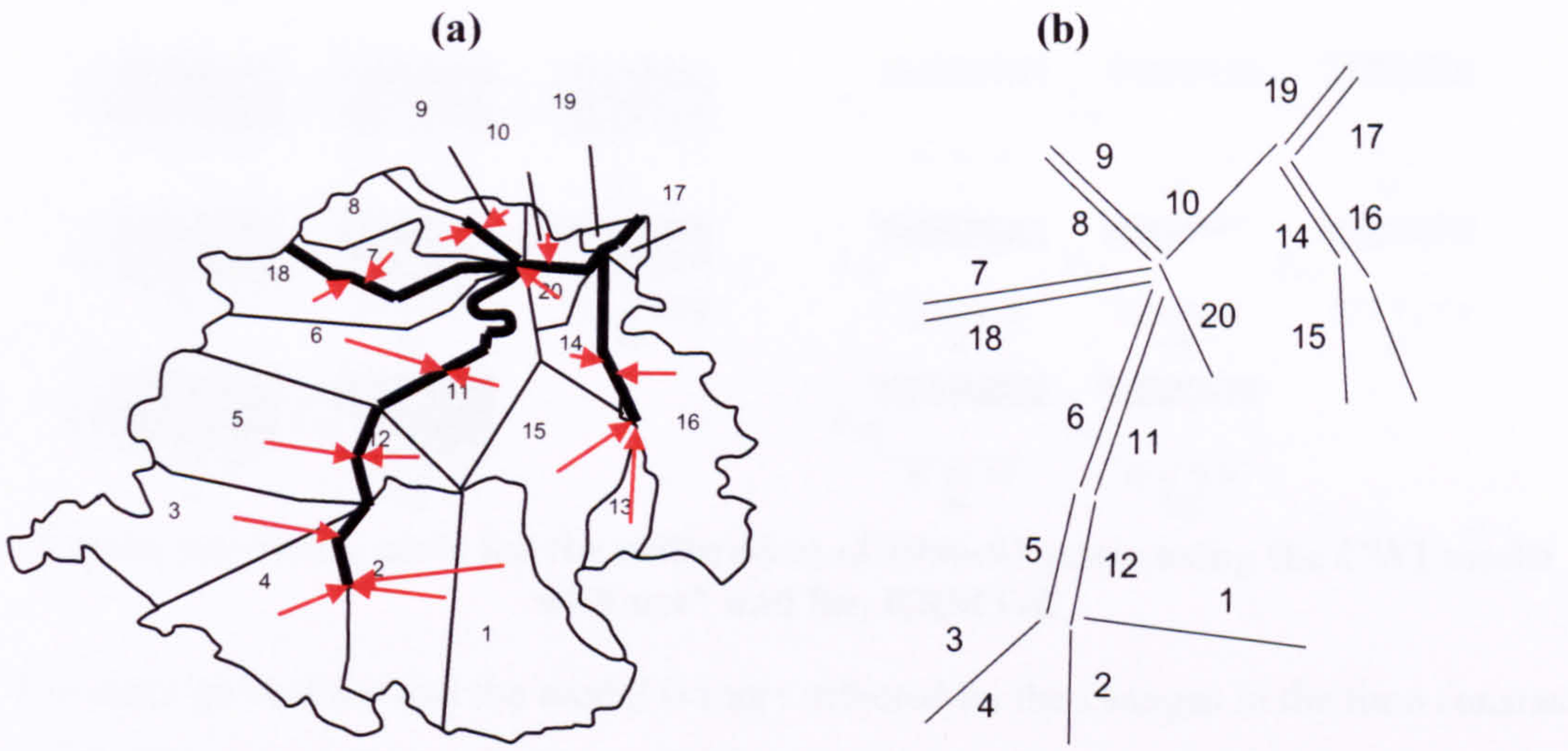


Figure 8.5: The division of Wadi Ahin into required subcatchments showing the effective hilllopes runoff pathways, and the model's channel network layout

Table 8.3 shows the details of each subcatchment and channel. It should be noted that plane 21 has no actual subcatchment associated with it (hence has zero area and zero channel length) – it is included in RRMT-SD simply to add together the flows from 17 and 19.

Table 8.3: The subcatchments characteristics

Plane no	Area (km^2)	Length (m)	Width (m)	Channel length (m)	Slope
1	84.4	15127	5611	5526	0.04
2	66.4	12073	5534	5526	0.03
3	63.9	12459	5163	5526	0.03
4	66	10778	6157	5526	0.06
5	72.1	1789	40547	5887	0.35
6	54.3	14060	3884	14726	0.05
7	20	11175	1798	12646	0.06
8	24.4	8520	2882	8410	0.09
9	12.2	695	17618	8410	0.92
10	8.5	3473	2461	4618	0.05
11	40.3	12541	3233	14726	0.04
12	12.6	4276	2964	5887	0.09
13	14.9	7851	1907	5526	0.11
14	17.8	19674	910	10302	0.01
15	63.7	16305	3933	5526	0.06
16	66.4	18336	3645	10302	0.05
17	3.4	2616	1298	2922	0.06
18	36.3	12372	2952	12646	0.07
19	0.9	2710	326	2922	0.01
20	5.6	3429	1630	4618	0.05
*21	0	0	0	0	0

8.5 The Results of RRMT-L

8.5.1 Results using the CWI model

Figure 8.6 shows the dotty plots for nse* and fm.

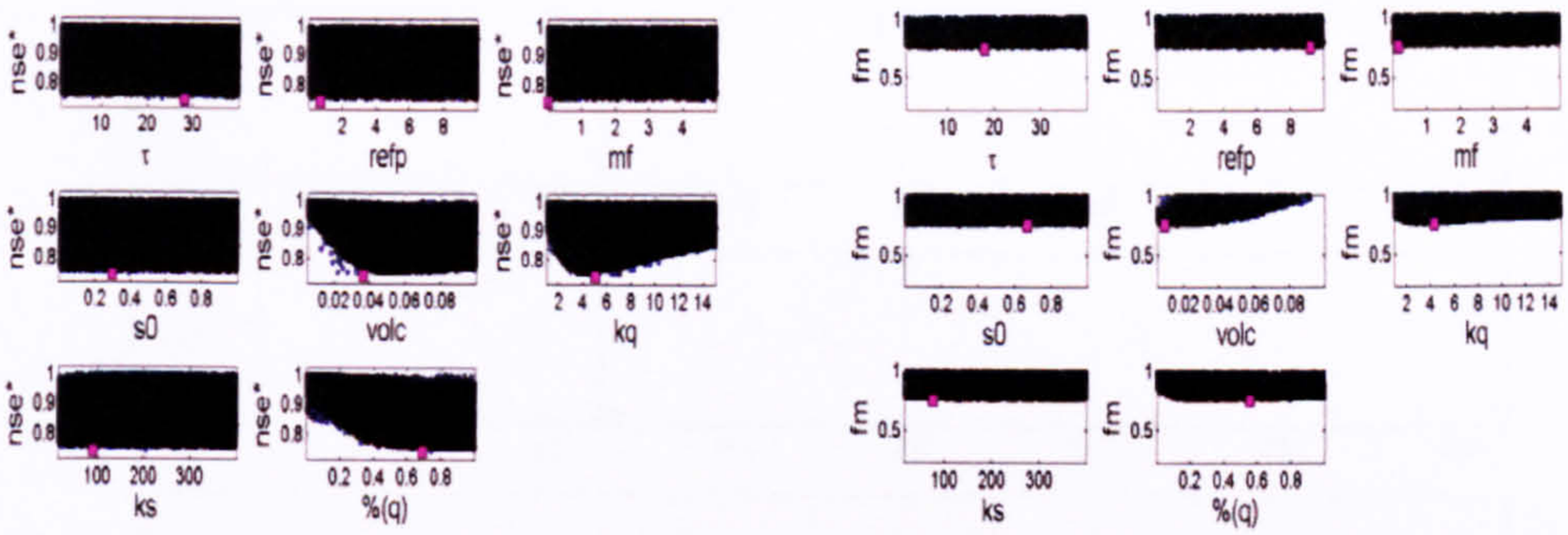


Figure 8.6: Dotty plots for the calibration of 1996-97 years using the CWI model with nse* and fm, RRMT-L

The dotty plots show that the model is more affected by the changes in the time constant quick flow k_q, the flow split *%q*, and the *volc*. It should be noted from the figures that the effects of these parameters and their optimum values are slightly different, using the two different objective functions.

The time-series results using nse* are shown in **Figure 8.7** for the calibration and validation periods, 1996-99. **Figure 8.8** shows the results when the events of March 1997 are excluded during calibration and validation. The figures have four sub-figures that show the rainfall, effective rainfall, calculated and observed flow, and the catchment wetness index, cwi (*s*). The selected scale does not show the observed flow of the March 1997 event, as it is very high compared to all the other events.

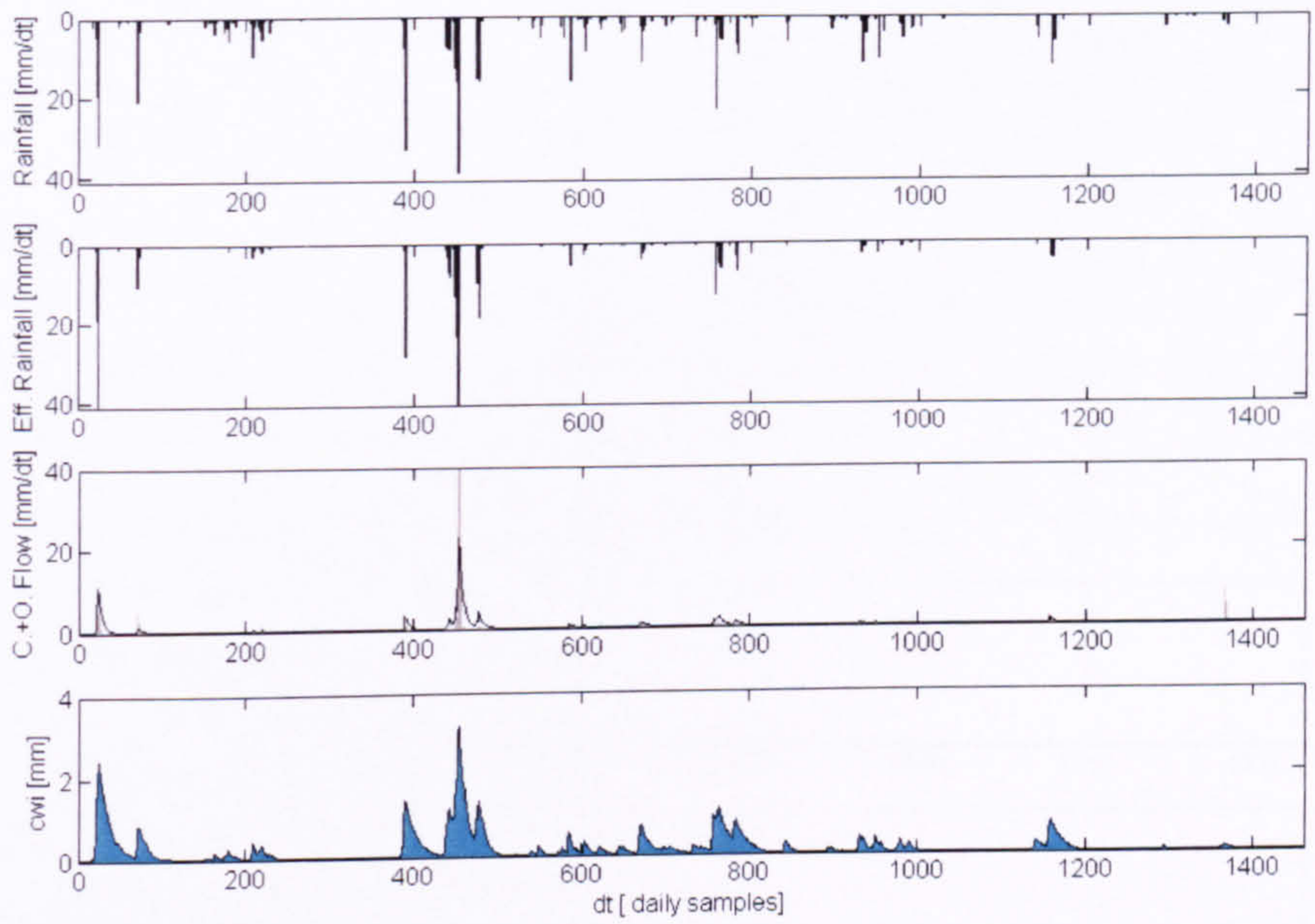


Figure 8.7: Model output for the 1996-99 years using the CWI model with nse*, RRMT-L

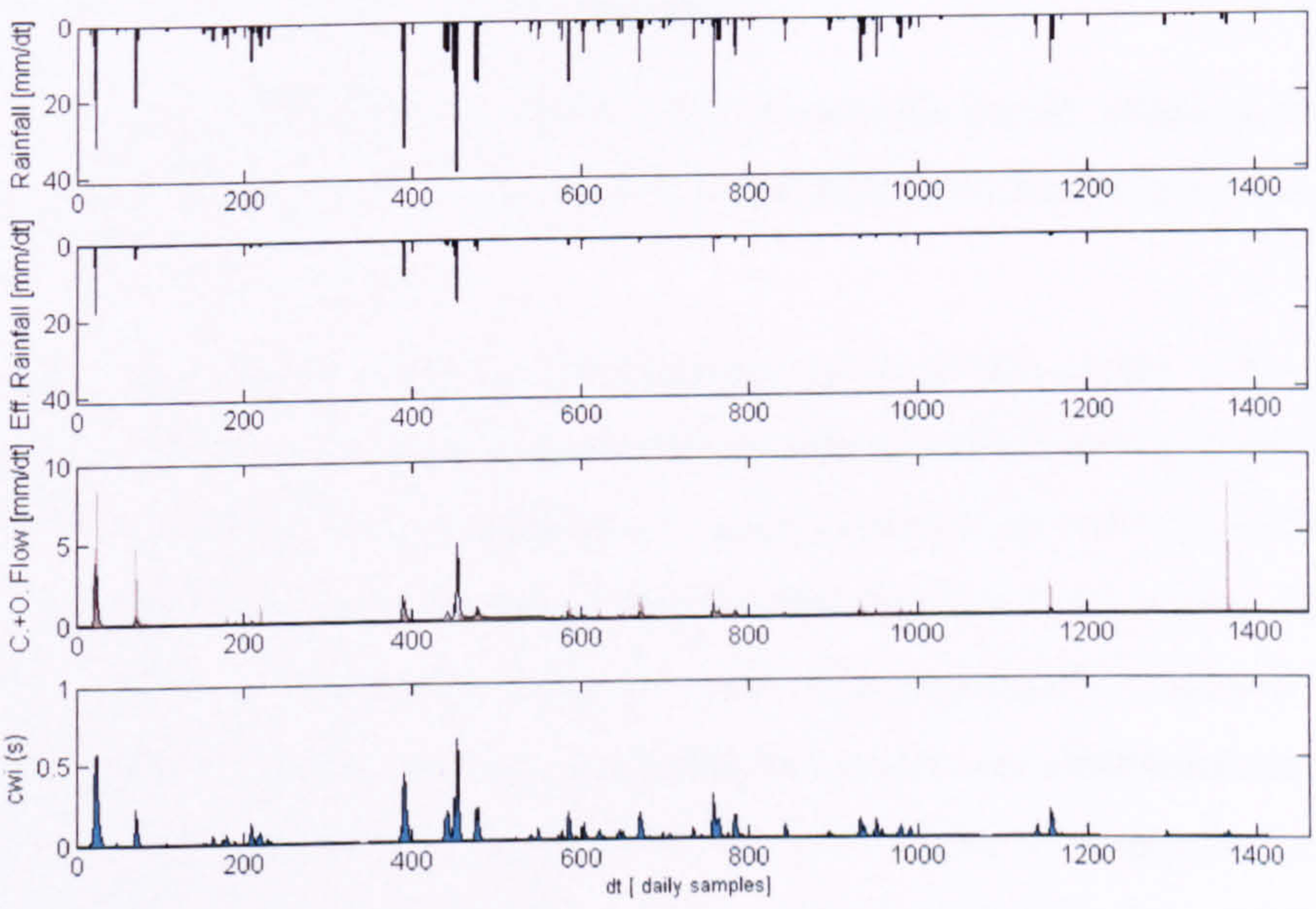


Figure 8.8: Model output for the 1996-99 years (missing out the March 1997 event) using the CWI model with nse*, RRMT-L

The results show that the model overestimates some of the events but underestimates others in both cases, including or excluding the March 1997 event. The figures show clearly that the CWI (*s*) and the effective rainfall are much higher when the March 1997 event was included. The model was forced to be wetter with higher effective rainfall in order to fit the high March 1997 event.

Figure 8.9 shows the results using the fm objective function, with the selected thresholds, where the model excludes the high flows of the March 1997 event.

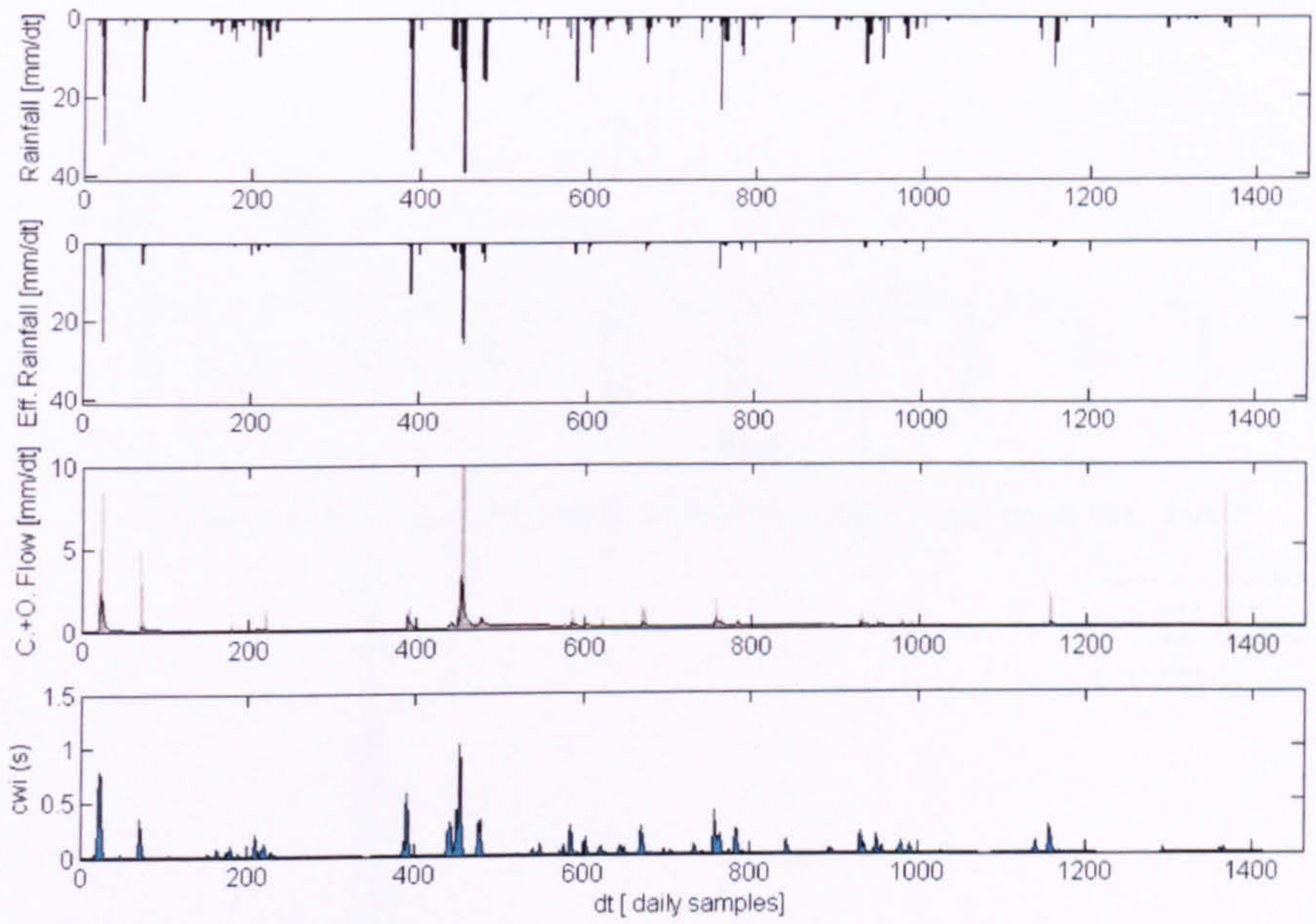


Figure 8.9: Model output for the 1996-99 years using the CWI model with fm, RRMT-L

In order to show more detail, a comparison between the results obtained using nse*, with and without March 1997, and that of fm, using the CWI model is shown in **Figure 8.10**, for each year individually.

The results show that the model overestimates some of the events using nse*, but underestimates most the events when excluding March 1997 event or when using fm. For the 1997 events, the model performance varied between one event to another but the March 1997 event was underestimated significantly. For the 1998 events, the January event was highly overestimated using the nse* but reasonably estimated for some others, but when the March 1997 was excluded, the model was underestimating most of the events, using either nse* or fm. In 1999, the nse* seems to obtain the best results, compared to other two methods. The general conclusion is that the model can only match the flow peaks by greatly exaggerating the volume of effective rainfall via adjusting the *volc* parameter. This effect is evident when the nse* objective function is used and the high flow event is included. The other objective functions are less weighted to extreme high flows and perform poorly for peak flows but it seems better for flow recessions and flow volume.

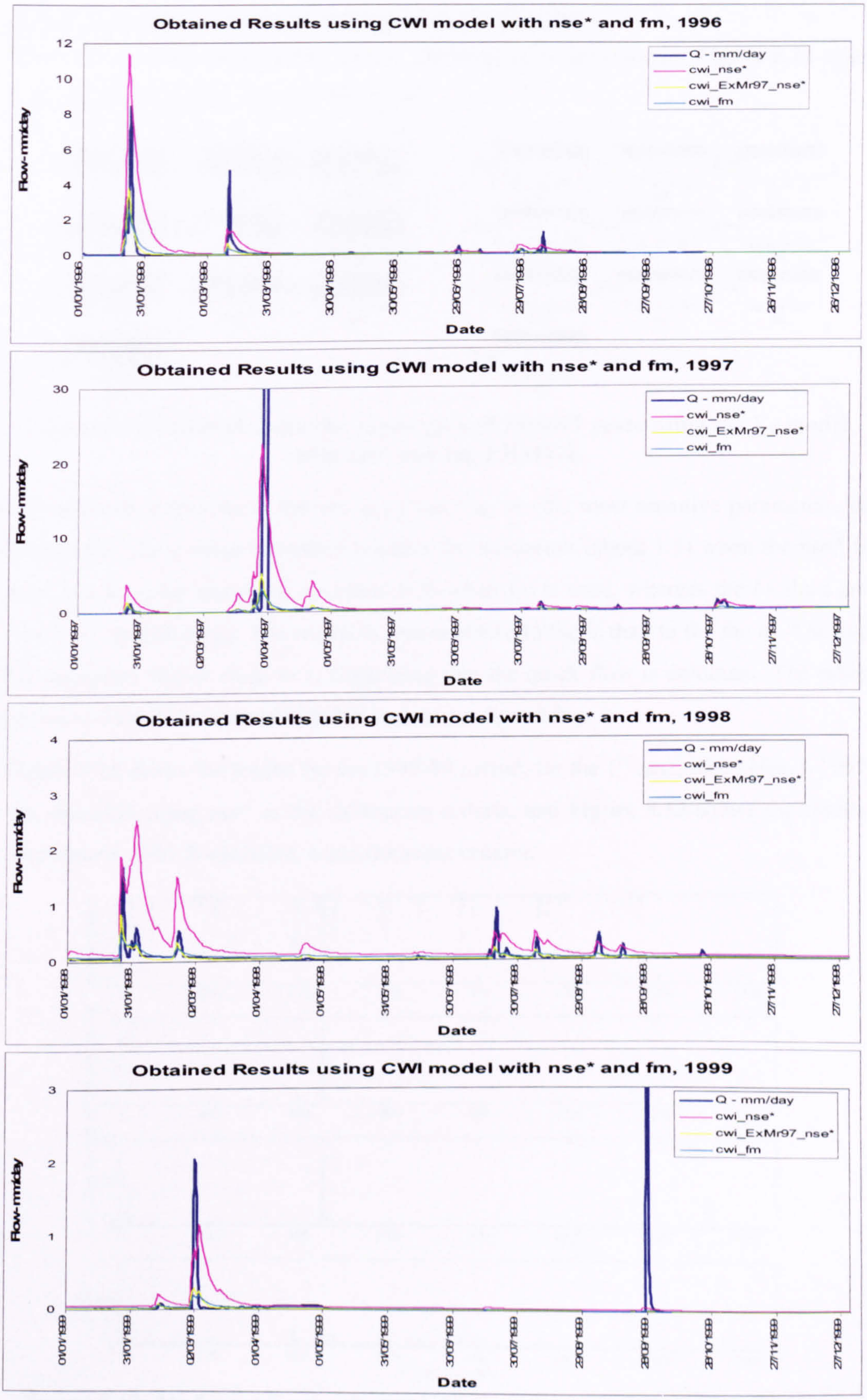


Figure 8.10: Calibration and validation results for each year from 1996 to 1999 period using the CWI model, with nse* and fm objective function, RRMT-L

8.5.2 Results obtained using the Ye model

The model was run using the Ye model. The dotty plots are shown in **Figure 8.11** using nse* and fm (including March 1997 event).

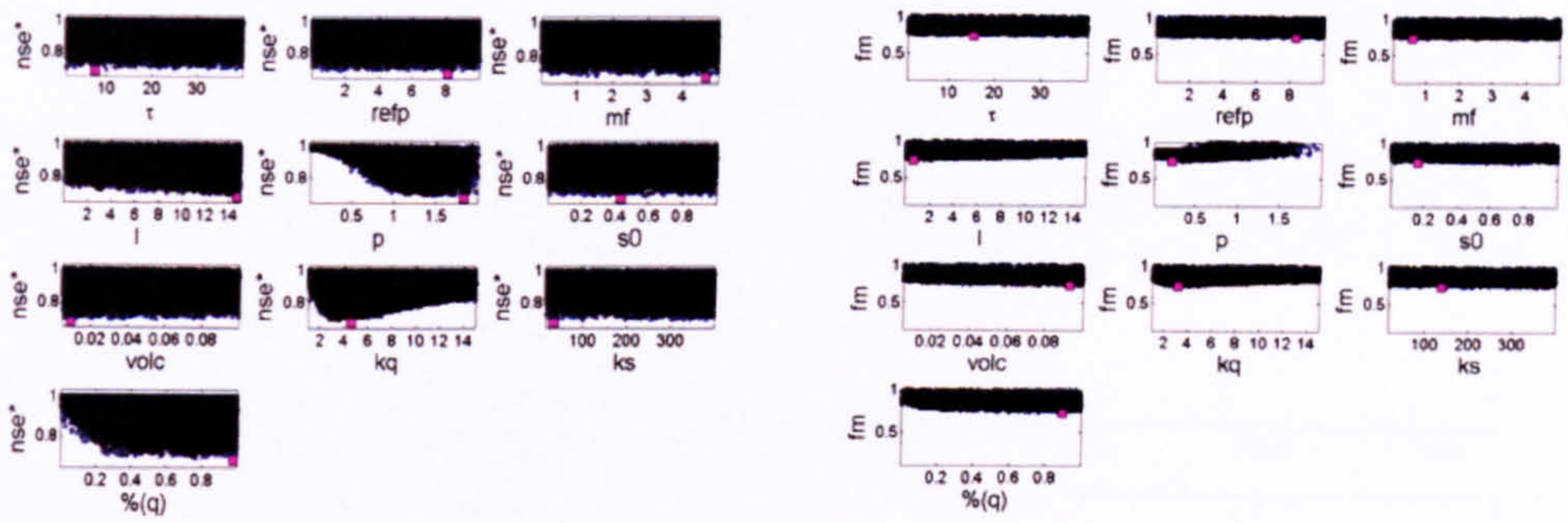


Figure 8.11: Dotty plots for the calibration of 1996-97 years using the Ye model with nse* and fm, RRMT-L

The obtained results show that the p, k_q and $\%q$, are the most sensitive parameters, in this model. The p value is pushed towards the maximum (about 1.8) when the nse* is used, but its value decreased (to about 0.3) when fm is used, whereas the l values are close to 1 in both cases. The model is less sensitive to the k_s than to the the k_q. The $\%q$ has opitimum values close to 1, suggesting that the quick flow is dominant. The other parameters do show some effects but less than p, k_q and $\%q$.

Figure 8.12 shows the results for the 1996-99 period, for the 1st case, when March 1997 was included, using nse* as the calibration criteria, and **Figure 8.13** shows the results when March 1997 is excluded, using the same criteria.

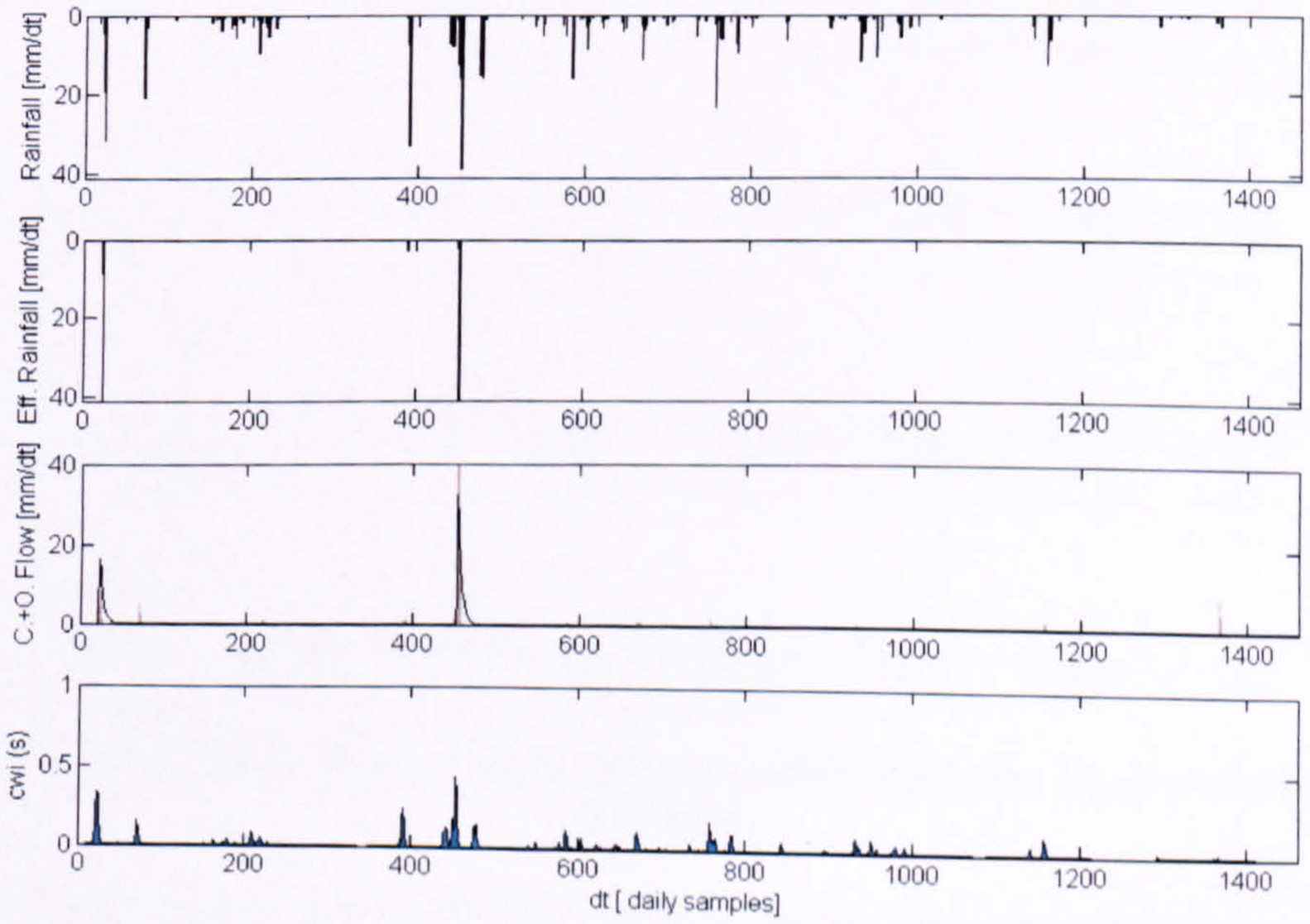


Figure 8.12: Model output for the 1996-99 years using the Ye model with nse*, RRMT-L

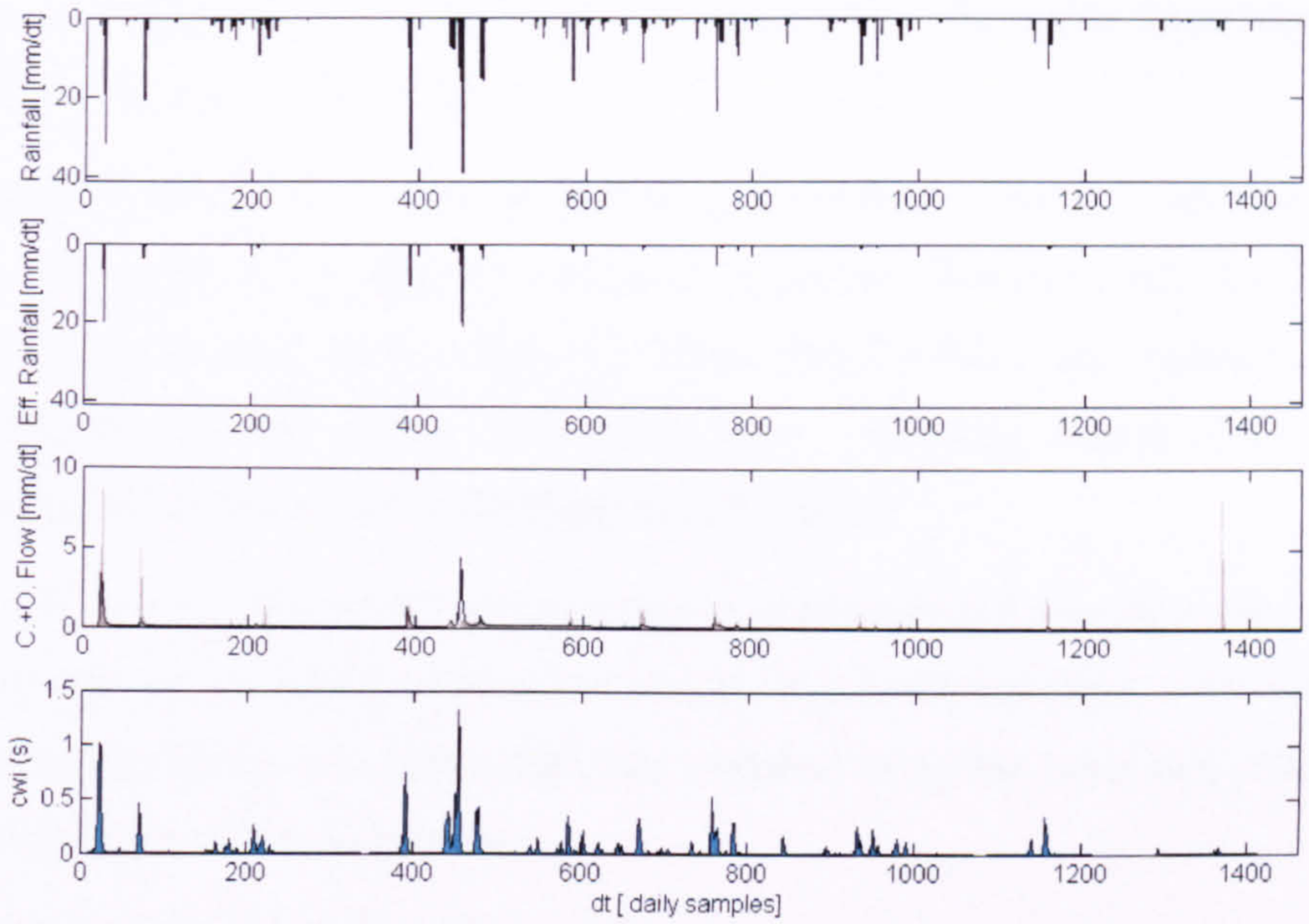


Figure 8.13: Model output for the 1996-99 years using the Ye model with nse* (missing out March 1997 event), RRMT-L

The result shows that the model is overestimating some events but underestimating the March 1997 event, when including the March 1997 event but underestimating the high events in the 2nd case and overestimating the other events.

The model output using fm is shown in **Figure 8.14**.

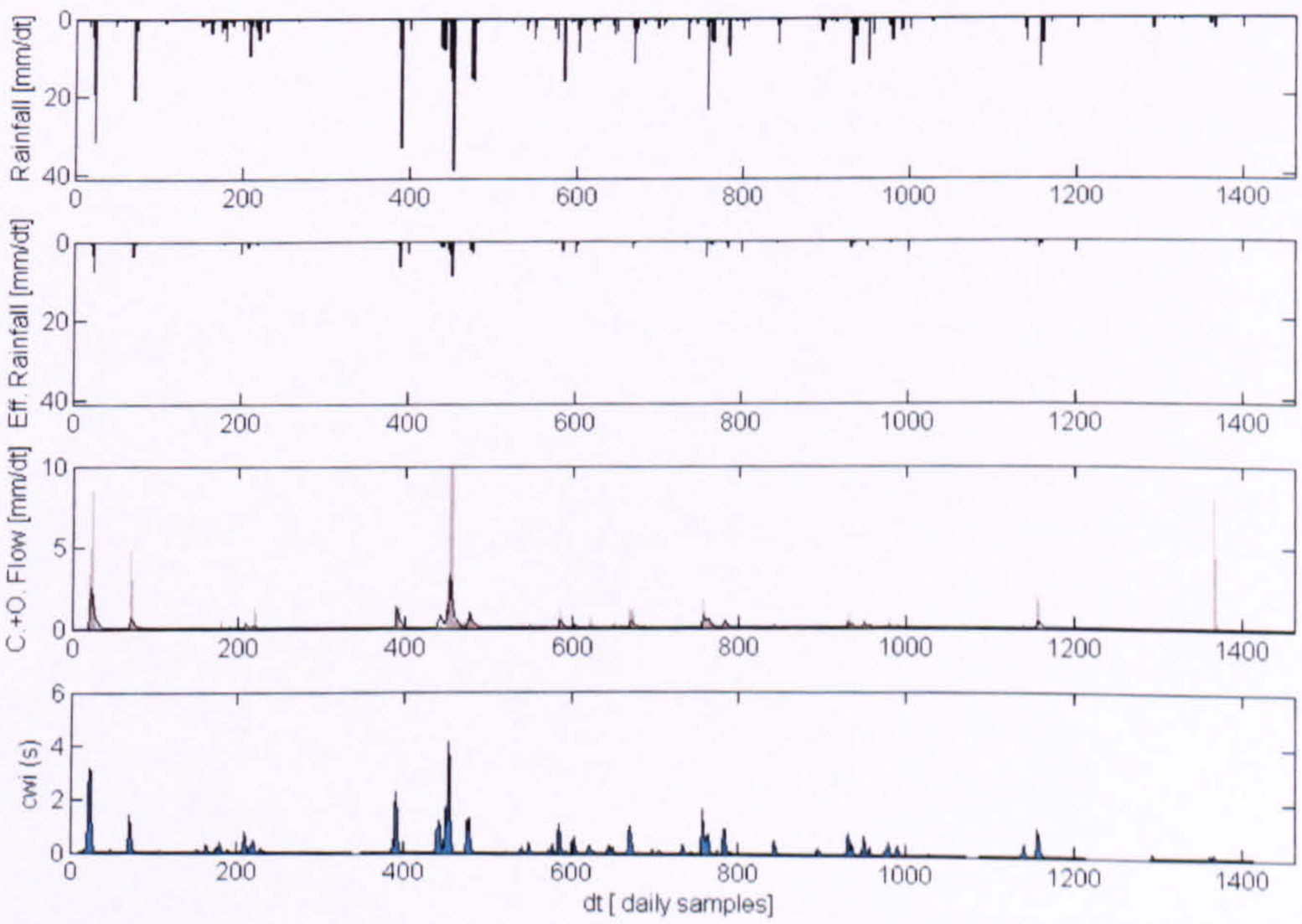


Figure 8.14: Model output for the 1996-99 years using the Ye model with fm, RRMT-L

The obtained results using the fm criteria show that the model is generally underestimating all the events.

Figures 8.15 shows the obtained results using the nse*, with and without March 1997, and the fm for each year, individually.

The obtained results show that the model's performance varies from one event to another, and with using different objective functions. However, for the 1996 year events, using the nse* shows that the model overestimates the January event but underestimates all the others. Using the nse*, excluding March 1997, and fm underestimated all the events as the **Figures 8.15** shows.

For the 1997 events, the model seems to vary in performance from one event to another. However, the severe March 1997 event was always underestimated, even thought the nse*, including March was better then that obtained using the other two criteria, nse* (excluding March 1997) and the fm.

The general conclusion is that a high value of the *p* parameter using nse* has aided in simulating the magnitude of the extreme March 1997 event and the January 1996 event, while the catchment wetness is not so exaggerated as it was using the CWI model. However this causes the lower events to be simulated especially poorly.

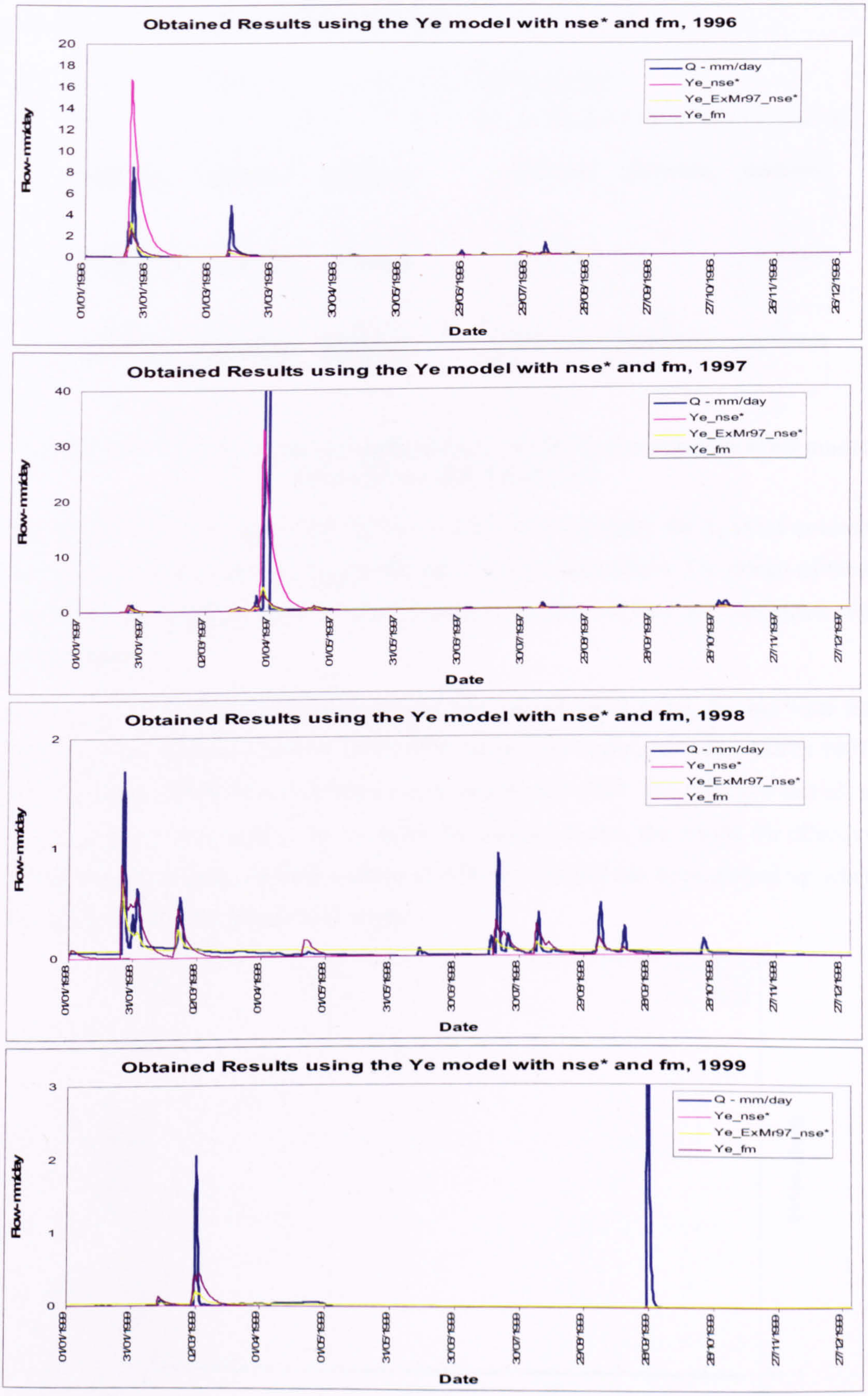


Figure 8.15: Calibration and validation results for 1996 to 1999 period using the Ye model, with nse* and fm, with and without March 1997 event, RRMT-L

8.6 The Results of RRMT-SD

8.6.1 Results obtained using the CWI model

The dotty plots obtained using the CWI are shown in **Figure 8.16**, using nse* and fm.

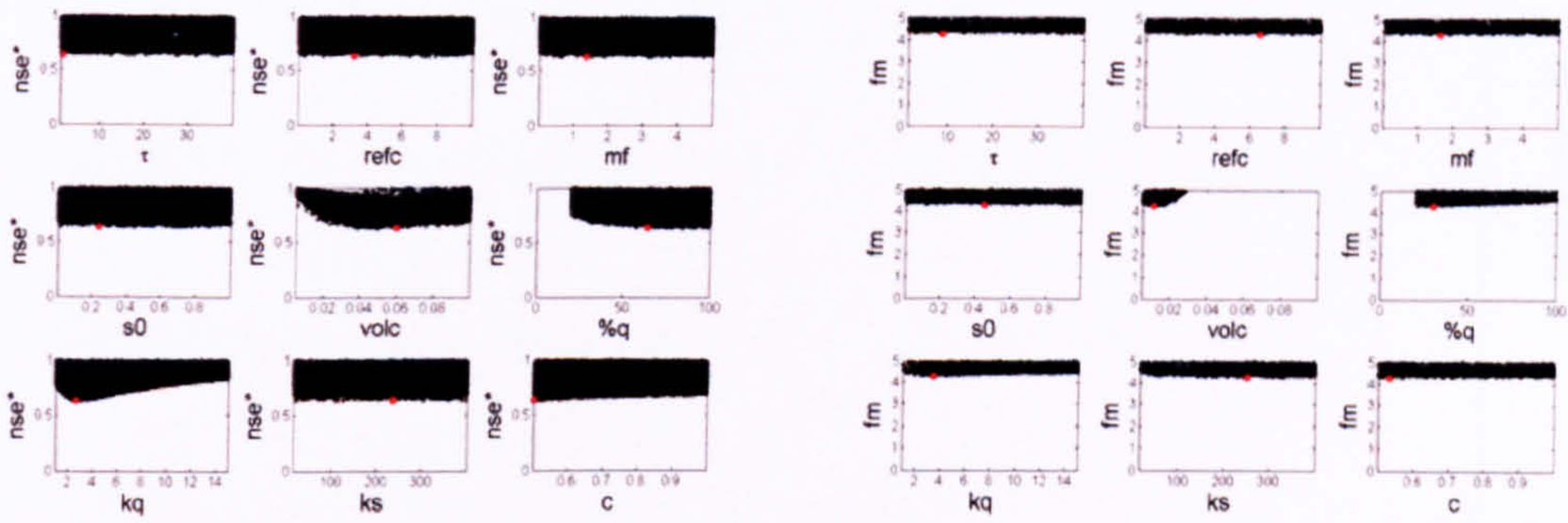


Figure 8.16: Dotty plots for the calibration of 1996-97 years using the CWI model with nse* and fm, RRMT-SD

The dotty plots show again that the *volc* (volumetric constant), the k_q (time constant quick flow reservoir) and the *%q* are the most sensitive parameters. The effects of these parameters are changing with the used objective function but they are consistently the most influential.

Figure 8.17 shows the simulation results that are obtained using the nse* for the calibration and validation period, 1996-1999, using CWI model, including March 1997, whereas **Figure 8.18** shows the results excluding March 1997. The effective rainfall is shown in the reverse y-axis. As found for the lumped model, the results for effective rainfall indicate clearly that the volume of effective rainfall has been pushed up when including the extreme March 1997 event.

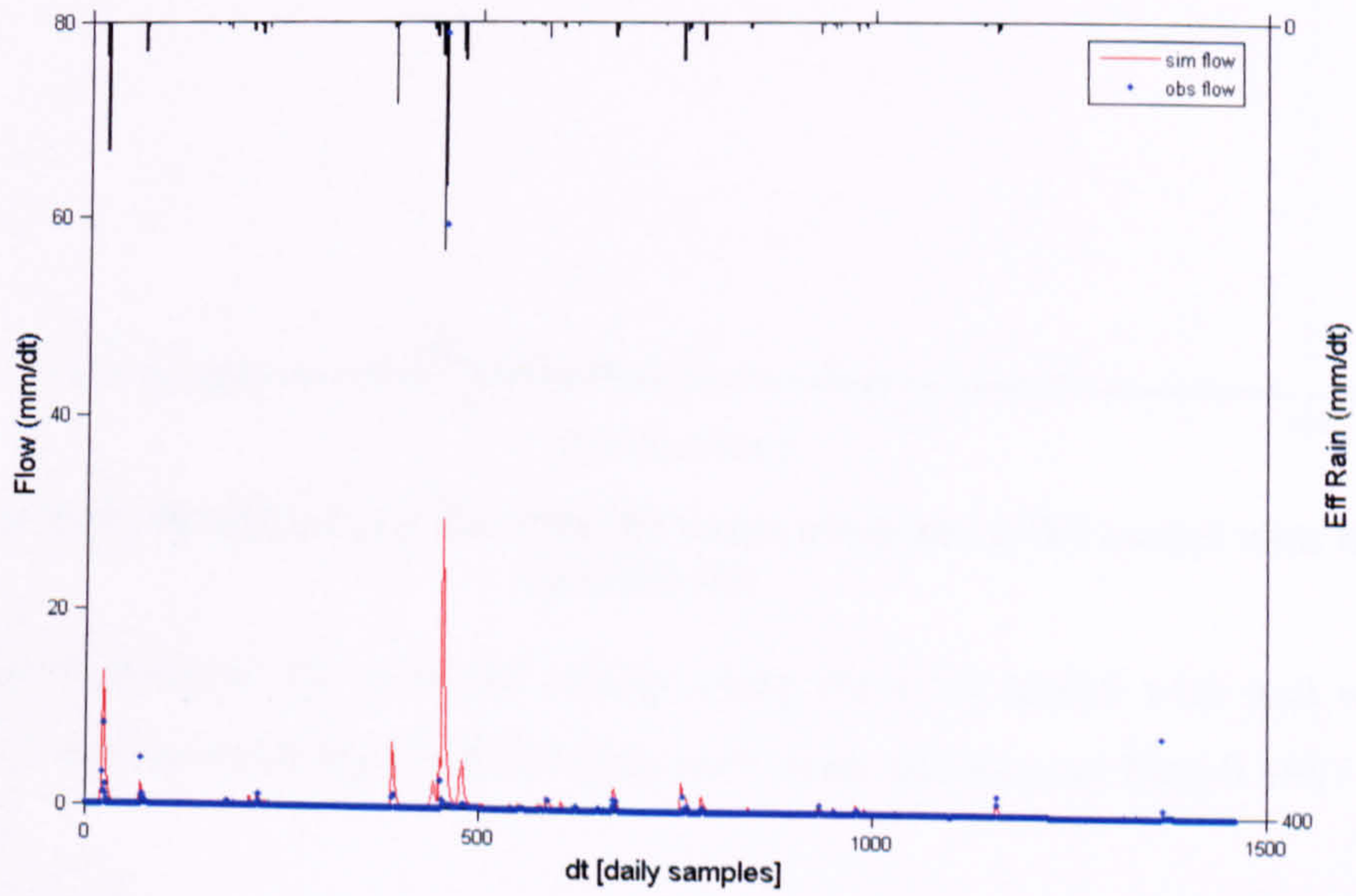


Figure 8.17: Model output for the 1996-99 years using the CWI model with nse*, RRMT-SD

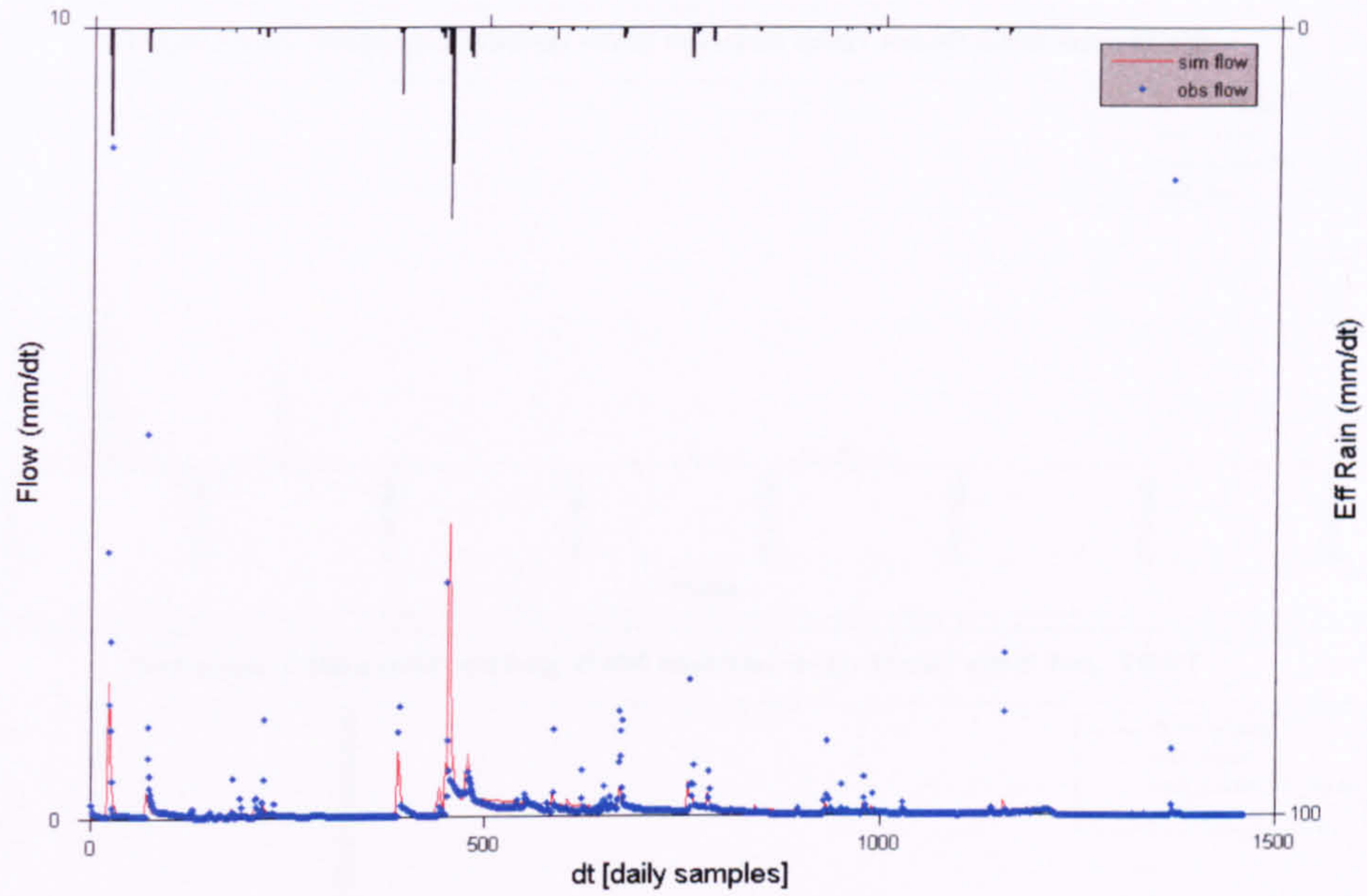


Figure 8.18: Model output for the 1996-99 years using the CWI model with nse* (missing out March 1997 event), RRMT-SD

Figure 8.19 shows the simulation results using CWI model but with fm as the calibration criteria.

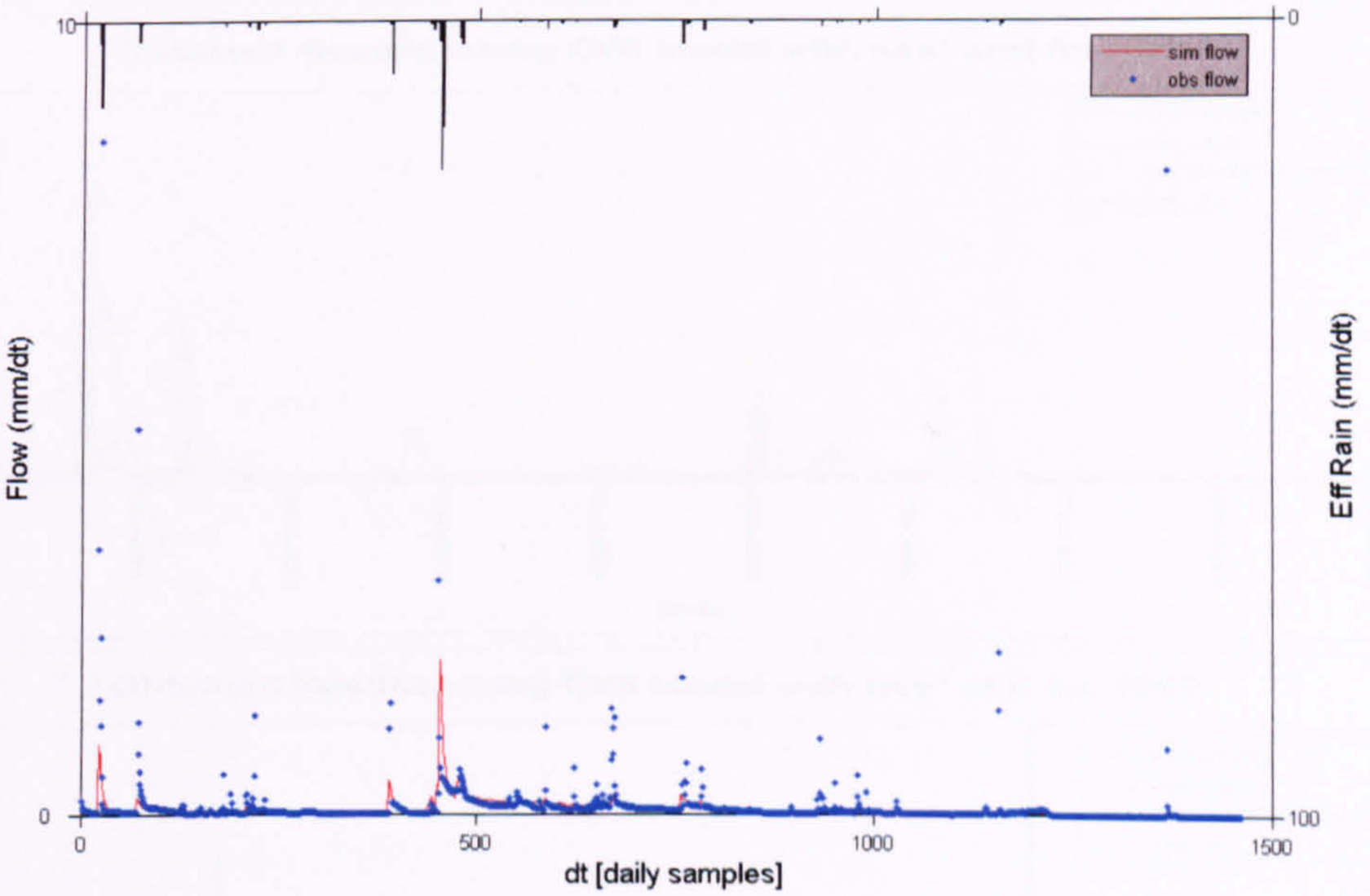


Figure 8.19: Model output for 1996-99 years using the CWI model with fm, RRMT-SD

A comparison between the obtained results using the CWI model with and without March 1997 are shown in **Figure 8.20** using nse*, with and without March 1997 event, and the fm.

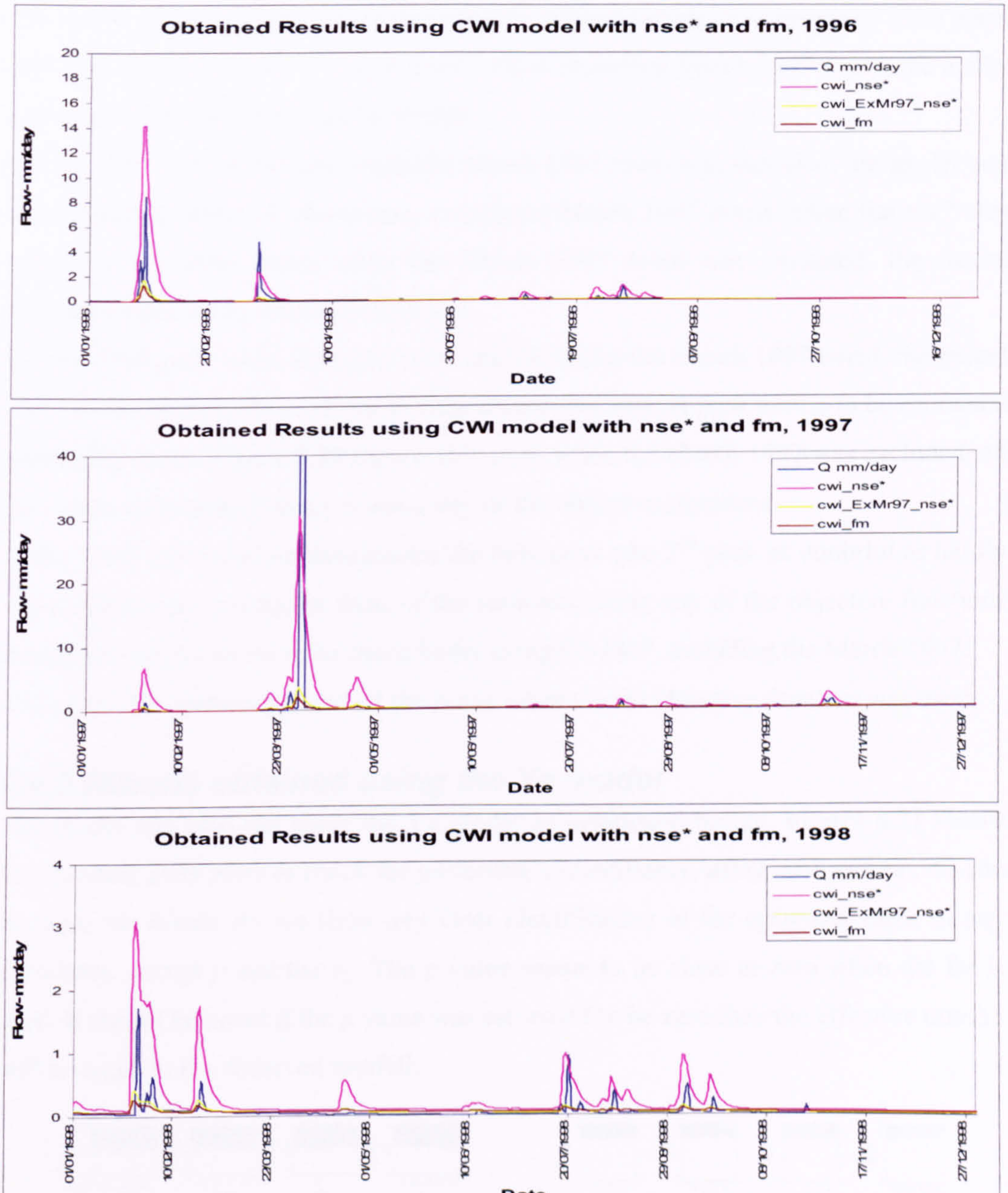


Figure 8.20: Calibration and validation results for 1996 to 1999 period using the CWI model, with nse* and fm, with and without March 1997, RRMT-SD

The results using nse* show that the model is overestimating most events of 1996 when including the March 1997 event, whereas when excluding March 1997 event, the model was underestimating about all the events.

For the 1997 year events and when the March 1997 event was included, the model was overestimating about all the events, except the March 1997 event, when the nse* was used. On the other hand, when the March 1997 event was excluded, the model underestimated all the events of this year.

For the 1998 year, when using the nse* and including the March 1997 event, the model was over estimating about all the events, though the August peak seems to be estimated reasonably as the **Figure 8.20** shows. However, when the March 1997 was excluded, all the events were underestimated using any of the objective functions.

In the 1999, the model underestimates the only peak (the 2nd peak as doubtful as hardly any rainfall was recorded in most of the stations), using any of the objective functions though the results seems to be much better using the nse*, including the March 1997.

The model has underestimated all the peaks when the fm objective function was used.

8.6.2 Results obtained using the Ye model

The model was also run using the Ye model as mentioned before. **Figure 8.21** shows the obtained dotty plots to check the parameter's identifiably, using nse* and fm. As can be seen, the results do not show any clear identification of the optimum value of any parameter, except p and the k_q. The p value seems to be close to zero when the fm is used. It should be noted if the p value was estimated to be zero then the effective rainfall will be equal to the observed rainfall.

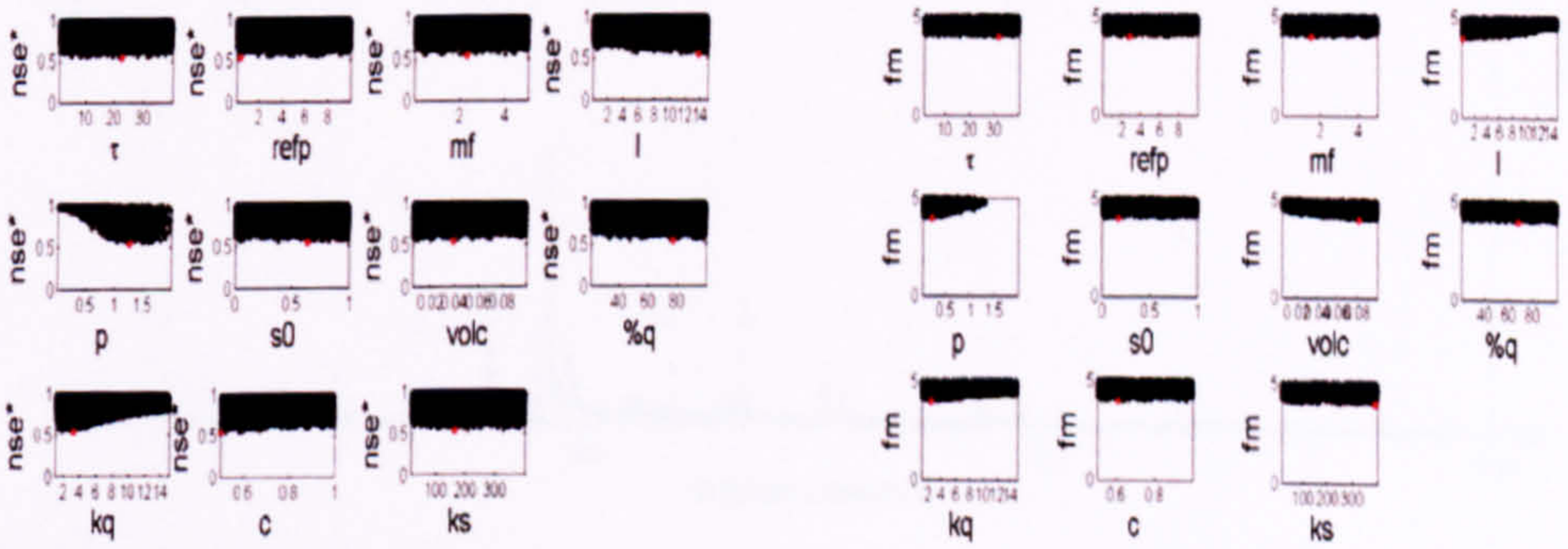


Figure 8.21: Dotty plots for the calibration of 1996-97 years using the Ye model with nse* and fm, RRMT-SD

Figure 8.22 shows the obtained results from the calibration when nse* was used, including March 1997 (though the figure was truncated at 40 mm/day so the smaller events can be noticeable), for the 1996-99 period, and **Figure 8.23** shows the obtained

results when March 1997 event is excluded. **Figure 8.24** shows the results when using fm.

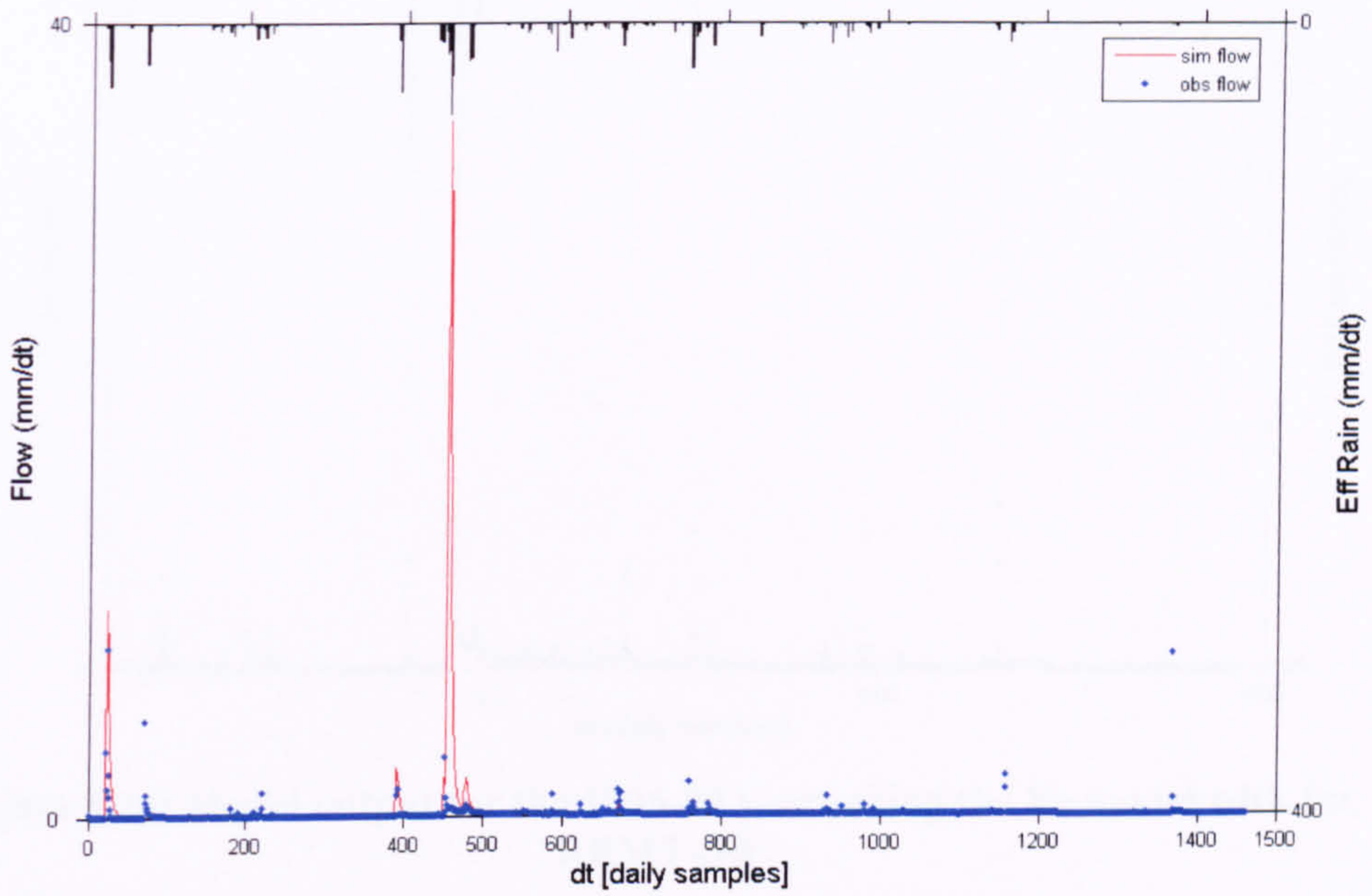


Figure 8.22: Model output for the 1996-99 years using the Ye model with nse*, RRMT-SD

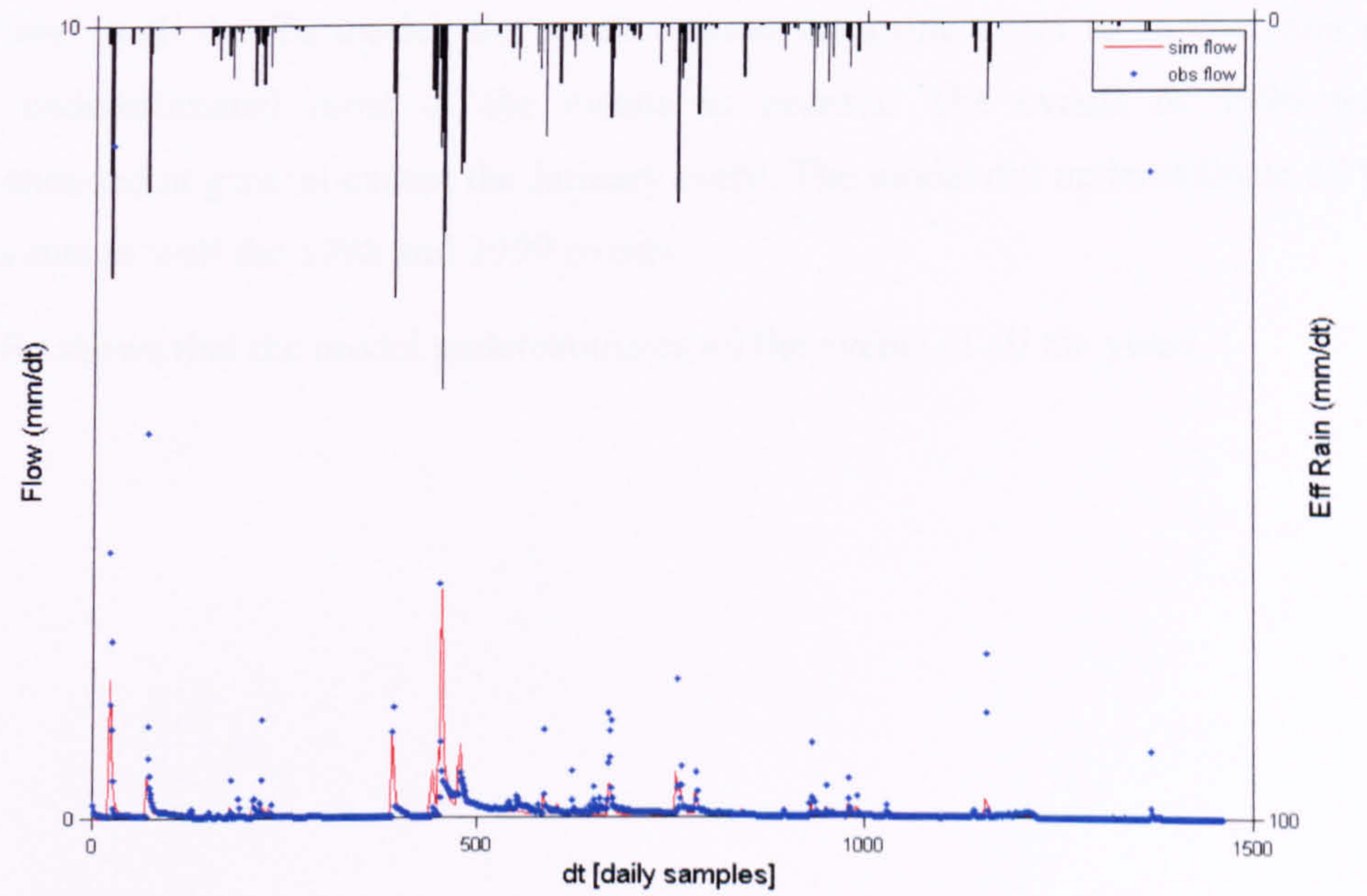


Figure 8.23: Model output for the calibration period of 1996-99 years using the Ye model, nse* (missing out March 1997 event), RRMT-SD

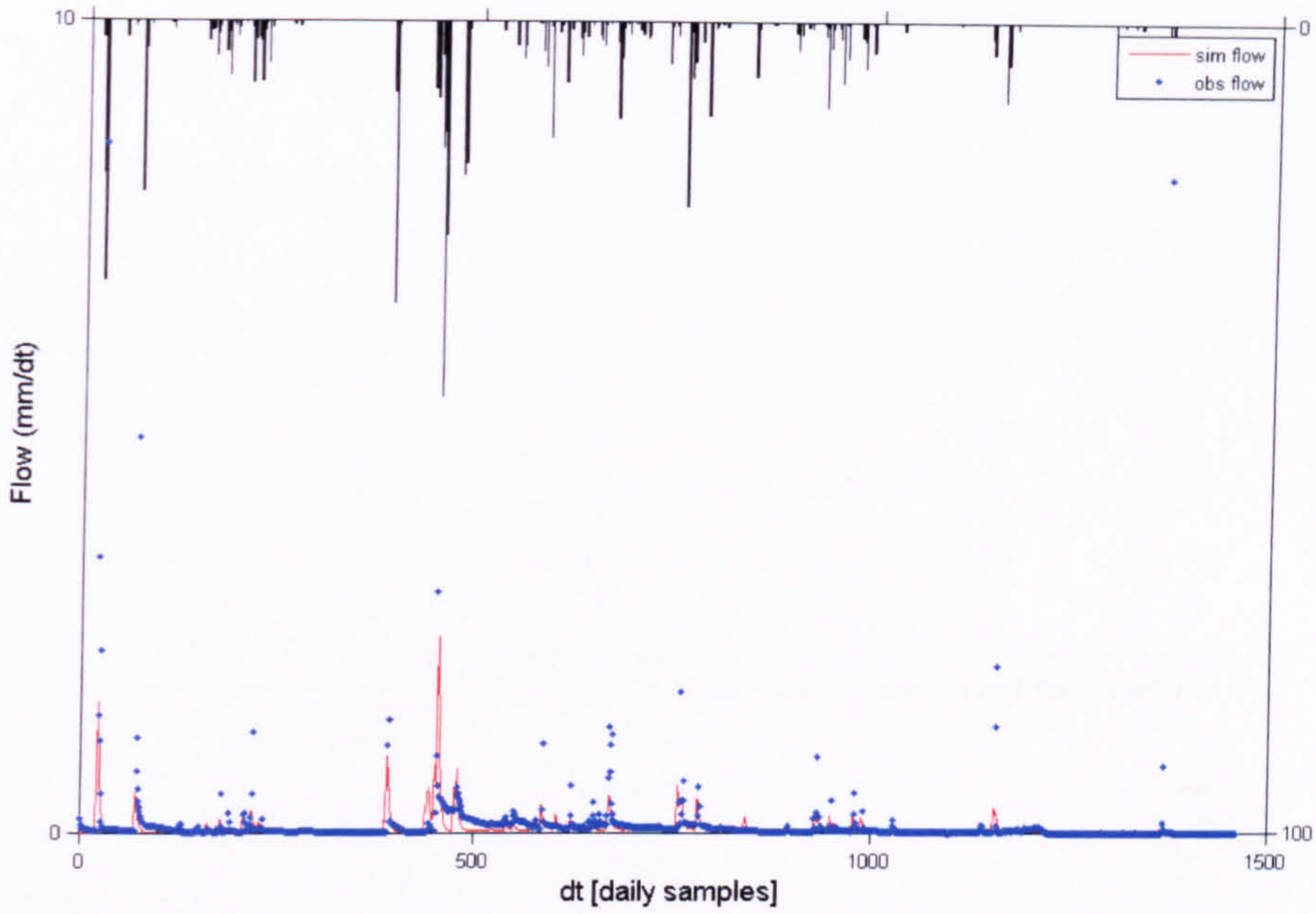


Figure 8.24: Model output for the 1996-99 years using the Ye model with fm, RRMT-SD

A comparison of the results obtained using the Ye model, using nse*, with and without March 1997 is shown in **Figure 8.25** when using nse* and fm.

Using nse* with the Ye model, the results varied from one event to another and the model underestimated most of the events in general. The events of 1996 were underestimated in general except the January event. The model did underestimate all the 1997 events as well the 1998 and 1999 events.

Using fm shows that the model underestimates all the events of all the years.

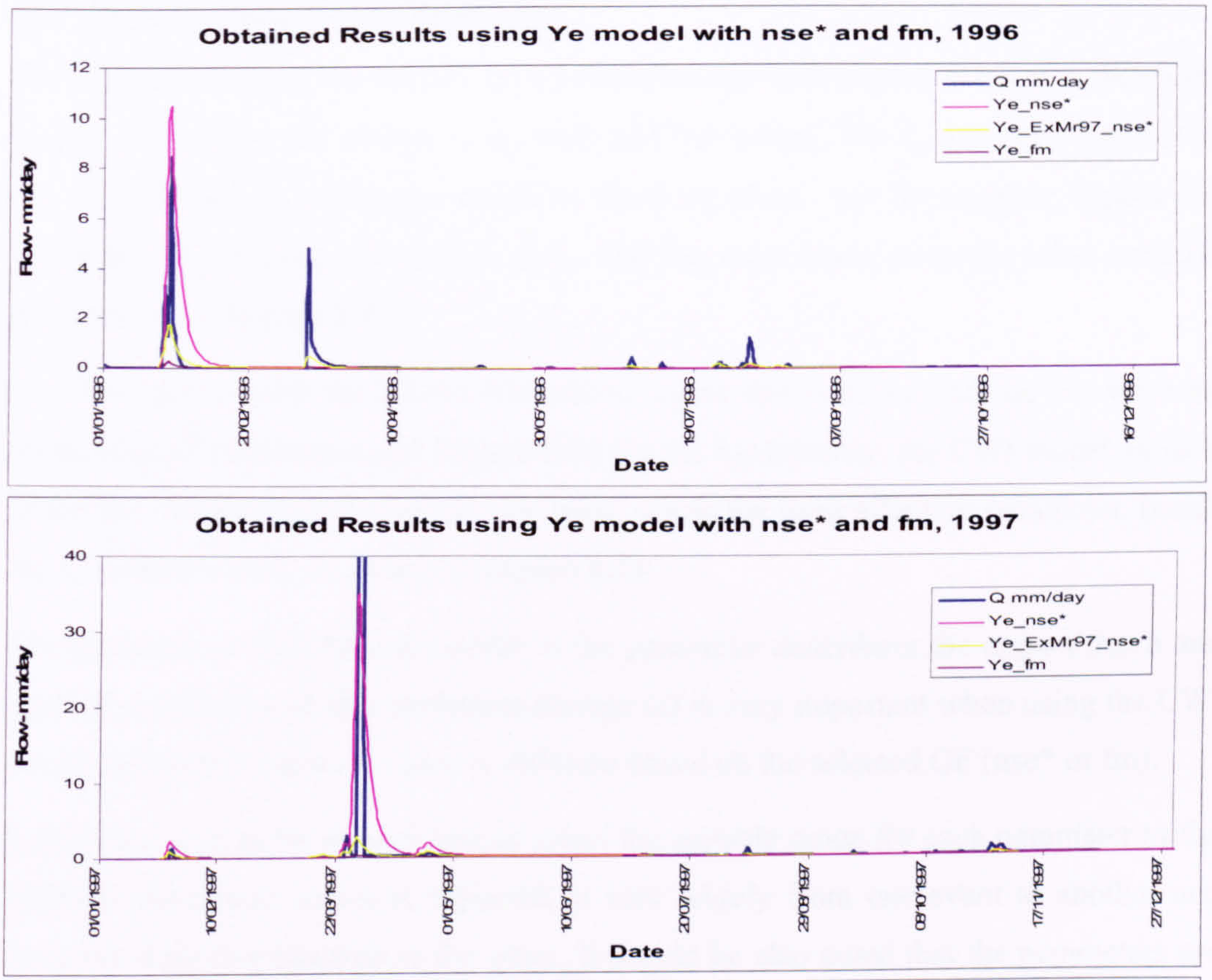


Figure 8.25: Calibration and validation results for 1996 to 1999 years using the Ye model, with nse* and fm with and without March 1997, RRMT-SD

8.7 Discussion of Results

The dotty plots, using the RRMT-L, 8-parameter, the CWI model, show that the model is most affected by the change in k_q, *volc*, and *%q* values. The k_q was also found to be the most identifiable parameter based on the dotty plots - see for example **Figure 8.6**. Using the 10-parameter Ye model, p, k_q, and *%q* were found to be the most sensitive parameters, see **Figure 8.11**.

The dotty plots using the RRMT-SD, shows again that *volc*, k_q, and the *%q* were the most sensitive parameters, see **Figure 8.16** for the 8-parameter, the CWI model version. When the 10-parameter Ye model was used, p was the most effective parameter, beside the k_q to some extent, as shown in **Figure 8.21**.

The results show that the *volc*, which is the parameter describing the impact that a unit input of rainfall has on the catchment storage (s) is very important when using the CWI model though the optimum value is different based on the selected OF (nse* or fm).

It does not seem to be an easy task to select the suitable range for each parameter as the optimum parameter values is expected to vary widely from one event to another and from one objective function to the other. It should be also noted that the parameters are interlinked to each other and to obtain the best set that can be suitable to all the events can be difficult. The used ranges for the purpose of this research are as suggested by Wagener et al. (2001), see **Table 8.1** and **8.2**.

The k_s in this research was found to be less important than the k_q suggesting the quick flow is the dominating. The insignificant effects of the slow flow might support the Ye et al. (1997) suggestion of using only one routing storage for ephemeral channels. However, this was not possible to be adopted in Wadi Ahin case as there was some base flow, hence, this could not be adopted directly from the beginning in this research and hence, two storage routing model was thought to be more appropriate to be adopted. It would be interesting to investigate the model's performance using one routing storage as was suggested by the Ye et al. (1997).

The obtained results are expected to be affected by the input data beside the used parameter values, such as rainfall, observed flow, and temperature. The interpolation rainfall method over the catchment for the lumped version will surely have effects on the obtained results, as was proven in **Chapter 7**. The obtained results from IHACRES showed that the model was not highly sensitive to the temperature, specially the lumped

version, but is controlled rather by the moisture/flow. This is evident from **Figure 8.6**, which shows that the *mf* values are close to zero.

The model was run using different SMA models as mentioned before. The obtained results show that the model performance is varying from one event to another, as was expected and the used soil moisture accounting model and the used objective functions have great effects on the obtained results. This is not a surprise as different models use different soil moisture concepts, as well as the effect using different OFs.

The flood peaks and volumes obtained using the Ye model were found to be higher in general than that obtained using CWI model when the nse* was used. However, the obtained flood peaks decreases when using the fm.

The CWI model using the nse* has obtained better calibration results period (1996-97) than the validation period (1998-99), where hardly any flood was estimated for the whole of the two validation years, as can be noticed from **Figure 8.26**. However, when using the fm, this does not seem to be the case. The model seems to perform better in 1998 (**Figure 8.27**), even though it underestimated nearly all the events for about all the simulated period.

The obtained nse* value for the calibration period, 1996-97 using CWI was 0.73, including the March 1997 event but was 0.658 when it was excluded. This drops to 1.34 for the validation period, 1998-99, including March 1997, but 0.96, when it was excluded. When using the fm, the obtained value was 0.74 for the calibration period but 1.49 for the validation period.

As nse* is more biased by high floods, it was not a surprise to obtain higher flood peaks when using the nse* compared to the fm, where a threshold value of 72 m^3/s (8.5 mm/day) was selected for the higher threshold value, and 0.8 m^3/s (0.1 mm/day) for the lower threshold value. The analysis shows that, using nse*, missing out the March 1997 event did improve the obtained results slightly. However, using fm was expected to do better as it was set to ignore the March 1997 event and the very low base flow and give more weight to the more typical events in both models.

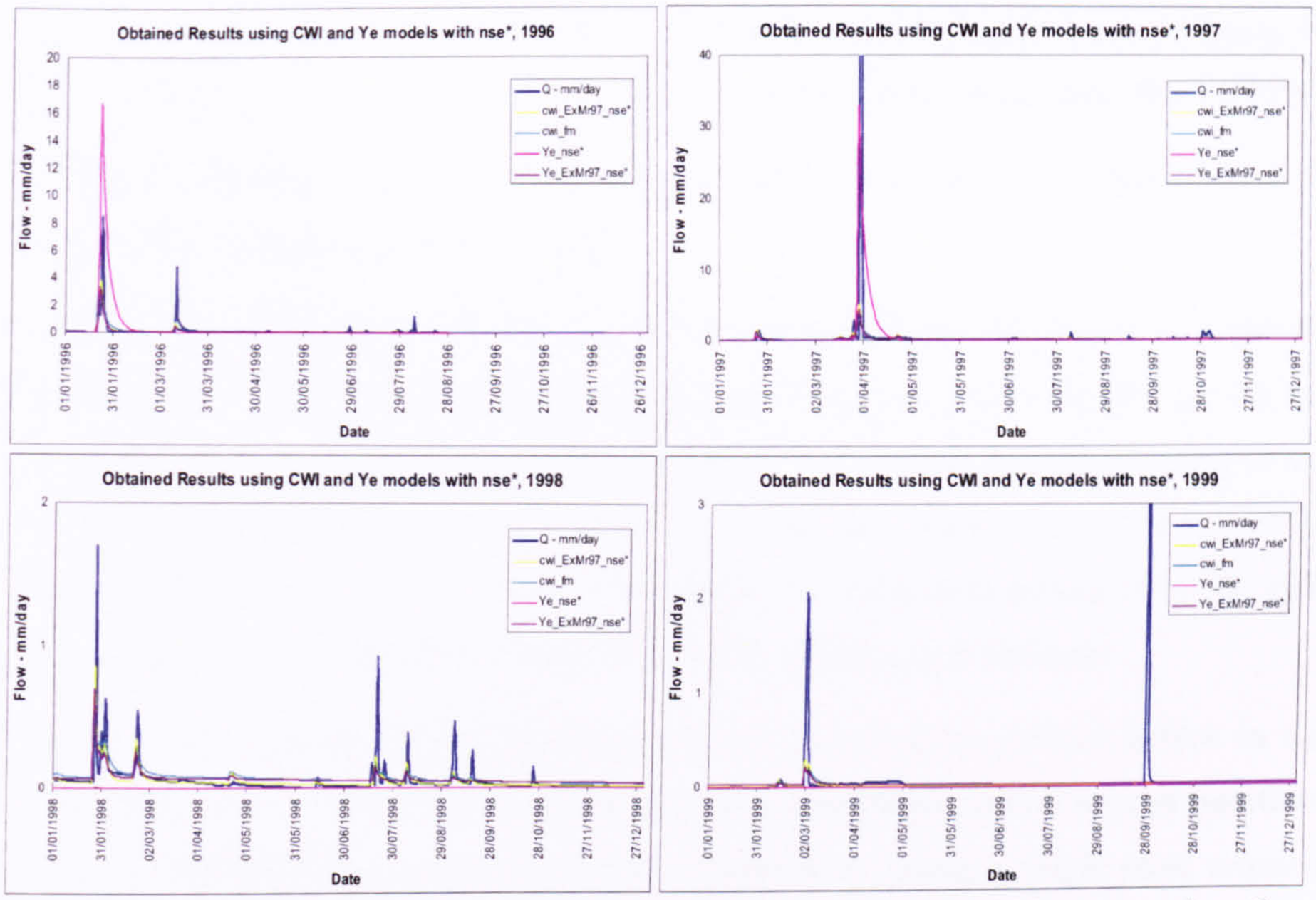


Figure 8.26: Calibration and validation results for 1996 to 1999 years using the CWI model and the Ye model, with nse*, RRMT-L

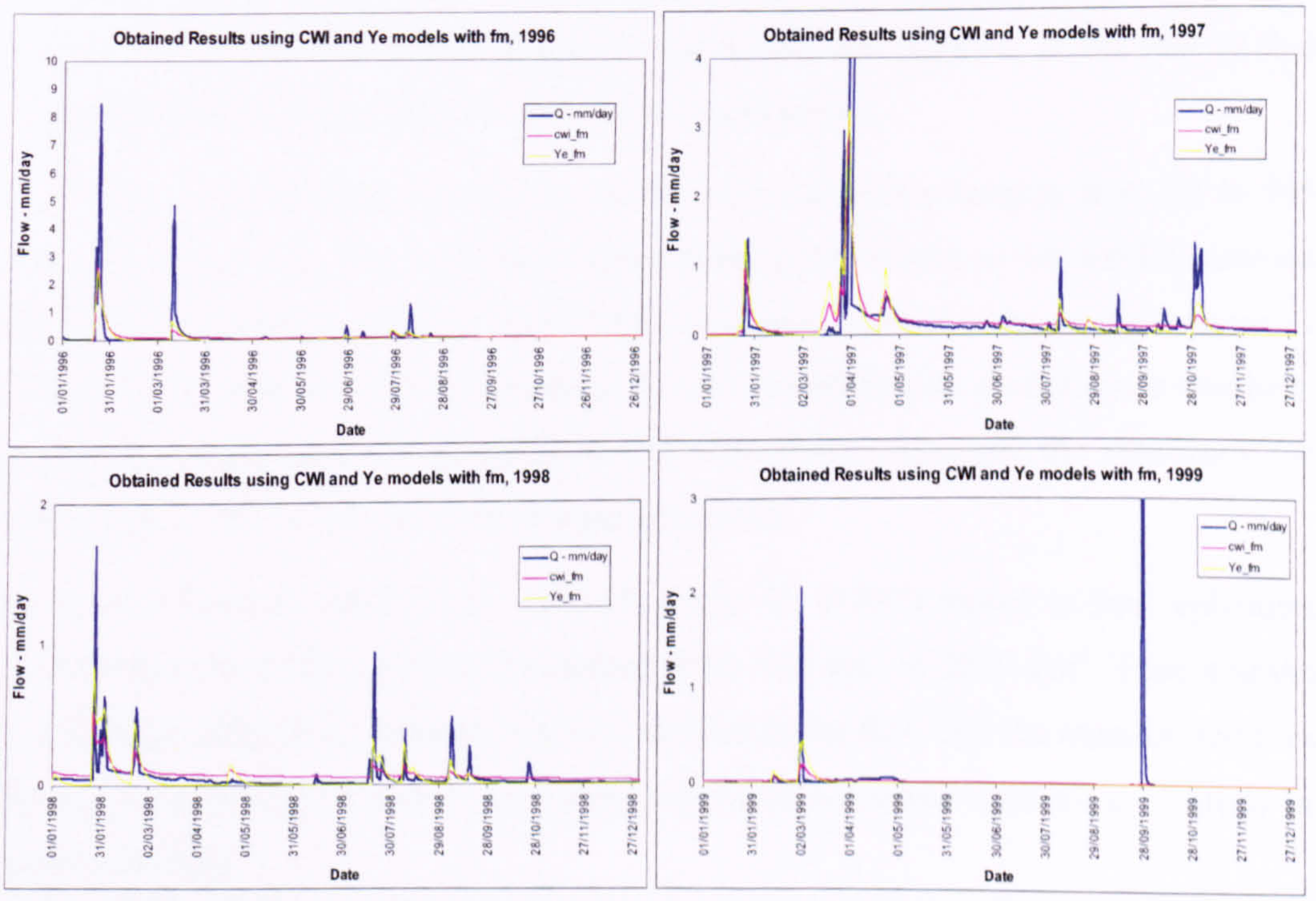


Figure 8.27: Calibration and validation results for 1996 to 1999 period using the CWI model and the Ye model, with fm, RRMT-L

When using the Ye model, the nse* obtained for the calibration period was 0.66 when including or excluding March 1997. For the validation period it was 1.02, including the March 1997 event, but 0.96 excluding it. The fm results, on the other hand, show that it

was 0.73 in the calibration period but 0.96 in the validation period. This means the obtained results using the fm with Ye model was slightly better than using the nse* OF.

The Wadi Ahin results are now compared with results from previous studies where the lumped IHACRES model has been used.

Ye et al. (1997) carried out their study using three low-yielding catchments in Australia. The model was calibrated using two periods, each of 5-years, where the first period was a drier than the second period. In Wadi Ahin case, two periods were used, each of two years only, but they both include wet and dry periods. The calibration period was 1996-97 in which 1996 was less wet than 1997, and in the validation period 1998-99, 1999 can be considered as a dry year, compared to 1998, which was a wet year.

Ye et al. (1997) introduced two more parameters (p and l) as defined before in this chapter. They also believed that in catchments with low yields and no regular baseflow, only one linear storage is needed to explain streamflow. Using a single store required only one additional parameter to the five in the loss model so that the total number of parameters they used was six. The Ye et al. model was tested in this research as the results shows. However, a two storage routing model was adopted, in our case as there was a base flow in Wadi Ahin for almost the whole period.

Ye et al.'s study obtained reasonable results with efficiency ranging from 82 to 90% when the model was used with daily data but the performance of the model increased when used for monthly analysis. IHACRES was found to be of adequate performance in all tested cases (the wet and dry periods). It was noticed that its performance was better for the dry period in terms of absolute mean deviation, bias, and the efficiency (see **Chapter 4** for the definition of these measurements).

Crock and Jakeman (2008) have used the Ye et al. (1997) model to four ephemeral catchments in Australia, with areas ranging from 181 km^2 to 2540 km^2. They assessed the model in terms of R^2 statistics that was applied to the flow and the transformed flow. The study obtained poor results for the dry years which contrast with Ye et al. study but agrees with ours.

Even though different performance assessment was used when the Ye model was applied to Wadi Ahin, the obtained results did not show good results for any of the simulated periods at least not for fm or nse* or through visual assessment. The 1999 year was one of the dry years in this case with only one small flood (the second flood is doubtful as hardly any rainfall was recorded at any of the rainfall gauges), but the model

highly overestimated the only event in that year in terms of peak and volume, when using nse* as **Figures 8.12** shows, and highly underestimated it when using fm, as **Figure 8.14** shows. 1997 and 1998 can be considered as wet years with more than 3 events per year, but the model overestimated some events and underestimated some others when nse* was used, but underestimated nearly all the events when using fm. The validation nse* value using the Ye model was 1.021 (0.98 when March 1997 event was excluded), and 0.96 using fm. On the other hand and as mentioned before, the nse* value obtained using the CWI model was 1.34 (0.96, excluding March 1997 event), and the fm was 0.96. Hence, there is hardly any improvement using this model in our case. The model in our case has not been tested using the monthly data as this is not thought to be adequate for our case as the flood mostly starts and ends in the same day, and monthly data can not reflect that.

Evans and Jakeman (1998) have also used IHACRES model but with some modifications. The authors introduced the catchment moisture deficit (CMD) to the model to utilise a water balance approach that extracts information from catchment-scale time series data available on precipitation, energy-related variables and stream discharge. This replaces the statistically based non-linear evapotranspiration loss module by a catchment moisture deficit accounting scheme.

Evans and Jakeman (1998) tested three small catchments, two of which are humid catchments (the Coweeta catchments in North Carolina, USA), and the other is a semiarid catchment (Scott Creek in South Australia). The results from the model calibration were found to be good in general even though the model had some difficulty reproducing hydrograph recessions in one of the humid catchments. However, the authors believed that by using this semi-physical approach, the physical interpretation of the parameters will be made easier than with the statistical approach in the unmodified IHACRES. Again this is difficult to compare with our study but this model can be recommended for future work.

In another study, Croke and Jakeman (2004) introduced a revised version of the non-linear part of IHACRES model that was used in the Evans and Jakeman (1998) study mentioned above. The new version was developed to aid in estimating flows in ungauged basins and for applications where time-series estimates of actual evapotranspiration are required. This modified model has only 3 parameters depending on the climate data used. This version was applied to the same catchments that were used by Evans and Jakeman (1998). The results showed lower R^2 values for the

calibration periods but better performance for the simulation period. It would be a good idea to test this version if the required time was available to compare the results as the required climate data can be made available.

For the purpose of our research, the semi-distributed version of IHACRES, was run using both the original and Ye et al. model structure to check the performance of IHACRES in comparison to the lumped version and KINEROS2 when the catchment was subdivided into 20 subcatchments, as mentioned above. In this case, it should be noted that only rainfall was allowed to vary spatially over the subcatchments, using the KINEROS2 rainfall interpolation method. The same catchment-average rainfall was maintained over all compared models. This means that only the effects of the spatial distribution of rainfall were tested rather than the spatial distribution of the subcatchments' characteristics. As there is not enough information on the variation of the parameter values over the different parts of the subcatchments this seems to be acceptable. It should be also borne in mind that there was only one meteorological station that temperature values were obtained from, and hence, its recorded temperature values were used over the whole catchment uniformly.

The obtained results were also found to be different using different SMA models, as well as using different objective functions. These can be illustrated in **Figures 8.28** and **8.29**. **Figure 8.28** shows a comparison between the obtained results of the CWI and the Ye models, using the nse*-optimal parameter sets, with the semi-distributed version whereas **Figure 8.29** shows the obtained results using fm.

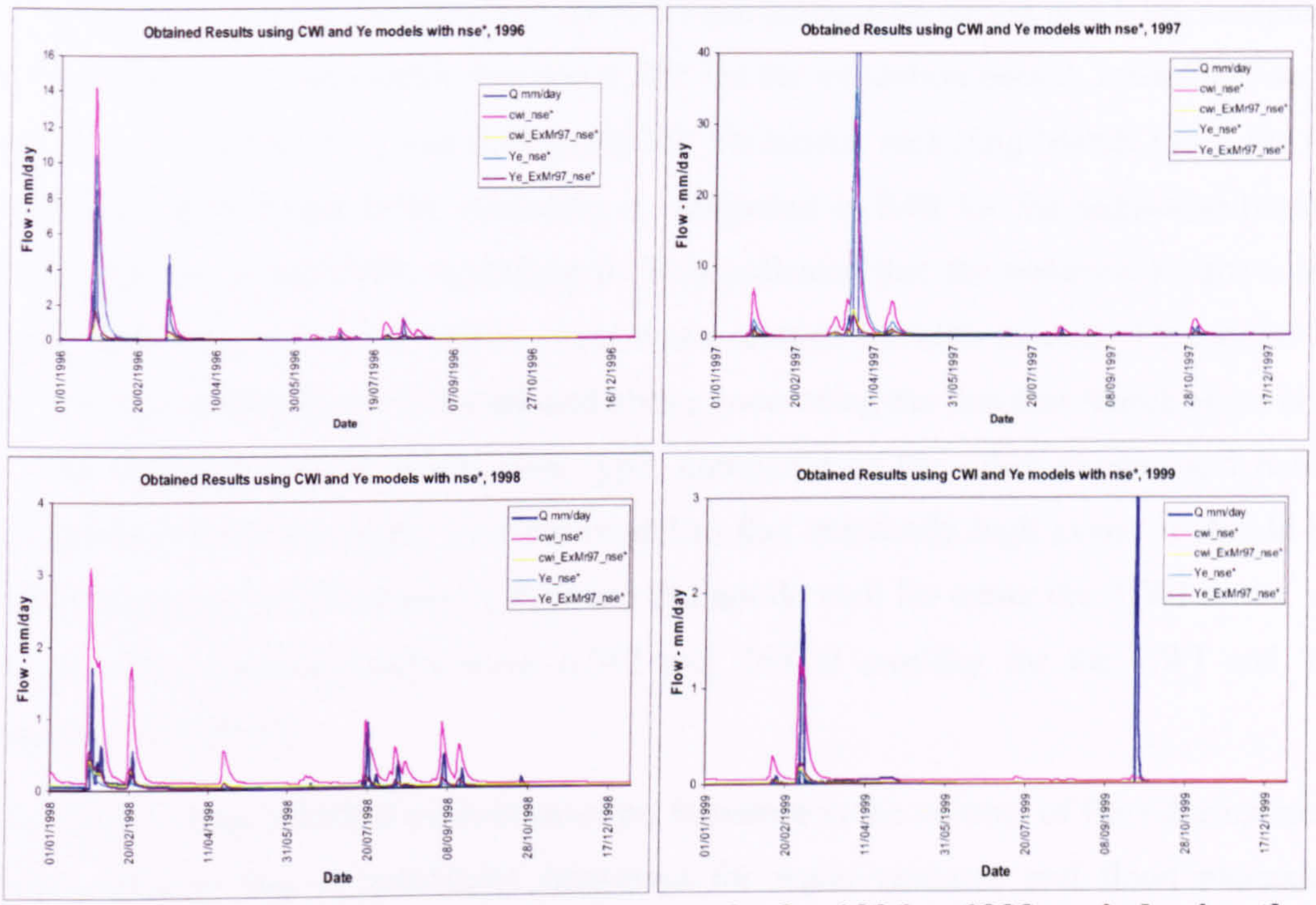


Figure 8.28: Calibration and validation results for 1996 to 1999 period using the CWI model and the Ye model, with nse*, RRMT-SD

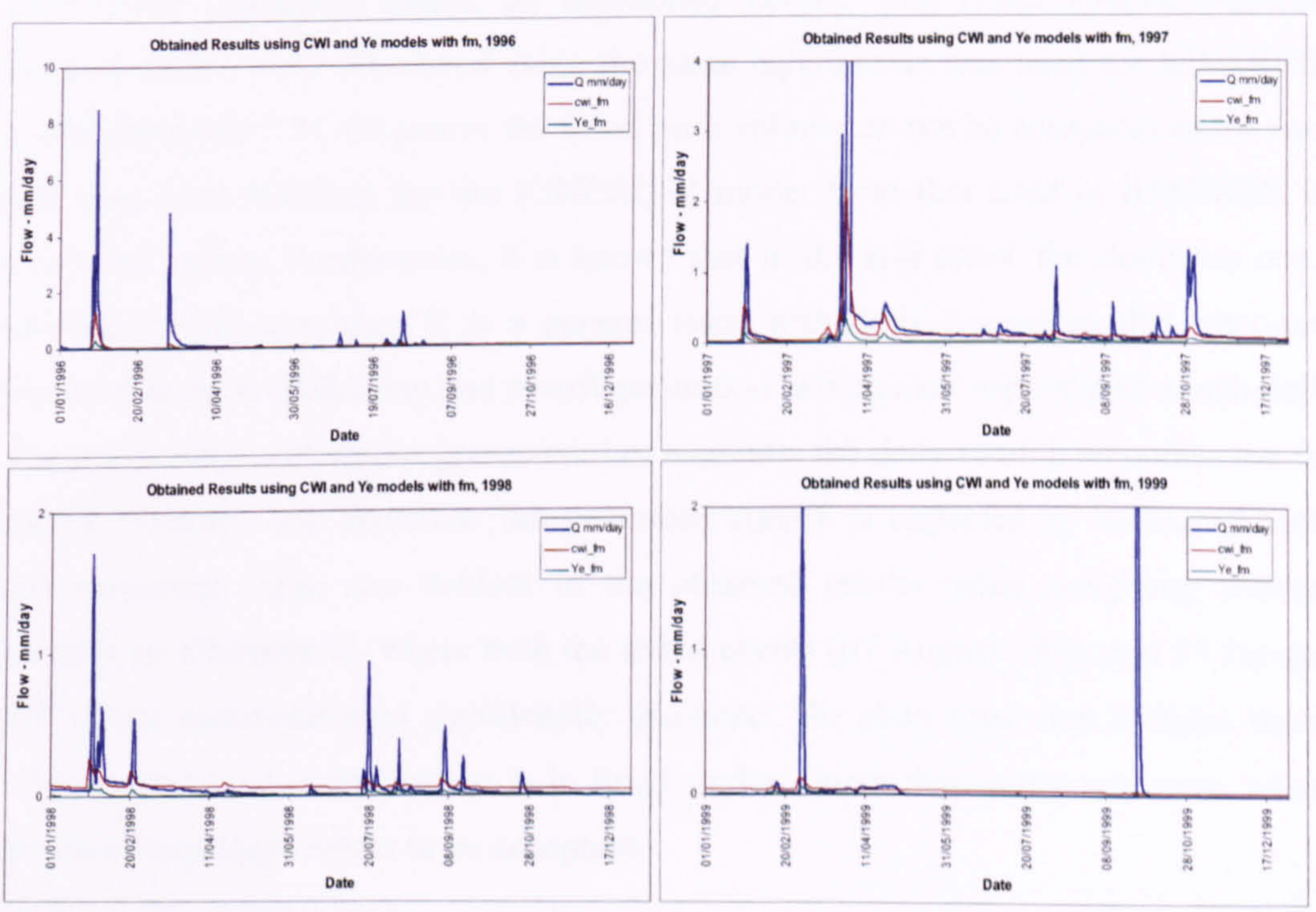


Figure 8.29: Calibration and validation results for 1996 to 1999 period using the CWI model and the Ye model, with fm, RRMT-SD

Performances of IHACRES have been evaluated so far in terms of visual inspection of fits and in terms of nse* and fm values. The obtained results were clearly different based on the used SMA model and the objective function. Including and excluding March 1997 when using nse* shows also some effects. The nse* value obtained, using

CWI model, including March 1997 event for the calibration period was 0.96, compared to 0.88 when it was excluded, but was 1.382 for the validation period, including March and 0.98, excluding it. It was 0.56 using the Ye model, including March 1997, for the calibration period, and 0.80, excluding it, compared to 0.99 for the validation period, including March and 0.97, excluding it. This indicates that the obtained results using nse* were better when the March event was excluded for both models. This might be for the same reason that was mentioned above concerning the fact that March event is of a very different rainfall mechanism type, compared to the other events, and hence excluding it does not highly bias the model to that extremely high event. It should be noted that using the fm objective function did not do well for either the; CWI or the Ye model. The obtained results were 6.042 and 26.639 mm/day for the CWI and Ye models, respectively.

However, a more practical evaluation of performance is the volume of flow during each event, OF_2, as this is potentially important for water resource and flood planning, Hence, it was calculated as an additional measure of performance and to compare with KINEROS2 validation results as mentioned before. The flood volume objective function values were calculated using the same equation as was used for KINEROS2 model (Equation 7.5). Of course the flood peak values can not be compared as the used time step were different for the KINEROS2 model from that used in IHACRES, as mentioned before. Furthermore, it is known that in the arid areas, the flood can occur and end in the same day. It is a general issue with daily time-steps that important processes such as infiltration and runoff generation, which may happen also at sub-daily time-scales, were not well-represented. For example, the daily rainfall smoothes out the rainfall intensity and therefore the generated runoff is expected to be significantly underestimated. This was evident in the obtained results using weighting average rainfall (see **Chapter 7**), where both the tested events (07 August 1996, and 25 January 1997) were underestimated significantly. However, the short time–step analysis seems to be more critical if the interest is in flood studies rather than water resources, where the larger time steps seems to be acceptable.

However, the values of OF_2 obtained using the RRMT-L with the CWI model fitted to nse*, including March 1997, show that 5 events out of 25 had values of OF_2 <0.3. This increased to 9 out of 25 when the March 1997 event was excluded. Using the Ye model with nse* produced poorer results. The results obtained using fm show that 7 events out of 25 had OF_2 <0.3, when the CWI was used, compared to 3 out of 25 when the Ye

model was used. This shows clearly that for the lumped version, both models did better when the March 1997 event was excluded, even though the CWI model did better than the Ye model when this event was included (5 events using CWI compared to none using the Ye model). This highlights the fact that the March 1997 event was a different rainfall type (perhaps caused by a cyclone) and including it might bias the model towards fitting to this significantly high event, with less weight given to the other medium to small events.

The results obtained using OF_2 for the RRMT-SD version show that 4 events out of 25 had $OF_2 < 0.3$, using the CWI model with nse*, when including March 1997 event, but 9 events when it was excluded. When the Ye model was used, with the nse*, 5 events out of 25 events had $OF_2 < 0.3$ when the March 1997 event was included, but 7 events when it was excluded. However, when using the fm objective function, 6 events out of 25 had $OF_2<0.3$, using the CWI, but only 5 events using the Ye. When the KINEROS2 model was used, the results were different depending on whether the 8-parameter, 4-parameter, 6-parameter, or 11-parameter case was applied. The results show that there were 7, 8, 5, and 8 events that have $OF_2 <0.3$ value, for the 8-parameter, 4-parameter, 6-parameter, and 11-parameter case, respectively. Hence, the results obtained with KINEROS2 were only slightly better than those obtained with IHACRES. The worse case in KINEROS2 was the 6-parameter case (the spatial variation case), where 5 events had $OF_2 <0.3$, whereas the worse case in IHACRES was the Ye model with nse*, including the March 1997 event, for the lumped version, where the model wasn't able to obtain any event with $OF_2<0.3$. The Ye model also obtained the 2nd worse result when the fm objective function was used (only 3 events out of 25 with $OF_2 <0.3$). The semi-distributed model seems to provide better results concerning the flood volumes, compared to the lumped version.

These means, in general, the CWI did better than the Ye model for both the lumped and the semi-distributed versions. The analysis also shows that using nse*, excluding the March 1997 event did better, in general, than the fm objective function.

As it was mentioned above, the obtained results depend highly on the used objective function but it should be noted that different objective function give different weight to different type of floods, e, g. the nse* give higher weight to the higher events than the lower ones which means a good fit might be obtained to the high events but poor fits to the low ones. The fm, depends on the selected threshold value which it uses to control the limits of the high and low flood peak of interest for the modeller. In our case the

high threshold was selected to ignore the March 1997 event and the low to ignore the base flow as it is not a result of the tested rainfall event but, most probably, is from the ground water. However, the poor results suggest that the selected threshold might need to be reviewed.

The modelling results also highlight the different behaviour of the event based models such as KINEROS2 and the continuous time-step models such as IHACRES. The event based models can do better for individual events and if the interest is on a specific flood event, for a flood study purpose compared to the continuous time-step models. However, both type of models, continuous and event based-models, can face difficulty in the validation process as a good set of parameters for one event can be inadequate for the others. This was evident from the obtained results in these analyses and the previous analysis using KINEROS2. Hence, each type of model should be selected based on the modelling aim, e. g. the continuous-time models are very useful tool in management and water resources assessment but the event based model can be particularly good for the flood events analysis.

- ***Running IHACRES using hourly data***

An important study that was carried out by McIntyre and Al-Qurashi (2008), applying IHACRES to Wadi Ahin for the same period that was used in this research, but running the model using hourly data during and around events and daily data in-between. 27 events for the 1996 to 1999 period were simulated using both lumped and semi-distributed IHACRES versions. Sensitivity analysis was carried out on the Ye model based on uniform random sampling of the used parameter values (20,000 samples). The analysis shows that the model was not sensitive to the *l*, and *mf* was found to be close to zero implying that the losses are not temperature dependent. In addition, the values of *%q*, k_q and k_s were found to have minor effects on the model performance. These findings led to simplifying the model to remove the four less effective parameters (*l, mf, %q,* and k_s) (see McIntyre and Al-Qurashi, 2008), leaving $\tau(T_k)$, *p*, k_q, *c,* and *volc*. Furthermore, it was suggested that $\tau(T_k)$ might also be usefully fixed to a value equal to one implying that the catchment model has little or no memory of wetness and that the catchment wetness index model might be simplified to a power law relationship between effective rainfall and rainfall (McIntyre and Al-Qurashi, 2008). Hence, the model was run with 4 parameters only (*volc, p,* k_q and *c).*

The objective functions that were used were the same as those used for running KINEROS2 (absolute relative errors in flow peaks (OF_1), flow volumes (OF_2) and time-

to-peaks (OF_3) - see **Chapter 7**). The IHACRES validation performances for flow peaks and volumes were compared to those of the KINEROS2 and a 2 parameter regression model (McIntyre et al., 2007). IHACRES was found to perform the best, especially the 5 parameter model. For example, there were 13 events out of the 27 events have obtained OF_2 <0.3 in validation when using the semi-distributed version (in event-based mode) but 11 using the lumped version. In the PhD research the validation performances were significantly poorer and semi-distributed version of IHACRES did not show any better performance than the lumped version. This might because of using different objective functions than what were adopted in the paper, or because hourly data was also not used but the daily and only on a continuous time series basis. Wadi Ahin has a time of concentration much less than a day (6 hours using Kirpich or 12 hours using Bransby-Williams) though it was found to be 4 hours by McIntyre and Al-Qurashi (2008).

8.8 Conclusions

The IHACRES model was run through the RRMT (Wagener et al., 2004). The model was run using the lumped version (RRMT-L) and the semi-distributed version (RRMT-SD) (Orellana et al., 2008).

The loss models used in both cases were the CWI model by Jakeman et al. (1990) and its modification for ephemeral channels by Ye et al. (1997). The model was calibrated using uniform random sampling, with and without the highest recorded event of March 1997, using Nash Sutcliffe Efficiency (nse*) and a medium-flow objective function (fm).

The results show that soil moisture accounting model and the used objective function have great effects on the results.

The global sensitivity analysis shows that the CWI model was most affected by the change in k_q, *volc*, and *%q* values, using any of the RRMT versions (RRMT-L, or RRMT-SD). Using the Ye model, the p, k_q, and *%q*, were found to be the most sensitive parameters. Using the Ye model with RRMT-SD, p was the most effective parameter beside k_q to some extent.

The obtained results using the RRMT-L shows that the CWI model has obtained a better nse* value when the March 1997 event was excluded than when it is included (1.34 for the validation period, including the March 1997 event, compared to 0.96 when it was excluded). The obtained results using the RRMT-SD version were 0.96, including

the March event, compared to 0.98 when it is excluded) for the same period. On the other hand, the simulation result using the fm was 1.49, using the RRMT-L and 11.86 using the RRMT-SD. This indicates that the RRMT-L did much better than the RRMT-SD.

The obtained results using the Ye model with the nse* objective function show also that excluding the March 1997 events did improve the results slightly (1.02, using RRMT-L, including the March 1997 events but 0.96 when it was excluded and 0.99, using the RRMT-SD, including March 1997, but 0.97, when the March 1997 was excluded).

The results obtained using the fm shows that the RRMT-L did much better than the RRMT-SD (was 0.96, using the RRMT-L, but 11.53 using the RRMT-SD).

The overall results did not prove the benefit of using the semi-distributed version over the lumped version in this case. However, it should be noted that only rainfall was allowed to vary in the RRMT-SD but all the other parameters were uniformly distributed over the catchment.

The poor performance obtained can be referred to different factors that include; inappropriate objective functions, rainfall errors with poor network coverage, and errors associated with using a daily time-step. Hourly flow data would obviously have been better to achieve good correlation as the obtained results by McIntyre and Al-Qurashi (2008).

The limitations of what has been done in the used process of IHACRES, can be due to the selection of the objective functions which might be improved if the same volume and peak objective functions that were used in the KINEROS2, while including the low flow using a low-flow objective function. Using hourly data rather than daily data could be improved the performance too (see McIntyre and Al-Qurashi, 2008).

Chapter 9

Summary and Conclusions

9.1 Introduction

The hydrological features of arid areas are different in many respects from those of humid areas because of different climate, and hence rainfall regime. Hence, these aspects need to be considered when carrying out rainfall-runoff modelling in arid areas. However, there are not enough studies that cover all the different hydrological aspects of arid areas and few special modelling techniques have been developed specifically to suit the unique hydrological characteristics and responses of arid areas. Therefore, techniques used for hydrological design and water resources management have mainly been those developed originally for application in humid areas.

As rainfall-runoff modelling is a very important tool that can be used in assessment and management of hydrological systems (Beven, 2000; Singh et al., 2002; Wheater et al., 2002), many attempts have been carried out recently to test these models and to investigate their performance in different arid areas with development of certain tools to cover some of the critical aspects. An attempt has been made in this PhD research to use some advanced tools of model analysis to test some of the current models that have been used to consider arid area hydrological characteristics. Two models, KINEROS2 and IHACRES, have been selected and applied to the Wadi Ahin catchment in the Sultanate of Oman.

This chapter provides a brief summary of the outcome of this research, shedding light on the problems, and providing some recommendations where possible. Some guidelines are provided for improved rainfall-runoff modelling in arid areas in general and Oman in particular.

9.2 Effect of the Hydrological Features of Arid Areas on Rainfall-Runoff Modelling

Arid areas have distinctive hydrological features which should be considered in rainfall-runoff modelling (see **Chapter 2**). The most important features that need to be considered include the climate effects such as the high temperature, potential evapotranspiration, and humidity (although it depends on the location of the area relative to the coast).

The rainfall characteristics in arid areas are also rather different. The dominant mechanisms of rainfall generation in arid areas are different from those in humid areas and the rainfall tends to vary highly in space and time. Some studies show clearly the effects of seasonality (Al-Qurashi, 1995; Hofman & Rambo, 1995; Drissel & Osborn, 1968; Mourits & Saleh, 2002), where the summer events seem to be more intense and localized than winter ones (Al-Qurashi, 1995). Elevation affects the rainfall in both the number of the rain days and the rainfall depth.

Arid areas generally do not have continuous stream flow but when runoff does occur it can be very high with floods that are very flashy in nature. Variation of runoff in space and time and partial-area runoff can be significant in arid areas. The flood hydrographs in arid areas typically show rapid rise to peak flow and short recessions, often lasting for a few hours only. Relative to catchment area, flood peak magnitudes can also be very high (more than 10,000 m^3/s in Wadi Ghudun in Oman has been recorded). Flood volumes also can be very large, for example more than a million cubic meters have been recorded in one day in Egypt (Abu Zeid, 1997).

Rainfall-runoff relationships in arid areas seem to be more complex (**Chapter 2**). Hydrological processes such as the type of runoff-producing storm, rainfall characteristics, runoff characteristics, transmission losses, all have great effects on rainfall-runoff relationships. In addition, watershed physical characteristics, such as elevations, stream length, slope, catchment size, soil type, fans and reliefs, and vegetation cover, need to be well understood as they all have effects on the rainfall-runoff relationships.

The difficulty in understanding rainfall-runoff relationships is reflected in the difficulty of obtaining a runoff coefficient. Transmission losses in arid areas are high in typical permeable wadi courses and the runoff rate reduces downstream in such circumstances, and so no unique runoff coefficients can be expected. The literature review for arid areas showed that it was very difficult to obtain any runoff coefficient that can be used in hydrological analysis with confidence.

The transmission losses are very important for groundwater recharge and should not be ignored in any surface or groundwater modelling. However, this phenomenon is not yet fully defined, and further investigation is necessary. It is also very important that this phenomenon is taken into account when selecting a suitable model for use in any arid areas.

Overall, it is clear that any hydrological study that ignores the special hydrological features of arid regions can easily obtain misleading or wrong results. Hydrological models should take into account these features, and models that were originally developed for humid areas should be reviewed and modified as necessary when used in arid areas.

9.3 Effects of Rainfall on Rainfall-Runoff Modelling

When carrying out rainfall-runoff modelling it should be borne in mind that rainfall is a very important input to rainfall-runoff models. Good knowledge of rainfall and selecting the best interpolation method for determining the average rainfall over the study area will help in obtaining better results and evaluating the selected rainfall-runoff model performance. It can also aid in understanding the resulting simulated runoff and the rainfall-runoff relationships.

Rainfall data quality is also very important to consider when carrying out rainfall-runoff modelling. Poor data quality can arise from errors in observations, or from inadequate density of observations. Rainfall errors can be caused by instrument malfunction and accuracy, human errors, etc., and given the nature of the rainfall, capturing the spatial variability with conventional raingauge networks is problematic, if not impossible. Rainfall data quality has been found to have remarkable effects on the results of rainfall-runoff modelling. Errors in defining rainfall will affect the calculated runoff and will lead to variable accuracy of outflow results. Investigation of the rainfall data to find out the source of this variability before using it in any model is advisable. However, it is very important to bear in mind that, although the rainfall errors are important, there are some other errors such as those caused by the model structure and the estimation of the parameters values (Michaud & Sorooshian, 1994b) that can affect the simulation results.

From the literature review that was carried out for the purpose of this research, it can be seen that it is obvious that rainfall errors will affect the rainfall-runoff modelling results but determination of the exact amount of error is not an easy task. The data quality in arid areas is generally questionable and this makes it even more difficult when modelling arid areas.

The spatial and temporal variations of the rainfall are very high and need to be well understood. These variations have great effects on the resulting runoff and make the rainfall-runoff relationship difficult to define. However, it is difficult to measure the rainfall that falls in different parts of any catchment, and even studies using relatively high density networks have shown how difficult that could be. Using radar seems to be

a good alternative, potentially able to capture any rainfall at any part of the catchment at any time though it depends on the radar resolution, and it should be borne in mind that radar technology is very expensive and not all arid areas can afford it; besides that, a dense coverage of rainfall gauges would still be preferable to apply any necessary correction for rainfall amounts recorded by the radar and in mountainous areas.

It can be concluded that rainfall characteristics in arid areas are more complicated in some aspects than in humid areas and have great influence on rainfall-runoff modelling. The quality and the network coverage make it a challenging task. Nevertheless, good knowledge of the rainfall characteristics together with a skilled modeller is important to obtain good rainfall-runoff relationships.

9.4 Rainfall-Runoff Modelling and their Application in Arid Areas

Watershed models are important in water resources assessment, development and management (Singh et al., 2002). Beven (2001) stated there is a limited range of measurement techniques and a limited range of measurements available in space and time, therefore there is a need to extrapolate from the available measurements to assess the likely impact of future hydrological change. The models can generate a long representative time series of streamflow volumes from which water supply schemes can be designed. They can be used to analyse the quantity and quality of streamflow, reservoir system operations, groundwater development and protection, surface water and groundwater conjunctive use management, water distribution systems, water use, and a range of water resources management activities (Wurbs, 1998). Watershed models are also used to quantify the impacts of watershed management strategies, linking activities within the watershed to water quantity and quality for environmental and water resources protection (Singh et al., 2002) and design floods.

The review showed that the different types of models each have their advantages and disadvantages, though some of the models seem to be inappropriate to be used in arid areas as they do not consider the important hydrological characteristics such as the spatial and temporal variation of the rainfall and runoff or the infiltration losses beside other factors.

The review that has been carried out on rainfall-runoff aspects in arid areas concluded that the model performance can be affected by many factors which include:

- The purpose of the study and how suitable the selected model is for fulfilling this purpose
- The model type (metric, conceptual or physically-based model)
- The complexity of the model structure and the parameters used
- The hydrological characteristics of the studied areas
- The data availability
- The data quality
- The sufficiency of the modeller's experience in using the model and understanding of the studied area

9.5 Selected Models and the Obtained Results

Based on the review that was carried out, two different model types were selected for the research: the physically based type model (KINEROS2), and a hybrid metric conceptual type model (IHACRES). An attempt was made to study the benefits and the limitations of each of these models using the Wadi Ahin data. In the following section, the obtained results are discussed.

9.5.1 KINEROS2

The KINEROS2 model (Woolhiser et al., 19990) was run for a simple synthetic catchment (a series of planes of total length 20,000m, feeding a short channel) using different configurations, different numbers of planes in series, different rainfall distributions, and different rainfall time intervals. It was also run with and without infiltration to test the model's performance under different conditions. The model responses were compared to study the effects of the numerical errors on the flood peak values obtained.

The results show that using different numbers and sizes of planes have different effects based on the configuration but no clear pattern emerged. However, the tests showed that KINEROS2 was having problems in coping with a single plane length of 20,000m in some cases but seemed to give reasonable results in other cases for both 5- and 60-min time intervals for the uniform rainfall distribution test.

It was also found from the test that using large input time steps may cause a loss of information regardless of whether the time step is adjusted using the Courant adjustment. One possible explanation is that, when larger numbers of planes are used, such as in some cases when 16 and 32 planes, the duration of flows from the upper planes is short relative to the time step, resulting in large distortion of the hydrographs.

In some other cases, there is a combined effect of large time step and Δx. It is believed that the large time step will impact the shorter planes to a greater degree and can cause some problems in determining the right location of the advancing front. The longer planes will be more affected by the large Δx. Hence, the user might need to run the model with different sizes of planes with close observation of the obtained hydrographs and the percent of errors until the optimum length is reached for the subject study area. The accepted errors should not exceed 10% in theory, based on the developer's advice. However, this might not be always possible and the user might need to accept a higher percent of errors if the obtained results look reasonable. In our case, up to 30% can be thought reasonable due to the quality of the data and the rainfall network coverage.

Local sensitivity analysis was carried out using two recorded events: 07 Aug 1996, and 25 Jan 1997, which have different rainfall distributions and intensities (**Chapter 7**). Using a default set of parameters, three different rainfall interpolation methods were tested: the KINEROS2 method (called the centroid method in the thesis), the weighted average method, and the selected gauge method. The results show that the used interpolation method has a considerable effect on the model output. The simulations also show clearly that spatial distribution of the rainfall input over the catchment has significant effects on the results, and a suitable method of calculating areal rainfall from gauged rainfall is a very important factor.

Parameters were then perturbed to test sensitivity of the simulated flood peaks to different parameter values. It was found that the most important parameters were K_s, *n*, *Rel*, *Slp*, *G*, and *S*, which were selected for further investigation by carrying out a global sensitivity analysis through the uniform random sampling method (Monte Carlo, with 20,000 parameter sample numbers). A new rainfall parameter, *f*, which controls the weight given to the nearest gauge when calculating the rainfall over a plane, was also included.

The global sensitivity analysis was for the 25 events, which were found adequate for further investigation, from the Wadi Ahin for 1996-1999, using different objective functions representing peak flow, flow volume and time to peak performances.

The sampling experiment also provided an ensemble of the optimum set with respect to the individual objective functions (peak, volume, and time-to-peak) and the combined objective functions (peak and volume; peak, volume and time to peak). It was noticed that when each event was treated independently, using the best of the sampled parameter sets, KINEROS2 was able to accurately simulate independently flow peak,

flow volume and time to peak, for almost all events. However, the parameter sets which were estimated to be optimal for individual events did not perform well when transferred to other events. Furthermore, the parameter set which gave best calibration performance over any combination of 24 events did not generally produce acceptable performance (defined as within 30% of observed) when used to predict the 25th event. The parameter sets identified for the events individually were used to produce an ensemble of predictions. This produced very high uncertainty and the average of the ensemble was a very poor representation of the observed flow data.

In a second experiment, the infiltration model was substantially simplified, and a third experiment allowed spatial variability in the infiltration rate, but the same general conclusions were reached. Conclusions are consistent with these reached when KINEROS was applied to Walnut Gulch (Mishaude and Soroushian, 1994a, b; Yatheendradas et al., 2007).

These analyses show that the model performed differently for different events, but it was difficult to relate that to the rainfall distribution pattern, even though it was found from the dotty plots using the combined peak, volume and the time to peak objective functions that some parameters were better defined for the rainfall events which were relatively uniformly distributed over the catchment.

A question is posed here on how beneficial is using a complex model such as KINEROS2 which can take much more time and effort compared to a simpler model such as the regression analysis of McIntyre et al. (2007). However the differences in complexity of the modelling approaches and corresponding resource cost are clearly wide, yet the differences in prediction performances and the insights into key processes seem to be small, or in favour of the simpler approach. In addition, the selection of a model should depend on the aim of the modelling process, and the availability and quality of data. In the Wadi Ahin case, there was only one flow gauge in the selected upper catchment with poor spatial coverage of rain gauges, very limited prior information on soil hydraulic properties, canopy cover, and no detailed channel network survey. The data quality, in some cases, was also questionable (e.g. floods with hardly any recorded rainfall as was seen in the Sep 1999 event, or rainfall after the flood event occurrence, as was seen in the April 1996 event).

9.5.2 IHACRES

IHACRES (Jakeman et al., 1990) was used to investigate the behaviour of the catchment using daily data with its two available versions: the lumped version, and the

semi-distributed version through the RRMT software (Wagner et al., 2004; Orellana et al., 2007). The semi-distributed version was applied using the same sub-catchments that were used for KINEROS2, using the same data period (1996-97 for calibration and 1998-99 for validation). The model was run using CWI and its modified version of Ye et al. (1997) which was modified to suit the ephemeral channels. The model is run with and without the highest recorded event of March 1997, using two objective functions: the Nash Sutcliffe Efficiency, nse*, and a least-squares objective function which omits especially high flows and especially low flows, fm.

A global sensitivity analysis (again using 20,000 uniform random samples) shows that the CWI model result was most affected by the change in k_q, *volc*, and *%q* values, using any of the RRMT versions (the lumped version, RRMT-L; or the semi-distributed version, RRMT-SD). Using the Ye model, the p, k_q, and *%q*, were found to be the most sensitive parameters. The model showed that the k_s has no clear effect on the model sensitivity suggesting one routing model might be adequate. Ye et al. (1997) suggested using one routing storage in ephemeral channels but this was not thought appropriate in our case as we have some baseflow, and therefore, two storages in parallel were adopted to represent the slow flow and the quick flow.

The simulation results were found to be affected significantly by the used objective function, and excluding the high event of March 1997 did show slight improvement in the results in the case of using the nse*. However, the results did not show clearly which version of the IHACRES (the lumped or the semi-distributed version) was better as this varied from one case to another. However, the study that was carried out by McIntyre and Al-Qurashi (2008), where an hourly time step was used and with different objective functions (same objective functions that were used in KINEROS2), showed that the semi-distributed version has in general obtained better results compared to the lumped version. Hence, the adopted time step and the objective functions seem to have notable effects on the results obtained. The soil moisture accounting model was found to have some effects too.

However, it should be noted that only rainfall was allowed to vary spatially in the RRMT-SD but all the other parameters were uniformly distributed over the catchment. The poor results using this version can be partly explained by the poor rainfall and flow gauge network as well as the objective functions that are used in this PhD research which might need to be reviewed in the light of the obtained results.

9.5.3 Comparison of the performance of the tested models

Two different types of models were investigated of different complexity and structure: KINEROS2 and IHACRES.

The selected models have performed differently due to many different factors such as the model type and structure, the rainfall input and its interpolation methods, the parameter uncertainty, and the time interval used. These factors are discussed in some details below:

- ***Effects of model type and structure***

This idea is also discussed by Jakeman and Hornberger (1993) who believed that 3 to 5 parameters are sufficient to reproduce most required hydrological process as it is very dangerous to fit the used parameters that are required to simulate the hydrological process through optimisation against the observed flow in the over-parameterised models.

KINEROS2, as mentioned previously, is an event-based model with more than 20 parameters. The event-based models as can be seen here can be calibrated easily in most cases to obtain good results for individual events for any objective function. The difficulties occur when an attempt is made to find the optimum parameter set for the whole calibrated and validated periods, as has been seen in **Chapter 7.**

In running KINEROS2 model, the only available distributed data was the rainfall, even though there was no rain gauge to cover all the planes, and the neighbouring gauges were to be used in some cases, allowing the model to use the provided rainfall interpolation. This problem was outlined by Hughes (1995) in his study, where the rainfall is the only available variable to vary among the different subdivisions. However, since in arid areas, rainfall is highly spatially and temporally distributed, this can still be considered as an advantage, even though the other parameters are uniformly distributed due to the lack of data.

On the other hand, IHACRES is a hybrid metric/conceptual, simple model of average complexity, as previously mentioned. The model undertakes identification of hydrographs and component flows from rainfall, evaporation, and streamflow data.

IHACRES model was run through the RRMT using both the lumped version and the new semi-distributed version, RRMT-SD. Only rainfall was allowed to be spatially distributed. However, the representation of spatial rainfall produced no significant improvements in the results.

This may be due to many factors, including the assumption of spatially uniform parameter values and the rainfall data quality. In addition, it can be also due to the poor rainfall coverage. However, there are questions about whether the additional parameters required for a semi-distributed application are supported by the information in the data, and whether typically-available rainfall data sets will support useful estimation of spatial rainfall.

McIntyre and Al-Qurashi (2008), applying the physically-based model, found that KINEROS2 performance did not significantly change when moving from an 11 parameter-calibration to a 6 parameter calibration, and they found no benefit in representing spatial variations in the parameters. The same study found also that running IHACRES (the semi-distributed version), via the Ye model, using 5 parameters only obtained better results than using all 9 parameters.

KINEROS2 is a complex model both conceptually and numerically, with non-linear routing, and is prone to numerical errors and instabilities when applied to the large spatial units used for Wadi Ahin (Al Qurashi et al., 2008). It may be these numerical issues which allowed the simpler IHACRES model to out-perform KINEROS2, or it may be the increased sensitivity to input errors due to the non-linear routing (Michaud and Sorooshian 1994a), however it is suspected that the more empirical nature of the IHACRES loss model allows it to better compensate for errors in the rainfall estimation. Despite the potential benefits of KINEROS2 in many other circumstances as the study of Al Qurashi et al. (2008) shows, the use of a 5-parameter semi-distributed IHACRES was preferred for the Wadi Ahin application.

It should be noted that IHACRES was used in this PhD research in its continuous form and not on event based form as the KINEROS2, and hence the whole calibration period was simulated at once. It was expected in this way to obtain optimum parameters that are suitable to the whole period and not to each event individually. This was found difficult due to the fact that the initial conditions and rainfall distributions can be different from one event to another.

In general, continuous models can be more suitable to be used for management purposes where the available water resources and its volume for a certain period are more important than individual events. The spatial and temporal rainfall distribution in arid areas and the long dry periods between events makes it more difficult when these types of models are used with the expected change in the ground water storage having some effects on the surface runoff. The latter is difficult to assess in such conditions.

However, the success of the event-based models for predicting flow volumes is contingent on them using the observed flow to estimate the baseflow component. If OF_2 is based on comparing simulated stormflow with observed stormflow (i.e. observed flow minus the assumed baseflow) then the event-based models become slightly inferior to the continuous-time models. Therefore, for the purpose of flow volume prediction, the event-based models need to be supported by a good groundwater model to generate baseflows.

The KINEROS2 model considers the plant interception, the infiltration, and transmission losses but not the evaporation. The neglect of evaporation is likely to be justified during a flood but not at the start of the event when the first drops can evaporate immediately from the land and no runoff can start before the soil's wetness can reach a certain point. Of course this can depend also on the rainfall intensity, duration and the ponding time.

On the other hand, in IHACRES the channel model does not include a loss parameter and so channel transmission losses are accounted for by the $\tau(T_k)$ parameter. The lumping of all losses in this way is consistent with the empiricism of the IHACRES loss model; furthermore, the hillslope and channel routing models are linear and so whether or not the losses come before or within them is inconsequential.

- ***Effects of rainfall distribution and used time intervals***

The rainfall in arid areas is known to be highly variable in space and time. Hence, a very dense gauging network is required to measure the spatial rainfall over the element. In cases where gauges are sparse, the rainfall interpolation methods are more critical. This is an evident in the results of this research.

A test was carried out to assess the effects of using different rainfall interpolation methods over the catchment in **Chapter 6**. This illustrated how important it is to select a suitable method, and the potential uncertainty of predictions associated with rainfall estimates.

The quality of the rainfall data was also found to have significant effects on the model's performance and the results obtained. Some events had to be excluded where the rainfall occurred after the flood, or there was a flood with no recorded rainfall.
When using a lumped model, for example the lumped IHACRES, an average rainfall is used over the whole catchment. Hence, the rainfall intensity is smoothed out, and as a result the flood peaks tend to be underestimated. The obtained results using IHACRES-

L were evidence of this beside the other affecting factors such as the objective function used. However, IHACRES may be applied at any time-step, even though it seems the only sub-daily application so far has been that of Schreider and Jakeman (2001) and Schreider et al. (2001), who used a 4-hourly input-output time-step and recently, McIntyre and Al-Qurashi (2008).

The rainfall time intervals used have some effects on the results obtained, especially, when it concerns the flood peak and the time to peak. In this research this was tested through the use of 5-min and 60-min data with KINEROS2. Even though there was no significant difference found in that case, there is little doubt that there is a big difference between using hourly data and daily data such as that used to run IHACRES. This is due to the fact that the flood can start and end in the same day in arid areas, and hence, the flood peak value cannot be determined or the time to peak from daily data. In addition to that, the shape of the hydrograph can not be determined, bearing in mind that hydrographs in arid areas have sharp inclines and short recessions with a very short time to peak. Volumes may also be affected by the smoothing of intensities.

- ***Effects of parameter uncertainty***

One of the problems that should be considered when evaluating the results of any of the tested models is parameter values and how realistic and suitable they are for the study area.

It should be remembered that most parameters, in this case, were not identified through measurements and were based on previous studies, in particular the parameters that were related to the soil characteristics, except for some parameters that related to the geometry of the channels, which were based on the topographic maps and survey. However, the survey results were not available except in the adjacent area to the flow gauge. It is not clear whether all of these values were based on measurement or calibration. However, even if these values were obtained through measurements, they will be at certain points and will not reflect the characteristic of each individual plane. In addition, the optimum parameters in our case were obtained using a Monte Carlo optimisation method through uniform random search method. The parameters' bounds were determined from the literature.

In the case of IHACRES, the parameter values were all selected based on the calibration results using uniform random sampling with Monte Carlo simulation. The rainfall was interpolated using the KINEROS2 method, and the temperature was based on the

closest metrological gauge, Sohar Station. Hence, the obtained results were estimated based on the number of the samples used for the calibration period, which was short (only two years).

In general, the calibration of models is a very important process to select the appropriate parameter set but care should be taken to not get good results for the wrong reasons, in which case the predictions can be misleading. Therefore, it is very important that the modeller has a good understanding of the calibration techniques and how to use them together with suitable knowledge about the study area. Verification should always be carried out whenever possible to test the adopted assumptions and values. In our case, this was carried out for only two years, which might not be enough.

The study of McIntyre and Al-Qurashi (2008) showed that using an ensemble of parameter sets estimated from different events has been useful as it allows us to visualise the degree of uncertainty in predictions, and potentially it provides a basis from which to investigate how much the uncertainty may be reduced, for example by improved rainfall estimation. It also provides a framework for adding sources of uncertainty, for example the uncertainty which may arise from introducing a more comprehensive set of plausible rainfall inputs or more than one parameter set from each event. At present the uncertainty is unsatisfactory - so high and the runoff coefficients within each ensemble prediction range on average from 0.04 to 0.79, so that it is practically useless for decision-support. This is consistent with the simultaneous results of Yatheendradas et al. (2008) in their application of KINEROS2 to Walnut Gulch.

9.6 Conclusions and Recommendations

Two different types of model have been tested for the purpose of this research: a physically-based model, KINEROS2, and a hybrid metric/conceptual model, IHACRES. The model structure and complexity, the description of the hydrological process, and the time-scale that is used differ for each model. The models were applied to an arid catchment located in the Sultanate of Oman. The results obtained from both models were found to be poor in general. There are many reasons for this, as discussed throughout the thesis, but the main reason could be the inadequate quantity and quality of data. It should be noted that the version of KINEROS2 that was used, which has more than 20 parameters, is more complex than the version that was previously applied in Oman by Wheater (1983) and Mott MacDonald (1992).

The poor model results in our case seem to suffer from such circumstances which affected the model's performance beside the other possible reasons as discussed above.

However, the model seems to be successful in the calibration period when individual objective functions were used; OF_1, OF_2, and OF_3, but the results obtained using combined objective functions such as OF_4 and OF_5 did not show good results in most cases. However, this does not have great use in terms of prediction performance.

KINEROS2 is believed to be a useful model if the interest is in individual outputs, e.g. peaks only or volumes only such as in flood studies, or in a particular event (see Wheater, 1983) as it is an event based model, where events can be simulated individually in detail. However, the data shortage problem will remain a problem unless better rainfall coverage is provided and measurements for the model parameters are carried out at different parts of the catchment.

Even though the value of KINEROS2 is questionable in the context of Wadi Ahin, it could have three advantages in the following circumstances:

- Firstly, it contains parameters which, in design at least, are physically-based and in some cases may be related to soil classifications (Michaud & Sorooshian, 2004b). Therefore it may be applicable to represent physical change, or for catchments with good spatial data on soil properties (although this was found to be of limited value by Michaud & Sorooshian, 2004b; also see Grayson et al., 1992).

- Secondly, the ability of KINEROS2 to represent distributed runoff processes and generate spatially continuous runoff may be attractive for some applications, for example simulation of the effects of local interventions such as storage reservoirs or inundation mapping, whereas it was only used in this research to predict flow variables at the catchment outlet.

- Thirdly, the model generates temporally continuous runoff within each event, while what was assessed here was only the prediction performance for volumes, peaks and times-to-peaks of the hydrographs (although the full hydrograph can sometimes be predicted from the peak and/or volume (e.g. Sharma & Murthy, 1996), and this is somewhat evident in **Figure 5.15**.

In general, physically based models are an adequate tool to study the different scenarios of land use change and their possible effects on the flood impacts and water resources.

In the case of IHACRES, both lumped, and semi-distributed versions were tested. The model did not obtain good results overall, as has been shown above, with no clear improvement of the semi-distributed version over the lumped version. The interesting finding was that the Ye modified version did not show better performance than the CWI

model, in general, even though it was mainly modified to improve prediction in ephemeral channels.

The daily time intervals that were used for running the model make it difficult to depend on the model to simulate flood peaks, as floods in arid areas are very flashy and can occur and disappear in the same day. The model was tested through the semi-distributed version of IHACRES using hourly data to simulate the response of individual events. The results were found to be much more promising as compared to the results obtained using the daily data with a continuous time step (McIntyre and Al-Qurashi, 2008). However, using a continuous time step was found to be suitable for simulating the flood volumes and hence, they can be adequate for the purpose of water resources assessment.

The potential advantages of IHACRES can be summarised with the following points:

- It is parsimonious, in its simple form
- In continuous simulation mode, it simulates the antecedent conditions (although in some of the simulations, the antecedent wetness was zero, and hence of no benefit)
- It simulates the baseflow, which may be important for water resources
- It adjusts the effective rainfall, on the basis of the volume balance (*volc*) and non-linearity (*p*) parameters. This can compensate for rainfall measurement errors (however, this may be regarded as a disadvantage, as the mass balance is violated).

More investigation needs to be carried out with the IHACRES model, and the suggested one storage routing model (Ye et al., 1997). Selecting the appropriate *p* range seems to be critical and more investigation might be required to select the suitable range for each area. Further investigation is also advisable to study any possible modification to the model structure to improve the model performance. Adding the kinematic wave equation for channel routing, to test its implications for the model results, needs to be explored. Adding a facility for the assessment of transmission losses, which is a very important phenomenon in arid areas, is advisable. This would allow the model to represent some of the physical characteristics of the catchments, and check how these affect the model performance.

In general, further investigation using different types of model with larger catchments is required to decide on the better type of models to be used in arid areas. It is difficult based on this study to judge which type of models should be used as this depends on the available data and the aim of the modelling as mentioned before. However, the data shortage will remain a problem and the adopted model should be selected based on the availability of data.

However, it is also difficult to see how a useful level of accuracy can be achieved in arid and semi-arid regions using typically available data sets which suffer from the poor quality and network coverage. In this case different suggestions can be made as shown below:

- Detailed study of the different hydrologic characteristics on the hydrologic response in arid areas needs to be carried out to aid in improving the current model structure to consider the effects of the most important parameters and phenomena such as the transmission losses, and the spatial variation of rainfall and runoff and the effects of the partial area runoff on the infiltration process.

- Use of regression relations for better understanding of the relationships between the main parameters such as the rainfall, runoff, and the physical characteristics of the catchments, which can then be used to improve the parameter estimation and their complex interaction when running any model.

- In case of event-based models, the events can be grouped, based on their common characteristics. The seasonality effects can also be studied to be used in grouping and the classification of these events. The optimum parameters for these events can then be used in the validation process where similar groups can be validated together.

- A study on the effect of the size of the catchment is advisable as the small size catchments might have some different hydrologic characteristics from that of the medium and large ones. Hence, the appropriate model can be selected where these characteristics are considered and also to avoid numerical error problems.

- Better uncertainty analysis, to produce confidence limits on all predictions is suggested. Due to dominant influence of rainfall, this would require a stochastic rainfall model to generate rainfall realisations-based on gauged values and associated research (Wheater et al., 2007).

- Better methods of rainfall observation, which would require investment in radar and/or satellite estimation products, and associated technical/theoretical challenges.

- Use of a simpler model which may be more suitable given the data limitations for the areas where no adequate data is available for use of more sophisticated models.

- Different hydrological data can be collected through measurements and different models can be tested, and hence the produced results can be used as a guide in other catchments of similar characteristics. This can overcome the high cost of equipping all

the catchments in the country which can be very costly and can aid in carrying out hydrological studies with more confidence.

- A data base for arid areas where data and different studies and modelling experiences can be exchanged which can be done through the Wadi Hydrology Group (UNESCO).

The above recommendations are general recommendations to be used in most arid areas. Regarding Oman, few more points might need to be considered as shown below:

- Selecting and establishing some experimental catchments is advisable which can be provided with intense required equipment to study different hydrological aspects and detailed studies can be carried out.

- The monitoring network coverage needs to be improved further as no adequate rainfall and flow gauges were found in the Wadi Ahin which is considered among those catchments with best coverage.

- Detailed survey of the main wadi channel geometry is required which is very important in using the physically based models. It should be borne in mind that the behaviour of waves depends heavily on the channel characteristics such as slope, roughness, shape, width, and depth (Fogel et al., 1991). Currently the available survey data are available only in areas adjacent to the flow gauge.

- More flow gauges are required among the main channels for transmission loss assessment.

It should be noted, regardless that, the results obtained in this research show that reproducing observed response of individual events or continuous response of specific years is problematic. Nevertheless, due to different reasons, modelling will stay a very important tool in most hydrological studies, though care is required to select the suitable model type.

References

1. Abbott, M. B., Bathurst, J. C., Cunge, J. A., O'Connell, P. E., and Rasmussen, J. (1968a), 'An introduction to the European Hydrologic System-Systems, SHE, 1: History and philosophy-based, distributed modelling systems', J. Hydrolol., 87, 45-59

2. Abbott, M. B., Bathurst, J. C., Cunge, J. A., O'Connell, P. E., and Rasmussen, J. (1968b), 'An introduction to the European Hydrologic System-Systems, SHE, 2: Structure of a physically-based, distributed modelling systems', J. Hydrolol., 87, 61-77

3. Abrahams, A. D., Parsons, A. J., and Wainwright, J., (1995), 'Effects of vegetation change in interrill runoff and erosion', Walnut Gulch, southern Arizona, Geomorphology, 13, 37-48

4. Abu Zeid, Khaled, (1997),'Floods and watershed analysis', CEDARE Chronicle, Mar/Apr 1997.

5. Allam, M. N., Sorman, A. U., Ishaq, A. M., and Khan, A. M., (1989), 'Geomorphologic rainfall-runoff models for infiltrating watersheds', Final Report No. AR-7-85. KACST, Riyadh, Saudi Arabia

6. Al-Sulaimani, Z., and Al-Obaidani, S, (2003), 'Integrated water resources management experience of sultanate of Oman', In 3rd World Water Forum, Kuoto, Japan

7. Al-Qurashi, Aisha M. (1995),'Rainfall-runoff relationships in arid areas', MSc thesis, Heriot-Watt University, Edinburgh, UK.

8. Al-Qurashi, Aisha M., Mcintyre, Neil, Wheater, H., and Carl Unkrich, (2008), 'Application of a distributed rainfall-runoff model to an arid catchment in Oman', Journal of Hydrology, Vol 355, 91-105.

9. Andreassian, V., Perrin, Ch., Michel, C., Ustar-Sanchez, I, and Lavabre, J. (2001), 'Impact of imperfect rainfall knowledge on the efficiency and the parameters of watershed models', Journal of Hydrology, 250, 206-223.

10. Bedient, P. B., Wayn, C. H., (1988), 'Hydrology and floodplain analysis', Addison-Wesley Publishing Company.

11. Beck, M. B., (1987), 'Water quality modelling: a review of the analysis of uncertainty', Water Resources Research, 23(5), 1393-1441

12. Beven, K. J., (1989), 'Changing ideas in hydrology. The case of physically-based models', J. Hydrlogy, 105, 172

13. Beven, K. J. (2001),'Rainfall-runoff modelling', John Wiley & Sons, LTD, West Sussex, England.

14. Beven, K., and Binley (1992), 'The future of distributed models: Model calibration and predictive uncertainty', Hydrol. Processes, 6, 279–298

15. Brown, J. A.H., (1987), 'Estimating streamflows for water development projects in tropical regions', Proc. Engineering Conf. Darwin, Inst. Eng. Aust. Canberra, Nat Conf. Publ. 87/1, 343-349

16. Boughton, W. C., (1984), 'A simple model for estimating the water yield of ungauged catchments', Civ. Eng. Trans., Inst. Eng. Aust., CE(26), 83-88

17. Cameron, D. , Beven, K. J. and Naden, P, (2000a), ' Flood frequency estimation under climate change (with uncertainty) HESS, 4, 3, 393-405

18. Cameron, D. , Beven, K. J. and Tawn, J, (2000b), 'An evaluation of three stochastic rainfall models', J. Hydrology, 228, 130-149

19. Cameron, D., Beven, K. J. and Tawn, J, (2001), 'Modelling extreme rainfalls using a modified random pulse Bartlett-Lewis stochastic rainfall model (with uncertainty)', Adv. Water Resour., 24, 203-211

20. Chandler, R. E, Wheater, H. S, Isham, V. S., Onof, C., Bate, S., Northrop, P. J., Cox, D. R., Koutsoyiannis, D., (2002), Generation of spatially consistent rainfall data', BHS Occasional paper No.13.

21. Chiew, F., and McMahon, T., (1990), 'Estimating groundwater recharge using a surface watershed model:sensitivity analysis', J. Hydrol., 114, 305-325

22. Chiew, F., and McMahon, T., (1991), 'Improved modelling of the groundwater processes in MODHYDROG', Proc. Int. Hydrology and Water Resour. Symp.' Perth, Western Australia, Ins. Eng. Aust., Silverspring, MD, Nat. Conf. Publ. 91/22(2), 492-497

23. Chiew, F., and McMahon, T., (1993a), 'Australian data for rainfall-runoff modelling and the calibration of models against streamflow data recorded overdifferent time period', Civ. Eng. Trans., Aust., CE35(3), in press

24. Chiew, F., and McMahon, T., (1993b), 'Assessing the quality of catchment streamflow yield estimates', Aust. J., Soil Res., in press

25. Chiew, F. H., Whetton, P. J., McMahon, T. A., and Pittock, A. B., (1993), 'Simulation of the impact of climatic change on runoff and soil moisture in Australia catchments.

26. Chiew, F., and McMahon, T. (1994),'Application of the daily rainfall-runoff model MODHYDROLOG to 28 Australian catchments', Journal of Hydrology, 153, 383-416

27. Chow, V. T., (1978),'Stochastic modelling of watershed systems', Advances in Hydroscience, Vol II, 1-93, edited by Chow, V. T., Academic, San Diego, Calif.

28. Chow, V. T., Maidment, D. R., Mays, L. W., (1988), 'Applied hydrlogy', McGrow-Hill International Edition, Civil Engineering Series.

29. Cooke, R. U., Warren, A., and Goudie, A. S., (1993), 'Desert geomorphology', University College London Press, London

30. Cordery, I. (1970),'Initial loss for flood estimation and forecasting', Journal of Hydraulics Division, HY12, Proceedings of the American Society of Civil Engineers, 2447-2465.

31. Cordery, I, and Pilgrim, D. H. (1970), 'Design hydrograph methods of flood estimation for small rural catchments', Civil Engineering Transaction, CE12, 2, Australia.

32. Cordery, I, and Pilgrim, D. H., and Doran, D. G., (1983), 'Some hydrological characteristics of arid western New South Wales', Hydrology and Water Resources Symposium 1983, 287-292, Inst. Engrs. Austral., National Conference Publ. No. 83/13

33. Corradini, C. F., Melon, and Smith, R.E, (1994), 'Modelling infiltration during complex rainfall sequences', Water Resources Research, 30(10), 2777-2784

34. Correl, C., Sempere-Torres, D., Revilla, M., and Berenguer, M. (2000),'A semi-distributed hydrological model using rainfall estimates by radar application to Mediterranean basins', Phys. Chem. Earth (B), Vol. 25, No. 10-12, 1133-1136.

35. Cowperwait, P. S. P., and O'Connel, P. E., (1994), 'A generalised point process model for rainfalls', Proc. R. Soc. Lond., A447, 23-37

36. Cox, D. R., and Isham, V., (1988), 'A simple spatial-temporal model of rainfall', Proceedings of the Royal Society, London, A415, 317-328.

37. Cox, D. R., and Isham, V., (1994), 'A stochastic model of precipitation', In statistics for environment 2; Water related issues, (Eds. V. Barnett and K. Turkman), 3-18. Wiley. Chichester, UK.

38. Crawford, N. H., and Linsley, R. K. (1966), 'Digital simulation in hydrology: Stanford Watershed Model IV.' Tech. Rep. No 39, Stanford Univ., Palo Alto., Calif.

39. Croke, B. F. W., and Jakeman, A. J. (2004),'A catchment moisture deficit module for the IHECRES rainfall-runoff model', Environmental Modelling & Software, 19, 1-5.

40. Dams and Moore, (1988), 'Representative basin study for wadis Yiba, Habawnah, Tabalah, Liyyah, and Lith', Report for Ministry of Agricultural and Water, Riyadh, Saudi Arabia.

41. Dawdy, D., R., and Bergman, J. M., (1969), 'Effect of rainfall variability on streamflow simulation, Water Resources Researches, 5(5), 958-966.

42. De Vera, M. R., (1984), 'Rainfall-runoff relationship of some catchments with karstic geomorphology under arid and semi-arid conditions', J. Hydrol. 68, 85-94

43. Diaz-Graados, Bras, R. L., and Valdes, J. B., (1983), 'A derived flood frequency distribution based on GIUH and the density function of rainfall excess', TR 292, Massachusetts Institute of Technology, Cambridge, Mass.

44. Drissel, J. C., and Osborn, H. B. (1968),'Variability in rainfall producing runoff from a semiarid rangeland watershed, Alamogordo Creek, New Mexixo', Journal of Hydrology 6, 194-201.

45. Domingo, F., Villagarcia, L., Boer, M. M., Alados-Arboedas, L., and Puigdefabregas (2001),'Evaluating the long-term water balance of arid zone stream bed vegetation using evaporation modelling and hillslope runoff measurements', Journal of Hydrology, 243, 17-30.

46. Dooge, J. C. I., (1959), 'A general theory of the unit hydrograph', J. Geophys. Res., 64(2), 241-256

47. Duan, Q., Gupta, V., and Sorooshian, S., (1992), 'Effective and efficient global optimization for conceptual rainfall-runoff models', Water Resources Research, 28(4), 1015-1031

48. Duan, Q., Gupta, V., and Sorooshian, S., (1993), 'A shuffled Complex Evaluation Approach for Effective Global Minimization', Journal of Optimization Theory and Applications, 76(3), 501-521

49. Duan, Q., Sorooshian, S., and Gupta, V., (1994), 'Optimal use of the SCE-UA global optimisation method for calibrating catchment models', Journal of Hydrology, 158, 265-284.

50. El-Hames, A. S. and Richards, K. S. (1998), 'An integrated, physically based model for arid region flash flood prediction capable of simulating dynamic transmission loss', Hydrological Processes 12, 1219-1232.

51. Evans, J. P., and Jakeman, A. J. (1998), 'Development of a simple, catchment-scale, rainfall-ET-runoff model', Environmental Modelling and Software, 13, 385-393.

52. FAO, (1981), 'Arid zone hydrology', Irrigation and drainage paper, 37, Food and Agriculture Organization of the United Nations. Rome.

53. Faures, J.-M., Goodrich, D. C., Woolhister, D. A, and Sorooshian, S. (1995),'Impact of small-scale spacial rainfall variability on runoff modelling', Journal of Hydrology, 173, 309-326.

54. Fentie, B., Yu, B., Silburn, M. D., and Ciesiolka, C. A. A (2002), 'Evaluation of eight different methods to predict hillslope runoff rates for a grazing catchment in Australia', Journal of Hydrology, 261, 102-114.

55. Florsheim, J. L., Keller, E. A., and Best, D. W., (1991), 'Fluvial sediment transport in response to moderate storm flows following chaparral wildfire', Ventura Country, South California, Bulletin Geological Society of America, 103, 504-511

56. French, R. H., (1987), 'Hydraulic processes on alluvium fans', Developments in Water Science no. 31, Elsevier, Amsterdam.

57. Fogel, M. M., and Duckstein, L., (1973) 'Prediction of convective storm runoff in semiarid regions', IAHS, No 96, Wellington Symposium.

58. Fowler, H. J., Kilsby, C. G., and O'Connel, P. E., (2000), 'A stochastic rainfall model for the assessment of regional water resources systems under changed climatic conditions', HESS, 4(2), 263-282

59. Freeze, R. A, (1972), 'Role of subsurface flow in generating surface runoff. 2:Upstream source areas', Water Res., 8, 5, 1272-1283

60. Sir Alexander Gibb and Parteners, (1976),'Water Resources Survey of Northern Oman', Final Report.

61. Graf, W. L., (1983), 'Downstream changes in stream power in the Henri Mountains', Utah, Annual of the Association of American Geographers, 73, 373-387

62. Grayson, R. B., I. D. Moore, and T. A. McMahon, (1992a), 'Physically based hydrological modelling, 1, A terrain-based model for investigative purposes', Water Resources Research 26, No. 10

63. Grayson, R. B., I. D. Moore, and T. A. McMahon, (1992b), 'Physically based hydrological modelling, 2, Is the Concept realistic' Water Resources Research 26, No. 10, 2659-2666

64. Green, W. H., and Amp, C. A., (1911), 'Studies on soil physics: Flow of water and air through soils', J. Agri. Sci., 4, 1024

65. Goodrich, D. C., (1990), 'Geometric simplification of distributed rainfall-runoff model over a range of basin scales' PhD, dissertation, University of Arizona, Tucson.

66. Goodrich, D. C., (1991), 'Catchment hydrology', Rev. Geophys., 29, 202-209

67. Gupta, V. K., Waymire, E. and Wang, C. T., (1980), 'A representation of an instantaneous unit hydrograph from geomorphology', Water Resour. Res., 16, No. 3, 855-862.

68. Hamlin, M. J., (1983), 'The significance of rainfall in the study of hydrological processes at basin scale', Journal of Hydrology, 65, 73-94.

69. Hasofer, A. M., and Lind, N. C., (1974), 'Exact invariant second-moment code format', J. of the Engineering Mechanics Division, ASCE, 100(EM1), 111-121

70. Holder, R. L., (1985).'Multiple Regression in Hydrology'. Wallengford, Institute of Hydrology, 120.

71. Hofman, G., and Rambo, J., (1995), 'Spatial and temporal rainfall characteristics of Wadi Al-Jizi Basin in Northern Oman', Proceedings, Water Resources Management in Arid Countries, Muscat, Mar 1995, 2, 411-414

72. Hornberger, G. M., and Boyer, E. W., (1995), 'Recent advances in watershed modelling', U. S. national report to IUGG, 1991-1994, Rev. Geophys., American Geophysical Union, Suppl., 949-957

73. Horton, R. E. (1945), 'Erosional development of streams and their drainage basins: Hydrological approach to quantitative geomorphology', Bull., Geol. Soc. Am., 56, 275-370

74. Hromadka, T. V. (2000, II),'A unit hydrograph rainfall-runoff model using MATHEMATICA', Environmental Modelling & Software, 15, 151-160.

75. Hromadka, T. V., Whitley, R. J., (2000), 'On formalization of HEC-1 and related systems', ASCE Journal of Hydrologic Engineering.

76. Hughes, D. A (1995),' monthly rainfall-runoff models applied to arid and semiarid catchments for water resource estimation purposes', Hydrological Sciences, 40, 6, 751-769.

77. Hughes, D. A., and Sami, K., (1992), 'Transmission losses to alluvium and associated moisture dynamics in a semiarid ephemeral channel system in Southern Africa', Hydrological Processes, Vol. 6, 45-53

78. Hydrologic Engineering Centre (HEC), (1968), 'HEC-1 Flood hydrograph package, user's manual', U. S. Army Corps of Engineers, Davis, Clif.

79. Izzard, C. F., (1944), 'The surface profile of overland flow', Trans., Am. Geophys. Union, 25(VI), 959-968

80. Jakeman, A. J, Hornberger, G. M. (1993), 'How much complexity is warranted in rainfall-runoff model?', Water Resources Research, Vol. 29, No. 8, 2637-2649.

81. Jakeman, A. J, Hornberger, G. M., Littlewood, I. G., Whithead, P. G., Harvey, J. W., and Bencala, K. E., (1992), 'A systematic approach to modelling the dynamic linkage of climate, physical catchment descriptors and hydrologic response components', Mathematics and Computer in Simulation, 33, pp 359-366

82. Jakeman, A. J, Littlewood, I. G., and Whitehead, P. G. (1990), 'Computation of the instantaneous unit hydrograph and identifiable component flows with application to two small upland catchments', Journal of Hydrology, 117, 275-300.

83. Jakeman, A. J, Littlewood, I. G., and Symon, H. D., (1991), 'Features and applications of IHACRES: A pc program for identification of unit hydrographs and component flows from rainfall, evapotranspiration and streamflow data', Proceedings of the 13th IMACS World Congress on Computation and Applied

Mathematics, Vol. 4, edited by R. Vichnevetsky and J. J. H. Miller, 1963-1967, Criterion, Dublin, Ireland

84. Jakeman, A. J, Littlewood, I. G., and Whitehead, P. G., (1993a), 'An assessment of dynamic response characteristics of stream flow in the Balquhidder catchments', Journal of Hydrology, 145, pp 337-355

85. Jakeman, A. J, Littlewood, Chen, T. H. Post, D. A., Hornberger, G. M., Littelewood, I. G., and Whitehead, P. G., (1993b), 'Assessing uncertainties in hydrological response to climate change at large scale', In W. B. Wilkinson Macroscale Modelling of the Hydrosphere, Proceedings of Yokohama Symposium, July 1993, IAHS Publications, no 214, pp 37-47

86. Jakeman, A. J, Post, D. A. and Beck, M. B. (1994a), 'From data and theory to environmental model; the case of rainfall runoff', Environmentrics, 5, 297-314.

87. Jakeman, A. J., Post, D. A., Post, D. A., Schreider, S. Y., and Ye, W., (1994b), 'Modelling environmental systems: Partitioning the water balance at different catchment scales', Computer Techniques in Environmental Studies, Vol, 2, Environmental Systems, edited by P. Zannetti, 157-170, Comput. Mech., Publ., Southampton, England

88. Jordan, P. R (1977),'Streamflow transmission losses in Western Kansas', Journal of Hydraulics Division, HY8, 905-919.

89. Jolley, T., (1995),'A water resource model for groundwater recharge studies'.

90. Julien, P. Y, and Saghafian, B, (1991), CASC2 manual- a two-dimensional watershed rainfall-runoff model, Civil Engineering Rep, CER90-91PYJ-BS-12, Colorado State University, Fort Collins, 66 pp.

91. Julien, P. Y., and Moglen, G. E., (1990), 'Similarity and length scale for spatially varied overland flow', Water Resour., Res., 26(8), 1819-1832

92. Julien, P. Y., and Moglen, G. E., and Sunada, G. U., (1988), CASC users manual – A finite element model for spatially varied overland flow simulation, Centre for Geosci., Rep., CER 87-88 GEO7, Colo, State Univ., Fort Collins.

93. Keulegan, G. H., (1994), 'Spatially variable discharge over a sloping plane', Trans., Am. Geophys. Union, 25 (VI), 959-965

94. Kibler, D. F, and Woolhiser, D. A, (1970),' The kinematic cascade as a hydrologic model', Hydrology pap 39, Colorado State University, Fort Collins

95. KINEROS2 website, (2005), 'http://www.tucson.ars.ag.gov/kineros', Agricultural Research Centre, United States Department of Agriculture.

96. Kirkparick, S. C., Gellatt D., and Vecchi, M.P., (1983), 'Optimisation by simulated annealing' Science, 220, 671-680

97. Krajewski, W. F., Lakshmi, V., Geogakakos, K. P., and Jain, S. C., (1991), 'A Monte Carlo study of rainfall sampling effect on a distributed catchment model', Water Resources Research, 27 (1), 119-128.

98. Laird, J. R., Harvey, M. D., (1986), 'Complex-response of drainage basin to fire', Drainage Basin Sediment Delivery, IAHS Publication, No. 159, 165-184

99. Lane, L. J, Diskin, M. H., and Renard, K. J., (1971),'Input-output relationships for am ephemeral stream channel system', J. Hydrology, 13, 22-40

100. Lane, L. J. (1990),'Transmission losses, flood peaks, and groundwater recharge', Reprinted from Hydraulics/Hydrology of Arid Lands, Proceedings of Int'l Symposium, HY &IR Div./ ASCE, San Diego, CA.

101. Lange, J., Leibundgut, C., and Asher-P. Schick, (2000), ' The important of single events in arid zone rainfall-runoff modelling', Physics Chemistry Earth (B), Vol 25, No 708, 673-677

102. Leavesley, G. H., Lichty, R. W., Troutman, B. M., and Saindon, L. G., (1983), 'Precipitation-runoff modelling system user's manual', USGS Water Resources Investigations, Rep. No. 83-4238, Denver

103. Leonard, J., Lane, M., (1990), 'Transmission losses, flood peaks, and groundwater recharge', Hydraulics/Hydrology of Arid Lands, PROCEEDINGS OF Ont'l. Symposium, HY &IR Div./ASCE, San Diego, CA/July 30 Aug 2

104. Lebel, T., Taupin, J.D. and D'Amato, N., (1997), ' Rainfall monitoring during HAPEX-Sahel: 1. General rainfall conditions and climatology', Journal of Hydrology. 188-189, 74-96.

105. Lighthill, M. J., and Whitham, G. B., (1955), 'On kinematic waves: 1. Flood movement in long rivers', Proc. R. Soc. London, Ser. A., 229, 281-316

106. Linsley, R. K., Kohar, M. A., and Paulus, J. L. H., (1949), 'Applied Hydrology', McGraw-Hill Book Company, 414-415

107. Littlewood, I.G., Down, K., Parker, J. R., and Post. D.A., (1997), 'User Guide', Centre for Ecology and Hydrology, Wallingford UK &Integrated Catchment Assessment and Management Centre, Australia, National University, Canberra, 99pp.

108. Lopes, V. L., (1996), 'On the effect of uncertainty in spatial distribution of rainfall on catchment modelling', Catena, 28, 107-119

109. McCarthy, G. T., (1938), 'The unit hydrograph and flood routing, North Atlantic Div., U.S., Corps of Engineers, New London, CT.

110. Mcintyre, Neil, Al-Qurashi, Aisha M., Wheater, H. (2007), 'Regression analysis of rainfall-runoff data from an arid catchment in Oman', Hydrological Science, Special Section: Dryland Hydrology in Mediterranean Regions, 52(6), 1103-118.

111. McIntyre, N., Jackson, B., Wade, A.J., Butterfield, D. Wheater, H., 2005. Sensitivity analysis of a catchment-scale nitrogen model. Journal of Hydrology 315, 71–92.

112. McIntyre, N., Al-Qurashi, A., Wheater, H.S., 2007, 'Analysis of rainfall-runoff events from an arid catchment in Oman', Hydrological Sciences Journal, Vol 5 (6), Special Section; Dryland Hydrology in Mediterranean Regions.

113. McKay, M. D., Beckman, R. J., and Conover, W. J., (1979), 'A comparison of three methods for selecting values of input variables in the analysis of output from a computer code' Technometrics, 21(2), 239-245

114. Ministry of Water Resources, (1995), 'Water Resources of the Sultanate of Oman; An introduction guide', Sultanate of Oman.

115. Michaud, J. & Sorooshian, S. (1994a), 'Comparison of simple versus complex distributed runoff models on midsized semiarid watershed', Water Research, Vol. 30, No. 3, 593-605.

116. Michaud, J. & Sorooshian, S. (1994b),'Effect of rainfall-sampling errors on simulations of desert flash floods', Water Resources Research, Vol. 30, No. 10, 2765-2775,

117. Melching, C.S., (1995), 'Reliability Estimation', Computer Models of Watershed Hydrology, edited by Singh, V. P., Water Resources Publications, USA

118. Metcalf and Eddy, Inc., Univ. of Florida, and Water Resources Engineers, Inc. (1971), 'Storm water management model, Vo. 1-Final report', EPA Rep. No. 11024doc07/71 (NITS PB-203289), EPA, Washington D. C.

119. Mimikou, M. A. (1983), 'Kalman filter empirical fitting on monthly rainfall-runoff responses', Nord, Hydrol. Vol 14 (2), 93-112.

120. Mimikou, M. A., Kouvopoulos, Y. S., and Cavadias, G. and Vayiannos, N. (1991), 'Regional hydrological effect of climate change', J. Hydrol., Vol. 132, 119-146

121. Mimikou, M. A., Kouvopoulos, Y. S., and Anagnostou (1992), 'The influence of basin aridity on the efficiency of runoff predicting models', Nordic Hydrology, 23, 105-120.

122. Ministry of Regional Municipalities, Environment and Water Resources (MRMEWR), (2001), 'Design flood estimation guide for Oman', Sultanate of Oman, Unpublished study, Sultanate of Oman

123. Ministry of Water Resources (MWR), (1995), 'Water Resources of the Sultanate of Oman An introduction guide', Sultanate of Oman.

124. Ministry of Water Resources (MWR), (1998), 'Rainfall intensities in Oman, Greatest recorded events and frequencies'. Unpublished report, Sultanate of Oman.

125. Ministry of Water Resources (MWR), (2000a), 'National Water Resources Master Plan', Sultanate of Oman

126. Ministry of Water Resources (MWR), (2000b), 'Wet periods in Oman in recent decades', Unpublished report, Sultanate of Oman

127. Minshall, N. E., (1960), 'Prediction storm runoff on small experimental watersheds', J. of Hydraul Div., Am. Soc. Civil Engrs.

128. Moore, I. D., and Mein, R. G., (1975), 'An evaluation of three rainfall-runoff models', Proc. Hydrology Sym., Sydney, Nat. Conf. Publ., 75/3, 122-126

129. Morgali, J. R, (1970), 'Laminar and turbulent overland flow hydrographs', Journal of the Hydraulics Division, Proceedings of the American Scociety of Civil Engineers, 91 (HY2), pp 441-460.

130. Morris, E. M., (1980), 'Forecasting flood flows in grassy and forested basins using a deterministic distributed mathematical model', IAHS Publications No. 129 (Hydrological forecasting), International Association of Hydrological Sciences, Wallingford, U.K., 247-255

131. Morris, E. M., and Woolhiser, D. A., (1980), 'Unsteady one-dimensional flow over a plane: Partial equilibrium and recession hydrograph', Water Resour. Res., 16(2), 355-360

132. Mosapha, M. F., (2001),'Development and regionalisation of rainfall-runoff models for the semi-arid Southern Africa catchments', PhD thesis, University of London, Imperial College of Science, Technology and Medicine.

133. Mott MacDonald International Ltd in association with Watson Hawksley, (1991), 'National water resources, Mater Plan', Vol. 2, Main Report, Ministry of Water Resources, Oman

134. Mott MacDonald International Ltd in association with Watson Hawksley, (1991), 'National resources modelling, Mater Plan', Vol. 3, Ministry of Water Resources, Oman

135. Mott MacDonald International Ltd, (1992),'Groundwater recharge Schemes for Saham-Sohar Area', Data Analysis Report, Hydrology 3/1B of 3 (Final), Ministry of Agriculture and Fisheries.

136. Mourits, L. J. M., and Salih, A. M.A (2002),'Wadi Hydrology and water resources management', Proceedings of UNESCO/NWRC/ASSAD, Technical Document in Hydrology, N.1, UNESCO, Cairo Office

137. Nash, J. E., (1957), 'The form of instantaneous unit hydrograph', Hydrol. Sci. Bull., 3, 114-121

138. Nash, J. E., and Sutcliffe, J. V., (1970), 'River flow forecasting through conceptual models', I. A. discussion of principles, J. Hydrol., 10, 282-290

139. Neil, H., Paturel, J-E, and Sevat, E (2003),' Study of parameter stability of a lumped hydrologic model in a context of climatic variability', Journal of Hydrology, 278, 213-230.

140. Northrop, P., (1996), 'Modelling and statistical analysis of spatial-temporal rainfall fields', PhD thesis, Department of Statistical Science, University College, London

141. Northrop, P., (1997), 'A clustered spatial-temporal model of rainfall' Proce. Roy. Soc., London, A545, 1875-1888

142. Nouh, M., (1986), 'A construction damages due to floods in Wadi Ad-dilah', Technical report prepared on the National Project Number AR-5-62 for King Abdul Aziz City for Science and Technology, Riyadh, Saudi Arabia

143. Nouh, M., (1990), ' Flood hydrograph estimation from arid catchment morphology', Hydrological Processes, Vol. 4, 103-120

144. Ogden, F. L., and Julien, P. Y., (1993),'Runoff sensitivity to temporal and spatial rainfall variability at runoff plane and small basins', Water Resources Research, Vol 29, No 8, 2589-2597.

145. Ogden, F. L., and Julien, P. Y., (1994),'Runoff model sensitivity to radar rainfall resolution', Journal of Hydrology, 158, 1-18

146. Onof, C., and Wheater, H. S., (1993), 'Modelling of British rainfall using a random parameter Bartlett-Lewis Rectangular Pulse Model', J. Hydrology, 149, 67-05

147. Onof, C., and Wheater, H. S., (1994), 'Improved fitting of the Bartlett-Lewis Rectangular Pulse Model for hourly rainfall', J. Hydrologic Science, 39(6), 663-680

148. Orellana, B, McIntyre, N., Wagner, T., Jackson, B.,'A modular framework for the development of semi-distributed rainfall-runoff models', waiting for publication

149. Osborn, H. B., Hickok, R. B, (1968), 'Variability of rainfall affecting runoff from a semiarid rangeland watershed', Water Resources Res., 4(1), 199-203.

150. Osborn, H. B., Lane, L. J. (1969),'Precipitation-runoff relations for very small semiarid rangeland watersheds, Water Resources Research, Vol. 5, No. 2, 419-425.

151. Osborn, H. B., Lane, L. J. (1971),'Depth-area relationships for thunderstorms rainfall in South-eastern Arizona', American Society of Agricultural Engineers, Vol. 15, No. 4, 670-680.

152. Osborn, H. B., Lane, L. J., and Myers, V. A (1979),'Rainfall/watershed relationships for Southwestern thunderstorms', Soil and Water Division of ASAE, No. 77, 81-91.

153. Osborn, H. B. and Renard, K. G (1973), 'Thunderstorm runoff on the Walnut Gulch experimental watershed, Arizona, U. S. A., Journal of Hydrological Division, Proceeding, ASCE 99, 1129-1145.

154. Osborn, H. B. (1983),'Timing and duration of high rainfall rates in the Southwestern United States', Water Resources Research, Vol. 19, 1036-1042.

155. Palacios-Velez, O. L., and Cuevas-Renaud, B., (1992), 'SHIFT: a distributed runoff model using irregular triangular facets', J. Hydrol., 134, 35-55

156. Parlange, J-Y, Rose, CW, Sander, G., (1981), 'Kinematic flow approximation of runoff on a plane: an exact analytical solution', Journal of Hydrology, 52, 1-2, p171

157.

158. Parrisopoulos, G. A., and Wheater, H. S. (1990), 'Numerical study of the effects of layers on unsaturated-saturates two-dimensional flow', Water Res. Plan. Manage., 4, 97-122

159. Parrisopoulos, G. A., and Wheater, H. S. (1992a), 'Experimental and numerical infiltration studies in a wadi stream-bed', J. Hydr, Science, 37, 27-37

160. Parrisopoulos, G. A., and Wheater, H. S. (1992b), 'Effects of hysteresis on groundwater recharge from ephemeral flows', Water Resour. Res., 28(1), 3055-3061

161. Penman, H. L., (1948), 'Natural evaporation from open water, bare soil and grass', Proc. R. Soc. London, Ser. A., 193, 120-145

162. Perrin, C., Michel, C., Andreasian, V., (2001), 'Does a large number of parameters enhance model performance? Comparative assessment of common catchment model structures on 429 catchments', J. Hydrology, 242, 275-301

163. Pilgrim, D. H., Chapman, T. G., and Doran, D. G. (1988),'Problems of rainfall-runoff modelling in arid and semiarid regions', Hydrological Sciences, 33, 4, 8/1988, 379-400.

164. Pilgrim, D. H., Cordery, I., and Boyd, M. J., (1982), 'Australian developments in flood hydrograph modelling', in rainfall-runoff relationships, 37-48, Water Resources Publications, Litton, Colorado, USA

165. Pitman, W. V (1973), 'A mathematical model for generating monthly river flows from meteorological data in South Africa', Report no 2/73, Hydrological Research Unit, University of the Witwatersrand, Johannesburg, South Africa.

166. Porter, J. W and McMahon, T. A. (1971), 'A model for the simulation of streamflow records from climatic records', J. Hydrology, 33, 297-324.

167. Porter, J. W and McMahon, T. A., (1975), 'Application of a catchment model in south eastern Australia', J. Hydrol., 24, 121-134

168. Porter, J. W and McMahon, T. A. (1976), The Monash model:user manual for daily program, Hydrolg. Res. Rep. 2/76, Department of Civil Engineering, Monash University, Victoria, 41pp

169. Post, D. A. and Jakeman, A. J. (1999),'Predicting the daily streamflow of ungauged catchments in S. E. Australia by regionalising the parameters of lumped conceptual rainfall-runoff model', Ecological Modelling, 91-104.

170. Press, W. H., Teukosky, S. A., Vetterling, W. T., and Flannery, B. P. (1992), 'Numerical recipes in Fortran: The art of scientific computing', 2nd addition, Cambridge Univ. Press, New York

171. Puls, L. G., (1928), 'Flood regulation of the Tennessee River', Proc. 70th Congress, 1st Session, H. D., 185, Part 2, Appendix B

172. Rackwitz, R., (1976), 'Practical probabilistic approach to design', Comite Eurpean du Beton, Paris, Bulletin No. 112

173. Renard, K. G., Drissel, J. C., and Osborn, H. B. (1970), 'Flood peaks from small southwest range watershed', Journal of Hydraulics Division (Proceedings of the American Society of Civil Engineers), HY 3, 7161-785.

174. Renard, K. G, Asce, M, and Keppel, R. V (1966),'Hydrographs of ephemeral streams in the southwest', Journal of Hydraulics Division (Proceedings of the American Society of Civil Engineers), HY 2, 33-53.

175. Rodier, J. A (1985),'Aspects of Arid Zone Hydrology', Facets of Hydrology, Vol. II, Edited by Rodda, J. C., John Wiley & Sons Ltd.

176. Rodriguez-Iturbe, I., Cox, D. R., and Isham, V., (1987), 'Some models for rainfall based on stochastic point processes', Proceedings of Royal Society, London, A410, 269-288.

177. Rodriguez-Iturbe, I., Cox, D. R., and Isham, V., (1988), 'A point process model for rainfall; further developments', Proceedings of Royal Society, London, A417, 283-298.

178. Rodriguez-Iturbe, I., and Eagleson, P. S., 'Mathematical models of rainstorm events in space and time', Water Resour., Res., 23(1), 181, 181-190

179. Rodriguez-Iturbe, I., and Valdes, J. B., (1979), 'The geomorphologic structure of hydrologic structure of hydrologic response' Water Resour. Res., 15, 1409-1420

180. Rose, C. W. (1968), 'Water transport in soil with a daily temperature wave', Australian Journal of Soil Res., 6, 31-57

181. Rovey, E. W., Woolhiser, D. A., and Smith, R. E., (1977a), 'Urban storm runoff model', Journal of Hydraulics Division, American Society of Engineers, 103 (HY11), pp1339-1351.

182. Rovey, E. W, D. A. Woolehiser, and R. E. Smith, (1977b), 'A distributed kinematic model of upland watersheds', Hydrology paper 93, Colorado State University, Fort Collins.

183. Saleh, Abdin M. A., (1988), 'Arid lands: Evapotranspiration under extremely arid climates', in Water Resources Environmental, Civil Engineering Practice, Ch 10, pp305-324

184. Saleh, Abdin M. A., and Uygur Sendil, (1984), Evapotranspiration under extremely arid climates', J. of Irrigation and Drainage Engineering, Vol. 110, No 3, pp 289-303

185. Samuel, C. R, (1999), 'Stochastic rainfall modelling of convective storms in Walnut Gulch, Arizona', PhD thesis, Imperial College London.

186. Schick, A. P. (1988), 'Hydrologic aspects of flood in extreme arid environments ', Flood Geomorphology, ed, by V. R. Baker, R. C Kochel & P. C. Patton, 189-203, Wiley, New York.

187. Schreiber, D. L, (1970), 'Overland flow simulations by a nonlinear distributed parameter model', Ph.D. thesis, Washington State University, Pullman

188. Schreiber, D. L, and Kincaid, D. R., (1967), 'Regression models for predicting on-site runoff from short-duration convective storms, Water Resources Res., 3(2), 389-395

189. Schwartz, M., and Show, L., (1975), 'Signal processing, discrete spectral analysis, detection and estimation ', McGraw Hill Co., New York, 331-387

190. Shaw, Elizabeth M, Lynn, P. P. (1972),'Areal rainfall evaluation using two surface fitting techniques', Bulletin of International Association of Hydrological Sciences, XVII, 4, 12

191. Sharma, K. D. and Murthy, J. S. R. (1998), ' A practical approach to rainfall-runoff modelling in arid zone drainage basins', Hydrological Science, Journal 43, 331-348.

192. Sharma, K. D. and Murthy, J. S. R. (1996), 'Ephemeral flow modelling in arid regions', J. Arid Environments, 33, 161-178

193. Sharma, K. D., Choudhary, J.S. and Vangani, N. S., (1984), 'Transmission losses and quality changes along a desert stream, the Luni Basin in NW India , Journal of Arid Environments, 7, 255-262

194. Sharma, K. D., and Vangani, N. S., (1982), 'Flash flood of July 1979 in the Luni Basin: a rare event in the Indian desert', Hydrological Science Journal, 27, 365-377

195. Sherman, L. K (1932), 'Streamflow from rainfall by the unit-hydrograph method', Engineering News Record, 108, 501-505.

196. Simmers, I (2003),'Understanding water in a dry environment, Hydrological process in arid and semiarid zones', International Contribution to Hydrogeology, 23, International Association of Hydrogeologists, UNESCO.

197. Semmens, D.J., Goodrich, D.C., Unkrich, C.L., Smith, R.E., Woolhiser, D.A., Miller, S.N., 2005. KINEROS2 and the AGWA Modeling Framework. Chapter 6, Proceedings of the GWADI International Modelling Workshop, Roorkee, India, 30p. www.gwadi.org/shortcourses

198. Singh, V. P., and Woolhiser, D. A., (2002), 'Mathematical modelling of watershed hydrology', American Society of 150th Annirversary, Civil Engrs. Paper, Journal of Hydrologic Engineering, Vol. 7, No. 4.

199. Singh, V. P., and Woolhiser, D. A., (1976), 'Sensitivity of linear and nonlinear surface runoff models to input errors', Journal of Hydrology, 29, 243-249.

200. Singh, V. P, (1995), 'Computer models of watershed hydrology', Water Resources Publications, Colorado, U.S.A.

201. Singh, V. P, and Amenian, H., (1984), 'A rainfall-runoff model for ungauged basins' Proc. Fourth Congress of Asian and Pacific Regional Div., IAHR, Chiang Mai, Thailand, 1095-1109

202. Sir Alexander Gibb and Partners and the Institute of Hydrology, (1976), 'Water Resources Survey of Northern Oman', Final Report and Appendices, Ministry of Water Resources, Oman

203. Sivapalan, M., and N. R. Viney, (1994a), ' Application of nested catchment model predicting the effects of changes in forest cover', in Proceedings International Symposium on Forest Hydrology, edited by T. Ohta, 315-322, Int. Union of For. Res. Org., Vienna, Austria

204. Sivapalan, M., and N. R. Viney, (1994b), ' Large scale catchment modelling to predict the effects of land use changes', Water J., 21 (1), 33-37

205. SMEC (1991), Botswana National Water Master Plan Study, Vol. 6; Hydrology, Prepared by Snowy Mountains Engineering Corporation Ltd., WLPU Consultant and Swedish Geological International AB. Government of Botswana, Department of Water Affairs, Gaborone

206. Smith, R. E., '(1983), 'Flux infiltration theory for use in watershed hydrology', in Procs. National Conference on Advances in Infiltration, American Soc. Agricultural Engs., 313-323

207. Smith, R. E., '(1990), 'Analysis of infiltration through a two-layer soil profile', Soil Science Soc. of America J., 54, 1219-1227

208. Smith, R.E., Corradini, C., and Melone, F., (1993), 'Modelling infiltration for multistorm runoff events', Water Resources Research, 29(1), 133-144

209. Smith, R.E., Goodrich, D.C., Woolhiser, D.A., Unkrich, C.L., 1995, KINEROS - A kinematic runoff and erosion model. In: Singh, V.J., (Ed.), Computer Models of Watershed Hydrology. Water Resources Publications, Highlands Ranch, Colorado, pp. 697-732.

210. Smith, R.E., and Paralange, J-Y, (1978), 'A parameter-efficient hydrologic infiltration model', Water Resources Research, 14(3), 533-538

211. Soil Conservative Service (SCS), (1956), 'Supplement A, Section 4, Chapter 10, Hydrology', National engineering handbook, USDA, Washington, D. C.

212. Sorman, A. U., and Abdulrazzaq, J. (1993a),'Infiltration-recharge through wadi beds in arid region', Hydrological Sciences, 38, 3, 6/1993, 173-186.

213. Sorman, A. U., and Abdulrazzaq, J. (1993b), 'Flood hydrographs estimation for ungauged wadis in Saudi Arabia, L. Water Res. Plan. & Manag., 119-1, 45-63

214. Sophocleous, M., and Perkins, S. P. (2000),'Methodology and application of combined watershed and groundwater models in Kansas', Journal of Hydrology, 236, 185-201.

215. Sorooshian, S., Gupta, V. K. (1995), 'Model Calibration', Computer Models of Watershed Hydrology, edited by Singh, V. P., Water Resources Publications, USA

216. Stewart, E., (1986), 'A modelling study of the spatial and temporal variability of rainfall in south-west Saudi Arabia', MSc thesis, Univ. of London, 175 pp.

217. Storm, B., Jensen, K. H., and Refsgaard, J. C., (1988), 'Estimation of catchment rainfall uncertainty and its influence on runoff prediction, Nordic Hydrology, 19(2), 77-88.

218. Sugawara, M. (1967), 'The flood forecasting by a series storage type model', Int. Symposium Floods and their Computation, International Association of Hydrologic Sciences, 1-6

219. Sugawara, M. (1974), 'Tank model and its application to Bird Creek, Wollombi Brook, Bikin River, Kitsu River, Sanga River, and Nam Mune', Research Note, National Research Centre for Disaster Prevention, No 11, Kyoto, Japan, 1-64

220. Syed, K H., Goodrich, D. C., Myers, D. E., Sorooshian, S. (2003),' Spatial characteristics of thunderstorm rainfall fields and their relation to runoff', Journal of Hydrology, 271, 1-21

221. Telvari, A., Cordery, I., and Pilgrim, D.H., (1998), 'Relations between transmission losses and bed alluvium in an Australian arid zone stream', In Hydrology in changing environment, Eds. Howard Wheater and Celia Kirby, Wiley, Vol. II, pp 361-36

222. Thornes, J. B., (Ed.), (1990), 'Vegetation and erosion', Processes and Environments, Willey, Chichester

223. Thornes, J. B., (1994), 'Catchment and channel hydrology' In: Abrahams, A. D., Parsons, A. J., (Eds), Geomorphology of Desert Environments, Chapman & Hall, London, 257-287

224. Thornwait, C. W., (1948), 'An approach towards a rational classification of climate', Geogr., Rev., 38, 55-94

225. Toth, E., Montanari, A. Brath, (2000), 'Comparison of short-term rainfall prediction models for real-time flood forecasting', Journal of Hydrology, 239, 132-147

226. Tooth, S. (2000),'Process, form and change in dryland rivers: a review of recent research', Earth Science Review, 51, 67-107.

227. Travers Morgan, (1993), 'Detailed hydrotechnical recharge studies in Wadi Ghulaji', Final Report to Ministry of Water Resources, Oman

228. Taylor, G. I., (1938), 'Statistical theory of turbulence ', Proc. Roy. Soc., London, A164-490

229. UNESCO, (1979), 'Map of the world distribution of arid regions', Accompanied by explanatory note, MAB Technical Notes; no. 7, Paris: UNESCO. 54 p.

230. United States Department of Agriculture, Agricultural Research Service (USDA), (1990), KINEROS; A kinematic runoff and erosion model: Documentation and user manual, US, ARS-77, 130p.

231. Wagner, T, Lees, M. J., and Wheater, H. S., (1999), 'A generic rainfall-runoff modelling toolbox', Eos. Trans. AGU, 80(17), Fall Meet. Suppl., F203. Wheater H. S., Jakeman, A. J., and Beven, K. J., (1993). Chapter 5-Process and directions in rainfall-runoff modelling, In Jakeman, A. J., Beck, M. B., and McAleer, M. J., (1993), 'Modelling change in environmental systems', John Wiley & Sons Ltd, UK, 101-132.

232. Wagner, T, Lees, M. J., and Wheater, H. S. (2001a), 'A framework for the development and application of parsimonious hydrological models', To appear in Sing, Frevert and Meyer (Eds.), 'Mathematical models of small watersheds hydrology', Vol 2., Water Resources Publication, LLC, USA.

233. Wagner, T, and Lees, M. J., (2001),'Rainfall-runoff modelling toolbox user manual', Imperial College, London.

234. Wagner, T, Wheater, H. S., and Gupta, V., (2004), 'Rainfall-runoff modelling in gauged and ungauged catchments', Imperial College Press, London.

235. Wallace and Lane, L. J., (1978), 'Geomorphic features affecting transmission losses potential on semiarid watersheds', Hydrol. Water Resour., Arizona Southwest 8, 157-164

236. Walters, M. O. (1989), 'A unique flood event in an arid zone', Hydrological Processes, Vol. 3, 15-24.

237. Walters, M. O. (1990), 'Transmission losses in arid region', Journal of Hydraulic Engineering, 116, 1, 127-138

238. Weeks, W. D., and Hebbert, R. H. B., (1980), 'A comparison of rainfall-runoff models', Nord. Hydrol., 11, 7-24

239. Wheater, H.S, (1981), 'Northern Oman Flood Study', Imperial College-London.

240. Wheater, H.S. (2005),'Modelling hydrological processes in arid and semi-arid areas'. G-Wadi Asia Workshop, Global Network for Water and Development Information in Arid and Semi-Arid Regions of Asia, Roorkee, India

241. Wheater, H.S., Al-Qurashi, A. M. H, McIntyre, N., (2008) 'Hydrological process in wadis-scientific and practical aspects', Proceedings of the 4th International Conference on Wadi Hydrology, Seeb, Oman, 2-4 December 2007, publisher - Ministry of Regional Municiplaities and Water Resources

242. Wheater, H. S., and Bell, N. C, (1983),'Northern Oman flood study', Proceedings Inst of Civil Eng., 2, 57, 453-473.

243. Wheater, H.S. and Brown, R. P. C. (1989), 'Limitations of design hydrographs in arid areas-an illustration from south west Saudi Arabia', British Hydrological Society National Symposium, Sheffield, Sep 1989.

244. Wheater, H.S., Butler, A. P, Stewart, E. J., and Hamilton, G. S. (1991a),'A multivariate spatial-temporal model of rainfall in southwest Saudi Arabia. I. Spacial rainfall characteristics and model formulations', Journal of Hydrology, 125, 175-199.

245. Wheater, H.S., Butler, A. P, Onof, C., and Hamilton, G. S. (1991b),'A multivariate special-temporal model of rainfall in southwest Saudi Arabia. II. Regional analysis and long-term performance', Journal of Hydrology, 125, 201-220.

246. Wheater, H.S., Jakeman, A. J., and Beven, K. J. (1993),'Progress and Directions in rainfall-runoff modelling', Modelling Change in Environmental Systems, edited by Jakeman, A. J., Beck, M. B. and McAleer, M. J., Ch. 5, 101-132, John Wily, New York

247. Wheater, H. S., Jolly., T. J. and Peach, D. (1995),'A water resources simulation model for groundwater recharge studies: An application to Wadi Ghulaiji, Sultanate of Oman', Proc, Int. Conf. on Water Resources Management in Arid Countries, Muscat, 502-510.

248. Wheater, H. S., Isham, V. S., Cox, D. R., Chandler, R. E., Kakou, A., Northrop, P. J., Oh, L., Onof, C., Rodriguez-Iturbe, I. (2000), 'Spatial-temporal rainfall fields; modelling and statistical aspects', Hydrology and Earth System Sciences, 4(4), 581-601.

249. Wheater, H. S., Larentis, P. and Hamilton, G. S (1989), 'Design rainfall characteristics for south-west Saudi Arabia', Proc. Instn. Civ. Engrs, Part 2, 87, 517-538.

250. Wheater, H. S, Woods Ballard, B. and Jolly, T. J (1997), 'An integrated model of arid zone water resources: evaluation of rainfall-runoff simulation performance', Sustainability of Water Resources under Increasing Uncertainty (Proceeding of the Rabat Symposium) IAHS Publ, No 240, 395-05.

251. Wheater, H. S. (2002a),'Hydrological processes in Arid and semiarid areas', Hydrology of Wadi Systems, IHP Regional Network on Wadi Hydrology in the Arab Region, IHP-V, No. 55.

252. Wheater, H. S. (2002b), 'Progress in and prospects for fluvial flood modelling', Proc. Royal Society, 360, 1409-1431.

253. Wheater, H. S, and Al-Weshah, R. A. (2002),'Hydrology of Wadi Systems', IHP-V, No. 55, UNESCO, Paris

254. Wills, W.G., (1981), 'Some effects of brushfires on erosion pro-cesses in coastal Southern California', In: Davies, T. R. H., Pears, A. J. (Eds.), Erosion and Sediment Transport in Pacific Rim Steeplands, IAHS-AISH, Publication No. 132, 305-342

255. Wilson, C. B., Valdes, J. B., and Rodriguez-Iturbe, (1979), 'On the influence of the spatial distribution of rainfall on storm runoff', Water Resources Research, 15 (2), 321-328.

256. Wong, T. H. F., and Mustinov, M., (1987), 'Parameter optimisation of Monash Model in an arid catchment', Civ. Eng. Aust., CE29(4), 205-210

257. Woolhiser, D. A, C, L. Hanson, and A, R. Kuhlman, (1970), 'Overland flow on rangeland watersheds', Journal of Hydrology, New Zealand, 9 (2), pp 336-356

258. Woolhiser, D. A, and Liggett, J. A., (1967), 'Unsteady, one-dimensional flow over a plane—the rising hydrohraph', Water Resour. Res., 3(3), 753-771

259. Woolhiser, D.A., Smith, R.E., Goodrich, D.C., (1990), 'KINEROS, A Kinematic Runoff and Erosion Model: Documentation and User Manual', U S, Department of Agriculture, Agricultural Research Service, ARS-77, 130p.

260. Woolhiser, D.A., Smith, R.E., and Giraldez, J.-V., (1997), 'Effects of spatial variability of saturated hydraulic conductivity on Hortonian overland flow', Water Resources Research, Vol 32(3), 671-678

261. Wurbs, R. A., (1988), 'Dissemination of generalized water resources models in the United States', Water Int., 23, 190-198

262. Yang, C., Chandler, R.E., Isham, V.S. and Wheater, H.S., 2005. Spatial-temporal rainfall simulation using generalized linear models. Water Resources Research, Vol. 41, W11415, doi 10.1029/2004 WR003739.

263. Yatheendradas, S., Wagener, T., Gupta, H., Unkrich, C., Goodrich, D., Schaffner, M., Stewart, A., 2007. Investigating uncertainty in distributed flash-flood forecasting for semi-arid regions. Water Resources Research, in review.

264. Ye, W., Bates, B. C., Viney, Sivapalan, N. R. and Jakeman, A. J. (1997), 'Performance of conceptual rainfall-runoff models in low-yielding ephemeral catchment' Water Resources Research, Vol. 33, No. 1, 153-166.

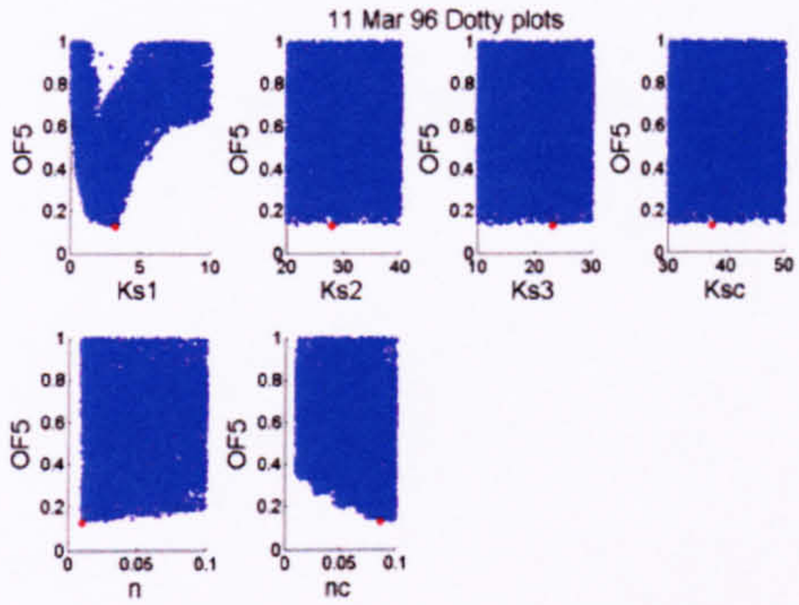
Appendix A

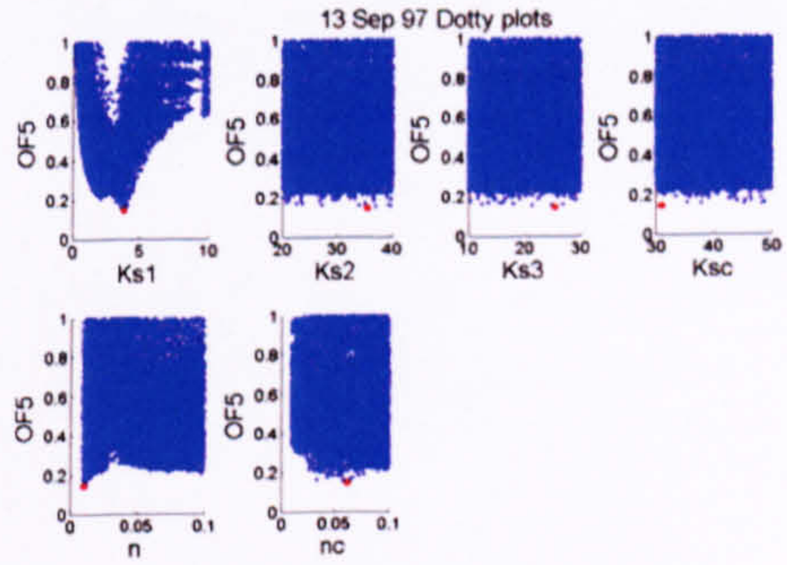
KINEROS2

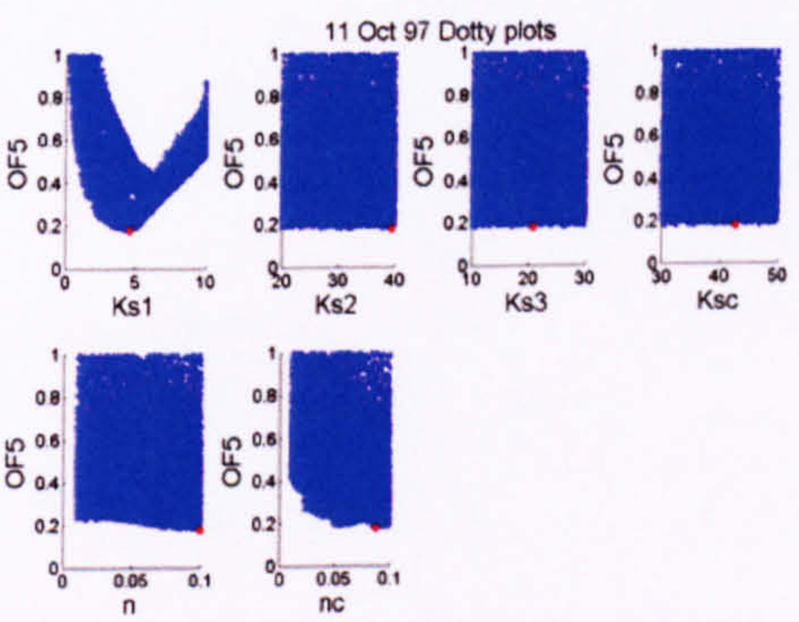
Dotty Plots

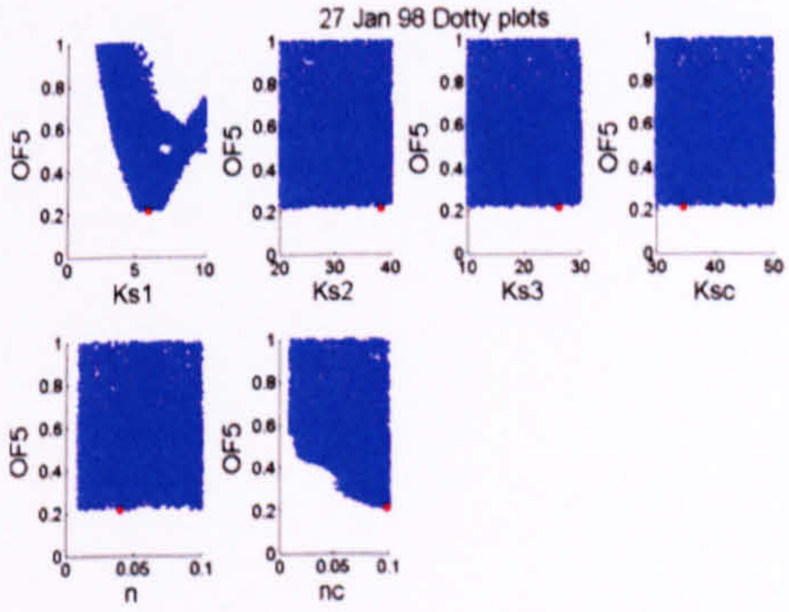
(Selected Events)

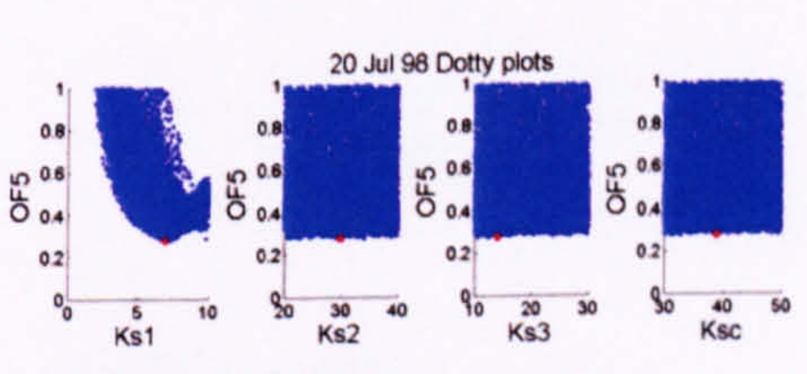
8-parameters, G=0

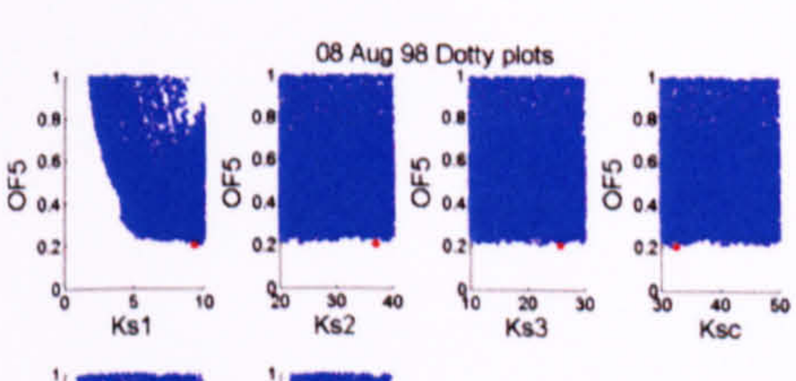


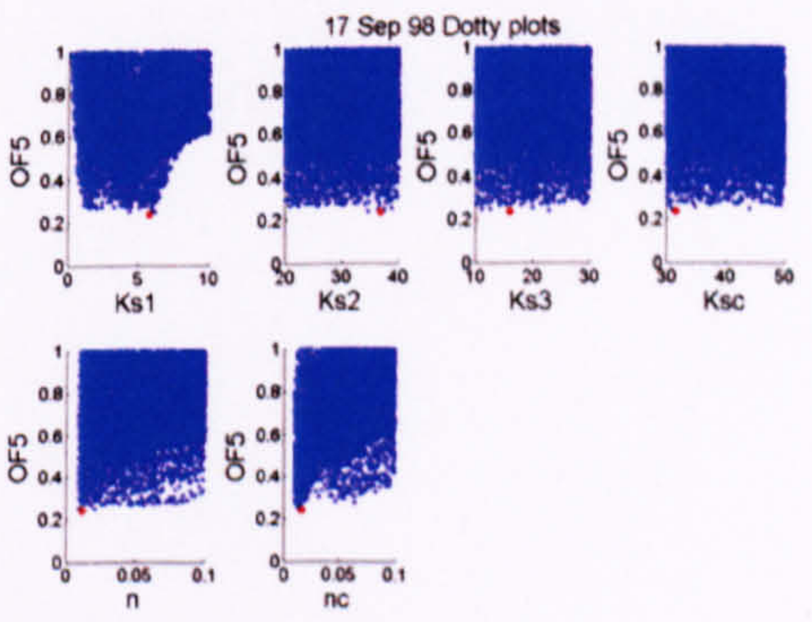


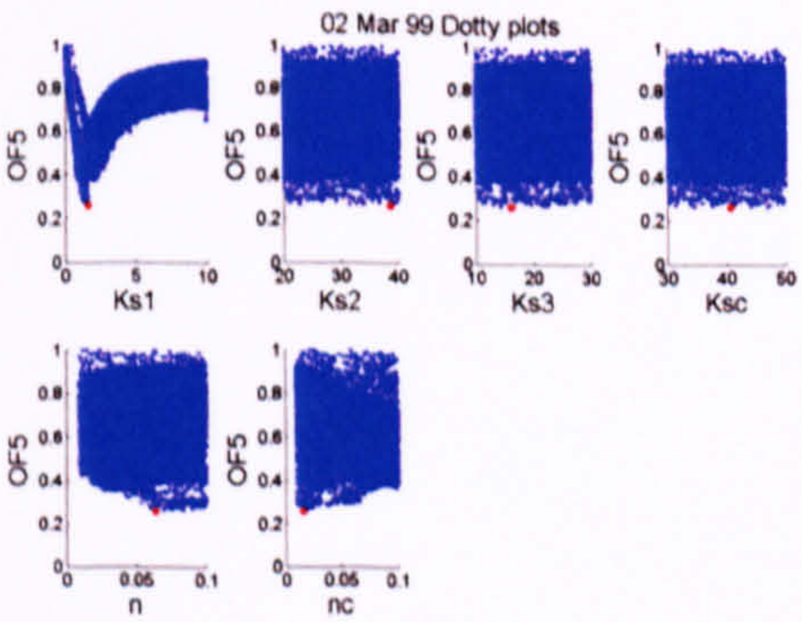




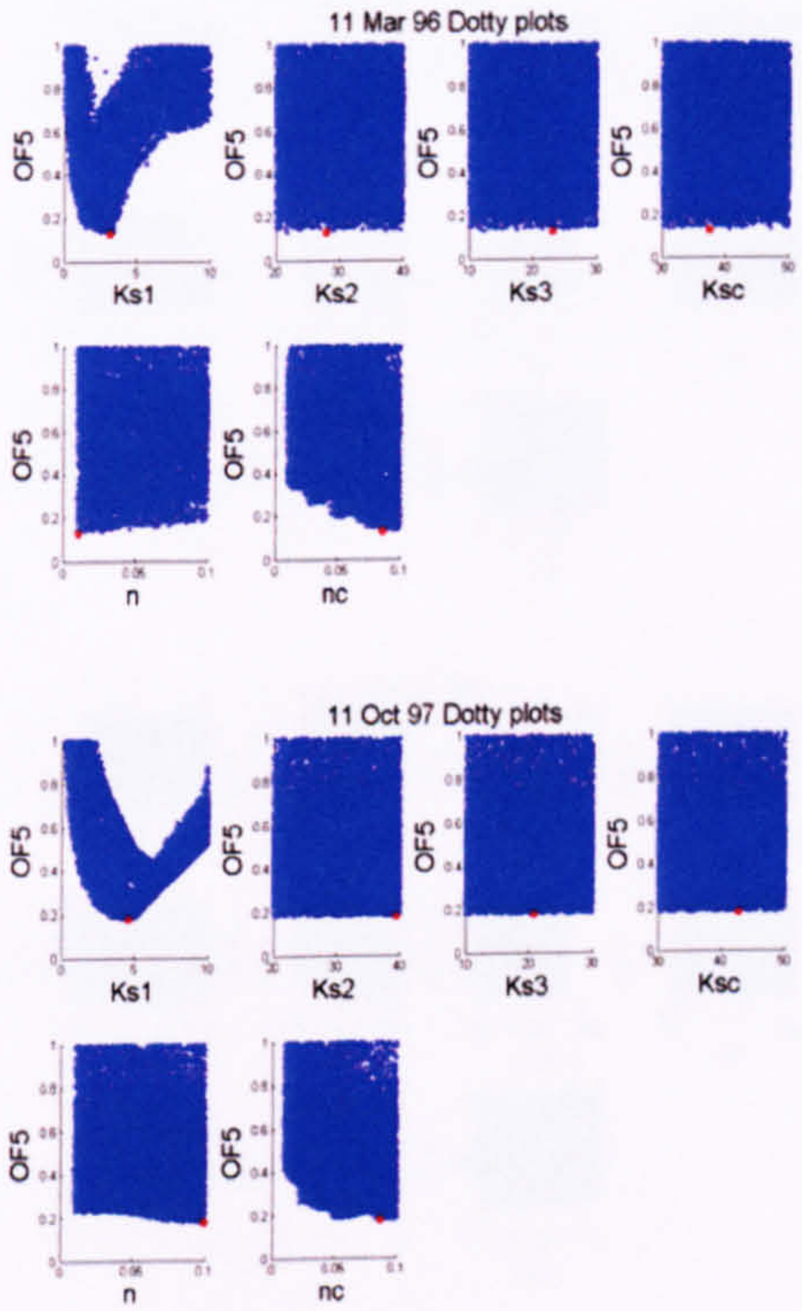


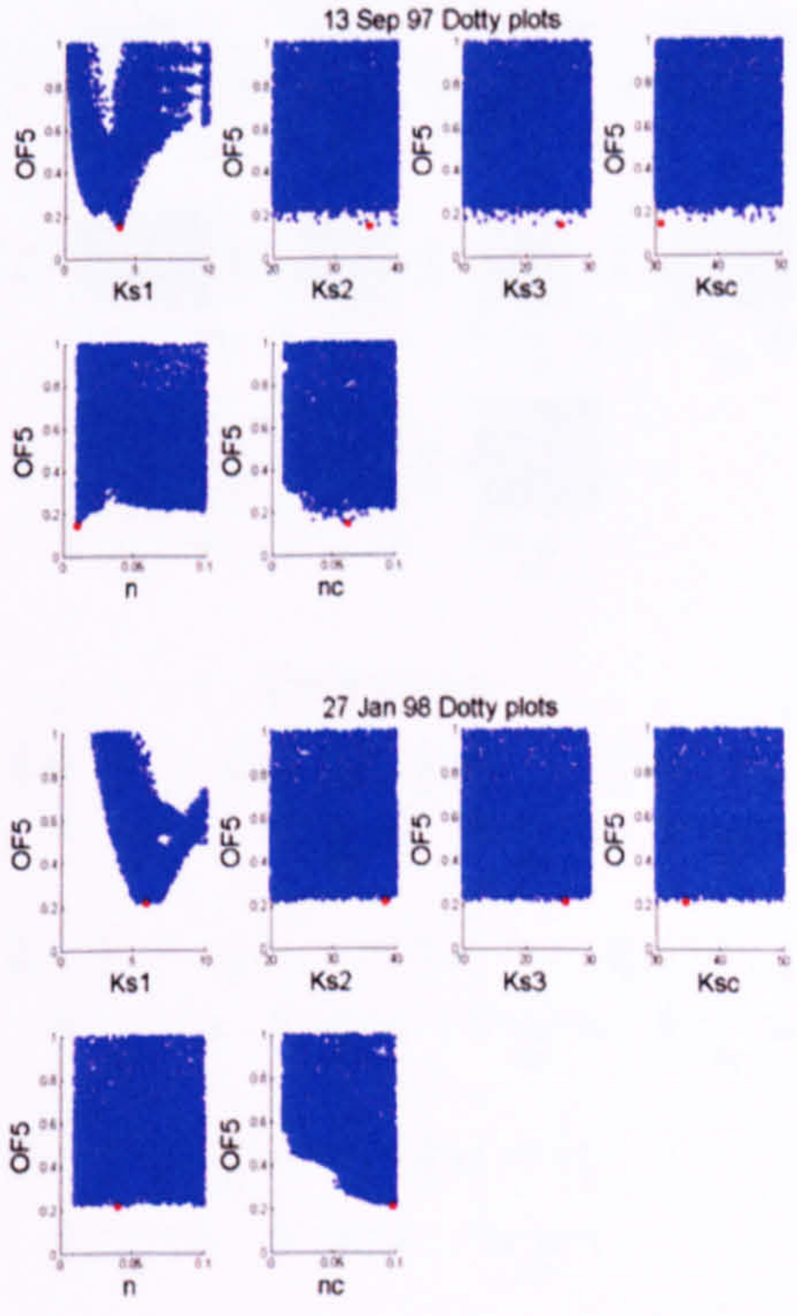


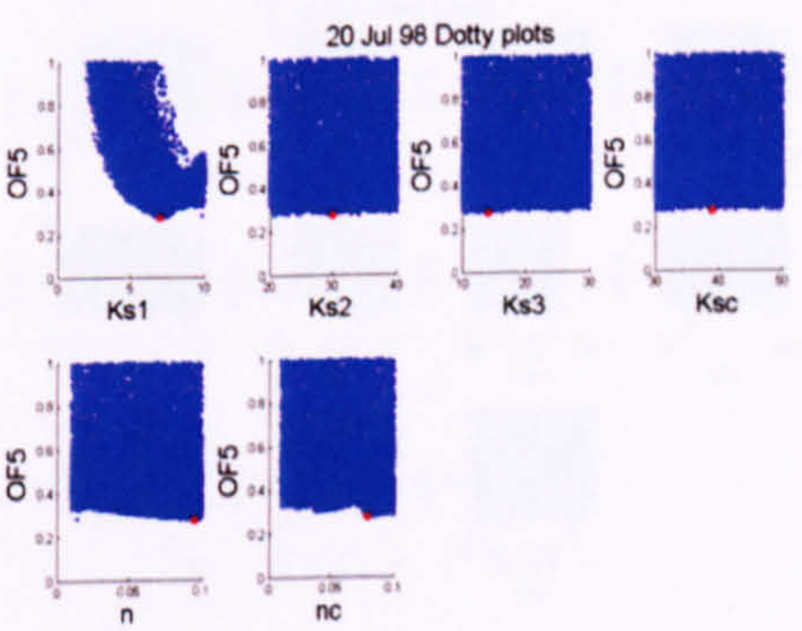


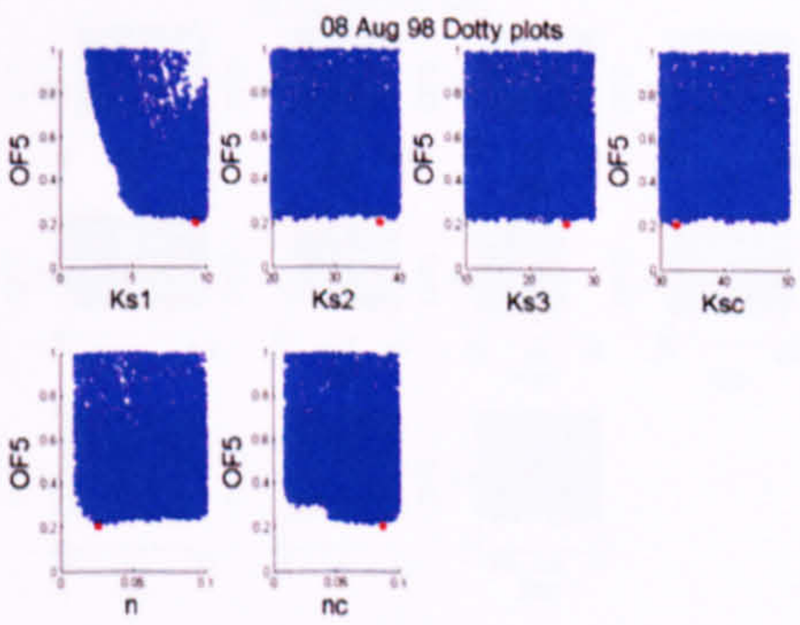


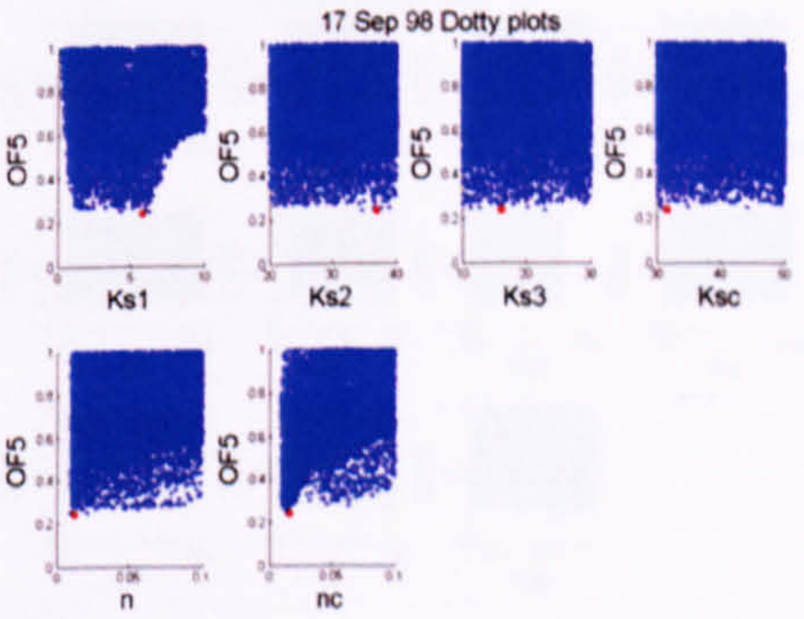
6-parameters, G=0

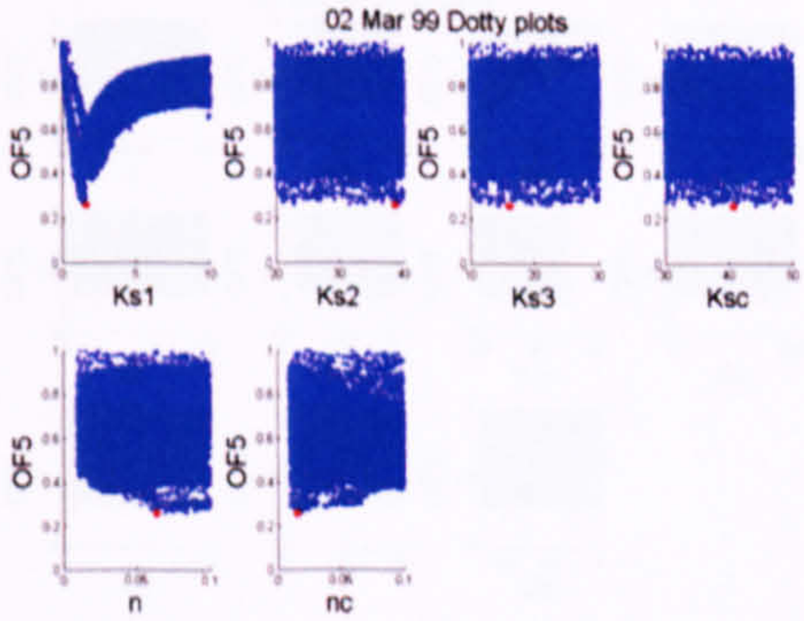




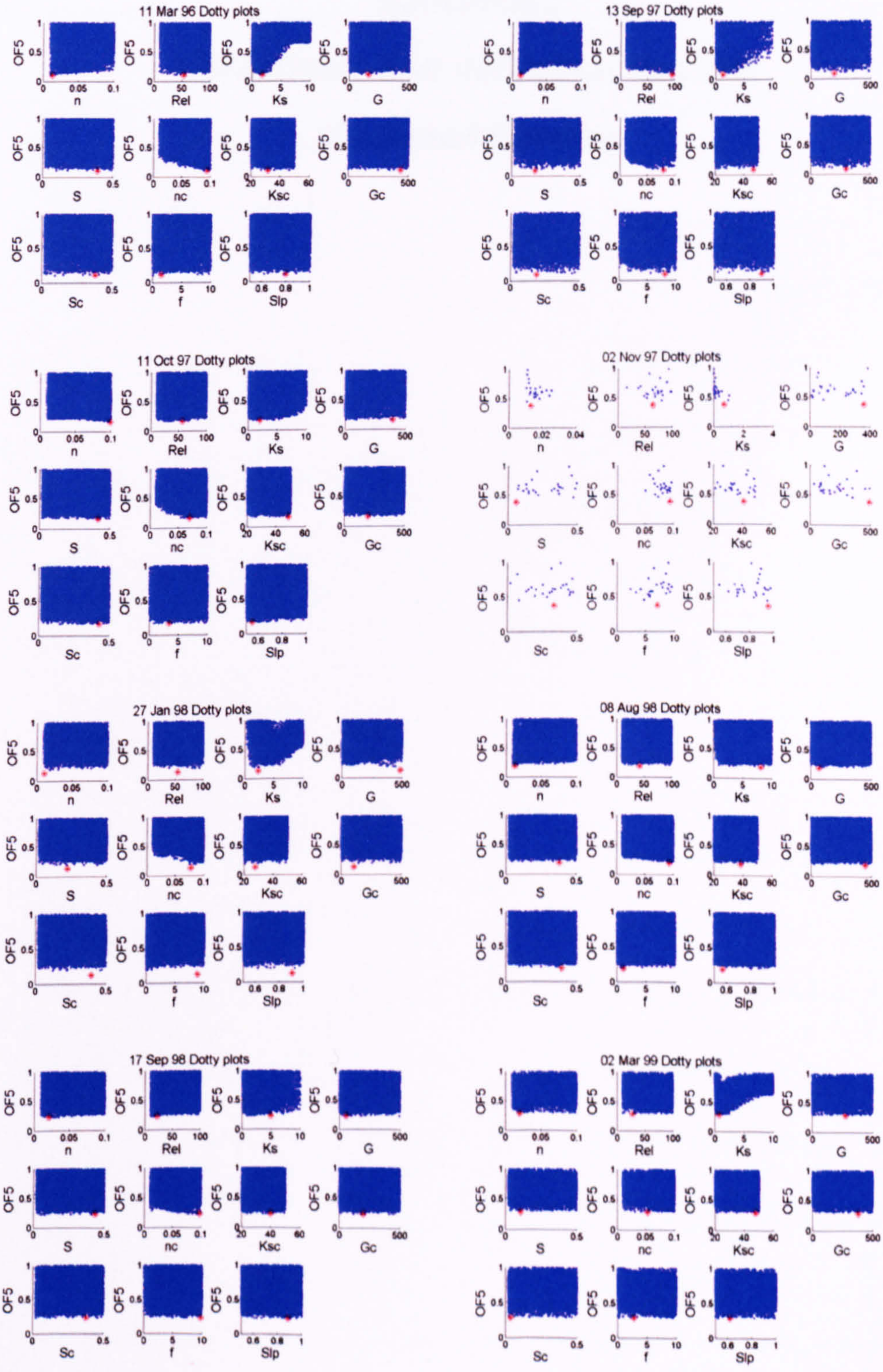








11-parameters, G>0



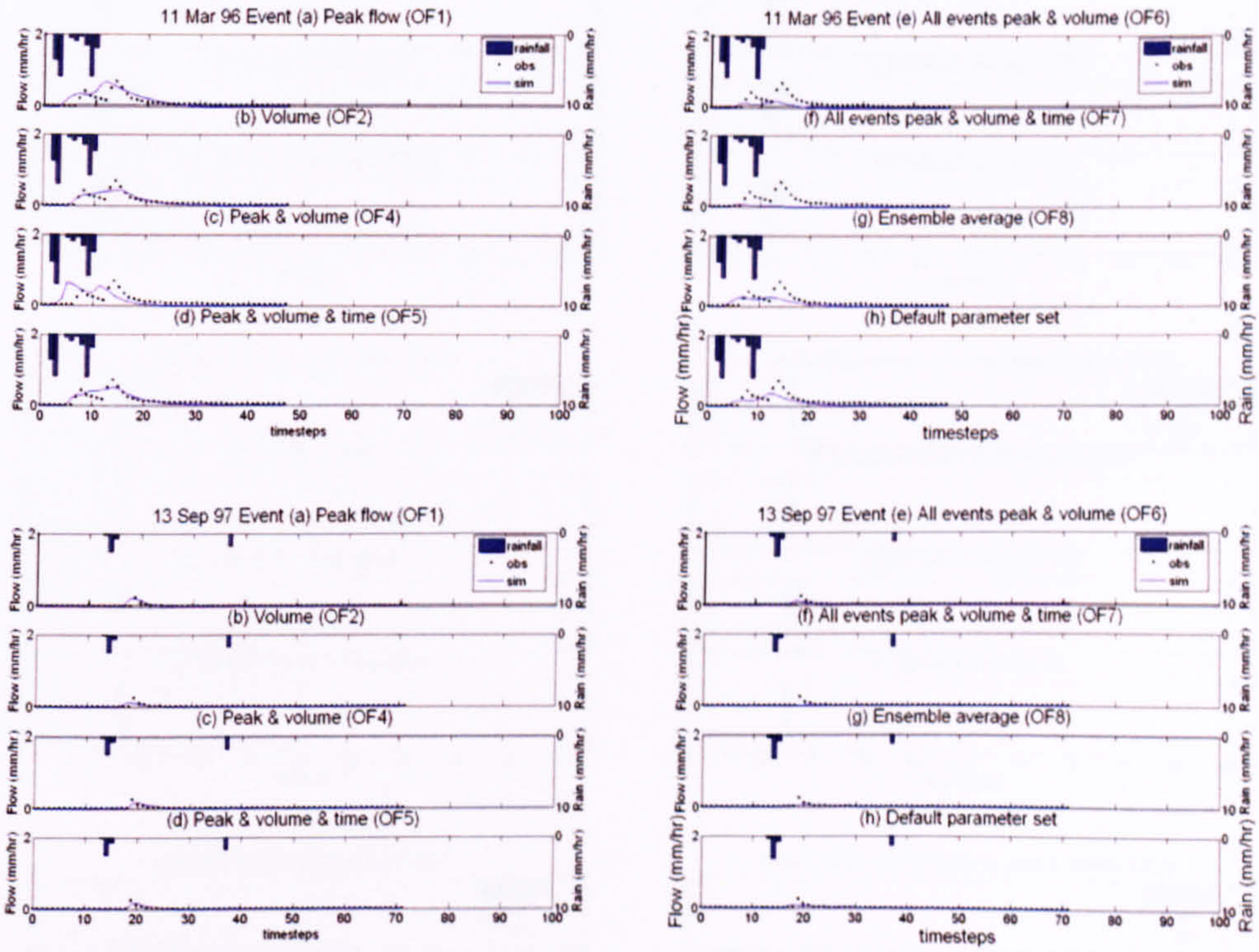
Appendix B

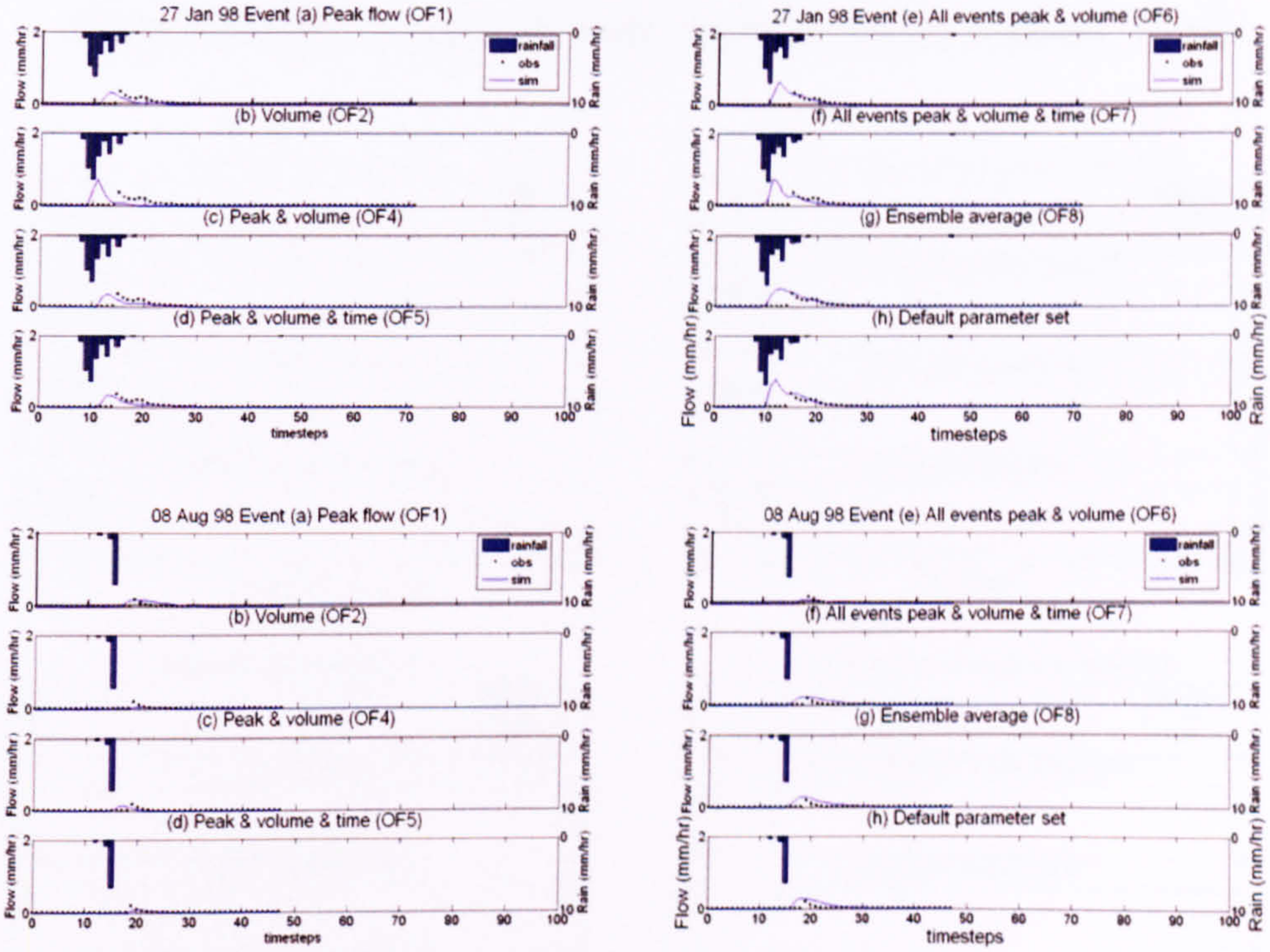
KINEROS2

Calibration and Validation Results

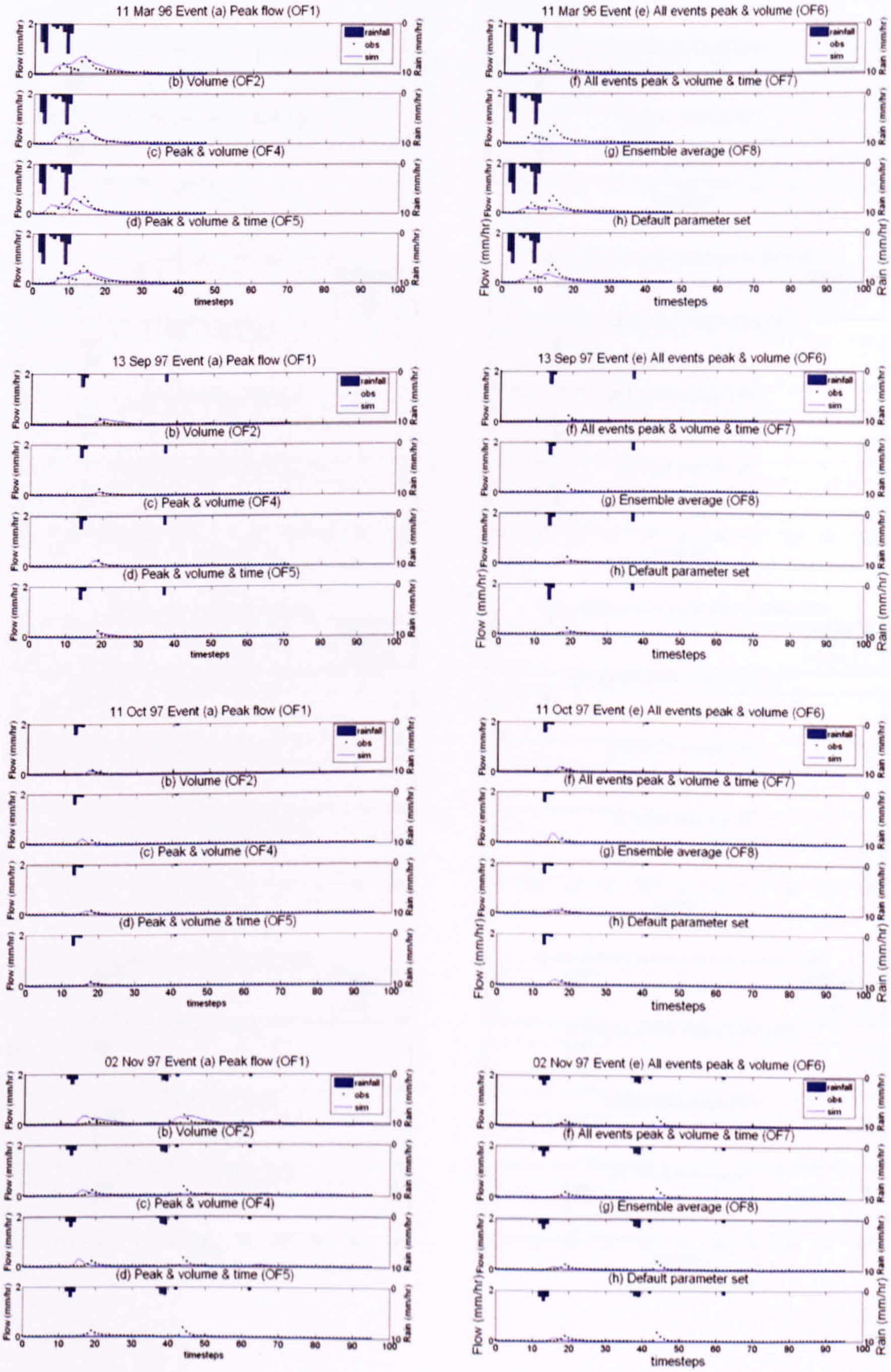
(Selected Events)

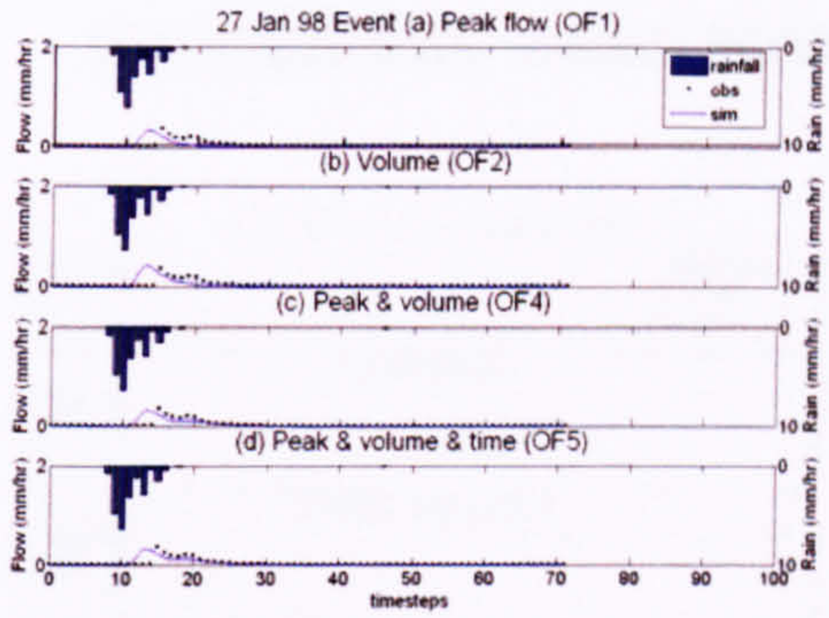
8-parameter case, G=0

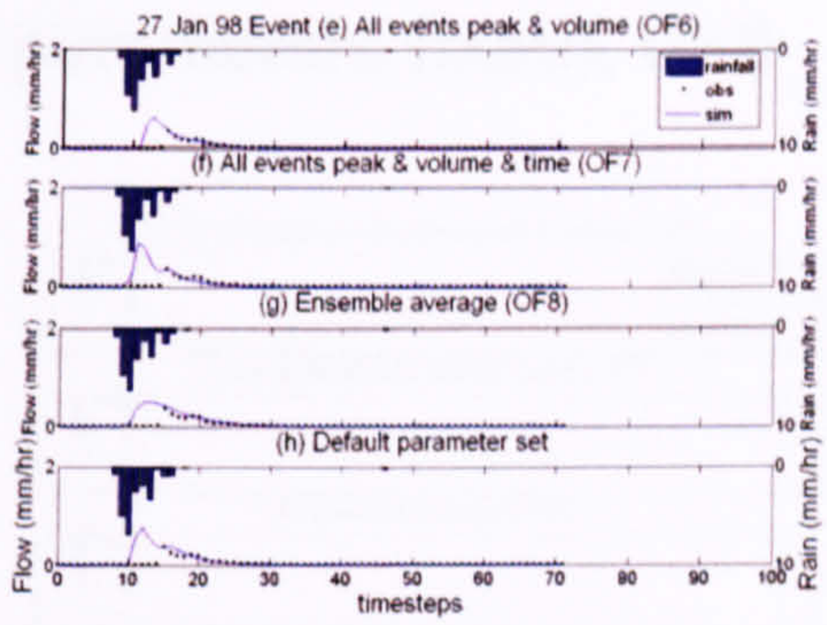


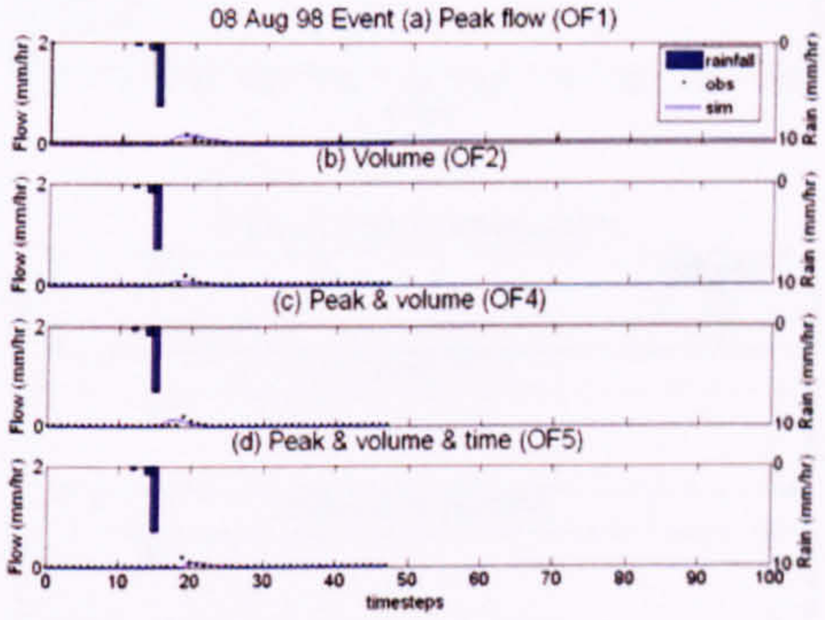

27 Jan 98 Event (a) Peak flow (OF1)
(b) Volume (OF2)
(c) Peak & volume (OF4)
(d) Peak & volume & time (OF5)
(e) All events peak & volume (OF6)
(f) All events peak & volume & time (OF7)
(g) Ensemble average (OF8)
(h) Default parameter set
08 Aug 98 Event (a) Peak flow (OF1)
(b) Volume (OF2)
(c) Peak & volume (OF4)
(d) Peak & volume & time (OF5)
(e) All events peak & volume (OF6)
(f) All events peak & volume & time (OF7)
(g) Ensemble average (OF8)
(h) Default parameter set
17 Sep 98 Event (a) Peak flow (OF1)
(b) Volume (OF2)
(c) Peak & volume (OF4)
(d) Peak & volume & time (OF5)
(e) All events peak & volume (OF6)
(f) All events peak & volume & time (OF7)
(g) Ensemble average (OF8)
(h) Default parameter set
02 Mar 99 Event (a) Peak flow (OF1)
(b) Volume (OF2)
(c) Peak & volume (OF4)
(d) Peak & volume & time (OF5)
(e) All events peak & volume (OF6)
(f) All events peak & volume & time (OF7)
(g) Ensemble average (OF8)
(h) Default parameter set
rainfall
obs
sim
Flow (mm/hr)
Rain (mm/hr)
timesteps

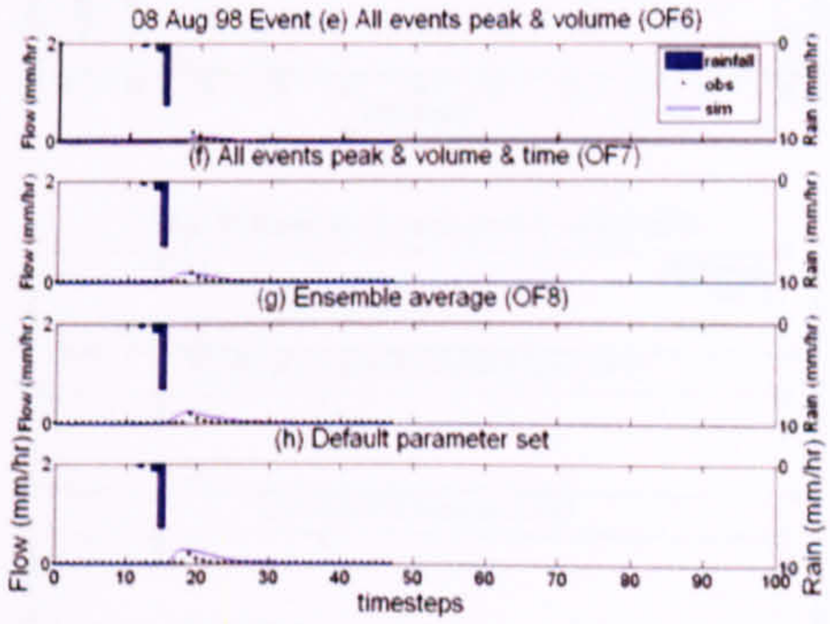
4-parameter case (some parameters fixed), G=0

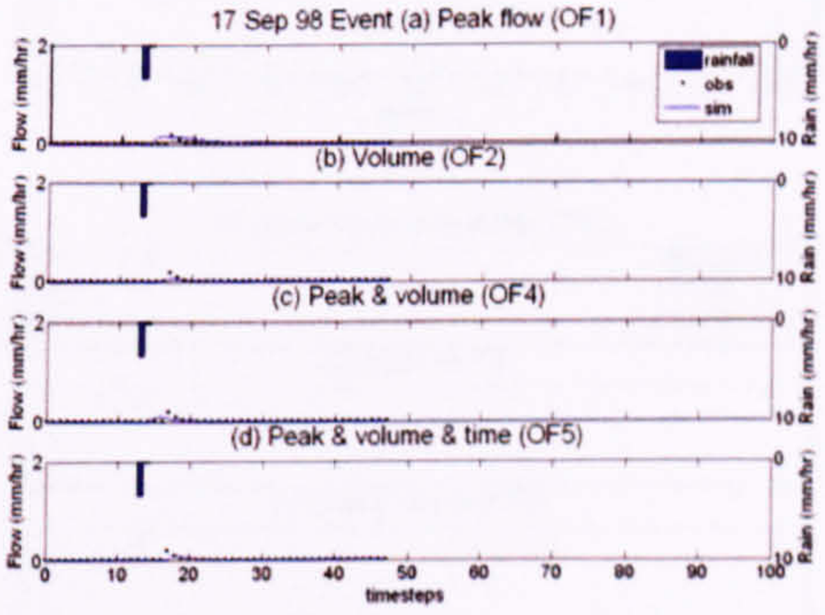


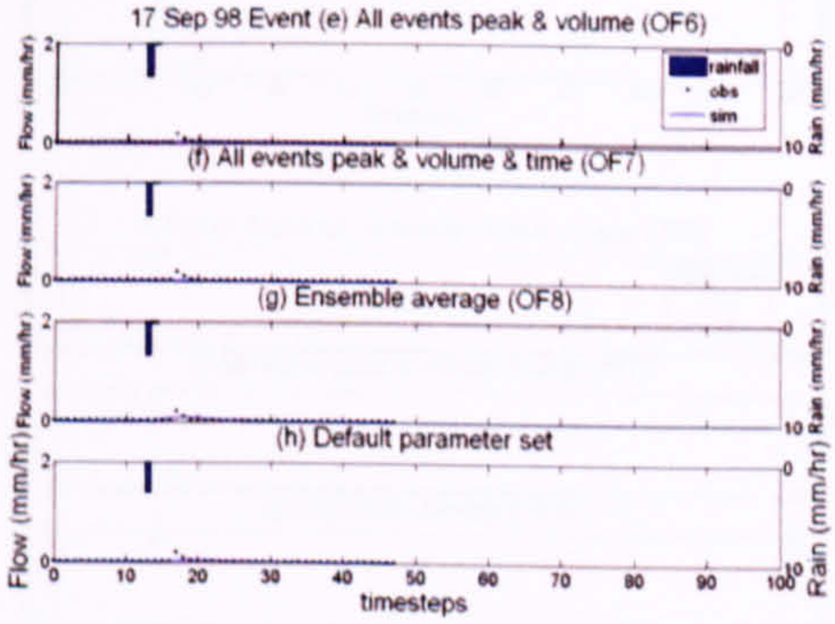

27 Jan 98 Event (a) Peak flow (OF1)
(b) Volume (OF2)
(c) Peak & volume (OF4)
(d) Peak & volume & time (OF5)
rainfall
obs
sim
Flow (mm/hr)
Rain (mm/hr)
timesteps

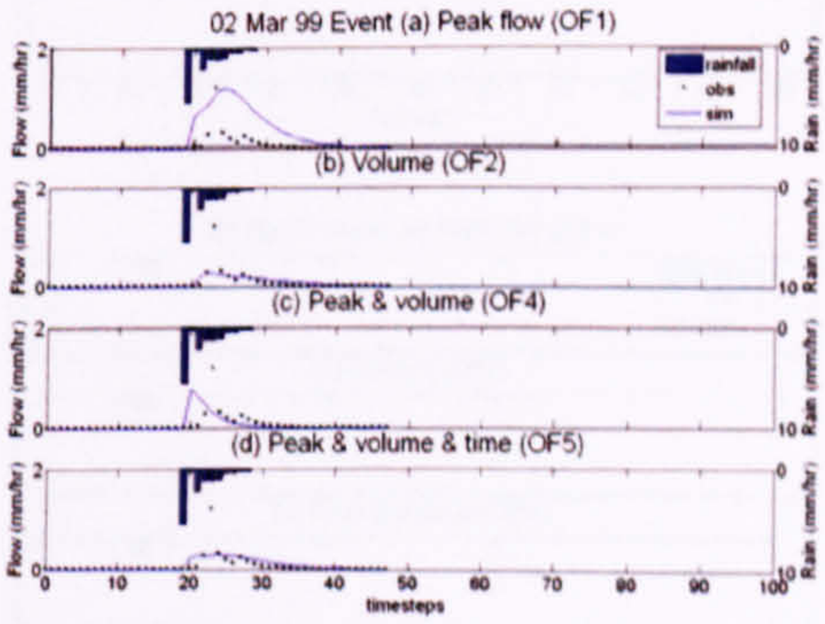

27 Jan 98 Event (e) All events peak & volume (OF6)
(f) All events peak & volume & time (OF7)
(g) Ensemble average (OF8)
(h) Default parameter set
rainfall
obs
sim
Flow (mm/hr)
Rain (mm/hr)
timesteps

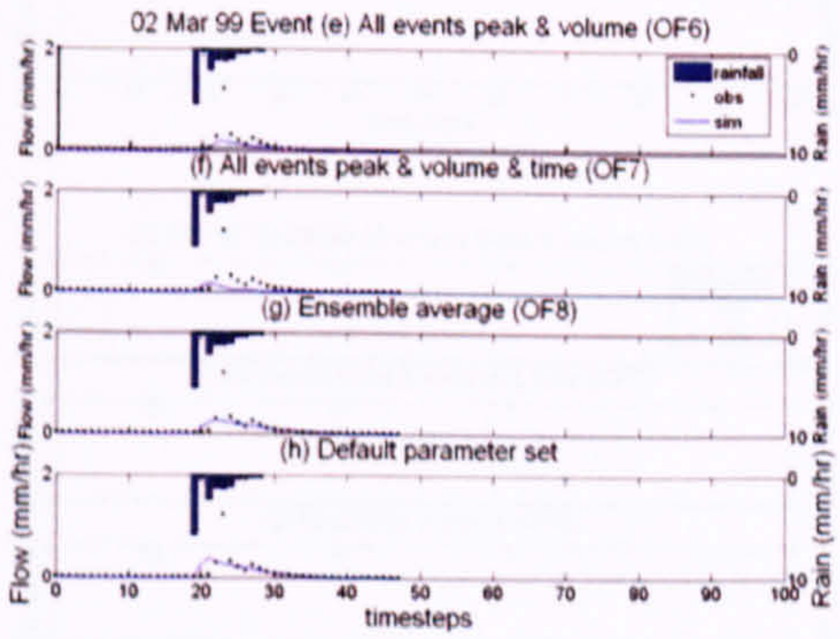

08 Aug 98 Event (a) Peak flow (OF1)
(b) Volume (OF2)
(c) Peak & volume (OF4)
(d) Peak & volume & time (OF5)
rainfall
obs
sim
Flow (mm/hr)
Rain (mm/hr)
timesteps


08 Aug 98 Event (e) All events peak & volume (OF6)
(f) All events peak & volume & time (OF7)
(g) Ensemble average (OF8)
(h) Default parameter set
rainfall
obs
sim
Flow (mm/hr)
Rain (mm/hr)
timesteps

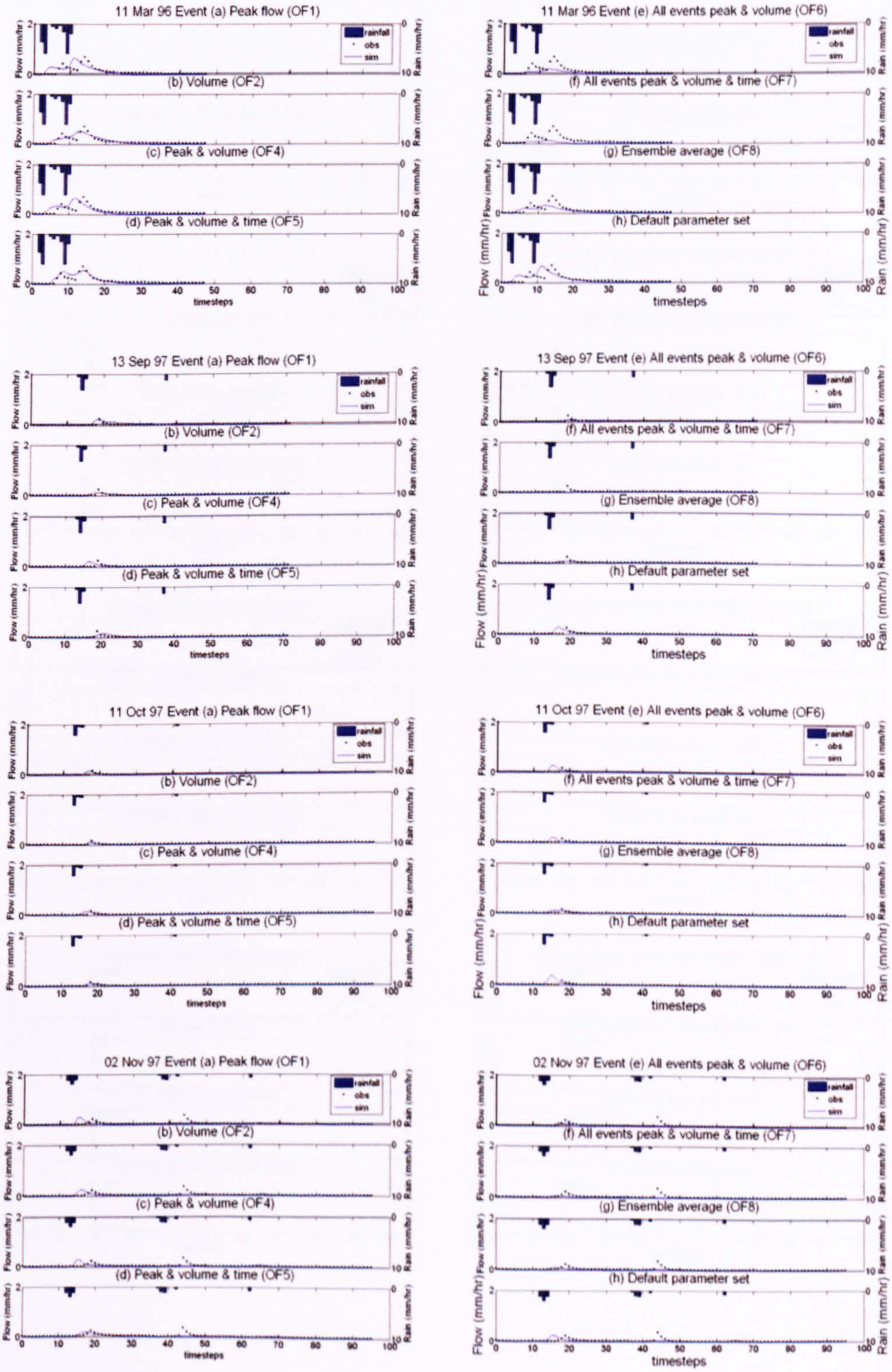

17 Sep 98 Event (a) Peak flow (OF1)
(b) Volume (OF2)
(c) Peak & volume (OF4)
(d) Peak & volume & time (OF5)
rainfall
obs
sim
Flow (mm/hr)
Rain (mm/hr)
timesteps

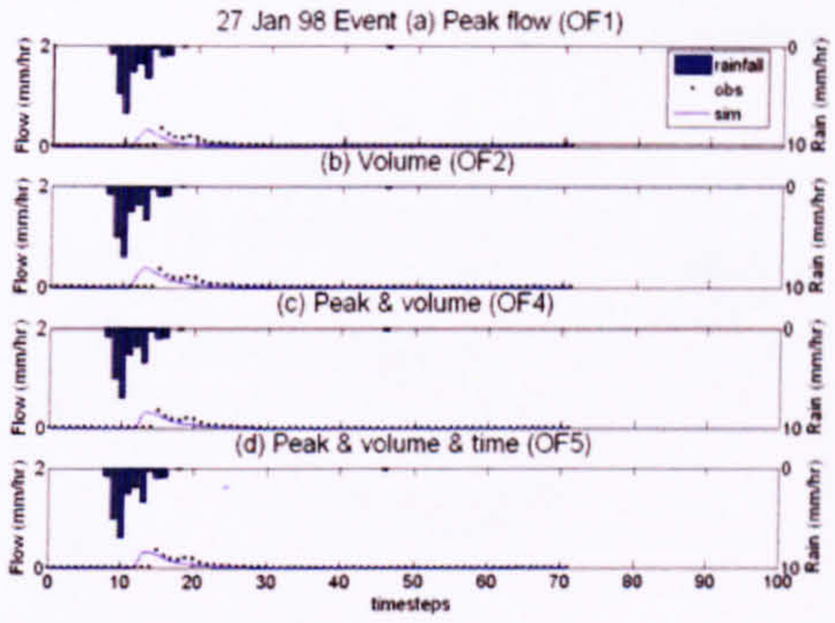

17 Sep 98 Event (e) All events peak & volume (OF6)
(f) All events peak & volume & time (OF7)
(g) Ensemble average (OF8)
(h) Default parameter set
rainfall
obs
sim
Flow (mm/hr)
Rain (mm/hr)
timesteps

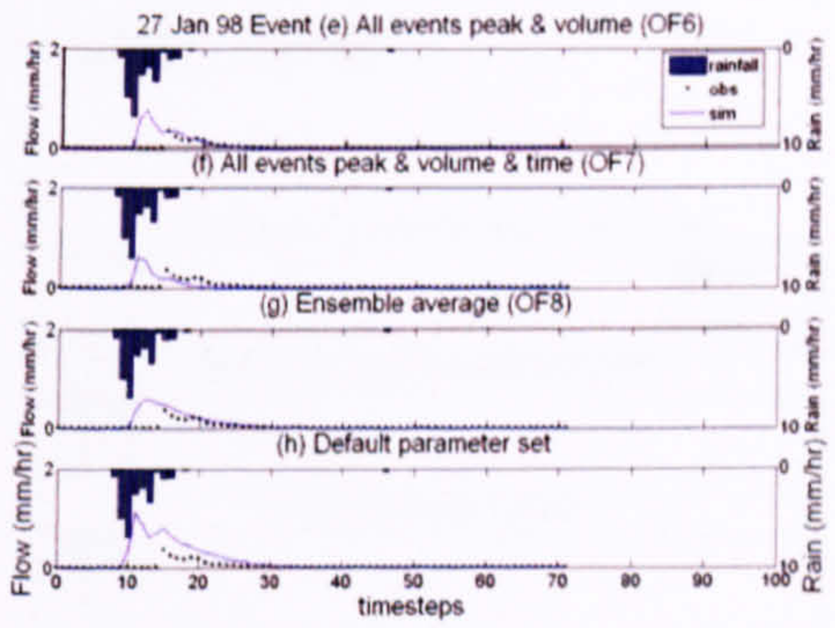

02 Mar 99 Event (a) Peak flow (OF1)
(b) Volume (OF2)
(c) Peak & volume (OF4)
(d) Peak & volume & time (OF5)
rainfall
obs
sim
Flow (mm/hr)
Rain (mm/hr)
timesteps

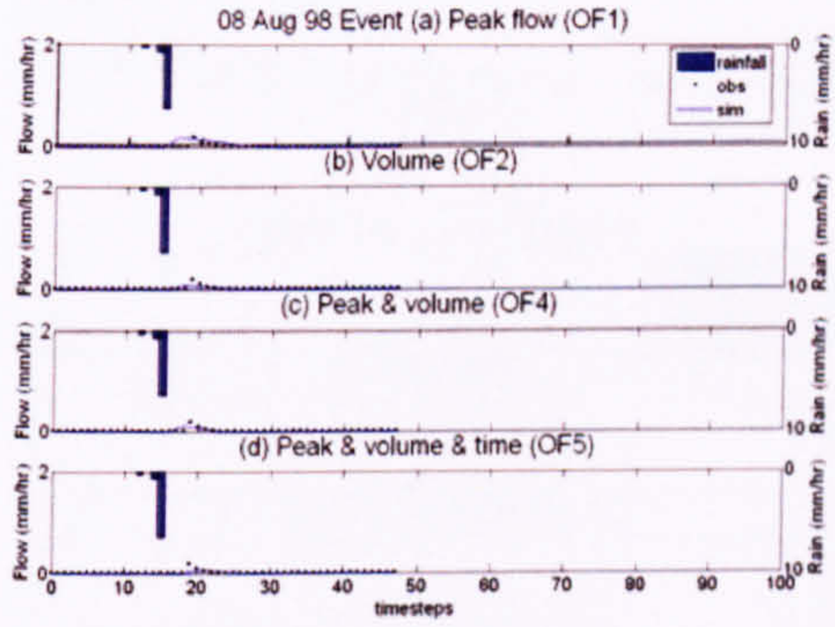

02 Mar 99 Event (e) All events peak & volume (OF6)
(f) All events peak & volume & time (OF7)
(g) Ensemble average (OF8)
(h) Default parameter set
rainfall
obs
sim
Flow (mm/hr)
Rain (mm/hr)
timesteps

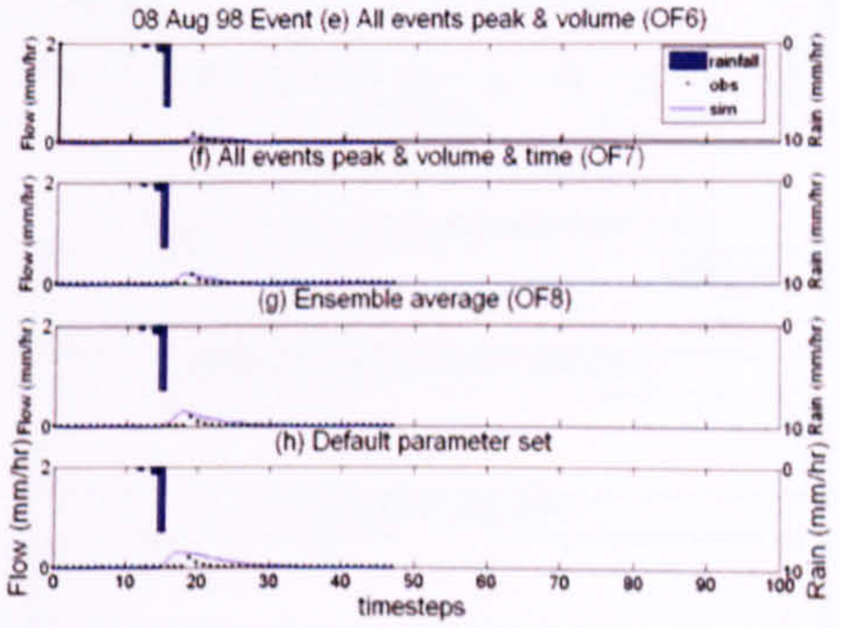
6-parameter case (some parameters fixed), G=0

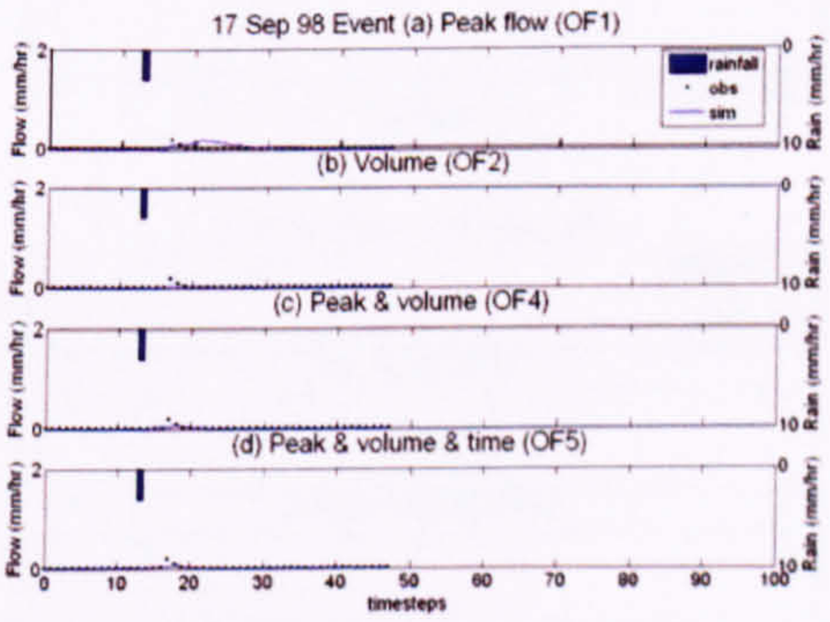


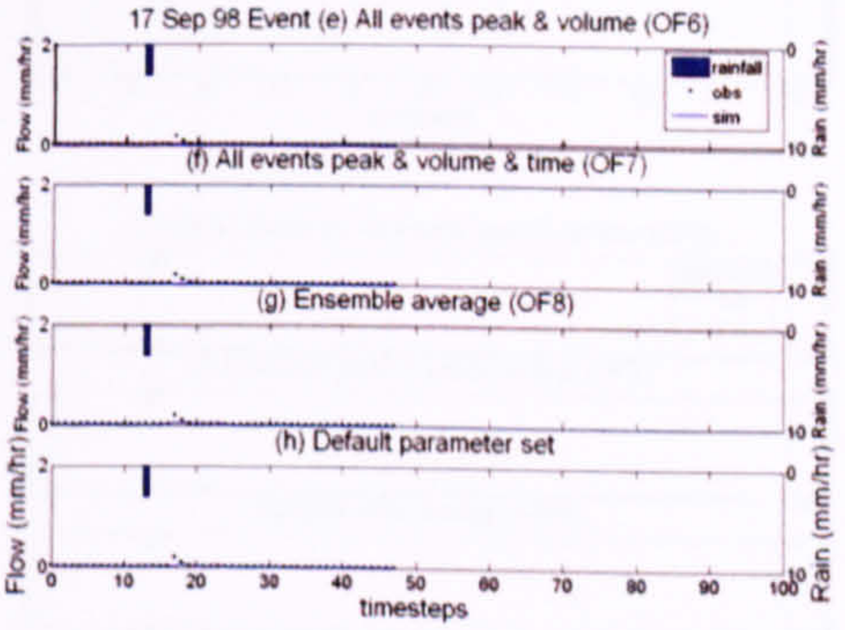

27 Jan 98 Event (a) Peak flow (OF1)
(b) Volume (OF2)
(c) Peak & volume (OF4)
(d) Peak & volume & time (OF5)
rainfall
obs
sim
Flow (mm/hr)
Rain (mm/hr)
timesteps

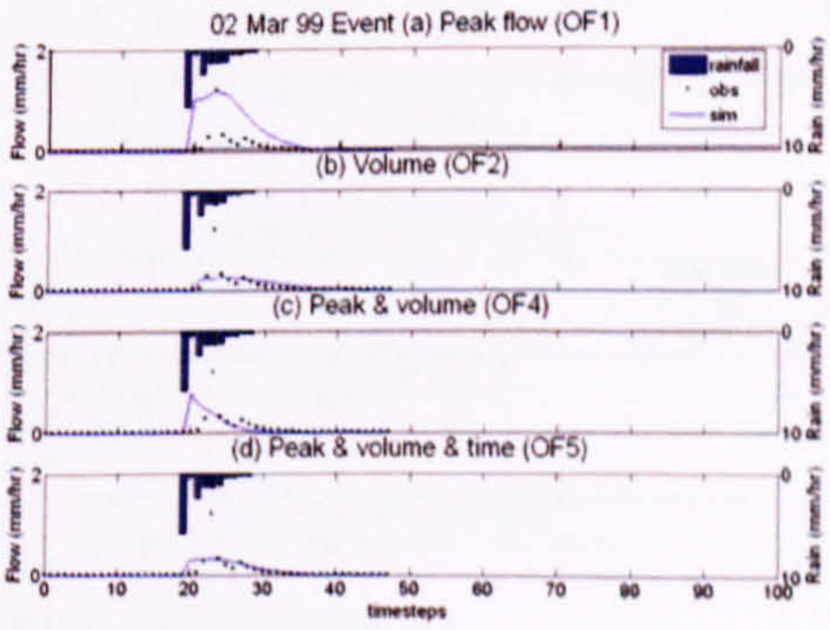

27 Jan 98 Event (e) All events peak & volume (OF6)
(f) All events peak & volume & time (OF7)
(g) Ensemble average (OF8)
(h) Default parameter set
rainfall
obs
sim
Flow (mm/hr)
Rain (mm/hr)
timesteps

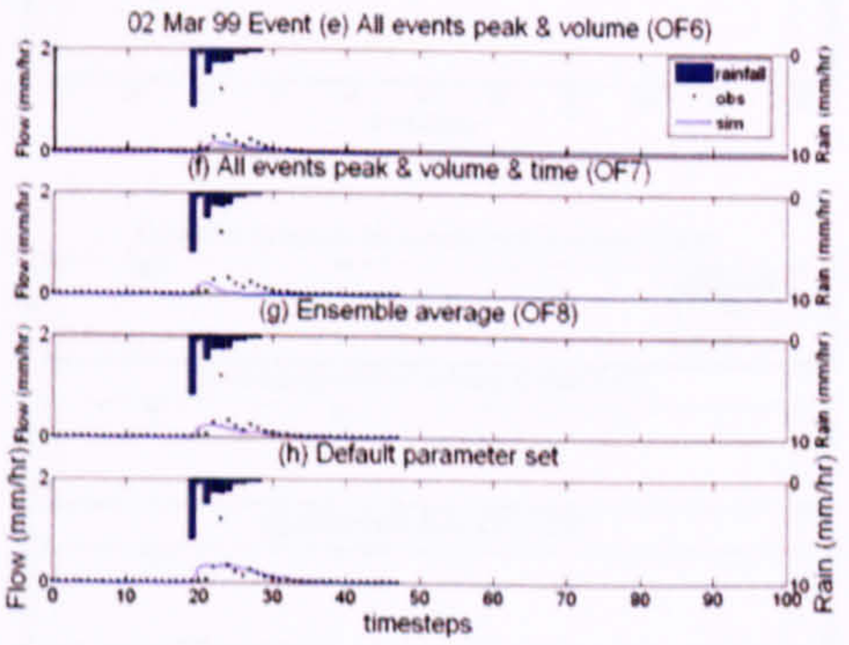

08 Aug 98 Event (a) Peak flow (OF1)
(b) Volume (OF2)
(c) Peak & volume (OF4)
(d) Peak & volume & time (OF5)
rainfall
obs
sim
Flow (mm/hr)
Rain (mm/hr)
timesteps


08 Aug 98 Event (e) All events peak & volume (OF6)
(f) All events peak & volume & time (OF7)
(g) Ensemble average (OF8)
(h) Default parameter set
rainfall
obs
sim
Flow (mm/hr)
Rain (mm/hr)
timesteps

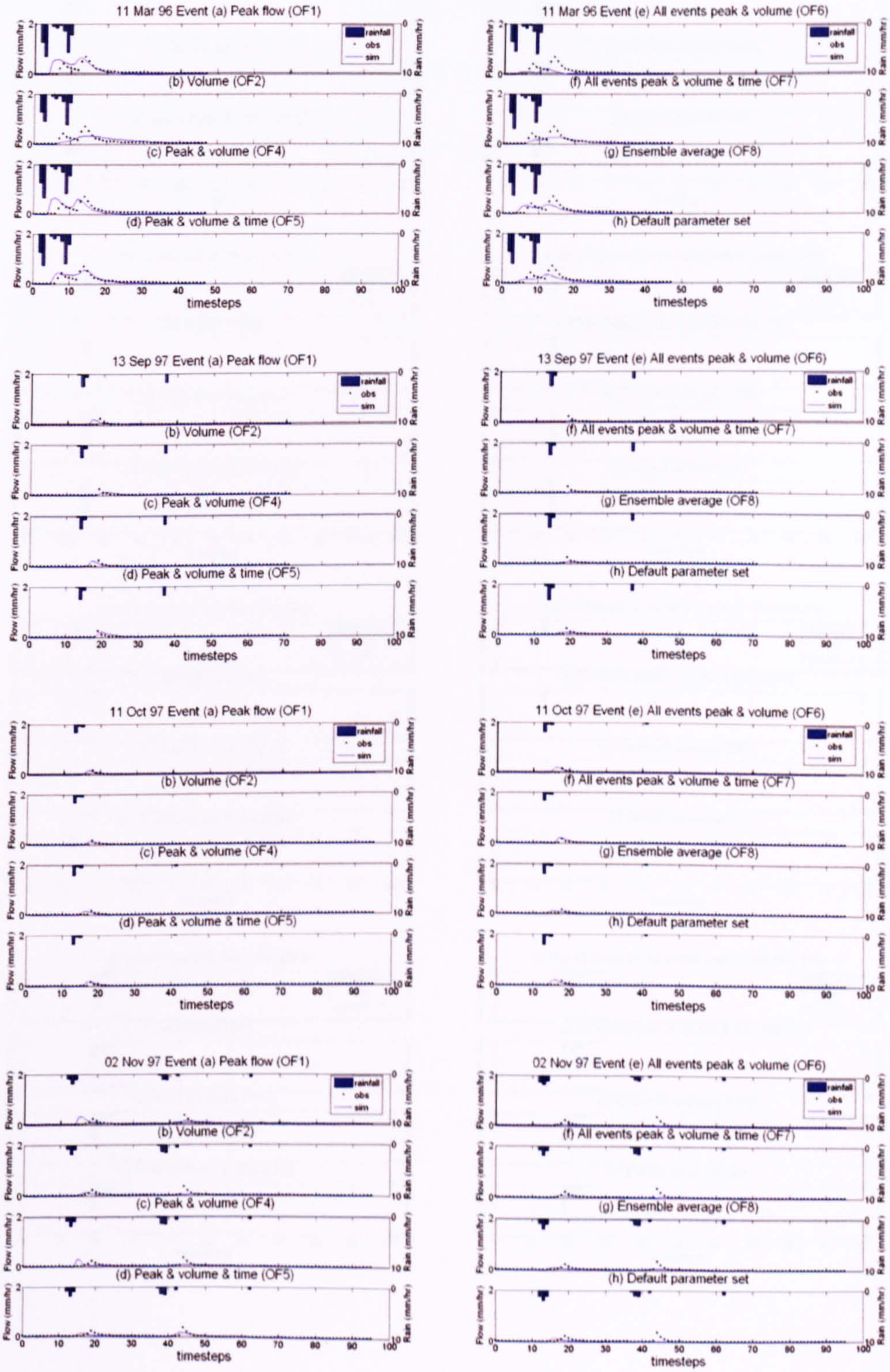

17 Sep 98 Event (a) Peak flow (OF1)
(b) Volume (OF2)
(c) Peak & volume (OF4)
(d) Peak & volume & time (OF5)
rainfall
obs
sim
Flow (mm/hr)
Rain (mm/hr)
timesteps

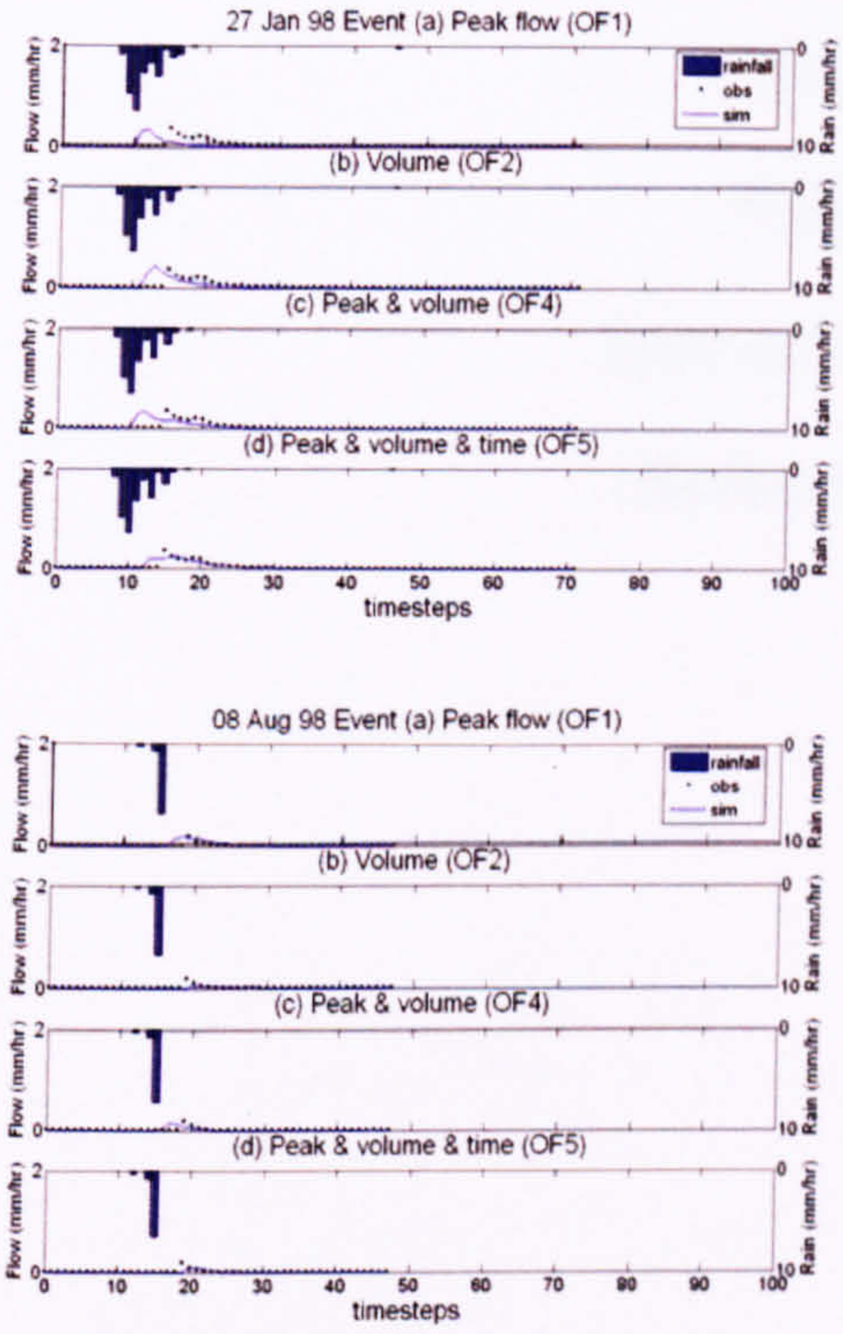

17 Sep 98 Event (e) All events peak & volume (OF6)
(f) All events peak & volume & time (OF7)
(g) Ensemble average (OF8)
(h) Default parameter set
rainfall
obs
sim
Flow (mm/hr)
Rain (mm/hr)
timesteps

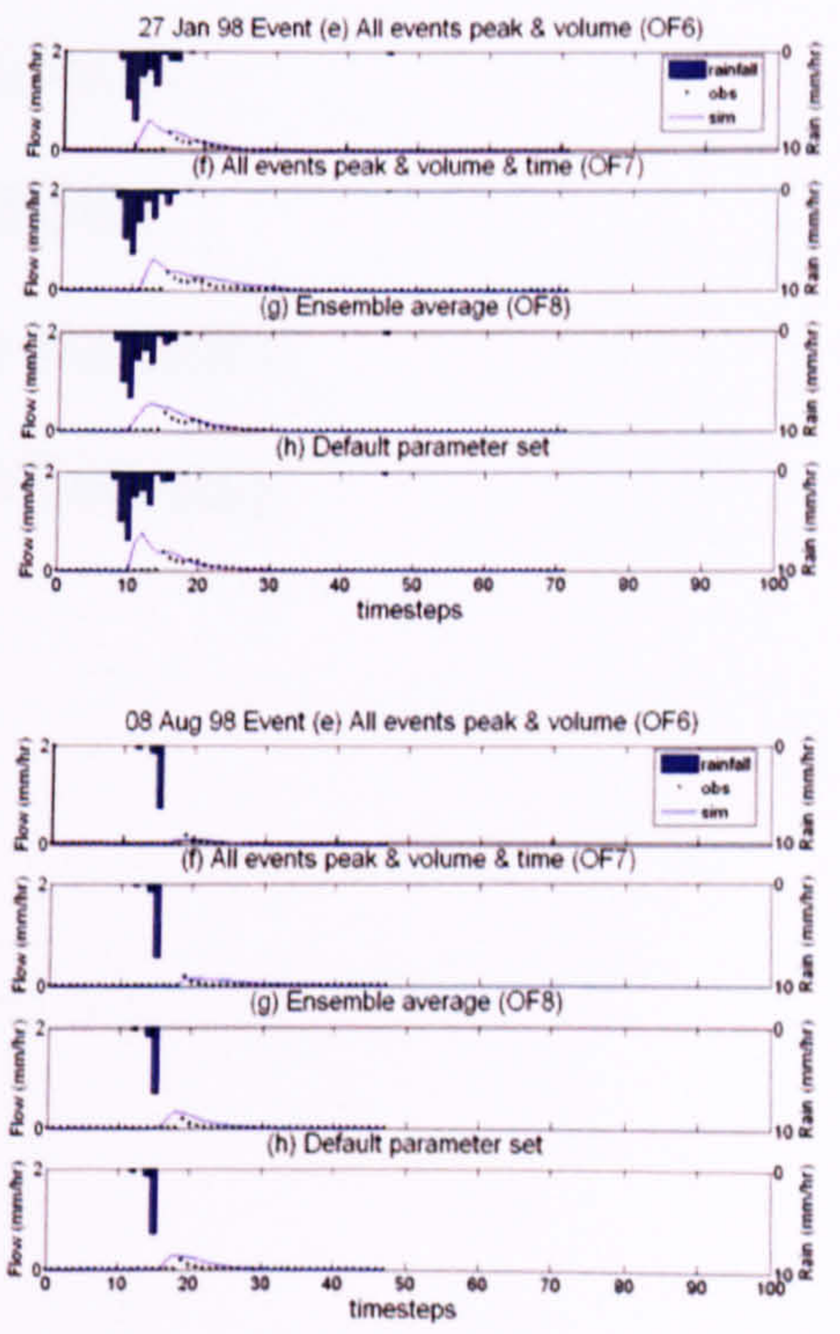

02 Mar 99 Event (a) Peak flow (OF1)
(b) Volume (OF2)
(c) Peak & volume (OF4)
(d) Peak & volume & time (OF5)
rainfall
obs
sim
Flow (mm/hr)
Rain (mm/hr)
timesteps


02 Mar 99 Event (e) All events peak & volume (OF6)
(f) All events peak & volume & time (OF7)
(g) Ensemble average (OF8)
(h) Default parameter set
rainfall
obs
sim
Flow (mm/hr)
Rain (mm/hr)
timesteps

11-parameter case, G>0




27 Jan 98 Event (a) Peak flow (OF1)
(b) Volume (OF2)
(c) Peak & volume (OF4)
(d) Peak & volume & time (OF5)
08 Aug 98 Event (a) Peak flow (OF1)
(b) Volume (OF2)
(c) Peak & volume (OF4)
(d) Peak & volume & time (OF5)
17 Sep 98 Event (a) Peak flow (OF1)
(b) Volume (OF2)
(c) Peak & volume (OF4)
(d) Peak & volume & time (OF5)
02 Mar 99 Event (a) Peak flow (OF1)
(b) Volume (OF2)
(c) Peak & volume (OF4)
(d) Peak & volume & time (OF5)
rainfall
obs
sim
Flow (mm/hr)
Rain (mm/hr)
timesteps


27 Jan 98 Event (e) All events peak & volume (OF6)
(f) All events peak & volume & time (OF7)
(g) Ensemble average (OF8)
(h) Default parameter set
08 Aug 98 Event (e) All events peak & volume (OF6)
(f) All events peak & volume & time (OF7)
(g) Ensemble average (OF8)
(h) Default parameter set
17 Sep 98 Event (e) All events peak & volume (OF6)
(f) All events peak & volume & time (OF7)
(g) Ensemble average (OF8)
(h) Default parameter set
02 Mar 99 Event (e) All events peak & volume (OF6)
(f) All events peak & volume & time (OF7)
(g) Ensemble average (OF8)
(h) Default parameter set
rainfall
obs
sim
Flow (mm/hr)
Rain (mm/hr)
timesteps

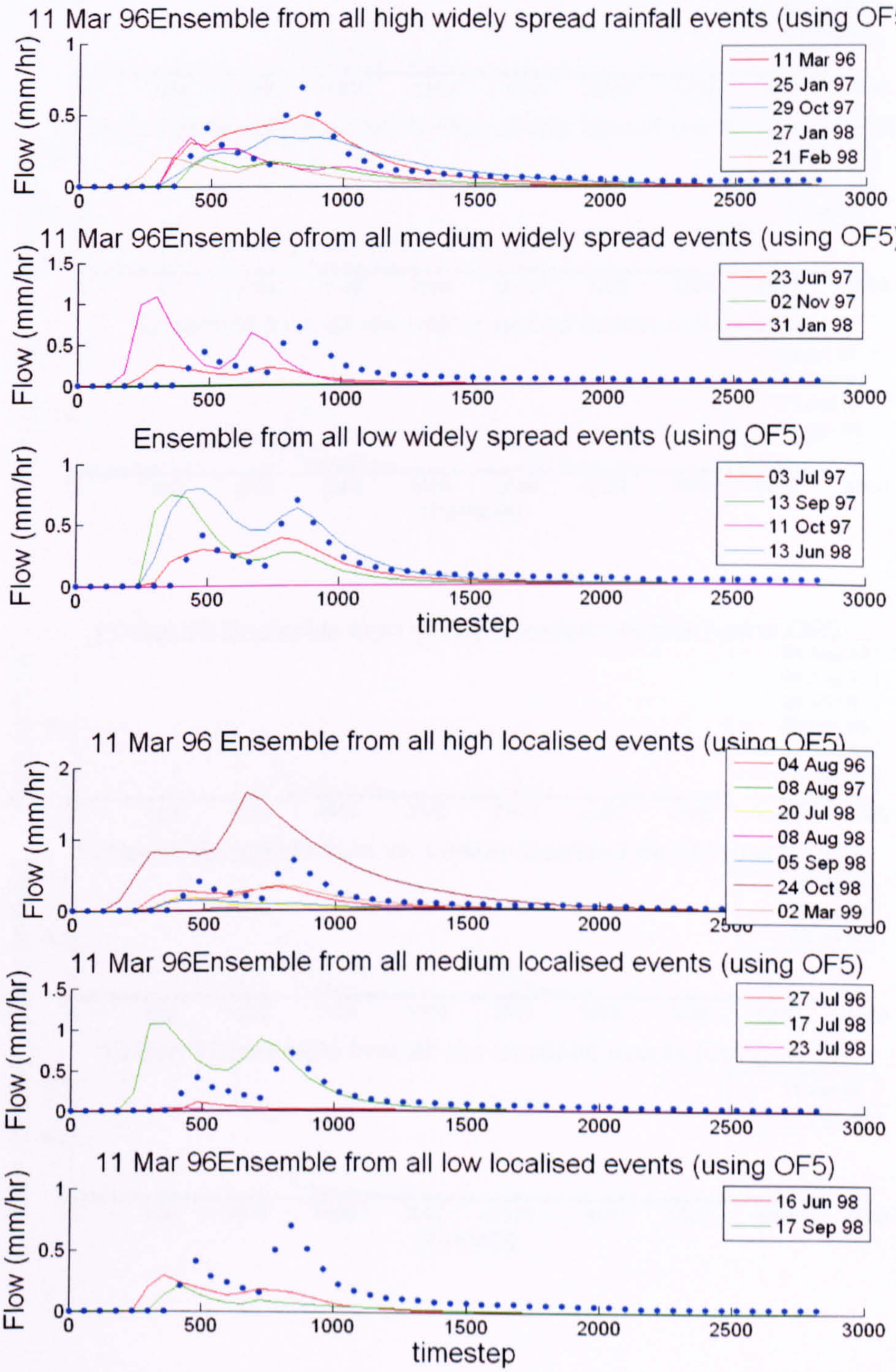
Appendix C

KINEROS2

Ensemble Results

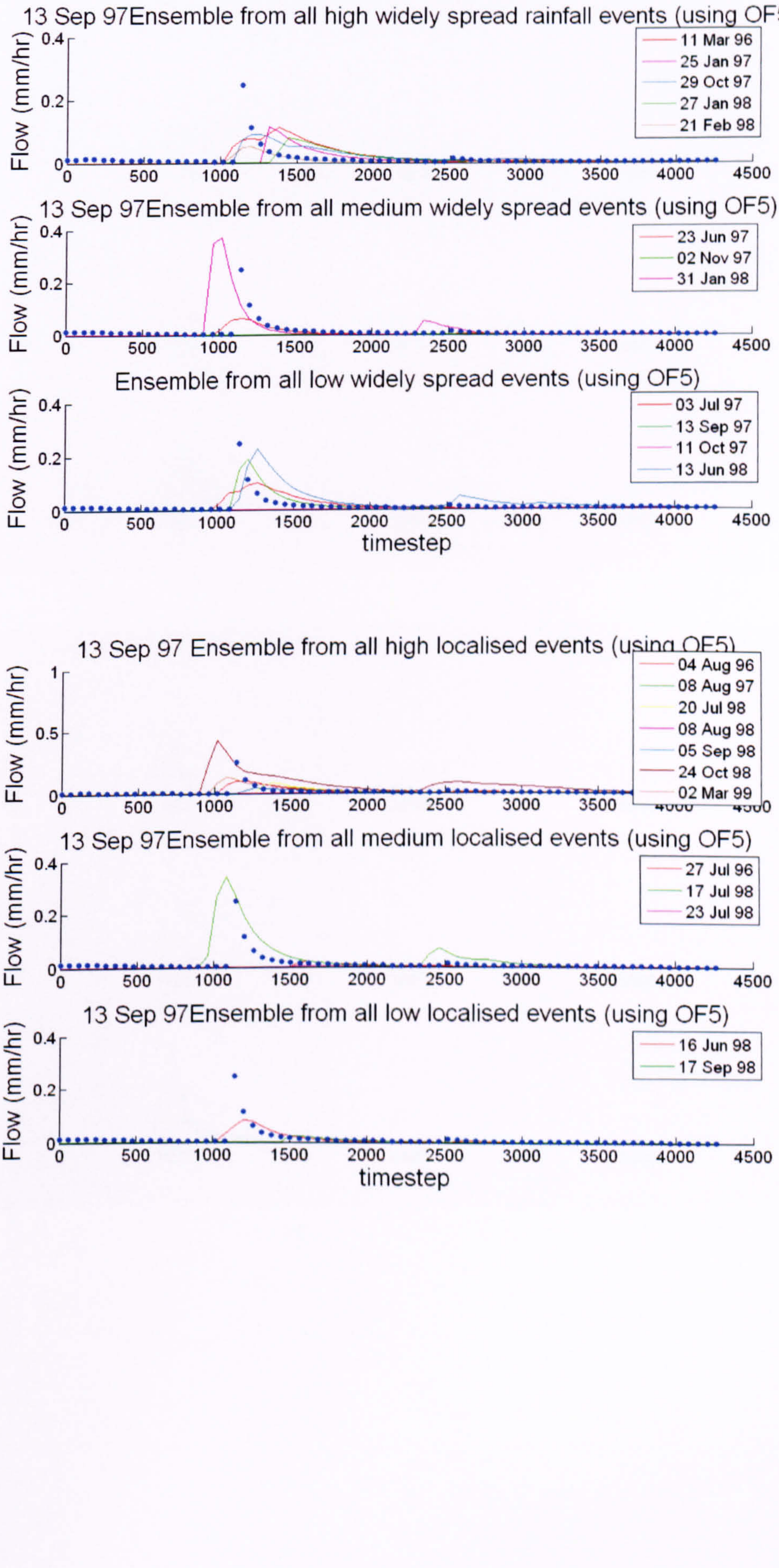
(Selected Events)

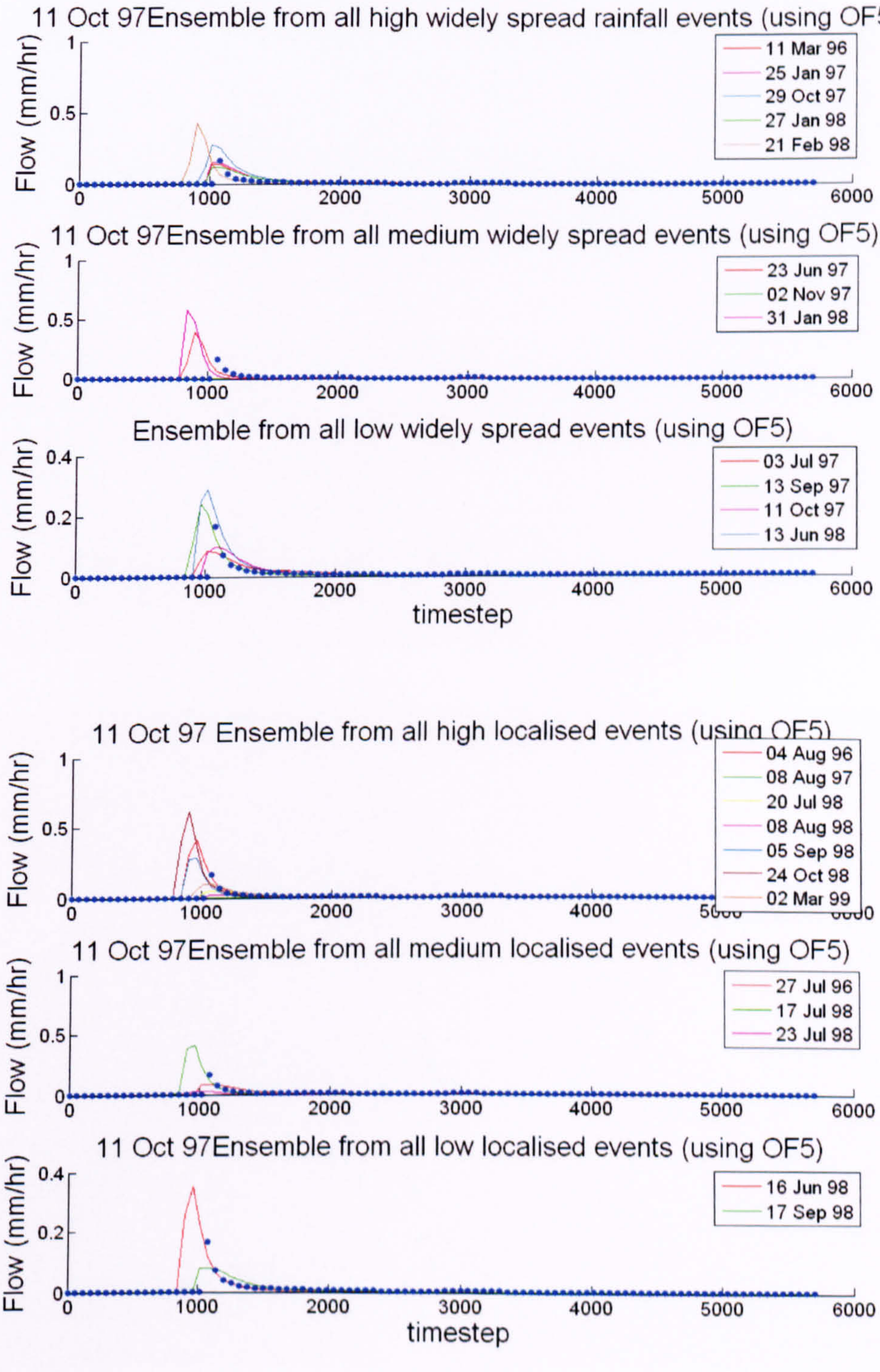
8-Parameters, G=0

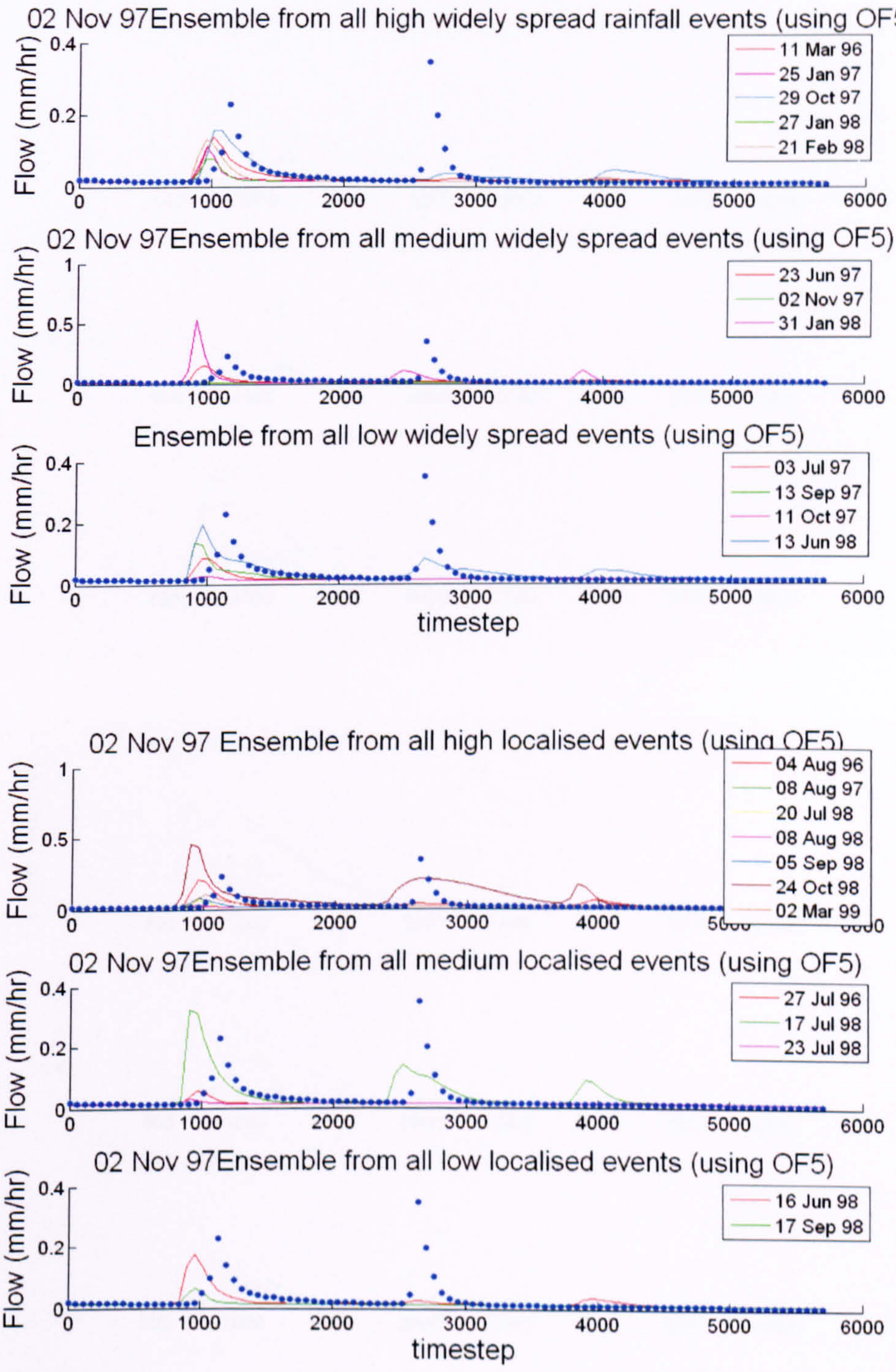


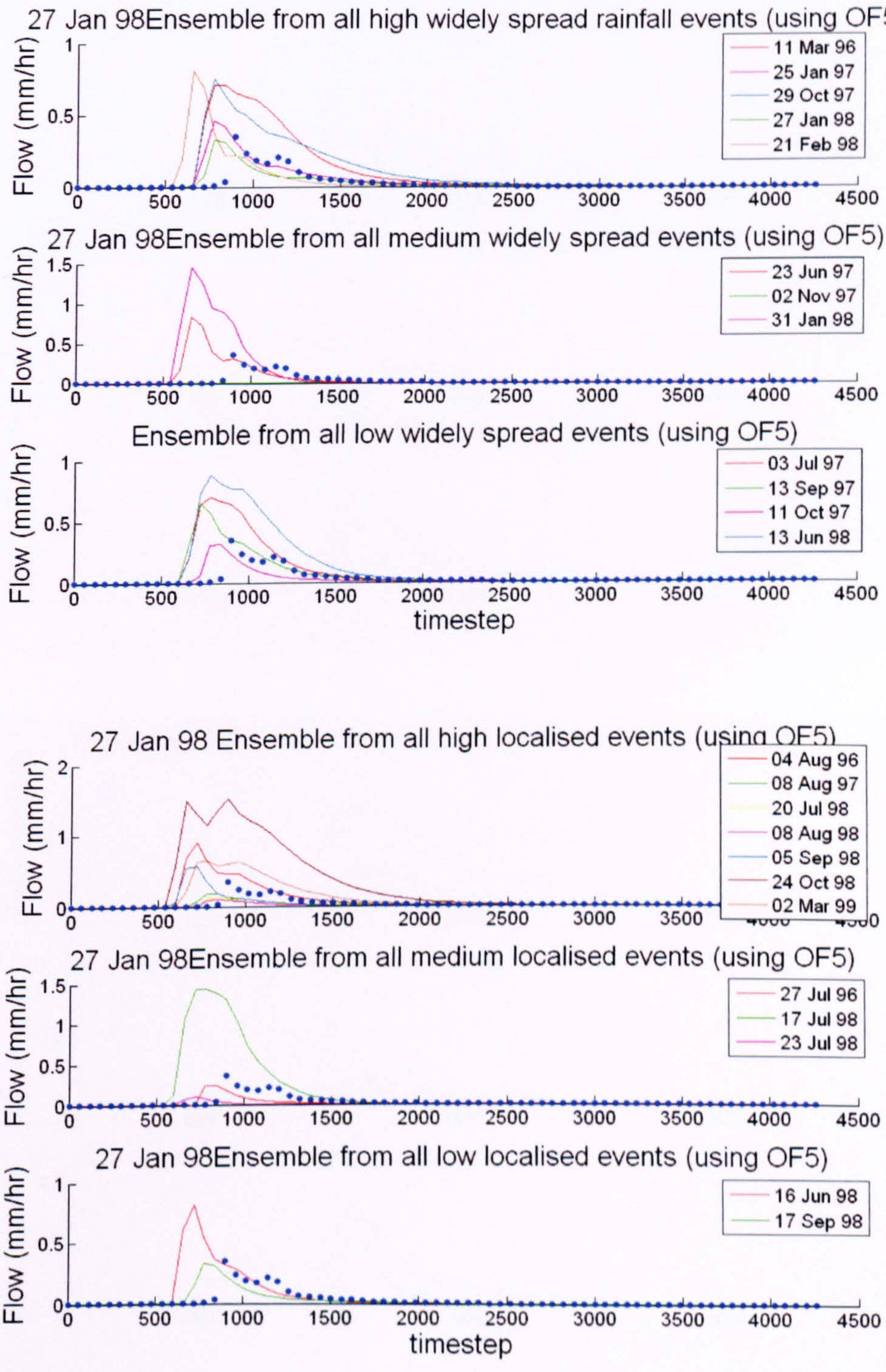
Note:

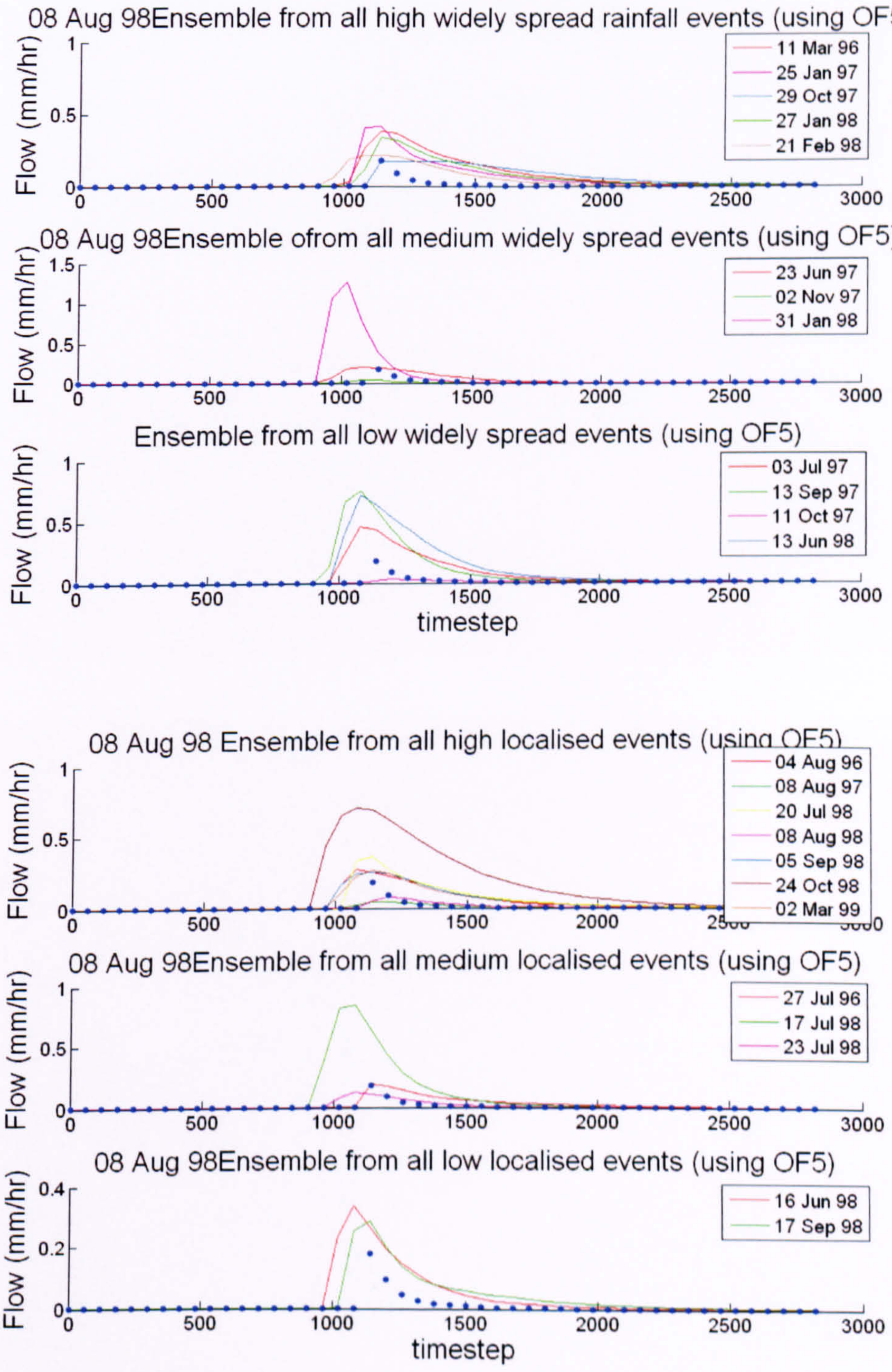
Timestep is in hours for all these simulation results

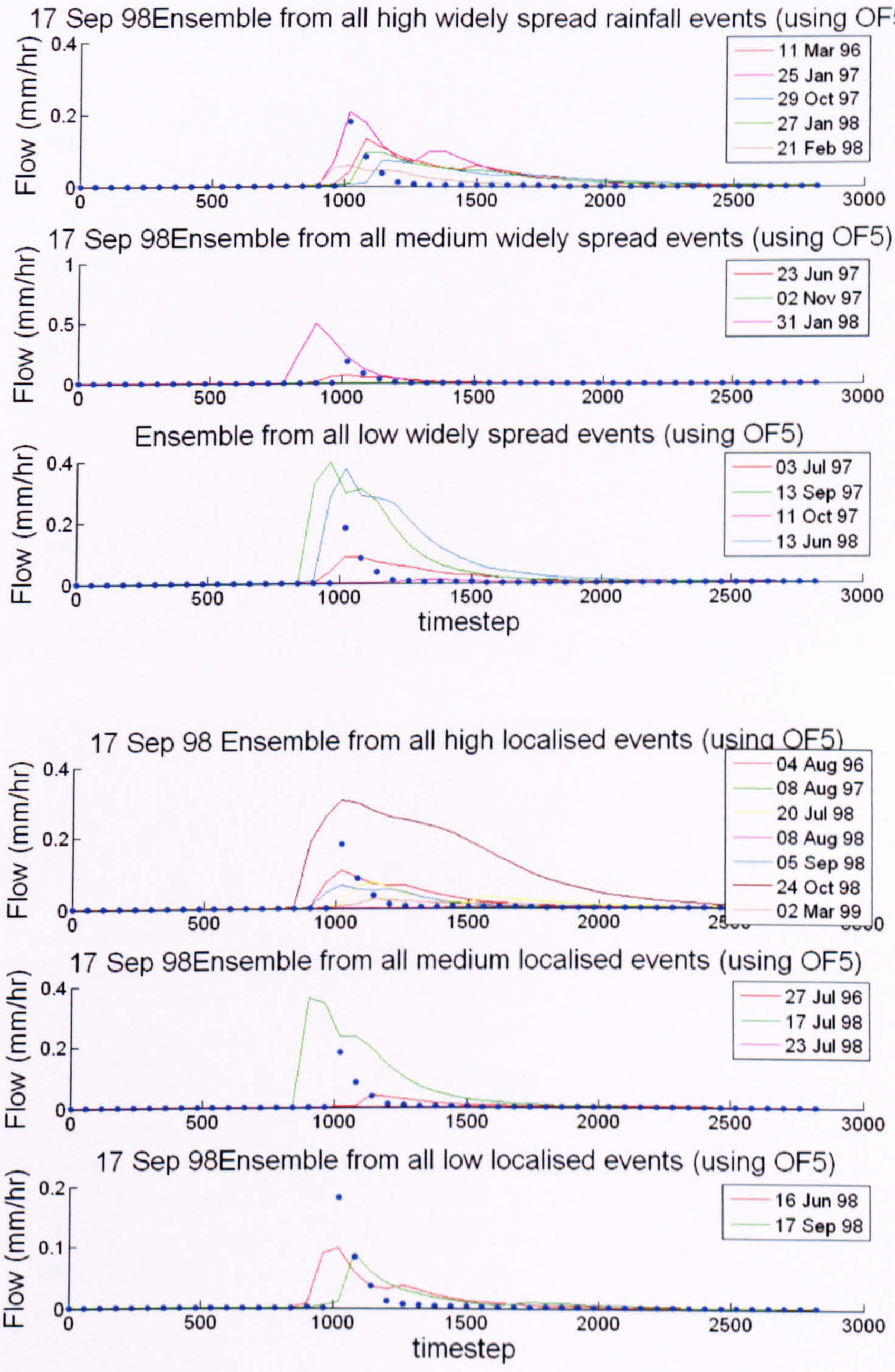

13 Sep 97Ensemble from all high widely spread rainfall events (using OF5)
Flow (mm/hr)
0.4
0.2
0
0
500
1000
1500
2000
2500
3000
3500
4000
4500
11 Mar 96
25 Jan 97
29 Oct 97
27 Jan 98
21 Feb 98
13 Sep 97Ensemble from all medium widely spread events (using OF5)
Flow (mm/hr)
0.4
0.2
0
0
500
1000
1500
2000
2500
3000
3500
4000
4500
23 Jun 97
02 Nov 97
31 Jan 98
Ensemble from all low widely spread events (using OF5)
Flow (mm/hr)
0.4
0.2
0
0
500
1000
1500
2000
2500
3000
3500
4000
4500
timestep
03 Jul 97
13 Sep 97
11 Oct 97
13 Jun 98
13 Sep 97 Ensemble from all high localised events (using OF5)
Flow (mm/hr)
1
0.5
0
0
500
1000
1500
2000
2500
3000
3500
04 Aug 96
08 Aug 97
20 Jul 98
08 Aug 98
05 Sep 98
24 Oct 98
02 Mar 99
13 Sep 97Ensemble from all medium localised events (using OF5)
Flow (mm/hr)
0.4
0.2
0
0
500
1000
1500
2000
2500
3000
3500
4000
4500
27 Jul 96
17 Jul 98
23 Jul 98
13 Sep 97Ensemble from all low localised events (using OF5)
Flow (mm/hr)
0.4
0.2
0
0
500
1000
1500
2000
2500
3000
3500
4000
4500
timestep
16 Jun 98
17 Sep 98

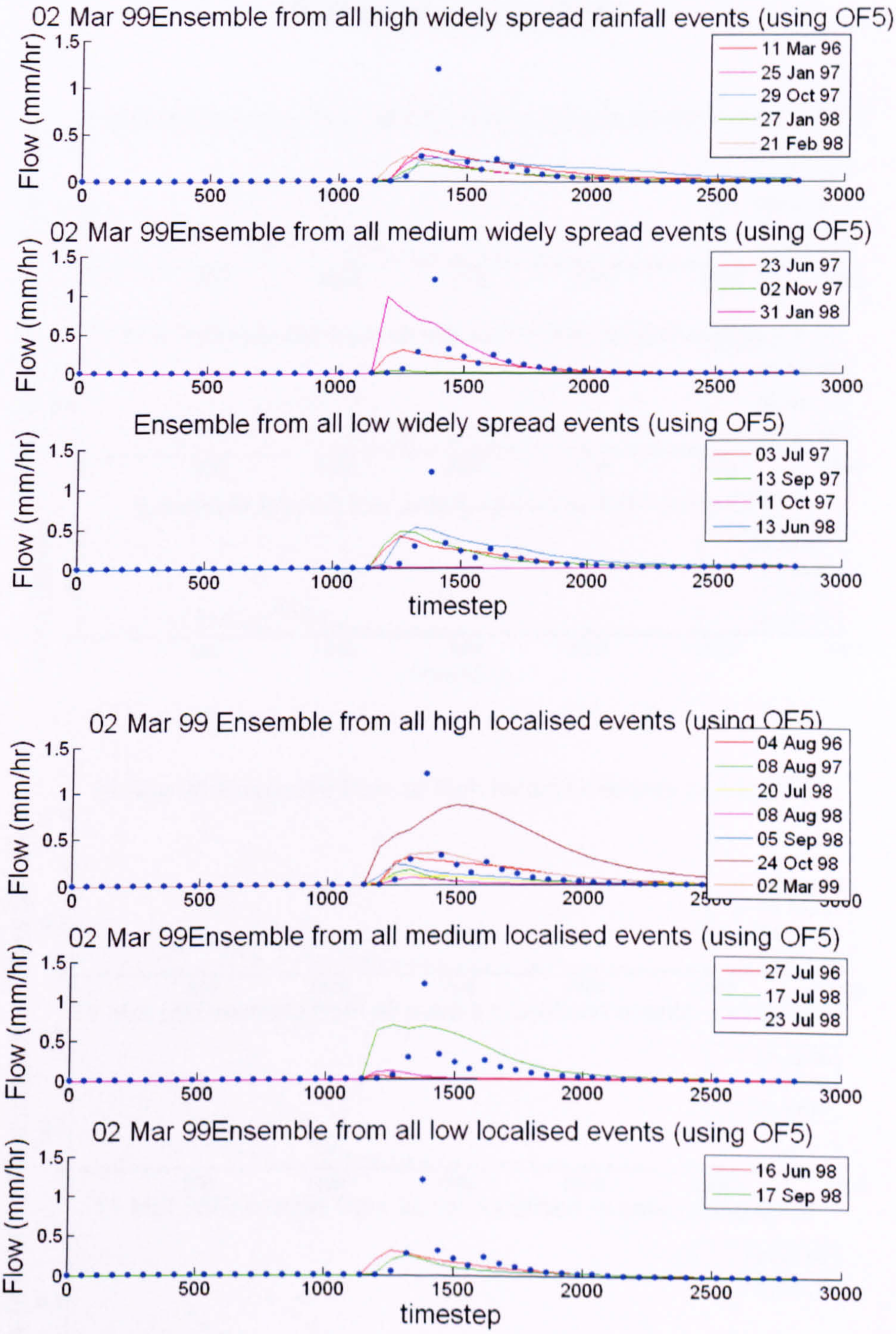

11 Oct 97Ensemble from all high widely spread rainfall events (using OF5)
Flow (mm/hr)
11 Mar 96
25 Jan 97
29 Oct 97
27 Jan 98
21 Feb 98
11 Oct 97Ensemble from all medium widely spread events (using OF5)
23 Jun 97
02 Nov 97
31 Jan 98
Ensemble from all low widely spread events (using OF5)
03 Jul 97
13 Sep 97
11 Oct 97
13 Jun 98
11 Oct 97 Ensemble from all high localised events (using OF5)
04 Aug 96
08 Aug 97
20 Jul 98
08 Aug 98
05 Sep 98
24 Oct 98
02 Mar 99
11 Oct 97Ensemble from all medium localised events (using OF5)
27 Jul 96
17 Jul 98
23 Jul 98
11 Oct 97Ensemble from all low localised events (using OF5)
16 Jun 98
17 Sep 98
timestep


02 Nov 97Ensemble from all high widely spread rainfall events (using OF5)
Flow (mm/hr)
11 Mar 96
25 Jan 97
29 Oct 97
27 Jan 98
21 Feb 98
02 Nov 97Ensemble from all medium widely spread events (using OF5)
23 Jun 97
02 Nov 97
31 Jan 98
Ensemble from all low widely spread events (using OF5)
03 Jul 97
13 Sep 97
11 Oct 97
13 Jun 98
02 Nov 97 Ensemble from all high localised events (using OF5)
04 Aug 96
08 Aug 97
20 Jul 98
08 Aug 98
05 Sep 98
24 Oct 98
02 Mar 99
02 Nov 97Ensemble from all medium localised events (using OF5)
27 Jul 96
17 Jul 98
23 Jul 98
02 Nov 97Ensemble from all low localised events (using OF5)
16 Jun 98
17 Sep 98
timestep

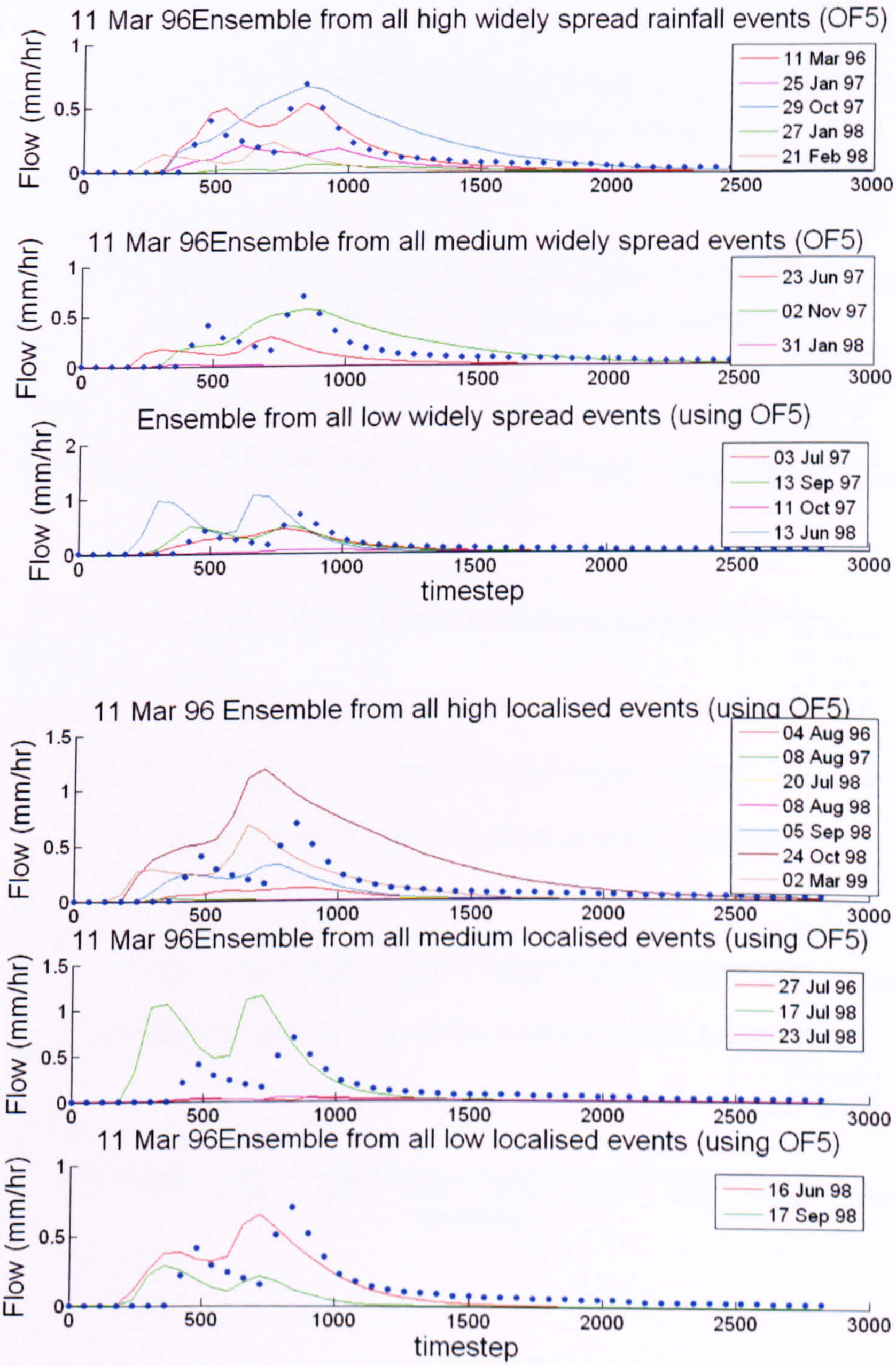

27 Jan 98Ensemble from all high widely spread rainfall events (using OF5)
Flow (mm/hr)
11 Mar 96
25 Jan 97
29 Oct 97
27 Jan 98
21 Feb 98
27 Jan 98Ensemble from all medium widely spread events (using OF5)
23 Jun 97
02 Nov 97
31 Jan 98
Ensemble from all low widely spread events (using OF5)
03 Jul 97
13 Sep 97
11 Oct 97
13 Jun 98
27 Jan 98 Ensemble from all high localised events (using OF5)
04 Aug 96
08 Aug 97
20 Jul 98
08 Aug 98
05 Sep 98
24 Oct 98
02 Mar 99
27 Jan 98Ensemble from all medium localised events (using OF5)
27 Jul 96
17 Jul 98
23 Jul 98
27 Jan 98Ensemble from all low localised events (using OF5)
16 Jun 98
17 Sep 98
timestep

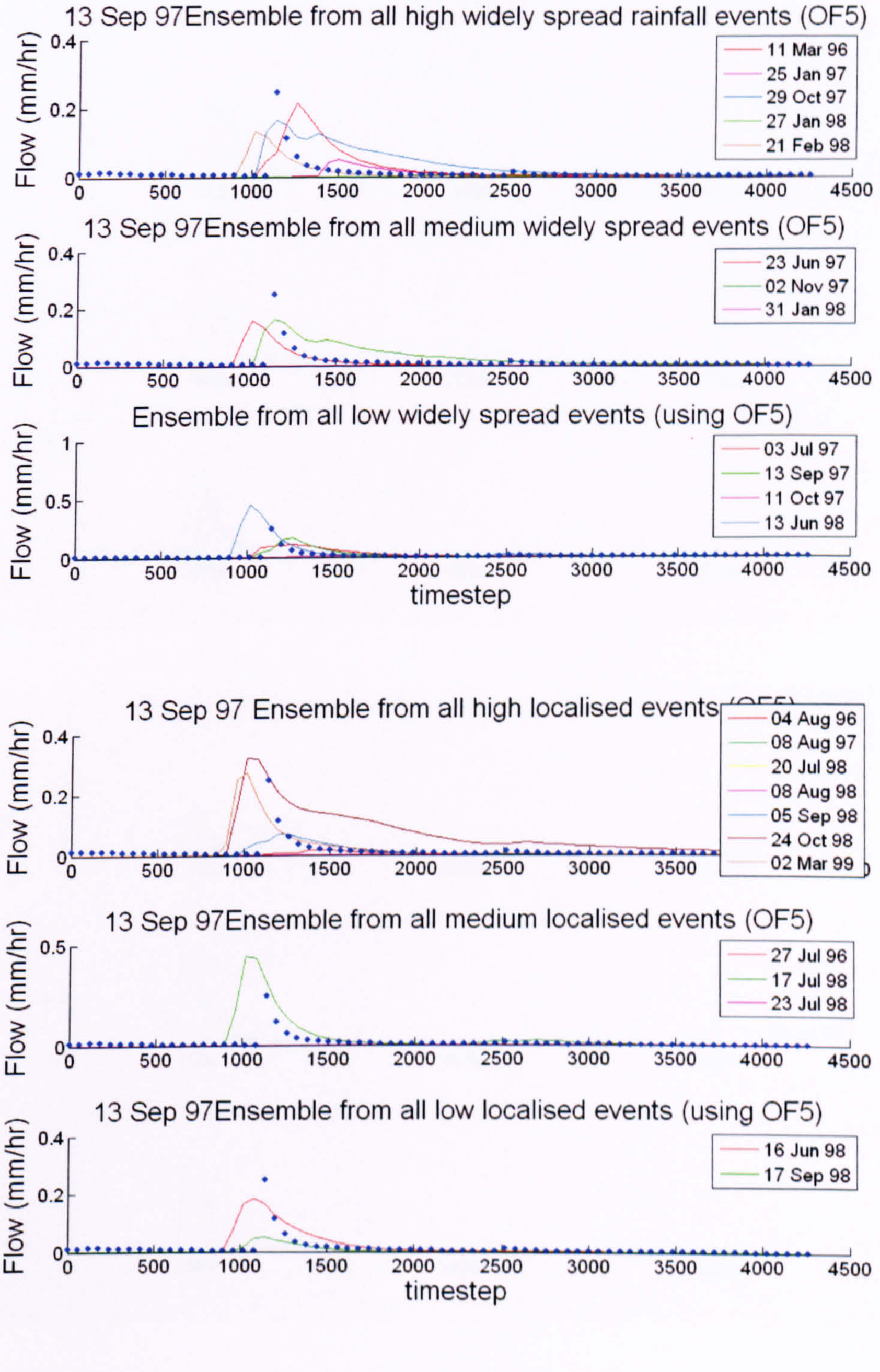

08 Aug 98Ensemble from all high widely spread rainfall events (using OF5)
Flow (mm/hr)
11 Mar 96
25 Jan 97
29 Oct 97
27 Jan 98
21 Feb 98
08 Aug 98Ensemble ofrom all medium widely spread events (using OF5)
23 Jun 97
02 Nov 97
31 Jan 98
Ensemble from all low widely spread events (using OF5)
03 Jul 97
13 Sep 97
11 Oct 97
13 Jun 98
08 Aug 98 Ensemble from all high localised events (using OF5)
04 Aug 96
08 Aug 97
20 Jul 98
08 Aug 98
05 Sep 98
24 Oct 98
02 Mar 99
08 Aug 98Ensemble from all medium localised events (using OF5)
27 Jul 96
17 Jul 98
23 Jul 98
08 Aug 98Ensemble from all low localised events (using OF5)
16 Jun 98
17 Sep 98
timestep

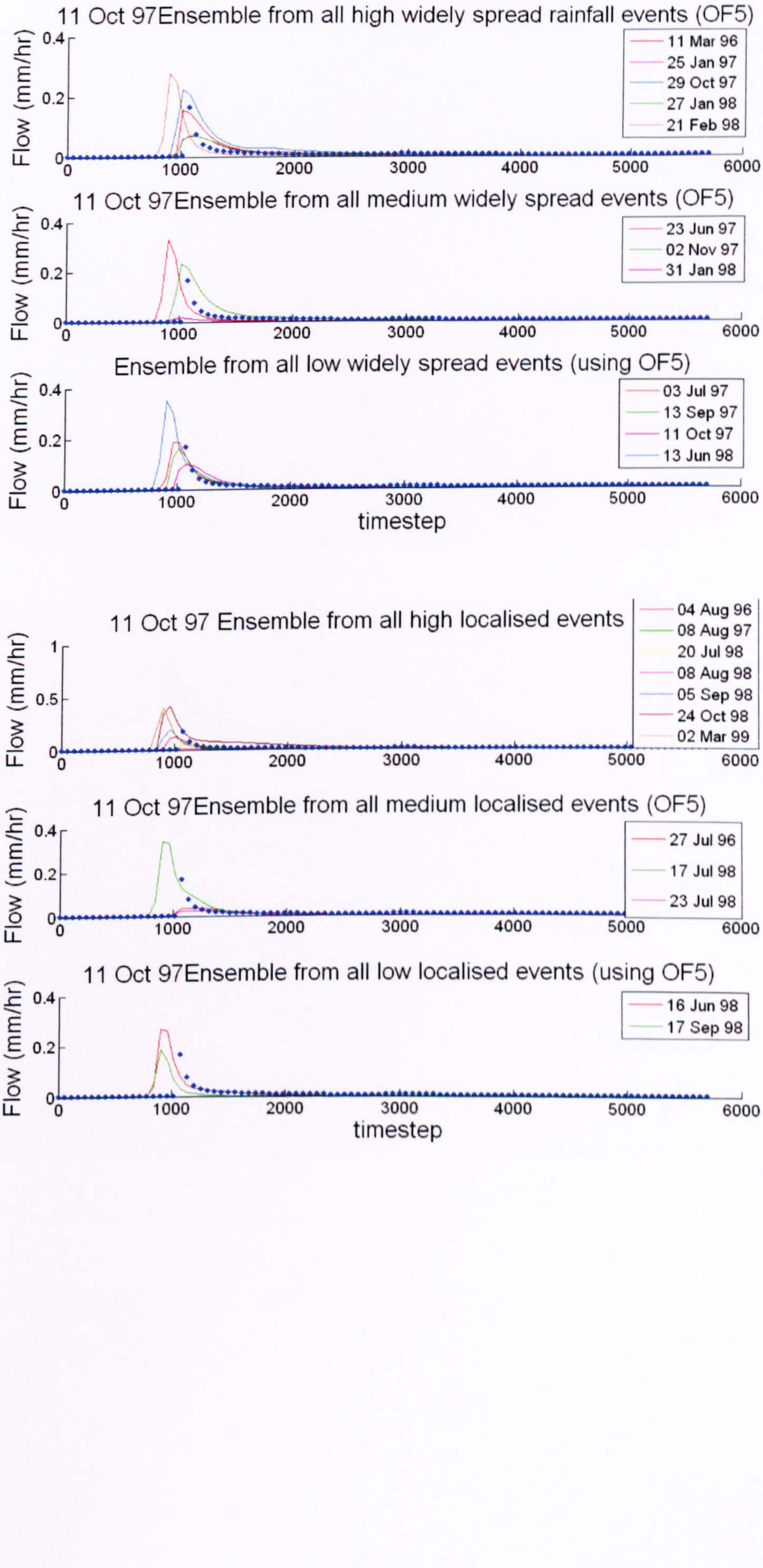

17 Sep 98Ensemble from all high widely spread rainfall events (using OF5)
Flow (mm/hr)
0.4
0.2
0
0
500
1000
1500
2000
2500
3000
11 Mar 96
25 Jan 97
29 Oct 97
27 Jan 98
21 Feb 98
17 Sep 98Ensemble from all medium widely spread events (using OF5)
Flow (mm/hr)
1
0.5
0
0
500
1000
1500
2000
2500
3000
23 Jun 97
02 Nov 97
31 Jan 98
Ensemble from all low widely spread events (using OF5)
Flow (mm/hr)
0.4
0.2
0
0
500
1000
1500
2000
2500
3000
timestep
03 Jul 97
13 Sep 97
11 Oct 97
13 Jun 98
17 Sep 98 Ensemble from all high localised events (using OF5)
Flow (mm/hr)
0.4
0.2
0
0
500
1000
1500
2000
04 Aug 96
08 Aug 97
20 Jul 98
08 Aug 98
05 Sep 98
24 Oct 98
02 Mar 99
17 Sep 98Ensemble from all medium localised events (using OF5)
Flow (mm/hr)
0.4
0.2
0
0
500
1000
1500
2000
2500
3000
27 Jul 96
17 Jul 98
23 Jul 98
17 Sep 98Ensemble from all low localised events (using OF5)
Flow (mm/hr)
0.2
0.1
0
0
500
1000
1500
2000
2500
3000
16 Jun 98
17 Sep 98
timestep

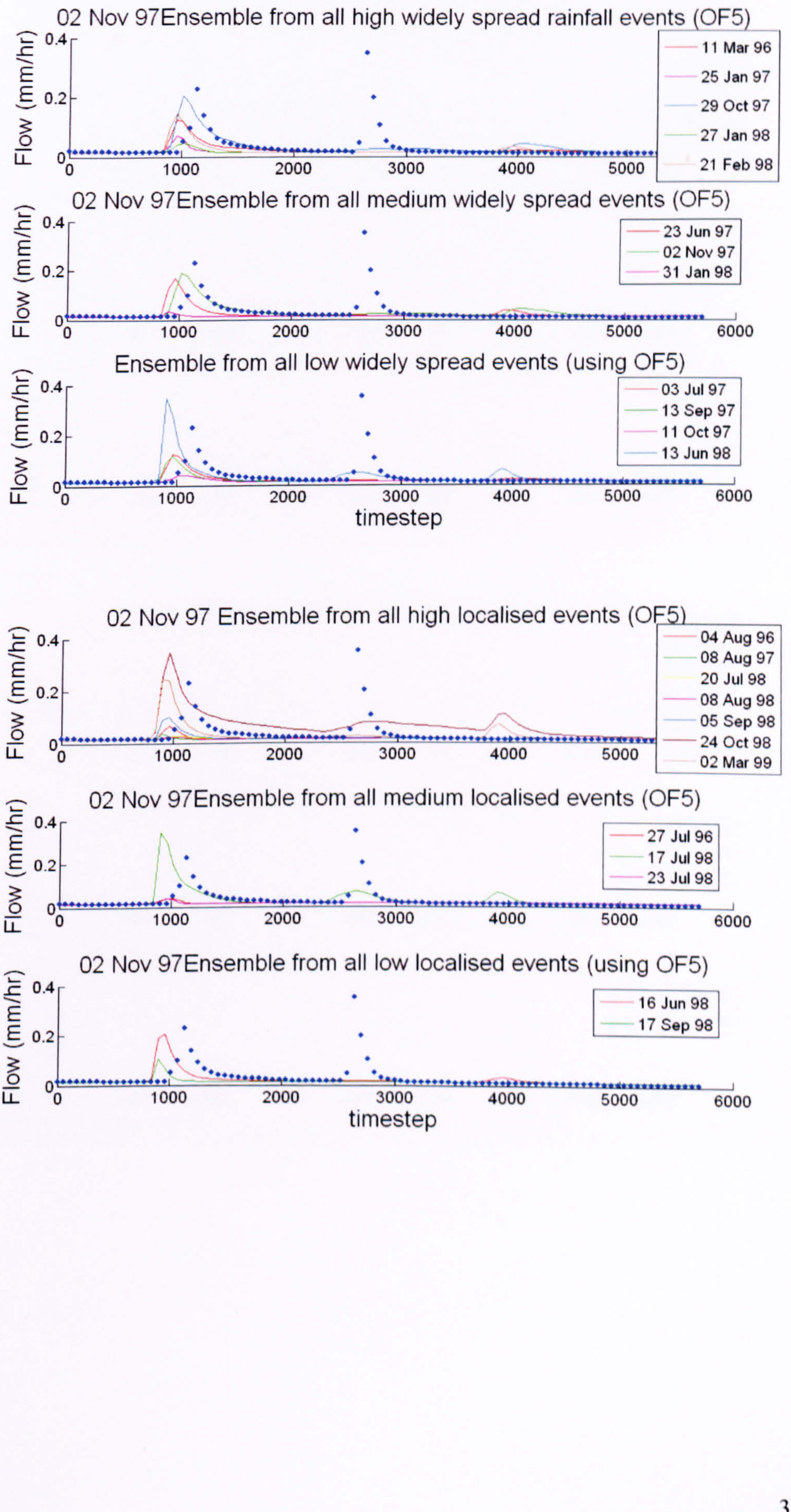

02 Mar 99Ensemble from all high widely spread rainfall events (using OF5)
Flow (mm/hr)
11 Mar 96
25 Jan 97
29 Oct 97
27 Jan 98
21 Feb 98
02 Mar 99Ensemble from all medium widely spread events (using OF5)
23 Jun 97
02 Nov 97
31 Jan 98
Ensemble from all low widely spread events (using OF5)
03 Jul 97
13 Sep 97
11 Oct 97
13 Jun 98
timestep
02 Mar 99 Ensemble from all high localised events (using OF5)
04 Aug 96
08 Aug 97
20 Jul 98
08 Aug 98
05 Sep 98
24 Oct 98
02 Mar 99
02 Mar 99Ensemble from all medium localised events (using OF5)
27 Jul 96
17 Jul 98
23 Jul 98
02 Mar 99Ensemble from all low localised events (using OF5)
16 Jun 98
17 Sep 98
timestep

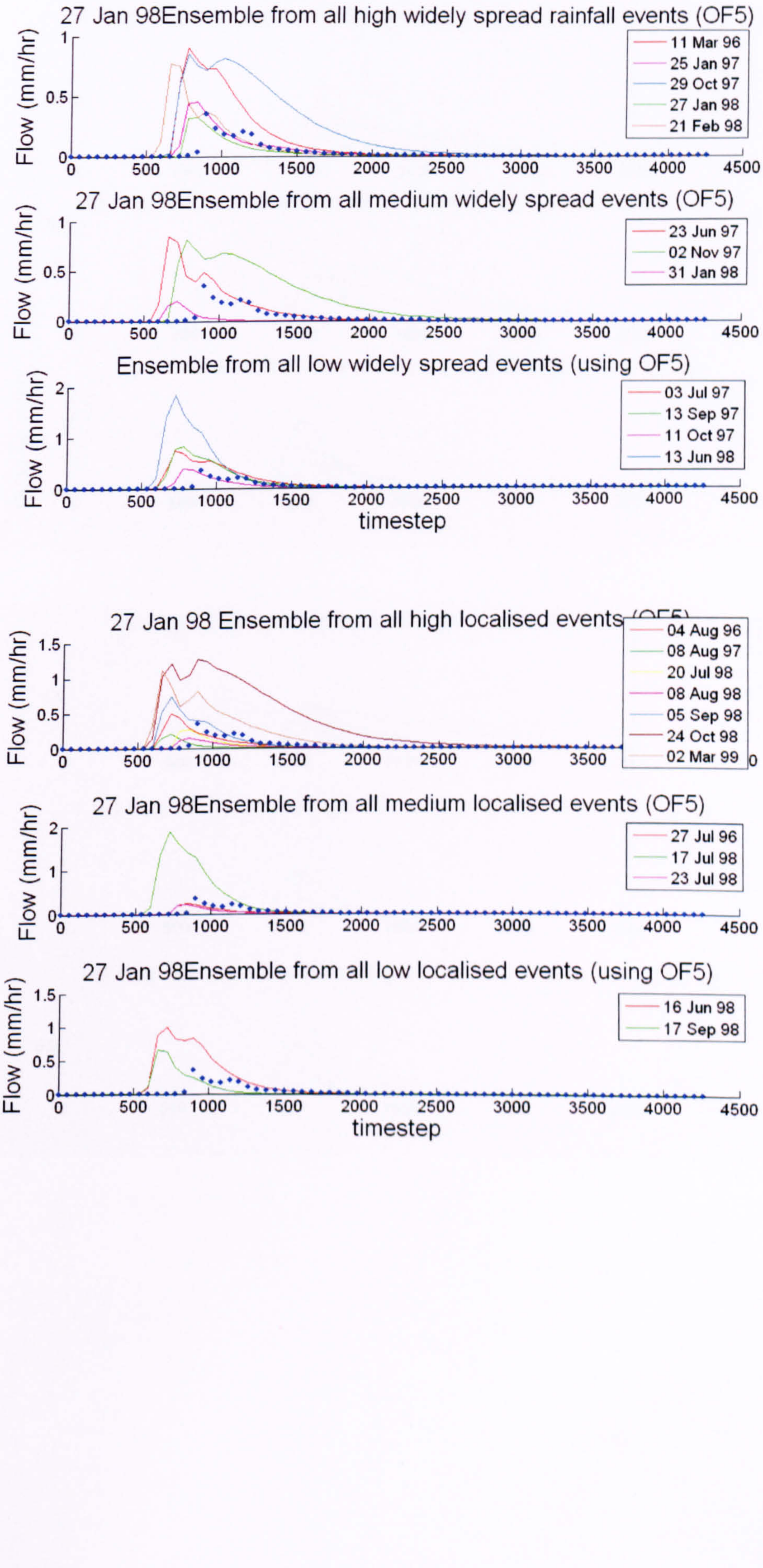
6-Parameters, G=0

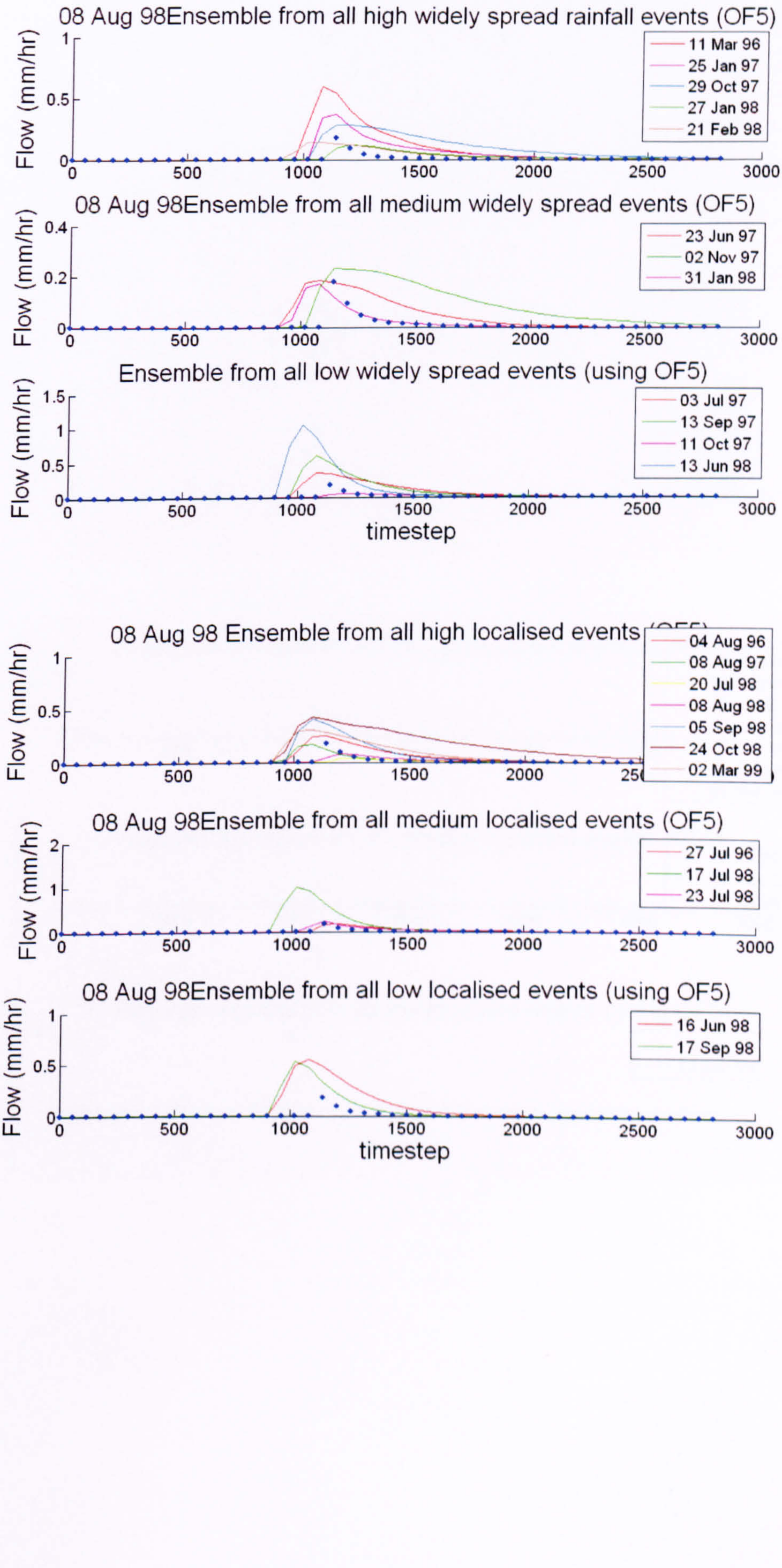


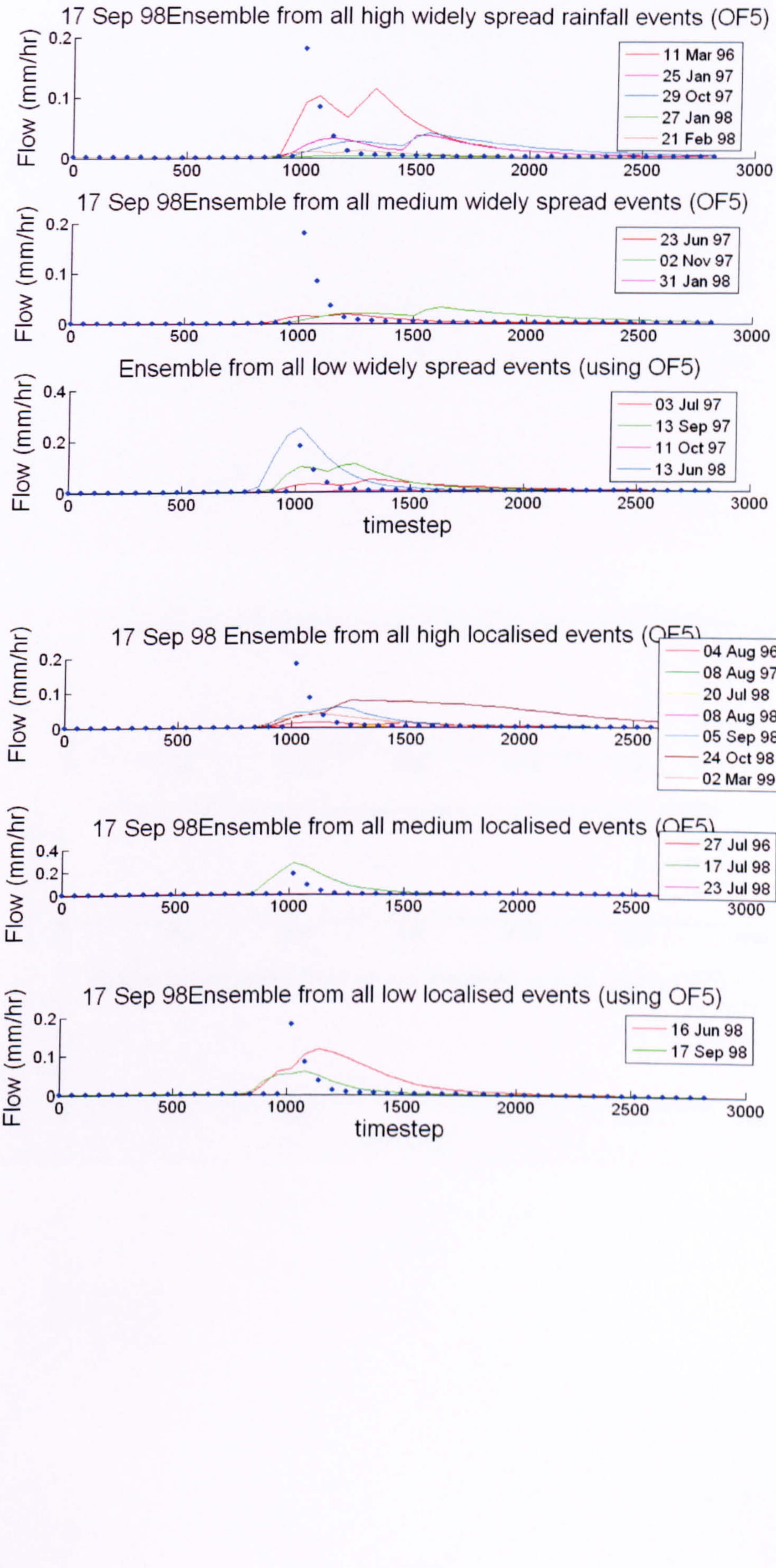

13 Sep 97Ensemble from all high widely spread rainfall events (OF5)
Flow (mm/hr)
0.4
0.2
0
0
500
1000
1500
2000
2500
3000
3500
4000
4500
11 Mar 96
25 Jan 97
29 Oct 97
27 Jan 98
21 Feb 98
13 Sep 97Ensemble from all medium widely spread events (OF5)
Flow (mm/hr)
0.4
0.2
0
23 Jun 97
02 Nov 97
31 Jan 98
Ensemble from all low widely spread events (using OF5)
Flow (mm/hr)
1
0.5
0
03 Jul 97
13 Sep 97
11 Oct 97
13 Jun 98
timestep
13 Sep 97 Ensemble from all high localised events (OF5)
Flow (mm/hr)
0.4
0.2
0
04 Aug 96
08 Aug 97
20 Jul 98
08 Aug 98
05 Sep 98
24 Oct 98
02 Mar 99
13 Sep 97Ensemble from all medium localised events (OF5)
Flow (mm/hr)
0.5
0
27 Jul 96
17 Jul 98
23 Jul 98
13 Sep 97Ensemble from all low localised events (using OF5)
Flow (mm/hr)
0.4
0.2
0
16 Jun 98
17 Sep 98
timestep

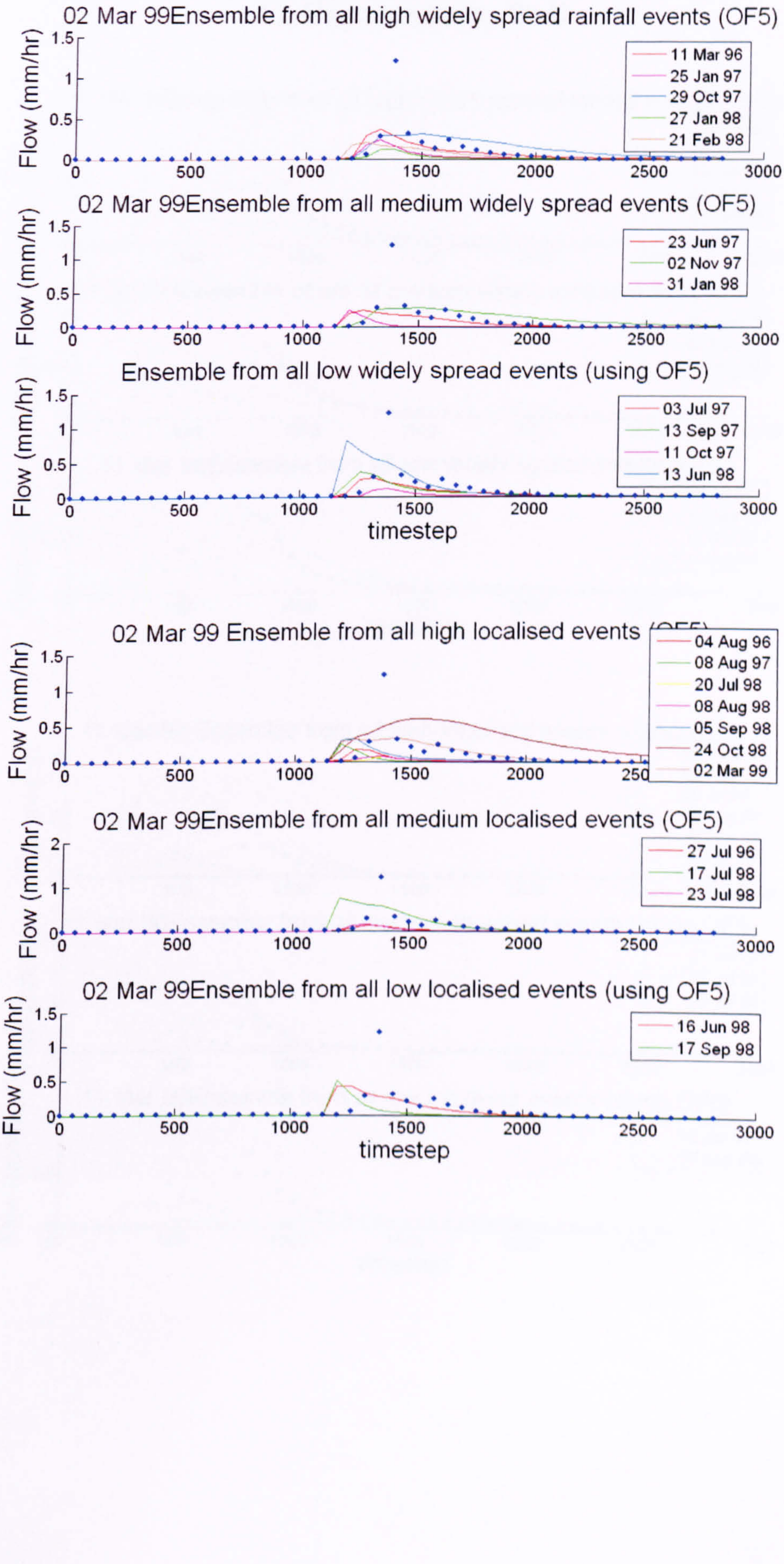

11 Oct 97Ensemble from all high widely spread rainfall events (OF5)
Flow (mm/hr)
0.4
0.2
0
0
1000
2000
3000
4000
5000
6000
11 Mar 96
25 Jan 97
29 Oct 97
27 Jan 98
21 Feb 98
11 Oct 97Ensemble from all medium widely spread events (OF5)
Flow (mm/hr)
0.4
0.2
0
0
1000
2000
3000
4000
5000
6000
23 Jun 97
02 Nov 97
31 Jan 98
Ensemble from all low widely spread events (using OF5)
Flow (mm/hr)
0.4
0.2
0
0
1000
2000
3000
4000
5000
6000
timestep
03 Jul 97
13 Sep 97
11 Oct 97
13 Jun 98
11 Oct 97 Ensemble from all high localised events
Flow (mm/hr)
1
0.5
0
0
1000
2000
3000
4000
5000
6000
04 Aug 96
08 Aug 97
20 Jul 98
08 Aug 98
05 Sep 98
24 Oct 98
02 Mar 99
11 Oct 97Ensemble from all medium localised events (OF5)
Flow (mm/hr)
0.4
0.2
0
0
1000
2000
3000
4000
5000
6000
27 Jul 96
17 Jul 98
23 Jul 98
11 Oct 97Ensemble from all low localised events (using OF5)
Flow (mm/hr)
0.4
0.2
0
0
1000
2000
3000
4000
5000
6000
timestep
16 Jun 98
17 Sep 98


02 Nov 97Ensemble from all high widely spread rainfall events (OF5)
Flow (mm/hr)
0.4
0.2
0
0
1000
2000
3000
4000
5000
11 Mar 96
25 Jan 97
29 Oct 97
27 Jan 98
21 Feb 98
02 Nov 97Ensemble from all medium widely spread events (OF5)
Flow (mm/hr)
0.4
0.2
0
0
1000
2000
3000
4000
5000
6000
23 Jun 97
02 Nov 97
31 Jan 98
Ensemble from all low widely spread events (using OF5)
Flow (mm/hr)
0.4
0.2
0
0
1000
2000
3000
4000
5000
6000
timestep
03 Jul 97
13 Sep 97
11 Oct 97
13 Jun 98
02 Nov 97 Ensemble from all high localised events (OF5)
Flow (mm/hr)
0.4
0.2
0
0
1000
2000
3000
4000
5000
04 Aug 96
08 Aug 97
20 Jul 98
08 Aug 98
05 Sep 98
24 Oct 98
02 Mar 99
02 Nov 97Ensemble from all medium localised events (OF5)
Flow (mm/hr)
0.4
0.2
0
0
1000
2000
3000
4000
5000
6000
27 Jul 96
17 Jul 98
23 Jul 98
02 Nov 97Ensemble from all low localised events (using OF5)
Flow (mm/hr)
0.4
0.2
0
0
1000
2000
3000
4000
5000
6000
timestep
16 Jun 98
17 Sep 98

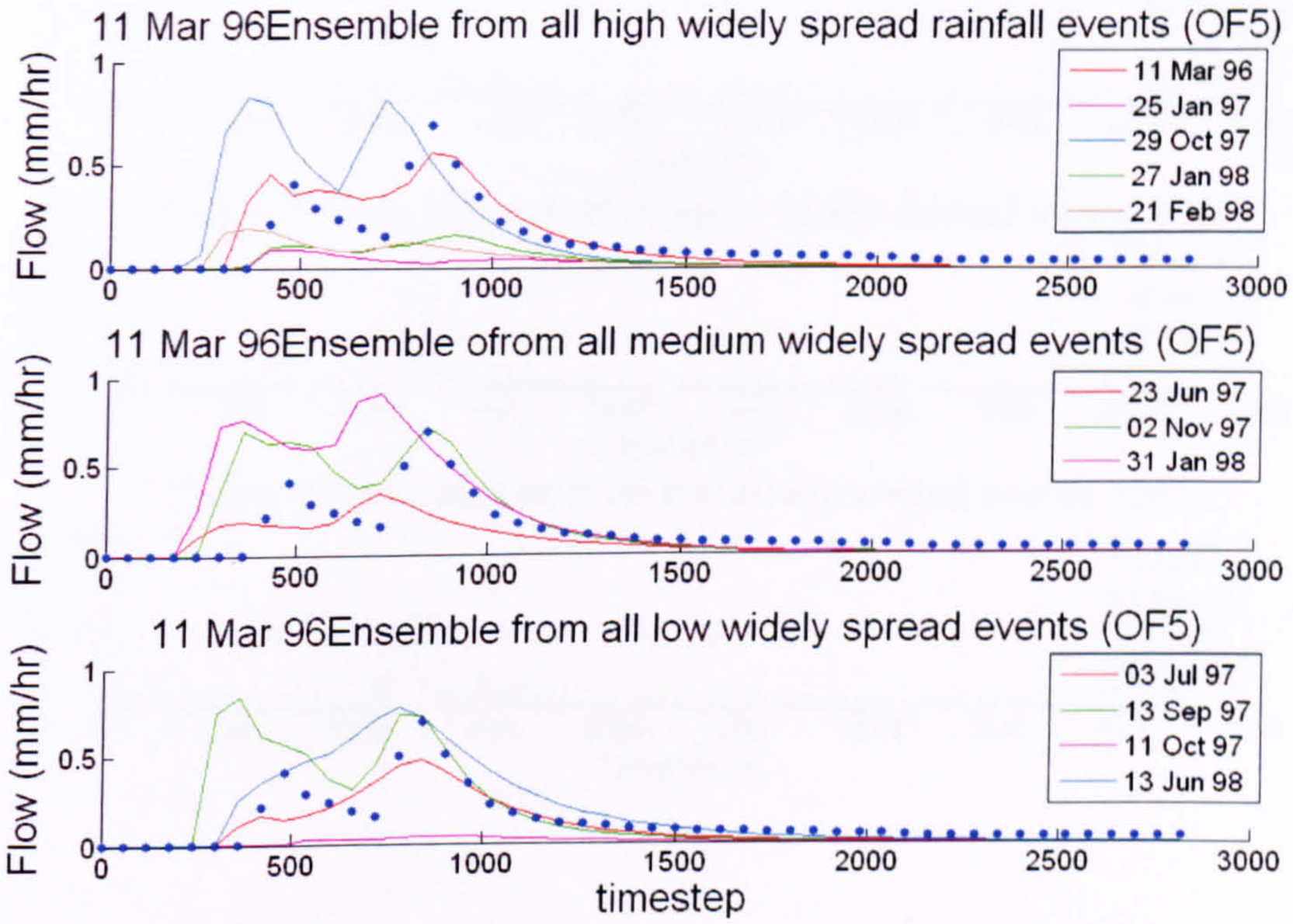

27 Jan 98Ensemble from all high widely spread rainfall events (OF5)
Flow (mm/hr)
11 Mar 96
25 Jan 97
29 Oct 97
27 Jan 98
21 Feb 98
27 Jan 98Ensemble from all medium widely spread events (OF5)
23 Jun 97
02 Nov 97
31 Jan 98
Ensemble from all low widely spread events (using OF5)
03 Jul 97
13 Sep 97
11 Oct 97
13 Jun 98
timestep
27 Jan 98 Ensemble from all high localised events (OF5)
04 Aug 96
08 Aug 97
20 Jul 98
08 Aug 98
05 Sep 98
24 Oct 98
02 Mar 99
27 Jan 98Ensemble from all medium localised events (OF5)
27 Jul 96
17 Jul 98
23 Jul 98
27 Jan 98Ensemble from all low localised events (using OF5)
16 Jun 98
17 Sep 98
timestep

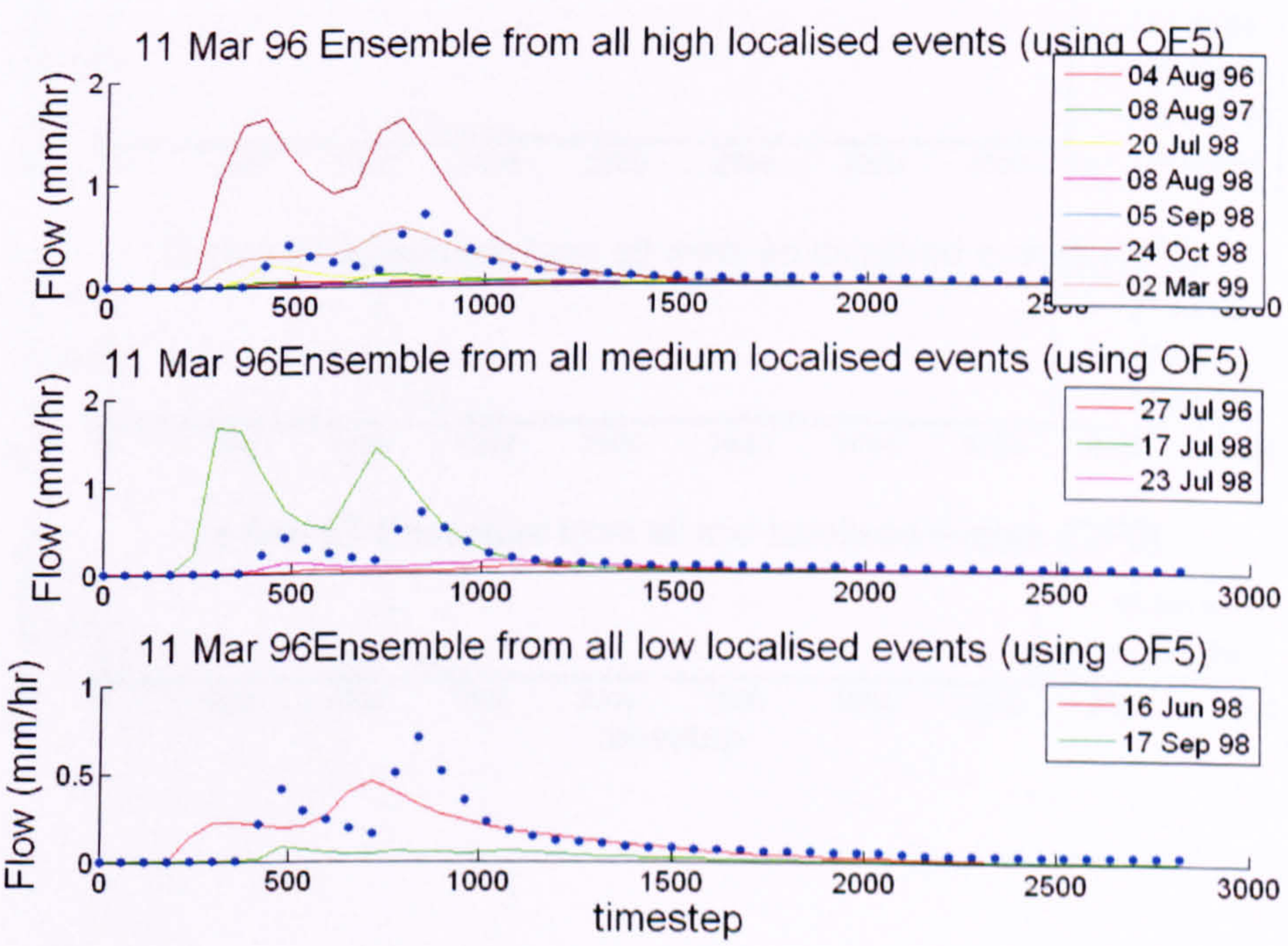

08 Aug 98Ensemble from all high widely spread rainfall events (OF5)
Flow (mm/hr)
11 Mar 96
25 Jan 97
29 Oct 97
27 Jan 98
21 Feb 98
08 Aug 98Ensemble from all medium widely spread events (OF5)
23 Jun 97
02 Nov 97
31 Jan 98
Ensemble from all low widely spread events (using OF5)
03 Jul 97
13 Sep 97
11 Oct 97
13 Jun 98
timestep
08 Aug 98 Ensemble from all high localised events
04 Aug 96
08 Aug 97
20 Jul 98
08 Aug 98
05 Sep 98
24 Oct 98
02 Mar 99
08 Aug 98Ensemble from all medium localised events (OF5)
27 Jul 96
17 Jul 98
23 Jul 98
08 Aug 98Ensemble from all low localised events (using OF5)
16 Jun 98
17 Sep 98
timestep

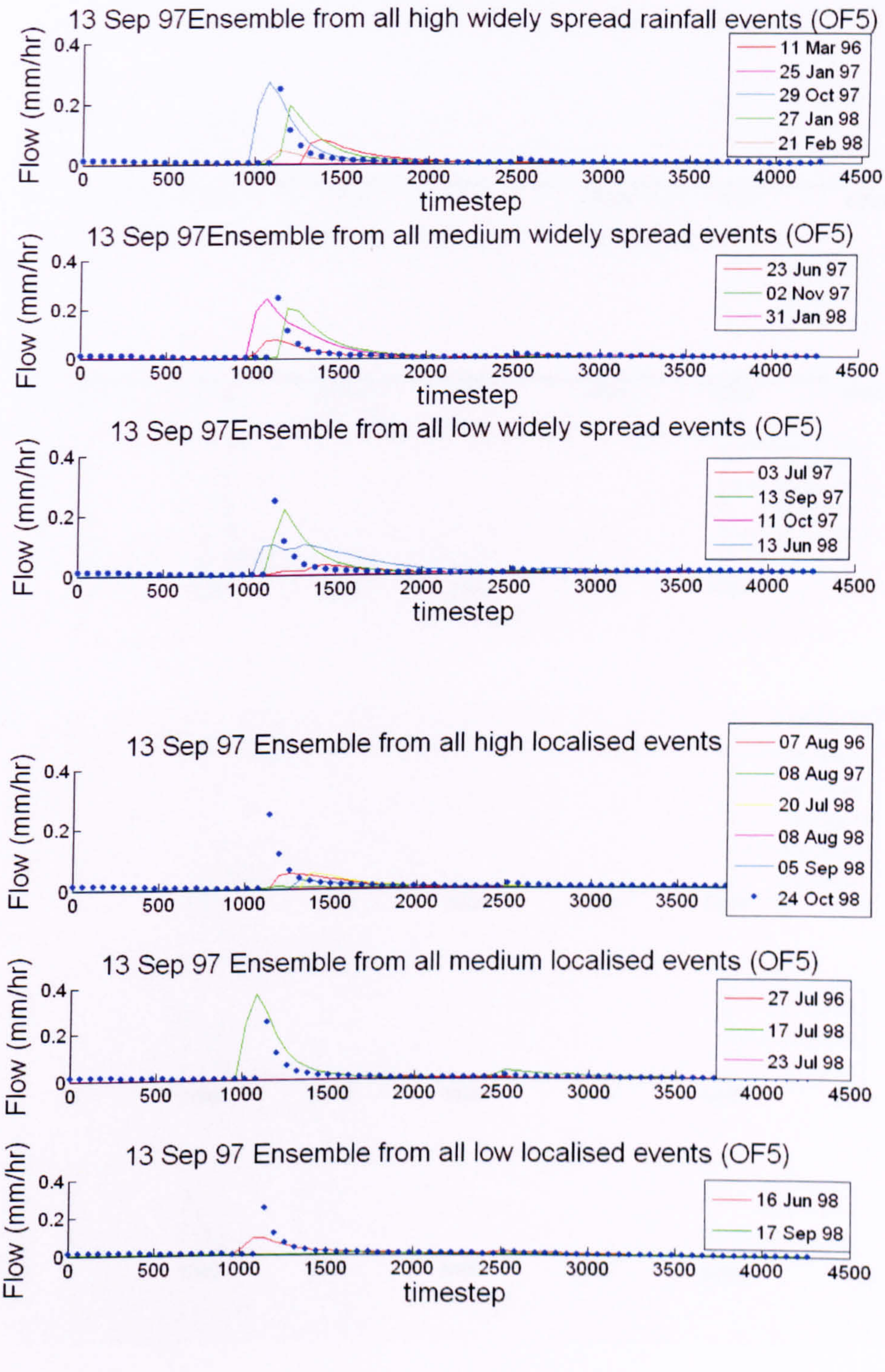

17 Sep 98Ensemble from all high widely spread rainfall events (OF5)
Flow (mm/hr)
0.2
0.1
0
0
500
1000
1500
2000
2500
3000
11 Mar 96
25 Jan 97
29 Oct 97
27 Jan 98
21 Feb 98
17 Sep 98Ensemble from all medium widely spread events (OF5)
Flow (mm/hr)
0.2
0.1
0
0
500
1000
1500
2000
2500
3000
23 Jun 97
02 Nov 97
31 Jan 98
Ensemble from all low widely spread events (using OF5)
Flow (mm/hr)
0.4
0.2
0
0
500
1000
1500
2000
2500
3000
timestep
03 Jul 97
13 Sep 97
11 Oct 97
13 Jun 98
17 Sep 98 Ensemble from all high localised events (OF5)
Flow (mm/hr)
0.2
0.1
0
0
500
1000
1500
2000
2500
04 Aug 96
08 Aug 97
20 Jul 98
08 Aug 98
05 Sep 98
24 Oct 98
02 Mar 99
17 Sep 98Ensemble from all medium localised events (OF5)
Flow (mm/hr)
0.4
0.2
0
0
500
1000
1500
2000
2500
3000
27 Jul 96
17 Jul 98
23 Jul 98
17 Sep 98Ensemble from all low localised events (using OF5)
Flow (mm/hr)
0.2
0.1
0
0
500
1000
1500
2000
2500
3000
timestep
16 Jun 98
17 Sep 98

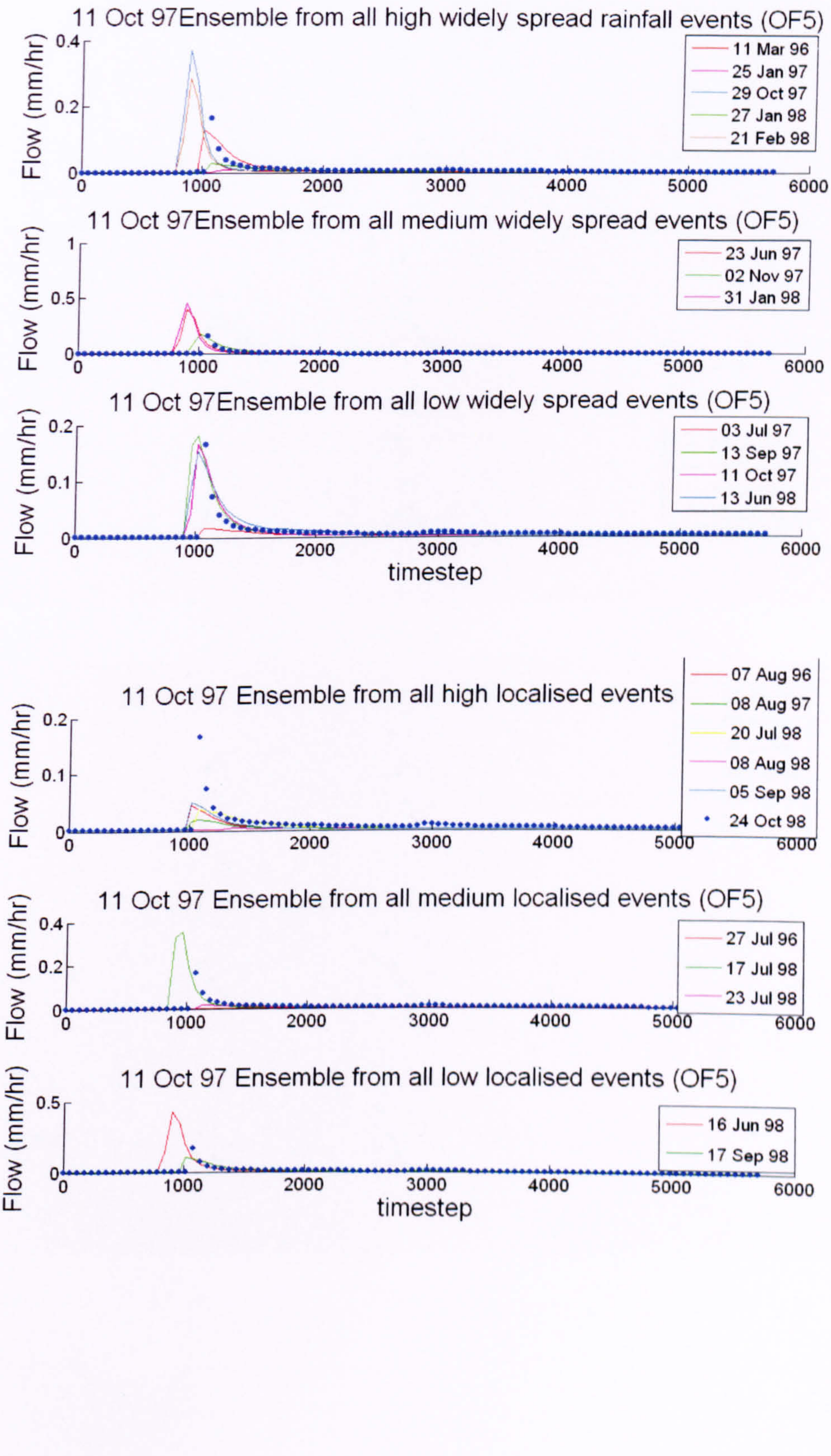

02 Mar 99Ensemble from all high widely spread rainfall events (OF5)
Flow (mm/hr)
11 Mar 96
25 Jan 97
29 Oct 97
27 Jan 98
21 Feb 98
02 Mar 99Ensemble from all medium widely spread events (OF5)
23 Jun 97
02 Nov 97
31 Jan 98
Ensemble from all low widely spread events (using OF5)
03 Jul 97
13 Sep 97
11 Oct 97
13 Jun 98
timestep
02 Mar 99 Ensemble from all high localised events
04 Aug 96
08 Aug 97
20 Jul 98
08 Aug 98
05 Sep 98
24 Oct 98
02 Mar 99
02 Mar 99Ensemble from all medium localised events (OF5)
27 Jul 96
17 Jul 98
23 Jul 98
02 Mar 99Ensemble from all low localised events (using OF5)
16 Jun 98
17 Sep 98
timestep

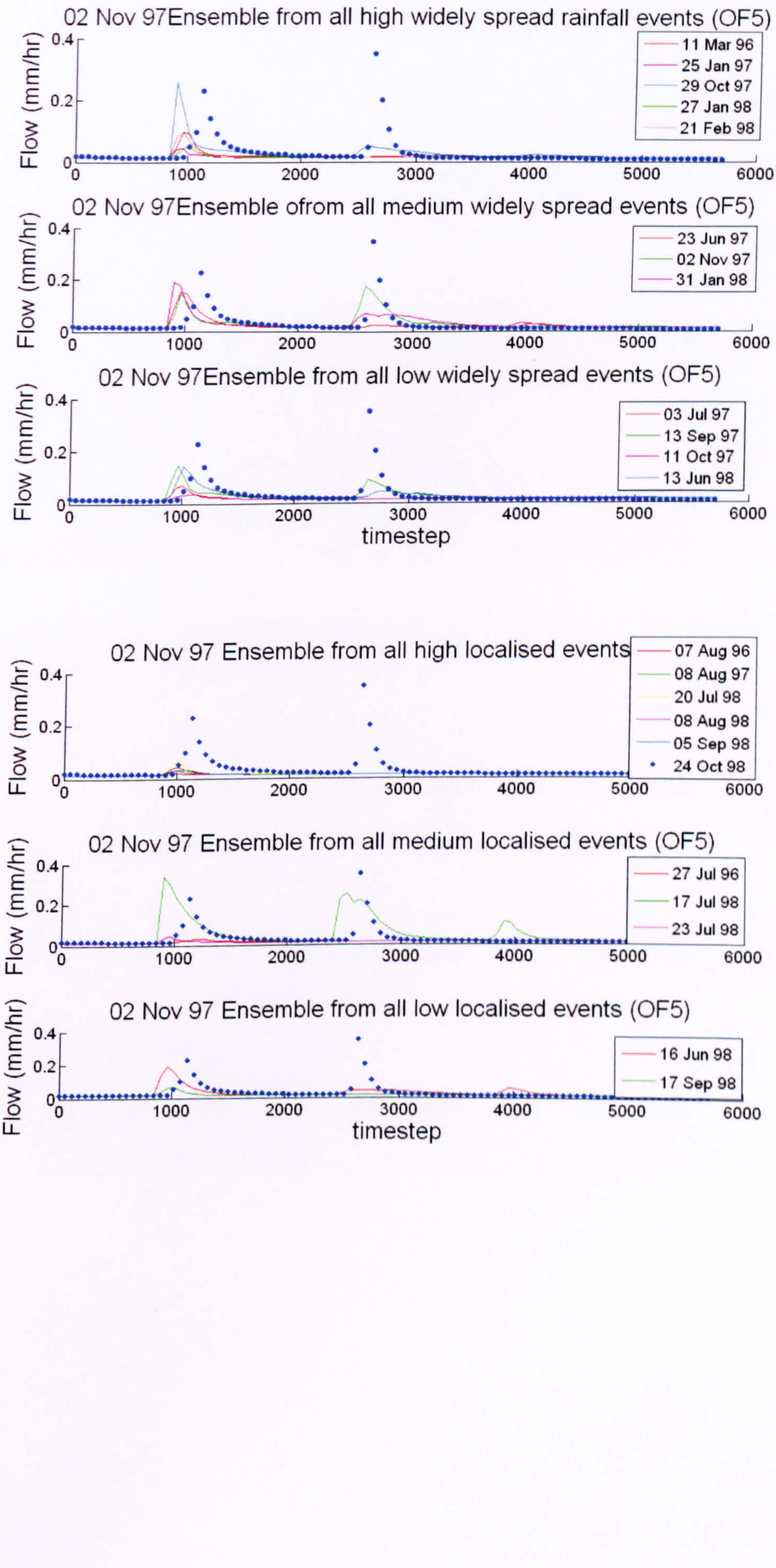
11-Parameters, G=0

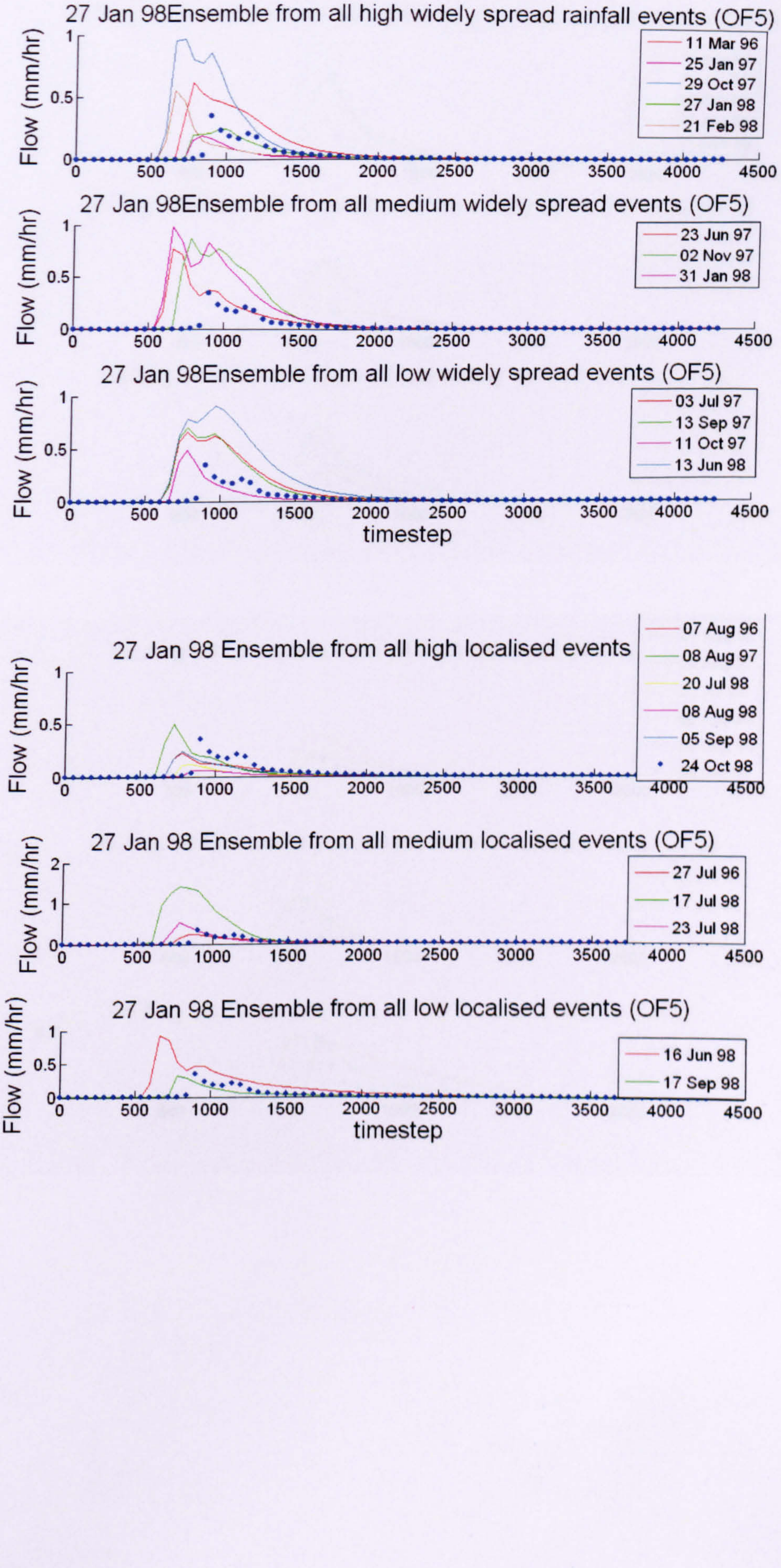


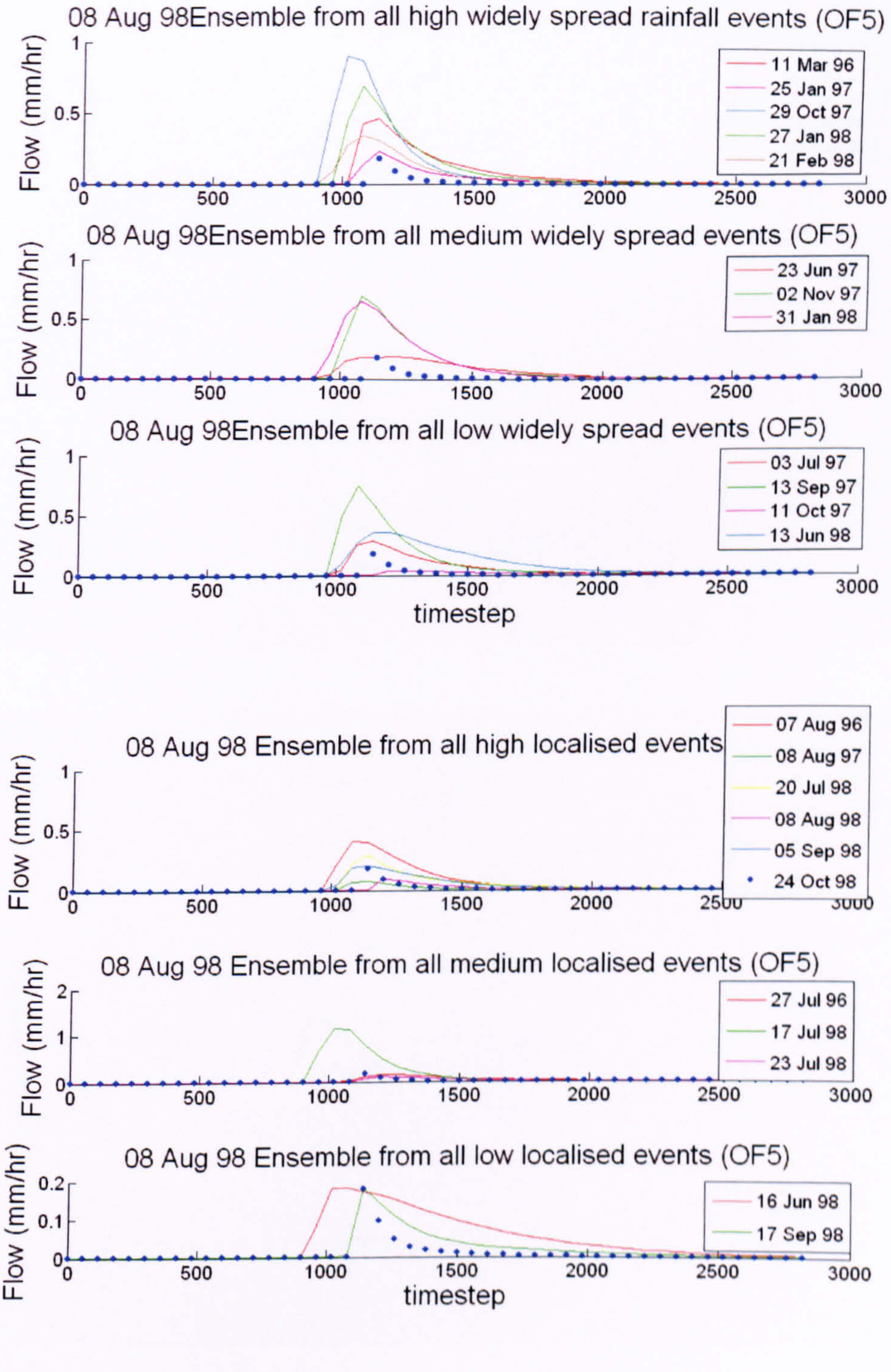


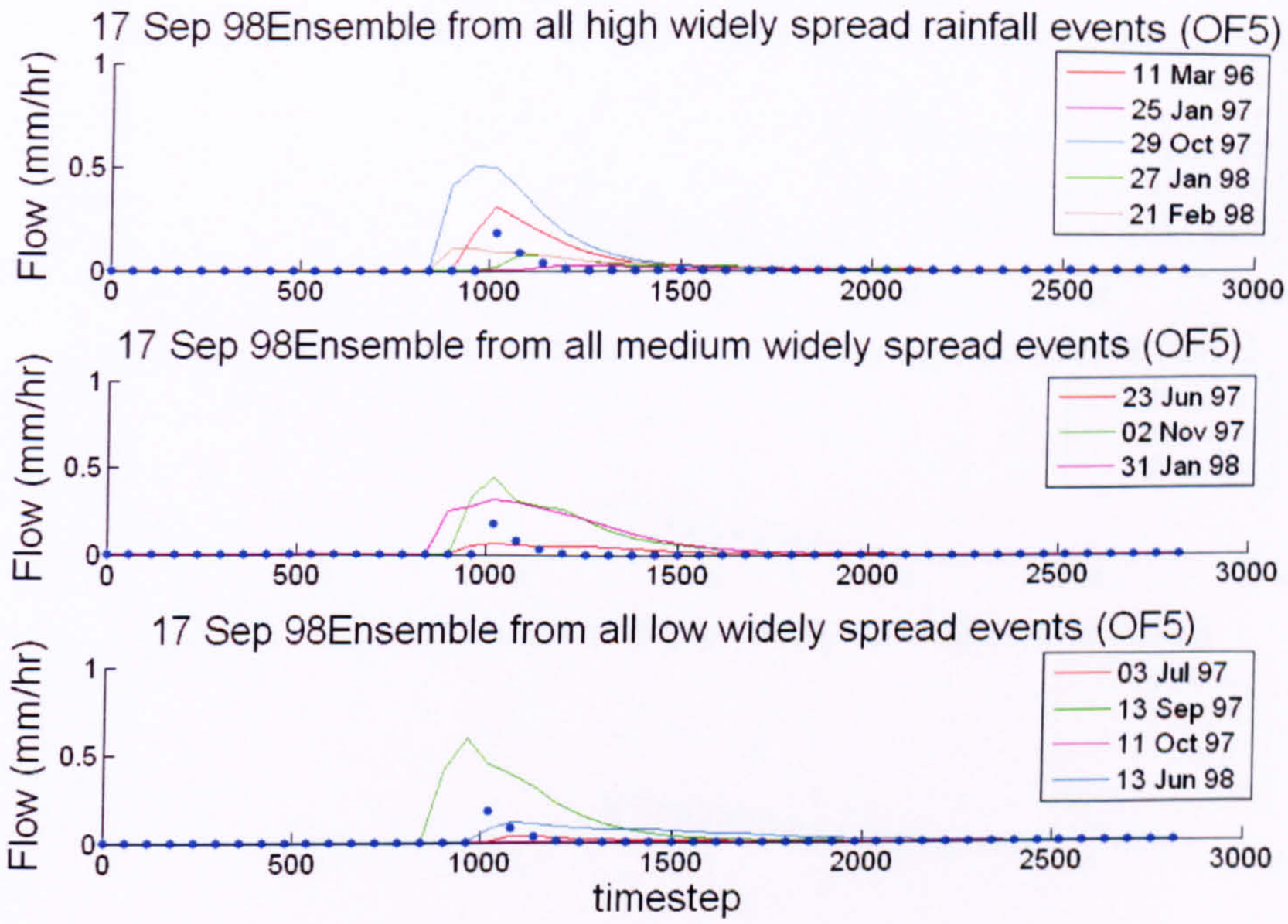

13 Sep 97Ensemble from all high widely spread rainfall events (OF5)
Flow (mm/hr)
timestep
11 Mar 96
25 Jan 97
29 Oct 97
27 Jan 98
21 Feb 98
13 Sep 97Ensemble from all medium widely spread events (OF5)
23 Jun 97
02 Nov 97
31 Jan 98
13 Sep 97Ensemble from all low widely spread events (OF5)
03 Jul 97
13 Sep 97
11 Oct 97
13 Jun 98
13 Sep 97 Ensemble from all high localised events
07 Aug 96
08 Aug 97
20 Jul 98
08 Aug 98
05 Sep 98
24 Oct 98
13 Sep 97 Ensemble from all medium localised events (OF5)
27 Jul 96
17 Jul 98
23 Jul 98
13 Sep 97 Ensemble from all low localised events (OF5)
16 Jun 98
17 Sep 98

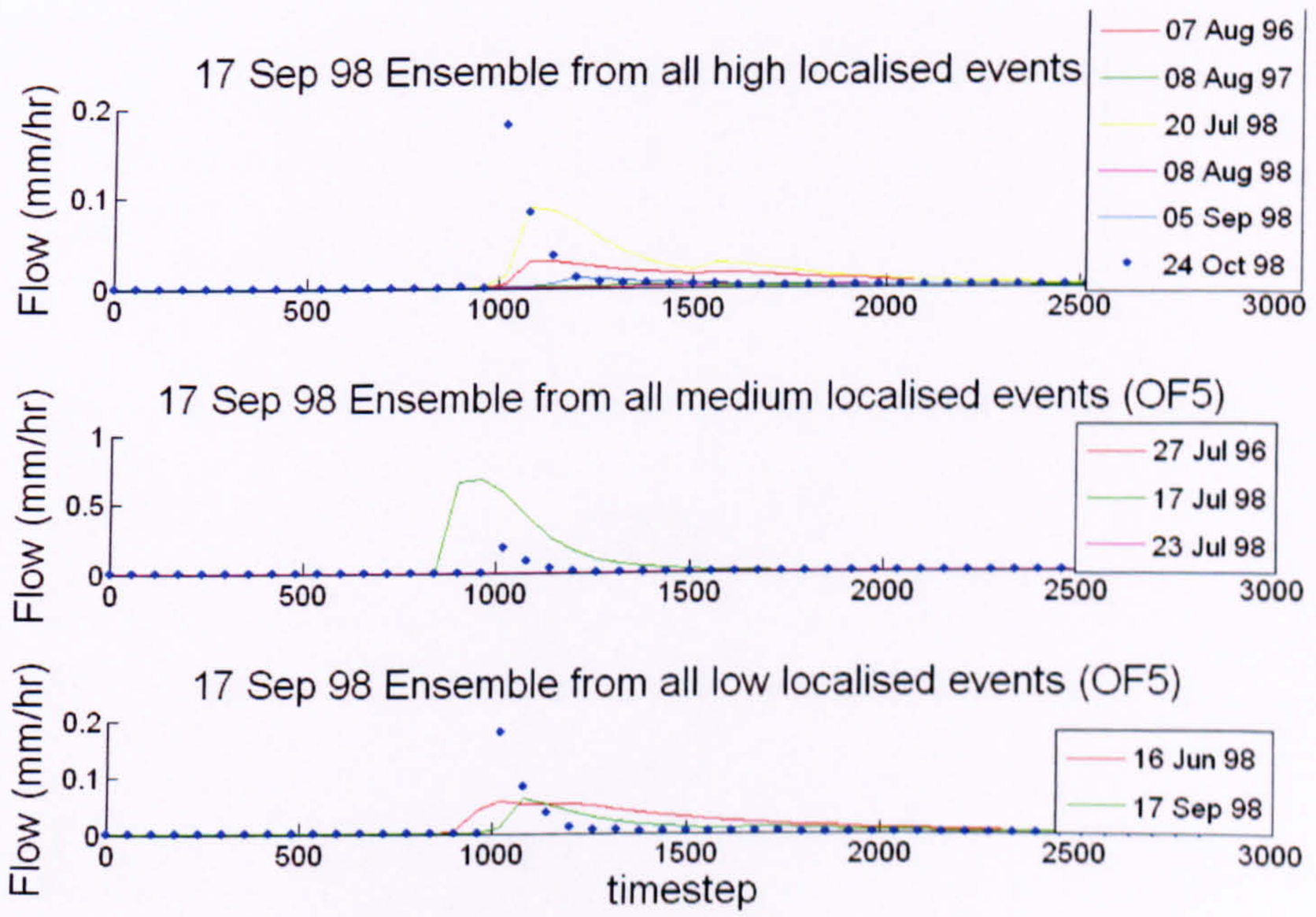

11 Oct 97Ensemble from all high widely spread rainfall events (OF5)
Flow (mm/hr)
11 Mar 96
25 Jan 97
29 Oct 97
27 Jan 98
21 Feb 98
11 Oct 97Ensemble from all medium widely spread events (OF5)
23 Jun 97
02 Nov 97
31 Jan 98
11 Oct 97Ensemble from all low widely spread events (OF5)
03 Jul 97
13 Sep 97
11 Oct 97
13 Jun 98
timestep
11 Oct 97 Ensemble from all high localised events
07 Aug 96
08 Aug 97
20 Jul 98
08 Aug 98
05 Sep 98
24 Oct 98
11 Oct 97 Ensemble from all medium localised events (OF5)
27 Jul 96
17 Jul 98
23 Jul 98
11 Oct 97 Ensemble from all low localised events (OF5)
16 Jun 98
17 Sep 98
timestep

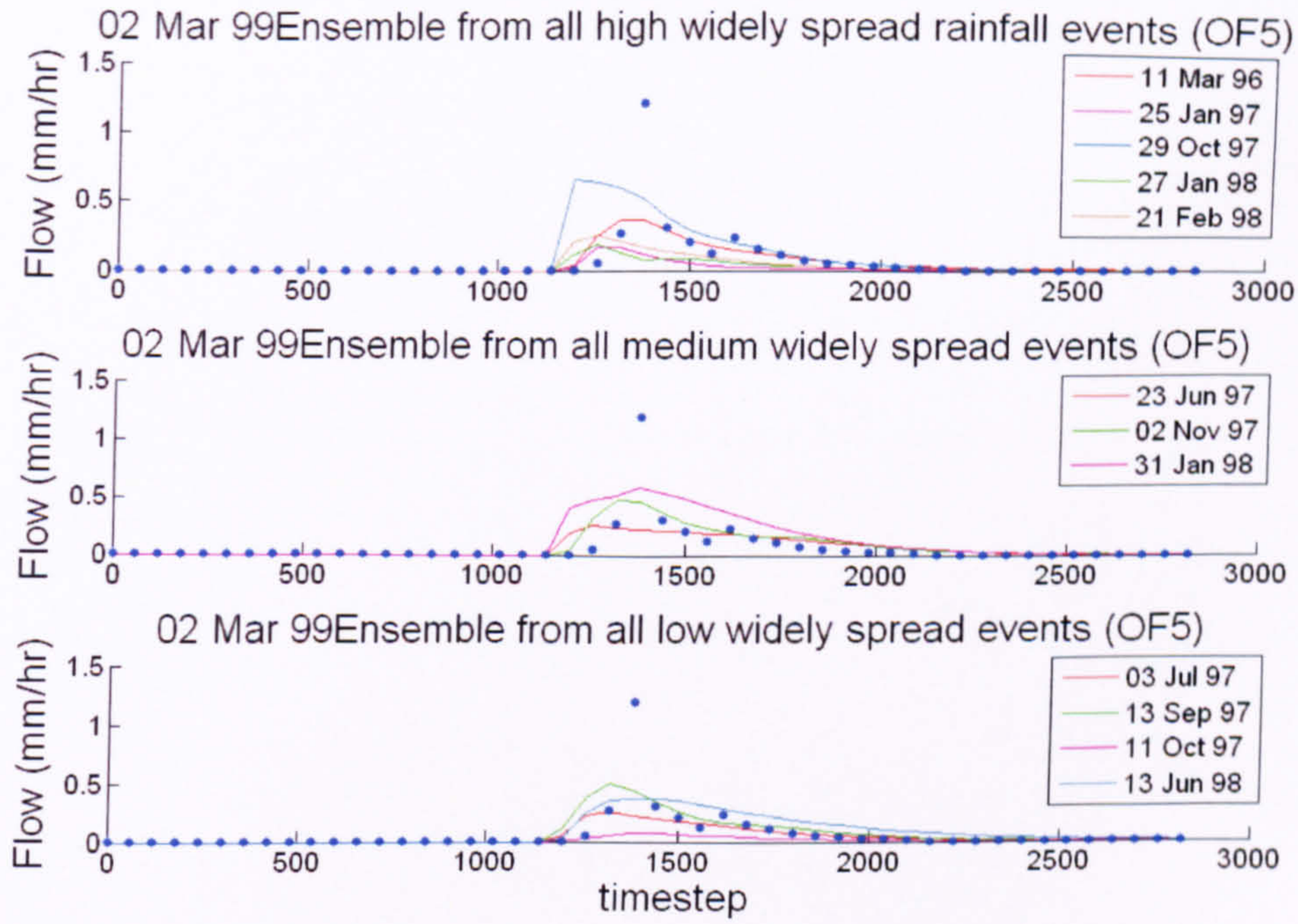

02 Nov 97Ensemble from all high widely spread rainfall events (OF5)
Flow (mm/hr)
0.4
0.2
0
0
1000
2000
3000
4000
5000
6000
11 Mar 96
25 Jan 97
29 Oct 97
27 Jan 98
21 Feb 98
02 Nov 97Ensemble ofrom all medium widely spread events (OF5)
Flow (mm/hr)
23 Jun 97
02 Nov 97
31 Jan 98
02 Nov 97Ensemble from all low widely spread events (OF5)
Flow (mm/hr)
03 Jul 97
13 Sep 97
11 Oct 97
13 Jun 98
timestep
02 Nov 97 Ensemble from all high localised events
Flow (mm/hr)
07 Aug 96
08 Aug 97
20 Jul 98
08 Aug 98
05 Sep 98
24 Oct 98
02 Nov 97 Ensemble from all medium localised events (OF5)
Flow (mm/hr)
27 Jul 96
17 Jul 98
23 Jul 98
02 Nov 97 Ensemble from all low localised events (OF5)
Flow (mm/hr)
16 Jun 98
17 Sep 98
timestep

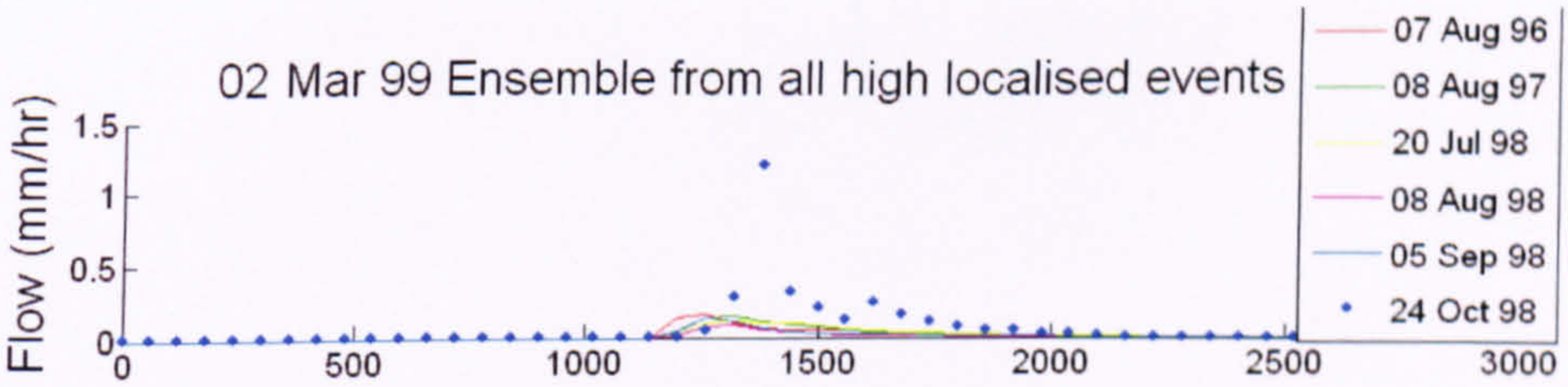

27 Jan 98Ensemble from all high widely spread rainfall events (OF5)
Flow (mm/hr)
11 Mar 96
25 Jan 97
29 Oct 97
27 Jan 98
21 Feb 98
27 Jan 98Ensemble from all medium widely spread events (OF5)
23 Jun 97
02 Nov 97
31 Jan 98
27 Jan 98Ensemble from all low widely spread events (OF5)
03 Jul 97
13 Sep 97
11 Oct 97
13 Jun 98
timestep
27 Jan 98 Ensemble from all high localised events
07 Aug 96
08 Aug 97
20 Jul 98
08 Aug 98
05 Sep 98
24 Oct 98
27 Jan 98 Ensemble from all medium localised events (OF5)
27 Jul 96
17 Jul 98
23 Jul 98
27 Jan 98 Ensemble from all low localised events (OF5)
16 Jun 98
17 Sep 98
timestep


08 Aug 98Ensemble from all high widely spread rainfall events (OF5)
Flow (mm/hr)
11 Mar 96
25 Jan 97
29 Oct 97
27 Jan 98
21 Feb 98
08 Aug 98Ensemble from all medium widely spread events (OF5)
23 Jun 97
02 Nov 97
31 Jan 98
08 Aug 98Ensemble from all low widely spread events (OF5)
03 Jul 97
13 Sep 97
11 Oct 97
13 Jun 98
timestep
08 Aug 98 Ensemble from all high localised events
07 Aug 96
08 Aug 97
20 Jul 98
08 Aug 98
05 Sep 98
24 Oct 98
08 Aug 98 Ensemble from all medium localised events (OF5)
27 Jul 96
17 Jul 98
23 Jul 98
08 Aug 98 Ensemble from all low localised events (OF5)
16 Jun 98
17 Sep 98
timestep


17 Sep 98Ensemble from all high widely spread rainfall events (OF5)
Flow (mm/hr)
11 Mar 96
25 Jan 97
29 Oct 97
27 Jan 98
21 Feb 98
17 Sep 98Ensemble from all medium widely spread events (OF5)
23 Jun 97
02 Nov 97
31 Jan 98
17 Sep 98Ensemble from all low widely spread events (OF5)
03 Jul 97
13 Sep 97
11 Oct 97
13 Jun 98
timestep


17 Sep 98 Ensemble from all high localised events
Flow (mm/hr)
07 Aug 96
08 Aug 97
20 Jul 98
08 Aug 98
05 Sep 98
24 Oct 98
17 Sep 98 Ensemble from all medium localised events (OF5)
27 Jul 96
17 Jul 98
23 Jul 98
17 Sep 98 Ensemble from all low localised events (OF5)
16 Jun 98
17 Sep 98
timestep





KING'S COLL. LONDON UNIV.